

2016

# Cell-free fetal DNA (cffDNA) enrichment for non-invasive prenatal testing (NIPT): a comparison of molecular techniques

Sillence, Kelly

<http://hdl.handle.net/10026.1/5319>

---

<http://dx.doi.org/10.24382/4051>

Plymouth University

---

*All content in PEARL is protected by copyright law. Author manuscripts are made available in accordance with publisher policies. Please cite only the published version using the details provided on the item record or document. In the absence of an open licence (e.g. Creative Commons), permissions for further reuse of content should be sought from the publisher or author.*

**Cell-free fetal DNA (cffDNA) enrichment for non-invasive prenatal testing  
(NIPT): a comparison of molecular techniques**

by

**Kelly A Sillence**

A thesis submitted to the University of Plymouth  
in partial fulfilment for the degree of

DOCTOR OF PHILOSOPHY

(December 2015)

School of Biomedical and Healthcare Sciences

### **Copyright Statement**

*This copy of the thesis has been supplied on condition that anyone who consults it is understood to recognise that its copyright rests with its author and that no quotation from the thesis and no information derived from it may be published without the author's prior consent.*

Cell-free fetal DNA (cffDNA) enrichment for non-invasive prenatal testing (NIPT):  
a comparison of molecular techniques

Kelly Sillence

**ABSTRACT**

Prenatal assessment of fetal health is routinely offered throughout pregnancy to ensure that the most effective management can be provided to maintain fetal and maternal well-being. Currently, invasive testing is used for definitive diagnosis of fetal aneuploidy, which is associated with a 1% risk of iatrogenic fetal loss. Developing non-invasive prenatal testing (NIPT) is a key area of research and methods to increase the level of cell-free fetal DNA (cffDNA) within the maternal circulation have been discussed to improve accuracy of such tests.

In this study, three strategies; co-amplification at lower denaturation temperature polymerase chain reaction (COLD-PCR), inverse-PCR and Pippin Prep™ gel electrophoresis, were analysed to identify a novel approach to selectively enrich shorter cffDNA fragments from larger maternal cell-free DNA (cfDNA). The sensitivity of droplet digital PCR (ddPCR) against real-time PCR (qPCR) was compared for fetal sex and *RHD* genotyping. In addition *RHD* zygosity testing was carried out for non-maternal samples. Consequently, Pippin Prep™ gel electrophoresis was combined with ddPCR analysis for the NIPD of Down Syndrome (DS) in pseudo-maternal samples.

The results revealed that the Pippin Prep™ gel electrophoresis enrichment approach successfully demonstrated 2-fold to 5-fold increases in the cffDNA fraction. However, further optimisation assays of COLD-PCR and inverse-PCR using actual maternal samples were required. The spike experiments for DS detection revealed that with the present assay



overrepresentation of the chromosome 21 target could be significantly detected for samples with  $\geq 15\%$  'cffDNA fraction'. In conjunction with the Pippin Prep<sup>TM</sup> enrichment method, this would have enabled assessment of all 10 maternal samples. Alternatively, fetal sex and *RHD* genotyping results determined that ddPCR provides a more sensitive platform compared to qPCR approaches, particularly for samples that express low cffDNA fractions (<2%). The ddPCR platform also proved to be a rapid and accurate system for the determination of *RHD* zygosity.

This study highlights that ddPCR could be used as opposed to qPCR for accurate determination of fetal sex and *RHD* status. While sequencing approaches currently provide the most sensitive platforms for NIPT of fetal aneuploidy, high costs (>£400) prevent universal application. The combination of cffDNA enrichment with ddPCR analysis could provide a cheaper and more widely available platform for NIPD. However, further large scale validation studies using actual maternal samples are required.

## Table of Contents

List of figures and tables.....	1
Acknowledgements.....	10
Declaration.....	11
Conferences attended, academic prizes and publications.....	12
List of Abbreviations.....	13
Dedication.....	17
<b>Chapter 1 .....</b>	<b>18</b>
<b>Introduction.....</b>	<b>18</b>
1.1 Prenatal screening .....	19
1.1.1 Definitions.....	19
1.1.2 Prenatal screening for fetal aneuploidy.....	21
1.1.2.1 Historical overview and current practice for prenatal screening for fetal aneuploidy.....	21
1.1.2.2 Developments of Sonographic Markers.....	28
1.1.2.3 Development of Serum/Plasma and Urine Biomarkers .....	33
1.1.2.4 NGS for NIPT of Fetal Aneuploidy .....	38
1.1.3 Prenatal screening for monogenic disorders .....	41
1.2 Invasive testing.....	45
1.3 Prenatal diagnosis.....	47
1.3.1 Fetal cells .....	47
1.3.2 Fetal RNA .....	49
1.3.3 Cell-free fetal DNA (cffDNA).....	51
1.3.3.1 Fetal sex determination .....	55
1.3.3.2 Fetal RHD genotyping .....	57
1.3.3.3 Determining fetal aneuploidy.....	62
1.3.3.3.1 Digital PCR.....	64
1.3.3.3.2 MPS .....	71
1.3.3.4 Determining fetal monogenic disorders .....	80
1.3.3.5 cffDNA enrichment.....	82
1.4 Ethical considerations .....	86
<b>Chapter 2.....</b>	<b>91</b>
<b>Materials and methods.....</b>	<b>91</b>
2.1 Sample collection .....	92

2.1.1	Pre-ordered samples .....	92
2.1.2	Human whole blood samples .....	92
2.1.2.1	DNA extractions of whole blood samples.....	92
2.1.2.2	DNA extraction of buffy coat from whole blood samples .....	93
2.1.3	Pseudo-fetal DNA samples .....	94
2.1.4	Pseudo-maternal samples .....	96
2.1.5	Maternal samples .....	97
2.2	Primer Design.....	98
2.2.1	Polymorphic STR amplicon (D21S1890).....	98
2.2.2	Non-polymorphic amplicon regions .....	99
2.3	Conventional and COLD PCR .....	102
2.3.1	Conventional PCR .....	102
2.3.2	COLD-PCR.....	102
2.4	Agarose gel electrophoresis .....	103
2.5	Gel Extraction .....	104
2.6	Assessment of DNA quality and concentration .....	105
2.6.1	Quantification by UV spectrophotometry.....	105
2.6.2	Quantification by fluorescence .....	105
2.6.3	DNA analysis .....	106
2.7	Real-time PCR (qPCR) .....	107
2.7.1	qPCR.....	107
2.7.2	qPCR to determine critical denaturation temperature.....	108
2.7.3	Quantifying DNA targets using Cq values .....	109
2.8	Inverse PCR.....	110
2.8.1	<i>Eco</i> R1 Restriction Digest to obtain purified <i>RH</i> fragment .....	110
2.8.2	Ligation using T4 DNA Ligase.....	112
2.8.3	Inverse PCR .....	113
2.8.4	Sequencing .....	116
2.9	Droplet digital PCR (ddPCR).....	116
2.9.1	ddPCR reaction .....	116
2.9.2	Droplet generation .....	117
2.9.3	ddPCR amplification.....	118
2.9.4	Analysing droplets following PCR amplification.....	118
2.9.5	Statistical analysis.....	122
2.10	Cloning.....	122
2.10.1	Producing PCR products.....	122
2.10.2	Producing Luria Bertani Media (LB Media) .....	122

2.10.3	Producing Luria Bertani Agar Plates (LB Plates).....	123
2.10.4	Cloning into pCR <sup>®</sup> 2.1 .....	123
2.10.5	Transforming competent cells.....	126
2.10.6	Colony PCR .....	126
2.10.7	Isolation of Plasmid DNA.....	127
2.10.8	Sequencing.....	129
2.10.8.1	Out of house sequencing.....	129
2.10.8.2	In house sequencing.....	129
2.11	Pippin Prep <sup>™</sup> size selective enrichment.....	131
2.11.1	Pippin prep <sup>™</sup> size selective gel electrophoresis.....	131
2.11.2	Analysis of Pippin Prep <sup>™</sup> enrichment .....	132
2.12	Analysis of T21 spike samples using ddPCR .....	132
<b>Chapter 3 .....</b>		<b>134</b>
<b>Selective enrichment of shorter psfDNA fragments by co-amplification at lower denaturation temperature- polymerase chain reaction (COLD-PCR) in pseudo-maternal samples.....</b>		<b>134</b>
3.1	Introduction .....	135
3.2	Results .....	139
3.2.1	Cloning of an STR fragment (D21S1890) on chromosome 21 for analysis of product formation at the optimal (95°C) and the critical (80°C) denaturation temperature. ....	139
3.2.2	Optimisation of critical T <sub>d</sub> for amplicons that do not contain STR regions 144	
3.2.3	Real-time PCR optimisation .....	147
3.2.4	psfDNA spiking experiments for singleplex and multiplex reactions .....	153
3.2.5	Optimisation of COLD-PCR for multiplex reactions using ddPCR.....	166
3.3	Discussion .....	179
3.3.1	COLD-PCR for selective amplification of D21S1890 STR psfDNA .....	179
3.3.2	COLD-PCR for the selective enrichment of non-polymorphic DNA target regions	182
3.3.3	Conclusion .....	189
<b>Chapter 4 .....</b>		<b>191</b>
<b>Inverse PCR (IPCR) for self-ligation of shorter psfDNA fragments.....</b>		<b>191</b>
4.1	Introduction .....	192
4.2	Results .....	195
4.2.1	Production of purified 285bp <i>RHD</i> and <i>RHCE</i> fragments.....	195
4.2.1.1	PCR amplification using consensus primers for RHD and RHCE exon 7 .....	195

4.2.1.2	Colony PCR for Fragment Insertion Analysis .....	196
4.2.1.3	Sequencing results of single white colonies.....	198
4.2.2	IPCR analysis of sticky-ended fragments .....	205
4.2.2.1	<i>EcoR</i> 1 digest .....	205
4.2.2.2	Ligation and IPCR.....	206
4.2.2.3	Sequencing results of IPCR product .....	208
4.2.3	Self-ligation of blunt ends.....	211
4.3	Discussion .....	218
<b>Chapter 5</b>	<b>.....</b>	<b>225</b>
<b><i>RHD</i> zygosity testing for non-maternal samples and maternal <i>RHD</i> genotyping using droplet digital PCR (ddPCR).....</b>		<b>225</b>
5.1	Introduction .....	226
5.1.1	<i>RHD</i> Zygosity Testing .....	226
5.1.2	Fetal <i>RHD</i> genotyping .....	228
5.2	Results .....	232
5.2.1	Optimising of ddPCR multiplex reactions .....	232
5.2.2	Sex determination of non-maternal samples and spiked samples using ddPCR	241
5.2.3	Determination of <i>RHD</i> zygosity for non-maternal samples .....	247
5.2.4	Testing sensitivity of ddPCR and qPCR for fetal sex determination and <i>RHD</i> genotyping in samples expressing optimal and suboptimal cfDNA fractions	258
5.3	Discussion .....	275
5.3.1	<i>RH</i> zygosity testing for non-maternal samples .....	275
5.3.2	ddPCR vs qPCR for the NIPT of fetal sex and <i>RHD</i> genotyping.....	280
<b>Chapter 6</b>	<b>.....</b>	<b>288</b>
<b>Determining the feasibility of Pippin Prep™ (PP) size selective gel electrophoresis for cfDNA enrichment in conjunction with ddPCR analysis for the detection of T21 in spiked samples.....</b>		<b>288</b>
6.1	Introduction .....	289
6.2	Results .....	291
6.2.1	Pippin Prep™ gel electrophoresis enrichment.....	291
6.2.1.1	Initial PP size-selective experiments using qPCR and ddPCR analysis	291
6.2.1.2	ddPCR analysis of PP gel electrophoresis cfDNA enrichment using a multiple-copy Y-specific target ( <i>TSPY1</i> ).....	298
6.2.1.3	ddPCR analysis of PP gel electrophoresis cfDNA enrichment using a single copy <i>RHD</i> specific targets for samples extracted using Streck BCTs .....	304
6.2.2	Spiking Experiments.....	323

6.2.2.1	Male gDNA spike experiments to determine detection of low copy targets 323	
6.2.2.2	T21 gDNA spike experiment to determine the minimal cffDNA fraction required for NIPT of fetal T21 .....	331
6.3	Discussion .....	342
6.3.1	Pippin Prep™ Size Selective Enrichment.....	342
6.3.2	Determining cffDNA fraction for aneuploidy detection.....	346
6.3.3	Future work.....	348
6.3.4	Conclusion .....	350
<b>Chapter 7</b>	.....	<b>351</b>
<b>Discussion</b> .....	.....	<b>351</b>
7.1	Size-selective enrichment of cffDNA .....	352
7.2	Determination of <i>RHD</i> zygosity.....	358
7.3	NIPD of fetal sex and <i>RHD</i> genotype .....	362
7.4	NIPD/ NIPT of fetal aneuploidy .....	364
7.5	Potential gene therapy for fetal aneuploidy.....	367
7.6	Future Work .....	368
7.7	Conclusion.....	370
<b>Appendices 1</b> .....	.....	<b>371</b>
<b>Appendices 2</b> .....	.....	<b>374</b>
<b>References</b> .....	.....	<b>379</b>

## List of Figures

Figure 1-1: The screening process, potential outcomes and measures of accuracy.....	21
Figure 1-2: The estimated risk of DS according to maternal age.....	22
Figure 1-3: Timeline summarising the key developments in DS screening.....	23
Figure 1-4: Incidence of sonographic features in Euploid, T21, T18 and T13 fetuses...31	
Figure 1-5: Principle of dPCR.....	65
Figure 1-6: Determining target concentration using the Poisson algorithm.....	68
Figure 1-7: Cost per raw Mb of DNA sequencing from 2001 to 2014.....	71
Figure 1-8: SNP analysis for the determination of T21: an example of the general principle.....	78
Figure 2-1: D21S1890 STR fragment amplicon region on chromosome 21 (21q22.3).....	99
Figure 2-2: Sequence alignment of <i>RHD</i> and <i>RHCE</i> for exon 7.....	101
Figure 2-3: pCR®2.1 Vector and <i>EcoR</i> I restriction site to excise region of interest containing PCR insert and produce sticky-ended fragments following cloning.....	111
Figure 2-4: The dilute ligation process.....	113
Figure 2-5: Hypothesised sequence following restriction digest ( <i>EcoR</i> I), ligation (T4 DNA polymerase) and inverse PCR (internal primers Table 2-3).....	115
Figure 2-6: Loaded DG8™ cartridge for QX100 system.....	118
Figure 2-7: 2D-Amplitude plot for male gDNA.....	119
Figure 2-8: Estimating target concentration using Poisson distribution to ddPCR data.....	120
Figure 2-9: Map of the linearized pCR®2.1 multiple cloning site (MCS).....	125
Figure 2-10: Pippen Prep™ Gel Electrophoresis.....	132
Figure 3-1: Representation of denaturation of shorter fetal DNA fragments and longer maternal DNA fragments at critical $T_d$ .....	137
Figure 3-2: COLD-PCR for D21S1890 fragment using $T_d$ gradient from 83°C to 73.2°C.....	140
Figure 3-3: Real-Time PCR amplification of D21S1890 psfDNA fragment and control Female gDNA at 95°C and 80°C $T_d$ .....	140

Figure 3-4: 2% agarose (w/v) gel of colony PCR for pseudo-fetal fragments using M13 forward and reverse primers.....	142
Figure 3-5: Sequence alignment of cloned psfDNA product amplified at 95°C and 80°C Td. Both sequences were mapped against a region of the linearized vector (pCR®2.1), which included the D21S1890 PCR product insert (reference).....	143
Figure 3-6: 2% agarose (w/v) illustrating initial COLD-PCR gradient (from 70°C to 95°C) for APP (A) and <i>EIF2C1</i> (B).....	145
Figure 3-7: 2% agarose (w/v) gel illustrating secondary COLD-PCR gradient (from 75°C to 80°C) for APP (A) and <i>EIF2C1</i> (B).....	146
Figure 3-8: qPCR amplification to determine drop out of psfDNA against Male gDNA for APP target on chr21 from 78°C down to 77°C.....	148
Figure 3-9: qPCR amplification to determine drop out of psfDNA against Male gDNA for <i>EIF2C1</i> target on chr1 from 78°C down to 77°C.....	149
Figure 3-10: Optimisation of the Td for the amplification of psfDNA for target APP (FAM) and target <i>EIF2C1</i> (HEX).....	150
Figure 3-11: Further optimisation of the Td for the amplification of psfDNA for target APP (A) and target <i>EIF2C1</i> (B) from 75.8°C to 76.6°C using qPCR.....	151
Figure 3-12: qPCR Amplification of APP (FAM) (A) and <i>EIF2C1</i> (HEX) (B) at 76.7°C for Male gDNA, psfDNA and NTC.....	153
Figure 3-13: qPCR amplification at optimum Td (95°C) and lowered Td (76.7°C) to determine the selective amplification of 5% Spike psfDNA (refer to 2.4.1).....	155
Figure 3-14: Amplification of multiplex reaction APP (FAM)/ <i>EIF2C1</i> (HEX) for samples amplified at 95°C Td (A-F) and 78°C Td (G-L).....	158
Figure 3-15: Amplification of dye-swap multiplex reaction ( <i>EIF2C1</i> (FAM)/ APP (HEX)) for samples amplified at 95°C Td (A-F) and 77.5°C Td (G-L).....	160
Figure 3-16: Clustered bar charts illustrating the concentration (ng/ µL) of APP-FAM (blue) and <i>EIF2C1</i> -HEX (green) with ratio analysis (black) for the following samples; NTC, Male gDNA, psfDNA (APP), psfDNA ( <i>EIF2C1</i> ), Plasma extracted DNA, 5% 'DS'-spike and 5% 'normal'-spike.....	162
Figure 3-17: 2% agarose (w/v) gel showing sexing results for 14 unknown samples. M= 100bp DNA ladder. Lane 8 and 16 represent NTC controls.....	164
Figure 3-18: Amplification of <i>SRY</i> (H.P.T) (FAM) / Xp22.3 (HEX) multiplex reaction at 95°C Td and 76°C Td for samples; Male gDNA (2ng/µL) (A), male plasma extracted DNA (8023) (B), psfDNA (Xp22.3) (C) and psfDNA ( <i>SRY</i> <sup>H.P.T</sup> ) (D).....	165



Figure 3-19: 1D amplitude plots illustrating Ta gradient from 61.6°C to 56°C for target genes (blue, left), APP and <i>SRY</i> , and reference genes (green, right), <i>EIF2C1</i> and Xp22.3.....	167
Figure 3-20: Bar chart demonstrating ratios achieved for APP/ <i>EIF2C1</i> multiplex reactions (black) and <i>SRY</i> /Xp22.3 multiplex reactions (grey) at varying T <sub>a</sub> s (62°C to 56°C.....	168
Figure 3-21: Bar chart showing the concentration (copies/μL) of APP (FAM), <i>EIF2C1</i> (HEX) and Xp22.3 (HEX) in singleplex reactions for Td gradient (78°C to 74.9°C).....	177
Figure 3-22: 1D amplitude plot illustrating droplet separation for Male gDNA, T21 gDNA, maternal sample 1B and NTC for singleplex reactions APP, <i>EIF2C1</i> and Xp22.3 at 95°C T <sub>d</sub> and expected T <sub>c</sub> .....	178
Figure 3-23: Schematic diagram showing the fragment length of alleles from a heterozygous fetus, alongside the alleles of the heterozygous mother and heterozygous father.....	180
Figure 4-1: 2% (w/v) agarose gel electrophoresis showing PCR products amplified at multiple T <sub>a</sub> s (56.4°C, 58.4°C and 60.4°C) using RH7 external primers (Table 2-2)...	196
Figure 4-2: 2% (w/v) agarose gel electrophoresis using M13 primers to check for product insert in 15 white colonies.....	198
Figure 4-3: Alignment of in-house sequencing results for colonies 2 (A), 6 (B) and 12 (C) against <i>RHD</i> and <i>RHCE</i> exon 7 285bp fragments.....	200
Figure 4-4: Alignment of external sequencing results for colonies 4 (A and B), 5 (C and D) and 9 (E and F) against <i>RHD</i> and <i>RHCE</i> exon 7 285bp fragments using M13 forward and reverse primers, respectively.....	203
Figure 4-5: 2% (w/v) agarose gel demonstrating restriction digested ( <i>EcoRI</i> ) and non-digested results for colonies 2, 4, 5, 9 and 12.....	206
Figure 4-6: 2% (w/v) agarose gel illustrating IPCR amplification of ligated RH fragments for three ligation dilutions (refer to 2.8.2).....	208
Figure 4-7: Alignment of colony 12 following self-ligation and IPCR (Col12IPCR) against hypothesised sequence generated for <i>RHD</i> insert ( <i>RHD</i> +MCS) and <i>RHCE</i> insert ( <i>RHCE</i> +MCS).....	210
Figure 4-8: 2% (w/v) agarose gel illustrating annealing temperature gradient (56 - 60°C) for colonies 2 and 5 using oligonucleotides containing <i>EcoRV</i> restriction site.....	212
Figure 4-9: qPCR analysis to determine the presence of DNA in maternal samples Rh47 and Rh61 (non-ligated).....	215

Figure 4-10: 2% (w/v) agarose gel for IPCR amplification of maternal samples Rh47 and Rh61 using 2x Fast TaqMan Universal MasterMix (top row) and IMMOLASE™ DNA Polymerase (bottom row).....	217
Figure 5-1: The four multiplex reactions used for sexing (multiplex reactions 1 and 2) and <i>RHD</i> genotyping (multiplex reactions 3 and 4).....	233
Figure 5-2: ddPCR data showing annealing temperature gradient (from 62°C down to 56°C) results for <i>SRY</i> (H.P.T) (FAM) and Xp22.3 (HEX) multiplex reactions.....	234
Figure 5-3: ddPCR data showing the annealing temperature gradient (62°C, 59.8°C, 58.4°C and 56°C) results for <i>TSPY1</i> (FAM) and Xp22.3 (HEX) multiplex reactions....	235
Figure 5-4: ddPCR data showing the annealing temperature gradient (62°C, 58.4°C, 57.4°C and 56°C) results for <i>RHD5</i> (FAM) and <i>EIF2C1</i> (HEX) multiplex reaction.....	237
Figure 5-5: ddPCR data showing the annealing temperature gradient (62°C, 58.4°C, 57.4°C and 56°C) results for <i>RHD7</i> (FAM) and <i>EIF2C1</i> (HEX) multiplex reaction.....	238
Figure 5-6: ddPCR 1D amplitude plots (1), histogram plots (2) and 2D amplitude plots (3) showing results for lower (300nM) and higher (900nM) primer concentrations for <i>SRY</i> <sup>H.P.T</sup> (FAM) and Xp22.3 (HEX) targets.....	240
Figure 5-7: Bar chart illustrating the concentration (copies/ μL) of the <i>SRY</i> <sup>H.P.T</sup> (FAM) target (blue) and the Xp22.3 (HEX) reference (green). The scatter plot illustrates the ratio of <i>SRY</i> /Xp22.3 (black).....	242
Figure 5-8: Bar chart illustrating the number of events (positive droplets) for <i>SRY</i> (H.P.T) (FAM), Xp22.3 (HEX) and the total (FAM + HEX positive droplets) in a generated by ddPCR in a multiplex experiment.....	244
Figure 5-9: ddPCR results for <i>TSPY1</i> Spike experiments.....	246
Figure 5-10: ddPCR data for <i>RHD5</i> (FAM)/ <i>EIF2C1</i> (HEX) multiplex reaction for control samples (NTC, Male gDNA and Female gDNA) and four unknown DNA samples extracted from plasma of human whole blood (refer to 2.1.2).....	248
Figure 5-11: ddPCR data for <i>RHD7</i> (FAM)/ <i>EIF2C1</i> (HEX) multiplex reaction for control samples (NTC, Male gDNA and Female gDNA) and four unknown DNA samples extracted from plasma of human whole blood (refer to 2.1.2).....	249
Figure 5-12: Bar chart demonstrating the mean concentration (copies/ μL) and SD for <i>RHD5</i> (FAM), <i>RHD7</i> (FAM) and <i>EIF2C1</i> (HEX) for DNA samples extracted from the plasma (A) and buffy coat (B) of human whole blood (refer to 2.1.2 and 2.1.3).....	253
Figure 5-13: Bar chart illustrated ratio analysis generated by ddPCR to determine <i>RHD</i> zygosity using multiplex reaction 3 ( <i>RHD5</i> (FAM) / <i>EIF2C1</i> (HEX)) (grey) and multiplex reaction 4 ( <i>RHD7</i> (FAM) / <i>EIF2C1</i> (HEX)) (black).....	257

Figure 5-14: Experimental overview of fetal sex determination and fetal <i>RHD</i> genotyping for maternal samples collected in both EDTA tubes (n=22) and Streck BCTs (n=24).....	259
Figure 5-15: Box Plot of raw Ct values obtained from qPCR analysis showing <i>SRY</i> , <i>TSPY1</i> (multiple copy target), <i>RHD5</i> and <i>RHD7</i> targets for A) samples collected in EDTA tubes and B) samples collected in Streck BCTs.....	265
Figure 5-16: ddPCR 2D amplitude plots for fetal sex determination (A) and <i>RHD</i> genotype (B) for samples collected in Streck BCTs (left) and EDTA tubes (right).....	268
Figure 5-17: ddPCR results showing concentration (copies/ $\mu$ L) of <i>RHD5</i> , <i>RHD7</i> and <i>EHF2C1</i> to determine the fetal <i>RHD</i> genotyping from 46 maternal plasma samples.....	270
Figure 5-18: A comparison of mean cfDNA fraction (based on <i>SRY</i> , <i>TSPY1</i> , <i>RHD5</i> and <i>RHD7</i> ) and mean concentrations of the reference targets (Xp22.3 and <i>EIF2C1</i> ) for maternal samples collected in EDTA tubes and Streck BCTs.....	274
Figure 6-1: qPCR amplification of <i>TSPY1</i> (A-D) and <i>HBB</i> (E-H) for non-maternal sample 147W (A and E), maternal sample 8 (female fetus) (B and F), maternal sample 9 (male fetus) (C and G) and Male and Female gDNA control samples (D and H).....	295
Figure 6-2: Bar Chart illustrating the concentration (copies/ $\mu$ L) of <i>SRY</i> (H.P.T) (FAM) target (blue) and Xp22.3 (HEX) reference (green) generated by ddPCR platform.....	297
Figure 6-3: Agilent 2100 Bioanalyzer electropherograms for four maternal samples (13AB, 24AB, 36AB and 43AB) before (non-PP, left column) and after (PP, right column) PP gel electrophoresis.....	299
Figure 6-4: Electrophoresis gel-like image generated by the Bioanalyzer showing the ladder (L) and results for all four maternal samples (13AB, 24AB, 36AB and 43AB) before (non-PP) and after PP gel electrophoresis (PP).....	300
Figure 6-5: Bar chart illustrating the number of Events (positive droplets) for <i>SRY</i> <sup>H.P.T</sup> (FAM, blue) and Xp22.3 (HEX, green) generated by ddPCR for maternal samples 13AB (A), 24AB (B), 36AB (C) and 43AB (D) before and after PP selective enrichment.....	302
Figure 6-6: Bar chart illustrated the mean $\pm$ SD fold-decrease in number of Events (positive droplets) for <i>TSPY1</i> (FAM, blue) and Xp22.3 (HEX, green) generated by ddPCR following PP size selective gel electrophoresis.....	303
Figure 6-7: Bar chart illustrating the cfDNA fraction calculated using the <i>TSPY1</i> multiple-copy target equation (refer to 2.9.4) for maternal samples before (non-PP, plain colour) and after (PP, striated colour) PP gel electrophoresis.....	304
Figure 6-8: Agilent 2100 Bioanalyzer electropherograms for three maternal samples (117, 118 and 119) and non-maternal sample (2454) before (non-PP, left column) and after (PP, right column) PP gel electrophoresis.....	309

Figure 6-9: Electrophoresis gel-like image generated by the Agilent 2100 Bioanalyzer showing the ladder (L) and results for three maternal samples (117, 118 and 119) and one non-maternal sample (2454) before (non-PP) and after (PP) PP gel electrophoresis.....310

Figure 6-10: Bar chart illustrating the cffDNA fraction (%) for maternal samples collected in Streck BCTs (n=11) before (non-PP (plain colour)) and after (PP (striated colour)) PP gel electrophoresis using concentrations (copies/  $\mu$ L) generated by ddPCR.....313

Figure 6-11: Bar chart illustrating the cffDNA fraction (%) change following PP gel electrophoresis for nine maternal samples (117, 118, 120, 122, 123, 124, 131, 132 and 133).....314

Figure 6-12: 2D Amplitude plots generated by ddPCR for maternal samples 119 (A-D) and 132 (E-H) for non-PP aliquots (A, C, E and G) and PP aliquots (B, D, F and H)...318

Figure 6-13: Bar chart illustrating the cffDNA fraction (%) for maternal samples 131HIJ, 132HIJ and 133HIJ based on calculations using the *RHD5* (A) and *RHD7* (B) fetal target concentrations (copies/  $\mu$ L) generated by ddPCR for a single non-PP aliquot (black) and two repeats of the PP aliquot (grey).....321

Figure 6-14: Clustered bar-chart illustrating the number of positive droplets (Events) for *SRY* (FAM) (blue), Xp22.3 (HEX) (green) and the total (grey) generated by ddPCR for NTC, 100% male gDNA, 100% female gDNA and male gDNA spikes from 50% (wt/wt) down to 1% (wt/wt).....324

Figure 6-15: 1D amplitude plots showing *SRY* (FAM) (blue) and Xp22.3 (HEX) (green) positive droplets (events) for NTC, female gDNA (100%), male gDNA (100%), 50% male spike, 10% male spike, 5% male spike, 3% male spike and 1% male spike.....326

Figure 6-16: Clustered bar-chart illustrating the number of positive droplets (Events) for *TSPY1* (FAM) (blue), Xp22.3 (HEX) (green) and the total (grey) generated by ddPCR for NTC, 100% male gDNA, 100% female gDNA and male gDNA spikes from 50% down to 0.1%.....328

Figure 6-17: Concentration (copies/  $\mu$ L) of *TSPY1* (blue) and Xp22.3 (green) for NTC, 100% female gDNA, 100% male gDNA, 50% male spike, 10% male spike, 5% male spike, 0.5% male spike and 0.1% male spike.....329

Figure 6-18: 1D amplitude plots showing *TSPY1* (FAM) (blue) and Xp22.3 (HEX) (green) positive droplets (events) for NTC, female gDNA (100%), male gDNA (100%), 50% (wt/wt) Male gDNA spike down to 0.1% (wt/wt) Male gDNA spike.....330

Figure 6-19: Concentration (copies/  $\mu$ L) of *DSCR3* (FAM) (blue) and *EIF2C1* (HEX) generated by ddPCR for D21 and T21 samples set up in both singleplex and multiplex reactions. The graph also illustrated the *DSCR3/ EIF2C1* ratio for all samples.....332

Figure 6-20: Concentration (copies/ $\mu$ L) of <i>DSCR3</i> (blue) and <i>EIF2C1</i> (green), and the <i>DSCR3/ EIF2C1</i> ratio (red) generated by ddPCR for disomy sample 110W at 57.8°C, 56.7°C, 56°C and 55°C.....	333
Figure 6-21: 2D amplitude plot for multiplex reaction ( <i>DSCR3</i> (FAM)/ <i>EIF2C1</i> (HEX)) showing droplet separation for Male gDNA amplification at 56°C Ta (top) and 57.8°C Ta (bottom).....	334
Figure 6-22: Mean concentration (copies/ $\mu$ L) $\pm$ SD of <i>APP</i> (FAM) (dark blue) and <i>EIF2C1</i> (HEX) (green) generated by ddPCR for disomy (pooled) female gDNA (2ng/ $\mu$ L) and disomy (pooled) male gDNA (2ng/ $\mu$ L).....	335
Figure 6-23: Clustered bar chart illustrating the mean ratio $\pm$ SD calculated from quadruplet replicates based upon the <i>DSCR3/ EIF2C1</i> (blue) assay and the <i>APP/EIF2C1</i> assay (purple) compared to the expected ratio for each T21 spike and controls (black).....	340
Figure 6-24: Bar chart illustrating the <i>APP/ EIF2C1</i> expected ratio (black) and actual ratio (purple) for NTC, 100% D21, 100% T21 and spike samples (50% down to 10%).....	341
Figure 6-25: <i>RHD</i> exons (black) and <i>RHCE</i> exons (white) of hybrid genes in some D variants.....	345

## List of Tables

Table 1-1: National UK Standards for T21, T18 and T13 screening.....	28
Table 1-2: Carrier frequencies of various autosomal recessive disorders within different populations.....	43
Table 1-3: Fetal specific target/ universal markers and universal DNA markers, purpose and method(s) of detection.....	54
Table 1-4: List of commercially available dPCR platforms.....	69
Table 1-5: Summary data for NIPT/ NIPD of fetal aneuploidy using shotgun massively parallel sequencing (s-MPS).....	75
Table 1-6: Summary data for NIPT/ NIPD of fetal aneuploidy using target massively parallel sequencing (t-MPS) for specific chromosomes.....	76
Table 1-7: Summary data for NIPT/ NIPD of fetal aneuploidy using targeted massively parallel sequencing (t-MPS) for SNP based analysis.....	77
Table 2-1: Summary of primers used. External and internal primer sequences and product sizes (bp) for multiple regions on chromosomes 1, 13, 18, 21, X and Y.....	95

Table 2-2: Internal primers and probes for <i>RHD</i> exon 5 ( <i>RHD5</i> ), <i>RHD</i> exon 7 ( <i>RHD7</i> ) and CCR5.....	100
Table 2-3: Inverse PCR internal and external primers for RH7.....	100
Table 2-4: Recipe for LB Media.....	122
Table 2-5: PCR conditions for IMMOLASE™ PCR Polymerase.....	127
Table 3-1: Oligonucleotides for D21S1890 STR fragment (HPLC purified (Eurofins MWG Operon) (for mapped sequences refer to Figure 2-1).....	139
Table 3-2: Summary of T <sub>d</sub> and T <sub>a</sub> optimisation experiments for all chromosomes of interest.....	147
Table 3-3: Summary of the T <sub>c</sub> determined for Male gDNA and psfDNA for targets APP and <i>EIF2C1</i> .....	152
Table 3-4: ddPCR results for <i>SRY</i> (H.P.T) (FAM)/ Xp22.3 (HEX) multiplex reaction at 95°C T <sub>d</sub> , 78°C T <sub>d</sub> and 76°C T <sub>d</sub> .....	170
Table 3-5: ddPCR results for <i>SRY</i> (H.P.T) (FAM)/ <i>EIF2C1</i> (HEX) multiplex reactions at 95°C T <sub>d</sub> , 78°C T <sub>d</sub> and 76°C T <sub>d</sub> .....	171
Table 3-6: ddPCR results for APP (FAM)/ <i>EIF2C1</i> (HEX) multiplex reactions at 95°C T <sub>d</sub> , 77.5°C T <sub>d</sub> , 76.8°C T <sub>d</sub> and 75.5°C T <sub>d</sub> .....	176
Table 4-1: RH determination of six colonies (2, 4-6, 9 and 12) by alignment of in house and external sequencing data to the external <i>RHD</i> and <i>RHCE</i> exon 7 285bp fragments.....	204
Table 4-2: <i>EcoRV</i> oligonucleotides for MCS of pCR®2.1. The primers used to amplify product insert in the pCR®2.1 vector containing <i>EcoRV</i> restriction site in the forward primer (shown in red).....	212
Table 4-3: T4 DNA Polymerisation reaction.....	213
Table 5-1: <i>SRY</i> (FAM) and Xp22.3 (HEX) multiplex ddPCR results for control samples and female samples spiked with Male gDNA (50% (wt/wt) down to 1% (wt/wt)).....	243
Table 5-2: The concentration of each target and the ratio generated for each multiplex reaction; <i>RHD5</i> (FAM)/ <i>EIF2C1</i> (HEX) and <i>RHD7</i> (FAM)/ <i>EIF2C1</i> (HEX).....	250
Table 5-3: Concentration of DNA extracted from the plasma of human whole blood...	251
Table 5-4: Zygosity testing results for multiple samples extracted from both the plasma and buffy coat of human whole blood samples.....	255
Table 5-5: Fetal sexing and <i>RHD</i> genotyping results obtained from both ddPCR and qPCR against results recorded following delivery.....	261

Table 5-6: Sensitivity, specificity and accuracy results of maternal samples collected in EDTA tubes and Streck BCTs on both ddPCR and qPCR platforms for fetal sex and <i>RHD</i> genotyping.....	264
Table 5-7: Rh Nomenclature and incidence of common haplotypes for Caucasian, African black and Asian populations.....	276
Table 6-1: DNA concentration of maternal sample aliquots.....	291.
Table 6-2: Sample concentration following qPCR analysis and cffDNA fractions for maternal sample 9.....	296
Table 6-3: cffDNA fractions for maternal samples before (non-PP) and after (PP) PP gel electrophoresis.....	307
Table 6-4: Results for repeat ddPCR experiment for maternal samples 131-133HIJ (PP) showing cffDNA fractions based on concentration of target (FAM) and reference ( <i>EIF2C1</i> ) genes for multiplex reactions <i>RHD5</i> (FAM)/ <i>EIF2C1</i> (HEX) and <i>RHD7</i> (FAM)/ <i>EIF2C1</i> (HEX).....	320
Table 6-5: Number of samples acceptable for T21 analysis (with at least one target above threshold) before (non-PP) and after (PP) PP gel electrophoresis for cffDNA fraction cut-offs of 15%, 20% and 25%.....	323
Table 6-6: Events (positive droplets) for <i>SRY</i> (FAM) and Xp22.3 (HEX) illustrating the actual fractional abundance of <i>SRY</i> against the expected fractional abundance.....	325
Table 6-7: Expected concentrations (copies/ $\mu$ L) of <i>TSPY1</i> based on concentration value for 100% male gDNA and actual concentration (copies/ $\mu$ L).....	330
Table 6-8: Summary of results illustrating the concentration (copies/ $\mu$ L) of DSCR3 (FAM) and <i>EIF2C1</i> (HEX) and the ratios calculated based upon concentration for each triplicate reaction and the mean concentration.....	337
Table 6-9: Summary of results illustrating the concentration (copies/ $\mu$ L) of APP (FAM) and <i>EIF2C1</i> (HEX) and the ratios calculated based upon concentration for each triplicate reaction and the mean concentration.....	338

## **Acknowledgements**

I would like to acknowledge and express sincere gratitude to the following people for their help during the completion of my PhD.

Professor Neil Avent, my director of studies, for his support, guidance, encouragement, consistent optimism, and most importantly for his enthusiasm, drive and passion for science which has inspired me to pursue a career in scientific research.

Dr Tracey Madgett, my second supervisor, for her guidance, support- both inside and outside the lab, solicited and valued advice and for her friendly and approachable nature, which has enabled me to build my confidence within the lab.

To all my family for their endless love and support. Special thanks to my Mum, Michelle Kent, and Grandparents, Clive and Sandra Sillence, whom without I wouldn't be where I am today- This is for you!

To my little brother, Tyler Kent, for making me smile, and for just being you!

Dr Michele Kiernan, for providing additional lab support, but also for being someone I could always go to if I needed advice.

Dr Llinos Roberts, who worked extremely hard to achieve ethical approval, which enabled us to convert my studies onto actual maternal samples.

Heidi Hollands and Dr Llinos Roberts, for their efforts in recruiting maternal samples and enthusiasm to contribute to my studies.

Mr Ross Welch, for his collaboration which enabled us to start recruiting maternal samples and also for his novel ideas for future studies.

Dr Paul Waines, for providing technical and emotional support throughout difficult periods.

Professor Dennis Lo for allowing me to visit his lab at the Chinese University of Hong Kong and carry out two weeks work experience under the guidance of Dr Yu-kwan Tong, who was welcoming, friendly and very helpful.

To all my friends and colleagues that have supported me through difficult periods, and who have also made my PhD an enjoyable and memorable life experience.

Special thanks to all the patients at Plymouth Hospital NHS trust who were willing to donate blood samples and participate in my study.



## **AUTHOR'S DECLARATION**

At no time during the registration for the degree of Doctor of Philosophy has the author been registered for any other University award without prior agreement of the Graduate Committee.

Work submitted for this research degree at the Plymouth University has not formed part of any other degree either at Plymouth University or at another establishment. This study was financed jointly with funded studentships from the School of Biomedical and Healthcare Science at Plymouth University and Eurogentest, Belgium.

Word count of main body of thesis: 69,127

Signed .....

Date .....

## Conferences Attended

Prenatal Molecular Diagnostics Europe. Lisbon, Portugal. April 2015. Poster presented entitled: Droplet Digital PCR for the Non-Invasive Prenatal Diagnosis (NIPD) of Fetal *RHD* Genotype: Potential for Routine Clinical Application.

Plymouth University Peninsula Annual Postgraduate Research Event. Cornwall, UK. October 2014. Oral Presentation entitled: Comparison of Droplet Digital PCR and Real-Time PCR for the Non-Invasive Prenatal Determination of Fetal Sex and *RHD* genotype.

Integrating Digital PCR. Cambridge Health Institute's Inaugural, Boston, USA. April 2013. To research digital PCR technologies to determine which platform our lab should purchase.

Moving Next Generation Sequencing into Diagnostics. Eurogentest, Prague, Czech Republic. March 2013. To discuss recent updates of Eurogentest (funded by the European commission).

## Academic Prizes

Centre for Research in Translational Biomedicine Annual Research Days, July 4<sup>th</sup> 2015, Plymouth University, UK. Awarded 1<sup>st</sup> Prize for poster presented entitled: *Droplet Digital PCR for the Non-Invasive Prenatal Diagnosis (NIPD) of Fetal RHD Genotype: Potential for Routine Clinical Application*.

Plymouth University Peninsula Annual Research Event 22<sup>nd</sup> October 2014. Awarded 1<sup>st</sup> prize for oral presentation on: *Comparison of droplet digital PCR and real-time PCR for the non-invasive prenatal determination of fetal sex and RHD genotyping*.

Centre for Research in Translational Biomedicine Annual Research Days, July 4<sup>th</sup> 2013, Plymouth University, UK. Awarded 1<sup>st</sup> Prize for poster presented entitled: *Selective enrichment of cell free fetal DNA using COLD-PCR for the non-invasive diagnosis of foetal aneuploidy*.

Centre for Research in Translational Biomedicine Annual Research Days, July 4<sup>th</sup> 2012, Plymouth University, UK. Awarded 2<sup>nd</sup> Prize for poster presented entitled: *The application of selective enrichment of cell free-foetal DNA for non-invasive prenatal diagnosis*.

## Publications

Sillence, K. A., Roberts, L. A., Hollands, H. J., Thompson, H. P., Kiernan, M., Madgett, T. E., Welch, C. R and Avent. N. D. Fetal sex and *RHD* genotyping using Digital PCR demonstrates greater sensitivity compared to real-time PCR. *Clinical Chemistry* 2015, 61(11):1399-407.

Sillence, K.A., Madgett, T.E., Roberts, L.A., Overton, T.G and Avent, N.D. Non-Invasive Screening Tools for Down's syndrome: A Review. *Diagnostics* 2013, 3:291-314.

Webb, A., Madgett, T. E., Miran, T., Sillence, K. A., Kaushik, N., Kiernan, M and Avent, N. D. 2012. Non Invasive Prenatal Diagnosis of Aneuploidy: Next Generation Sequencing or Fetal DNA Enrichment? *BJMG* 2011, 15: 17-26.

## Abbreviation List

2D – Two-dimensional  
2D-DIGE - Two-dimensional - difference gel electrophoresis  
3D- Three-dimensional  
A1BG - alpha-1b-glycoprotein  
ADAM12 - Disintegrin and metalloprotease domain-containing protein 12  
AFP – Alpha-fetoprotein  
APCS - Serum amyloid P-component  
AS-APEX - Allele specific arrayed primer extension  
 $\beta$ -hCG – Beta- human chorionic gonadotropin  
BHQ1- Black hole quencher 1  
BMI – Body mass index  
BP – base pair  
CAH – Congenital adrenal hyperplasia  
cfDNA – Cell-free DNA  
cffDNA – Cell-free fetal DNA  
CGIs - CpG islands  
Chr21 – Chromosome 21  
Chr18 – Chromosome 18  
Chr13 – Chromosome 13  
Chr1 – Chromosome 1  
ChrX – Chromosome X  
ChrY- Chromosome Y  
CNA Kit - QIAamp Circulating Nucleic Acid kit  
COBRA – Combined bisulfite and restriction analysis  
COLD-PCR – Co-amplification at lower denaturation temperature- polymerase chain reaction  
CRL – crown-rump length  
Ct – Cycle threshold  
CVS – Chorionic villus sampling  
D21 – Disomy 21  
DANSR – Digital Analysis of Selected Regions  
ddPCR – Droplet digital PCR  
Del – Severely weak D  
DMD – Duchenne muscular dystrophy  
DMR – Differentially methylated region  
DNA – Deoxyribonucleic acid  
dNTP – Deoxynucleotide mix  
dPCR – Digital PCR  
DR – Detection rate  
DS – Down Syndrome  
DS-DEMSPs – Down Syndrome differentially expressed maternal serum proteins  
EDTA - Ethylenediaminetetraacetic acid

ELISA – Enzyme-linked immunosorbent assay  
FACS – Fluorescent-activated cell sorting  
FASP – Fetal Anomaly Screening Programme  
FFF – Frontal fetal facial  
FISH – Fluorescent *in situ* hybridisation  
FNRBCs – Fetal nucleated red blood cells  
FORTE – Fetal-fraction Optimise Risk of Trisomy Evaluation  
FOQ – Family origin questions  
FPR – False positive rate  
FSN – False screen negative  
FSP – False screen positive  
gDNA – genomic DNA  
GE – Genomic equivalent  
HA – Hepatic Artery  
HDFN – Haemolytic disease of the fetus and newborn  
HPLC - High performance liquid chromatograph  
HPSF – high purity salt free  
HS – High sensitivity  
IEAs – Irregular erythrocyte antibodies  
IPCR – Inverse polymerase chain reaction  
ISPD – International Society for Prenatal Diagnosis  
LMICs – Lower middle income countries  
LR-PCR – Long range polymerase reaction  
MACS – Magnetic charge flow separation  
MALDI ToF MS- matrix-assisted laser desorption/ionisation time of flight mass spectrometry  
MCS – Multiple cloning site  
MeDIP - Methylation DNA immunoprecipitation  
MEN2A - Multiple endocrine neoplasia type 2A  
M-HLCS - methylated form of *the holocarboxylase synthetase gene*  
Min – Minute  
miRNAs – Micro RNAs  
MLPA – Multiplex ligation-dependent probe amplification  
MPS – Massively parallel sequencing  
mRNA – Messenger RNA  
MS – Mass spectrometry  
NCVs – Normalised chromosome values  
NHS – National Health Service  
NHS BT – National Health Service Blood and Transfusion  
NIPD – Non-invasive prenatal diagnosis  
NIPT – Non-invasive prenatal testing  
NPV – Negative predictive values  
NoE – Network of excellence  
NSCG – National Society of Genetic Counselors

NT- Nuchal translucency  
NTC – Non-template control  
NTD – Neural tube defects  
OAPR – Odds of a positive result  
PAPP-A – Plasma associated plasma protein A  
PCR – Polymerase chain reaction  
PCR-SSP – polymerase chain reaction- sequence-specific polymorphism  
PHE – Public Health England  
PIV – Pulsatility index of veins  
PIGF – Placental growth factor  
PNAs – Peptide nucleic acids  
PP – Pippin Prep  
PPV – Positive predictive values  
PsfDNA – Pseudo-fetal DNA  
QF-PCR – quantitative fluorescent polymerase chain reaction  
qPCR – real-time polymerase chain reaction  
RAADP - routine antenatal anti-D prophylaxis  
RCD – Relative chromosome dosage  
*RHD5* – *RHD* exon 5  
*RHD7* – *RHD* exon 7  
*RHDΨ* – *RHD* pseudogene  
RMD – Relative mutation dosage  
RNA – Ribonucleic acid  
ROI – Region of interest  
RT – Reverse transcriptase  
S - Second  
SAFE - The Special Non-Invasive Advances in Fetal and Neonatal Evaluation  
SELDI ToF MS - surface enhanced laser desorption ionisation time of flight mass spectrometry  
s-MPS – shotgun massively parallel sequencing  
SPR – Screen positive rate  
SPRI - Solid Phase Reversible Immobilization  
SNP – Single nucleotide polymorphism  
Streck BCTs – Streck Cell-Free DNA™ Blood Collection Tubes  
STR – Short tandem repeats  
SURUSS – Serum, Urine and Ultrasound Screening Study  
T21 – Trisomy 21  
T18 – Trisomy 18  
T13 – Trisomy 13  
 $T_a$  – Annealing temperature  
 $T_c$  – Critical denaturation temperature  
 $T_d$  – Denaturation temperature  
 $T_m$  – Melting temperature  
t-MPS – Targeted massively parallel sequencing

TSP – True screen positive

TSN – True screen negative

UCH – University College Hospital

UK NSC – UK National Screening Committee

uE3- Unconjugated estriol

ZFN – Zinc finger nuclease

## **Dedication**

I would like to dedicate my thesis to my Mum and Grandparents for all their love and support – I couldn't have done it without you

# Chapter 1

## Introduction



## 1.1 Prenatal screening

Prenatal screening is used to determine women at high risk for many specific pregnancy related disorders, such as aneuploidy, neural tube defects, congenital heart disease and autosomal recessive disorders. It has been estimated that there is around a 2-3% baseline risk that a child will be born with a congenital or genetic disorder, although, the probability of having an affected child is increased when there is a family history of the disorder (Teeuw *et al.*, 2010). Incorporation of a screening programme within the clinic enables invasive testing, such as chorionic villus sampling (CVS) and amniocentesis (refer to 1.2), to be targeted at women who are more likely to display a positive result. Despite the relative success of current screening approaches (80-90% detection rate (DR)), advances in screening tools could further improve the specificity and sensitivity, thus reducing the number of women offered invasive diagnostic tests and increasing the DR, respectively.

### 1.1.1 Definitions

To determine the success of a screening programme, various measurements are used, including; the DR, the false positive rate (FPR) or more recently the screen positive rate (SPR), and the odds of a positive result (OAPR). The DR refers to the sensitivity of the test and therefore identifies the proportion of affected cases successfully determined by the screening programme. Low FPR (the rate of occurrence of positive results in non-affected cases) are also required in addition to high DRs. The SPR, an alternative to the FPR, includes both the false positive and true positive results. The SPR illustrates the chance that a test will be above the cut off risk (for example 1 in 200) and the result will be reported as screen-positive (McEwan, Godfrey and Wilkins, 2012). Lower FPR's/SPR's are required to reduce the number of pregnancies unnecessarily exposed to CVS or

amniocentesis. The OAPR refers to the likelihood that women seen to be high risk after screening will actually display a positive result following definitive diagnosis (Wald, 2008).

The threshold used to determine the cut-off point at which invasive testing is offered influences the DR and the FPR/ SPR. Ideally, screening tests would display a high DR (>90%) and a low (<2%) FPR/ SPR (McEwan, Godfrey and Wilkins, 2012). However, both the DR and FPR/ SPR will be lowered if the threshold is increased (for example 1 in 100) and elevated if the threshold is decreased (for example 1 in 300) (Sillence *et al.*, 2013). Figure 1-1 displays the screening process, potential outcomes and measures of accuracy of prenatal screening for Down Syndrome (DS).

The positive predictive values (PPV) and negative predictive values (NPV) can also be used to determine the performance of diagnostics tests, with high results being indicative of improved accuracy. The PPV and NPV refer to the proportions of positive and negative results that are true positive and true negative results, respectively (Pencina *et al.*, 2008). However, the PPV and NPV are also dependent upon the prevalence of a 'positive' result, for example Trisomy 21 (T21) fetuses in a given population.

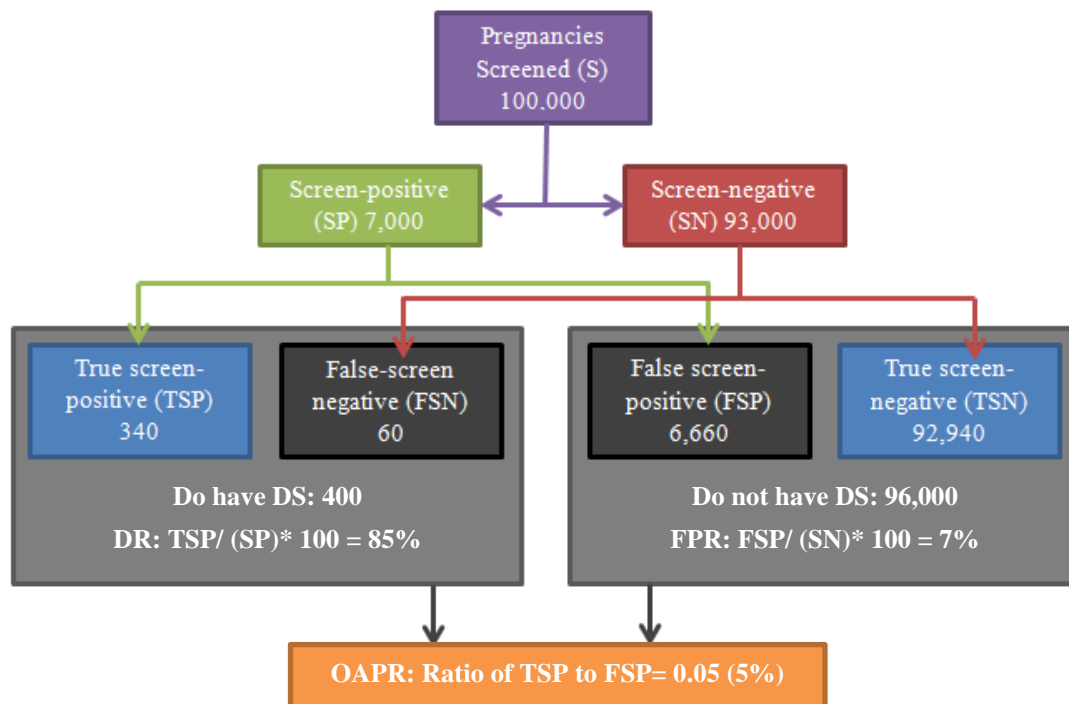


**Figure 1-1: The screening process, potential outcomes and measures of accuracy.** DR is the proportion of affected cases successfully identified by the screening test. True screen positive (TSP) / (TSP + false screen negative (FSN)) = 85%. FPR: Proportion of positive results in non-affected cases identified by the screening test. False screen positive (FSP) / (FSP + (true screen negative (TSN))) = 7% [adapted from Sillence *et al.* (2013) and Buckley and Buckley (2008)].

### 1.1.2 Prenatal screening for fetal aneuploidy

#### 1.1.2.1 Historical overview and current practice for prenatal screening for fetal aneuploidy

Aneuploidy, a divergence from the normal number of chromosomes ( $n=46$ ), results in significant morbidity and mortality. Chromosomal abnormalities occur in 1 of 160 live

births and additional copies of chromosomes 21 (DS), 18 (Edwards syndrome) and 13 (Patau syndrome) account for the majority of aneuploidies that are not associated with sex chromosomes at birth (Nussbaum *et al.*, 2007; Driscoll and Gross, 2009). DS (T21) is the most common fetal aneuploidy and the leading cause of developmental delay, with an incidence around 1 in 800 live births (Ehrich *et al.*, 2011). However, the risk of fetal aneuploidy is directly related to maternal age, from the age of 34 the risk begins to increase exponentially (Figure 1-2) to around 1 in 35 live births for women in their late 40s (Morris, Mutton and Alberman, 2002). In the early 1980s, maternal age was effectively the only screening tool available for detection of fetal chromosomal imbalance such as DS and invasive diagnostic tests were offered to all women aged 35 years and above. Women younger than 35 years were only offered testing if there was a known family history of the disorder (Buckley and Buckley, 2008).

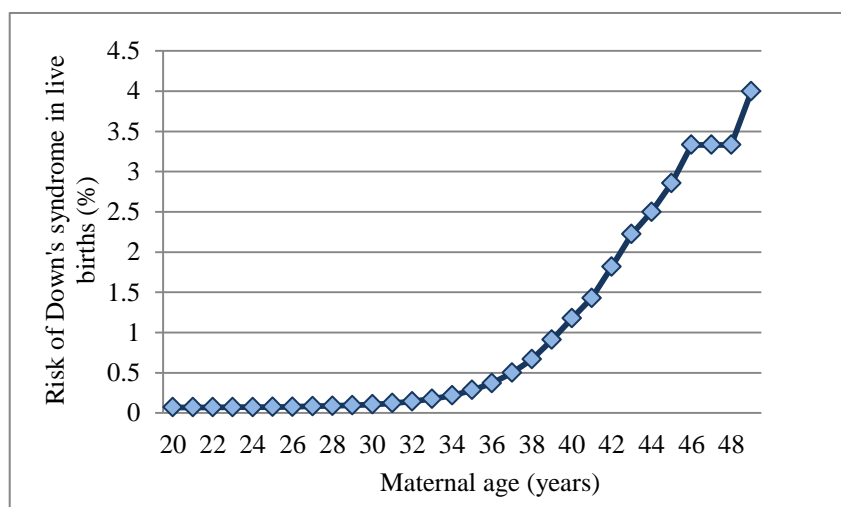


**Figure 1-2: The estimated risk of DS according to maternal age.** The risk of having a DS fetus in live births gradually increases up until around 34 years of age. The risk then increases exponentially, and women in their late 40's have a risk >3%. [Adapted from Morris, Mutton and Alberman (2002)].

Since maternal age alone only provides a DR of <35%, most aneuploidy fetuses were undetected and an abundance of unaffected fetuses were exposed to unnecessary invasive testing (Haddow *et al.*, 1992). In addition, due to increases in the average maternal age, resources to perform invasive testing in a growing number of patients were unavailable. Between 1989 and 2008, the percentage of mothers aged 35 years and above increased from 9% to 20%, respectively, making screening based on maternal age alone unsustainable. The gradual introduction of various biochemical and sonographic markers since the early 1980s has greatly improved the sensitivity of current screening programs to around 95% (Rozenberg *et al.*, 2006; Ehrich *et al.*, 2011) (Figure 2-3).

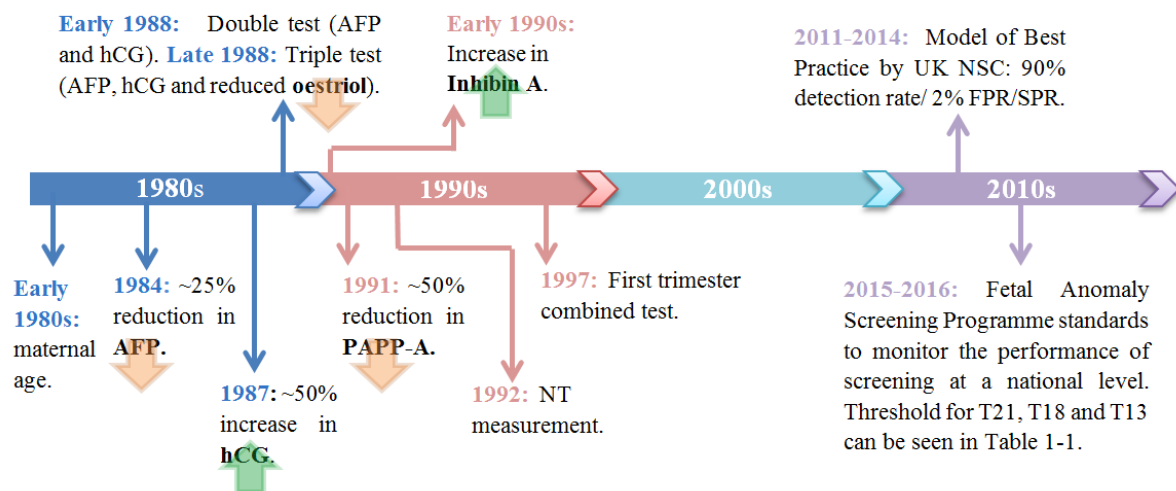


**Figure 1-3: Timeline summarising the key developments in DS screening.** Since the early 1980's multiple serum and sonographic markers have been identified to increase the sensitive and specificity of maternal screening. This figure highlights key markers, which have been introduced into the screening programme overtime, summarising the UK National Screening Committee (UK NSC) Model of Best Practice for 2011 to 2014 (Sillence *et al.*, 2013).

The development of sonographic and maternal serum biomarkers enabled marked improvements to the sensitivity and reliability of screening compared to maternal age

alone. The discovery of different biochemical markers for aneuploidy screening, such as reduced alpha-fetoprotein (AFP), raised Beta- human chorionic gonadotropin ( $\beta$ -hCG), raised Inhibin A and reduced pregnancy associated plasma protein A (PAPP-A), and the introduction of various screening tests are illustrated in Figure 1-3. The most common first trimester test is the combined test, which combines maternal age, NT measurement and serum biomarkers, PAPP-A and  $\beta$ -hCG. In addition to fetal aneuploidy, AFP was historically used for the biochemical screening of open neural tube defects (NTD). However, raised AFP is not visible in fetuses that express closed NTD (10% of lesions) and is also associated with other abnormalities such as gastroschisis, omphalocele, congenital nephrosis and fetal demise (Cameron and Moran, 2009). Therefore, biochemical screening of NTD is not effective and has consequently been surpassed by sonographic methods using two-dimensional (2D) and more recently, three-dimensional (3D) ultrasound techniques (refer to 1.1.2.2).

For prenatal screening of fetal aneuploidy, nuchal translucency (NT) is the most vital and only sonographic marker used clinically. The NT measures the thickness of the skin fold behind the nape of the neck and is carried out between 11 and 14 weeks gestation. All fetuses display some fluid at the back of the neck, which increases with gestation, and as a consequent the NT measurement must take into consideration the crown-rump length to calculate the posterior risk (Souka *et al.*, 1998). However, fetuses with chromosomal abnormalities, such as DS, are associated with increased NT as a result of nuchal edema due a delay in lymphatic vascular development (Haak *et al.*, 2002; Burger *et al.*, 2015). In euploid pregnancies, fetuses that express increased NT often have a healthy outcome (Souka *et al.*, 2005), but in some cases it can also be associated with structural malformations (predominantly cardiac defects), genetic syndromes, skeletal dysplasia and intrauterine fetal demise (Hyett, Moscoso and Nicolaidis, 1997; Souka *et al.*, 1998).

Many studies have identified a strong correlation of enlarged NT and cardiac defects in both aneuploidy and euploid fetuses (Hyett, Moscoso and Nicolaides, 1995; Hyett *et al.*, 1996; Zosmer *et al.*, 1999; Jouannic *et al.*, 2011). Similarly to aneuploidy, the risk of cardiac malformations is positively correlated with increasing NT (Ghi *et al.*, 2001). Nicolaides *et al.* (1992) determined that fetal NT  $\geq 3$  mm was a useful marker for fetal chromosomal abnormalities between 10 and 14 weeks gestation. The study revealed that the presence of NT was associated with  $>10$ -fold increase and the absence of translucency ( $<3$  mm) was associated with a 3-fold decrease in risk of chromosomal abnormality (Nicolaides *et al.*, 1992). NT is still an important marker for risk assessment of fetal aneuploidy. However, invasive testing is now offered if the NT is  $\geq 3.5$  mm or if the risk determined by the combined test is  $\geq 1$  in 150 (Lichtenbelt *et al.*, 2015). The first trimester combined test was first introduced in 1997, which integrates the NT measurement, maternal age and early detectable serum biomarkers, free beta human chorionic gonadotropin (f $\beta$ -hCG) and pregnancy associated plasma protein A (PAPP-A) (Wald and Hackshaw, 1997) (Figure 1-3). Studies have identified that with the first trimester combined test around 85-90% of all DS cases could be detected with a 5% FPR (Spencer and Nicolaides, 2003; Nicolaides *et al.*, 2005; Jaques *et al.*, 2007; Valinen *et al.*, 2007).

Integrated testing requires first and second trimester screening results to determine the risk of aneuploidy. In conjunction with maternal age, the NT and serum levels of PAPP-A are tested between 10+3 and 13+6 weeks gestation, and serum levels of AFP, f $\beta$ -hCG, unconjugated estriol (uE3) and Inhibin A are measured between 15 and 18 weeks gestation (Benn, 2002). Between 2003 and 2004 an audit of the integrated test at two London hospitals, University College Hospital (UCH) and St Mary's Hospital was carried out based on 15,888 women (Wald *et al.*, 2009). The results revealed a DR of 87% (95% CI, 74-95) and a

FPR of 2.1% (95% CI, 1.9-2.3) illustrating the feasibility of this test. In an alternative study, the results of the Serum, Urine and Ultrasound Screening Study (SURUSS) for DS were assessed (Wald *et al.*, 2003). The results revealed that for women who attend first trimester screening, the integrated test offered the most effective approach. In a summative report, Wald *et al.* (2004) revealed that the integrated test, which illustrated DRs of 85% and a FPR of 0.9%, demonstrates greater accuracy than the combined test (4.3% FPR) and the quadruple test (6.2% FPR). However women who miss first trimester screening can only be offered second trimester quadruple testing, which has a slightly lower sensitivity and thus a higher SPR than the first-trimester combined test (McEwan, Godfrey and Wilkins, 2012).

Although the Integrated test increases test sensitivity in conjunction with a reduction in FPR, there are concerns that some women who indicate high risk (1 in 150) following first trimester screening have to wait until after second-trimester testing before they are offered invasive procedures for definitive diagnosis, which is associated with ethical complications (refer to 1.4). Secondly, a step-wise approach was developed. Consequently, high risk patients following the first trimester combined screening test are offered CVS, and low/intermediate cases are offered second trimester screening (AFP, uE3 and free  $\beta$ -hCG). If the combined risk is high, patient is offered second trimester amniocentesis (Nicolaidis, 2011). This led to the development of Contingency screening, which only offers second trimester serum screening to women that present intermediate risk values between 1 in 50 and 1 in 1000. Women who indicate significantly high risk following first-trimester screening are consequently offered invasive diagnostic tests immediately. Alternatively,



pregnant women that indicate extremely low risk after first trimester screening are not offered subsequent second-trimester tests. Currently, the UK National Screening Committee (UK NSC) has not supported either the Integrated or Contingency screening tests despite improvements to DR and FPR/SPR, because of the complexity associated with both techniques (McEwan, Godfrey and Wilkins, 2012). In addition, the integrated test was also not recommended by the UK NSC as the combined test was more cost effective, and as an additional appointment in the second trimester is required for the Integrated test, failure to attend would make the test invalid.

In 2003 the UK NSC provided evidence for the first DS screening policy called a 'Model of Best Practice'. During 2004 to 2005 all trusts were expected to provide a screening programme that demonstrated  $\geq 60\%$  DR for a  $\leq 5\%$  FPR (Wald *et al.*, 2003). Through investment in sonographic training, improved quality control methods for biochemical analysis and development of ultrasound technology the sensitivity of screening and specificity of screening began to improve. In 2008 and 2011 the core screening standard set by the UK NSC for England was a DR of  $>90\%$  and a SPR of  $<2\%$  for women undergoing combined screening, and a DR of  $>75\%$  and a SPR of  $<3\%$  for women undergoing quadruple screening (Figure 1-3) (The UK National Screening Committee, 2008; The UK National Screening Committee, 2011). The only change made to the Model of Best Practice in 2011 was that the cut-off/ threshold for the quadruple test (second trimester), which was reduced from 1 in 200 to 1 in 150 in line with the combined test (first trimester) cut-off.

The National Health Service (NHS) Fetal Anomaly Screening Programme (FASP) published by Public Health England (Public Health England, 2015) is

responsible for implementing screening policies set by the UK NSC. The aim of FASP is to ensure equal access of quality assured screening throughout the UK, which provides high quality Information to enable women to make an informed choice about their screening options and consequent pregnancy choices (The UK National Screening Committee, 2015). Table 1-1 illustrates the national standards for T21, Trisomy 18 (T18) and Trisomy 13 (T13) screening.

**Table 1-1: National UK Standards for T21, T18 and T13 screening (PHE, 2015).**

Screening Strategy	Thresholds	
	Acceptable	Achievable
<b>T21</b>	Standardised DR 85%	
<b>Combined Test</b>	Standardised SPR 1.8-2.5%	Standardised SPR 1.9-2.4%
<b>T18/T13</b>	Standardised DR 80%	
<b>Combined Test</b>	Standardised SPR 0.1-0.2%	Standardised SPR 0.13-0.17%
<b>T21/T18/T13</b>	Standardised DR 80%	
<b>Combined Test</b>	Standardised SPR 1.8-2.5%	Standardised SPR 1.9-2.4%
<b>Quadruple (T21)</b>	Standardised DR 80%	
	Standardised SPR 2.5-3.5%	Standardised SPR 2.7-3.3%

### 1.1.2.2 *Developments of Sonographic Markers*

Pregnancy ultrasound scans are primarily carried out to determine the viability, gestational age and number of fetuses, but is also used as a tool to detect major structural abnormalities (Blaas, 2014). Sonographic imaging plays an important role in prenatal screening and has succeeded serum screening for detection of NTD's. Classic 2D ultrasound can be used to detect cranial signs, such as lemon shaped head, banana cerebellum and ventriculomegaly, for the presence of spinal bifida (Van den Hof *et al.*, 1990). However, the prognosis of spinal bifida can vary depending on the location of the lesion, with higher lesions being

associated with an increased chance of being wheelchair bound. The development of 3D ultrasound has improved diagnostic accuracy (to within one vertebral body in up to 80% of patients) and enables improved prediction of outcome and more directed genetic counselling (Cameron and Moran, 2009).

The role of sonographic imaging in the risk assessment of aneuploidy, particularly DS (T21), has been extensively investigated during the first and second trimester (Benacerraf, Frigoletto and Cramer, 1987; Stoll *et al.*, 1993; Hill, 1996; Nyberg and Souter, 2001; Rozenberg *et al.*, 2006; Kagan *et al.*, 2009; Abele *et al.*, 2015). Thickened nuchal fold was the first ultrasound marker identified for DS and currently the only sonographic marker included in the combined screening test (Figure 1-3). Increase NT can also be used as a marker for other chromosomal abnormalities, such as Edwards Syndrome (T18) and Patau's Syndrome (T13) (Cicero *et al.*, 2003). In addition to fetal aneuploidy, NT measurement is important since it is associated with adverse prenatal outcomes caused by a variety of fetal conditions, including cardiac defects (Hyett *et al.*, 1997), dysplasias and genetic syndromes (Souka *et al.*, 1998). Similarly to aneuploidy detection, a thicker NT is associated with an increased probability of associated anomalies.

More subtle sonographic markers for the second-trimester screening of T21 were evaluated (Stressig *et al.*, 2011; McEwan, Godfrey and Wilkins, 2012; Blaas, 2014). The results revealed that the combination of maternal age with either ductus venous (DV), tricuspid blood flow or nasal bone abnormalities only demonstrated a marginal improve in DR (33.8%, 32.4% and 31.4%) compared to maternal age alone (29%) (Stressig *et al.*, 2011). It has also been shown that these sonographic markers are also useful for the determination of other aneuploidies and structural abnormalities (Blaas, 2014). Figure 1.4 illustrates the occurrence of these additional sonographic markers alongside NT, for euploid and aneuploidy fetuses. However, some of these markers express inter-racial

variation and therefore incorporation into the screening programme may be population specific. For example, hypoplasia of the nasal bone in Caucasians occurs in only 1-3% of normal pregnancies during late first-trimester screening, whereas this increase to around 10% in African populations (McEwan, Godfrey and Wilkins, 2012). Therefore, if integrated into first trimester screening a lower FPR would be associated with Caucasian populations. Kagan *et al.* (2009) determined that it would be possible to increase the DR to 93-96% (with a FPR of 2.5%) by incorporating DV and tricuspid regurgitation markers to first-trimester combined screening test. However, checking for these additional markers is not only challenging, which results in variation of interpreting results, but also very time consuming. Therefore these markers have not been adopted into routine clinical practice for widespread screening. They may have a role, but in a contingent screening model whereby they are offered to women with an intermediate risk from combined screening, In these situations further information is needed before deciding whether to opt for invasive testing (Nicolaidis *et al.*, 2005).

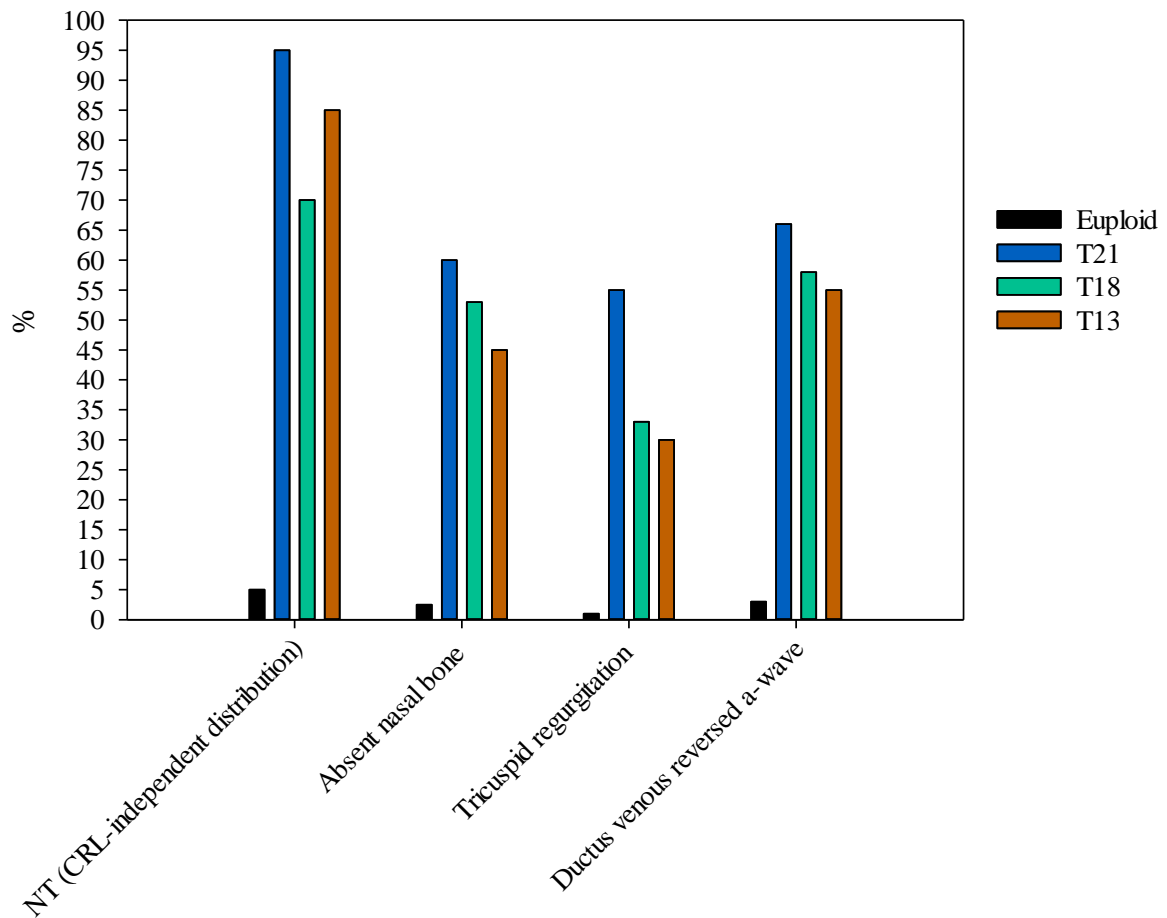


**Figure 1-4: Incidence of sonographic features in Euploid, T21, T18 and T13 fetuses.**

The incidence of sonographic markers including NT measurement, absent nasal bone, tricuspid regurgitation and ductus venous reversed a-wave for pregnancies carrying euploid (black), T21 (blue), T18 (green) and T13 (orange) fetuses. (Adapted from (Nicolaidis, 2011). (CRL; crown-rump length).

Various structural abnormalities can be seen using ultrasound and a combination of certain sonographic makers can be used to differentiate between aneuploidies. In T18, onset intrauterine growth restriction and bradycardia (Cicero *et al.*, 2003) are visible. In addition, in around 30% of cases small and large exomphalos can also be seen by ultrasound (Sherod *et al.*, 1997). Exomphalos is also associated with heart defects and

other chromosomal abnormalities such as T13 (Groves *et al.*, 2006). In T13, holoprosencephaly or exomphalos is observed in about 30% of cases (Souka *et al.*, 1998), along with fetal tachycardia and early onset intrauterine growth restriction in around 65% of cases (Cicero *et al.*, 2003). Detection of these structural anomalies during either first or second trimester screening does not provide a definitive diagnosis and consequently, invasive testing should be offered. Other second trimester sonographic markers for the detection of T21 have been determined, including choroid plexus cysts, dilated cisterna magna and echogenic cardiac foci and a two vessel cord. However, due to low levels of sensitivity and specificity (McEwan, Godfrey and Wilkins, 2012), in 2008 the UK NSC recommended that a prior risk for DS should not be adjusted based on the presence or absence of one or more of these markers (The UK National Screening Committee, 2008). This was reiterated in 2015, when FASP recommended that an established screening test result should not be recalculated at the 18+0 to 20+6 fetal anomaly scan, as stated in previous report (Public Health England, 2015). However, the document stated that along with NT, ventriculomegaly, echogenic bowel, renal pelvic dilation and small measurements (compared to dating scan) should be reported and consequently women should be referred for further assessment (The UK National Screening Committee, 2015).

Although chromosomal aneuploidy can be effectively detected by 2D ultrasound, particularly by the identification of increased NT in the first and second trimester, the use of 3D and 4D ultrasound to observe sonographic markers seems to provide better detection and identification rates (Malhotra *et al.*, 2014). Recently, a comparative study between conventional 2D ultrasound and a novel volume NT™ technique (3D ultrasound) revealed that the latter improves the Herman score by obtaining a better sagittal plane, even in the hands of a less experienced operator (Haddad *et al.*, 2015). Therefore, this platform should be available whenever 2D assessment is difficult to

obtain. This illustrates that the improved resolution associated with 3D and 4D ultrasound scanning can be used to improve the detection of some of the previously mentioned sonographic markers. Alternatively, if novel sonographic techniques facilitate increased sensitivity and specificity, the introduction of additional second trimester ultrasound markers within the current screening programme could be re-evaluated. In a recent study, the frontal fetal facial (FFF) angle in 80 normal fetuses and 42 T21 fetuses were compared using 3D ultrasound for women between 14 and 27 weeks gestation (Merz and Pashaj, 2015). The results revealed that the T21 fetuses demonstrated higher FFF angles compared to normal fetuses and that FFF angles  $>145^{\circ}$  should be considered as a potential marker for T21. However, values  $\leq 145^{\circ}$  does not exclude the possibility of carrying a T21 fetus in the second trimester (Merz and Pashaj, 2015). Alternatively, an evaluative study revealed that the addition of DV and hepatic artery (HA) Doppler measurements to the first trimester combined screening test could increase the accuracy for DS detection (Togrul *et al.*, 2014). However, further large scale validation is required since only the DV Pulsatility index of veins (PIV) illustrated significantly higher measurements ( $P= 0.03$ ) in women who illustrated high risk for fetal aneuploidy following the combined test.

#### *1.1.2.3 Development of Serum/Plasma and Urine Biomarkers*

In addition to identifying new possible ultrasound markers, novel biochemical screening markers to improve current DRs and FPRs/SPRs (Table 1-1, Page 28) have also been extensively studied (Cowans *et al.*, 2011; Du *et al.*, 2011; Akinlade *et al.*, 2012; Munnangi *et al.*, 2014; Iles *et al.*, 2015). Serum biomarkers presently incorporated within different screening programmes include; PAPP-A, AFP, hCG (and its subunits), uE3 and Inhibin A (Wald *et al.*, 1996) (1.3.2.1).

Initially, the criteria for selecting proteins for analysis as potential novel biomarkers were based on logical reasoning and up-regulation or down-regulation in alternative pregnancy disorders. For example, placental growth factor (PIGF) plays a key role in placental development and previous studies have also illustrated significant decreases of PIGF in the first trimester for pregnancies associated with pre-eclampsia (Akolekar *et al.*, 2008). The assessment of this biomarker for fetal aneuploidy screening revealed a significant increase in PIGF for T21 pregnancies compared to unaffected pregnancies at 8 weeks gestation, but significant increases were no longer detected at 10 weeks gestation (Cowans *et al.*, 2011). Therefore, this biomarker would only be beneficial to screening in early pregnancy. Consequently, PIGF has not been incorporated into the combined screening test, which is carried out at between 10 and 14 weeks gestation.

Microarray techniques, initially determined seven differentially expressed genes (Crosley *et al.*, 2013). PAPP-A2, one of the identified genes, was selected for follow up analysis since previous data had also detected up-regulation in pre-eclampsia (Crosley *et al.*, 2013). The results revealed that PAPP-A2 was significantly increased and could serve as an additional serum marker for T21 screening during the second trimester (Munnangi *et al.*, 2014). Alternatively, some biomarkers were selected based on incidental discovery by western blotting. Disintegrin and metalloprotease domain-containing protein 12 (ADAM12) was detected by western blotting in pregnant serum but not in non-pregnant serum (Shi *et al.*, 2000). Investigation of ADAM12 revealed significant reduction in early trimester ( $\leq 8$  weeks) in T21 cases compared to normal controls (Christiansen *et al.*, 2010). However, since this protein is almost non-



existent by 9-10 weeks, like PIGF, this biomarker is unsuitable for the combined screening test.

Improved proteomic technological developments have created the potential to identify new panels of serum biomarkers (Koster *et al.*, 2010). The Special Non-Invasive Advances in Fetal and Neonatal Evaluation (SAFE) Network of Excellence (NoE) was established by the European Union (EU) in 2004 to provide worldwide cost effective routine NIPD and screening through long term partnerships. (Chitty *et al.*, 2008; Maddocks *et al.*, 2009). One of the major goals of the SAFE NoE was to identify a more informative panel of T21 markers. Since improved DR and lower FPR are currently achieved during first trimester screening, classification of more suitable markers for the second trimester is of paramount importance (Kagan *et al.*, 2010; Miguelez *et al.*, 2010).

Heywood *et al.* (2011) set out to identify potential new plasma protein biomarkers using a two-dimensional - difference gel electrophoresis (2D-DIGE) approach. The 2D-DIGE approach uses amine reactive dyes, which assures that proteins common to both samples (ran on the same gel) express the same relative mobility regardless of tagged-dye used and consequently prevents the need to compare multiple 2D gels (Ünlü, Morgan and Minden, 1997) However, the study highlighted the inadequacies of gel-based proteomics for identification of plasma biomarkers for T21 and suggested that gel-free approaches may be more effective (Heywood *et al.*, 2011). Kang *et al.* (2012) identified 31 DS differentially expressed maternal serum proteins (DS-DEMSPs) in the maternal serum of women carrying a DS fetus, and out of these ten were considered as potential biomarkers (Alpha-2-macroglobulin, Apolipoprotein A1, Apolipoprotein E, Complement C1s subcomponent, Complement component 5,

Complement component 8, alpha polypeptide, Complement component 8, beta polypeptide and Fibronectin).

In 2012, a preliminary study evaluated the application of combining 2D-DIGE and mass spectrometry for determining different levels of expression of proteins in normal fetuses ( $n=6$ ) and T21 fetuses ( $n=6$ ) (Yu *et al.*, 2012). Bioinformatics was then used to analyse the proteins and subsequently, candidates of interests were further analysed by enzyme-linked immunosorbent assay (ELISA). Out of the 29 proteins successfully identified in the maternal serum of women carrying a T21 fetuses, the top 5 up-regulated included serotransferrin, alpha-1b-glycoprotein (A1BG), desmin, alpha-1-antitrypsin and ceruloplasmin, while the most down regulated protein was serum amyloid P-component (APCS). Yu *et al.* (2012) revealed that ceruloplasmin and complement factor B were significantly higher in the T21 cases compared to the normal cases ( $P < 0.05$ ). This study demonstrated down-regulation of APCS in second trimester samples. However, in an alternative study using protein chip technology/ surface enhanced laser desorption ionisation time of flight mass spectrometry (SELDI ToF MS), APCS was found to be significantly up-regulated in second trimester maternal plasma samples carrying T21 fetuses ( $P < 0.004$ ) (Heywood *et al.*, 2012).

SELDI ToF MS is a variation on matrix-assisted laser desorption/ionisation (MALDI) that is used for the analysis of protein containing samples such as plasma or serum (Tang, Tornatore and Weinberger, 2004). SELDI is associated with an additional separation phase, which enables bound proteins to be analysed with more ease. The use of SELDI ToF MS for the investigation of differentially expressed proteins in maternal plasma samples taken in both first and second trimester carrying normal and T21 fetuses has been described (Heywood *et al.*,

2011; Heywood *et al.*, 2012; Narasimhan *et al.*, 2013). The results revealed that the proteomic profile of maternal serum varied from first trimester (10 to 14 weeks and second trimester (14 to 20 weeks). For first trimester samples, a significant up-regulation of plasma protease C1 inhibitor was identified in the T21 group compared to the controls ( $P = <0.004$ ). In the second trimester subset, as previously mentioned APCS was found to be up-regulated, along with a significant up-regulation of transthyretin ( $P= <0.006$ ) and a significant down-regulation of complement C3- $\alpha$  chain ( $P= 0.0005$ ). Transthyretin was also shown to be up-regulated in an independent study, which also used SELDI ToF MS to test normal cases (n=85) and trisomy cases (n=23) (Narasimhan *et al.*, 2013). In total, Narasimhan *et al.* (2013) determined 37 unique hydrophobic proteomic features for T21, T18 and T13 fetuses, highlighting the improved accuracy, sensitivity and specificity of proteomic spectrum-based screening.

Recently, the application of direct MALDI ToF MS on maternal urine samples for the detection of T21 was evaluated (Iles *et al.*, 2015). The study revealed spectral profile differences between T21 (n=8) and normal (n=39) groups between 12 and 14 weeks gestation, but illustrated poor discrimination between 15 and 17 weeks gestation. While, this approach may provide rapid results at lower costs than expensive immunoassays for serum/plasma biomarker profiling, the accuracy is likely to be lower and urine samples are more likely to become contaminated.

Currently, no additional serum, plasma or urine markers have been incorporated into first or second trimester screening programmes. However, developments in proteomic platforms currently available enables detection of an increased number of potential markers rather than 'selection at random' or choosing

proteins that demonstrate variation in expression in other pregnancy related disorders.

#### *1.1.2.4 NGS for NIPT of Fetal Aneuploidy*

The technological aspects of massively parallel sequencing (MPS) using maternal plasma containing cell-free DNA (cfDNA) for NIPT/NIPD will be discussed under ‘*Determining Fetal Aneuploidy- MPS*’ (refer to 1.3.3.3.2), since it was first developed as a diagnostic tool for the replacement of invasive procedures. However, currently it is only offered as an advanced screening tool and many women who receive a positive NIPT prefer to also undergo invasive testing for a definitive diagnosis.

Since the introduction of NIPT for fetal aneuploidy into clinical practice in Hong Kong in 2011, the American College of Obstetrics and Gynecology published a statement indicating that cfDNA testing should only be offered to high-risk women (Choi *et al.*, 2013). This is essential since NIPT only tests the placental DNA, thus confined placental mosaicism (CPM), caused either by mitotic non-disjunction in a trophoblastic cell or trisomic rescue (in the fetus), results in a trisomic cell line in the placenta and not in the fetus. Therefore, CPM, as well as twin pregnancies and maternal tumours, can give rise to FPRs, thus it is essential that if prospective parents select to abort fetus following a positive NIPT test, confirmation of aneuploidy should be conducted using invasive tests. In 2013 the International Society for Prenatal Diagnosis (ISPD) defined that cfDNA testing using MPS may be considered in high-risk cases based on first or second trimester screening results (International Society for Prenatal Diagnosis, 2013).

Since the current standard is to offer NIPT of fetal aneuploidy as an intermediate screening step, it is not economically viable to introduce this as part of an NHS clinical service. It was suggested that the cut-off to offer cfDNA testing could be set to manage numbers and reduce costs. However, this would result in more cases of fetal aneuploidy being missed compared to implementing MPS screening as part of the combined screening (Soothill, 2014). By integrating cfDNA testing within the combined test is also not currently economically viable. Therefore, it was suggested that MPS could replace the serum screening aspect of the combined test to reduce costs. However, this decreases the information available for other pregnancy complications such as pre-eclampsia, which is associated with low levels of PAPP-A (Spencer, Cowans and Nicolaides, 2008). The availability of MPS as the primary screening method is currently commercially available. By screening the entire pregnancy population based on cfDNA sequencing alone results in high levels of sensitivity and specificity (Ehrich *et al.*, 2011; Lau *et al.*, 2013; Liang *et al.*, 2013; Li *et al.*, 2015), although the costs of cfDNA sequencing within the NHS are not yet known (Soothill, 2014).

It is a possibility that cfDNA testing using MPS could replace the current combined screening test in the near future. However, currently, the number of tests which do not provide a result would lead to an increase in the number of women offered invasive testing. In 2014 a study conducted across 21 centres within the United States (1914 women) was published, which compared DNA sequencing to standard prenatal aneuploidy screening (Bianchi *et al.*, 2014). This study tested a general obstetrical population rather than just targeting high risk cases, since the performance of cfDNA testing in low risk populations was

unknown. The results revealed that the FPR was significantly lower for the cfDNA testing compared to standard screening for T21 (0.3% vs. 3.6%,  $P < 0.001$ ) and T18 (0.2% vs. 0.6%,  $P < 0.03$ ). In addition, all cases of trisomy were detected using DNA sequencing, resulting in higher PPV for cfDNA testing compared to standard screening for T21 (45.5% vs 4.2%) and T18 (40% vs. 8.3%) (Bianchi *et al.*, 2014). Since higher cfDNA fractions have been associated with fetal aneuploidy (Lee *et al.*, 2002), it was expected that higher sensitivities would be visible for high-risk populations. However, these results revealed that the performance of cfDNA sequencing in a general obstetric population corresponded to the performance previously seen in high-risk pregnancies alone (Bianchi *et al.*, 2014). Although it is important to note that 0.9% of cfDNA tests were also unable to provide results.

In a similar study, two European centres determined the feasibility of a SNP-based NIPT for determining the risk of fetal aneuploidy in a general pregnant population (Comas *et al.*, 2014). The results supported clinical implementation of NIPT as a safe, early and accurate option for the general obstetrical population. However, it is also revealed that for Centre A and Centre B, only 2023/2155 (93.9%) and 311/319 (97.5%) samples, respectively, received a NIPT result that was able to determine the risk of aneuploidy (Comas *et al.*, 2014).

Initially, it was thought that cfDNA sequencing tests were less reliable for T13 detection (Ashoor *et al.*, 2013a). Although recent improvements for the detection for T18 and primarily T13 have been shown (Ashoor *et al.*, 2013b). However, the UK NSC must review emerging evidence and evaluate the feasibility of MPS screening and whether it can be used to replace current screening or be offered as an additional screening test. Due to the high sensitivity and specificity associated with shotgun MPS (s-MPS) and targeted

MPS (t-MPS) sequencing it is possible that once clinical stability is established, cfDNA analysis could replace both combined screening tests and invasive tests currently available (Allyse *et al.*, 2015). Presently, the National Society of Genetic Counselors (NSGC) support NIPT as an option for high-risk patients but encourages that it is only offered where there is informed consent and additional counselling support is provided (Devers *et al.*, 2013). Patients that display abnormal results, or if results are unable to be determined, should also receive counselling and be offered invasive testing.

### 1.1.3 Prenatal screening for monogenic disorders

X-linked monogenic disorders are linked to single gene mutations on the X chromosome and as a consequence male and female fetuses are affected unequally. Therefore, NIPD of fetal sex (refer 1.4.3.1) is an important screening tool for couples with known disease status or previous family history (Hill *et al.*, 2011). For each recessive X-linked disorder, such as Duchenne's muscular dystrophy (DMD) and haemophilia, each pregnancy has a 25% chance of an affected male fetus and a 25% chance of a carrier daughter. Thus identifying a female fetus predominantly indicates that the fetus will not express the disorder and invasive testing is not required. The incidence of affected females is considerably lower than males since a mutation would need to occur in two copies of the gene to cause the disorder. For example, the prevalence of DMD is around 1 in 7000 (Romitti *et al.*, 2015), therefore, the prevalence of an affected female in an unrelated population would be around 1 in 49,000,000. However, consanguineous mating causes individuals to inherit segments of their genomes from each parent which are homozygous and consequently this increases the incidence of X-linked and autosomal recessive disease within these sibships (Woods *et al.*, 2006). Alternatively, a women with an X-linked dominant disorder has a 50% chance of having an affected daughter or son with each pregnancy, whereas only female fetuses will be affected (100%) if the father carried

the affected X-mutation (Hartl and Jones, 2005). Therefore, determination of a female fetus if the father expresses the disorder allows for indirect diagnosis of the disease. In addition, fetal sex determination is important for conditions associated with ambiguous development of the external genitalia, such as congenital adrenal hyperplasia (CAH), since dexamethasone treatment can be targeted to female fetuses (Forest, Morel and David, 1998) (refer to 1.3.3.1).

Autosomal disorders are not sex-linked and therefore males and females are equally affected. Autosomal recessive disorders occur when two copies of an abnormal gene are inherited from phenotypically normal parents who are carriers for a specific disorder. The risk of having an affected child if both parents are carriers for the disease is  $1/4$  (Woods *et al.*, 2006). For autosomal dominant disorders only a single affected copy of the gene is required for disease manifestation and if a single parent carries this mutation the risk of having an affected child is  $1/2$ . Since the disorder is dominant in most cases the affected parent will show symptoms of the disease. However, in Huntington's disease, a neurodegenerative autosomal dominant disorder, physical symptoms do not usually begin until 35 years of age and as a consequence the parental status at time of conception and throughout pregnancy is not known (Langbehn *et al.*, 2004). Therefore, couples with known family history of Huntington's or specific autosomal recessive disorders can be offered preconception risk assessment. Defining the presence of mutated gene for Huntington's disease indicates a 50% risk that the fetus will also express the mutated allele. For autosomal recessive disorders, determining the carrier status of each parent, or maternal carrier status, prior to conception enables fully informed reproductive choices to be made. This can include pre-implantation diagnosis and *in vitro* fertilisation, or alternatively allow for counselling to psychologically prepare prospective parents, preventing couples, or individuals, having to make quick and difficult choices during the



antenatal screening period, such as potential termination of pregnancy (Hussein *et al.*, 2013). Due to the low prevalence of recessive disorders, the likelihood of a couple expressing the same recessive allele is low. However, as previously mentioned the likelihood is increased if mating is consanguineous.

The carrier frequencies of some autosomal recessive disorders vary between individuals of specific ethnic backgrounds and as a consequence different carrier screening programmes are recommended for different populations (Table 1-2). Cystic fibrosis, Tay-Sachs disease and sickle cell anaemia are more prevalent in Caucasians (Northern European origin), Ashkenazi Jewish and African populations, respectively (Wailoo and Pemberton, 2008). For example, the carrier prevalence of sickle cell anaemia ranges from 1 to 40 percent from different populations (Hussein *et al.*, 2013). Within the NHS, women are offered antenatal screening for sickle cell anaemia and thalassaemia with follow up analysis on the newborn as part of the bloodspot program (Cavanagh, McHugh and Coppinger, 2015). In low prevalence populations, family origin questions (FOQ) are used to determine if screening is necessary, but in high prevalence populations all pregnant women are offered screening for all haemoglobinopathies. The prenatal screening blood test for sickle cell anaemia and thalassaemia is carried out before 10 weeks gestation to increase time available for parents to make an informed decision. The test determines the carrier status of each parent and if both are identified to be carriers of concerned haemoglobinopathy, genetic counselling is offered.

**Table 1-2: Carrier frequencies of various autosomal recessive disorders within different populations.**

<b>Population</b>	<b>Condition</b>	<b>Carrier Frequency*</b>
African-American	Sickle Cell Anaemia	1 in 10
	Cystic Fibrosis	1 in 65

	Beta-Thalassaemia	1 in 75
	Gaucher Disease	1 in 15
	Cystic Fibrosis	1 in 26 - 1 in 29
Ashkenazi Jewish	Tay-Sachs Disease	1 in 30
	Dysautonomia	1 in 32
	Canavan disease	1 in 40
Asian	Alpha-Thalassaemia	1 in 20
	Beta-Thalassaemia	1 in 450
European-American	Cystic Fibrosis	1 in 25- 1 in 29
French Canadian	Tay-Sachs Disease	1 in 30
Hispanic	Cystic Fibrosis	1 in 46
	Beta-Thalassaemia	1 in 30- 1 in 50
Mediterranean	Beta-Thalassaemia	1 in 25- 1 in 29
	Cystic Fibrosis	1 in 29
	Sickle Cell Anaemia	1 in 40

\*Carrier frequencies obtained from Oregon Health and Science University (OHSU) Department of Health Services Oregon Health and Science University (OHSU) (2005,

Section 1.3.3.4 describes various methods that have been developed for the NIPD of monogenic disorders, including, detection of paternally inherited mutations, relative mutation dosage (RMD) analysis for determination of individual monogenic disorders and MPS for detection of multiple monogenic disorders. Similarly to aneuploidy analysis, it is reasonable to suggest that these fetal specific genetic-based tests may be used as advanced intermediate screening tools and allow confirmatory invasive tests to be directed at women that are highly likely to carry an affected fetus.

## 1.2 Invasive testing

Despite recent advances of t-MPS for NIPT of fetal aneuploidy (1.3.4), invasive tests, such as CVS and amniocentesis, are currently the only approaches clinically available for definitive diagnosis. CVS is carried out between 10 and 12 weeks gestation and involves the collection of placental tissue (chorionic villi) (Olney *et al.*, 1995). This can either be achieved using a transcervical procedure, which obtains the tissue by inserting a catheter through the cervix and into the placenta, or alternatively by a transabdominal procedure, which collects the tissue by inserting a needle through the abdomen and uterus and into the placenta. The type of CVS procedure carried out is dependent upon the route accentuated through the physicians training and also gestational age, since the placenta moves away from the cervix as it increases, restricting the transcervical approach (Hallak *et al.*, 1992).

Contrastingly, amniocentesis is performed between 15 and 18 weeks gestation and involves the collection of amniotic fluid using a transabdominal approach into the amniotic sac (Olney *et al.*, 1995). For both CVS and amniocentesis, ultrasound is used to monitor and guide the needle/ catheter to the correct location. For analysis of fetal genetic material for detection of chromosomal aberrations, karyotyping has been considered the gold standard for over 30 years, and is highly accurate and reliable (Los *et al.*, 2001; Boormans *et al.*, 2008). However, analysis is labour intensive and results can take between 14 to 21 days to arrive (Boormans *et al.*, 2008). Thus, this approach is being progressively replaced by alternative rapid aneuploidy tests, such as quantitative fluorescent polymerase chain reaction (QF-PCR), fluorescent *in situ* hybridisation (FISH) and multiplex ligation-dependent probe amplification (Choy *et al.*, 2014).

Direct analysis of fetal genetic material enables accurate (100%) definitive diagnosis. However, irrespective of the downstream processing used for detection of chromosomal aberrations, the invasive methods used (CVS or amniocentesis) to obtain fetal genetic material are associated with a 1% risk of iatrogenic fetal loss (Ferguson-Smith, 2003; Chiu, Cantor and Lo, 2009; Ehrich *et al.*, 2011). Despite considerable developments within the field of NIPD, improved PPVs (refer to 1.1.1) are required before invasive tests can be replaced. In addition, the cost benefits, ethical considerations and practicality of implementing NIPD into the clinic must be evaluated on a wide scale.

### 1.3 Prenatal diagnosis

Screening is an effective tool to determine risk of pregnancy related disorders and fetal chromosomal abnormalities. However, it cannot be used for a definitive diagnosis. In order for a diagnosis to be made, direct analysis of fetal genetic material is required. Currently, confirmation of specific fetal disorders can only be routinely achieved using invasive tests (1.2), which are associated with a small but significant risk of miscarriage. Therefore, developing a reliable and highly accurate NIPD test has long been sought after. The discovery of fetal cells (Walknowska, Conte and Grumbach, 1969), fetal RNA (Poon *et al.*, 2000) and predominantly cfDNA (Lo *et al.*, 1998a) within the maternal circulation has made NIPD viable and multiple techniques have been researched over the last two decades. Although none of these techniques have replaced invasive testing at present, due to high levels of sensitivity (100%) achieved by MPS, it is likely that non-invasive testing will be implemented within the clinic in the near future.

#### 1.3.1 Fetal cells

The presence of fetal cells within the maternal circulation (Walknowska, Conte and Grumbach, 1969) demonstrates that the placenta does not form an impermeable barrier between the mother and fetus, enabling bidirectional trafficking. Therefore, this highlights the application of intact fetal cells as a target for NIPD. Multiple complex fetal cell enrichment techniques have been described for purification and diagnostic analysis, including density gradient centrifugation (Cupp *et al.*, 1984), Fluorescence-activated cell sorting (FACS) (Herzenberg *et al.*, 1979), magnetic-activated cell sorting (MACS) (Gänshirt *et al.*, 1998), charge flow separation (Wachtel *et al.*, 1998), and immunomagnetic colloid systems (Lim, Tan and Goh, 1999). However, the relative rarity and fragility of fetal cells makes isolation difficult (Bianchi, 1999).

The first fetal cell identified within maternal plasma using PCR was the fetal leucocyte, which was identified in 1969 by detecting the presence of Y-chromosome targets in mitogen-stimulated lymphocytes (Walknowska, Conte and Grumbach, 1969). However, initial studies revealed that these cells can persist within the maternal circulation for 1 (Schroder, Tilikai and Chapelle, 1974) and 5 (Ciaranfi, Curchod and Odartchenko, 1977) years following delivery. It was later revealed that rare male fetal progenitor cells can persist in maternal blood for up to 27 years postpartum (Bianchi *et al.*, 1996). Therefore, nucleated fetal cells are unlikely to become an effective diagnostic tool since cells from previous pregnancies, previous miscarriages or maternal microchimerism can lead to false positive results in subsequent pregnancies.

Consequently, research has focused on terminally differentiated cell types, such as trophoblastic sprouts and erythrocytes. Trophoblasts have a unique morphology, which makes them easy to identify and are rapidly cleared from the circulation following delivery. However, the sparsity of monoclonal antibodies specific for trophoblastic markers have made isolation difficult (Bertero *et al.*, 1988). One of the fundamental problems associated with trophoblastic sprouts is that these cells are not generally expressed in healthy pregnancies, but are detectable in pre-eclampsia (Sargent *et al.*, 1994). Though this may appear as an attractive marker for pre-eclampsia, absence may be a result of limited sensitivity as opposed to a healthy fetus.

Fetal nucleated red blood cells (FNRBCs) are ideal for NIPD since they have a limited lifespan, contain a full representation of the fetal genome, are more predominant than leucocytes (improving isolation) and contain specific fetal cell identifiers (Bianchi, 1999; Choolani, Mahyuddin and Hahn, 2012). In a recent publication, the application of whole genome sequencing (WGS) of single FNRBCs from villi demonstrated 100% accuracy in first trimester samples (Hua *et al.*, 2014). In addition, further analysis of FNRBCs from

post-termination of pregnancy maternal blood, which confirmed three unaffected cases, illustrates the feasibility of this approach to target cells from maternal blood. However, the utility of FNRBCs for NIPD has currently not reached clinical implementation due to rarity of the cells and inconsistencies in enrichment strategies. Research into the improved isolation of FNRBCs, along with other cell types is currently ongoing (Huang *et al.*, 2011; Ponnusamy *et al.*, 2012; Emad *et al.*, 2014; Hua *et al.*, 2014; Parikh *et al.*, 2014; Lo, 2015) and recent sequencing data provides a promising platform for true non-invasive diagnostic testing, providing successful isolation of fetal cells. Although research into developing advanced cell sorting techniques is ongoing, predominantly research has focused on the application of cffDNA in the maternal circulation (refer to 1.3.3), which is present in significantly higher quantities (Lo *et al.*, 1998b).

### 1.3.2 Fetal RNA

The discovery of fetal-derived messenger RNA (mRNA) within the maternal circulation in 2000 (Poon *et al.*, 2000) generated an alternative class of molecular markers for potential non-invasive testing as opposed to fetal cells (1.4.1) and cffDNA (1.4.3). Similarly to cffDNA, circulating RNA has a relatively short half-life (~16 minutes) and is rapidly cleared from the circulation (Nigam *et al.*, 2012). Lo *et al.* (2007a) identified an approach using digital PCR for the noninvasive detection of T21. The report identifies a digital RNA-SNP strategy, which uses digital PCR to determine the imbalance of a single nucleotide polymorphism (SNP) on *PLAC4* mRNA, a placentally-expressed transcript on chromosome 21 (chr21), in women bearing DS fetuses. The study successfully detected 90% of T21 cases and excluded 96.5% of euploid control cases (Lo *et al.*, 2007a). The main advantage of targeting mRNA that is placentally-expressed only is that target amplification is free of maternal background. However, this means that the fetus has to be informative for SNP analysis. Despite DNA being more stable than RNA, one advantage

of using RNA for NIPD is that DNA is present in low copy numbers, whereas several subclasses of RNA (including mRNA) are highly abundant (Ladomery, Maddocks and Wilson, 2011). Despite the abundance of RNA in the circulation, usually, RNA is unstable and susceptible to nuclease attack (Lichtenstein *et al.*, 2001). However, it has been postulated that ‘free’ fetal mRNA within the maternal circulation is encapsulated within a syncytiotrophoblast-derived microvesicle, which protects it from RNase.

Studies have also identified microRNAs (miRNAs) within the maternal circulation, providing yet another set of molecular markers (Chim *et al.*, 2008b; Kotlabova, Doucha and Hromadnikova, 2011; Ladomery, Maddocks and Wilson, 2011). miRNAs are short (19-25bp) non-coding regulatory RNAs that are capable of silencing gene expression (Bartel, 2009). The discovery of some miRNAs, such as *miR-141*, were found to be more stable than *CSH1*, a typical placentally-expressed mRNA (Ladomery, Maddocks and Wilson, 2011) identifying it as a more stable alternative for NIPD. Lim *et al.* (2015) set out to identify a panel of miRNAs as potential biomarkers for NIPT of T21 and successfully identified elevated levels of two miRNAs (*miR-1973* and *miR-3196*) in T21 cases compared to control placentas. This research is not diagnostic, but has the potential to improve the sensitivity and specificity of current screening tests (refer to 1.1.2.1). Because of the complexity associated with RNA processing, and the uncertainty of RNA stability, in conjunction with higher cffDNA being available than originally thought, the majority of research has focused on the application of analyzing cffDNA for NIPD for fetal aneuploidy. However, both types of free nucleic acids could potentially be used for NIPD of fetal genetic abnormalities. In addition, detecting specific miRNAs that are upregulated or down-regulated in T21, and potentially other aneuploidies, miRNA analysis may play an important role in future screening.



### 1.3.3 Cell-free fetal DNA (cffDNA)

In addition to fetal cells, cffDNA has also been shown to cross the placenta and enter the maternal circulation (Lo *et al.*, 1997). The levels of cffDNA within the maternal plasma were originally said to comprise around 3% to 6% during early and late pregnancy, respectively (Lo *et al.*, 1998b). However, in one study digital PCR analysis of maternal samples has revealed that the median fractional concentration of cffDNA was  $\geq 2$  times higher across all three trimesters (Lun *et al.*, 2008). Currently, cffDNA is the gold standard for NIPT since the entire fetal genome is represented in the maternal circulation (Lo *et al.*, 2010), and in comparison it is more readily available than fetal cells (refer to 1.3.1) and more stable than RNA (refer to 1.3.2). In addition, the use of cffDNA instead of intact fetal cells avoids complexities such as microchimerism, since these cells occur at low numbers, thus their contribution to the cffDNA is insignificant (Nelson, 2008). The fetal proportion of free DNA in maternal plasma is derived from syncytiotrophoblasts that have undergone apoptosis and as previously stated cffDNA is rapidly cleared from the circulation making it a specific marker for each pregnancy (Lo *et al.*, 1999; van der Schoot *et al.*, 2006).

When cffDNA was initially discovered, it was identified that it constituted around 3-6% of the total cfDNA from early to late gestation, respectively (Lo *et al.*, 1998a). However, more recent reports have identified that levels may be higher than first described (10-12 % average at early second trimester) (Nicolaidis *et al.*, 2014). The levels of cffDNA within the circulation can also vary due to alternative factors other than gestational age. Some studies have identified the following; maternal weight (Wataganara *et al.*, 2004), ethnicity (Ashoor *et al.*, 2013a), pre-eclampsia (Hahn, Huppertz and Holzgreve, 2005), pre-term labour (Farina *et al.*, 2005), physical activity (Schlütter *et al.*, 2014), blood processing protocols (including time before processing and storage conditions) (Chiu *et*

*al.*, 2001), method of collection (Sparks *et al.*, 2012b) and even fetal aneuploidy itself (Lee *et al.*, 2002).

Delays in transportation for samples collected in Ethylenediaminetetraacetic acid (EDTA) tubes, results in maternal leucocyte apoptosis, which results in an increase in maternal cfDNA (Norton *et al.*, 2013). Women with an increased Body Mass Index (BMI) also express higher levels of maternal cfDNA as obese women shed more maternal DNA from adipose tissue (Wang *et al.*, 2013). Therefore, increases in maternal cfDNA results in a decline in cffDNA fraction (Sillence *et al.*, 2015). Alternatively, the extraction method used to isolate cfDNA can affect the proportion of cffDNA. Brojer *et al.* (2005) determined that (cycle threshold) Ct values for automated extractions were significantly lower than those for manual extractions (indicating increased gene copy number) when starting with  $\leq 2$  mL of maternal plasma. Previous data has also identified that manual extractions yield 23.4% more total cell-free DNA, however, automated approaches yield 40.7% more cffDNA (Houfflin-Debarge *et al.*, 2000). The level of cffDNA available can affect detection of fetal specific targets, therefore it is important to include universal fetal markers (Table 1-3) to ensure presence of cffDNA.

Detection of paternally inherited (fetal specific) sequences, such as those on the Y chromosome (chrY) and those on the *RHD* gene in *RHD*-negative mothers, enables successful determination of fetal sex (refer to 1.3.3.1) and *RHD* genotype (refer to 1.3.3.2), respectively. Furthermore, detection of variable regions, such as short tandem repeats (STRs) (Rong *et al.*, 2012) and single nucleotide polymorphisms (SNPs) (Nicolaidis *et al.*, 2013a), can also be used to detect paternally inherited sequences. However, both methods rely on the fetus inheriting a paternal sequence that is absent from the maternal genome. In addition, for SNPs (and some STRs), the maternal and fetal

specific sequence will only differ by a single nucleotide base. Therefore, highly sensitive detection methods are essential and often selective enrichment of cffDNA (refer to 1.3.3.5) is required (Wright and Burton, 2009).

Alternative fetal markers such as mRNA (1.4.2) and epigenetic modifications, in particular DNA methylation variations, were identified. Both *maspin* (chromosome 18) (Chim *et al.*, 2005) and *RASSF1A* (chromosome 3) (Chan *et al.*, 2006) were found to be hypermethylated in the fetus and hypomethylated in the mother, providing the first clinically viable universal markers for fetal DNA. Both are useful for the determination of fetal DNA in female and *RHD*-negative fetuses, but only *maspin* can be used as a marker for the detection of fetal aneuploidy (T18). Recently, various studies have set out to identify more fetal epigenetic markers (Chim *et al.*, 2008a; Papageorgiou *et al.*, 2009; Tong *et al.*, 2010; Lun *et al.*, 2013). Since CpG islands (CGIs) often undergo DNA methylation, an initial study investigated CGIs located on chromosome 21 and identified a panel of 22 fetal epigenetic markers that illustrated methylation differences between the mother and fetus (Chim *et al.*, 2008a). Out of the 22 markers identified, it included the unmethylated form of the *phosphodiesterase 9A gene*, which was later developed by Lim *et al.* (2011) as a potential marker for the NIPT of T21. An alternative approach using combined bisulfite and restriction analysis (COBRA), which evaluated genome beyond CGIs, identified that the *holocarboxylase synthetase gene (M-HLCS)* is hypermethylated in placental tissue (Tong *et al.*, 2010). Chromosome dosage of *M-HLCS* against a Y-specific sequence using various platforms has been labelled the ‘epigenetic-genetic approach (EGG)’ and initial results highlight its potential as a NIPD test for T21 (Tong *et al.*, 2010; Lim *et al.*, 2014). Table 1-3 summarises various fetal specific sequences within the maternal circulation, alongside universal DNA markers, their application and method(s) of detection.

**Table 1-3: Fetal specific target/ universal markers and universal DNA markers, purpose and method(s) of detection [adapted from Wright and Burton (2009)].**

<b>Purpose</b>	<b>Sequence detected</b>	<b>Detection method(s)</b>
<b>Sex determination</b>	<i>SRY, DYS14, DYZI, DYZ3, DAZ, ZFY, amelogenin</i>	PCR (conventional, nested, real-time)
<b>Haemolytic Disease of the Fetus and Newborn (HDFN)</b>	<i>RHD, RHC, RHc, RHE, Kell, ABO</i>	PCR (conventional, nested, real-time)
<b>Single gene disorders</b>	<i>HD, FGFR3, DMPK, CFTR, globin, CYP21</i>	PCR (conventional, nested, real-time); PCR with mass spectrometry (MS)
<b>Aneuploidy</b>	SNPs <i>maspin</i> <i>U-PDE9A</i> <i>M-HLCS</i>  PLAC4 RNA	PCR Methylation sensitive PCR with MS Methylation sensitive PCR with MS Methylation sensitive PCR with MS; dPCR; bisulphate conversion RT-PCR with MS; Digital PCR
<b>Universal fetal markers</b>	Fetal RNA (PLAC4, GCM1, ZDHHC1, PAPP, PSG9, PLAC1, TFP12, KISS1)  STRs, biallelic insertion/deletion polymorphisms, SNPs	RT-PCR; microarray  Bisulphate conversion or methylation-sensitive PCR with MS
<b>Universal DNA markers</b>	<i>GAPDH, CCR5, β-globin, β-actin, β-hCG, albumin, ATL1</i> Hypermethylated <i>RASSF1A</i>	PCR (conventional, nested, real-time) Methylation-sensitive qPCR

Currently, detection of fetal specific targets is achieved using qPCR and routine testing of fetal gender, *RHD* genotype and even some paternally inherited sequences for single gene disorders (refer to 1.3.3.4) has been implemented within the clinic (Chitty *et al.*, 2008). However, some studies have identified that digital PCR (dPCR) platforms can detect rare sequences, such as cffDNA, with improved sensitivity (Strain *et al.*, 2013; Kim, Jeong

and Cho, 2014; Sillence *et al.*, 2015) (refer to 1.3.3.3.1). With regard to the EGG approach previously mentioned, qPCR analysis revealed lower sensitivity for detection of T21 fetuses (90%) (Lim *et al.*, 2014) compared to an alternative study using dPCR (100%) (Tong *et al.*, 2010). However, both studies used small sample sizes for analysis and further large scale validation studies are required.

Due to the variation and relatively low amounts of cffDNA in an overwhelming background of maternal cfDNA, non-polymorphic analysis of fetal aneuploidy is significantly more challenging, especially when considering that half of the fetal genome is inherited from the mother (Wright and Burton, 2009). Unlike sexing and *RHD* genotyping, which involve the detection of foreign genetic sequences in the maternal blood, diagnosis of fetal aneuploidy requires accurate quantification of sequences that are shared by the maternal genome, to determine if there is under- or over-representation of a particular chromosome. Currently, only MPS approaches can reliably detect fetal aneuploidy (refer to 1.3.3.3.2). However, selective enrichment of cffDNA (refer to 1.3.3.5) combined with improved dPCR technology (refer to 1.3.3.3.1) could potentially provide a cheaper and more rapid NIPT for aneuploidy detection.

#### *1.3.3.1 Fetal sex determination*

Fetal sexing can be ascertained by detecting the presence of Y-specific targets within the maternal circulation. Many studies have achieved high accuracy (100%) using Y-specific primers for a region on the *SRY* gene (Costa *et al.*, 2001; Sekizawa *et al.*, 2001; Honda *et al.*, 2002). However, detection of single-copy targets using conventional qPCR can sometimes be close to the limits of detection especially if the cffDNA concentration is low, which can lead to reduced sensitivity and false-negative results (Avent and Chitty, 2006). Therefore, detection of low copy targets can be improved by using primers

specific for a multiple-copy target (DYS14) located on the *TSPY1* gene of the Y-chromosome (Zimmermann *et al.*, 2005). Since single-copy targets are more reliable for the detection of copy-number polymorphisms, clinical assays for fetal sex determination often incorporate both targets.

NIPD of fetal gender during the first trimester enables early assessment of pregnancies with known familial risk of sex-linked disorders and is also important for the management of CAH, a monogenic inherited recessive disorder (New *et al.*, 2001) (refer to 1.3.3.1). In 90% of cases CAH is caused by a defect in the *CYP21A2* gene that encodes for 21-hydroxylase, preventing effective synthesis of cortisol and as a consequence can cause female fetuses to become virilised by the overproduction of androgens (Speiser and White, 2003). However, NIPT for fetal sex can allow for dexamethasone treatment to be targeted to female fetuses only (New *et al.*, 2014). The prevalence of CAH and sex linked –disorders in the UK are 5 per 10,000 live births and 1 per 10,000 live births, respectively (NHS, 2010). By determining fetal gender, up to 50% of women can avoid invasive testing since only male fetuses are at risk of X-linked recessive genetic disorders for heterozygous carriers and only female fetuses can develop ambiguous genitalia in pregnancies with a familial risk of CAH. Alternatively, for X-linked dominant genetic disorders all female fetuses will be affected if the father has the disorder, whereas both males and females will have a 50% chance of inheriting the affected allele if the mother has the disorder (Section 1.3.3). However, dominant X-linked disorders are often associated with infertility (Zechner *et al.*, 2001).

The combination of multiple- and single-copy targets using qPCR already provides adequate sensitivity and specificity (see above). However, dPCR has the potential to be used as a secondary test for inconclusive results, since the partitioning nature of dPCR (refer to 1.3.3.3.1) has been shown to increase sensitivity for maternal samples that

express low cfDNA fractions (Sillence *et al.*, 2015). Adversely, the application of MPS for fetal sexing is not cost effective since accurate quantification is unnecessary and current PCR platforms (qPCR and dPCR) are sufficient for the detection of Y-specific targets.

#### 1.3.3.2 *Fetal RHD genotyping*

Haemolytic disease of the fetus and newborn (HDFN) is caused when maternal IgG antibodies of *RHD*-negative mothers are exposed to the RhD positive antigens on fetal red blood cells. Subsequently allo-anti-D is produced, which crosses the placenta and results in destruction of the fetal red blood cells (Urbaniak and Greiss, 2000). This can cause mild anaemia or in more severe cases, HDFN can lead to total body edema, hepatosplenomegaly and heart failure, consequently resulting in intrauterine death (Eder, 2006; Van der Schoot *et al.*, 2006). Prior to 1970, HDFN was a major cause of fetal mortality with a prevalence of almost 5 per 10,000 live births in the UK alone (Bowman, 1996). However, since the introduction of routine antenatal anti-D prophylaxis (RAADP), which prevents RhD alloimmunisation and consequently HDFN, the incidence has reduced nearly tenfold (Kumar and Regan, 2005; Fyfe *et al.*, 2014).

Currently, all *RHD*-negative women are offered RAADP in the third trimester (between 28 and 34 weeks of pregnancy) and repeatedly following delivery in concordance with UK NICE guidelines (Alfirevic and Callaghan, 2014), but this is costly as it is produced from the plasma of hyperimmunised male volunteers. According to the National Institute for Health and Clinical Excellence (NICE) approximately 97,000 women receive RAADP each year, which costs between £54 per patient to £313.50 per patient, depending on the technology used (NICE, 2008). However, targeted administration of RAADP to women carrying *RHD*-positive fetuses only, has been routinely implemented in the Netherlands

since 2011 using qPCR (De Haas *et al.*, 2012) and NICE has recommended the exploration of routine antenatal fetal *RHD* genotyping within the UK (NICE, 2008). Providing routine NIPT of fetal genotype enables administration to be targeted to women who are known to be carrying an *RHD*-positive fetus (van der Schoot *et al.*, 2003). Since around 38% of pregnancies will be carrying an *RHD*-negative fetus this approach has clear financial benefits (Chitty *et al.*, 2014). In addition, although donors are carefully screened for blood-borne pathogens the risk of transmitting an infection is remote, since it is obtained from human blood the risk is not eliminated. In the 90s anti-D IgG was associated with isolated cases of hepatitis C (The UK National Screening Committee, 2013). Reducing the number of women undergoing RAADP treatment will lower the number of women exposed to possible infection and also mothers with *RHD*-negative fetuses avoid the discomfort of the injection.

The various antigens of the Rh system that are present on the surface of the erythrocytes are coded for by two paralogous genes, *RHD* and *RHCE*, which are located on chromosome 1 (p34-p36). The *RHD* gene is essentially a duplicate of the *RHCE* gene, and the two Rh proteins differ in only 36 of the 417 amino acids of which they each comprise (Flegel, 2007). In Caucasian populations, the RhCcEe protein is almost universally present (Daniels *et al.*, 2009a), but the frequency of the D+ phenotype is predominantly lower in this ethnicity group (70-85%) compared to sub-Saharan African (95%) and eastern Asian (99.5%) populations (Finning *et al.*, 2008; Daniels, 2013). However, although most people are D+ or D-, the presence of D variants creates a grey area.

Most D-negative phenotypes are a result of a complete *RHD* deletion and therefore the entire RhD protein is absent from the erythrocyte membrane (Wagner and Flegel, 2000). Since the entire *RHD* gene is absent from the maternal plasma in D-, diagnosis is



relatively simple in this instance. However, the tandem arrangement of the *RHD* and *RHCE* genes has led to the frequent evolution of aberrant *RH* alleles. Some of the aberrant *RHD* alleles do not result in RhD antigen expression and consequently a significant number of D-negative phenotypes determined by serological analysis actually possess fragments or mutated *RHD* genes (Daniels *et al.*, 2009a). The most predominant is the *RHD* pseudogene (*RHD*Ψ), which possess an inactive *RHD* gene due to a 37bp insert prior to exon 4, three missense mutations in exon 5, and a nonsense mutation and a missense mutation in exon 6 (Singleton *et al.*, 2000; Avent, 2008). The RhD negative blood is only found in 3-5% of black Africans, and is even rarer in Chinese populations (Bianchi *et al.*, 2005). In one study which tested 82 D-negative black Africans only 18% of D-negative individuals are a result of *RHD* deletion (Singleton *et al.*, 2000). Instead, 66% had *RHD*Ψ and 15% had the RHD-CE-DS (or r'S,) variant, respectively (Singleton *et al.*, 2000). Though the majority of the *RHD* gene is present, neither variant produces any epitopes of D (Daniels *et al.*, 1998; Rouillac-Le Sciellour *et al.*, 2004).

In addition to D-negative serological phenotypes, hybrid *RHD-RHCE* genes (and also SNPs) can produce weak D and partial D variants (Daniels, 2013) (refer to 5.1.1). Both weak D and partial D will produce all or some of the conventional antigens, respectively, but with a weakened expression (Rizzo *et al.*, 2012). Although production of alloanti-D is more common in individuals with partial D since a number of D epitopes are not expressed, although some weak D variants have also been shown to produce alloanti-D (Wagner *et al.*, 2000). Confirming the RhD variant status of each mother during pregnancy prevents women with partial D being incorrectly labelled as *RHD* positive by serological tests and therefore enables RAADP to be targeted to women that require treatment (refer to 5.1.1). Though this review focuses on the prevention of RhD alloimmunisation since it is predominantly the major cause of HDFN, it is important to

note that other alloantibodies can sometimes lead to HDFN. Therefore, first trimester screening of other antigens become more of a focus and in 2002 screening for irregular erythrocyte antibodies (IEAs) in all pregnant women was introduced in the Netherlands (van der Schoot *et al.*, 2003). The most frequent IEAs after anti-D are anti-E, anti-K1, -D, -c and -C, however, occurrence of these antibodies is less common (1 in 300) and not all alloantibodies will induce HDFN (van der Schoot *et al.*, 2003).

The presence of *RHD* pseudogenes and D-variants complicates NIPT of fetal genotype, since all or part of the *RHD* gene may be present but phenotypically the fetus is considered to be *RHD* negative. Therefore, assays have been developed to target sequences that will distinguish between *RHD*-positive and *RHD* $\Psi$ /*RHD-CE-DS* genotypes (Finning *et al.*, 2008; Müller *et al.*, 2008; De Haas *et al.*, 2012; Banch Clausen *et al.*, 2014). With regard to Caucasian populations multiple studies have illustrated accuracies close to 100% by amplifying sequences from two or three exons (Rouillac-Le Sciellour *et al.*, 2007; Müller *et al.*, 2008). However, higher false negative rates can occur for first trimester screening and limited data is available on *RHD* genotyping in mixed ethnic populations for the determination of *RHD* variants. Grande *et al.* (2013) determined that by including assays that amplified sequences on *RHD* exons 5, 7 and 10, high accuracy (>99%) of fetal *RHD* genotype during the second trimester could be achieved in a mixed ethnic population. This also included detection of seven cases that were compatible with *RHD* variants and only a single false positive result was observed due to twin pregnancy. Consequently, administration of RAADP was avoided in 95% of *RHD* negative fetuses.

The qPCR platform is the current gold standard for detection of fetal specific targets and many studies have reported the used of the StepOnePlus™ Real-Time PCR System for fetal *RHD* genotyping (Daniels *et al.*, 2009b; Scheffer *et al.*, 2011; Sillence *et al.*, 2015;

Thurik *et al.*, 2015). The system uses an LED-based optical detection system that can record four colour fluorescent readings (FAM™/SYBR® Green, VIC®/JOE™, NED™/TAMRA™, and ROX™ dyes), which enables multiple targets to be analysed in a single reaction, providing a high throughput and cost-effective platform. While four separate colour references are available, often only three targets can be multiplexed in a single reaction since ROX™ is often used as a passive reference dye.

The use of standards in each qPCR assay also allows for indirect absolute quantification of starting DNA. However, the exponential nature of amplification on this platform only permits detection differences down to a 2-fold change in copy number. High throughput methods using robotic isolation of plasma DNA and qPCR analysis revealed higher accuracies for determining fetal *RHD* status at 30 weeks gestation the Netherlands (99.4%) (Van der Schoot *et al.*, 2006) compared to samples tested at 28 weeks gestation in the UK (95.7%) (Finning *et al.*, 2008). Similar accuracies have been recorded in France (Rouillac-Le Sciellour *et al.*, 2004), however, initial false-negative results were all re-tested making the test uneconomical. Though highly sensitive, all studies revealed false-negative results even though third trimester samples were tested. Early testing during the first trimester, as previously stated, will only increase the number of false negative results encountered (Lo *et al.*, 1998c). This is detrimental since if applied in a clinical setting, mothers would not receive RAADP and would be at risk of HDFN, particularly if a previous sensitisation event has occurred. Sensitisation events can arise during previous pregnancies, threatened miscarriage, ectopic pregnancy, invasive testing, antepartum haemorrhage, closed abdominal injury, and intrauterine injury (Kumar and Regan, 2005).

Consequently, third generation dPCR approaches were developed (refer to 1.3.3.3.1). Recent publications have described the application of dPCR for the detection of low-level targets with improved precision, resulting in reliable quantification well below the limit

of quantification of qPCR (Strain *et al.*, 2013; Miotke *et al.*, 2014). In addition, Lun *et al.* (2008) illustrated that higher cfDNA fractions were calculated when using dPCR, highlighting the capability of this platform to detect more fetal specific targets as a result of its partitioning nature (refer to 1.3.3.3.1). Recent data published by our research lab has also shown that increased sensitivity is achieved using dPCR (100%) compared to qPCR (83.4%) for determining fetal *RHD* genotype (Sillence *et al.*, 2015). Therefore, it is possible that dPCR could replace qPCR for non-invasive testing of fetal sexing and *RHD* genotyping, or alternatively, it could be used as a secondary platform for conformation of inconclusive/ negative results.

In addition, multiplex ligation-dependent probe amplification (MLPA) which can target many more regions of interest, enables determination of various Rh and other blood group antigens in a single reaction (refer to 5.3.1). Whilst fetal genotype can be determined with 100% accuracy using DNA microarray and MPS (Fichou *et al.*, 2013; Halawani *et al.*, 2014; McBean, Hyland and Flower, 2014), at present it is not economically viable. T-MPS assays for developing a full panel of blood group genes, which can be used to screen blood prior to transfusion, is a key area of interest and as costs continue to decrease it is likely that this approach will become more utilized. However, due to the high levels of sensitivity associated with dPCR and various qPCR approaches, it is currently unnecessary and not economically viable since 1/3 of all women will require NIPT for targeted administration of antenatal and postnatal anti-D.

### 1.3.3.3 *Determining fetal aneuploidy*

The majority of fetal aneuploidies result in spontaneous miscarriage during early pregnancy, since the over- or under-representation of certain genes causes alterations in the stoichiometry of multi-protein complexes and disrupts normal cellular functions

(Huettel *et al.*, 2008). Some chromosomal imbalances are viable but are associated with multiple birth defects, and the most frequent include; Monosomy X (Turner syndrome), T21 (DS), T18 (Edward's syndrome) and T13 (Patau syndrome). T21 is the most common aneuploidy (refer to 1.1.2.1), and consequently is the most predominant reason why women choose to undergo invasive testing if identified to be high risk following screening for a definitive diagnosis (refer to 1.1.2.1).

Over the last decade research has focused on developing a highly accurate (100%), cost-effective and robust platform for the NIPD of fetal aneuploidy, which enables accurate quantification and identification of chromosomal imbalances without the need for invasive tests. The most successful results for non-invasive detection of fetal aneuploidy have been achieved using both s-MPS and t-MPS (refer to 1.3.3.3.2), which typically express >99% DR with a false positive of 0.1-1% (Ashoor *et al.*, 2012; Norton *et al.*, 2012; Sparks *et al.*, 2012a; Futch *et al.*, 2013; Liang *et al.*, 2013). Despite the decline in costs of MPS in recent years, routine testing is currently not economically viable and tests are only available through commercial providers costing between £400 and £900 (Antenatal Results and Choices, 2013). Initially, these tests were developed for definitive diagnosis of fetal aneuploidy by directly assessing fetal material. However, at present it has been established that NIPT of aneuploidy should be offered as an advanced screening tool (Morris *et al.*, 2014). Though this is currently only available commercially (Allyse *et al.*, 2015), in time, it is likely that this test will become the primary screen for detection of chromosomal abnormalities or alternatively replace invasive testing. However, further assessment of the costs and benefits of MPS testing are required to determine its place within the screening programme before NIPT can be implemented into routine practice (refer to 1.3.3.3.2).

As further large scale validation studies are carried out, it is possible the reliability of NIPT may become consistent with that achieved by CVS and amniocentesis, and thus could potentially replace invasive testing as the primary diagnostic procedure. Though research has focused on the application of MPS for NIPT/ NIPD, other cheaper alternative platforms have been studied, such as dPCR (Lo *et al.*, 2007b; Lun *et al.*, 2008; Tsui *et al.*, 2011), which could provide rapid assessment of fetal aneuploidy at a fraction of the cost.

#### 1.3.3.3.1 Digital PCR

To detect the presence of a T21 fetus, NIPD tests must be capable of detecting a 1.5-fold increase in only a fraction (around 5-10%) of the total cfDNA (Zimmermann *et al.*, 2002). Conventional qPCR can only detect a difference of one Ct value, which corresponds to a 2-fold change in copy number, thus making detection of a 1.5-fold increase of chr21 in only  $\leq 10\%$  of the total cfDNA unattainable on this platform. Contrastingly, dPCR enable quantification of nucleic acids from single molecules by means of sample partitioning. Thermal cycling is used to amplify DNA which will be present in some, but not all, of the individual partitions ready for end-point analysis (Figure 1-5). Subsequently, the concentration of each target is calculated by determining the fraction of positive droplets (for example see 2.9.4) (Pinheiro *et al.*, 2011). Figure 1-5 highlights the principle of dPCR.

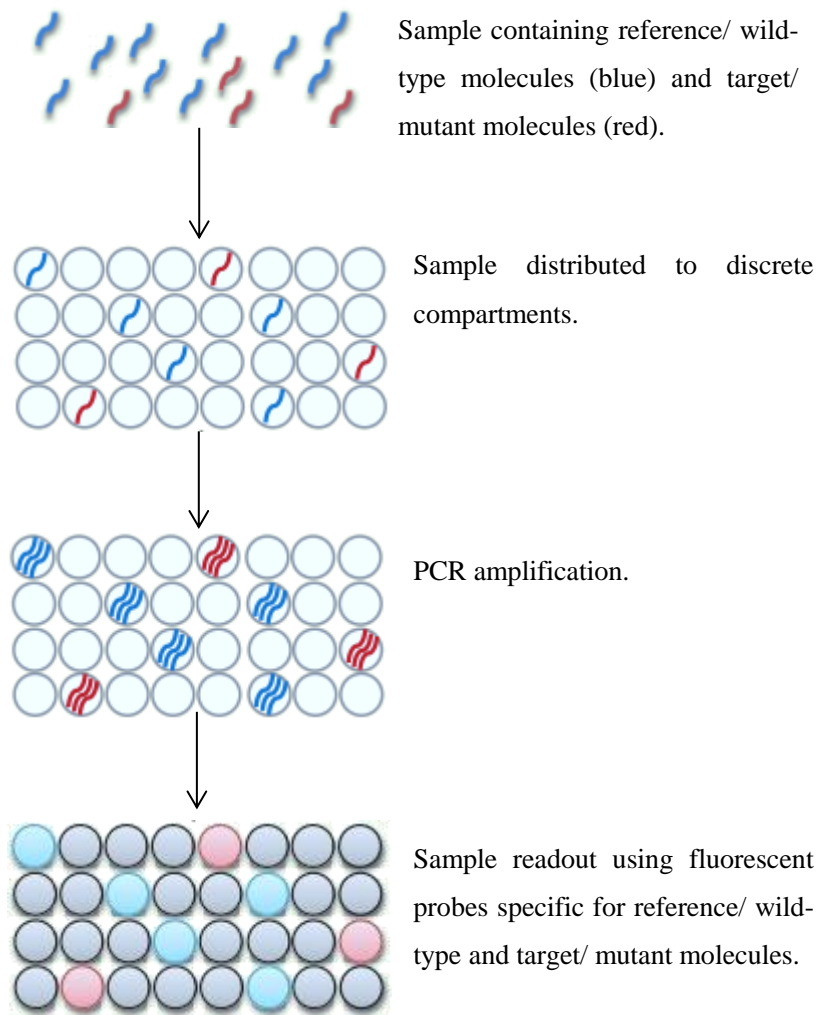


**Figure 1-5: Principle of dPCR.** Initially DNA is diluted so that the average concentration of target DNA in each compartment is less than 0.5 molecules to ensure only a single target is present in a single compartment. However, due to the low levels of cfDNA maternal plasma samples are not diluted. Once diluted (or following maternal plasma DNA extraction), samples are separated into the discrete compartments. Subsequently, partitioned molecules are amplified by PCR using fluorescent probes to detect the reference/ wild-type (blue) and the target/ mutant (red) molecules in a single reaction. [Adapted from Sun, Jiang and Chan (2015)].

In 2006 Fluidigm launched the first commercial microfluidic system for dPCR analysis (BioMark HD) using integrated fluidic circuits (Baker, 2012). Lo *et al.* (2007b) revealed

two approaches for the NIPD of fetal aneuploidy using this platform; the RNA-SNP strategy and the digital relative chromosome dosage (RCD) method. The SNP-RNA approach (see 1.4.2), uses dPCR to determine the imbalance of a SNP on placentally derived mRNA in women bearing DS fetuses. An alternative method for aneuploidy detection using SNPs located in the *PLAC4* gene has also been described using reverse transcriptase (RT) MLPA (Deng *et al.*, 2011). This study used five SNP loci on *PLAC4* and using RT-MLPA, followed by capillary electrophoresis and demonstrated diagnostic sensitivity and specificity of 92% and 100%, respectively (Deng *et al.*, 2011). Though this highlights the application of SNP-RNA dPCR and RT-MLPA analysis, both methods rely on the presence of heterozygous SNPs (Lo *et al.*, 2007a; Lo *et al.*, 2007b; Deng *et al.*, 2011).

The RCD method is not reliant on heterozygous SNPs and instead determines the relative dosage by calculating the aggregate (maternal and fetal) number of copies of the aneuploidy chromosome against a reference diploid chromosome in maternal plasma. For example, in a T21 pregnancy, the chr21 dose will be 50% higher than the reference for the fetus (3:2 ratio, respectively). Therefore, for maternal plasma samples expressing 10% cffDNA, a 5% increase in the chr21 target is expected (Chiu and Lo, 2012). By dividing the target loci concentration by the reference loci concentration the RCD ratio is calculated, and for a maternal plasma sample containing a cffDNA fraction of 10% a ratio of 1.05 would be expected due to the 5% increase of the chr21 target. However, Lo *et al.* (2007a) determined that a minimum cffDNA fraction of 25% (giving a ratio of 1.125) was required for accurate detection of T21 using the Fluidigm system.

Microfluidic systems, such as the BioMark HD (Fluidigm) and the QuantStudio 3D Digital PCR System (Life Technologies), were initially developed to automate the original dPCR manual approach, which was labour intensive and the number of replicates



were limited to 96 or 384, depending on plates used (Table 1-4) (Sykes *et al.*, 1992). Typically, each microfluidic chip contains a few thousand nano-litre sized reaction vessels, and thus has greatly improved the throughput of dPCR (Chang *et al.*, 2006). In a study by (Fan *et al.*, 2009), this method of microfluidic dPCR accurately identified all cases of fetal trisomy in all of the 40 specimens analysed, however the results were obtained from CVS samples and not maternal blood samples. To achieve this level of accuracy using maternal plasma samples is significantly more challenging due to the high level of background maternal DNA.

Microfluidic chips are expensive, which has limited its widespread use for routine clinical practice. The emergence of droplet-based dPCR, primarily the QX200 (advanced version of the QX100) Droplet Digital PCR™ System (Bio-Rad), has provided a cost-effective platform for analysis of a large number of molecules. The QX200 uses an oil-emulsion approach under a vacuum to separate each sample into a maximum of 20,000 1nL droplets per well (see 2.9.2). Each droplet serves as an individual compartment for PCR amplification, which are read using a dual fluorescent detection system (VIC/HEX and FAM) to determine the fraction of positive droplets for both the reference and target (chr21) DNA molecules (Figure 1-5). The fraction of positive droplets (p), from 0 (all droplets are negative) to 1 (all droplets are positive), for each sample is automatically aligned to a Poisson algorithm (Figure 1-6) to determine the absolute copy number (copies per  $\mu\text{L}$ ) using the following equation (Pinheiro *et al.*, 2011);

$$\text{Copies per droplet} = -\ln(1-p)$$

It is important that Poisson corrections are applied, since the number of targets can exceed the number of positive droplets if high concentrations are used (Figure 1-6). Thus without aligning samples to the Poisson algorithm, quantification is incorrect as we

assume each positive droplet only contains 1 target molecule. However, when low concentrations of target DNA are present it is likely that each positive droplet will contain a single target (Figure 1-6). Consequently, the automatically calculated concentration of the reference and target gene loci can be used to determine the digital RCD as previously described.

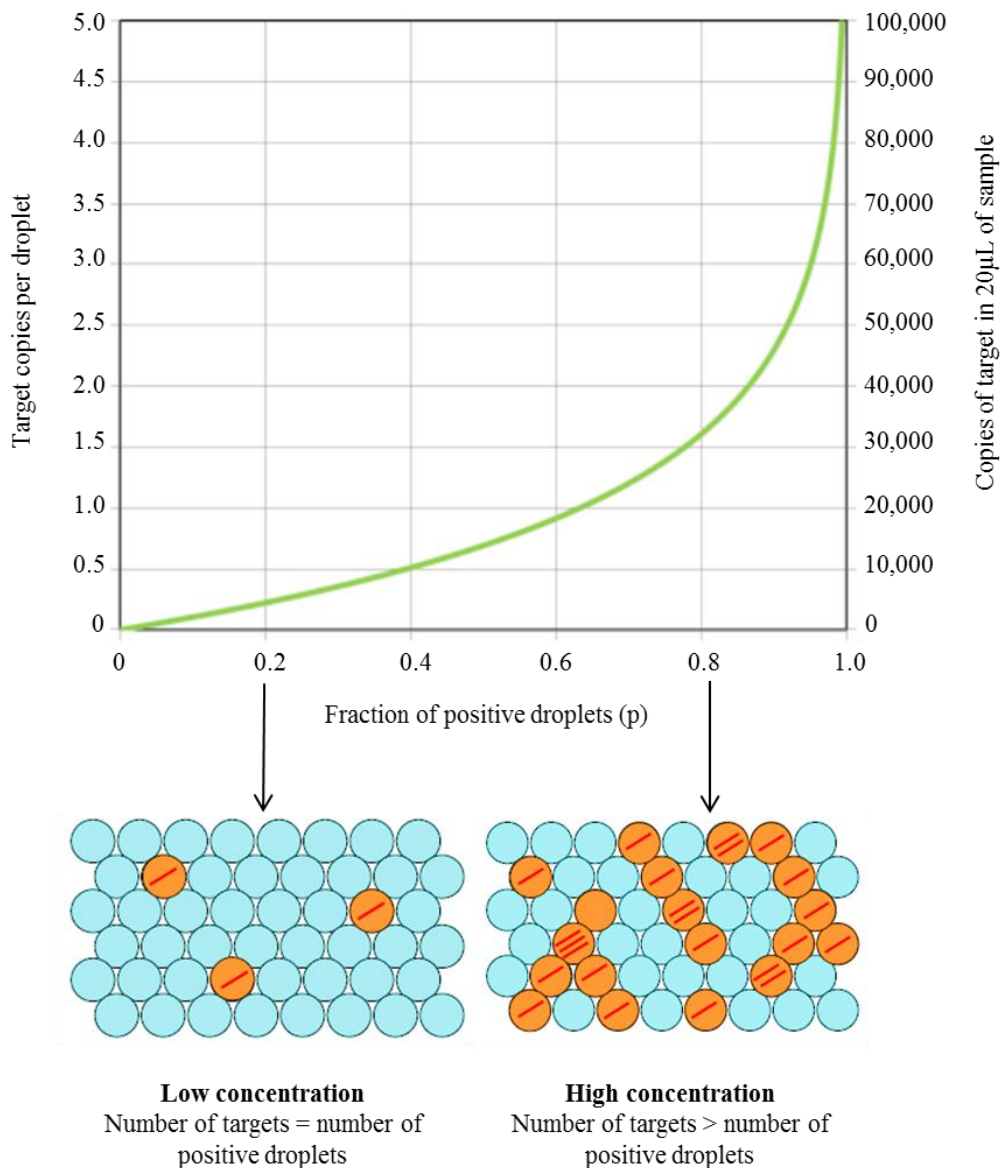


**Figure 1-6: Determining target concentration using the Poisson algorithm.** For samples that contain low concentrations of target molecules, the number of targets is equal to the number of positive droplets, since each droplet contains a single molecule.

Contrastingly, for samples that contain high concentrations of target molecules, the number of targets present exceeds the number of droplets, and thus some droplets contain multiple (2 to 3) target molecules. In order to calculate the correct quantification the number of positive droplets (p) is aligned to the Poisson algorithm. [Adapted from Koo (2014)].

The RainDance® Digital PCR System (RainDance™ Technologies) also uses droplet-technology to produce up to 10,000,000 PCR reactions per sample. This system far exceeds the number of partitions per sample than any other dPCR platform available, although the claimed detection sensitivity is comparable to the QX200 system (Table 1-4). In addition, the throughput of the QX200 is far greater than the RainDrop (Table 1-4) and costs are 10-fold less per sample (\$3 and \$30, respectively) (Roberts, 2014). Table 1-4 summarises the various commercially available digital PCR platforms.

**Table 1-4: List of commercially available dPCR platforms** [adapted from Sun, Jiang and Chan (2015)].

System	Maximum no. of samples per run	No. of PCR reactions per sample	Reaction volume per sample (µL)	Claimed detection sensitivity
Fluidigm BioMark HD	48	770	0.65	Single copy
Life Technologies QuantStudio 3D	24	20,000	14.5	<1% target in a reaction
RainDance	8	1,000,000-10,000,000	25-100	0.0001% target in a reaction
RainDrop				
Bio-Rad QX200/QX100	96	20,000	20	0.0001% target in a reaction

Studies have shown the application of dPCR for the detection of multiple haemoglobinopathies and other monogenic disorders (refer to 1.3.3.4) using the principle dPCR described in Figure 1-5 for the detection of wild-type and mutant molecules. Due to the increased sensitivity of more recent, droplet-based, platforms it is likely that lower cffDNA (<25%) are feasible for the detection of fetal aneuploidy using the RCD method

as opposed to detection of fetal specific targets. The magnitude of chromosome dosage alterations in maternal plasma is dependent upon the cfDNA fraction, since lower cfDNA fractions are associated with less chromosome dosage aberrations (as previously described). Therefore, when lower cfDNA fractions are present, more molecules must be analysed to achieve the same diagnostic accuracy as samples expressing higher cfDNA fractions.

Computer simulation models have determined that around four-times more molecules are required to attain the same diagnostic accuracy using dPCR when the cfDNA concentration in maternal plasma is halved (Lo *et al.*, 2007a). Further computer simulation analysis revealed that for 5% cfDNA fractions, a minimum of 100,000 molecules from the target chromosome (chr21) and reference chromosome would need to be analysed to achieve a sensitivity of 95% and specificity of 99% (Sun, Jiang and Chan, 2015). Technically, it would be difficult to achieve this many reads for a single target locus. Therefore, by increasing the number of targets per chromosome, it is feasible that dPCR could be used as an alternative platform to MPS (refer to 1.3.3.3.2) for aneuploidy detection, provided a reasonable volume of plasma is obtained. Although, at present, effective counting of a large number of molecules from maternal plasma is only achieved using MPS approaches. However, the PPV of this test is relatively low since there is a low prevalence of fetal aneuploidy (Sun, Jiang and Chan, 2015). Consequently, these tests are only available commercially as an advanced screening tool. Recent developments using targeted approaches has enabled accurate detection subchromosomal aberrations down to 2 Mb (Zhao *et al.*, 2015), which require less reads per sample making this approach more economically viable (see below).

### 1.3.3.3.2 MPS

The cost of massively parallel sequencing (MPS) has decreased dramatically since the beginning of the 21<sup>st</sup> century (Figure 1-7) (Wetterstrand, 2015). Three variations of sequencing methodologies are currently used for the detection of fetal aneuploidy, particularly T21. These include; s-MPS (Table 1-5), t-MPS for specific chromosomal segments (Table 1-6) and t-MPS for direct sequence analysis of SNPs (Table 1-7).

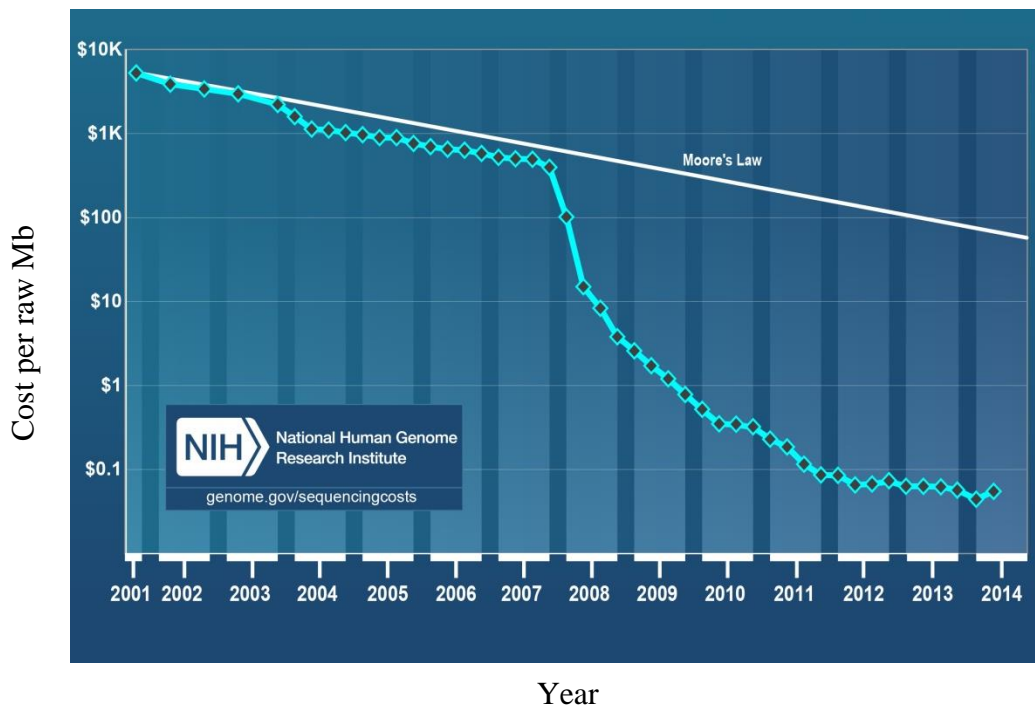


**Figure 1-7: Cost per raw Mb of DNA sequencing from 2001 to 2014.** The graph illustrated actual cost of sequence per Mb each year against the hypothetical data reflecting Moore's Law based upon the doubling of 'computer power' every two years. [Taken from Wetterstrand, (2015)].

The s-MPS approach allows cfDNA obtained from maternal plasma to produce millions of short-sequence tags that can be aligned and uniquely mapped to specific chromosomes against a human reference genome (Sonek *et al.*, 2012). The reliability for fetal aneuploidy detection using this method is determined by the depth of sequencing and

subsequent counting statistics. Fan *et al.* (2008) were the first to propose counting chromosomes using high-throughput s-MPS technology. In this initial small scale study 5 million sequence tags were obtained per patient on average, which provided sufficient data to detect the over- or underrepresentation of chromosomes and allow for correct classification of aneuploidy fetuses (Fan *et al.*, 2008).

Since the initial s-MPS study, variations in sequence analysis to further improve test accuracy have been developed. Studies determined that sequencing biases occurred relative to the GC-content of each chromosome in a linear fashion, and thus consequent studies have allowed for adjustments to be made with respect to the DNA base composition (Fan *et al.*, 2010; Liang *et al.*, 2013). Intra-run and inter-run variability caused by alterations in sample handling, DNA extraction or the sequence itself, were also shown to alter the chromosomal distribution of sequence reads for each sample (Turan *et al.*, 2010). To minimize the intra- and inter-run sequencing variation, normalised chromosome values (NCVs) from the sequence data were incorporated (Sehnert *et al.*, 2011). NCV values  $>4.0$  were required for classification of affected aneuploidy state, and NCV values  $<2.5$  were used to classify unaffected cases. NCV values between 2.5 and 4 were classified as ‘no call’. Using these parameters, Sehnert *et al.* (2011) demonstrated 100% correct classification of samples with T21 and T18, but was unable to detect the T13 case (‘no call’) (Table 1-5). Multiple studies have reported the success of using sequence tag mapping and chromosome counting to detect aneuploidies such as T21, T18 and T13, illustrating sensitivities  $>99\%$  for a FPR of  $<1\%$  in most cases (Table 1-5).

The chromosome-specific t-MPS approach, requires an additional step compared to the first approach, which allows for selective amplification of chromosome regions of interest (such as chr21, chromosome 18 (chr18) and chromosome 13 (chr13)) to determine the

excess of a particular chromosome relative to another (Sparks *et al.*, 2012b). The Illumina HiSeq® 2500, which uses reversible terminator-based sequencing-by-synthesis, delivers the highest daily throughput and total yield (160 Gb/ day) compared to all other sequencing platforms currently available (Illumina®, 2015). This consequently enables more samples to be simultaneously sequenced at greater depth. The primary advantage of t-MPS is lower sequencing costs, since fewer reads are required per patient, enabling more samples to be multiplex in a single run. For example, the HiSeq® 2500 can process 8 human genomes at 30x coverage, or alternatively, 150 human exomes can be processed per run (Illumina®, 2015). Therefore, by targeting an even smaller region of exomes (such as chr21, chr18 and chr13) even more samples can be processed with greater sequencing depth for each chromosome targeted (Table 1-6).

The third approach uses t-MPS that relies upon the analysis of SNPs, and thus determines paternally inherited sequences to assess the relative contribution of maternal and fetal DNA within the plasma (Benn, 2014). Similarly to the second approach described, an additional amplification step is required before sequencing, although SNP sequences rather than chromosome specific sequences are amplified. Figure 1-8 demonstrates the use of SNP analysis for determination of T21. By genotyping fathers to determine the SNP profile improved test accuracy can be achieved but paternal genotyping is not essential. The commercial test Panorama™ (Natera, 2015) provides NIPT using this approach, which uses multiplex PCR to amplify almost 20,000 SNPs in each individual reaction (Zimmermann *et al.*, 2012). Subsequently, SNPs are aligned to corresponding chromosomes and each product is evaluated based on the hypothesis that the fetus is monosomic, disomic or trisomic. Once the possibility of recombination has been considered, the maximum likelihood that the fetus is normal, aneuploid or triploid can be calculated (Benn, 2014). As there is identification of fetal specific fragments, this

approach can be used for detection of microdeletions and duplications (Wapner *et al.*, 2015). In addition, theoretically, NIPT using SNP analysis should also provide the most promising approach for determining fetal aneuploidy in multiple pregnancies and also for diandric triploidy, although such testing is not currently offered (Benn, 2014). Table 1-7 summarises data for determining fetal aneuploidy using t-MPS for SNP based analysis.



**Table 1-5: Summary data for NIPT/ NIPD of fetal aneuploidy using shotgun massively parallel sequencing (s-MPS).** [Adapted from Benn (2014)].

Study	Detection of T21 (DS)			Detection of T18 (ES)			Detection of T13 (PS)		
	DS DR	DS FPR	DS NR	ES DR	ES FPR	ES NR	PS DR	PS FPR	PS NR
(Fan <i>et al.</i> , 2008)	9/9 (100%)	0/9 (0.00%)	0/18 (0.00%)	2/2 (100%)	0/16 (0.00%)	0/18 (0.00%)	1/1	0/17 (0.00%)	0/18 (0.00%)
(Chiu <i>et al.</i> , 2011)	86/86 (100%)	3/146 (2.05%)	11/764 (1.4%)						
(Ehrich <i>et al.</i> , 2011)	39/39 (100%)	1/410 (0.24%)	18/467 (3.9%)						
(Palomaki <i>et al.</i> , 2011)	209/212 (98.6%)	3/1471 (0.20%)	13/1686 (0.8%)						
(Sehnert <i>et al.</i> , 2011)	13/13 (100%)	0/34 (0.00%)	1/48 (2.08%)	8/8 (100%)	0/39 (0.00%)	1/48 (2.08%)	0/1 (0.00%)	0/46 (0.00%)	1/48 (2.08%)
(Palomaki <i>et al.</i> , 2012)				59/59 (100%)	5/1688 (0.30%)	17/1988 (0.9%)	11/12 (91.7%)	16/1688 (0.95%)	17/1988 (0.9%)
(Liang <i>et al.</i> , 2013)	40/40 (100%)	0/372 (0.00%)	12/435 (2.8%)	14/14 (100%)	0/372 (0.00%)	12/435 (2.8%)	4/4 (100%)	1/408 (0.25%)	12/435 (2.8%)
(Song <i>et al.</i> , 2013)	8/8 (100%)	0/1733 (0.00%)	73/1916 (3.8%)	2/2 (100%)	1/1739 (0.01%)	73/1916 (3.8%)	1/1 (100%)	0/1740 (0.00%)	73/1916 (3.8%)
(Stumm <i>et al.</i> , 2014)	39/40 (97.5%)	0/430 (0.00%)	32/504 (6.3%)	8/8 (100%)	1/472 (0.21%)	32/504 (6.3%)	5/5 (100%)	0/472 (0.00%)	32/504 (6.3%)
(Bianchi <i>et al.</i> , 2014)	5/5 (100%)	6/1909 (0.31%)	17/2042 (0.8%)	2/2 (100%)	3/1905 (0.16%)	17/2042 (0.8%)	1/1 (100%)	1/899 (0.11%)	
	47/47 (100%)	0/136 (0.00%)	11/183 (4.8%)						

DS, Down syndrome; ES, Edward's syndrome; PS, Patau syndrome; T21, trisomy 21; T18, trisomy 18; T13, trisomy 13; DR, detection rate;

FPR, false positive rate; NR, no result.

**Table 1-6: Summary data for NIPT/ NIPD of fetal aneuploidy using target massively parallel sequencing (t-MPS) for specific chromosomes. [Adapted from Benn (2014)].**

Study	Detection of T21 (DS)			Detection of T18 (ES)			Detection of T13 (PS)		
	DS DR	DS FPR	DS NR	ES DR	ES FPR	ES NR	PS DR	PS FPR	PS NR
(Nicolaidis <i>et al.</i> , 2012)	8/8 (100%)	0/1939 (0.00%)	100/2049 (4.9%)	2/2 (100%)	2/1929 (0.01%)	100/2049 (4.9%)			
(Norton <i>et al.</i> , 2012)	81/81 (100%)	1/2888 (0.03%)	148/3228 (4.6%)	37/38 (97.4%)	2/2888 (0.06%)	148/3228 (4.6%)			
(Ashoor <i>et al.</i> , 2012)	50/50 (100%)	0/297 (0.00%)	3/400 (0.8%)	49/50 (98.0%)	0/297 (0.00%)	3/400 (0.8%)			
(Ashoor <i>et al.</i> , 2013a)							8/10 (80%)	2/1939 (0.05%)	53/2002 (2.6%)
(Verweij <i>et al.</i> , 2013)	17/18 (94.4%)	0/486 (0.00%)	16/520 (3.1%)						
(Fairbrother <i>et al.</i> , 2013)	-	0/284 (0.00%)	4/288 (1.4%)	-	0/284 (0.00%)	4/288 (1.4%)	-	0/284 (0.00%)	4/288 (1.4%)
(Gil <i>et al.</i> , 2013)	11/11 (100%)	0/946 (0.00%)	48/1005 (4.8%)	5/5 (100%)	1/952 (0.11%)	48/1005 (4.8%)	1/1 (100%)	0/956 (0.00%)	48/1005 (4.8%)
(Stokowski <i>et al.</i> , 2015)	107/108 (99.1%)	0/533 (0.00%)	8/799 (1.0%)	29/30 (96.7%)	0/611 (0.00%)	8/799 (1.0%)	12/12 (100%)	0/629 (0.00%)	8/799 (1.0%)

DS, Down syndrome; ES, Edward's syndrome; PS, Patau syndrome; T21, trisomy 21; T18, trisomy 18; T13, trisomy 13; DR, detection rate; FPR, false positive rate; NR, no result.

**Table 1-7: Summary data for NIPT/ NIPD of fetal aneuploidy using targeted massively parallel sequencing (t-MPS) for SNP based analysis.** [Adapted from Benn, (2014)].

Study	Detection of T21 (DS)			Detection of T18 (ES)			Detection of T13 (PS)		
	DS DR	DS FPR	DS NR	ES DR	ES FPR	ES NR	PS DR	PS FPR	PS NR
(Nicolaidis <i>et al.</i> , 2013a)	25/25 (100%)	0/204 (0.00%)	13/242 (5.4%)	3/3 (100%)	0/226 (0.00%)	13/242 (5.4%)	1/1 (100%)	0/228 (0.00%)	13/242 (5.4%)
(Pergament <i>et al.</i> , 2014)	58/58 (100%)	0/905 (0.00%)	88/1051 (8.4%)	24/25 (96%)	1/939 (0.11%)	87/1051 (8.3%)	12/12 (100%)	0/953 (0.00%)	86/1051 (8.2%)

DS, Down syndrome; ES, Edward's syndrome; PS, Patau syndrome; T21, trisomy 21; T18, trisomy 18; T13, trisomy 13; DR, detection rate; FPR, false positive rate; NR, no result.

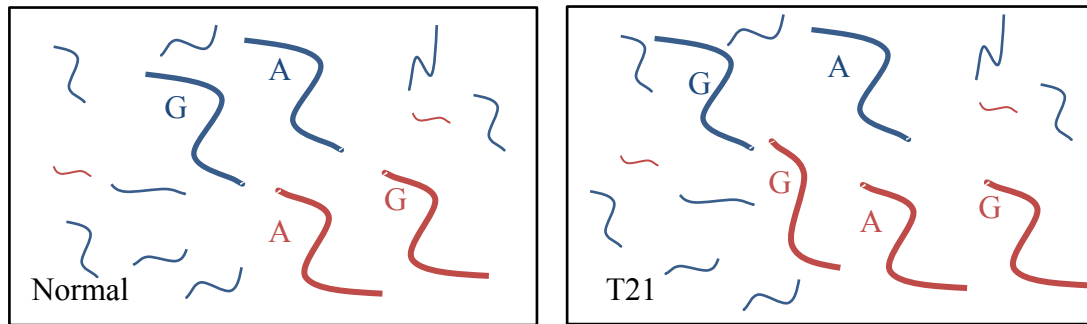


**Figure 1-8: SNP analysis for the determination of T21: an example of the general principle.** Fetal DNA (red) and maternal DNA (blue) SNP analysis for normal (left) and T21 (right) fetus. In this example the father is genotyped GG and the mother GA. For a normal pregnancy (left) if the fetus inherits a G allele from the father and an A allele from the mother, the G/A DNA fragment ratio will be 1.0, regardless of the cffDNA fraction. For a T21 fetus, who has inherited a G from the father and a G and an A from the mother due to a maternal non-disjunction, which gives rise to a fetus with the AGG genotype (right). Therefore for a fetal fraction of 15% the G/A DNA fragment ratio will be approximately  $((15\% \times 2) + (85\% \times 1))/((15\% \times 1) + (85\% \times 1)) = 1.15$  [Adapted from Benn, (2014)].

In 2011, NIPT was first released in Hong Kong (Lau *et al.*, 2012) and later introduced commercially in the USA (Agarwal *et al.*, 2013). In 2014, four predominant US companies provided commercial-based NIPT including; Materni21Plus™ (Sequenom, CA, USA), verifi™ (Illumina, CA, USA), Harmony™ (Ariosa Diagnostics, CA, USA) and Panorama™ (Natera, CA, USA) (Allyse *et al.*, 2015). While the verifi™ and Materni21Plus™ tests use s-MPS, the Harmony™ and Panorama™ tests use t-MPS, and the t-MPS based on SNP analysis, respectively. Prior to 2015, maternal samples collected within the UK were shipped to Hong Kong or the USA for commercial testing. However, in February 2015, Premaitha Health (Manchester, UK) launched the IONA® test; the first ever CE-marker NIPT product for pregnant women (Premaitha Health PLC, 2015). Therefore, Premaitha Health is currently the only company authorised by the European Regulatory agency to sell products to enable

laboratories to offer NIPT services within the UK. In a subsequent validation study, results revealed that the test enabled 100% accuracy for the determination of fetal T21, T18 and T13 (Poon *et al.*, 2015).

In a recent study, the results for NIPT of targeted cfDNA analysis using Digital Analysis of Selected Regions (DANSR) and Fetal-fraction Optimised Risk of Trisomy Evaluation (FORTE) with microarray quantification was combined with all published clinical performance studies, which also used the DANSR/FORTE methodology (Stokowski *et al.*, 2015). The consorted data included more than 23,000 pregnancies and revealed sensitivities >99% for T21, 97% for T18 and 94% for T13, with a specificity of >99.9% for all trisomies. This approach is also adopted by the Ariosa Diagnostics Harmony™ test.

Despite the success of NIPT, low cfDNA concentrations can result in false negative results, and placental mosaicism, vanishing twins or maternal tumours can alternatively give rise to false positive results (Dondorp *et al.*, 2015). In addition, because of the low prevalence of fetal aneuploidies, many studies that express high sensitivity and specificity (>99%), are associated with lower PPVs. For example, one study demonstrated 100% sensitivity and >99% specificity, but revealed a PPV of 45.5% (95% CI: 16.7-76.6) for T21, therefore over 50% of the general risk population were false alarms (Bianchi *et al.*, 2014). Despite this PPV being 10 times better than current first-trimester screening, PPVs of 100% are required for diagnostic testing (Dondorp *et al.*, 2015). Although the accuracy of NIPT is superior to conventional screening (see 1.3.2), unlike traditional methods, failure to obtain a result occurs in around 2% of all NIPT's performed (Benn, Cuckle and Pergament, 2013).

The costs for NIPT ranges from £400 to £900 (Allyse *et al.*, 2015), and with continued technological and statistical developments it is likely that not only will costs continue to decline but PPVs are likely to show improvement, which could build evidence for the

application of NIPD using MPS-based technologies. However, at present most studies have focused on high risk cases and consequently NIPT is only implemented as a commercial secondary screening test. The UK NSC is currently working with clinicians to assess the performance of NIPT in the NHS, and thus will make a recommendation on whether to introduce this screening based once results have been obtained (The UK National Screening Committee, 2015). Routine first trimester screening is being carried out as normal, and women identified as high risk are subsequently offered NIPT as a second screening test. Therefore, only women considered high risk following secondary screening will be offered diagnostic tests, and thus the number of women undergoing invasive testing should be reduced (refer to 1.1.2.1). In a recent press release, Benn (2015) determined that DRs for fetal aneuploidy would increase by implementing the universal application of NIPT. In addition, using NIPT as a replacement for conventional screening (refer to 1.1.2.4) would reduce health costs, provided that it can be carried out for \$744 (~£490) or less (Benn *et al.*, 2015). Further reports have also identified the use of NIPT as a cost effective screening option for all women, regardless of age or risk (Fairbrother *et al.*, 2015; Walker *et al.*, 2015).

#### *1.3.3.4 Determining fetal monogenic disorders*

Section 1.3.3 highlights the inheritance of multiple autosomal and sex-related monogenic disorders, and describes the importance of fetal sexing and determination of ethnic background within the screening programme. However, determination of fetal sex in pregnancy with previous family history of haemophilia, only illustrates a 25% chance of disease if the fetus is male and invasive testing is currently required for confirmation.

The application of NIPD for autosomal recessive disorders as well as other monogenic disorders, such as X-linked recessive DMD and autosomal dominant polycystic kidney disease, requires the detection of a paternally inherited mutation that is not present within the

maternal genome (Chiu *et al.*, 2002). For autosomal recessive disorders, the lack of a paternally inherited mutation suggests that the fetus is not homozygous for the disease-associated allele and confirmatory tests are not required. However, if the paternally inherited mutation is detected, invasive testing is required to confirm disease status of the fetus (Lo, 2013). For example, detection of mutated paternally inherited polymorphic STRs on the *CYP21A2* indicates that there is a 50% chance of CAH in female fetuses, whereas normal alleles indicate that female fetus will be unaffected (Krone and Arlt, 2009). In addition, exclusion of paternally inherited  $\beta$ -thalassaemia mutations using informative SNPs that differ between maternal and paternal alleles, can also determine unaffected fetuses. This approach has been well reported using multiple detection systems such as qPCR (Chiu *et al.*, 2002), allele specific arrayed primer extension (AS-APEX) technology (Papasavva *et al.*, 2006), conventional PCR - DGGE (Lazaros *et al.*, 2008) and MALDI-TOF MS (Li *et al.*, 2009). However, since maternally inherited sequences will be undistinguishable from the large background of maternal DNA, the main disadvantage of this approach is that disease status cannot be confirmed in cases where a paternally inherited sequence is detected. However, more sensitive techniques have been described for the determination of  $\beta$ -thalassaemia and other recessive haemoglobinopathies, such as dPCR (Barrett *et al.*, 2012), pyrophosphorolysis-activated polymerisation and melting curve analysis (Phylipsen *et al.*, 2012) and MPS approaches (Lam *et al.*, 2012), which allow dosage analysis for accurate diagnosis.

Many studies using MPS and digital PCR platforms have successfully discriminated between unaffected and affected fetuses for dominant and recessive traits, despite high background of maternal DNA signal (Lench *et al.*, 2013). Lun *et al.* (2008) described an approach for NIPD of essentially all monogenic disorders. The approach was defined as relative mutation dosage (RMD), and through the use of dPCR enabled the determination of slight differences in

concentration between either; a mutant and normal gene or between two alleles for a particular SNP. Currently, the application of this approach has been successfully implemented for the NIPD of fetal haemophilia (Tsui *et al.*, 2011) and sickle cell anaemia (Barrett *et al.*, 2012). This platform can be adapted for multiple monogenetic disorders, but it is likely that only one or a few disorders could be analysed in a single run dependent upon the platform used (refer to 1.3.3.3.1).

Alternatively, MPS platforms enable polymorphism dosage analysis and detection of paternally inherited mutations for multiple genes by sequencing millions of cfDNA molecules from maternal plasma. Consequently, the maternal inheritance of the fetus for recessive disorders can be determined in regions where the mother is heterozygous (Lo, 2013). Disease presence in the fetus can then be determined by mapping the SNP alleles to each of the maternal haplotypes and determining a significant increase in concentration of the mutant SNP. This method has previously been used for the NIPD of  $\beta$ -thalassaemia using both s-MPS (Lo *et al.*, 2010) and t-MPS (Lam *et al.*, 2012).

The advantage of digital PCR is that it is a simple and cheaper alternative to MPS. However, since MPS approaches analyse a substantially increased number of molecules, the robustness of digital PCR for NIPT is likely to be reduced (Lo, 2013). In addition, the decline in costs of MPS associated with target approaches could enable a conceivably cost-effective platform for clinical implementation. However, the application of digital PCR may still be a vital tool for prenatal screening and diagnosis for prospective parents with a risk of a known specific monogenic disorder.

#### *1.3.3.5 cffDNA enrichment*

The low concentration of cffDNA, particularly during the first trimester of pregnancy (1-3%), makes accurate quantification of chromosomal imbalance considerable more challenging and



is often the reason why false-negative results are encountered. Consequently, methods to selectively enrich the relative proportion of cffDNA have been developed.

Dhallan *et al.* (2004) identified that the addition of formaldehyde to maternal blood samples helped to increase the relative proportion of free fetal DNA, from 7.7% in untreated samples to 20.2% in the formaldehyde-treated samples. These results illustrate that the addition of formaldehyde yield higher cffDNA fractions by inhibiting maternal cell lysis during sample collection, transportation, handling and processing. It has been suggested that the formaldehyde allows for an increase in the percentage of free fetal DNA by two mechanisms, 1) it reduces the amount of background free maternal DNA by decreasing the amount of cell lysis through formaldehyde-mediated cell membrane stabilisation and 2) it helps to preserve free fetal DNA by nuclease inhibition. However, since this initial publication, different groups have attempted to replicate the preservation of cffDNA fractions using formaldehyde without success (Chinnapapagari *et al.*, 2005; Chung *et al.*, 2005). Alternatively, the introduction of Streck Cell-Free DNA™ Blood Collection Tubes (Streck BCTs, Streck, Omaha NE) has been shown to increase the preservation of both cffDNA (Wong *et al.*, 2013) and cffRNA (Qin, Bassett and Fernando, 2014) compared to standard EDTA tubes. Streck BCTs contain the anticoagulant K<sub>3</sub>EDTA and an unspecified cell preservative in liquid medium, which is used as an alternative to formaldehyde (Risberg, 2013). Das *et al.* (2013) determined that Streck Cell Preservative and Cell-Free DNA BCT reagents do not contain any free formaldehyde, and thus provide safer alternatives for preserving samples whilst protecting the integrity of the biomolecules. Similarly to formaldehyde, the preservatives in Streck BCTs are included to stabilise leukocytes, which prevent cellular degradation and subsequent release of maternal genomic DNA into the plasma (Wong *et al.*, 2013). Since the amount of maternal cfDNA is reduced, the cffDNA is less dilute resulting in higher overall cffDNA fractions. The most significant differences in cffDNA fractions have been observed

when samples have been stored for up to 72 hours (Barrett *et al.*, 2011), highlighting the application of this collection method for preservation of samples that may be transported over long distances. In addition, maternal blood collected in Streck BCTs yields higher cffDNA fractions at  $\geq 23^{\circ}\text{C}$  for up to seven days, and thus samples can be transported at room temperature (Wong *et al.*, 2013).

The application of cffDNA within the clinic rapidly expanded following its discovery in 1997 (Lo *et al.*, 1997). However, the molecular characteristics of cffDNA were not extensively studied until many years later. In 2004, it was reported that DNA derived from plasma consists of mainly shorter fragments and that maternal-derived cfDNA molecules are longer than cffDNA molecules (Chan *et al.*, 2004). Li *et al.* (2004) later compared the bands present in maternal and non-maternal plasma extracted DNA samples using southern blot analysis. The results identified that the major portion of cffDNA had an approximate size of  $<0.3\text{Kb}$ , whereas the majority of maternal cfDNA was  $>1\text{kb}$  (Li *et al.*, 2004).

Recent publications have identified that the size discrepancies between maternal cfDNA and cffDNA may not be as considerable as first described (Lo *et al.*, 2010; Stephanie *et al.*, 2014). Lo *et al.* (2010) studied the size distribution of fetal-derived and maternal-derived cfDNA at a single-base resolution using paired-end MPS. The results illustrated that both cffDNA and maternal cfDNA show a series of peaks, primarily a major peak at 166bp and a smaller peak at 143bp. However, cffDNA showed an increase of molecules  $<150\text{bp}$  and a reduced proportion of molecules at 166bp, illustrating that the larger 166bp peak is predominantly maternal in origin. Stephanie *et al.* (2014) also illustrated that samples which express higher cffDNA fractions illustrate a higher proportion of short fragments ( $<150\text{bp}$ ) and a lower proportion of larger fragments ( $\geq 166\text{bp}$ ) in comparison to samples expressing low cffDNA fractions. In 2010 an alternative study, also using paired-end sequencing for size distribution of fetal and maternal cfDNA, identified that cffDNA had a major peak at around

162bp and a minor peak at around 304bp (Fan *et al.*, 2010). The study revealed that selective analysis of shorter fragments led to an increase in cffDNA fraction, but did not increase the sensitivity of aneuploidy detection since less sequence reads were counted for quantification. This research illustrates that maternal plasma contains a complex mixture of short cffDNA fragments (predominantly <150bp), larger maternal cfDNA fragments >1kb; particularly if there is maternal leucocyte degradation (Sillence *et al.*, 2015), and smaller maternal cfDNA fragments of various sizes (166bp and 304bp have been shown). Previous data has also demonstrated that during pregnancy the fragmentation of plasma DNA shifts towards fragments of longer length compared to non-pregnant plasma DNA (Chan *et al.*, 2004). Since plasma DNA is thought to be derived from hematopoietic stem cells, which play an important role in the release of plasma DNA, it is likely that due to physiological and hormonal changes during pregnancy larger DNA molecules are released (Lurie, 1990; Lui *et al.*, 2002).

To help increase the relative proportions of cffDNA within the maternal circulation, methods exploiting the size difference between the maternal cfDNA and cffDNA have been developed (Li *et al.*, 2004; Li *et al.*, 2005; Li *et al.*, 2008; Galbiati *et al.*, 2011). In addition to cffDNA, it has also been identified that tumour-derived circulating cell-free DNA fragments are shorter than nuclear DNA in plasma (Diehl *et al.*, 2005; Jiang *et al.*, 2015). Both cffDNA and tumour DNA are present in low proportions in a maternal cfDNA or wild-type backgrounds, respectively, and are often undetectable by conventional PCR. Methods that allow for an increase in the percentage cffDNA would make it easier to distinguish cffDNA from maternal cfDNA and increase test reliability, particularly for the determination of fetal aneuploidy where accurate quantification is imperative (Lo *et al.*, 1998b).

Initial studies focused on the use of separating smaller cffDNA from larger maternal cfDNA using gel electrophoresis (Li *et al.*, 2004). Although, this approach has been shown to successfully enrich cffDNA for detection of point mutations in  $\beta$ -

thalassaemia (Li *et al.*, 2005), widespread use is not feasible since this approach is associated with extensive loss of total cfDNA, time consuming and prone to contamination (Go, van Vugt and Oudejans, 2010). Subsequently, an alternative size-selective enrichment strategy known as co-amplification at lower denaturation temperature- polymerase chain reaction (COLD-PCR) was described (refer to 3.1), which exploits differences in the melting temperature ( $T_m$ ) of variant or mismatched sequences compared to wild-type ones (Li *et al.*, 2008; Galbiati *et al.*, 2011). Consequently, by using a critical denaturation temperature ( $T_c$ ) lower than the melting temperature ( $T_m$ ) minority mutated alleles are selectively amplified. However, one disadvantage of this approach is that selective amplification relies upon the fetus displaying mutations that are unique to maternal mutations within chromosome region of interest.

#### **1.4 Ethical considerations**

Providing highly sensitive screening and non-invasive testing for pregnancy related disorders reduces or eradicates the risk of miscarriage that is associated with invasive techniques (refer to 1.2), respectively. However, the implementation of safer non-invasive tests within the clinic also raises many ethical concerns.

Fundamentally, there is a growing concern that the ease and safety of NIPT may increase the number of women undergoing diagnostic testing, and thus increase the uptake of abortions for women carrying affected fetuses (Hall, Bostanci and Wright, 2010). This is evident, particularly in many lower middle income countries (LMICs), such as China and Mexico, where giving birth to a baby with a genetic abnormality is often seen as a burden (Wang and Michaels, 2010). Offspring with disabilities are seen to threaten the family support network as children are expected to provide care to parents/ grandparents in old age. In one Chinese

study it was reported that 83% would consider abortion if diagnosis revealed that the fetus had a disability (Su and Macer, 2003). In such countries, prenatal testing is seen as necessary for the prevention of giving birth to an affected child. Therefore, the wider availability of NIPT is likely to increase the number of women seeking abortions not just legally but also illegally, which is often unsafe and poses a risk to maternal health (Allyse *et al.*, 2015). In addition, activists have argued that lowering the number of individuals with disabilities in society reduces society's ability to value such individuals and prevents the provision of necessary services (Kellogg *et al.*, 2014).

Concerns have also been raised regarding the implementation of safer non-invasive diagnosis as it could potentially create a platform for selective abortion of fetuses with minor abnormalities, undesired sex or unwanted paternity (de Jong *et al.*, 2010). Technological developments associated with many non-invasive techniques allow for a broad spectrum of abnormalities to be detected compared to current karyotyping, and thus the potential clinical introduction of these techniques raises further ethical challenges. However, the application of NIPD could enable broad or narrow testing. Broad testing allows for the detection of any disorder but it is suggested that only severe disabilities are brought to attention (de Jong *et al.*, 2010). Increasing the diagnostic scope of NIPD is seen as ethically problematic, essentially because of the difficulty associated with defining which disorders are severe, and with regards to Down syndrome and other disorders, the severity of symptoms can vary dramatically. In addition, diagnosis of late onset disorders can be seen as an invasion of the autonomy of the child that has been prenatally diagnosed (Human Genetics Commission and the UK National Screening Committee, 2005).

Narrow testing of specific disorders reduces the occurrence of unexpected or unclear findings, which prevents difficult counselling situations arising. In a recent study, the ethical issues surrounding NIPD of autosomal recessive disorders were reviewed (Skirton,

Goldsmith and Chitty, 2014). Results determined that all mothers felt such tests should be available on request, but it is vital that fathers that declined carrier testing should also be made aware that the fetal result may reveal their status. In conclusion the paper suggested that consent forms for NIPD should be signed to reiterate the gravity of the test and guidance should be provided to manage sensitive information (Skirton, Goldsmith and Chitty, 2014). Despite fewer moral implications being associated with a narrow approach, withholding results would deprive a couple of their autonomous reproductive choice if they wish to attain all NIPD information (Ogilvie, Yaron and Beaudet, 2009). Therefore, it is likely generic consent for a broad NIPD test will be implemented, which enables mothers to indicate specific disorders they would prefer to be told about following counselling on categories of abnormalities (de Jong *et al.*, 2010). This approach requires comprehensive counselling, which will be problematic since it is probable that this will be too time consuming and costly to implement on a wide scale (Childbirth Connection, 2012).

First trimester testing can allow for early reassurance or enable longer time periods in order for women to make informed choices. Subsequently, if women do decide not to continue with pregnancy, termination may be physically and psychologically less encumbering when performed in early pregnancy (Hall, Bostanci and Wright, 2010). In addition, in most western countries the gradualist view is commonly adopted, where the moral status of the embryo/fetus progresses with its development (de Jong *et al.*, 2010). However, the timing of abortion is ethically irrelevant if the embryo is assigned with high moral status from the start, or alternatively, if no status is attributed.

It has been suggested that appropriate counselling and informed consent will become more challenging when offering NIPD on a wide scale (Schmitz, Netzer and Henn, 2009; Wright, 2009). While the replacement of the current two-step model (screening and invasive diagnosis) with a single NIPD tests creates a conceptually easier platform, it is likely that the

provision of adequate information and pre-test counselling will become increasingly difficult (Wright, 2009). This can result in normalisation of NIPD, which will occur if the test is portrayed as routine and uptake increases as a result of thoughtlessness or pressure to take the test due to its relative ease and safety, as opposed to making an informed decision (Hall, Bostanci and Wright, 2010). Thus, autonomous reproductive decision making is not promoted. Alternatively, it is feasible that high uptake could be a result of positive reception to the new NIPD test, which safely facilitates parental reproductive choice (Wright, 2009). Regardless of where NIPD fits into the current screening/ diagnosis procedure, it is vital that the quality of present guidelines for informed consent and pre-test counselling does not diminish. Additionally, since screening programmes in current practice have shown that the uptake of testing is not always a result of adequate understanding (Green *et al.*, 2004), improvements to current guidelines of pre-test screening should also be considered.

## Study Aims

- To test various molecular techniques for the selective enrichment of cffDNA from maternal plasma using either pseudo-maternal samples or actual maternal samples, including; COLD-PCR, inverse-PCR and Pippin prep size selective methods.
- To develop a novel assay for the quick assessment of *RHD* zygosity in non-maternal samples using ddPCR.
- To compare the sensitivity of ddPCR for the determination of fetal sex and *RHD* status using ddPCR compared to conventional q-PCR platforms.
- To combine size-selective enrichment of cffDNA and ddPCR analysis to provide a novel and cost-effective test for the NIPT/ NIPD of fetal aneuploidy.



# Chapter 2

## Materials and methods

## 2.1 Sample collection

### 2.1.1 Pre-ordered samples

Male genomic DNA (gDNA) (G1471, Promega, Southampton, UK) and female gDNA (G1521, Promega) each pooled from multiple anonymous donors were used as templates for standards, control samples and optimisation experiments throughout this study. Samples were diluted to 20ng/μL and stored as 50μL aliquots at -20°C for up to 10 months.

T21 gDNA 5μg (100ng/μL) samples (PHE Culture Collection, Salisbury, UK) was used as a positive DS control sample. Samples were diluted to 50ng/μL and stored as 5x 20μL at -80°C for up to 6 months.

### 2.1.2 Human whole blood samples

Human whole blood was supplied by the National Health Service Blood and Transplant (NHS BT) (Bristol, UK). Samples were collected in EDTA tubes (5 mL total blood volume). The blood was spun at 3500 x g for 5 minutes (mins) and plasma was removed using a sterile Pasteur pipette and placed in a clean 2 mL microcentrifuge tube. The plasma was then re-centrifuged at 16 000 x g for 5 mins and the second supernatant was then removed and placed in a clean 2 mL microcentrifuge tube. Subsequently, the buffy coat layer was also removed using a fresh Pasteur pipette and placed in a clean 2 mL microcentrifuge tube with 200 μL 1x phosphate buffer saline (PBS) to dilute the starting material.

#### *2.1.2.1 DNA extractions of whole blood samples*

DNA was extracted from 1 x 2mL aliquot of plasma using the QIAamp Circulating Nucleic Acid kit (CNA kit) (Qiagen, Hilden, Germany) within 24-72 hours of collection.

The extraction process was carried out using QIAamp mini columns on the QIAvac 24 Plus vacuum manifold (Qiagen). Although longer lysis incubation periods have not been associated with increased DNA extraction, samples were lysed for 45 mins as opposed 30 minmins to maximise yield. After the wash stages using buffer ACB, buffer ACW1 and ACW2, a final wash phase was carried out using Molecular Biology Grade Ethanol (99.5%) (BPE2818-4, Fisher Scientific, Loughborough, UK). Samples were then spun down (20 000 x g for 3 mins) and incubated for 5 mins with 50-70  $\mu$ L of Buffer AVE (RNase free water containing 0.04% (w/v) sodium azide). Finally, DNA samples were eluted by centrifugation (20 000 x g for 1 minute) into 1.5mL elution tubes. Following DNA extraction, samples collected during early experimentation were quantified using the NanoVue Plus Spectrophotometer (GE Healthcare, Life Sciences, Buckinghamshire, UK) (2.6.1). However, due to the variation in readings associated with this approach, quantification was subsequently carried out using the Qubit® 2.0 Fluorometer (Life Technologies, Paisley, UK) (2.6.2). The method used for DNA quantification in each assay has been specified throughout. Samples expressing DNA concentrations  $>25\text{ng}/\mu\text{L}$  were diluted to  $10\text{ng}/\mu\text{L}$ . All samples were stored at  $-20^{\circ}\text{C}$ .

#### *2.1.2.2 DNA extraction of buffy coat from whole blood samples*

DNA was extracted from buffy coat in 200  $\mu$ L PBS using the QIAamp DNA Blood Mini Kit (Qiagen) following manufacturer's instructions for the spin protocol. The additional centrifugation step in a clean 2 mL collection tube following wash phase with Buffer AW2, was carried out to help reduce the chance of possible Buffer AW2 carryover. To elute the DNA, the QIAamp mini spin column was placed in a clean 1.5 mL microcentrifuge and 200  $\mu$ L of Buffer AE was added to the column. This was incubated at room temperature for 5 mins in an attempt to increase DNA yield. Samples were

quantified using the NanoVue Spectrophotometer (GE Healthcare) (2.6.1) and stored at -20°C as 4 x 50 µL aliquots.

### 2.1.3 Pseudo-fetal DNA samples

The external primers (Table 2-1) were used to amplify 280-320 bp fragments from the Male gDNA (2.1.1), to produce the pseudo-fetal DNA (psfDNA) samples. Following PCR amplification (2.3.1) and agarose gel electrophoresis (2.4), psfDNA fragments were excised from the agarose gel and purified using the QIAquick gel extraction protocol (Qiagen, Hilden, Germany) (refer to 2.5).

**Table 2-1: Summary of primers used.** External and internal primer sequences and product sizes (bp) for multiple regions on chromosomes 1, 13, 18, 21, X and Y.

Chr	Gene	External Primers (5'-3')	Product size (bp)	Internal Primers (5'-3')	Product size (bp)	Probes (5' - 3')
1	<i>EIF2C1F</i>	AAAGCATCAGA GCTGGCATT <sup>1</sup>	317	GTTCGGCTTTCA CCAGTCT <sup>1</sup>	81	CTGCCATGTGG AAGATGATG <sup>1</sup>
	<i>EIF2C1R</i>	AGTGTGGTCACT GGACTTGG <sup>1</sup>		CTCCATAGCTCT CCCCACTC <sup>1</sup>		
13	<i>SPG20 F</i>	TGGGTGGGAATC TGCTAGAC	297	GCACCAGGCTGG AAATTCT	80	TGCCACTTCTC TGCAGAATG
	<i>SPG20 R</i>	GCTGGACAACCTT TGTGATGG		TGGATATAACTT GGGCACCTC		
13	<i>ZIC2 F</i>	GCAACTCCACAA CCAGTACG	297	GGTGCCTTTTTTC CGCTATATG	90	AATCTGCAAGT GGATCGACC
	<i>ZIC2 R</i>	CACTCCTCCAG AAGCAGAC		CTTGGGATTGCT CAGTTGCT		
13	<i>ATPZB F</i>	AGGATCTTGGGC ATGACTTG	300	TTCCAATTTGAA AGGCATCA	82	AAGGTTTCCCT GGAACAAGG
	<i>ATPZB R</i>	TTCAATGGAGCT GACACAGG		CACAACCGATGG CACATATT		
18	<i>APCDD1 F</i>	CAAAGGCAGAC CTGACCATC	297	CACCCACCTTC TCCATCTA	97	GTCCTCTCGTC CAGGGTCAT
	<i>APCDD1 R</i>	AGGGCTGTTTAT TGGCTGTG		TCCTACCTTTGA ACACGAACTC		
18	<i>TTR F</i>	CACCAATCCAA GGAATGAG	282	ACCTGAAGGACG AGGGATG	98	CTAAAGCAGT GTTTTCACCTC A
	<i>TTR R</i>	GCGTTCTGCCCA GATACTTT		TGCCTGGACTTC TAACATAGCA		
18	<i>TNFRSF11A F</i>	GAAGATGCCAG GATGCTCTC	285	CAGATGCCCACA GAAGATGA	85	CCAGCCCACA GACCAGTTAC
	<i>TNFRSF11A R</i>	CATGGGAGTCCA ATCAGTCC		ATTTGCTTCCAG GCTCAGTG		
21	<i>DSCR3 F</i>	GCGTGGTGGTCA TATCGAGT	315	CCAACACCAGGG AGTGTCTT	87	TAAACCTCCAG CTCAGTGCC
	<i>DSCR3 R</i>	ATGGGGTCTTGC TATGTTGC		GCTTCAAACACA CCCACACTT		
21	<i>RCAN1F</i>	TGACCCTGCGAT TATTTTCC	292	AGTACACGCCGA TCCACCT	97	GAGGACGCAT TCCAAATCAT
	<i>RCAN1R</i>	CCACCTCCGAAG AAGTCGT		ACCAGCCACCTC CACAGTAA		
21	<i>APP F</i>	GAGGAGGAAGA AGTGGCTGA	286	AAGAAGCCGAT GATGACGAG	96	GAGGAAGAGG CTGAGGAACC
	<i>APP R</i>	ATGTTTTTGATT GGGAAGG		TGCTGGTGGTTC TCTCTGTG		
X	<i>FOXP3 F</i>	GAAAGGAGGAT GGACGAACA	288	AAACTGGTGGGA GGCAGAG	94	GATGATAGGC CCTGGATGTG
	<i>FOXP3 R</i>	CTGTGTGGCTGG TTGTGAAG		CAGGCAAGACA GTGGAAACC		
X	<i>NROB1 F</i>	CCCACGAGCACA AATCAAG	293	CGCTCAAGAGTC CACAGGT	89	GTTGAAGACG CTGCGCTT
	<i>NROB1 R</i>	GGCTCCGAGACT TCCACAGT		CTGGAAGCAGG GCAAGTA		
X	<i>PRPS1 F</i>	CCATATTGGTCA GGCTGGTC	259	GCTTTCTACATC CCACATCAGG	88	TGGGAATAAG CTCGCTTTTT
	<i>PRPS1 R</i>	GGGAGGCTGAA GAAGGAGAA		AGGTAGGAGGTC CCAGCAGT		

X	Xp22.3 F	CACAAGCTCGCT TAGCAACA	315	GATGAGGAAGG CAATGATCC <sup>1</sup>	86	CTGTTTCTCTC TGCCTGCA <sup>1</sup>
	Xp22.3 R	TAGCCCTTAGGC ACTCGAAA		TTGGCTTTTACC AAATAGGG <sup>1</sup>		
Y	<i>SRY</i> F (K.A.S.)	GGCACCTTCAA TTTTGTCTG	300	CGGAGAAGCTCT TCCTTCCT	89	TCAGTGTGAA ACGGGAGAAA
	<i>SRY</i> R (K.A.S.)	TTTCGCATTCTG GGATTCTC		TCCTGGACGTTG CCTTTACT		
Y	<i>SRY</i> F (H.P.T.)	GAATGCGAAACT CAGAGATCA	287	TGGGATACCAGT GGAAAATG	96	ATTCTTCCAGG AGGCACAGA
	<i>SRY</i> R (H.P.T.)	CTGGTGCTCCAT TCTTGAGT		TCGGGTATTTCT CTCTGTGC		
Y	<i>TSYPI</i> F	TACATGGTCAGC CTGGAGGT	293	GGGGAGGGTAA GGGAAATAA	88	CAAGAGTGAG CACCTCACCC
	<i>TSYPI</i> R	TCCTTCCACTAC CCATCCTG		CAGGACAAGGT GGAGAAAGC		
Y	<i>DDX3Y</i> F	AGCAGCCTAACC CTGTCAAG	296	CCACTCAGCTTT CCTCAGGT	89	ATCCTGCAGA GGGACCTTCT
	<i>DDX3Y</i> R	CCAACTAGCCGT CACCTACC		CAATCTTCAGGT TAGGGAGGTG		

<sup>1</sup>Taken from Fan *et al.* (2009)

#### 2.1.4 Pseudo-maternal samples

PsfDNA samples (2.1.3) and Female gDNA (2.1.1) were used to produce the pseudo-maternal samples containing 5% ‘fetal’ DNA using a dilution approach and a genomic equivalent (GE) approach.

For the dilution approach both the psfDNA samples and the female gDNA (‘maternal’ cfDNA portion) were diluted to 2ng/μL. Spike samples containing one psfDNA gene regions (e.g. target gene region; *APP*) were produced by adding 5% psfDNA (2ng/μL) to 95% Female gDNA (2ng/μL). This dilution was used to test each fragment and to produce pseudo-maternal samples carrying a ‘female fetus’ (5% Xp22.3). Spike samples containing two psfDNA gene regions (e.g. *APP* (target gene) and *EIF2C1* (reference gene)) were produced by adding 2.5% psfDNA target fragment (2ng/μL) and 2.5% psfDNA reference fragment (2ng/μL) to 95% female gDNA (2ng/μL). This dilution was used to produce pseudo-maternal samples carrying a ‘male fetus’ (2.5% *SRY* (target) and 2.5% Xp22.3 (reference)) and a ‘normal fetus’ (2.5% *APP* (target) and 2.5% *EIF2C1*

(reference)) to give a ratio of 1. To produce pseudo-maternal samples carrying a 'DS fetus', 3% psfDNA *APP* target and 2% psfDNA *EIF2C1* reference was added to 95% Female gDNA to give a ratio of 1.5 in the 5% 'fetal' proportion.

For the GE approach, the initial step was to calculate the molecular equivalent of gDNA (Plasma extracted sample (2.1.2)) and psfDNA for a 5% spike (Appendices 1). Subsequently, the molecular mass of the fake fetal DNA fragment was calculated in order to determine the moles per microliter of fetal fragment using Avogadro's constant. This was then used to dilute the fetal fragment to determine how much of each fragment was required per 1  $\mu\text{L}$  of plasma DNA. A worked example is illustrated in Appendices 1. To produce the pseudo 'DS'-spike, the *APP* psfDNA fragment constituted 3/5 of the 5% fetal spike GE/ $\mu\text{L}$  and the *EIF2C2* psfDNA fragment constituted 2/5 of the 5% 'fetal' spike GE/ $\mu\text{L}$  (Appendices 1). To produce the pseudo 'normal'-spike, *APP* and *EIF2C1* psfDNA fragments constituted 1/2 of the 5% 'fetal' spike GE/ $\mu\text{L}$  each (Appendices 1).

#### 2.1.5 Maternal samples

Maternal samples were recruited at Plymouth Hospitals NHS Trust, Plymouth, UK with informed consent, from October 2013 to January 2015. Ethics approval was granted by the United Bristol Healthcare and Trust Research and Ethics Committee (REC) (ref: 13/SW/0148).

Maternal peripheral blood samples were collected in EDTA tubes (5-10 mL total blood volume) and centrifuged at 1 600 x g for 10 mins at room temperature. The plasma was carefully removed and transferred to a 15 mL tube. The plasma was then re-centrifuged at 16 000 x g for 10 mins. All samples were processed within 4 hours of collection and plasma aliquots (1 mL) were stored at  $-80^{\circ}\text{C}$ .

Maternal peripheral blood samples collected in Streck BCTs (10-20 mL total blood volume) were centrifuged at 1 600 x g for 15 mins at room temperature. The plasma was carefully removed and transferred to a 50 mL tube. The plasma was then re-centrifuged at 2 500 x g for another 10 mins. All samples were processed within 48 hours of collection and plasma aliquots (1 mL) were stored at -80°C.

DNA was extracted from two 1 mL aliquots of plasma (mixed) using the CNA kit (Qiagen) on the QIAvac 24 Plus vacuum manifold (Qiagen). The extraction process was carried out according to the manufacturer's protocol as previously described (2.1.2) and each sample was eluted in 60 µL of Buffer AVE (RNase free water containing 0.04% (w/v) sodium azide). No DNase or RNase treatment was used. Following DNA extraction, samples were quantified on the Qubit® 2.0 Fluorometer (Life Technologies) using the Qubit® dsDNA high sensitivity (HS) assay kit (Life Technologies) (2.6.2). Samples were stored at -20°C as single 60 µL aliquots for up to four weeks. Due to the fragmented nature of cfDNA, template DNA was expected to be in a primary linear structure, therefore no template modification steps such as sonication or restriction digest were necessary.

## **2.2 Primer Design**

### **2.2.1 Polymorphic STR amplicon (D21S1890)**

The chosen region of interest was a fragment on chromosome 21 (D21S1890), which contained a CA- STR region. Primers for amplification (Figure 2-1) were designed by Alice Bruson (Universita delgi di Padova, Italy) using the Primer3 software (<http://fodo.wi.mit.edu/primer3>). Following primer design the sequences were subsequently BLASTed to ensure primer specificity for chromosome using Primer-BLAST on the NCBI website (<http://www.ncbi.nlm.nih.gov/>). Figure 2-1 shows the



amplicon region, highlighting the internal primers (blue), external primers (green) and the probe (pink), which was labelled with a 5'FAM reporter label and a black hole quencher 1 (BHQ1) quencher dye attached to the 3' end. All primers and probe were high performance liquid chromatograph (HPLC) purified (Eurofins MWG Operon, Acton, London, UK).

```

GTATTTTTTAAGCCTGAGGACCCATTTGGGAGTTAGATTCTGGATCGAGCCTAGGGTC
AGTTTTTCCTTGTGTTAAATAACACTACTTCACAGAAGGGGGAACGAGAATTCAGGGG
AGTTGGCACAAAACCTTGAACCCTTCTCGGGAGGCTTTCCTGCCTGGACGGACGCCT
GGGAGGAGGGCCCGGAGAAACGAGGATGAGCTTCTCCTCATTCGCCCGAGGGTCTGA
CCACAGATTTCCCAATCGCCACACACACACACACACACACACACACACACACACA
CACGGGTTGTTTGGGAGTCAGTTGGTTTTCAAAGGCTTTC AAGGAAATGAAGAGTCC
CAAAGTTTTCCCTTAATCGTTCAGAGTGTTTTTCTTTGTCCCAGGTTTATATACCAAGAA
TACGGGGGAATATTTTTAGTTCCTTTCAGCTGAACAGTGTACAACACTGCCTTTTTTTCCTT
TTGGAGGTCCCAACACCCTGTTAATCCGCTCCTAGGAGAACTAAACAAAAACAAGGC
TGGACGTCGTGTCTCCCGCCTGTAATCCCAGTGCTTTGGGAGGCTGAGGCAGGAGGA
TCAGTTGAGCTCAGGAGTTTGAG

```

**Figure 2-1: D21S1890 STR fragment amplicon region on chromosome 21 (21q22.3).**

External primers (green), internal primers (blue) and probe (5'FAM and 3' BHQ1) (pink) for D21S1890. The underlined sequence illustrates the CA STR region.

### 2.2.2 Non-polymorphic amplicon regions

Internal primers, external primers and probes for various regions on five different chromosomes (chromosomes; 13, 18, 21, X and Y) were designed using Primer3 software (<http://frodo.wi.mit.edu/primer3/>) (Table 2-1). Internal primers for chromosome 1 (*EIF2C1*) were taken from Fan *et al.* (2009, ), but the external primers and probe were designed using Primer3 software (Table 2-1). In addition, the internal primers and probe for the Xp22.3 amplicon on chromosome X were also taken from Fan *et al.* (2009, ), unless stated otherwise. Internal primers and probes for two *RHD*-specific gene regions

(*RHD* exon 5 and *RHD* exon 7) were taken from Finning et al. (2008, (Table 2.1). For inverse PCR experiments internal and external primers that were consensus for both *RHD* and *RHCE* exon 7 (*RH7*) were designed in house using Primer3 software (<http://frodo.wi.mit.edu/primer3/>) (Table 2-2, Figure 2-2). Unlike conventional primer pairs which face inward to overlap amplification of the region of interest (ROI), the internal inverse PCR forward and reverse primers (purple) were designed to be facing away from each other (Figure 2-2).

**Table 2-2: Internal primers and probes for *RHD* exon 5 (*RHD5*), *RHD* exon 7 (*RHD7*) and *CCR5*.**

Amplicon location	Primer	Sequence (5' - 3')	Dual-Labelled Hydrolysis Probe (5' - 3')	Length (bp)
1p36.11 Exon (5)	<i>RHD5</i> Forward*	CGCCCTCTTCTTG TG GATG	FAM- TCTGGCCAAGTTTCA	82bp
	<i>RHD5</i> Reverse*	GAACACGGCATTCTT CCTTTC	ACTCTGCTCTGCT- BHQ1	
1p36.11 Exon (7)	<i>RHD7</i> Forward*	CAGCTCCATCATGGG CTACAA	FAM- AGCTTGCTGGGTCTG	75bp
	<i>RHD7</i> Reverse*	AGCACCAGCAGCAC AATGTAGA	CTTGGAGAGATC- BHQ1	
3p21.31	<i>CCR5</i> Forward	TACCTGCTCAACCTG GCCAT	FAM/HEX**-	91bp
	<i>CCR5</i> Reverse	TTCCAAAGTCCCACT GGGC	TTTCCTTCTTACTGTC CCCTTCTGGGCTC- BHQ1	

\*Taken from Finning *et al.* (2008). \*\* Two version of the *CCR5* (FAM- and HEX-labelled).

**Table 2-3: Inverse PCR internal and external primers for *RH7*.**

<i>RH7</i> Primer	Sequence (5' – 3')	Figure 2-2
External forward	GAAGGGCTTCTTTGAGGTGA	1
External reverse	GTAAGCCCAGTGACCCACAT	2
Internal (inverse) forward	TCAGCTTGCTGGGTCTGCTTG	3
Internal (inverse) reverse	GTGTTATTATAAGCAGATTGGCAGGTGAG	4

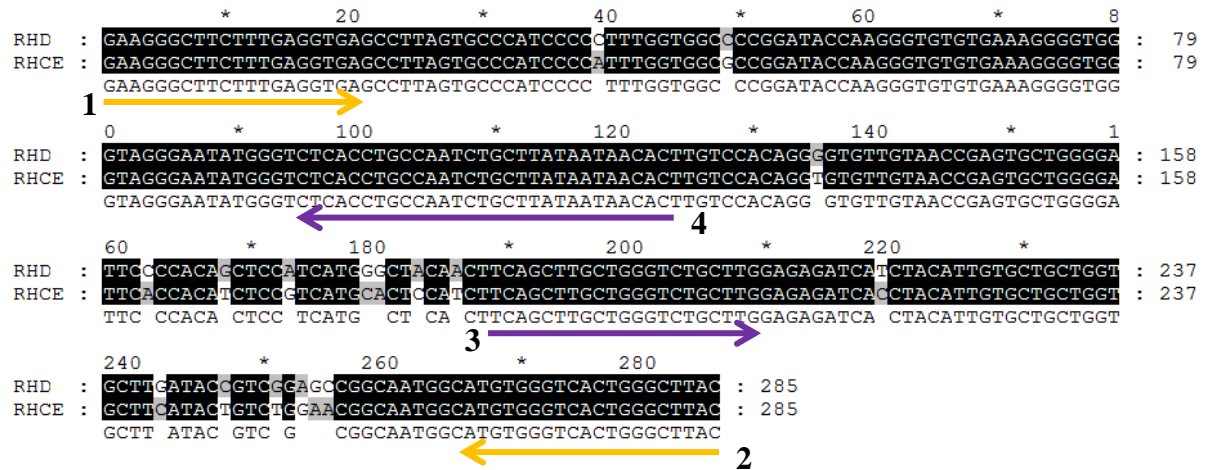


**Figure 2-2: Sequence alignment of *RHD* and *RHCE* for exon 7.** Illustrating sequence mapping of inward facing external primers (orange, forward (1) and reverse (2)) and outward facing internal primers (purple, forward (3) and reverse (4)).

All internal primers and probes were HPLC purified (Eurofins MWG Operon), and all external primers were HPSF (high purity salt free) purified (Eurofins MWG Operon, Acton, London, UK). Probes were labelled with a black hole quencher 1 (BHQ1) quencher dye attached to the 3' end and either a 5'FAM or 5'HEX fluorescent reporter label, unless stated otherwise (Appendices 2, Table 2-2, Table 3-2).

In house primers were analysed using OligoAnalyzer 3.1 (Integrated DNA technologies, <https://www.idtdna.com/calc/analyzer>) following recommended guidelines, including; primer length (18-22bp), primer melting temperature (52°C to 58°C), GC-content (40-60%), GC clamp ( $\leq 3$  G's or C's), hairpins ( $\Delta G \geq -2$  kcal/mol), self/cross primer-dimerization ( $\Delta G \geq -6$  kcal/mol), di-nucleotide repeats ( $\leq 4$ ), single-base runs ( $\leq 4$ ) and 3'end stability (less negative  $\Delta G$ ). Results for primer analysis are illustrated in Appendices 2. Following primer design/analysis the sequences were subjected to BLAST analysis to ensure primer specificity for each chromosome using Primer-BLAST on the NCBI website (<http://www.ncbi.nlm.nih.gov/>).

## 2.3 Conventional and COLD PCR

### 2.3.1 Conventional PCR

Conventional PCR reactions were performed in individual RNase-free PCR tubes (0.2 mL) (Life Technologies). Each reaction was carried out in a 25  $\mu$ L solution containing 12.5  $\mu$ L of 2x Fast TaqMan Universal MasterMix (Applied Biosystems), which contains a highly purified DNA polymerase (UP) which enables instant hot start and minimizes non-specific product formation, 300nM of each primer, Nuclease free Water (AM9937, Applied Biosystems) and a standard volume of template DNA/ non-template control (NTC) (5  $\mu$ L). However, reaction volumes were doubled for gel extraction experiments when producing psfDNA fragments (50 L) (refer to 2.5) and the total amount of DNA added per reaction was specified throughout each experimental chapter. PCR cycling was carried out on the Veriti® 96 Well Thermal Cycler (Applied Biosystems) at the following conditions; 50°C for 2 mins (optimization of UNG activity); 95°C for 10 mins (activation of TaqMan); 50°C for 2 mins (allows DNA to re-nature); 35 cycles of 95°C for 30 s (denaturation phase), optimised  $T_a$  for 30 s (annealing phase) and 72°C for 60 s (extension phase). The 35 cycles were then followed by 10 minutes at 72°C and a 4°C hold step. The annealing temperature used and any other variations from this standard PCR set-up were outlined in each experimental results section.

### 2.3.2 COLD-PCR

To determine the optimal annealing temperature of the internal primers (Table 2-1), the Male gDNA (used for all chromosomes except X) and Female gDNA (used for chromosome X) were amplified by conventional PCR for each primer set (2.3.1). Once the optimum annealing temperature had been determined, the denaturation temperature was tested using a fundamental gradient from 95°C down to 70°C. The following PCR

conditions were used; 50°C for 2 mins; 95°C for 10 mins; 50°C for 2 mins; 35 cycles of 95°C/ 90°C/ 85°C/ 80°C/ 75°C/ 70°C for 30 s, optimised  $T_a$  for 30 s and 72°C for 60 s. Samples were held at 4°C.

To establish the critical denaturation temperature ( $T_c$ ) down to 1°C, a consecutive gradient was carried out between the temperature at which product was last amplified and the  $T_d$  directly below this from the initial gradient experiment results (5°C below). The PCR reaction was the same as described above, but with a smaller range  $T_d$  gradient. The refined  $T_d$  gradient tested for each internal primer set is specified in Chapter 3 (3.2).

## **2.4 Agarose gel electrophoresis**

PCR amplicons were analysed using agarose gel electrophoresis. Samples were run on 2% agarose (*w/v*) gels, which were produced by mixing 1 x TAE buffer (40 mM Tris-acetate [pH 8.0], 1mM EDTA) with 1X GelRed Nucleic Acid Stain (Cambridge Bioscience, Cambridge, UK). 10  $\mu$ L of the PCR Ranger 100bp DNA Ladder (Norgen, Manchester, UK) was loaded and used as a marker for all gel electrophoresis runs. DNA gel loading buffer (100 mM Tris-HCl pH 8.3, 10% (*v/v*) glycerol and 0.05% (*w/v*) Orange G) was added to a proportion of the PCR reaction at a final concentration of 20% on Parafilm M Sealing Film (Fisher Scientific). The remainder of each PCR reaction was stored at 4°C for up to 48 hours for secondary gel electrophoresis analysis (if required). The PCR reaction- loading buffer mix was subsequently added to corresponding wells. Due to the large volume of loading buffer-mix added for gel extraction protocols for psfDNA fragments (50  $\mu$ L), two wells were taped together to double the maximum volume of each well (2 x 53  $\mu$ L). Electrophoresis was carried out at 120V for 45 mins in 1 x TAE buffer. Following the run, gels were removed and placed in the EC3 imaging

system (UVP BioImaging system, Cambridge, UK) and results were analysed using the Launch Vision WorksLS program (Chemi Doc 410).

## **2.5 Gel Extraction**

DNA fragments were excised from the agarose gel (2.4) using a clean sharp scalpel on the EC3 imaging system (UVP BioImaging system) under UV light rays. The gel segments containing each fluorescent band were then weighed and the DNA was purified using the QIAquick gel extraction protocol (QIAGEN, Hilden, Germany) according to manufacturer's instructions. To summarise, three volumes of buffer QG were added to one volume of gel and mix was incubated at 50°C for 10 mins, with repeated vortexing every 2-3 mins to help completely dissolve the gel. To increase the yield of DNA fragment obtained, one gel volume of isopropanol was added. Samples were then added to QIAquick spin columns (Qiagen) and centrifuged for 1 minute. The flow through was discarded and the recommended additional wash step using 0.5mL of Buffer QG was carried out. After the wash phase using buffer PE, the samples were finally eluted in 50µL of Buffer EB (10 mM Tris-Cl, pH8.5). Once DNA band had been extracted, the psfDNA samples were quantified using the NanoVue Plus Spectrophotometer (GE Healthcare) (refer to 2.6.1).

## 2.6 Assessment of DNA quality and concentration

### 2.6.1 Quantification by UV spectrophotometry

The NanoVue™ Plus Spectrophotometer (GE Healthcare) was used to measure DNA concentration and quality of samples for earlier experiments following manufacturer's instructions. The optical density was assessed at 260 nm and 280 nm and the DNA quality threshold for the A260/A280 ratio was set between 1.6 and 1.95.

### 2.6.2 Quantification by fluorescence

Because of the variation in results associated with the UV spectrophotometry approach due to non-selective quantification (2.7.1), the determination of DNA concentration was later assessed using the Qubit® dsDNA HS assay kit (Life Technologies). This method is highly selective for double stranded DNA (dsDNA), and therefore has a higher tolerance to contaminants, such as salts, free nucleotides, solvents, detergents or even protein. Quantification was carried out following manufacturer's instructions (Life Technologies). The total volume of Qubit® working solution and Qubit® standard/ sample is always 200 µL. 10 µL of the standard is added to 190 µL of working solution, but the amount of sample added can be anywhere between 1-20 µL. For all experiments 2 µL of sample was added to 198 µL of working solution. After 2 mins incubation at room temperature, the standards and samples were run on the on the Qubit® 2.0 Fluorometer (Life Technologies). The Qubit® Fluorometer generates concentration in ng/ mL, which corresponds to the concentration of the sample after dilution. To calculate the starting concentration of the sample, the following calculation was used:

$$\text{Concentration of sample (ng/ } \mu\text{L)} = \text{QF value} = \left( \frac{200}{x} / 1000 \right)$$

Where QF value = the value given by the Qubit<sup>®</sup> 2.0 Fluorometer and x = the number of microliters of sample added to the assay tube.

The type of quantification used for each experiment is stated throughout.

### 2.6.3 DNA Analysis

The Agilent 2100 Bioanalyzer system (Agilent Technologies, Cheshire, UK) was used for analysing maternal DNA samples before and after Pippin Prep selective enrichment (refer to 2.11). The samples were analysed using the High Sensitivity DNA Analysis Kit (5067-4626, Agilent Technologies) following the Agilent High Sensitivity DNA Kit Guide. To summarise, once the gel-dye mix was prepared, the mix was loaded into the well-marked 'G' (in a black circle) on the High Sensitivity DNA chip help by the chip priming station. Consequently, the plunger was lowered and held in position for 60 seconds (s) before slowly pulling the plunger back to the 1mL position. More gel mix was loaded into the remaining 'G' wells (no black circle) to complete loading of the gel-dye mix. Subsequently, the marker, ladder and samples were loaded into allocated wells. Once the chip had been vortexed for 1 minute at 2400 rpm it was loaded onto the Agilent Bioanalyser 2100 instrument within 5 mins. Results were generated on the 2100 Expert Software (version B.02.08, Agilent Technologies). Before reviewing individual sample Gels and Electropherograms, the Gel and Electropherogram of the High Sensitivity DNA Ladder was evaluated to ensure that; 15 peaks were visible, all peaks were well resolved, the baseline was flat and there was correct identification of both markers.



## 2.7 Real-time PCR (qPCR)

### 2.7.1 qPCR

qPCR measures DNA template at the exponential phase, as opposed to the plateau stage when using traditional PCR. This enables more accurate quantification since the cycle threshold (Ct) can be compared against a series of standards with known concentrations, whereas traditional PCR only provides a qualitative representation. In addition the use of fluorophores enables multiple targets to be amplified in a single reaction, which is known as multiplexing. Multiplex qPCR reactions were set up in MicroAmp fast optical 96-well reaction plates (0.1mL) (Life Technologies). Reactions were performed in a 25  $\mu$ L solution containing 12.5  $\mu$ L of 1x TaqMan Universal PCR Master Mix (Applied Biosystems), 300nM of forward and reverse primers for two separate targets, 250nM of each probe and a standard volume of template DNA (5  $\mu$ L). Maternal samples yielded low DNA concentrations; therefore a standard volume of template DNA was used. However, for other experiments, such as  $T_a$  optimisation, a known concentration of DNA was added. The total amount of DNA added per reaction is specified throughout each experimental chapter. For singleplex reactions the same reaction set-up as described for multiplexing was used, however the total volume of the second primer set and probe was replaced with Nuclease free Water (Applied Biosystems).

Standard curves were generated for each assay by completing a four step 10-fold serial dilution of Male gDNA (20ng/  $\mu$ L (S1), 2ng/  $\mu$ L (S2), 0.2ng/  $\mu$ L (S3) and 0.02ng/  $\mu$ L (S4)). Positive and negative control samples, as well as a NTC were included in each assay, the samples used as controls are detailed throughout. Analysis of all DNA samples, control samples and standards was performed in triplicate unless stated otherwise.

PCR cycling was carried out on a Life Technologies StepOnePlus™ qPCR System under the following conditions: 95°C for 10 mins, 45 cycles of 95°C for 15 s and optimised  $T_a$  for 1 min. Samples were held at 4°C. Data was collected during the exponential phase of PCR amplification and analysed using the StepOnePlus™ Software v2.3.

### 2.7.2 qPCR to determine critical denaturation temperature

To enable multiplexing of targets, the  $T_c$  was further optimised using the StepOnePlus Real-Time PCR (qPCR) System (Life Technologies). The qPCR reactions were set up in MicroAmp fast optical 96-well reaction plates (0.1mL) (Life Technologies). Reactions were performed in a 25  $\mu$ L solution containing 12.5  $\mu$ L of 1x TaqMan Universal PCR Master Mix (Applied Biosystems), 300nM of each primer, 250nM of each probe and 10ng DNA. Variations in the amount of DNA added have been specified through the results section of Chapter 3 (refer to 3.2). Standards and control samples used for each assay were the same as describe previously (refer to 2.8.1). All DNA samples, control samples and standards were performed in triplicate unless stated otherwise.

PCR cycling was carried out on a Life Technologies StepOnePlus™ qPCR System under the following conditions: 95°C for 10 mins, 50°C 2 mins, 45 cycles of 95°C/ $T_c$  for 15 s and optimised  $T_a$  for 1 min. Samples were held at 4°C. The  $T_d$  was altered based on results from previous experiments to determine the  $T_c$ . For each run, the lower  $T_d$  and optimum  $T_d$  (95°C) were tested on a single 96-well plate by enabling the VeriFlex™ Block on the StepOnePlus™ qPCR System. If the number of samples tested exceeded one plate, two separate plates were run, one at the optimum  $T_d$  and one at the lower  $T_d$ 's. Data was collected during the exponential phase of PCR amplification and analysed using the StepOnePlus™ Software v2.3.

### 2.7.3 Quantifying DNA targets using Ct values

To accurately determine the quantity of a particular target within a reaction it is important that the point of measurement be accurately determined. The point at which the fluorescence generated within a reaction crosses the threshold, is known as the Threshold Cycle (Ct), which is now more commonly referred to as the Quantification Cycle (Cq). To determine the Cq, first the baseline value and the threshold must be set. For many reactions the StepOnePlus™ Software automatically determined the threshold and the baseline value (3-15 cycles). However, for some experiments the threshold was manually set to ensure consistency across multiple runs for example when testing a large number of samples. The threshold levels set have been specified in the relevant sections. The baseline value was constantly kept at 3-15 cycles.

The Cq values generated from the standards by the StepOne Plus™ Software were exported to [Excel]. In [Excel] the mean Cq values of the four standards (S1-S4) were used to plot the linear standard curve. The linear trendline was selected to illustrate the equation for the regression line and the R<sup>2</sup> value. The DNA concentration of the unknowns was subsequently estimated using the following equation:

$$[\text{DNA}] = 10^{(\text{Cq}-b)/m}$$

Where Cq is the mean Cq value of each unknown, b is the Y-intercept and m is the slope of the linear regression line. The units of quantity are determined by the dilutions used to define the standard curve, which is 'ng/ μL' in this study.

The R<sup>2</sup> value illustrates how well the data fits the regression line. For all quantification experiments an R<sup>2</sup> value of >0.985 was accepted. The efficiency values were generated by the StepOnePlus™ Software. Efficiencies close to

100% illustrate that the assay is robust and reproducible. Low efficiencies can be caused by poor primer design or suboptimal conditions. Alternatively efficiencies >100% are more likely to be a result of co-amplification of non-specific product or pipetting errors in the serial dilution. For all quantification experiments an amplification efficiency of 90-110% was accepted, but for qualitative experiments lower efficiencies were tolerated (75-110%).

## **2.8 Inverse PCR**

### **2.8.1 EcoR1 Restriction Digest to obtain purified RH fragment**

The consensus *RH* 7 external primers (Table 2-3) were used to amplify the region of interest. Following PCR amplification (refer to 2.3.1) and agarose gel electrophoresis (refer to 2.4) samples were then gel extracted (refer to 2.5) to produce 285bp fragments. The 285bp *RH* fragments were then cloned to generate pure *RHD* and *RHCE* colonies (as described in 2.10).

The purified fragments were then excised from each plasmid using *EcoRI* restriction enzyme digest (Promega, Southampton, UK) (refer to 4.2.4). The restriction site and enzymatic reaction carried out is illustrated in Figure 2-3. Following restriction digest, fragments were run on a 2% agarose (w/v) gel (refer to 2.4) and products between 300-400bp were gel extracted (2.6). The extracted fragments were then ethanol precipitated; 2.5 volumes of cold 100% ethanol (Fisher Scientific) was added to 1 volume of sample followed by centrifugation at 14 000 x g for 30 mins at room temperature. The supernatant was then removed and rinsed with 70% ethanol (diluted with nuclease free water). Following re-centrifugation for 10 mins any remaining supernatant was removed and pellets were left to dry for 5 mins at room temperature. Samples were finally re-

suspended in 50  $\mu\text{L}$  of TE Buffer (10 mM Tris-HCl [pH 8.0], 1mM EDTA) and quantified using the NanoVue Plus Spectrophotometer (GE Healthcare) (refer to 2.6.1).

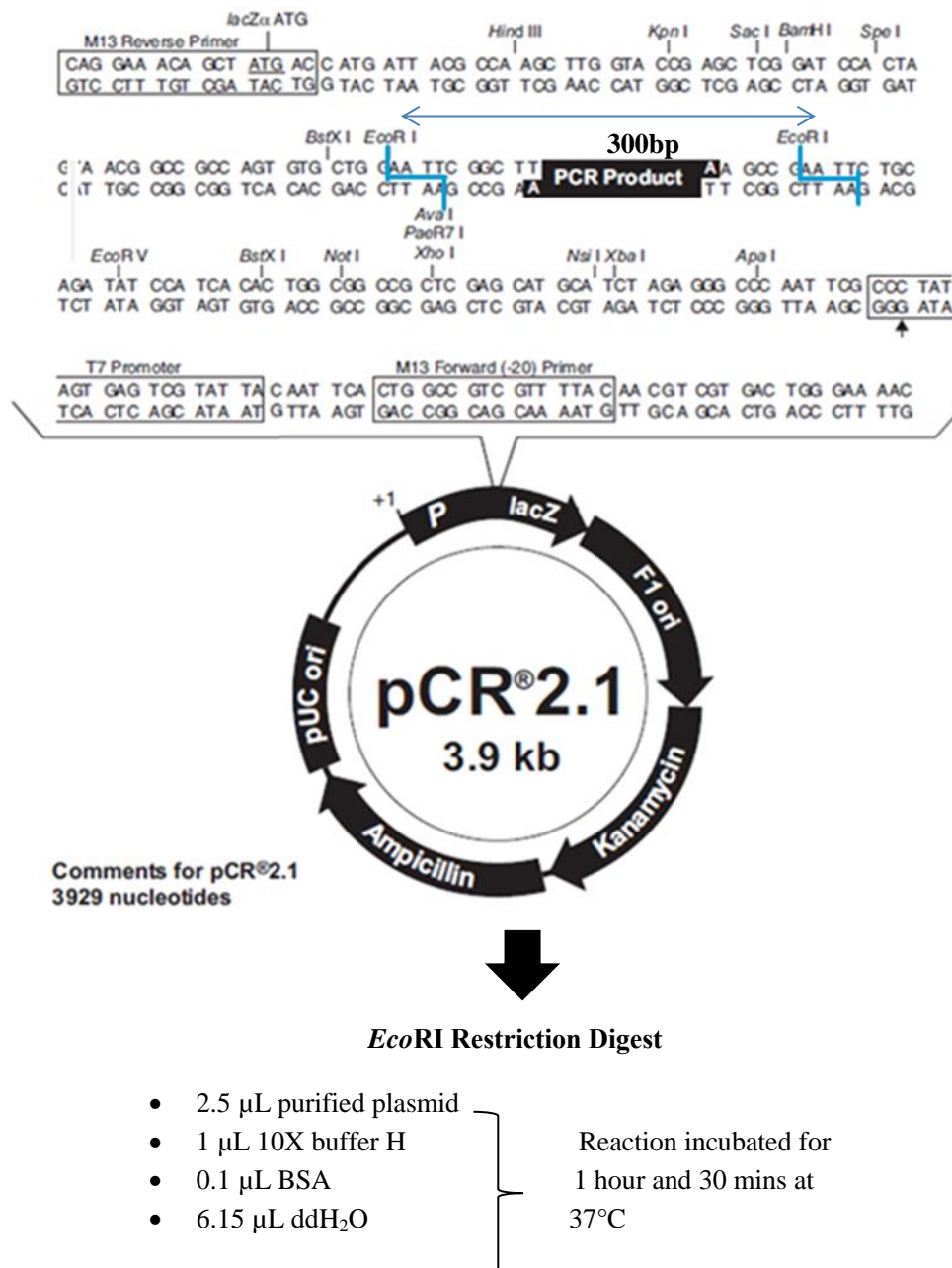


**Figure 2-3: pCR<sup>®</sup>2.1 Vector and *EcoR*I restriction site to excise region of interest containing PCR insert and produce sticky-ended fragments following cloning.** The pCR<sup>®</sup>2.1 vector incorporates the DNA sequence during transformation stage of cloning (refer to 2.10.5). This figure shows the vector and the multiple cloning site (MCS) sequence within the P lacZ region, highlighting the *EcoR*I restriction site, PCR insert

region and M13 primer sequences. Once fragments have been cloned and isolated, the DNA can be excised from the vector using restriction enzymes, such as *EcoR1*. The *EcoR1* restriction digest (shown below vector) subsequently produces fragments with 5' end overhangs of AATT, which are referred to as sticky ends (or cohesive ends) since they easily ligate to complementary sequences (or self-ligate). The combination of the *RH* external fragment (285bp) (refer to Table 2-3) and the incorporated MCS region following *EcoR1* digest (15bp) should produce a product 300bp in size.

### 2.8.2 Ligation using T4 DNA Ligase

100ng of the PCR products that were excised from the pCR®2.1 vector were subsequently ligated with T4 DNA Ligase (2 Weiss units/  $\mu$ L) (Promega, Southampton, UK) at three separate dilutions (4 Weiss units/ reaction, 2 Weiss units/ reaction and 1 Weiss unit per reaction) and incubated at 4°C overnight (O/N). Figure 2-4 illustrates the protocol carried out for fragment ligation and the three dilution reactions tested. Following O/N incubation the ligated DNA fragments were ethanol precipitated following the same procedure as described above (2.8.1).

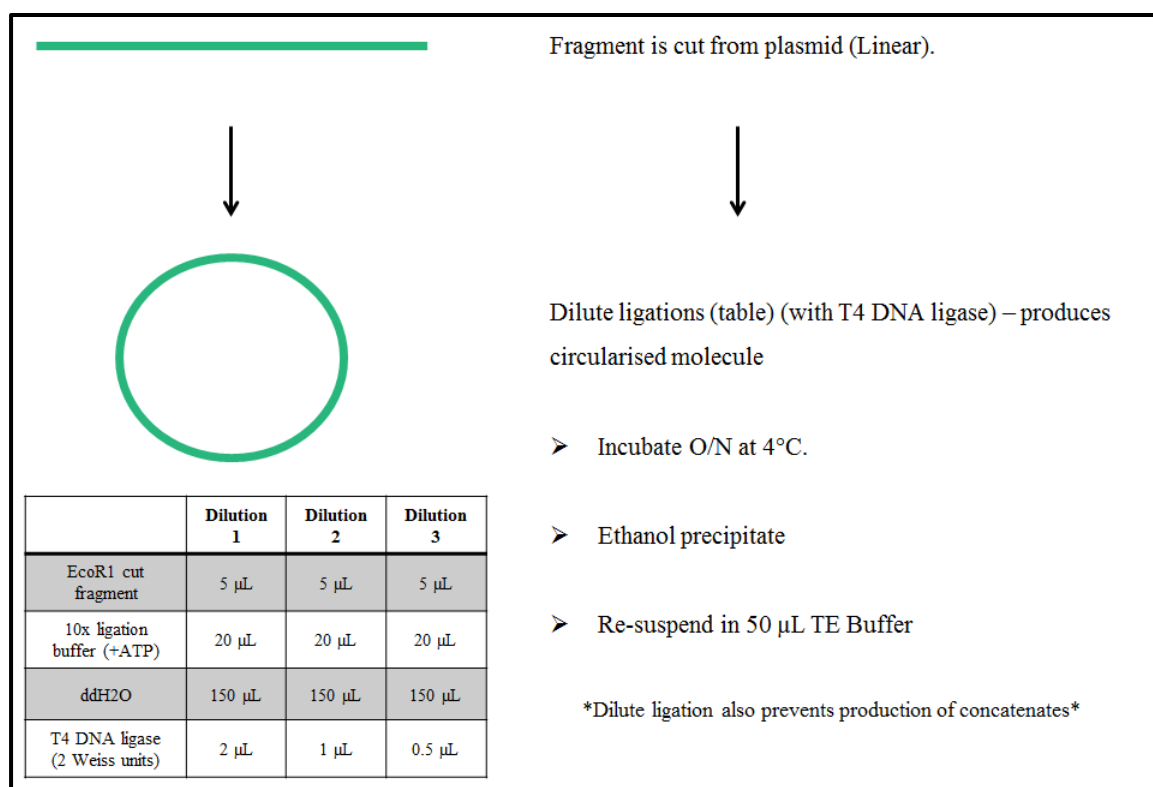


**Figure 2-4: The dilute ligation process.** Linear product generated from *EcoRI* restriction digest is hypothesised to self-ligate, rather than ligate to other fragments when the amount of T4 DNA ligase present is highly dilute. Following ligation incubation overnight (O/N), ligated product is subsequently ethanol precipitated and resuspended in TE Buffer.

### 2.8.3 Inverse PCR

The internal (inverse) primers for the *RH 7* fragment (Table 2-3) were added to 7.4 µL of 2X MyTaq DNA polymerase (Bioline, London, UK) and nuclease free water to a final concentration of 200nM each in a 40 µl total reaction volume. Follow ligation samples were not quantified and therefore a standard volume of DNA (10 µL) was added to the reaction mix to give a total volume of 50 µL. Reactions tested using IMMOLASE™ (Bioline), were set up as follows; 200nM (final concentration) of each internal inverse PCR primer (Table 2-3), 4 µL 10xImmoBuffer, 1 µL dNTP Mix (100mM), 1 µL MgCl<sub>2</sub> solution (100mM), 1 µL IMMOLASE™ made up to 50 µL with nuclease free water. A

standard volume of DNA (10  $\mu$ L) was added to the reaction mix to give a total volume of 50  $\mu$ L. Samples were run on the Veriti® 96 Well Thermal Cycler (Applied Biosystems) as follows; 95°C for 5mins (activation of 2X MyTaq); 35 cycles of 95°C for 30 s, 48°C for 1 min and 68°C for 2 mins. The samples were then subsequently run on a 2% agarose (w/v) gel (refer to 2.4) to check that amplification of the ligated fragments yielded a linear product ~230bp in size (Figure 2-5). Figure 2-5 also illustrates the sequence that should have been generated from the inverse PCR following successful restriction digest and ligation when using cloned Rh fragments. PCR products were quantified using the NanoVue Plus Spectrophotometer (refer to 2.7.1).



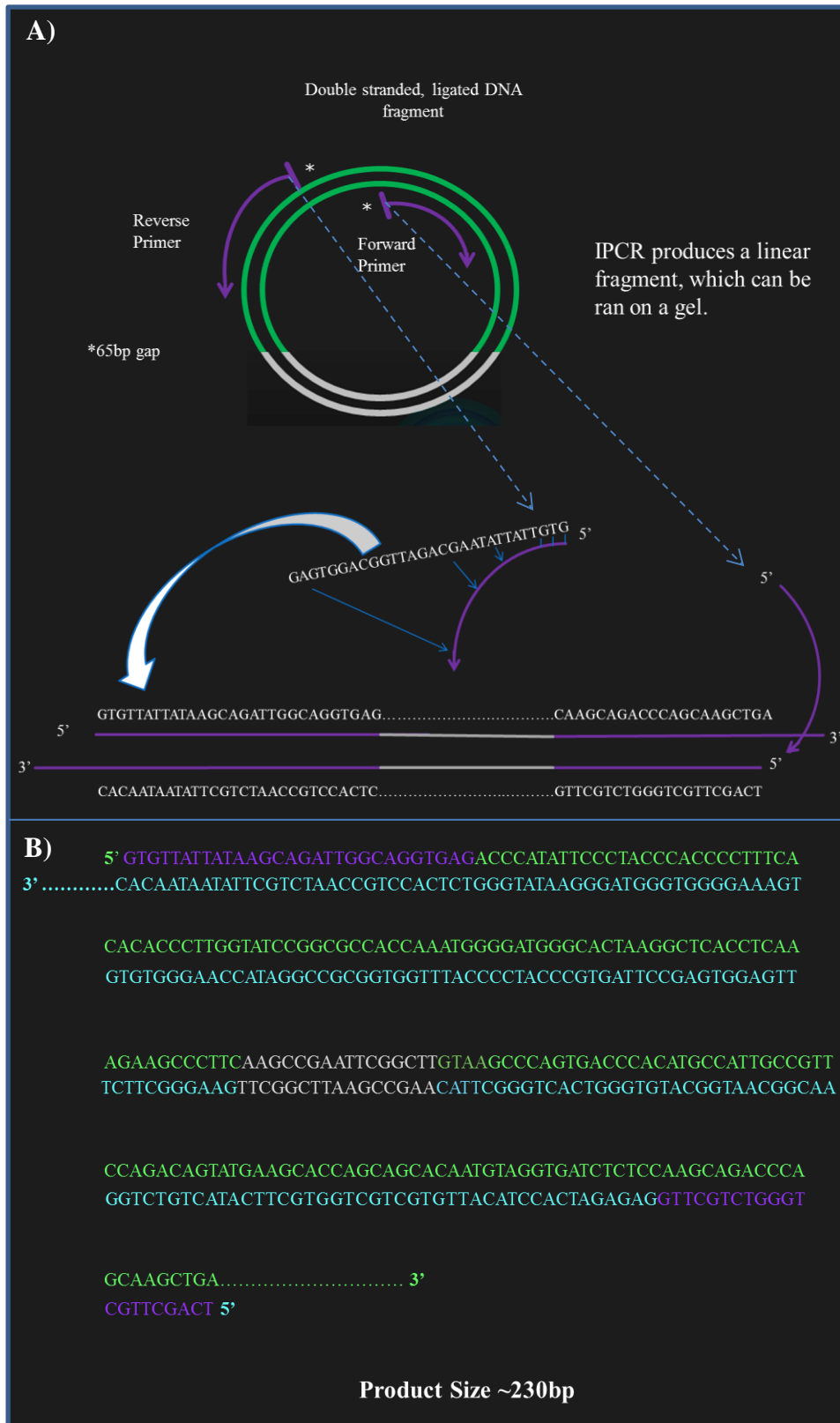


**Figure 2-5: Hypothesised sequence following restriction digest (*EcoRI*), ligation (T4 DNA polymerase) and inverse PCR (internal primers Table 2-3). A) Binding of the forward and reverse inverse PCR primers (*RH* exon 7) to the circularised product. B) 5' –**

3' nucleotide sequence that should be generated for each forward and reverse inverse PCR primer (indicated in purple). The 5'-3' Sequence generated by the forward primer is the bottom sequence, and the 5'-3' sequence generated by the reverse primer is the top sequence. The sequence region highlighted in white indicates where the sticky-ends produced by the *EcoRI* restriction digest should have self-ligated. The grey region illustrated part of the pCR®2.1 Vector (Figure 2-3) that should also be included in generated sequence.

#### 2.8.4 Sequencing

The gel extracted products (refer to 2.5) generated by inverse PCR, were consequently diluted to 10 ng/  $\mu\text{L}$  and sent for sequencing with 2  $\mu\text{L}$  of forward primer to Eurofins Genomics (Ebersberg, Germany) as described in section 2.10.7.

### 2.9 Droplet digital PCR (ddPCR)

#### 2.9.1 ddPCR reaction

The ddPCR reactions were performed in a 20  $\mu\text{L}$  solution containing 10 $\mu\text{l}$  ddPCR™ Supermix for Probes (Bio-Rad, Herfordshire, UK), 300nM primers, 250nM probes and 5  $\mu\text{L}$  DNA/ NTC sample in individual RNase-free PCR tubes (0.2 mL) (Life Technologies). The recommended dynamic range of DNA for the QX100™ Droplet Digital™ PCR System is from 1 to 120 000 copies/ 20  $\mu\text{L}$  reaction. For control samples such as Male and Female gDNA (2.2.1) or *RHD* positive and *RHD* negative samples (2.2.2) 30ng of DNA was added per reaction (equivalent of ~ 9 000 copies or 18 000 copies per haploid and diploid expressed genes). Alterations in the amount of DNA added for optimisation experiments are noted throughout each experimental chapter. Due to the low proportions of cffDNA circulating in maternal plasma, samples were not diluted and

a standard volume of template DNA (5  $\mu$ L) was added per 20  $\mu$ L reaction (range: ~150 to 300 copies/ 20  $\mu$ L reaction for Streck BCT samples and ~10 000 to 40 000 copies/ 20  $\mu$ L reaction for EDTA samples). In addition to control samples and maternal samples, NTCs were included in every assay to check for contamination. Each sample was tested in duplicate unless stated otherwise. The reaction mix was vortexed (15 s) and briefly centrifuged before droplet generation.

### 2.9.2 Droplet generation

The individual 20  $\mu$ L PCR reactions were transferred to the centre row of a DG8™ cartridge (186-4008, Bio-Rad) for use with the QX100™ Droplet Digital™ PCR System (Bio-Rad), which is held in place by the DG8™ Cartridge Holder (186-3051, Bio-Rad) (Figure 2-6). Any unused wells on the cartridge were filled with 1x ddPCR buffer control (186-3052, Bio-Rad). Once eight samples per cartridge had been loaded, 70  $\mu$ L of QX100 Droplet Generator Oil for Probes (186-3005, Bio-Rad) was loaded into the bottom row of the cartridge (Figure 2-6). The cartridge was then sealed using DG8™ Gaskets (186-3009, Bio-Rad) and loaded onto the QX100™ Droplet Generator (186-3002, Bio-Rad). Using an oil emersion approach the sample were drawn through the cartridge under a vacuum where ~20 000 1 nL droplets were formed in just under 3 mins/ eight samples. The generated droplets (40  $\mu$ L total volume) were then transferred to an Eppendorf Twin Tec PCR 96-well Plate (Sigma-Aldrich, Dorset, UK) by gentle pipetting using a multi-channel pipette. This process was repeated until all 20  $\mu$ L PCR reactions had been converted to droplets (ranging from 11,000 to 15,000 droplets/ reaction) in batches of eight and loaded onto the 96-well plate. The plate was then sealed using a Pierceable Foil Heat Seal (181-4040, Bio-Rad) on the PX1™ PCR Plate Sealer (181-4000, Bio-Rad).



**Figure 2-6: Loaded DG8™ cartridge for QX100 system.** A) Center row for 20  $\mu$ L PCR reaction. B) Bottom row for 70  $\mu$ L of Droplet Generation Oil. C) Collection well for droplet generation.

### 2.9.3 ddPCR amplification

The 96-well plate was subsequently loaded onto the C1000 Touch™ Thermal Cycler (185-1148, Bio-Rad) and cycling conditions were as follows; 95°C for 10 mins, 40 cycles of 95°C for 30 s and optimised  $T_a$  for 1 min, after which a final 98°C step for 10 mins was carried out (as recommended by Bio-Rad). Samples were held at 10°C. These cycling conditions were also used for COLD-PCR experiments; however, in addition to the control  $T_d$  (95°C), lower  $T_d$ 's were also tested (for temperatures tested see section 3.2.5). A 2.5°C/s ramp rate was used to ensure each droplet reached the correct temperature for each step during cycling.

### 2.9.4 Analysing droplets following PCR amplification

Experimental set up was created using the QuantaSoft™ Software v1.2 (Bio-Rad) following manufacturer's instructions. The software was used to designate the experiment type, sample name and which gene region corresponds to each fluorescent channel (FAM and HEX). All samples were tested using absolute concentration (ABS) analysis.

Following amplification samples were loaded onto the QX100™ Droplet Reader (186-3003, Bio-Rad). The droplet reader and QuantaSoft software were then used to count PCR-positive and PCR-negative droplets to provide ABS of target DNA. QuantaSoft software automatically determined the threshold above which droplets were considered positive. However, the threshold was manually adjusted using the 1D-amplitude plot and 2D-amplitude plot on a well-by-well basis for singleplex and multiplex reactions, respectively, unless stated otherwise. Thresholds were determined when intermediate droplets between two clusters did not alter the calculated concentration (Miotke *et al.*, 2014). Figure 2-7 illustrates a 2D amplitude plot and the manual thresholds set for both the FAM (*SRY* taken from Lo *et al.* (1997, ) and HEX (Xp22.3) signal for a Male gDNA sample (30 ng/ 20  $\mu$ L reaction).

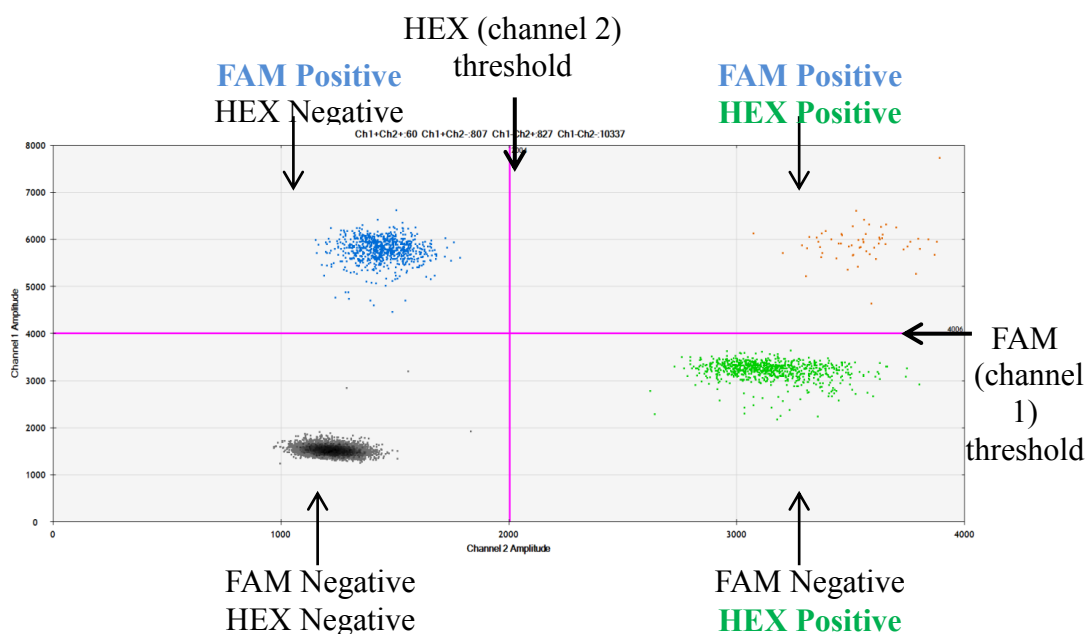


**Figure 2-7: 2D-Amplitude plot for male gDNA.** Sample illustrated negative droplets (grey), *SRY*-FAM positive droplets (blue), Xp22.3-HEX positive droplets (green) and dual positive droplets (Orange). The diagram also illustrated the threshold set manually for the *SRY*-FAM (channel 1) amplitude (horizontal) and the Xp22.3-HEX (channel 2) amplitude (vertical).

Target concentration is estimated using Poisson algorithm to fit the fraction of positive droplets, in order to determine the ABS concentration (Figure 2-8) (Poisson 95% confidence interval). This is automatically calculated by the QuantaSoft software using the following equation:

$$\text{Number of Molecules} = -\ln [(N - n)/N] \times N$$

Where  $N$  is the total number of wells counted and  $n$  is the number of target or reference positive wells.

Results are automatically converted from copies of target in 20 $\mu$ L reaction to copies/ $\mu$ L using the Poisson distribution. Poisson correction statistics are required since reactions with higher DNA concentrations ( $\geq 2$  copies per positive droplet) express a higher number of targets than number of positive droplets. However, the number of positive droplets is equal to the number of targets for samples expressing low concentrations of DNA (1 copy per positive droplet).

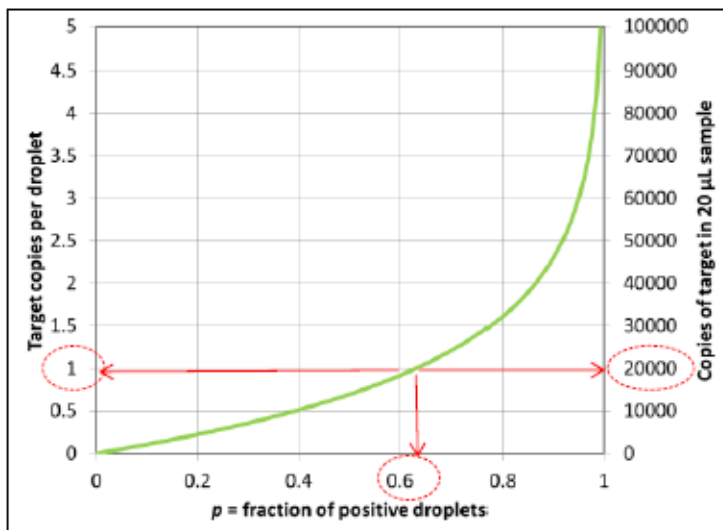


**Figure 2-8: Estimating target concentration using Poisson distribution to ddPCR data.** The curve represents the relationship

between the fraction of positive droplets, the number of target copies per droplet and the number of copies of target in a 20  $\mu$ L reaction.

The cfDNA fractions in maternal samples were calculated based on the concentrations (copies/  $\mu\text{L}$ ) of the target and reference genes generated by ddPCR. For single-copy targets (*SRY*, *RHD5* and *RHD7*) expressed by the fetus only, the following equation was used:

$$\left( \frac{2 \times \text{Target-FAM (copies/ } \mu\text{L})}{\text{Total copies/ } \mu\text{L}^*} \right) \times 100$$

Since we assume that there are 30 copies (Barrett *et al.*, 2012) of *DYS14* (where amplicon is located) on the *TSPY1* gene, the following equation was used for this multiple-copy target:

$$\left( \frac{2 \times (\text{Target-FAM (copies/ } \mu\text{L}) / 30)}{\text{Total copies/ } \mu\text{L}^*} \right) \times 100$$

\*Target-FAM (copies/  $\mu\text{L}$ ) + Reference-HEX (copies/  $\mu\text{L}$ ).

For samples tested in duplicate, the positive and negative droplets from both wells were combined by selecting the merged button. This enabled data to be analysed together as a single experiments, increasing the number of droplets per sample. In addition, the ratio of the target gene (FAM)/ reference gene (HEX) was calculated for multiplex experiments (FAM copies/  $\mu\text{L}$  / HEX copies/  $\mu\text{L}$ ).

### 2.9.5 Statistical analysis

Statistical analysis for comparing sample variation was carried out using the Mann Whitney U Test in SigmaPlot Version 12.5 and significance was accepted at  $p < 0.05$ . To

compare the expected and observed fractional abundance (%) generated in Chapter 6, the Chi-Squared test was carried out in [Excel].

## 2.10 Cloning

### 2.10.1 Producing PCR products

External primers were used to generate PCR fragments for insertion into the pCR<sup>®</sup>2.1 vector using the TOPO TA Cloning<sup>®</sup> kit with One Shot<sup>®</sup> TOP10 Chemically Competent *E. coli* (K2040-01, Invitrogen, Carlsbad, CA) following manufacturer's instructions. Conventional PCR experiments using external primers for; 1) the D21S1890 STR 229bp fragment (Table 3-1) and 2) the *RH7* 285bp fragment (Table 2-4), were carried out as described (2.3.1), but using higher final concentrations (500nM) of each external primer.

Following PCR amplification, PCR products were run on a 2% agarose (w/v) gel (refer to 2.4) and gel extracted using the QIAquick Gel Extraction Kit (Qiagen) (refer to 2.5). Fragments were then quantified using the NanoVue Plus Spectrophotometer (GE Healthcare) (refer to 2.6.1).

### 2.10.2 Producing Luria Bertani Media (LB Media)

The LB media was produced by recipe shown in Table 2-4. Once dissolved the solution was autoclaved and kept at room temperature until required.

**Table 2-4: Recipe for LB Media.**

Tryptone	5g
Yeast Extract	2.5g
NaCl	2.5g
Distilled water	Up to 500 mL



### 2.10.3 Producing Luria Bertani Agar Plates (LB Plates)

To produce LB Agar (LA), the same recipe was used (Table 2-4) with the addition of agar to a final concentration of 1.2%. The solution was then autoclaved for sterilization. If the LA had re-set, the mixture was re-heated in a boiling water bath for 1 hour (~100°C). Once the LA had cooled to 55°C (also using a water bath), kanamycin (Sigma-Aldrich) was added at a concentration of 50µg/ mL. Working near an opened Bunsen burner, ~20 mL of the LA containing kanamycin was added per 10cm polystyrene Petri dish (~25 plates in total/ 500 mL). Each plate was covered with lids and swirled to evenly distribute the LA-kanamycin mix. Plates were then left to cool for around 30-60 mins. Once solidified plates were inverted to avoid condensation on the agar and stored at 4°C O/N.

For Blue/White colony screening, 40 µL of 5-bromo-4-chloro-3-indolyl-β-D-galactopyranoside (X-gal) (Sigma-Aldrich) (which was produced from dissolving two tablets into 500 µL of Dimethylformamide (DMF) (Fisher Scientific)), was spread across the top of each Agar plates under aseptic conditions. Plates were then left to dry for a minimum of 30 mins before adding transformed competent cells (refer to 2.10.5).

### 2.10.4 Cloning into pCR<sup>®</sup>2.1

The following formula was used to estimate the amount of PCR product needed to ligate with 50 ng of pCR<sup>®</sup>2.1 vector:

$$X \text{ ng PCR product} = \frac{(\text{Y bp PCR product}) (50\text{ng pCR}^{\text{®}}2.1 \text{ vector})}{(\text{size in bp of the pCR}^{\text{®}}2.1 \text{ vector: } \sim 3900)}$$

Where X ng is the amount of PCR product of Y base pairs to be ligated for a 1:1 (vector: insert) molar ratio.

To perform the cloning reaction, 1  $\mu\text{L}$  of fresh, diluted (see above equation), PCR product was added to 1  $\mu\text{L}$  of 10X ligation buffer, 2  $\mu\text{L}$  of pCR<sup>®</sup>2.1 vector (25ng/  $\mu\text{L}$ ) and 1  $\mu\text{L}$  of T4 DNA ligase (4.0 Weiss units) and made up to a total volume of 10  $\mu\text{L}$  using nuclease free water. All reagents (except nuclease free water and PCR product) were supplied in the TA Cloning<sup>®</sup> Reagents (Invitrogen). Reactions were gently mixed and left O/N at 14°C. The map and features of the linearized pCR<sup>®</sup>2.1, within the *LacZ $\alpha$*  gene (1-545 bases), are illustrated in Figure 2-9.

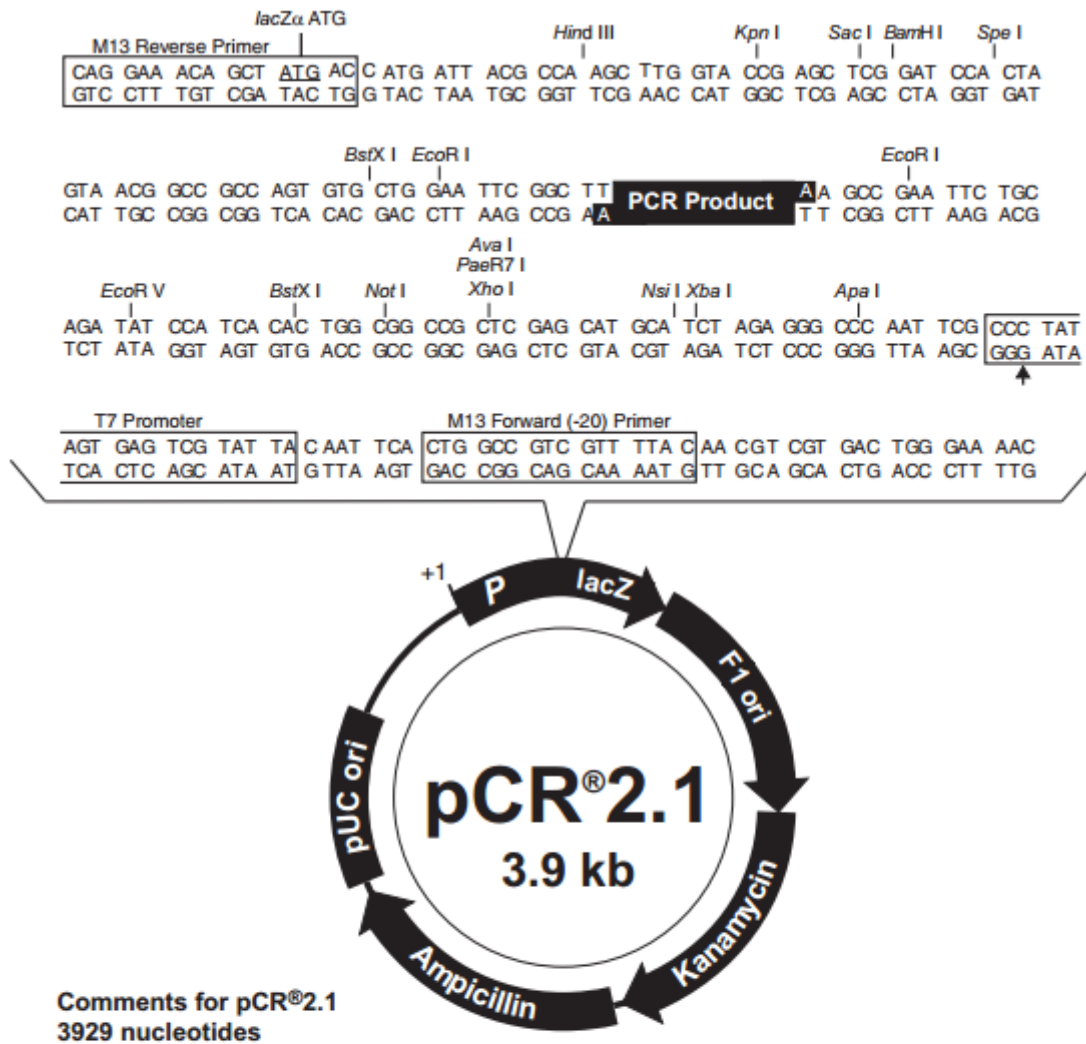


**Figure 2-9: Map of the linearized pCR<sup>®</sup>2.1 multiple cloning site (MCS).** The map highlights key features of the MCS including restriction enzyme sites, M13 primer binding sites and the T7 promoter site (Taken from Invitrogen TA Cloning<sup>®</sup> Kit Manual, Version V, April 2004). The complete sequence of the pCR<sup>®</sup>2.1 plasmid is available from the Invitrogen website ([www.invitrogen.com](http://www.invitrogen.com)).

### 2.10.5 Transforming competent cells

Once fragment was ligated into the pCR<sup>®</sup>2.1 vector, the construct was ready for transformation into competent *E.coli*. One Shot<sup>®</sup> cells (K2040-01). Before carrying out transformation, a water bath was set to 42°C and the S.O.C. medium (Super Optimal broth with Catabolite repression; 2% tryptone, 0.5% yeast extract, 10 mM NaCl, 2.5 mM KCl, 10 mM MgCl<sub>2</sub>, 10 mM MgSO<sub>4</sub>, and 20 mM glucose) (Life Technologies) was equilibrated to room temperature. S.O.C. medium is used to obtain maximum transformation efficiency of *E.coli*.

After a brief centrifugation, 2 µL of each ligation reaction was added to 50 µL vials of frozen One Shot<sup>®</sup> TOP10 Competent Cells (Invitrogen) (one for each transformation) and were gently mixed by pipetting. The vials were incubated on ice for 30 mins, and the remaining ligation reaction was stored at -20°C. The competent cells were then heat shocked for 30 s at 42°C to create pores in the competent cells and allow the supercoiled plasmid DNA to enter. Once the plasmid had been taken up by the cells, 250 µL of S.O.C. medium was added to each vial, which were then placed in a shaking incubator and shaken horizontally at 37°C for 60 mins at 225rpm. Consequently, 25 µL and 100 µL of each vial was spread across LA plates containing X-gal (refer to 2.10.3) and kanamycin (50 µg/ mL) (2.10.3) using aseptic conditions. The plate were then incubated O/N at 37°C, followed by 2-3 hours at 4°C to allow for proper colour development.

### 2.10.6 Colony PCR

Conventional PCR using M13 forward (5'-GTAAAACGACGGCCAGT-3') and reverse (5'AACAGCTATGACATG-3') primers was used to analyse positive transformants. Multiple white colonies and a single blue colony (negative control) were selected and resuspended in 300 µL of nuclease free water and then heated on a heat block at 95°C for

5 mins. Primers were used at a final concentration of 100 nM, the PCR reaction was carried out using IMMOLASE™ DNA Polymerase (Bioline, London, UK) and conditions are shown in Table 2-5. The cycle sequence was run on the Veriti® 96 Well Thermal Cycler (Applied Biosystems) as follows: 95°C for 10 mins followed by 40 cycles of 94°C for 30 s, 56°C for 30 s, then 72°C for 60°C. Succeeding 40 cycles, there was a final elongation step at 72°C for 5 mins before holding samples at 4°C. PCR samples were then run on a 2% agarose (w/v) gel (refer to 2.4) to check for product size ~300bp.

**Table 2-5: PCR conditions for IMMOLASE™ PCR Polymerase.**

10x ImmoBuffer	2 µL
100mM dNTP Mix	0.4 µL
50mM MgCl <sub>2</sub> Solution	1 µL
Forward primer (10 µM)	0.25 µL
Reverse primer (10 µM)	0.25 µL
IMMOLASE™	0.3 µL
ddH <sub>2</sub> O	15.8µL
Plasmid DNA*	5 µL

dNTP; deoxynucleotide mix (containing all four nucleotide bases; A, T, G, C)\*Suspended in nuclease free water

#### 2.10.7 Isolation of Plasmid DNA

Multiple white colonies were selected from each plate for plasmid isolation and restriction analysis. Each colony was resuspended in 5 mL LB Medium (2.10.2) containing 50 µg/ mL kanamycin and incubated O/N at 37°C at 180rpm (horizontally shaken). 2 mL of the bacteria/ LB medium/ kanamycin mix was pipetted into a 2 mL Eppendorf tube and centrifuged at 6 800 x g for 3 mins at room temperature (15-25°C). The supernatant was carefully removed using a 1 mL pipettor, leaving the bacterial pellet. The plasmid DNA was then purified using the QIAprep Spin Miniprep Kit (Qiagen) and a

microcentrifuge, following manufacturer's instructions. Briefly, the pelleted bacterial cells were resuspended in 250  $\mu$ L Buffer P1 and transferred to a microcentrifuge tube, ensuring no cell clumps remained. Buffer P2 (250  $\mu$ L) was added and mixed gently by inverting tube 10 times, which turned the solution a homogenous blue colour after enough inverting. Buffer N3 (350  $\mu$ L) was immediately added and mixed by inverting 10 times to avoid localised precipitation. Finally, the resuspended bacterial cells were centrifuged at 18 000 x g for 10 mins to produce a compact white pellet. The supernatant, which contained the precipitated plasmid DNA, was then removed and placed in a QIAprep spin column (Qiagen) and centrifuged for 30-60 s at 20 000 x g. Once centrifuged the flow through was discarded and the spin column was washed twice using buffer PB with an additional 1 minute centrifugation to remove any residual wash buffer. The QIAprep column was then placed in a clean 1.5 mL microcentrifuge tube. Finally 50  $\mu$ L of Buffer EB (10 mM Tris-Cl, pH 8.5) was added and left for 1 minute before the purified plasmid DNA was eluted by centrifugation at 20 000 x g for 1 min. Samples were then quantified (refer to 2.6.1) ready for dilution and sequencing.

Once the correct clones had been identified following sequencing, the original colony was re-streaked on LB plates containing 50  $\mu$ g/ mL kanamycin. A single colony was then isolated and inoculated into 2 mL of LB Medium containing 50  $\mu$ g/ mL kanamycin. 850  $\mu$ L of culture was mixed with 150  $\mu$ L of sterile glycerol and purified using the QIAprep Spin Miniprep Kit (Qiagen) (see above). Samples were eluted in 50  $\mu$ L Buffer EB (Qiagen) and stored at -80°C.

## 2.10.8 Sequencing

### *2.10.8.1 Out of house sequencing*

Purified plasmid DNA samples were sent to Eurofins Genomics (Ebersberg, Germany) for sequencing (refer to 2.10.7). Sequencing was carried out using internal oligonucleotides for both the D21S1890 STR (Table 3-1) and the *RH7* amplicons. Samples were first diluted to 10 ng/  $\mu\text{L}$  and then 15  $\mu\text{L}$  of each diluted sample was added to 2  $\mu\text{L}$  of internal forward primer and another 15  $\mu\text{L}$  was added to 2  $\mu\text{L}$  of internal reverse primer in separate 1.5 mL Eppendorf<sup>®</sup> safe lock microcentrifuge tubes (Sigma-Aldrich). All samples sent for sequencing were labelled with prepaid barcodes (Eurofins MWG Operon) and the barcode serial numbers were recorded with the corresponding sample. Results were analysed using ClustalW2 Multiple Sequence Alignment (<http://www.ebi.ac.uk/Tools/msa/clustalw2/>) and GeneDoc Software (v2.7.000) for alignment against expected sequence (Figure 2-3).

### *2.10.8.2 In house sequencing*

For the *RH* fragments (4.2.3), colonies that produced a band between 400 to 500bp were sequenced in house using the BigDye<sup>®</sup> Terminator v3.1 Cycle Sequencing Kit (Life Technologies) according to manufacturer's instructions by Dr Michele Kiernan. Briefly, 1.5  $\mu\text{L}$  of amplified product (10ng/  $\mu\text{L}$ ) was added to 4  $\mu\text{L}$  of Big Dye Terminator Mix, 3.5  $\mu\text{L}$  of Sequencing Buffer and 1  $\mu\text{L}$  of M13 forward primer (5pmol/  $\mu\text{L}$ ), made up to 20  $\mu\text{L}$  with nuclease free water. This was carried out for all samples IN A 96-well plate. Consequently, the plate was run on the Veriti<sup>®</sup> 96 Well Thermal Cycler (Applied Biosystems) under the following conditions; 96°C for 1 min, 35 cycles of 96°C for 10 s, 50°C for 5 s and 60°C for 4 mins, followed by 1 cycle at 60°C for mins and a 10°C hold step. The 20  $\mu\text{L}$  PCR reaction was then transferred to 1 clean 1.5 mL microcentrifuge

with 5  $\mu$ L of 125mM EDTA (pH8) and 60 $\mu$ L of ethanol. The reaction was then incubated at room temperature for 20 mins and centrifuged at top speed on the benchtop microcentrifuge at 4°C for 20 mins. The pellets formed, were washed with 100  $\mu$ L 70% ethanol and air dried for 10 mins. Finally samples were resuspended in 15  $\mu$ L HiDi Formamide and transferred to a 96-well sequencing plate for running on the Applied Biosystems ABI 3130 Genetic Analyzer (Applied Biosystems).

The data generated for each colony was downloaded as a .ABI file and the sequences generated were analysed using BioEdit Sequence Alignment Editor Software (Ibis Biosciences, CA, USA). Base calls recorded as 'N' were analysed and if a clear nucleotide was visible, the base was manually updated using the BioEdit Software. The sequence for each colony was individually aligned to the *RHD* and *RHCE* exon 7 external 285bp product using ClustalW2 Multiple Sequence Alignment (<http://www.ebi.ac.uk/Tools/msa/clustalw2/>) and GeneDoc Software (v2.7.000). The 17 SNPs between *RHD* and *RHCE* within this 285bp were used to determine the isolated gene fragment of each colony. The unpurified PCR products of colonies that were unsuccessfully sequenced in house were sent to Eurofins Genomics (Ebersberg, Germany) for sequencing (see above).



## **2.11 Pippin Prep™ size selective enrichment**

### **2.11.1 Pippin prep™ size selective gel electrophoresis**

DNA samples extracted from maternal samples (refer to 2.1.5) and non-maternal samples (2.1.2) were quantified using the Qubit® dsDNA HS assay kit (2.6.2) and subsequently loaded onto the Pippin Prep™ DNA Size Selection System (Sage Science, MA, USA) following manufacturer's instructions (Operation Manual Software v.6.00). Maternal samples were not diluted and based on individual sample concentration; 30-300ng of DNA was loaded per reaction well. Non-maternal samples were diluted and 500-1000ng of DNA was loaded per reaction well for maximum elution. Pippin Prep samples were run in pre-cast 2% agarose (w/v) gel cassettes, pre-stained with ethidium bromide (Sage Science). Once the gel cassette had passed the continuity test, the samples, which were pre-prepared with Pippin Prep loading solution (3:1) (Sage Science, Inc.), were loading into individual sample wells. Each cassette contained 5 wells, which enabled four samples plus the Marker B (100-600bp) (Sage Science) to be loaded per run. Following the LED calibration, samples were run using the Cassette 2% Marker B Overflow Detection Protocol and target size selection was set at 150bp (100bp start, 200bp end). The elution timer records the length of the time of the elution. When the elution is complete the elution timer will show the elapsed time of elution (~60 mins) and the elution indicator light will turn green on the lane status panel. Samples collected in the elution modules were recovered in a fixed volume of 40µL in TE buffer.

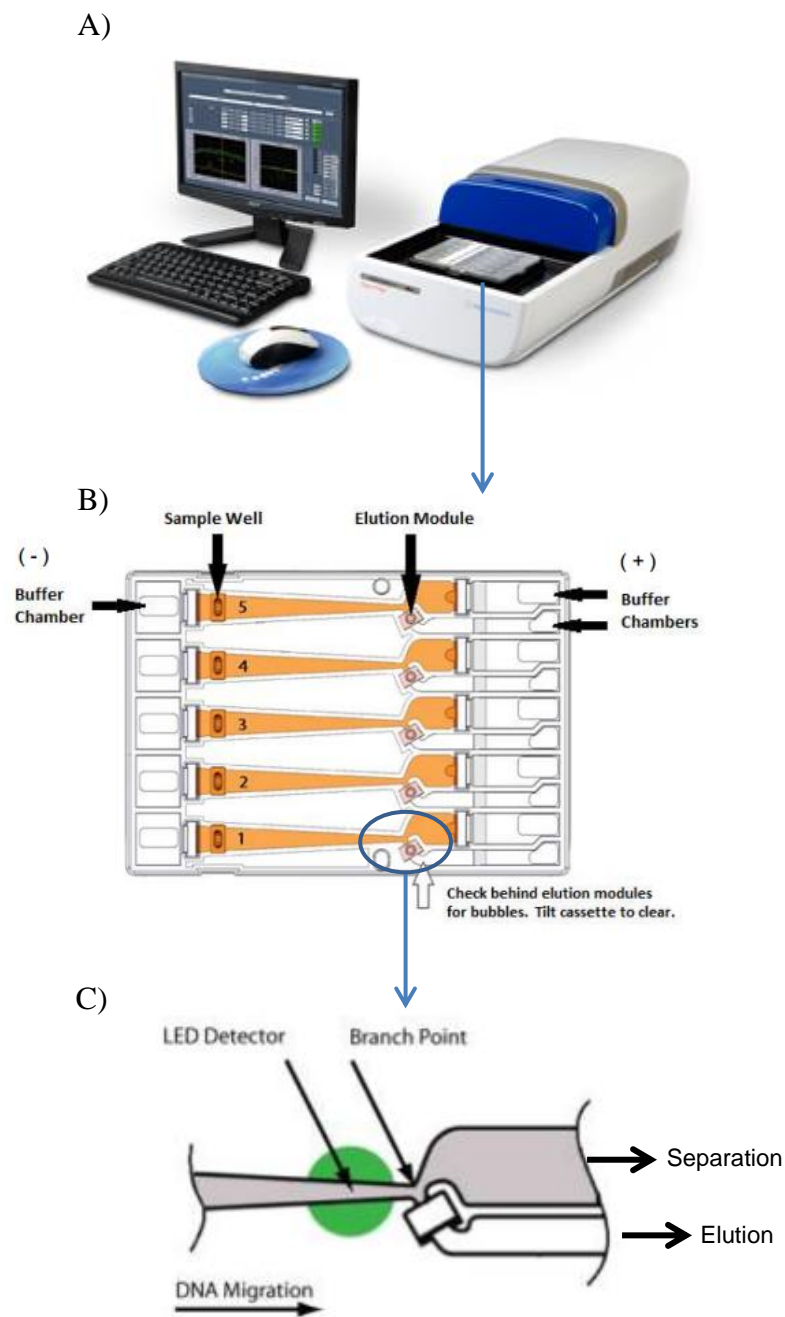


**Figure 2-10: Pippin Prep™ Gel Electrophoresis.** A) Image of the Pippin Prep™ DNA Size Selection System. B) A schematic diagram of a Gel Cassette. C) An illustration showing the DNA migration and the branch point between the separation and elution channels, which are downstream from the detector position (LED Detector). Following gel electrophoresis 40  $\mu$ L of eluted samples can be collected from the elution module (B) for subsequent analysis.

### 2.11.2 Analysis of Pippin Prep™ enrichment

Both the original sample aliquots and elution of each sample following Pippin Prep gel electrophoresis were analysed on the Agilent 2100 Bioanalyzer system (see 2.6.3). No purification step was carried out prior to run on the Bioanalyzer to preserve the amount of size-selected cfDNA. However, this resulted in unobtainable data for some samples following the Bioanalyzer run. To determine if enrichment had occurred, regardless of Bioanalyzer data, both sample aliquots were analysed using qPCR (see 2.7.1) and ddPCR (2.9) for the initial experiment. However, all consequent experiments for determining the proportion of selective enrichment were conducted using only the ddPCR platform for Y-specific targets (*TSPY1* and *SRY*) and *RHD*-specific targets (*RHD* exon 5 and *RHD* exon 7) (refer to chapter 6).

### **2.12 Analysis of T21 spike samples using ddPCR**

To determine the minimal cfDNA fraction required to identify a T21 fetus, T21 gDNA (2ng/  $\mu$ L) was used as psfDNA and spiked into male gDNA (2ng/  $\mu$ L), female gDNA (2ng/  $\mu$ L) or individual Disomy 21 (D21) cfDNA samples (2.1.2) from 50% down to 1% (assay dependent). Consequently, the spiked samples, 100% male/ female gDNA/ D21 cfDNA (2ng/  $\mu$ L), 100% T21 gDNA (2ng/  $\mu$ L) and non-template controls were run in quadruplets on the ddPCR platform (2.9) for analysis. The mean ratio of each T21 spiked-sample was analysed against the mean ratio of the D21 control to determine if significant differences were obtained using the comparative T-Test on SigmaPlot Version 13.0. Significance was accepted at  $P < 0.05$ .

## Chapter 3

Selective enrichment of shorter psfDNA fragments by  
co-amplification at lower denaturation temperature-  
polymerase chain reaction (COLD-PCR) in pseudo-  
maternal samples

### 3.1 Introduction

The presence of cffDNA within the maternal circulation has enabled routine NIPD of fetal sex and *RHD* genotype in many laboratories worldwide using qPCR analysis (Finning *et al.*, 2008; Avent & Chitty, 2006; De Haas *et al.*, 2012; Banch Clausen *et al.*, 2014). More recently, due to a decline in costs of NGS, the application of NIPT for fetal aneuploidy is also more readily available. NIPT for fetal aneuploidy is only offered privately as a secondary screening tool for high risk pregnancies and at present invasive-testing is still required for a definitive diagnosis (Hill *et al.*, 2014; Morris *et al.*, 2014; Quezada *et al.*, 2015). Despite the high levels of sensitivities associated with qPCR for fetal sex/*RHD* determination (>95.7%) and MPS for aneuploidy detection (>99%), it has been identified that both platforms can produce false negative or inconclusive results if low levels of cffDNA are present (<4%) (Finning *et al.*, 2008; Ashoor *et al.*, 2013; Porreco *et al.*, 2014).

The disparity in fragmentation between maternal cfDNA and cffDNA instituted the development of research into the application of size selective purification to improve detection and quantification of dilute fetal DNA fragments (refer to 1.3.3.5). One size-selective enrichment strategy described was COLD-PCR (Li *et al.*, 2008; Galbiati *et al.*, 2011), which selectively amplifies minority alleles from a background of wild-type alleles, based on the principle that even a single nucleotide difference will alter the critical denaturation temperature ( $T_c$ ). The  $T_c$  is defined as the optimum dissociation factor, at which the selective amplification of minority alleles is enriched. The COLD-PCR results illustrated exclusive amplification and isolation of the mutants from the wild-type, highlighting the capability of selective enrichment through sequence dissimilarities. Li *et al.* (2008) also highlighted in their discussion the possibility of the application of

COLD-PCR for selective amplification of other minority alleles such as cffDNA circulating in maternal plasma.

Macher et al. (2012) focused on the application of COLD-PCR in conjunction with HRM analysis for the NIPD of multiple endocrine neoplasia type 2A (MEN2A). Fetuses with MEN2A were non-invasively diagnosed by the presence of the C634Y mutation in the maternal plasma. The results illustrated 100% accuracy since all pregnancies carrying a fetus with the C634Y mutation matched the melt-curve analysis of the positive control. Presence of mutation was also confirmed by sequencing of the COLD-PCR amplified product. However, for detection of fetal aneuploidy mutations cannot be targeted due to sequence similarities, instead accurate quantification is required for detection of chromosomal imbalance.

Rather than exploiting SNPs for separation, it may be possible to selective enrich shorter cell-free DNA fragments (fetal and tumour) using the same approach. Figure 3-1 illustrates the proposed application of selective amplification using COLD-PCR. We hypothesized that the shorter cffDNA may be selectively amplified at the  $T_c$ , whereas larger maternal cfDNA fragments will remain partially double-stranded and therefore will not be amplified. By increasing the overall proportion of cffDNA it may be possible to determine allelic-imbalances using qPCR or dPCR platforms, which are considerably cheaper (~10-fold) than predominant MPS approaches currently available (refer to 1.3.3.3.2).

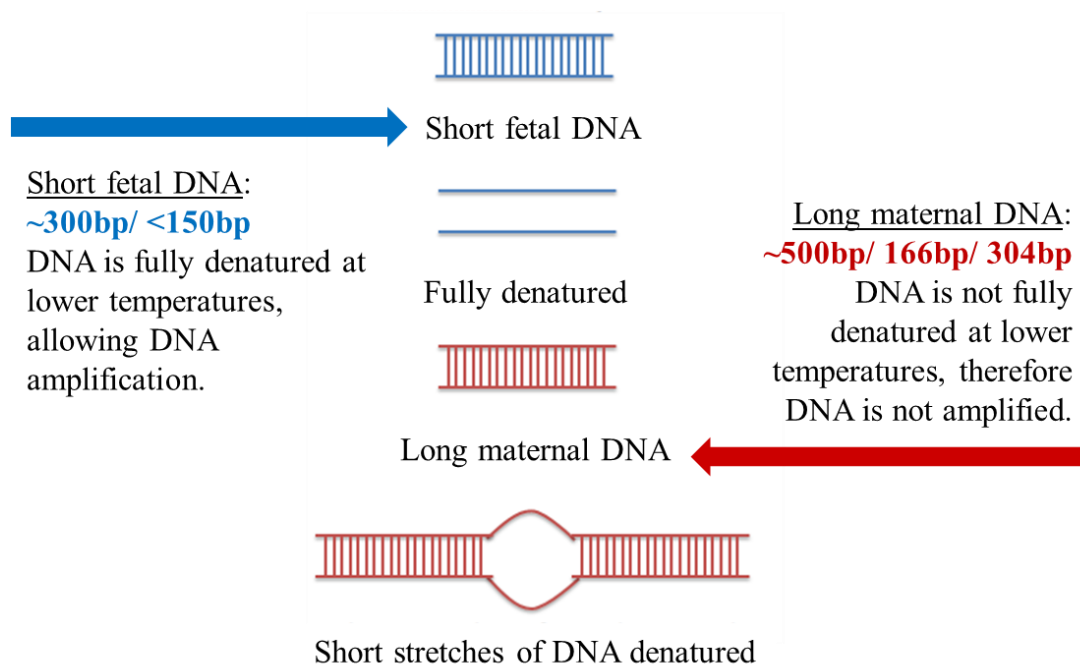


**Figure 3-1: Representation of denaturation of shorter fetal DNA fragments and longer maternal DNA fragments at critical Td.** Amplification at the critical Td illustrates full denaturation of the shorter fetal fragments and only short stretches of DNA denaturation for longer maternal fragments.

The aims of this study were:

- To determine why smaller products are formed at lower  $T_d$ s when amplifying pseudo-fetal DNA fragment containing a short-tandem repeat region (STR).
- To optimise the  $T_d$  of multiple internal primers for highly conserved regions of DNA, which do not contain an STR, on chromosomes X, Y, 1, 21, 18 and 13.
- To produce pseudo-maternal DNA samples and further optimise the  $T_d$  for two targets in singleplex and multiplex reactions using qPCR to selectively amplify the pseudo-fetal proportion.
- To transfer multiplex reactions onto a dPCR platform for accurate detection and quantification of selective enrichment.



## 3.2 Results

### 3.2.1 Cloning of an STR fragment (D21S1890) on chromosome 21 for analysis of product formation at the optimal (95°C) and the critical (80°C) denaturation temperature.

Initial experiments were continued from previous work carried out by Tara Miran (ResM student, Plymouth University, UK), which focused on the use of COLD-PCR to selectively amplify psfDNA (Miran, (2012)). The investigation focused on a fragment of chromosome 21 that contained a CA STR (D21S1890). The psfDNA fragments were produced using external primers designed by Alice Bruson (a visiting PhD student from Universita delgi di Padova, Italy) (Table 3-1) and spiked into female gDNA at 5% as described (refer to 2.1.4).

**Table 3-1: Oligonucleotides for D21S1890 STR fragment** (HPLC purified (Eurofins MWG Operon) (for mapped sequences refer to Figure 2-1).

	<b>Forward primer sequence (5'-3')</b>	<b>Reverse primer sequence (5'-3')</b>	<b>Hybridisation probe sequence (5'-3')</b>	<b>Size (bp)</b>
<b>D21S1890 internal oligonucleotides</b>	TCGCCCCGAGGG TCTGA	AAACCAACTGAC TCCCAAACAAC	FAM- AGATTTCCC	101
<b>D21S1890 external oligonucleotides</b>	GGAGAAACGAG GATGAGCTTC	TATTCCTCCCGTAT TCTTGGT	AATCGCCA- BHQ1	229

Optimisation of  $T_c$  was repeated by performing a denaturation temperature gradient ( $T_d$ ). Conventional PCR identified the  $T_c$  of D21S1890 to be 78.2°C (Figure 3-2). However, when repeated on a qPCR platform psfDNA fragment was not amplified at this  $T_d$ , therefore a higher gradient was tested and the  $T_c$  was determined to be 80°C on this platform (Figure 3-3), which comply with previous results achieved by Tara Miran (Miran, 2012).

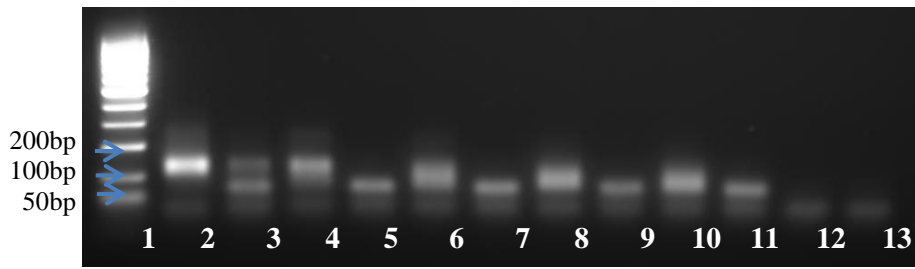


**Figure 3-2: COLD-PCR for D21S1890 fragment using  $T_d$  gradient from 83°C to 73.2°C.** Lane 1 represents marker (Ranger 100 bp DNA ladder), lanes 2, 4, 6, 8, 10 and 12 represent amplification of Male gDNA at  $T_d$  83°C, 78.8°C, 78.6°C, 78.4°C, 78.2°C and 73.2°C, respectively. Lanes 3, 5, 7, 9, 11 and 13 identify negative water controls at each temperature. Clear identification of 101bp product amplified at both 83°C and 78.8°C. Product was also amplified at  $T_d$  78.6°C, 78.4°C and 78.2°C but smaller than size of fragment DNA. There was no amplification at all presented at 73.2°C  $T_d$ . Lane 3 illustrated contamination of similar size to target. Lanes 5, 7, 9 and 11 all showed contamination of a secondary product <101bp.

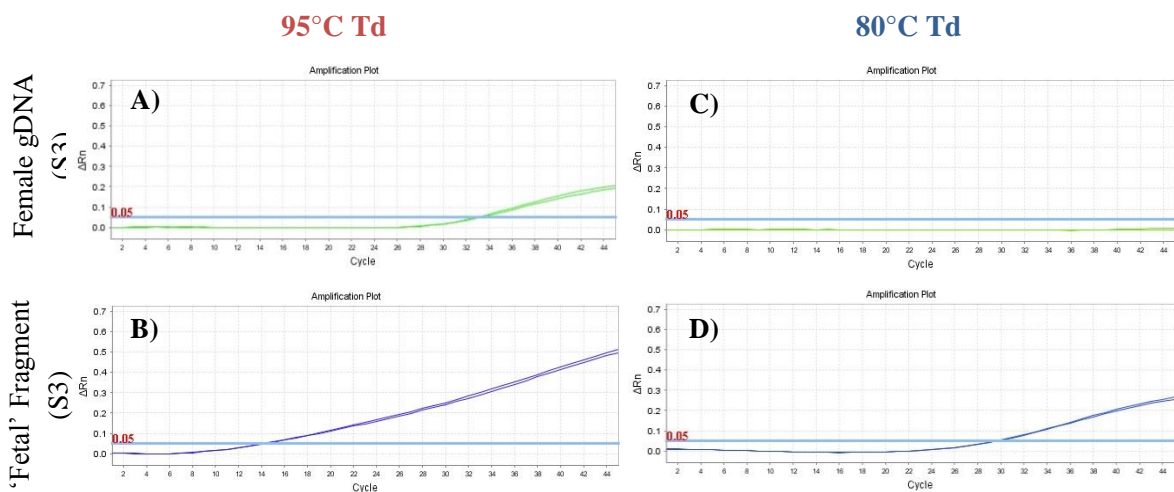


**Figure 3-3: Real-Time PCR amplification of D21S1890 psfDNA fragment and control Female gDNA at 95°C and 80°C  $T_d$ .** A) Amplification of female gDNA (0.2 ng/ $\mu$ L) at 95°C  $T_d$  (33.14 Ct). B) Amplification of 'fetal' fragment D21S1890 at 95°C  $T_d$

(14.21 Ct). C) Amplification of female gDNA (0.2 ng/  $\mu$ L) at the  $T_c$  80°C (undetermined Ct). D) Amplification of ‘fetal’ fragment D21S1890 at the  $T_c$  80°C (29.62 Ct).

Previous data for the same STR region illustrated that the psfDNA fragments presented lower melting temperatures ( $T_m$ ) at 80°C  $T_d$  compared to 95°C  $T_d$  using melt-curve analysis (78.06°C  $T_m$  and 81.3°C  $T_m$ , respectively), which also indicated smaller product formation (Miran, 2012). The presence of shoulder peaks from the melt-curve analysis demonstrated possible heteroduplex formation. In addition, fragment analysis (ABI Genetic analyser 3130 with Peak Scanner™ Software) carried out by a senior research technician showed multiple stutter peaks when only two peaks were expected for heterozygous samples since each individual expresses two alleles.

To continue on from this research, cloning experiments were carried out to compare psfDNA sequences amplified at 80°C and 95°C  $T_d$ . External primers were used to create the psfDNA fragment D21S1890, which was used as a template for conventional PCR amplification at 80°C and 95°C  $T_d$  using D21S1890 internal primers (refer to 2.3.2) (Table 3-1). Following PCR amplification products were gel extracted and quantified using the NanoVue Plus™ Spectrophotometer (GE Healthcare, Buckinghamshire, UK) (refer to 2.5 and 2.6.1, respectively). The psfDNA fragments yielded 14.7ng/ $\mu$ l and 18.8ng/ $\mu$ l of DNA at 80°C and 95°C  $T_d$ , respectively. Purified PCR products were then cloned into pCR®2.1 vectors and transformed into competent *E.coli*. One Shot® cells (TA Cloning Kit) (refer to 2.10). The pCR®2.1 cloning vector expresses single 3’ deoxythymidine (T) residues, which allow PCR inserts to ligate efficiently. Surrounding the PCR insert region of the vector are multiple restriction enzyme sites and M13 forward (-20) and reverse priming sites. For this experiment a single colony from each plate was analysed by colony PCR (refer to 2.10.6) using the M13 primers, and products were ran

on an agarose gel (refer to 2.4) (Figure 3-4). The results illustrate that the PCR product (~300bp) was only successfully inserted when 100  $\mu$ L of transformation vial was loaded for psfDNA amplified at 95°C  $T_d$ . However, the psfDNA amplified at the  $T_c$  (80°C) showed product insert from a single colony for one duplicate of each loading volume (Figure 3-4).

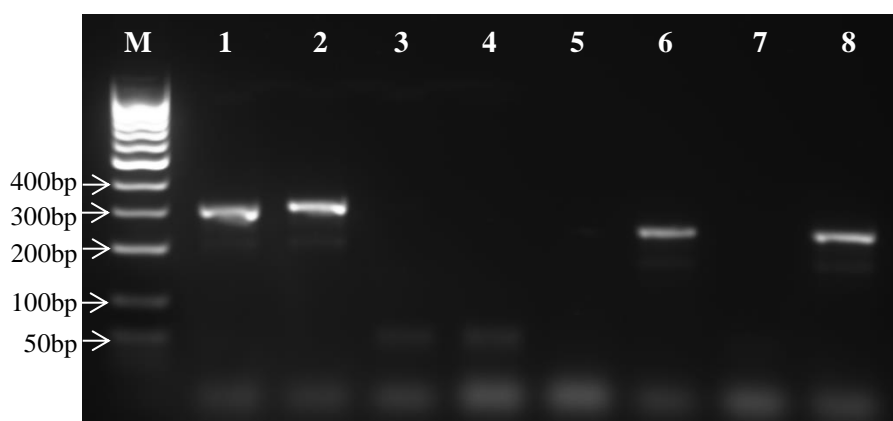


**Figure 3-4: 2% agarose (w/v) gel of colony PCR for pseudo-fetal fragments using M13 forward and reverse primers.** M= 100bp DNA ladder. Lanes 1-4 represent psfDNA amplified at 95°C and lanes 5-8 represent psfDNA amplified at 80°C. Lanes 1, 2, 5 and 6 represent colonies selected from LB agar plates that were spread with 100 $\mu$ l of transformation vial. Lanes 3, 4, 7 and 8 represent colonies selected from LB agar plates that were spread with 25 $\mu$ l of transformation vial.

These colonies were subsequently selected for plasmid DNA purification and sent for sequencing with the forward M13 primer (Prepaid barcodes, Eurofins Genomics, Wolverhampton, UK). The sequencing results were aligned to the M13 primer binding region of the pCR2.1 vector, which included the D21S1890 internal sequence, using ClustalW2 (<http://www.ebi.ac.uk/Tools/msa/clustalw2/>) and GeneDoc 2.7 Software. The results for alignment against this 301bp reference sequence for psfDNA amplified at 95°C

T<sub>d</sub> and 80°C T<sub>d</sub> are illustrated in Figure 3-5. The results show a 52-base deletion of the 3' end of the vector (including the M13 reverse primer binding region) for psfDNA amplified at both temperatures, which is a result of only sequencing samples in one direction (due to limited supply). For the remaining 249 bases, the PCR product amplified at 95°C T<sub>d</sub> shows complete (100%) alignment (Figure 3-5). However, the PCR product amplified at 80°C T<sub>d</sub> only illustrates 77% alignment (192/249), since 57 bases of the D21S1890 internal sequence (including CA-repeat region) were absent. These cloning results illustrated that when the psfDNA fragment was amplified at the T<sub>c</sub>, the CA-repeat region and surrounding nucleotide bases were deleted possibly as result of hairpin formation, which is why shorter products were presented at the lower 80°C T<sub>d</sub>.

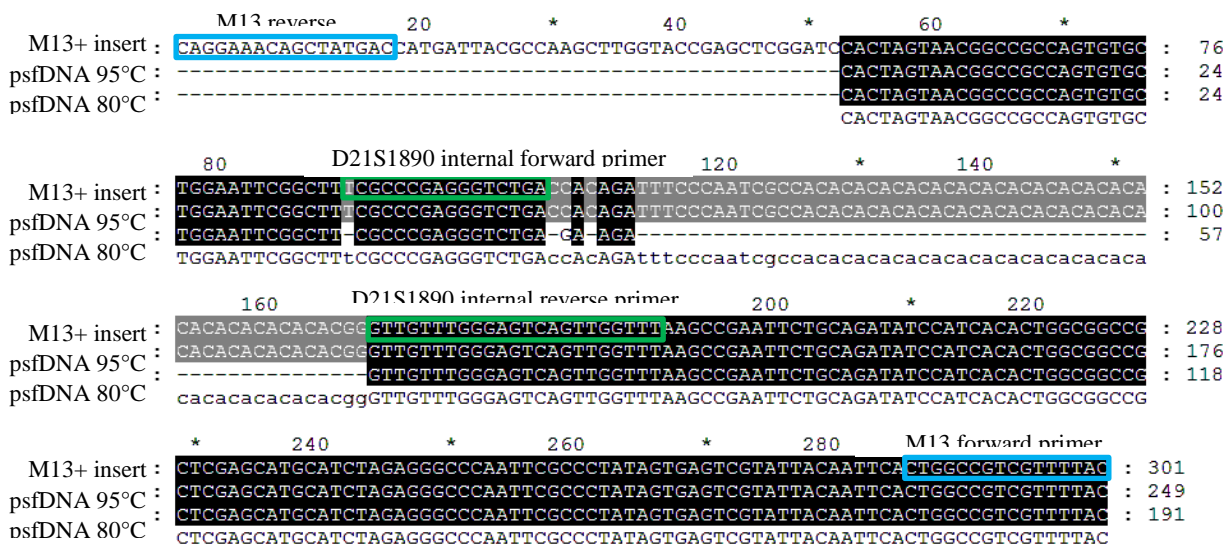


**Figure 3-5: Sequence alignment of cloned psfDNA product amplified at 95°C and 80°C T<sub>d</sub>.** Both sequences were mapped against a region of the linearized vector (pCR<sup>®</sup>2.1), which included the D21S1890 PCR product insert (reference). The M13 Primers are highlighted in blue and the internal D21S1890 primers are highlighted in green. The psfDNA product amplified at 95°C T<sub>d</sub> showed complete sequence alignment of the internal D21S1890 amplicon. The psfDNA product amplified at 80°C T<sub>d</sub> only

demonstrated 77% sequence alignment of the internal D21S1890 amplicon, since 57 bases were absent including the entire CA repeat region.

### 3.2.2 Optimisation of critical $T_d$ for amplicons that do not contain STR regions

Since the D21S1890 target illustrated sequence hairpin formation at 80°C  $T_d$ , internal and external primers were designed (or taken from previous publications), which did not contain any STRs, for multiple-targets on chromosomes 1, 13, 18, 21, X and Y (Table 2-1). Following annealing temperature ( $T_a$ ) optimisation of the primers, the  $T_c$  was optimised for two target regions *APP*, located on chromosome 21, and *EIF2C1*, located on chromosome 1 (Figure 3-6 and Figure 3-7). The  $T_c$  in these experiments is defined as the highest temperature at which Male gDNA (control for longer DNA fragments) is no longer amplified. The fundamental  $T_d$  gradient from 95°C down to 70°C (with a 5°C decline) for both targets illustrated product amplification at 80°C but no product amplification at 75°C (Figure 3-6). Consequently, the next temperature gradient for both *APP* and *EIF2C1* internal products was carried out between 75°C and 80°C  $T_d$  with a 1°C decline in temperature (Figure 3-7). The results demonstrated that the highest temperature at which Male gDNA is not amplified (the  $T_c$ ) is 78°C for both *APP* and *EIF2C1* internal products, respectively. In succession the optimal  $T_a$  and critical  $T_c$  was determined for all other targets (Table 3-2). The final column in Table 3-2 lists the rank of all primer pairs for each chromosome. The rank was decided based on the following criteria; a) the intensity of the fluorescent signal shown on a 2% agarose (w/v) gel, b) the appearance of any secondary bands and c) the primer concentration necessary for successful amplification. The oligonucleotide pairs for each gene were ranked within each chromosome sub-set. High ranking oligonucleotide pairs (Rank 1), such as *APP*, illustrated higher levels of fluorescence from low starting concentrations of primers (200-

300nM) and only expressed a single band. Low ranking oligonucleotide pairs (Rank 3), such as *TTR* (chromosome 18) and *FOXP3* (chromosome X), illustrated low fluorescence, secondary bands or required high starting concentrations of primers for amplification (Table 3-2).

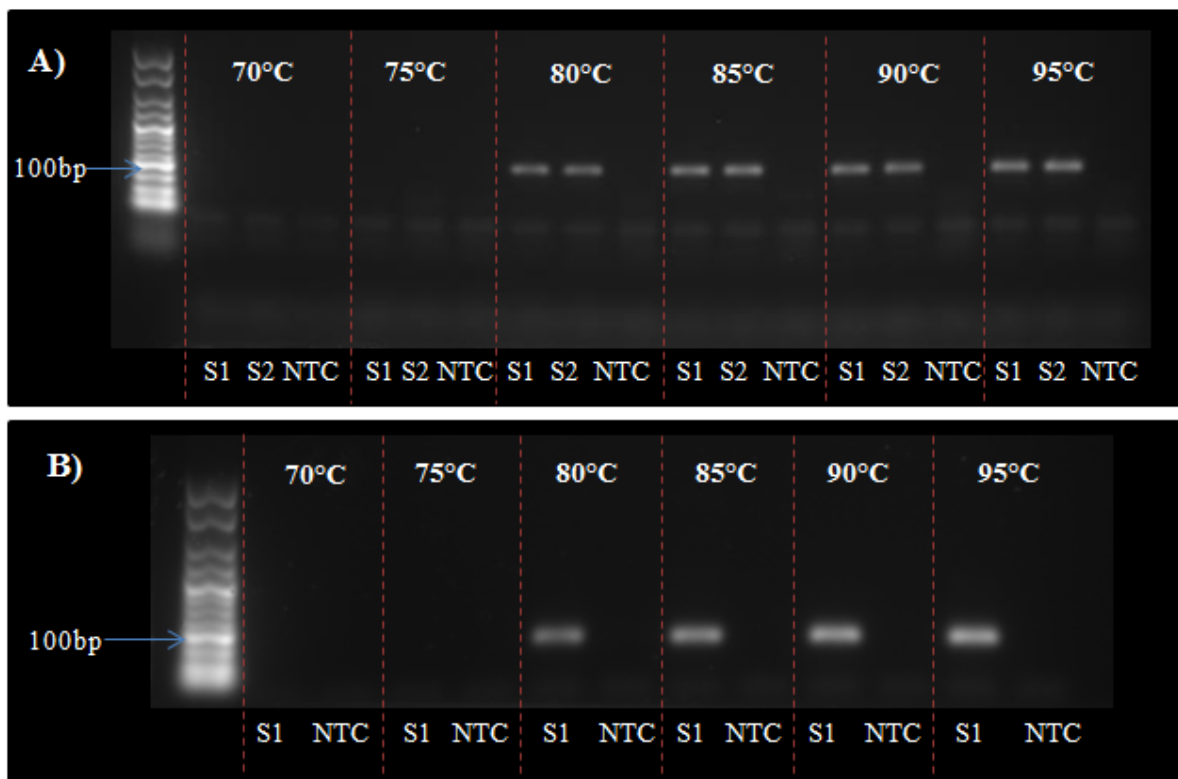


**Figure 3-6: 2% agarose (w/v) illustrating initial COLD-PCR gradient (from 70°C to 95°C) for *APP* (A) and *EIF2C1* (B).** The  $T_d$  was graded from 70°C to 95°C for Male gDNA and non-template controls (NTC) to optimise the critical  $T_d$  for the *APP* and *EIF2C1* internal primers (200 nM final concentration). A) The 96bp product produced by the *APP* internal primers. For each temperature Male gDNA was tested at S1 and S2 concentrations (20ng/  $\mu$ L and 2ng/  $\mu$ L) against NTC. B) The 81bp product produced by the *EIF2C1* internal primers. For each temperature Male gDNA was tested at S1 concentrations against NTC. The  $T_c$  for both *APP* and *EIF2C1* is 75°C.

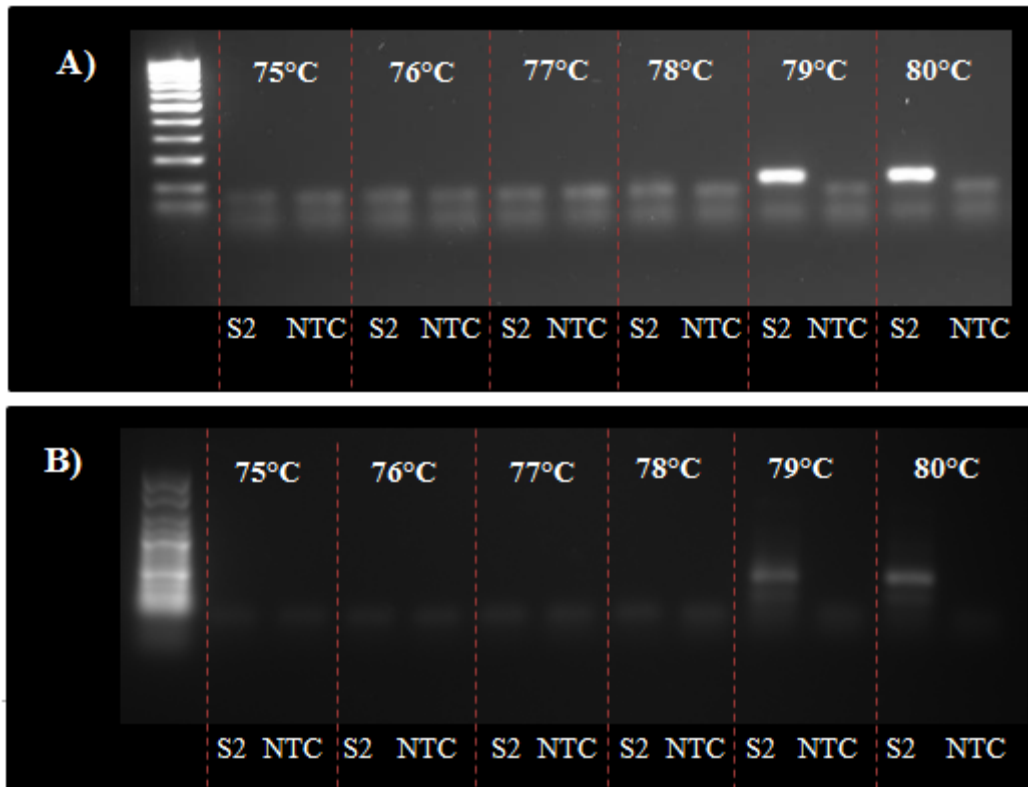


**Figure 3-7: 2% agarose (w/v) gel illustrating secondary COLD-PCR gradient (from 75°C to 80°C) for *APP* (A) and *EIF2C1* (B).** The denaturation temperature was graded from 75°C to 80°C, with a 1°C decline in temperature, for Male gDNA and non-template controls (NTC) to further optimise the critical  $T_d$  for the *APP* and *EIF2C1* internal primers (200 nM final concentration). A) The 96bp product produced by the *APP* internal primers. For each temperature Male gDNA was tested at S2 concentrations (2ng/  $\mu$ L) against NTC. B) The 81bp product produced by the *EIF2C1* internal primers. For each temperature Male gDNA was tested at S2 concentrations against NTC. The  $T_c$  for both *APP* and *EIF2C1* is 78°C.



**Table 3-2: Summary of optimisation experiments for all chromosomes of interest.**

Results for the optimisation of the  $T_a$ , primer concentration and the  $T_d$  for target regions on chromosomes 1, 21, 18, 13, X and Y.

Chr	Target Region	Optimal $T_a$ (°C)	Lowest Primer Concentration (nM)	Lowest $T_d$ at which product is amplified (°C)	$T_c$ (°C) <sup>1</sup>	Rank
1	<i>EIF2C1</i> <sup>2</sup>	60	200	79	78	1
21	<i>DSCR3</i>	60	100	78	77	2
	<i>RCANI</i>	56	100	79	78	3
	<i>APP</i>	60	100	80	79	1
18	<i>APCDD1</i>	60	200	75	74	1
	<i>TTR</i>	60	200	75	74	3
	<i>TNFRSF11A</i>	58	200	84	83	2
13	<i>SPG20</i>	58	200	77	76	1
	<i>ZIC2</i>	62	100	81	80	2
	<i>ATP7B</i>	58	400	Poor amplification	N/A	-
X	<i>FOXP3</i>	60	200	82	81	3
	<i>NROB1</i>	58	200	83	82	4
	<i>PRPS1</i>	60	100	75	74	2
	Xp22.3 <sup>2</sup>	58	100	76	75	1
Y	<i>SRY</i> (K.A.S) <sup>3</sup>	60	200	76	75	2
	<i>SRY</i> (H.P.T) <sup>4</sup>	60	200	76	75	2
	<i>TSYP1</i>	58	200	77	76	1
	<i>DDX3Y</i>	60	200	80	79	3

<sup>1</sup> The critical  $T_d$  at which only pseudo-fetal DNA is successfully amplified.

<sup>2</sup> Taken from Fan *et al.* (2009).

<sup>3</sup> Designed in house by Kelly A Sillence.

<sup>4</sup> Designed in house by Hannah P Thompson.

### 3.2.3 Real-time PCR optimisation

The  $T_c$  for Male gDNA was further optimised by qPCR using a  $T_d$  gradient from 78°C down to 77°C for targets *APP* and *EIF2C1* (Figure 3-8). Although this initial experiment was carried out in a singleplex reaction, different 5'-fluorescent-labelled probes were used for *APP* and *EIF2C1* targets (FAM and HEX, respectively), in preparation for consecutive multiplex reactions. In addition to the Male gDNA, psfDNA fragments (280-320bp) produced from external primers were also tested on the qPCR platform (Figure 3-

8 and Figure 3-9) (refer to 2.1.3). Amplification of both targets was also tested at 95°C  $T_d$ , which was used as a positive control temperature for all samples. Figure 3-8 and Figure 3-9 demonstrated successful amplification of *APP* and *EIF2C1*, respectively, for both samples at 95°C  $T_d$ . The *APP* and *EIF2C1* targets were also successfully amplified at all three lower  $T_d$ s (78°C, 77.5°C and 77°C) for the psfDNA samples (Figure 3-8 and Figure 3-9). Late amplification of Male gDNA at Ct 37.5 and Ct 40 for target *APP* (Figure 3-8), and Ct 39 and Ct 39.5 for target *EIF2C1* (Figure 3-9), was shown at 78°C  $T_d$  and 77.5°C  $T_d$ , respectively. Although the *EIF2C1* target did show some amplification of Male gDNA at 77°C  $T_d$ , because amplification occurred under the threshold (0.050 $\Delta R_n$ ), it can be stated that there was no amplification for this target at this temperature; equally, target *APP* also demonstrated no Male gDNA amplification at 77°C.

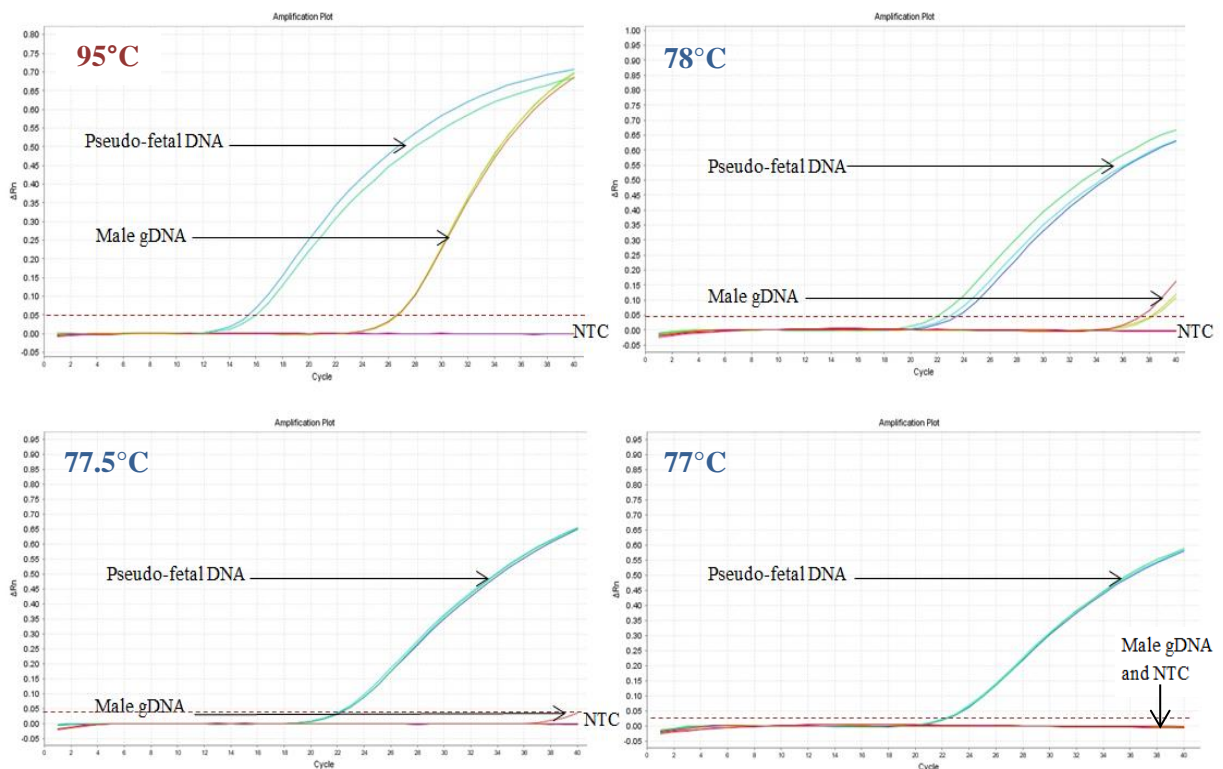


**Figure 3-8: qPCR amplification to determine drop out of psfDNA against Male gDNA for *APP* target on chr21 from 78°C down to 77°C. Amplification of Male**

gDNA (2ng/  $\mu\text{L}$ ) and psfDNA (2ng/  $\mu\text{L}$ ) using *APP* primers (200 nM concentrations) for the following  $T_d$ s; 95°C (control) 78°C, 77.5°C and 77°C.

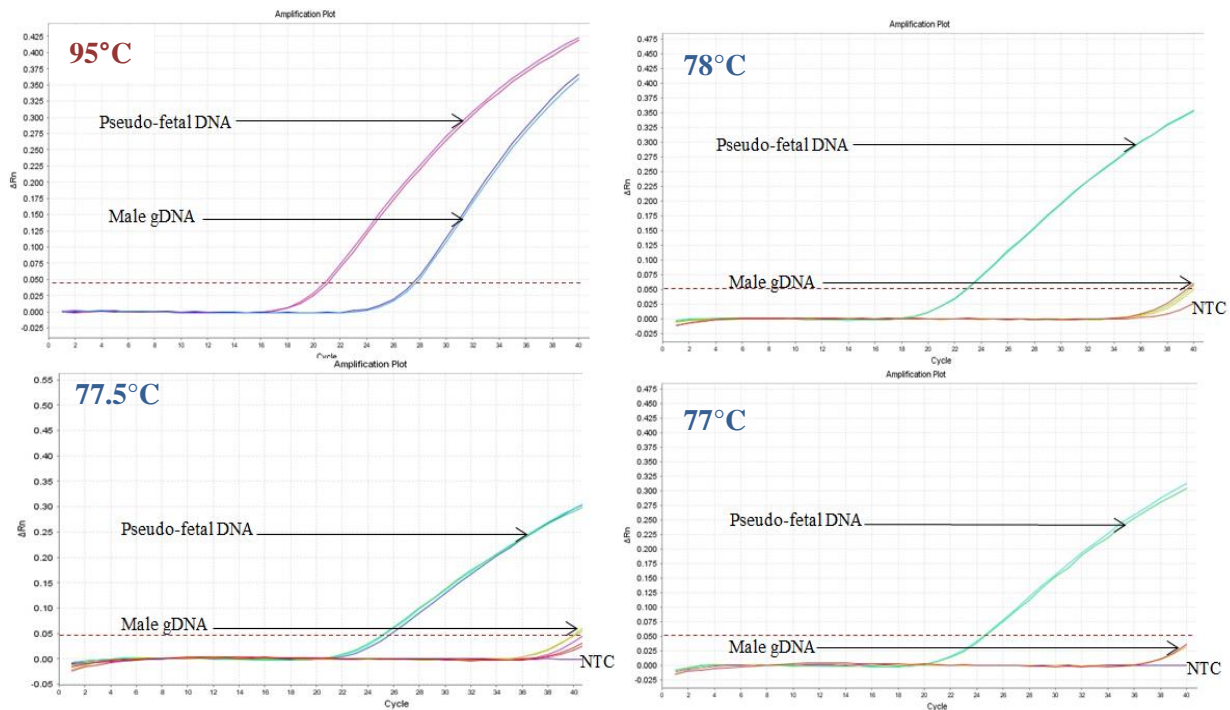


**Figure 3-9: qPCR amplification to determine drop out of psfDNA against Male gDNA for *EIF2C1* target on chr1 from 78°C down to 77°C.** Amplification of Male gDNA (2ng/  $\mu\text{L}$ ) and pseudo fetal DNA (2ng/  $\mu\text{L}$ ) using *EIF2C1* primers (200 nM concentrations) for the following  $T_d$ s; 95°C (control) 78°C, 77.5°C and 77°C.

Following the optimisation of the  $T_c$  for the Male gDNA, qPCR was ultimately used to optimise the critical denaturation temperature of the psfDNA (Figure 3-10). Figure 3-10A demonstrated that when the  $T_d$  was set to 73°C, 74°C, 75°C and 76°C there was no amplification of the psfDNA for both *APP* and *EIF2C1*. One psfDNA (*EIF2C1*) replicate did show amplification of the *EIF2C1* (HEX) target at 76°C  $T_d$  (36 Ct), but the other two replicates showed no amplification (Figure 3-10B). Successful psfDNA amplification was only illustrated when the  $T_d$  was increased to 77°C for *EIF2C1* and *APP* targets (25 Ct

and 26 Ct, respectively) (Figure 3-10C). The gradient was then further optimised from 75.8°C to 76.6°C (with a 0.2°C incline in temperature) to determine the critical T<sub>d</sub> of each target when amplifying psfDNA (Figure 3-11). Table 3-3 shows the final T<sub>c</sub> for psfDNA and Male gDNA.

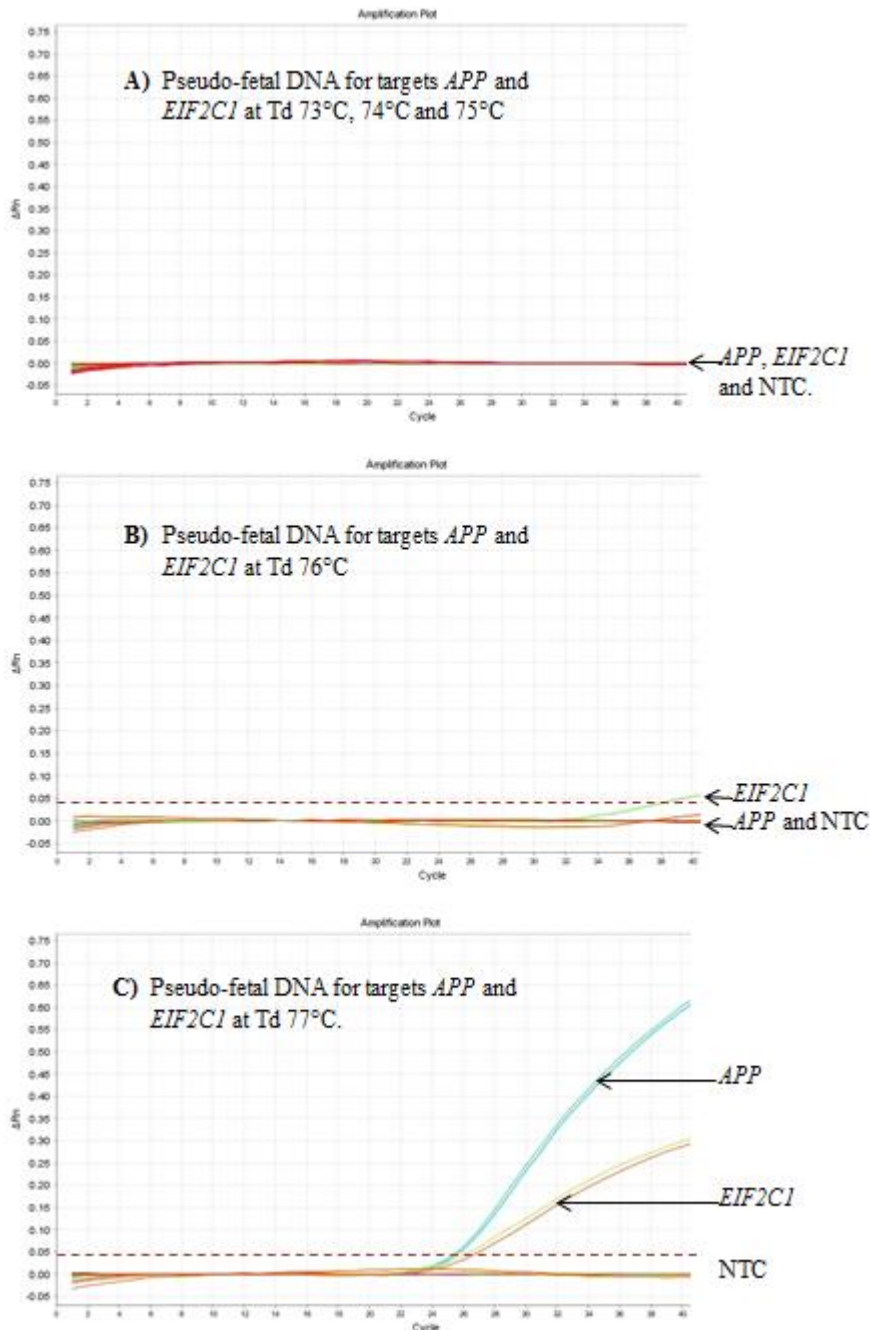


**Figure 3-10: Optimisation of the T<sub>d</sub> for the amplification of psfDNA for target *APP* (FAM) and target *EIF2C1* (HEX). A) qPCR amplification at 73°C, 74°C and 75°C, B)**

RT-PCR amplification at 76°C and C) RT-PCR amplification at 77°C. Cut-off thresholds were set at 0.05.

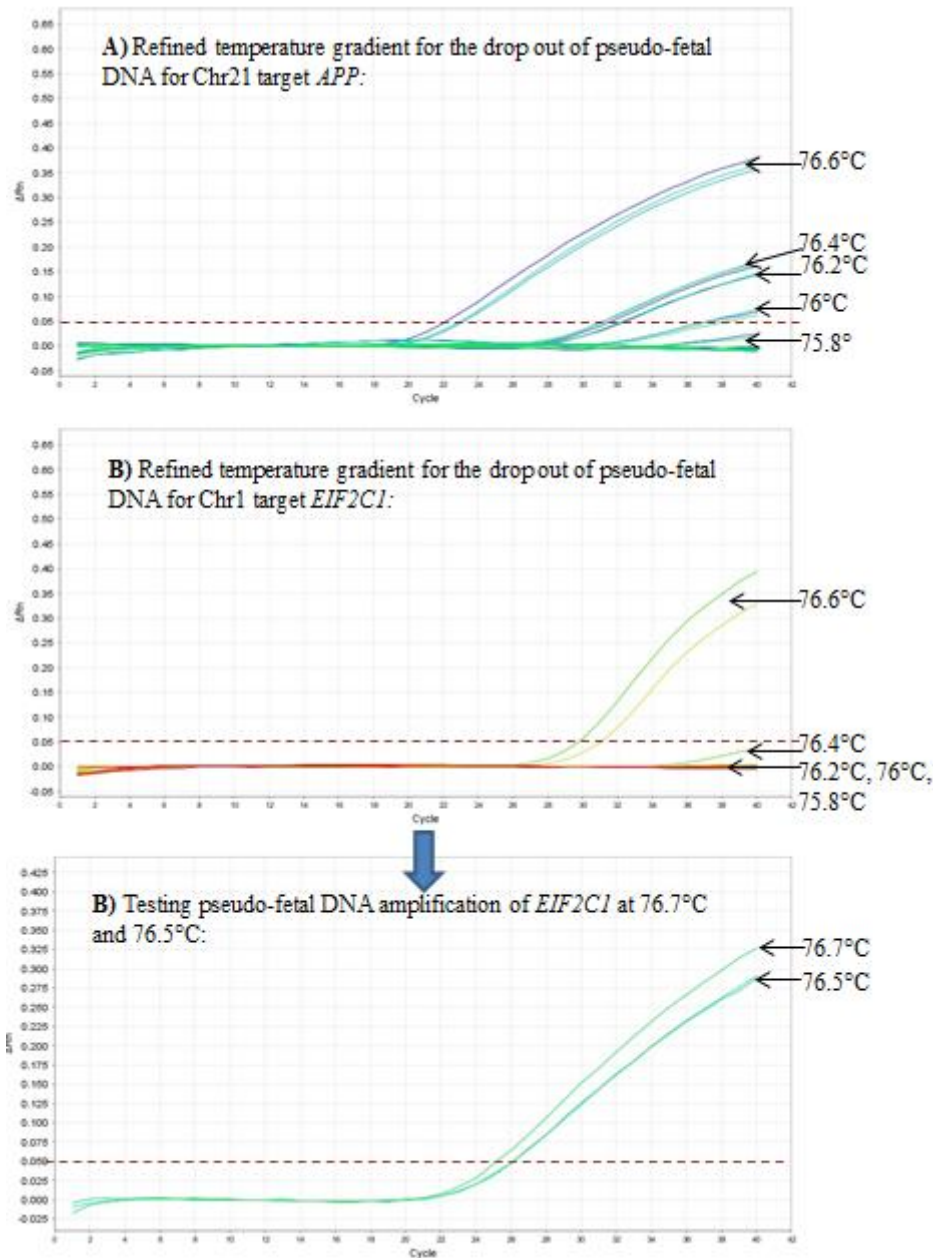


**Figure 3-11: Further optimisation of the  $T_d$  for the amplification of psfDNA for target *APP* (A) and target *EIF2C1* (B) from 75.8°C to 76.6°C using qPCR. For target *EIF2C1* the original gradient included the following temperatures; 75.8°C, 76°C, 76.2°C, 76.4°C and 76.6°C (same as target *APP*). The temperature was further optimised to**

determine if the psfDNA would be amplified at a temperature lower than 76.6°C. Cut-off thresholds were set at 0.05.

**Table 3-3: Summary of the  $T_c$  determined for Male gDNA and psfDNA for targets *APP* and *EIF2C1*.**

Target	Sample	Final $T_d$ at which product is amplified (°C)	$T_c$ (°C)
<i>APP</i>	Male gDNA	77.5	77
	psfDNA	76	75.8
<i>EIF2C1</i>	Male gDNA	77.5	77
	psfDNA	76.5	76.4

Following the optimisation of the  $T_c$  for the Male gDNA and psfDNA, qPCR was carried out at 76.7°C  $T_d$  for both Male and psfDNA. This temperature was chosen as it was in-between the highest psfDNA  $T_c$  (*EIF2C1* (76.5°C)) and the highest Male gDNA  $T_c$  (77°C for both *APP* and *EIF2C1*) (Table 3-3). At 76.7°C  $T_d$  both *APP* (FAM) and *EIF2C1* (HEX) targets illustrated successful amplification of pseudo-fetal fragments (23 Ct and 25 Ct, respectively), but showed no amplification of larger Male gDNA fragments (Figure 3-12). The results indicated that using the mean  $T_d$ , allowed for the most efficient selective amplification and 76.7°C  $T_d$  was defined as the  $T_c$  for non-spiked samples.

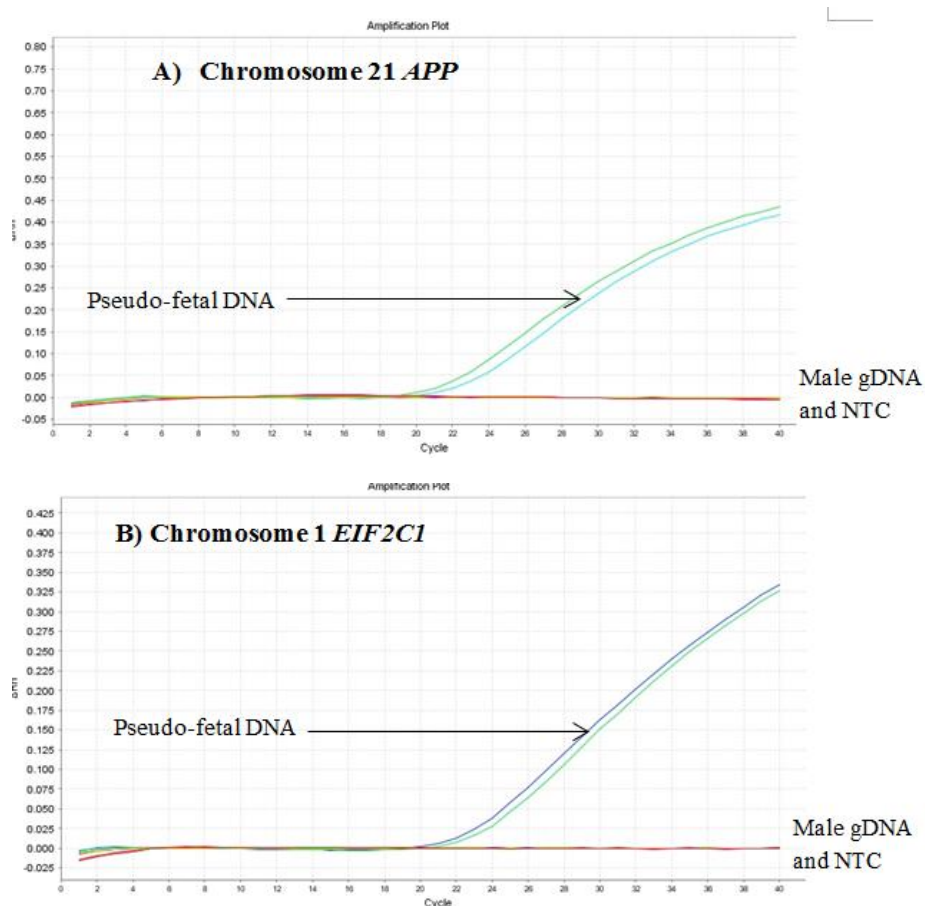


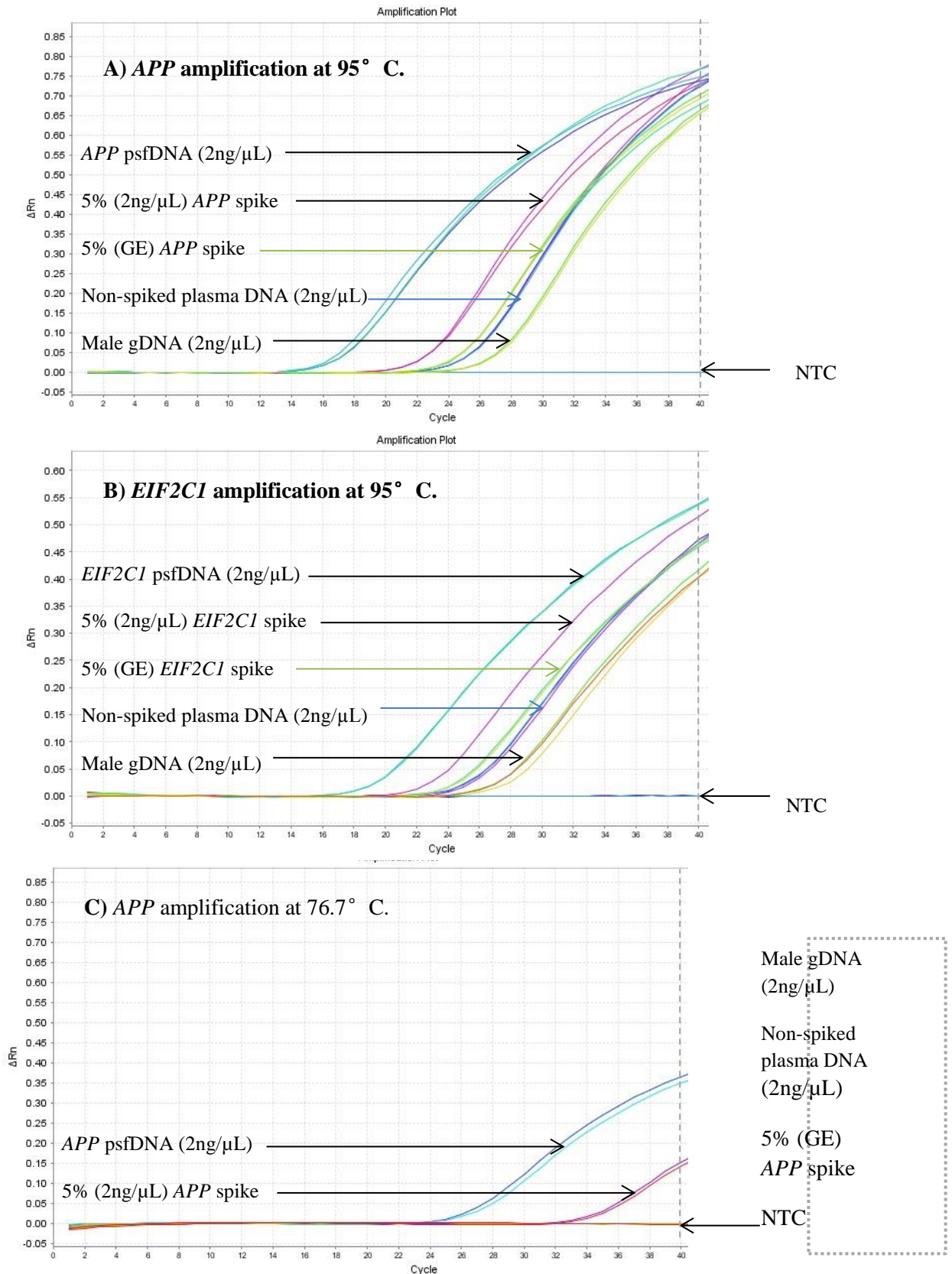
**Figure 3-12: qPCR Amplification of *APP* (FAM) (A) and *EIF2C1* (HEX) (B) at 76.7°C for Male gDNA, psfDNA and NTC.** The experiment was carried out in singleplex reactions and the results reveal that at 76.7°C on the psfDNA fragments are successfully amplified.

### 3.2.4 psfDNA spiking experiments for singleplex and multiplex reactions

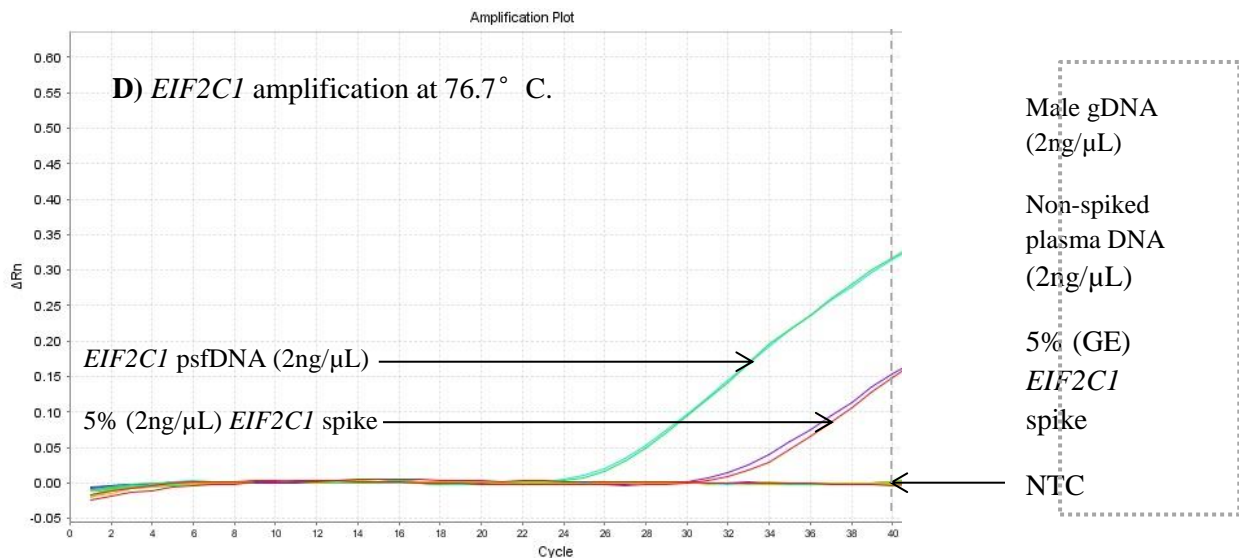
5% ‘fetal’ spikes (2.1.3) were subsequently tested at this  $T_c$  (76.7°C). Controls included; NTC, 100% psfDNA (*APP*) (2ng/μL), 100% psfDNA (*EIF2C1*) (2ng/μL), Male gDNA (2ng/μL) and 100% (non-spiked) plasma extracted DNA (2ng/μL). Figure 3-13A and Figure 3-13B demonstrated successful amplification of *APP* (FAM) and *EIF2C1* (HEX), respectively, for all samples, except the NTC. However, at the  $T_c$  (76.7°C) only the 100% psfDNA and the 5% ‘fetal’ spike were amplified for both targets (Figure 3-13C and



Figure 3-13D, respectively). The 5% GE spike did not show amplification at the  $T_c$  (Figure 3-13C, D) (2.1.4).







**Figure 3-13: qPCR amplification at optimum  $T_d$  (95°C) and lowered  $T_d$  (76.7°C) to determine the selective amplification of 5% Spike psfDNA (refer to 2.4.1).** The spikes were produced using both the dilution and genomic equivalent method (2.1.4). Male gDNA and non-spiked plasma DNA were used as controls to compare ‘fetal’ DNA amplification with genomic DNA amplification. NTC was used a negative control throughout. qPCR amplification was carried out for target *APP* (FAM) at 95°C  $T_d$  (A) and 76.7°C (C), and target *EIF2C1* (HEX) at 95°C (B) and 76.7°C (D).

The initial multiplex experiment for *APP*-FAM and *EIF2C1*-HEX, demonstrated no ‘fetal’ amplification at 76.7°C for both targets (data not shown). Therefore, the  $T_d$  was increased to 78°C. Since the GE spike did not illustrate any selective ‘fetal’ enrichment (sample too dilute), only the dilution spike was analysed. Figure 3-14 shows the amplification plots for all samples (Male gDNA, *EIF2C1* psfDNA, *APP* psfDNA, non-spiked plasma extracted DNA, 5% T21-spike, 5% D21-spike and NTC) (2.7.1). Before testing the samples at the new  $T_c$  (78°C), the control  $T_d$  (95°C) was tested. Male gDNA,

non-spiked plasma extracted DNA, 5% T21-spike and 5% D21-spike all illustrate successful amplification of both targets at the control  $T_d$ , whilst the NTC shows no amplification. The *APP* psfDNA fragment only showed amplification of *APP*-FAM. However, the *EIF2C1* psfDNA fragment illustrated amplification of *APP*-FAM in addition to *EIF2C1*-HEX at both temperatures (Figure 3-14C and Figure 3-14I). When the  $T_d$  was reduced to  $78^\circ\text{C}$  both the psfDNA fragments (100%) (Figure 3-14H and Figure 3-14), 5% 'DS'-spike (Figure 3-14K) and 5% 'normal'-spike (Figure 3-14L) showed successful amplification of both targets. The Male gDNA dropped below the threshold at  $78^\circ\text{C}$   $T_d$  ( $\Delta Rn0.05$ ), and therefore can be considered to be 'dropping-out' (Figure 3-14G). However, the non-spiked plasma DNA showed very last minute amplification (39 Ct) at this temperature just above the threshold (Figure 3-14J). Therefore, the experiment was repeated at  $77.5^\circ\text{C}$   $T_d$ . Due to the increased level of fluorescent emitted by the FAM-fluorescent dye for target *APP* compared to the HEX-fluorescent dye for target *EIF2C1* ( $0.4\Delta Rn$  and  $0.2\Delta Rn$ , respectively) a dye swap was carried out. Swapping over the fluorescent labels (*APP*-HEX and *EIF2C1*-FAM) was used to determine if the increased levels of fluorescence and lower Ct amplification of *APP*-HEX was a result of increased levels of fragmentation of chromosome 21 (in comparison to reference chromosome 1), or if this was caused by increased efficiency of the FAM-labelled reporter.

The result of this dye-swap experiment revealed that the increased Ct values are associated with the efficiency of the FAM-fluorescent reporter, since the results were inversed. In this run the *EIF2C1*-FAM target illustrated higher fluorescence compared to the *APP*-HEX target ( $1\Delta Rn$  and  $0.2\Delta Rn$ , respectively) for Male gDNA control at  $95^\circ\text{C}$   $T_d$  (Figure 3-15A). At the lowered  $T_d$  ( $77.5^\circ\text{C}$ ), the amplification of Male gDNA remained below the threshold limit, but the non-spiked plasma DNA still demonstrated late

amplification (38.5 Ct) (Figure 3-15J). Like the previous multiplex assay, this experiment also identified minimal change in amplification levels of target *APP* and target *EIF2C1* between the 'DS'-spike (Figure 3-15K) and 'normal'-spike (Figure 3-15L) at lower  $T_d$ .

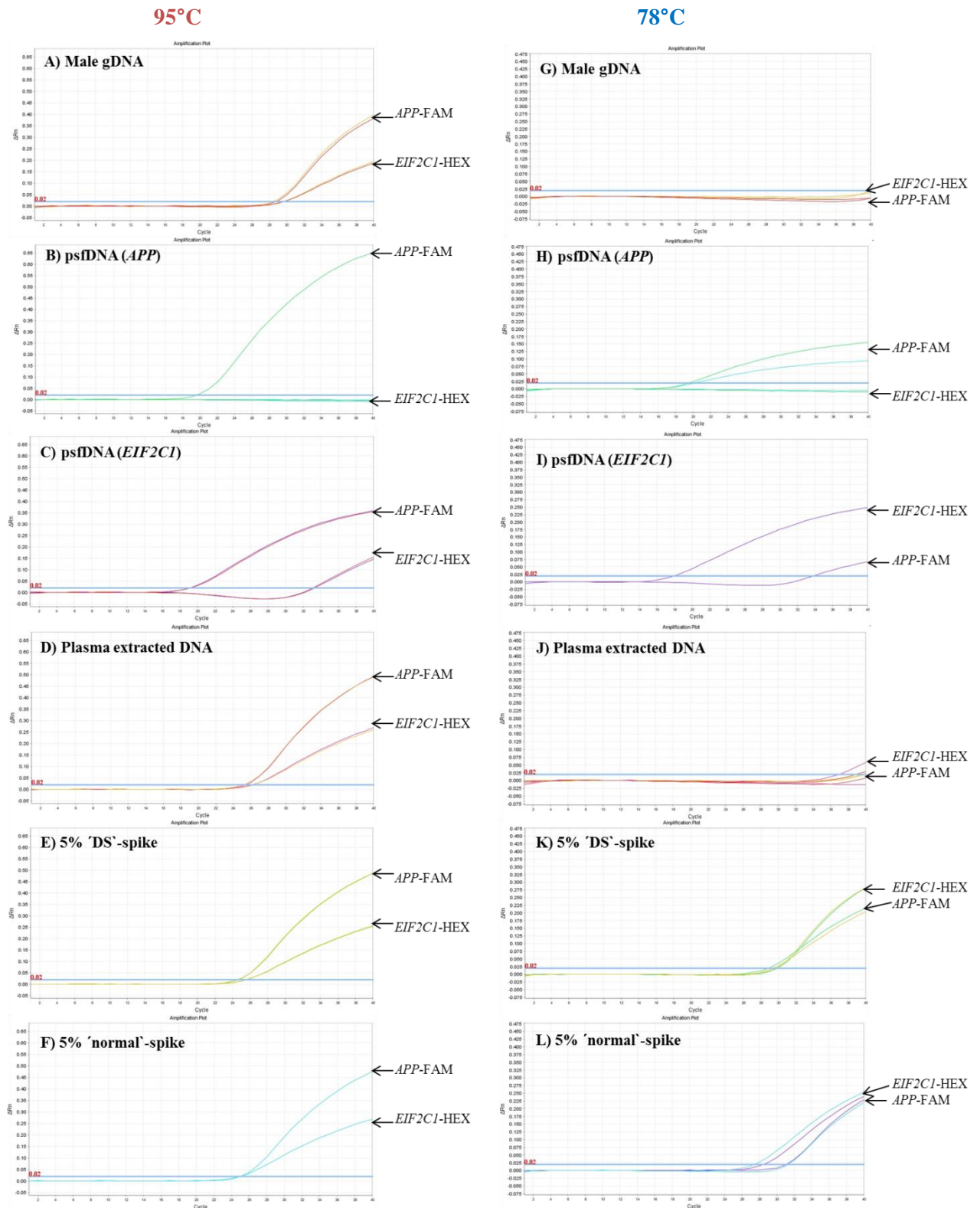


**Figure 3-14: Amplification of multiplex reaction *APP* (FAM)/ *EIF2C1* (HEX) for samples amplified at 95°C  $T_d$  (A-F) and 78°C  $T_d$  (G-L). When amplified at 95°C  $T_d$ , both Male gDNA (A) and plasma extracted DNA (D) sample illustrated successful amplification of both targets (*APP*/ *EIF2C1*), but also showed late amplification of**

*EIF2C1* at 78°C T<sub>d</sub> (39.9 Ct (G) and 37.4Ct (J), respectively). The psfDNA (*APP*) sample only displayed successful amplification of the *APP* target at 95°C T<sub>d</sub> (B) and 78°C T<sub>d</sub> (H). However, the psfDNA (*EIF2C1*) sample demonstrated amplification of both targets at 95°C T<sub>d</sub> (C) and 78°C T<sub>d</sub> (I) (33.1 Ct and 33.9 Ct, respectively), indicating sample contamination. The 5% ‘DS’-spike (E and K) and the 5%-'normal' spike (F and L) show amplification of both targets at both T<sub>d</sub>s (95°C and 78°C).

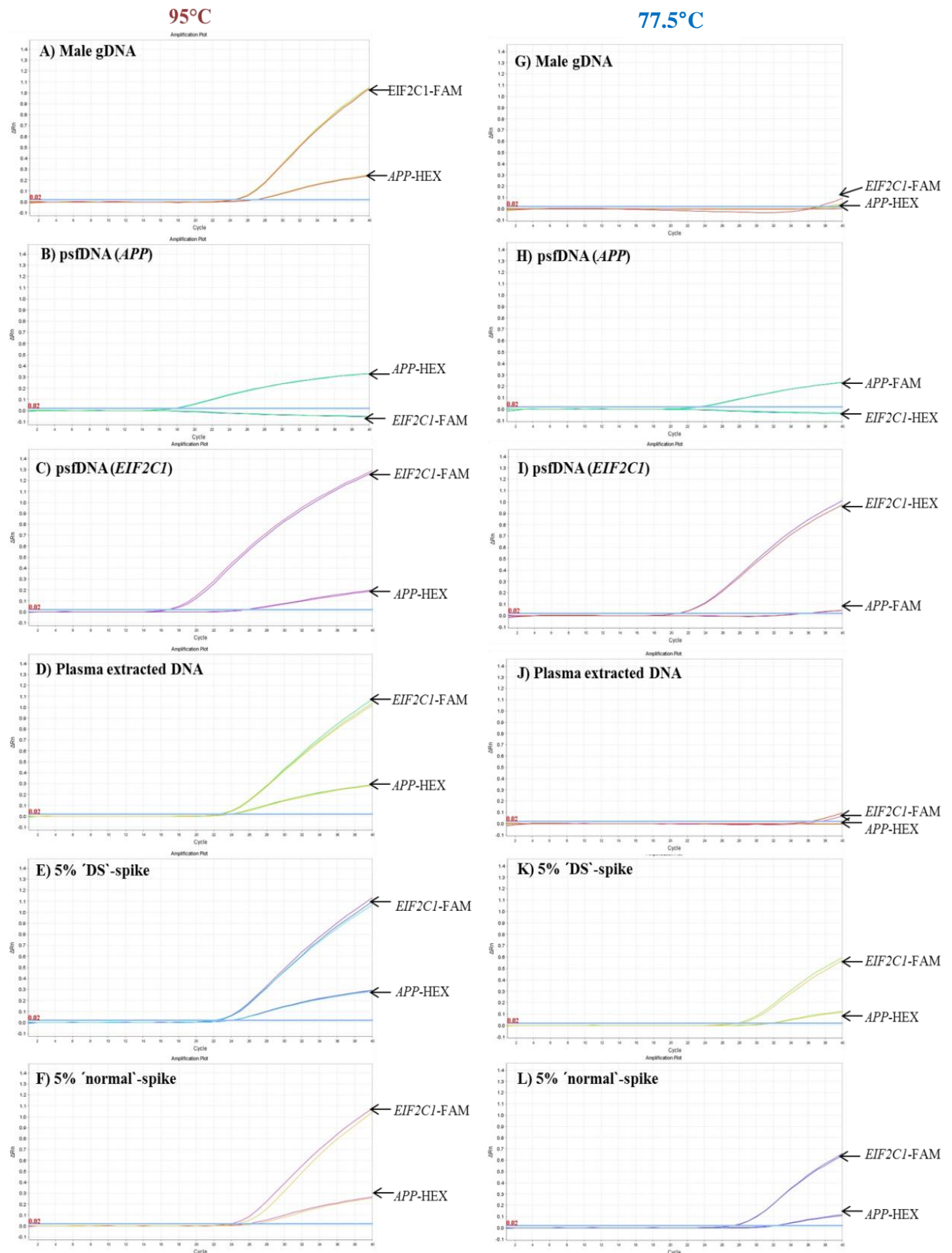


**Figure 3-15: Amplification of dye-swap multiplex reaction *EIF2C1* (FAM)/*APP* (HEX) for samples amplified at 95°C  $T_d$  (A-F) and 77.5°C  $T_d$  (G-L).**

When amplified at 95°C  $T_d$ , both Male gDNA (A) and plasma extracted DNA

(D) illustrated successful amplification of both targets (*APP/ EIF2C1*), but also showed late amplification of *EIF2C1* at 78°C T<sub>d</sub> (37.1 Ct (G) and 36.5 Ct (J), respectively). The psfDNA (*APP*) sample only shows successful amplification of the *APP* target at 95°C T<sub>d</sub> (B) and 77.5°C T<sub>d</sub> (H). However, the psfDNA (*EIF2C1*) sample shows amplification of both targets at 95°C T<sub>d</sub> (C) and 77.5°C T<sub>d</sub> (I) (26.3 Ct and 36.4 Ct, respectively), also indicating sample contamination. The 5% ‘DS’-spike (E and K) and the 5%-‘normal’ spike (F and L) show amplification of both targets at both T<sub>d</sub>s (95°C and 78°C).

Three new T<sub>d</sub> temperatures were tested; 77.2°C, 77.3°C and 77.4°C, and the results are shown in Figure 3-16. The *APP* fragment is also amplified in the psfDNA (*EIF2C1*) fragment at 95°C T<sub>d</sub>; this is likely due to contamination of the psfDNA (*EIF2C1*) since the NTC is clean (A-D). Both Male gDNA and plasma extracted DNA show no target amplification at 77.2°C, 77.3°C and 77.4°C T<sub>d</sub>. Spike samples and pure psfDNA fragments show successful amplification at all three T<sub>d</sub>s (77.2°C, 77.3°C and 77.4°C). The ratio of *APP/EIF2C1* for Male gDNA, plasma extracted DNA and 5% ‘normal’-spike all demonstrated ratios close to 1 (1.05, 1.02, and 1.04, respectively), but the 5% ‘DS’- spike sample illustrates a slighter higher ratio (1.14). When the T<sub>d</sub> was reduced the ratio for the 5% ‘normal’- spike sample should remain close to 1, however at 77.4°C, 77.3°C and 77.2°C is reduced (0.59, 0.55 and 0.69, respectively). The drop in ratio is a result of selective amplification of the *EIF2C1* target, which yields higher *EIF2C1* concentrations and subsequently reduces the ratio to <1 (0.39 – 0.75) (Figure 3-16A-C). Furthermore, if selective enrichment of shorter pseudo-fetal fragments is occurring, then the ratio for the 5% ‘DS’- spike sample should begin to increase (closer to 1.5). However, the results only illustrate a higher ratio for the ‘DS’ spike compared to the ‘normal’ spike

at 77.4°C T<sub>d</sub> (0.75 and 0.69, respectively) (Figure 3-16). 77.2°C T<sub>d</sub> and 77.3°C T<sub>d</sub> both illustrated high ratios for the 5% ‘normal’ spike (Figure 3-16).

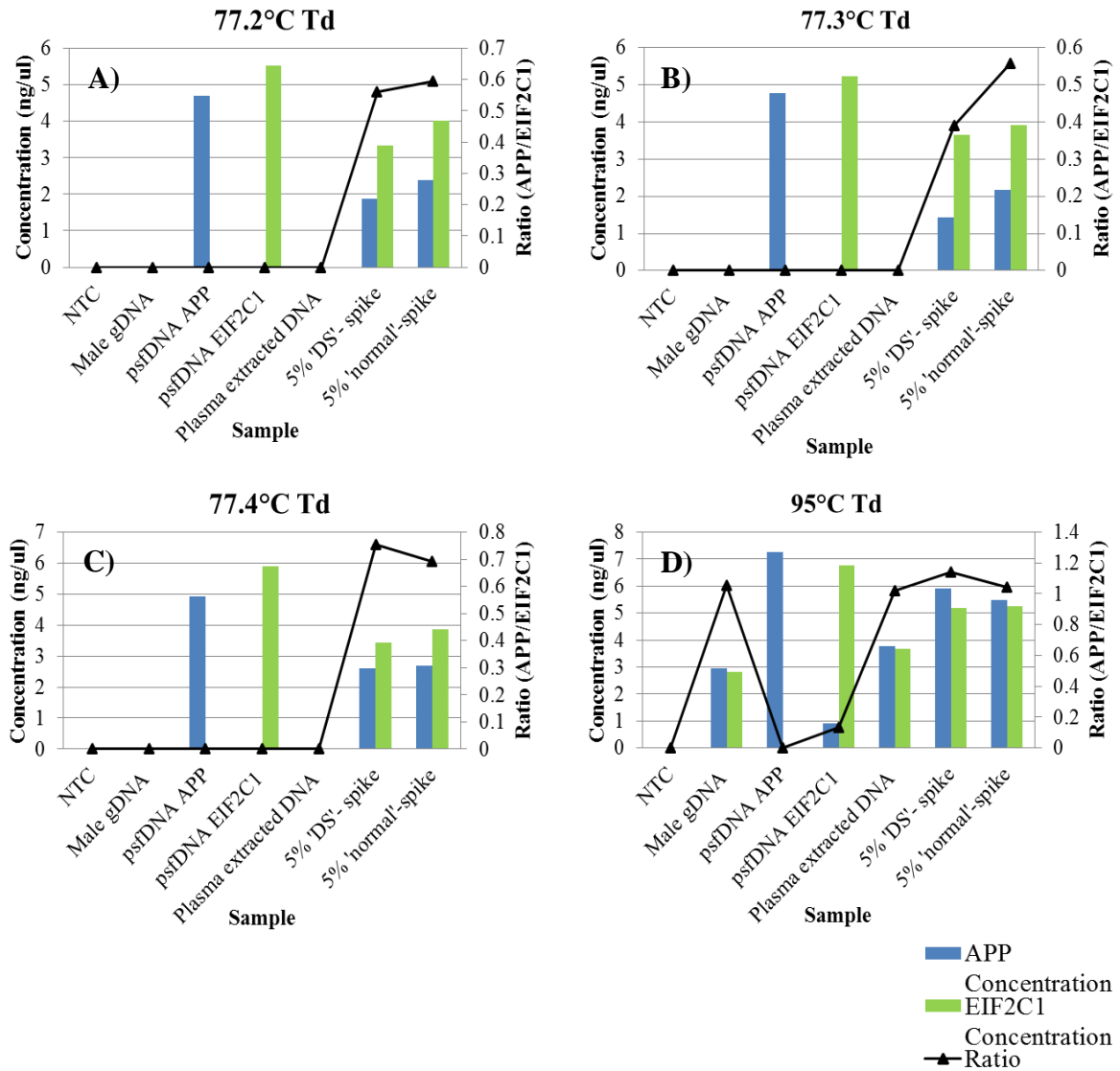


**Figure 3-16: Clustered bar charts illustrating the concentration (ng/  $\mu$ L) of *APP-FAM* (blue) and *EIF2C1-HEX* (green) with ratio analysis (black) for the following samples; NTC, Male gDNA, psfDNA (*APP*), psfDNA (*EIF2C1*), Plasma extracted DNA, 5% ‘DS’-spike and 5% ‘normal’-spike. The results for all samples were collected at three lower T<sub>d</sub>s; 77.2°C (A), 77.3°C (B), and 77.4°C (C), and at the optimal 95°C T<sub>d</sub> (D) for determination of the T<sub>c</sub> in a multiplex reaction. The psfDNA samples only showed amplification of the**



corresponding target at all three lower  $T_d$ s (A-C), however small amounts of *APP* (0.92ng/ $\mu$ L) were present in the psfDNA (*EIF2C1*) sample when amplified at 95°C  $T_d$  (D). Male gDNA and Plasma extracted DNA illustrate no DNA template amplification for both targets at 77.2°C and 77.3°C (A, B), but the plasma extracted sample did show minimal amplification of the *EIF2C1* target (0.007ng/ $\mu$ L) at 77.4°C (C). Both Male gDNA and plasma extracted DNA illustrate DNA template amplification of both targets at 95°C expressing a ratio of 1.05 and 1.02, respectively (D). Both DNA targets (*APP* and *EIF2C1*) are present for 5% 'DS'-spike and 5% 'normal'-spike at all temperatures (A-D). However, at the lower  $T_d$ s the ratios are reduced <1 (0.4 – 0.7) (A-C). When amplified at 95°C  $T_d$ , the 5% 'DS'-spike and the 5% 'normal'-spike samples illustrate ratios of 1.14 and 1.04, respectively.

In addition to the *APP* and *EIF2C1* multiplex reactions, Xp22.3 (HEX) and *SRY*<sup>(H.P.T)</sup> (FAM) were also tested. Initially, 14 unknown blood samples from NHSBT (Bristol, UK) were sexed using the *SRY*<sup>(H.P.T)</sup> internal primers by conventional PCR following genomic DNA extraction (Table 2-1) (refer to 2.3.1). Figure 3-17 shows the agarose gel image for all 14 samples and two NTCs. Eight samples illustrated a band between 50-100bp and were determined to be Male (976K, 386P, 671X, 8023, 936C, 279X, 141W and 708A). The other seven samples did not illustrate a band and were therefore classified as female (583G, 5510, 650F, 816G, 6547 and 155P) (Figure 3-17).

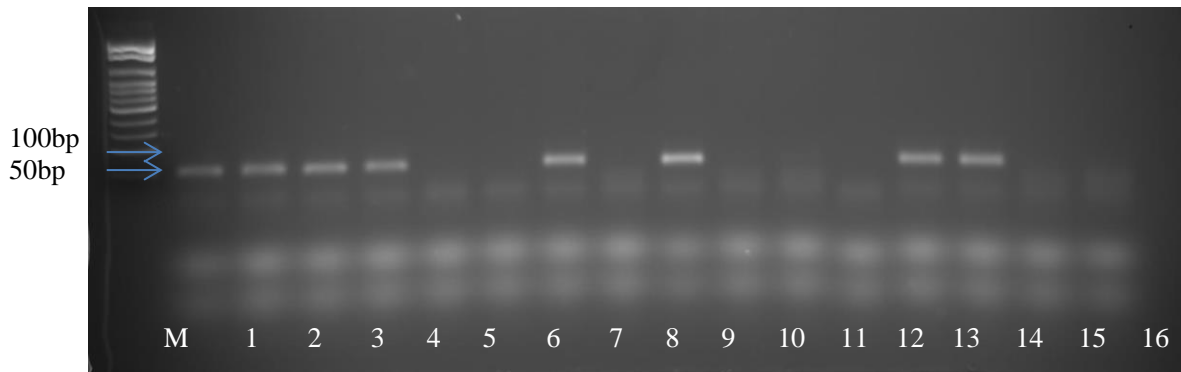


**Figure 3-17: 2% agarose (w/v) gel showing sexing results for 14 unknown samples.**

M= 100bp DNA ladder. Lane 8 and 16 represent NTC controls. Lanes 1, 2, 3, 4, 7, 9, 13 and 14 represent samples 976K, 386P, 671X, 8023, 936C, 297X, 141W and 708A, respectively. All these samples show *SRY*<sup>(H.P.T)</sup> amplification and were classified as Male samples. Lanes 5, 6, 10, 11, 12 and 15 represent samples 583G, 5510, 650F, 816G, 6547 and 155P, respectively. These samples did not show any *SRY* (H.P.T) amplification and were therefore classified as female samples.

The  $T_c$  was optimised for both Xp22.3 and *SRY*<sup>(H.P.T)</sup> in a singleplex reaction on the qPCR (data not shown) (Table 3-2). Even though the singleplex experiments revealed a  $T_c$  of 75°C, an initial  $T_d$  of 76°C was chosen due to the increase in  $T_d$  observed for the *APP/EIF2C1* multiplex reactions. The Xp22.3 (HEX) and *SRY*<sup>(H.P.T)</sup> (FAM) multiplexing results are illustrated in Figure 3-18. Samples were all diluted to 2ng/μL before amplification. The Male gDNA sample only showed amplification of both targets (*SRY*/Xp22.3) at 95°C  $T_d$  (Figure 3-18A). However, sample 8023 (Male) showed amplification of both targets at 95°C  $T_d$ , and also demonstrated late amplification of Xp22.3 (HEX) at 76°C (38.9 Ct) (Figure 3-18B). The psfDNA (Xp22.3) and psfDNA (*SRY*) only show amplification of corresponding targets at both  $T_d$  temperatures (95°C and 76°C), illustrating no sample contamination (Figure 3-18).

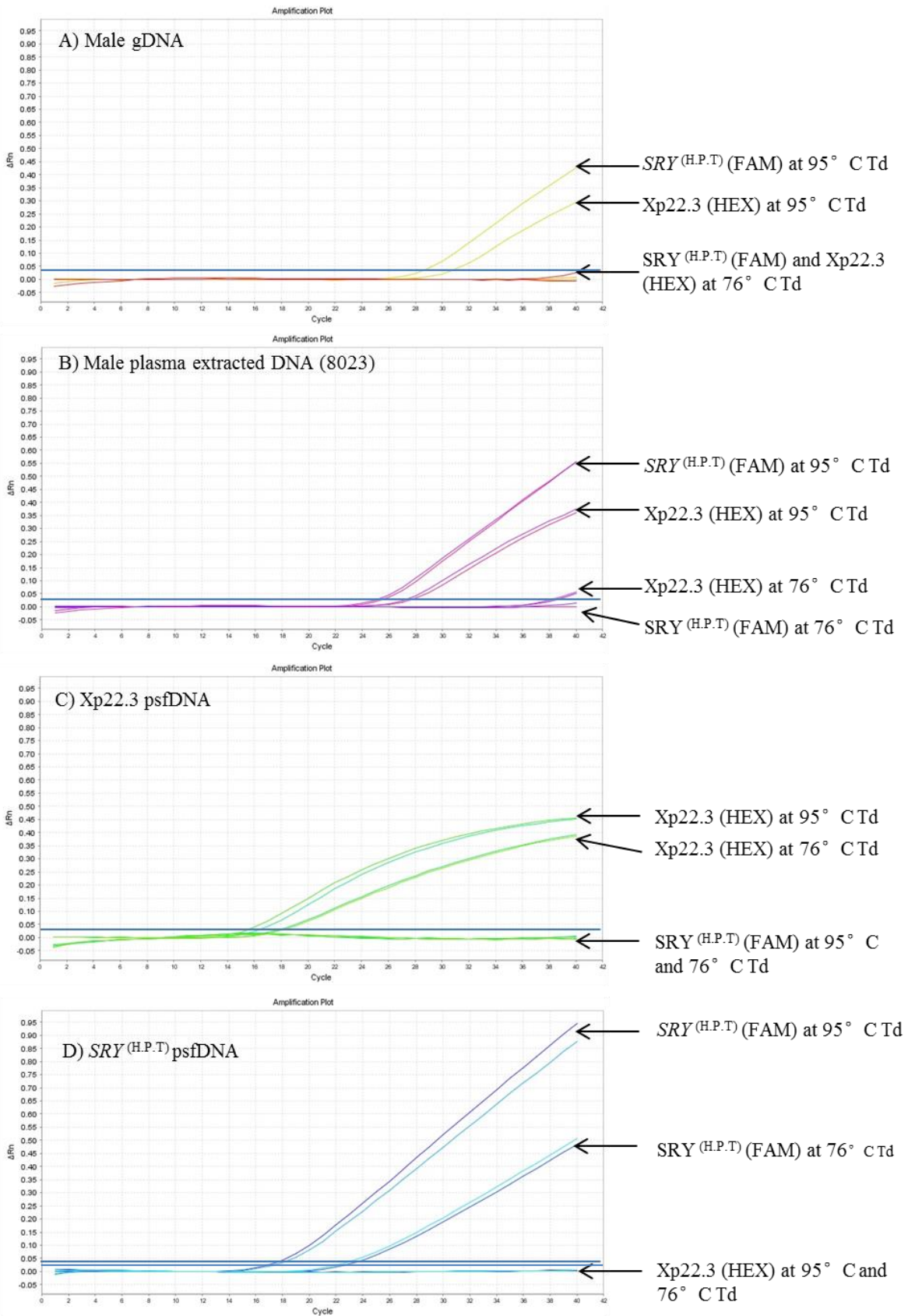


**Figure 3-18: Amplification of  $SRY^{(H.P.T)}$  (FAM) / Xp22.3 (HEX) multiplex reaction at 95°C T<sub>d</sub> and 76°C T<sub>d</sub> for samples; Male gDNA (2ng/μL) (A),**

**male plasma extracted DNA (8023) (B), psfDNA (Xp22.3) (C) and psfDNA (SRY<sup>H.P.T</sup>) (D).** Male gDNA only shows *SRY*<sup>(H.P.T)</sup> (FAM) and Xp22.3 (HEX) amplification at 95°C T<sub>d</sub> (28.7 Ct and 30.9 Ct, respectively) (A). However, plasma extracted DNA sample 8023 also shows amplification of Xp22.3 (HEX) amplification at 76°C T<sub>d</sub> (38.6 Ct) in addition to *SRY* (FAM) and Xp22.3 (HEX) amplification at 95°C T<sub>d</sub> (25.4 Ct and 27.7 Ct, respectively) (B). The psfDNA (Xp22.3) sample only shows amplification of Xp22.3 (HEX) at 95°C T<sub>d</sub> and 76°C T<sub>d</sub> (16.1 Ct and 18.3 Ct, respectively) (C). The psfDNA (*SRY*) sample only showed amplification of *SRY* at 95°C T<sub>d</sub> and 76°C T<sub>d</sub> (17.9 Ct and 23.6 Ct, respectively) (D).

### 3.2.5 Optimisation of COLD-PCR for multiplex reactions using ddPCR

Following qPCR analysis, the T<sub>a</sub> was re-optimised on the ddPCR platform for the following multiplex reactions; *APP* (FAM)/ *EIF2C1* (HEX) and *SRY*<sup>(H.P.T)</sup> (FAM)/ Xp22.3 (HEX) (2.9). Figure 3-19 illustrates the T<sub>a</sub> gradient tested (61.6°C to 56°C). All targets show improved separation of droplets at the two lowest annealing temperatures (56.5°C and 56°C). The expected ratio for both multiplex reactions was 1. The *APP/EIF2C1* multiplex reaction illustrated a ratio closer to 1 at 56.5°C T<sub>a</sub> compared to 56°C T<sub>a</sub> (1.11 and 1.13, respectively). The *SRY/Xp22.3* multiplex reaction also illustrated a ratio closer to 1 at 56.5°C T<sub>a</sub> compared to 56°C T<sub>a</sub> (0.978 and 0.976, respectively) (Figure 3-20). Therefore, 56.5°C T<sub>a</sub> was used for the initial T<sub>d</sub> gradient experiment. The *APP/EIF2C1* multiplex reaction was also carried out using higher primer concentrations (900nM) in an attempt to produce a ratio closer to 1. However, the ratio produced was slightly less sufficient (1.13) than the previous experiment using lower primer concentrations (300nM) (1.11, respectively).

Since the installation of the ddPCR in December 2013, ethical approval for maternal samples had been successfully granted (refer to 2.1.5). This allowed analysis of COLD-PCR to be determined using actual maternal samples on this platform as opposed to pseudo-maternal samples, which were used in previous qPCR analysis.

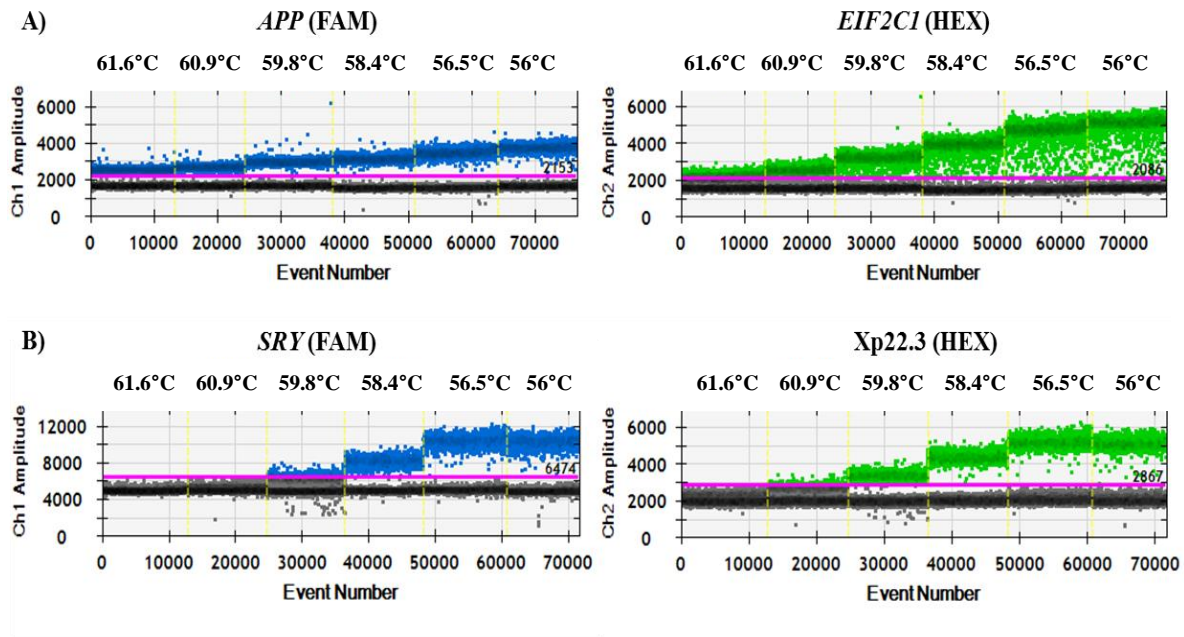


**Figure 3-19: 1D amplitude plots illustrating  $T_a$  gradient from 61.6°C to 56°C for target genes (blue, left), *APP* and *SRY*, and reference genes (green, right), *EIF2C1* and Xp22.3. A) *APP* (FAM)/ *EIF2C1* (HEX) multiplex reaction. B) *SRY*<sup>(H.P.T)</sup> (FAM)/ Xp22.3 (HEX) multiplex reaction. The pink line in all plots illustrates the threshold that was set manually for best separation of positive droplets (above threshold) and negative droplets (below threshold). All targets illustrate optimal separation at 56.5°C  $T_a$  and 56°C  $T_a$ .**

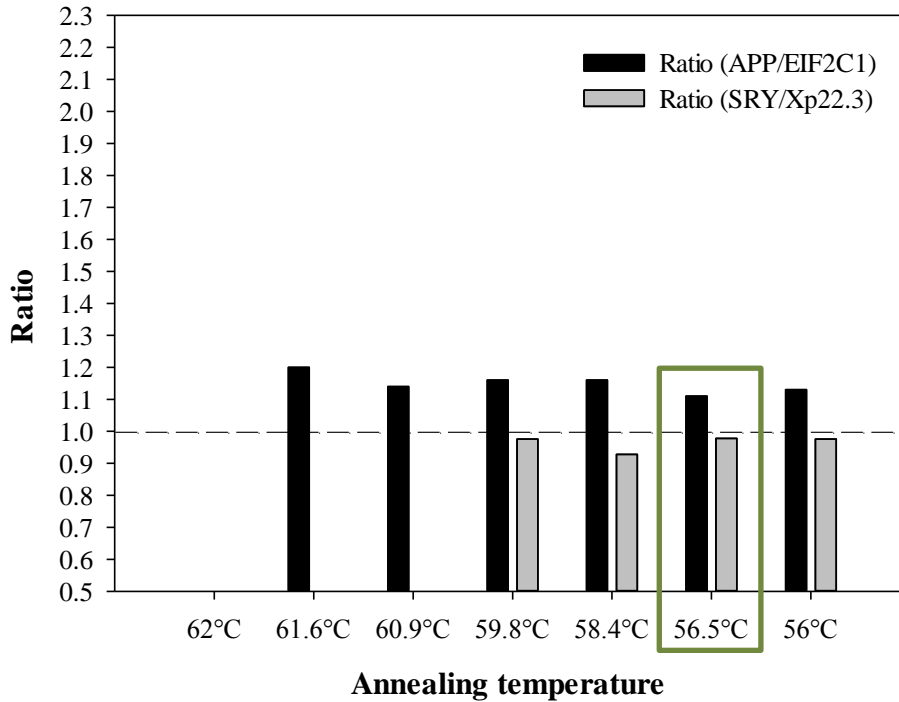


**Figure 3-20: Bar chart demonstrating ratios achieved for *APP/EIF2C1* multiplex reactions (black) and *SRY/Xp22.3* multiplex reactions (grey) at varying  $T_{as}$  (62°C to 56°C). The optimum  $T_a$  achieved was 56.5°C (highlighted green), since this  $T_a$  produced ratios closet to 1 (dashed line) for the *APP/EIF2C1* and *SRY/Xp22.3* multiplex (1.11 and 0.978, respectively). When amplified at 62°C, droplet separation for one amplicon, or both amplicons, was impaired and ratio could not be generated for either of the multiplex reactions.**

Following optimisation of primer concentration (300nM) and sample concentration (20-30ng/ reaction) (data not shown), three maternal samples (ST1, ST2 and 1A) were tested at 95°C  $T_d$  (control), 78°C  $T_d$  and 76°C  $T_d$ . In addition, Male gDNA (4ng/ $\mu$ L) and NTC were tested at all temperatures (2.9.3) and plasma extracted DNA from a female donor (583G) (4ng/ $\mu$ L) was tested at 95°C  $T_d$  as a negative control for *SRY* amplification. Despite qPCR optimisation of multiplex reactions (including *SRY*<sup>(H.P.T)</sup> (FAM)/ Xp22.3 (HEX)), the ddPCR results clearly highlights the variation in amplification efficiencies at

reduced temperatures (Table 3-4). The results illustrated depletion of both target-genes at the lower  $T_d$  (*SRY* and Xp22.3), but show increased efficiency for the Xp22.3 oligonucleotides, since there is a considerable decline in the ratio at 78°C/76°C  $T_d$  compared to 95°C  $T_d$  for the Male gDNA control (0.29/0.21 and 0.98, respectively) (Table 3-4). Furthermore, it is expected that the ratio for maternal samples carrying male fetuses will increase at the  $T_c$ , since the larger-maternal fragments of Xp22.3 should not be amplified (depleted), thus reducing the HEX-signal. However, maternal samples ST1 and 1A illustrate higher ratios at 95°C  $T_d$  (0.24 and 0.02, respectively) compared to 78°C  $T_d$  (0.122 and 0.014, respectively) (Table 3-4). Target concentrations can also be used to calculate cffDNA fractions (2.9.4). Higher ratios can also be equated to increased cffDNA fractions, therefore both ST1 and 1A maternal samples illustrated a reduction in cffDNA fractions at 78°C  $T_d$ , showing depletion of fetal DNA as opposed to enrichment (Table 3-4). The *SRY* target was not amplified for maternal samples (ST1 and 1A) at 76°C  $T_d$ , indicating that this temperature is too low for *SRY* amplification even though Xp22.3 (reference gene) was still successfully amplified at this  $T_d$  (15.6 copies/ $\mu$ L).

**Table 3-4: ddPCR results for *SRY*<sup>(H.P.T)</sup> (FAM)/ *Xp22.3* (HEX) multiplex reaction at 95°C T<sub>d</sub>, 78°C T<sub>d</sub> and 76°C T<sub>d</sub>. Results show the concentration (copies/ μL) of each target, the ratio generated (FAM / HEX) and calculated cffDNA fraction (refer to 2.9.4).**

	95°C T <sub>d</sub>				78°C T <sub>d</sub>				76°C T <sub>d</sub>			
	Concentration (Copies/μL)		Ratio	cffDNA fraction (%)	Concentration (Copies/μL)		Ratio	cffDNA fraction (%)	Concentration (Copies/μL)		Ratio	cffDNA fraction (%)
	<i>SRY</i>	<i>Xp22.3</i>			<i>SRY</i>	<i>Xp22.3</i>			<i>SRY</i>	<i>Xp22.3</i>		
Male gDNA (20ng) 583G (female) (20ng)	287	294	0.975	N/A	28.7	98.1	0.292	N/A	0.564	3.39	0.166	N/A
Maternal sample ST1 (male fetus)*	5.28	41.4	0.128	22.6%	1.91	37.6	0.0507	9.7%	0	15.6	N/A	N/A
Maternal sample ST2 (female fetus)*	0	17.4	N/A	N/A	0	12.5	N/A	N/A	0	3.58	N/A	N/A
Maternal sample 1A (male fetus)**	4.49	224	0.02	3.9%	1.38	102	0.014	2.7%	0	1.53	N/A	N/A

\*Obtained from Dr Svetlana Trivodalieva (2013), Research Center for Genetic Engineering and Biotechnology, Macedonian Academy of Sciences and Arts, Krste Misirkov 2, 100 Skopje, Republic of Macedonia. \*\* Maternal samples from Plymouth Hospitals NHS Trust (Plymouth, UK).

Therefore, the *SRY*<sup>(H.P.T)</sup> (FAM) target was multiplexed against the *EIF2C1* (HEX) reference, since this target illustrated higher T<sub>d</sub> dropout compared to *Xp22.3* (78°C and 75°C, respectively) from the initial conventional PCR results (Table 3-2). In this experiment only two maternal samples were tested (ST1 and ST2), alongside Male gDNA (5ng/ reaction), Female gDNA (4.8ng/ reaction) and a NTC at all three T<sub>d</sub> temperatures (95°C, 78°C and 76°C). Lower concentrations of Male and Female gDNA were tested



(5ng/ reaction) to be more representative of maternal sample concentrations (2-5ng/ reaction). The results in Table 3-5 showed that at 76°C T<sub>d</sub> there was no amplification of both targets, even though the *SRY* target was successfully amplified at this T<sub>d</sub> (for Male gDNA control only) in the previous experiment. This is likely to be attributed to the lower concentration of Male gDNA used.

**Table 3-5: ddPCR results for *SRY*<sup>(H.P.T)</sup> (FAM)/ *EIF2C1* (HEX) multiplex reactions at 95°C T<sub>d</sub>, 78°C T<sub>d</sub> and 76°C T<sub>d</sub>.** Results show the concentration (copies/ μL) of each target, the ratio generated (FAM / HEX) and calculated cffDNA fraction (refer to 2.9.4).

	95°C				78°C				76°C			
	Concentration (Copies/μL)		Ratio	cffDNA fraction	Concentration (Copies/μL)		Ratio	cffDNA fraction	Concentration (Copies/μL)		Ratio	cffDNA fraction
	<i>SRY</i>	<i>EIF2C1</i>		(%)	<i>SRY</i>	<i>EIF2C1</i>		(%)	<i>SRY</i>	<i>EIF2C1</i>		(%)
Male gDNA (5ng)	26.6	47.6	0.558	N/A	4.18	1.04	4.01	N/A	0	0	N/A	N/A
Female gDNA (5ng)	0	42.8	N/A	N/A	0	5.32	N/A	N/A	0	0	N/A	N/A
Maternal sample ST1 (male fetus)*	3.4	56.2	0.0605	12.1%	4.66	12.2	0.383	76.4%	0	0	N/A	N/A
Maternal sample ST2 (female fetus)*	4.22	22.6	N/A	N/A	2.41	3.32	N/A	N/A	0	0	N/A	N/A

\*obtained from Dr Svetlana Trivodalieva (2013), Research Center for Genetic Engineering and Biotechnology, Macedonian Academy of Sciences and Arts, Krste Misirkov 2, 100 Skopje, Republic of Macedonia.

Amplification of Male gDNA at 95°C illustrated a ratio of 0.558, which is close to the expected ratio (0.5), since male samples will express 1 copy of *SRY* and two copies of *EIF2C1*. The lower T<sub>d</sub> (78°C) displayed an increased ratio (4.01) for Male gDNA

indicating biased amplification of *SRY*<sup>(H.P.T)</sup> (FAM) over *EIF2C1* (HEX). Though there was selective amplification of the *SRY* target, the concentration was dramatically reduced for both *SRY* and *EIF2C1* targets at the lower  $T_d$  (78°C) (4.01 copies/ $\mu$ L and 1.04 copies/ $\mu$ L, respectively) compared to the optimal  $T_d$  (95°C) (26.6 copies/ $\mu$ L and 47.6 copies/ $\mu$ L, respectively) (Table 3-5). The maternal sample carrying a female fetus (ST2) should only indicate amplification of the *EIF2C1* reference gene, however at 95°C  $T_d$  and 78°C  $T_d$  there was *SRY* amplification (Table 3-5). In repeated experiments, with new sample aliquots it was identified that the *SRY*<sup>(H.P.T)</sup> (FAM) target was being amplified in random female samples. Therefore, future sexing experiments were carried out using *SRY* primers designed by Lo et al. (1997). The maternal sample carrying the male fetus (ST1) illustrated a decreased cffDNA fraction for the *SRY/EIF2C1* multiplex compared to the previous *SRY/Xp22.3* multiplex (12.1% and 22.6%, respectively). However, it is possible that multiple (2-3 times) freeze-thawing of the sample led to a decline in the cffDNA fraction.

In contrast to the previous *SRY/Xp22.3* multiplex reaction, the *SRY/EIF2C1* multiplex reaction saw an increase in ratio, and subsequently cffDNA fraction, at the lower  $T_d$  (78°C) compared to the optimum  $T_d$  (95°C) (0.0605 and 0.383 ratios, respectively) (Table 3-5). This resulted in a 6.3-fold increase in cffDNA fraction. Because the data is contradictory between the two multiplex reactions, it cannot be concluded that the increase in fetal proportion in the *SRY/EIF2C1* multiplex is a result of COLD-PCR selective amplification. It is likely that the difference is caused due to difference in primer efficiencies at the lower  $T_d$ , since the previous experiment illustrated biased amplification of the reference gene (Xp22.3), reducing the ratio and consequently cffDNA fraction. Whereas in the second multiplex reaction (*SRY/EIF2C1*) the target gene (*SRY*) showed biased amplification at 78°C  $T_d$ , increasing the ratio (Table 3-4 and Table 3-5). These

results illustrate that extensive primer optimisation is required to ensure equal ratios can be obtained even at 'critical'  $T_d$ . Because the overall aim is to selectively enrich shorter fetal fragments and subsequently determine chromosome imbalances (through ratio analysis) for aneuploidy detection (primarily T21), the *APP/EIF2C1* multiplex reaction  $T_d$  was optimised.

An initial  $T_d$  optimisation experiment using Male gDNA (20ng/ reaction) illustrated final amplification of *APP* and *EIF2C1* at 77.5°C  $T_d$  and 76.8°C  $T_d$  respectively (Table 3-6). In a secondary, singleplex,  $T_d$  optimisation experiment the lowest  $T_d$  at which product could be amplified was further refined and final amplification of *APP* and *EIF2C1* for Male gDNA was shown at 77.2°C  $T_d$  and 76.5°C  $T_d$ , respectively (Figure 3-21). Additionally, Xp22.3 was also tested and final amplification was shown at 75.7°C  $T_d$  (Figure 3-21). Therefore,  $T_d$ s below the point at which amplification last occurred (expected  $T_c$ s) were selected for *APP* (76.8°C), *EIF2C1* (76.2°C) and Xp22.3 (75°C) for the following experiment. In this experiment singleplex reactions were used to test the amplification of Male gDNA (30ng/ reaction), T21 gDNA (10ng/ reaction) and maternal sample 1B (30ng/ reaction) at the optimal  $T_d$  (95°C) and expected  $T_c$  (see above). NTCs were also tested for each singleplex reaction at both  $T_d$ s.

The Xp22.3 target illustrated successful amplification for all samples (except NTC) at 95°C  $T_d$ , but at 75°C  $T_d$  only the Male gDNA control and maternal sample 1B illustrated minimal amplification of Xp22.3 (HEX) (Figure 3-22). Although, it is important to note that the T21 gDNA was more dilute due to limited available and high costs of sample. The maternal sample 1B illustrates a higher number of Xp22.3 positive droplets compared to the Male gDNA control at 75°C (32 events and 6 events, respectively). This illustrates selective amplification in the maternal sample, however to completely eradicate amplification of the Xp22.3 target in Male gDNA this would require further reducing  $T_d$ .

Therefore, the experiment was repeated at 74.8°C  $T_d$  using Male gDNA (20ng/ reaction) and maternal sample 1D (20ng/ reaction). The results demonstrated Xp22.3 (FAM) amplification for both Male gDNA and maternal sample 1D (6 events and 5 events, respectively). This illustrated no selective amplification of shorter fragments in maternal sample (1D) compared to Male gDNA with only contains larger cfDNA fragments (results not shown). Previous experiments illustrated that at 74.9°C  $T_d$  Male gDNA was not amplified (Figure 3-21) using 5ng/ reaction of Male gDNA, but when higher concentrations were used (20ng/ reaction) Male gDNA was successfully amplified at 74.8°C  $T_d$ . This result illustrated that dropout is also dependant on starting quantity and not just  $T_d$ .

The *APP* target and *EIF2C1* target both show amplification of all samples (except NTC) at 95°C  $T_d$ . But at the expected  $T_c$  none of the samples illustrated successful amplification not even maternal sample 1B (Figure 3-22). The *EIF2C1* target demonstrated amplification of Male gDNA and maternal sample 1B at 76.5°C  $T_d$  (Figure 3-21) but did not show amplification of both samples at 76.2°C  $T_d$  (Figure 3-22). The *APP* target showed amplification of Male gDNA and maternal sample 1B at 77.2°C  $T_d$  (Figure 3-21) but did not show amplification of both samples at 76.8°C  $T_d$  (Figure 3-22). Therefore, amplification of *APP* at 77°C  $T_d$  was tested using the same samples, but both the maternal sample (1B) and the Male gDNA sample illustrated amplification (data not show). Although further  $T_d$ s between 76.2°C and 76.5°C for *EIF2C1* and  $T_d$  76.9°C for *APP* could have been tested, supplementary experiments were not carried out due to the following reasons; 1) The  $T_d$  dropout for Male gDNA is too close to  $T_d$  dropout of maternal samples, which prevents multiplexing of *EIF2C1* and *APP* for ratio analysis. 2) Further primer optimisation is required, since there is too much variation in the efficiencies of *APP* and *EIF2C1* oligonucleotides at the lower  $T_d$ s for accurate analysis of

chromosome imbalance (Table 3-6). However, such primer optimisation is likely to be highly challenging, especially when considering the close boundaries between maternal sample dropout and Male gDNA dropout.

**Table 3-6: ddPCR results for *APP* (FAM)/ *EIF2C1* (HEX) multiplex reactions at 95°C Td, 77.5°C Td, 76.8°C Td and 75.5°C Td. Results show the concentration (copies/  $\mu$ L) of each target and the ratio generated (FAM / HEX).**

	95°C			77.5°C			76.8°C			75.5°C		
	Concentration (Copies/ $\mu$ L)		Ratio	Concentration (Copies/ $\mu$ L)		Ratio	Concentration (Copies/ $\mu$ L)		Ratio	Concentration (Copies/ $\mu$ L)		Ratio
	<i>APP</i>	<i>EIF2C1</i>		<i>APP</i>	<i>EIF2C1</i>		<i>APP</i>	<i>EIF2C1</i>		<i>APP</i>	<i>EIF2C1</i>	
Male gDNA (40ng)	878	760	1.16	1.46	5.03	0.289	No call	3.08	N/A	No call	No call	N/A
Female gDNA (20ng)	475	444	1.07	1.69	3.39	0.5	No call	2.1	N/A	No call	No call	N/A
Female gDNA (40ng)	892	893	0.999	No call	5.91	N/A	No call	4.12	N/A	No call	No call	N/A
T21 gDNA (40ng)	218	152	1.45	0.61	0.915	0.667	No call	0.740	N/A	No call	No call	N/A
T21 gDNA (40ng)	462	310	1.49	1.62	1.93	0.84	No call	1.67	N/A	No call	No call	N/A

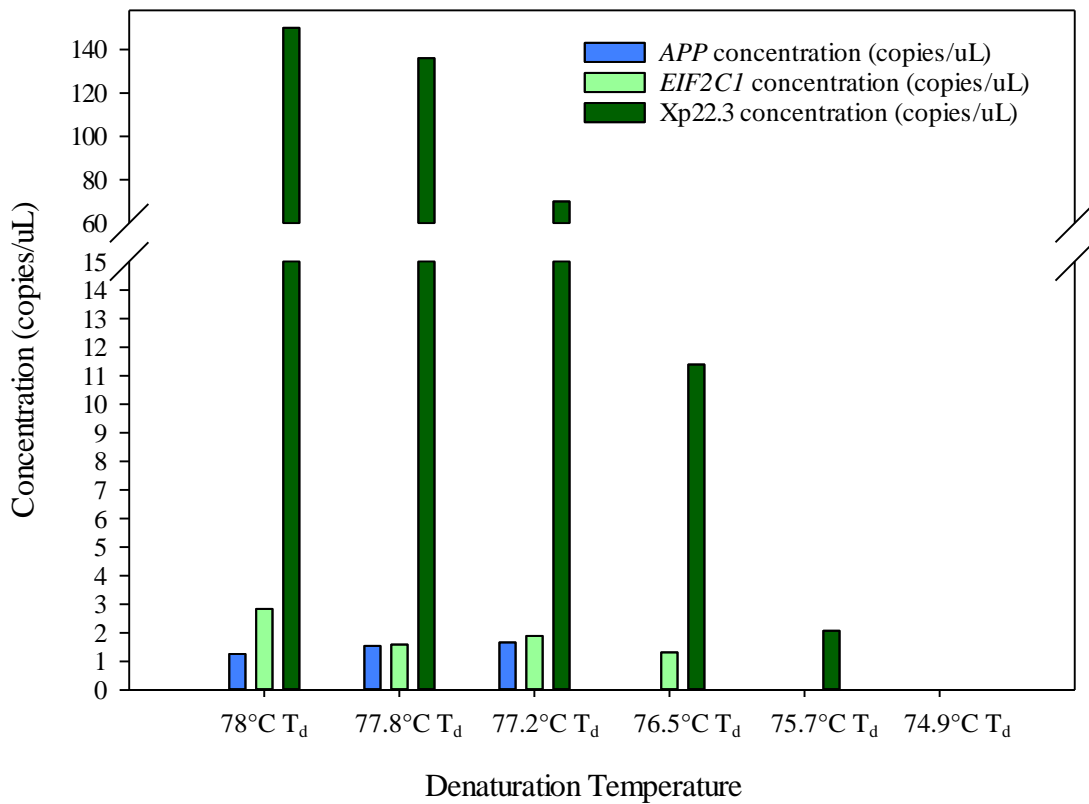


**Figure 3-21: Bar chart showing the concentration (copies/ $\mu$ L) of *APP* (FAM), *EIF2C1* (HEX) and *Xp22.3* (HEX) in singleplex reactions for  $T_d$  gradient (78°C to 74.9°C). *APP* (FAM) (blue) shows final amplification at 77.2°C  $T_d$ . *EIF2C1* (HEX) (green) shows final amplification at 76.5°C  $T_d$ . *Xp22.3* (HEX) (dark green) shows final amplification at 75.7°C  $T_d$ .**

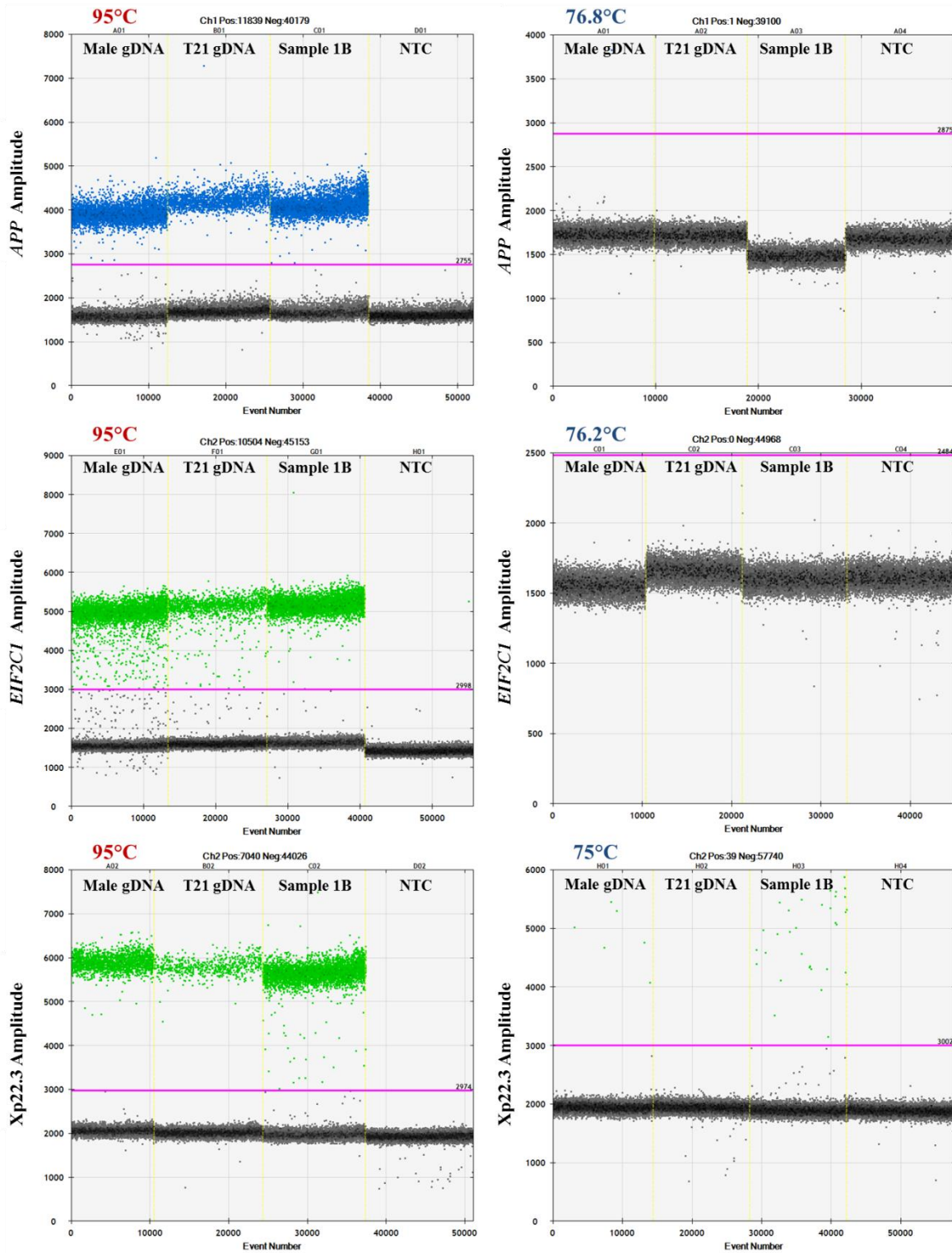


Figure 3-22: 1D amplitude plot illustrating droplet separation for Male gDNA, T21 gDNA, maternal sample 1B and NTC for singleplex reactions *APP*, *EIF2C1* and *Xp22.3*



at 95°C T<sub>d</sub> and expected T<sub>c</sub>. The pink line indicates threshold set manually for droplet separation.

### 3.3 Discussion

#### 3.3.1 COLD-PCR for selective amplification of D21S1890 STR psfDNA

Initial experiments revealed that amplification of the D21S1890 psfDNA fragment (containing CA-repeat STR) at the T<sub>c</sub> (80°C) produced a smaller product in comparison to product amplified at 95°C T<sub>d</sub> (Figure 3-4). Previous unpublished data also revealed that spike experiments showed multiple stutter peaks as oppose to expected three visible alleles (Figure 3-23), which further suggests size discrepancies between amplified products. Stutter peaks are a common biological artefact of STR analysis, and it is more common for stutter peaks to occur with di-nucleotide repeats as oppose to larger tri- or tetra-nucleotide repeat units (Murray, Monchawin and England, 1993). The proposed mechanism for the production of stutter peaks is known as slipped strand mispairing, which is suggested to occur if the polymerase falls off the extension strand during amplification. Subsequently, the template strand and extension strand breathe apart and as a consequence a single unit can be looped out during the re-annealing phase, resulting in the synthesis of an extended strand which contains one less repeat than the template strand (Walsh, Fildes and Reynolds, 1996).

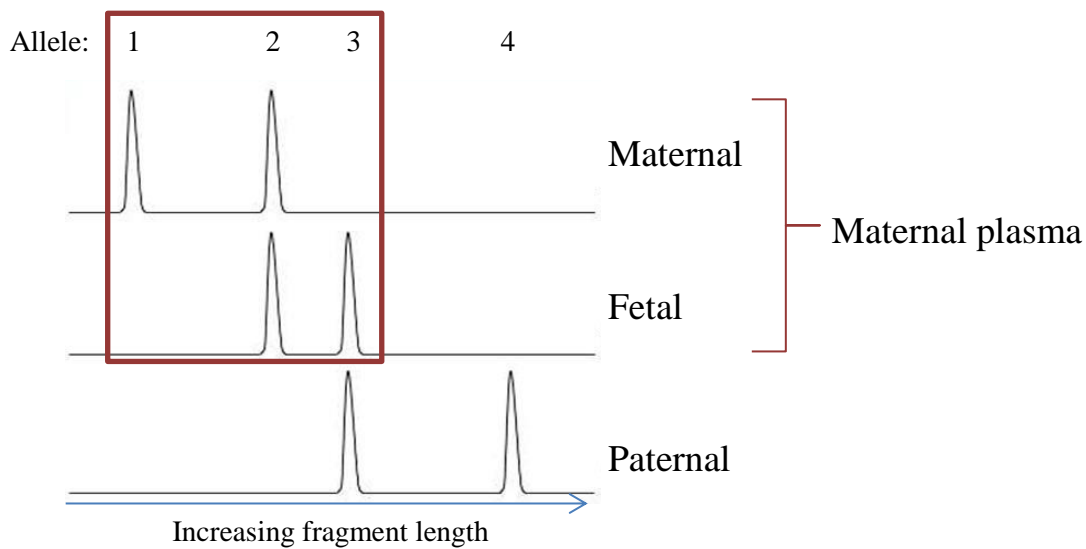


**Figure 3-23: Schematic diagram showing the fragment length of alleles from a heterozygous fetus, alongside the alleles of the heterozygous mother and heterozygous father.** The red square highlights the three alleles which should be represented in the maternal plasma sample, including; a pure maternal allele (1), a distinguishing paternally inherited fetal allele (3) and a matching allele, which is expressed by both fetus and mother (2).

Taq polymerase misreading and secondary DNA structures have also been associated with occurrence of stutter patterns (Miller and Yuan, 1997). The presence of stutter peaks can obscure results and interfere with analysis of allele determination. However, it was identified that the occurrence of stutter patterns could be reduced by optimising PCR conditions, such as primer concentration, in conjunction with hot-start PCR (Kellogg *et al.*, 1994). Prior to PCR amplification, mispriming on less specific sites and primer dimerization can occur at temperatures below the cycling conditions. Providing a hot-start prevents unwanted DNA synthesis, particularly for amplifications involving multiplex reactions (multiple primers), high GC content of amplicon or high cycle numbers (Kermekchiev, Tzekov and Barnes,

2003). Kellogg *et al.* (1994) illustrated that the higher the number of cycles the bigger the change visible in size distribution. This signifies that the occurrence of stutter peaks in this study were a result of Taq Polymerase misreading as opposed to secondary DNA structures, since the pattern would remain consistent during amplification if caused by secondary structures. More recently, it has been identified that higher stutter peaks have been associated with low copy number STR typing (Seo *et al.*, 2014). Results illustrated that lowering the annealing/extension temperature to 56°C enhances the stability of the polymerase and DNA template strand, reducing the likelihood of slippage during PCR amplification (Seo *et al.*, 2014).

In this study instead of decreasing the annealing temperature, the  $T_d$  was reduced in an attempt to selectively enrich the shorter psfDNA fragments. However, the optimum denaturation temperature for complete dissociation and strand separation is 95°C and at the lower  $T_d$  shorter products were visible (Figure 3-4). Therefore, the D21S1890 psfDNA fragments following PCR amplification at 80°C and 95°C were cloned and sequenced to determine the cause of stutter peaks and shorted fragment size. The sequencing results illustrated that at the lowest  $T_d$  the entire CA repeat region was deleted and an additional 15bp of the expected product using the internal primers (Figure 3-5). While at the optimal  $T_d$  (95°C) the entire D21S1890 psfDNA internal product was successfully amplified (Figure 3-5). This could have been a result of slippage due to reduced PCR efficiency at lower  $T_d$ , but additionally may have also been caused by possible hairpin-loop formation at the  $T_c$ .

The hairpin loop is a secondary structure caused by intramolecular base pairing that can be formed by DNA or RNA and often occurs when two regions of the same strand are complementary in nucleotide sequence. The D21S1890 internal sequence illustrates three C-nucleotides 26 bp downstream from the start of the forward primer and three complementary G-nucleotides 76 bp downstream from the start of the forward primer, which incorporate the

majority of the missing sequence (91%). However, just prior to the three C-nucleotides are three T-nucleotides that are missing from the sequence alignment (Figure 3-5). Polymerase slippage only occurs at repeat regions, since directly repeated sequences provide multiple re-annealing sites for the extension strand if the strands are separated. In addition, slippage to a matching repeat is often small, since slippage of multiple repeat units becomes energetically unfavourable as more bonds must be broken in the template than are reformed in the loop (McMurray, 1999). Therefore, due to the size of the deletion and the deletion of addition bases other than just the CA-repeat, it is likely that the shorter product amplified at the lower  $T_d$  is a result of hairpin-loop formation as oppose to slippage.

The polymorphic characteristic of STRs is the variation in the number of tandemly repeated units between alleles. These results have indicated that lowering the  $T_d$  reduces the PCR efficiency and as a result does not amplify the entire internal product. More importantly the entire region of interest (ROI) was deleted preventing allele analysis. Stutter peaks are a common factor of STR marker analysis, particular for di-nucleotide repeat regions. In order to reduce the occurrence of these peaks all aspects of PCR amplification should be optimal, including annealing temperature, primer concentration and Taq used. Therefore, selective enrichment of psfDNA using COLD-PCR for regions containing STR markers is not reliable since region of interest can be completely deleted. In addition, variations in CA-repeat regions between maternally inherited and paternally inherited alleles for each individual fetus may alter the  $T_c$  required for selective enrichment.

### 3.3.2 COLD-PCR for the selective enrichment of non-polymorphic DNA target regions

Currently, NGS is at the forefront of research for NIPD and its application in prenatal testing is currently used worldwide (Lo, 2015). However, despite the continual decline in costs this method is still not routinely available for all pregnancies (high and low risk) and is currently

only used as a private secondary screening tool rather than a replacement for invasive diagnosis. The accuracy of NGS is unrivalled (99%) but false negative results can still occur, often as a result of low cfDNA fractions (Lo, Chiu and Chan, 2014; Porreco *et al.*, 2014). Enriching the proportion of cfDNA would not only allow improved sample quality for NGS analysis, but could also improve detection of fetal aneuploidy on cheaper alternative platforms such as dPCR. The COLD-PCR selective enrichment approach was first described using single-nucleotide mismatch between mutant and wild-type dsDNA sequences. Depending on the location of the mismatch the  $T_m$  is usually altered by 0.2-1.5°C for products  $\geq 200$  bp (Liew *et al.*, 2004). The  $T_c$  is lower than the  $T_m$ , and at this lower temperature DNA sequences with one or two nucleotide mismatches will be amplified at different efficiencies. Rather than separate mutant and wild-type sequences, this study aimed to determine the selective enrichment of cfDNA based on size variance with maternal cfDNA. The rationale behind determining the  $T_c$  was to find the  $T_d$  at which only the shorter psfDNA was amplified but not the longer 'maternal' DNA (Figure 3-1).

Prior to multiplexing qPCR experiments, the  $T_c$  was determined by conventional PCR for multiple loci on chromosomes 1, 21, 13, 18, X and Y using Male gDNA (Table 3-2). With multiplexing in consideration, target and reference genes that expressed similar  $T_c$ s were selected for aneuploidy experiments (*APP* and *EIF2C1*, respectively) and sexing experiments (*SRY*<sup>(H.P.T)</sup> and Xp22.3, respectively). Consequently, the  $T_c$  was further optimised for each target on the qPCR platform. The  $T_c$  of *EIF2C1* psfDNA (76.4°C) was only marginally lower than the  $T_c$  for Male gDNA (77°C), however by selecting a mid-range  $T_d$  between these two temperatures (76.7°C) allowed for only the smaller psfDNA to be selectively amplified (Figure 3-16). Sexing experiments revealed a lower  $T_c$  of 76°C (Figure 3-18). The initial  $T_c$  for Male gDNA was higher when running conventional PCR (78°C), but at this  $T_d$  qPCR illustrated amplification of Male gDNA for both targets (*APP* and *EIF2C1*). This can be

attributed to an increased number of cycles carried out on the qPCR platform (40 cycles) compared to convention PCR run (35 cycles) since amplification occurred after the 35<sup>th</sup> cycle.

Initial singleplex spiking experiments were also carried out to determine selective amplification of psfDNA fragments (*APP* and *EIF2C1*) at 76.7°C. However, only spikes that were produced by dilution as oppose to the GE method (refer to 2.1.4) showed successful amplification. By using the genomic equivalent approach much lower concentrations of psfDNA fragments were added to represent the correct number of copies of template for the 5% fetal proportion of the spike. The results illustrated that this was too dilute for qPCR amplification. Since multiple dilution steps of very small volumes were required to produce the GE spike, it is possible that the psfDNA fragment was lost during this process, hence all consecutive experiments were carried out using the dilution approach.

Multiplex PCR can help to reduce cost, time and effort by simultaneously amplifying multiple targets in a single reaction (Elnifro *et al.*, 2000). However, combining multiple oligonucleotides requires further optimisation to prevent preferential amplification of one specific target and ensure successful amplification under the same reaction conditions. The results show that at 95°C samples which should express an equal proportion of *APP* and *EIF2C1* (Male gDNA, plasma extracted DNA and 5% ‘normal’- spike) all demonstrated ratios close to 1 (1.05, 1.02, and 1.04, respectively) (Figure 3-16). In addition, results also show ratios close to 1 for the *APP/EIF2C1* multiplex (0.999) and the *SRY/Xp22.3* multiplex (0.975) when amplified at 56.5°C  $T_d$  on the ddPCR platform (Figure 3-19). This illustrates that there is equal amplification of both targets at the optimal  $T_d$  on both platforms. However, when the  $T_d$  was reduced (77.2°C-77.4°C) so that only targets containing ‘fetal’ DNA were amplified, the ratios for the 5% ‘normal’-spike and 5% ‘DS’-spike were reduced (ranging from 0.39 to 0.75). This shows that at lower  $T_d$ s there is selective amplification of the

*EIF2C1* (HEX) reference target. Even though the 'DS'-spike demonstrated a slightly higher ratio at 77.4°C compared to the 'normal'-spike, this was reversed when the temperature was reduced by 0.1°C and at 77.3°C the 'normal'-spike showed a higher ratio (Figure 3-16). This illustrated that despite selective enrichment of the psfDNA, the selective amplification of the reference target at the lower  $T_d$  made ratio analysis unreliable and highly sensitive to temperature change.

The denaturation phase of PCR is responsible for strand separation and if the  $T_d$  is too low then the gDNA is prevented from being denatured, which inhibits amplification (Auer *et al.*, 1996). Shorter fragments that contain less G-C nucleotide bases are likely to denature at lower temperatures since less kinetic energy is required for strand separation. Yakovchuk, Protozanova and Frank-Kamenetskii (2006) determined that the two main factors primarily responsible for the stability of dsDNA are base pairing (between complementary bases) and stacking (between adjacent bases). Since the guanine-cytosine pair (GC pair) is bound by three hydrogen bases as opposed to two hydrogen bases between the adenine-thymine pair (AT pair), more energy is required to break the additional hydrogen bonds in amplicons with higher GC-content (Petruska *et al.*, 1988). Yakovchuk, Protozanova and Frank-Kamenetskii (2006) determined that higher GC pairing minimally contributed to increased stability, whereas AT pairing was always destabilizing. Producing oligonucleotides which target amplicons with a lower GC content could help to reduce the melting temperature and would possible increase strand separation of the *APP* target at the  $T_c$ . The differences in thermal stability of each target at lower  $T_d$ s is shown in this study (Figure 3-16). The *EIF2C1* fragment, which is shorter (81bp) than the *APP* fragment (96bp), which also has a marginally higher GC content (54.3% and 53.1%, respectively), dropped out at a lower  $T_d$  compared to the *APP* fragment (Figure 3-16). For the longer *APP* fragment an increased number of base-stacking and base-pairing interactions occur, stabilising the fragment, which prevents

denaturation at the lower  $T_d$ . Rather than altering the GC content (since both fragments are relatively similar), reducing the fragment size of the *APP* target would equalise the number of base-stacking interactions (and base pairing interactions), which could allow targets to display more comparable stability at the lower  $T_{ds}$ .

The  $R_n$  value given on the Y-axis of the qPCR amplification plot represents the reporter signal normalised to the fluorescence signal of ROX™ (Life Technologies), generally higher quantities of starting DNA will produce a higher  $R_n$  value (along with a lower  $C_t$  value) as more fluorescent signals will be generated. However, during the multiplex experiment samples that were considered to have an equal proportion of chromosome 1 (*EIF2C1*) to chromosome 21 (*APP*), for example; Male gDNA, non-spiked plasma DNA, and 5% 'normal'-spike DNA, all illustrated higher  $R_n$  values for target *APP*. This could have been observed for two reasons; Firstly, chromosome 21 may have been more fragmented than chromosome 1. Secondly, the FAM™ reporter dye (which was the label for the *APP* target) works with higher levels of efficiency compared to the HEX™ reporter dye (which was the label for the *EIF2C1* target). Therefore, to determine whether it was the latter of the two, the qPCR was repeated with a dye swap, so that *APP* was labelled with HEX™ and *EIF2C1* was labelled with FAM™ (Figure 3-14). The results of this dye swap experiment showed the opposite effects to the initial experiment; target *EIF2C1* produced higher  $R_n$  values in comparison to *APP* for all samples. Consequently, it can be concluded that this study indicates that FAM™ illustrates more intense fluorescence than HEX™. The Life Technologies website itself states that FAM™ is the most intense dye and it has been identified that FAM reagents have numerous benefits in comparison to other fluorophores, for example FAM reagents give carboxamides that are more resistant to hydrolysis and also give better conjugation yields with increased stability, which could allow for the increase in reporter signals observed in this study (Hahn, Wilhelm and Pingoud, 2001). Even though



there appears to be a more intense fluorescent signal with FAM reporter dyes, the overall aim of this study is to identify over- or under-representation on chromosome 21 using a dPCR platform. Therefore the optimisation of these reporter dyes is unnecessary as dPCR works by the principal that each well contains only 1 DNA strand, so a fluorescent signal is either generated or it is not, the intensity of the signal is irrelevant. However the dye swap experiment helps to confirm that chromosome 21 is not more fragmented than chromosome 1.

The COLD-PCR analysis on the ddPCR platform was carried out using actual maternal samples rather than pseudo-maternal samples, since ethical approval was granted just prior to installation of the ddPCR (December 2013). The results illustrated that when testing actual maternal samples on the ddPCR, the difference in  $T_d$  drop-out between the maternal cfDNA and the cffDNA (Table 3-6) was considerably less substantial than initial qPCR experiments with pseudo-maternal samples (Figure 3-16). The differences in primer efficiencies at lower  $T_{ds}$  were further highlighted on the ddPCR, since all targets dropped out at different temperatures and Xp22.3 showed significantly higher concentrations of target in singleplex reactions (Figure 3-21). Because of the efficiency differences at the lower temperatures multiplexing results were highly dependent upon which primer/probe sets were paired together. When the *SRY* target was multiplex with Xp22.3, the maternal sample carrying the male fetus (ST1) illustrated a decrease in cffDNA fraction (22.6% to 9.7%), but when the *SRY* target was multiplex with *EIF2C1*, the same sample illustrated an increase in cffDNA fraction (12.1% to 76.4%). The lower starting cffDNA fraction for the latter multiplex reaction is likely a result of freeze-thawing the sample 2-3 times. Because the data is contradictory between the two multiplex reactions, it cannot be concluded that the increase in fetal proportion in the *SRY/EIF2C1* multiplex is a result of COLD-PCR selective amplification. Instead the difference in cffDNA fraction between these two multiplex

reactions is attributed to variation in the primer efficiencies at the lower temperatures. If the reference oligonucleotides amplify more efficiently at the  $T_c$ , the cffDNA fraction will be reduced, and if the fetal-target oligonucleotides are more functional at the lower  $T_d$ , the cffDNA will be increased (Table 3-4 and Table 3-5). Both examples will not give a true representation of actual cffDNA fraction, and thus determining aneuploidy will be unreliable if the reference and target do not amplify with the same efficiency.

The singleplex Xp22.3 reaction did show an increased number of events at 75°C  $T_d$  for the maternal sample as opposed to the Male gDNA, however no temperature was identified in which only the maternal sample showed amplification. Since the qPCR samples were carried out using pure psfDNA fragments, higher concentrations of the ROI are likely to explain why such clear amplification differences were visible on the qPCR platform. Lun et al. (2008) compared male-DNA concentrations calculated using microfluidics dPCR, qPCR and mass spectrometry. The results illustrated that microfluidic dPCR demonstrated the least quantitative bias for measuring fetal fraction, with lower imprecisions and higher sensitivity compared with qPCR. The increase levels of sensitivity associated with ddPCR could also be responsible for improved detection of small amounts of fragments from male gDNA amplified at lower  $T_d$ s. The potential for increased sensitivity of ddPCR can be attributed to the partitioning of molecules, which is advantageous since rare events can be isolated from high levels of background DNA (in this case maternal cfDNA) (Strain *et al.*, 2013). In conventional PCR it is more challenging to distinguish one target molecule in large backgrounds of DNA.

Although further  $T_d$ s could have been tested, supplementary experiments were not carried out due to time constraints. However, finding a multiplex reaction, where the chromosome 21 target and chromosome 1 target maintain a ratio of close to 1, even at lower  $T_d$ , would set the

basis for temperature dropout determination of large maternal DNA fragments. The need to find an accurate  $T_c$  in a multiplex reaction is a downside to COLD-PCR, since the reaction becomes highly sensitive and changeable at lower temperatures. The major advantage of COLD-PCR is its ability to distinguish between cffDNA and maternal DNA. Additionally, insufficient detection of minority alleles has been reported by Sanger sequencing and pyrosequencing, following traditional PCR amplification (Li *et al.*, 2007). However, it has been identified that COLD-PCR has higher detection sensitivity than PCR alone for low level mutations (for example, KRAS) (Zuo *et al.*, 2009). The combination of COLD-PCR on a dPCR platform could be used as an alternative method of detection if a mutation, which is suspected in fetal DNA, is undetected by conventional PCR and Sanger sequencing. In addition, (Lo *et al.*, 2007) if cffDNA fractions of 25% can be achieved, digital RCD can determine T21.

Since the whole fetal and maternal genome have been found within maternal circulation, NGS can provide accurate detection of multiple mutations in a single run, provided optimum level of cffDNA is available ( $\geq 4\%$ ) (Lo *et al.*, 2010). Lo *et al.* (2010) suggests that genome-wide scanning could be used to diagnose fetal disorders and produce a genome-wide genetic map of the mutational status of the fetus non-invasively, provided maternal and paternal genetic information is available. However, despite the decline in costs of t-MPS, it is still too costly for routine implantation ( $>£400.00$ ) and is consequently only available to families of high economic status.

### 3.3.3 Conclusion

Fragments that contain STRs do not amplify efficiently at lower  $T_{ds}$ , which results in the formation of shorter mutated DNA products are produced. Thus, subsequent ratio analysis is unreliable. The initial experiments using conserved regions of DNA with no polymorphisms

showed the success of COLD-PCR for the selective amplification of psfDNA fragments from pseudo-maternal samples. However, the application of this approach using real maternal samples on a ddPCR platform showed similar dropout  $T_d$  for maternal samples and control samples. In addition, targets selected for multiplex reactions showed variation in temperature drop out. Despite the variation in primers, singleplex reactions have illustrated the potential for selective amplification. The size difference between fetal and maternal fragments is not as considerable as first identified; however alternative enrichment approaches have illustrated success enrichment based on size variation (Chapter 6). Therefore, provided further primer optimisation is carried out to ensure equal efficiencies of target amplification in a multiplex reaction at lower  $T_d$ s, COLD-PCR has the potential to allow for the selective amplification of shorter fetal DNA. Provided enrichment >25% cfDNA can be achieved, COLD-PCR on dPCR platforms (refer to 1.3.3.3.1) could provide cheaper alternatives to NGS for the NIPT of fetal aneuploidy.

## Chapter 4

Inverse PCR (IPCR) for self-ligation of shorter  
psfDNA fragments

## 4.1 Introduction

The discovery of the polymerase chain reaction (PCR) by Randall K. Saiki provided a revolutionary platform for the selective amplification and detection of DNA present in relatively low proportions (Saiki *et al.*, 1985). PCR is now a fundamental technique for clinical testing and is imperative in many research applications, such as DNA sequencing, DNA cloning, sequence-tagged siting, phylogenetic analysis and gene expression (Mullis *et al.*, 1986; Innis, Gelfand and Sninsky, 1999). However, the conventional approach first described using end-point gel electrophoresis analysis is limited since it only provides qualitative information and is associated with reduced levels of sensitivity. Despite developments in PCR technology (including qPCR and dPCR) to improve sensitivity, a major limitation of amplifying linear DNA using conventional primers is that only known sequences can be targeted (Ochman, Gerber and Hartl, 1988). Multiple modifications of the conventional PCR have been developed to facilitate the amplification and cloning of uncharacterised stretches of DNA upstream or downstream of regions that have already been cloned and sequenced (Weiss *et al.*, 1993; Loeb and Christians, 1996; Glaab and Tindall, 1997; Kaur *et al.*, 2002). Conceivably, the most straight forward approach identified was inverse PCR (IPCR) (Benkel and Fong, 1996).

Conventional PCR amplification requires oligonucleotides which adhere to opposite strands that face inwards to allow extension of the fragment between the forward and reverse primer. In contrast, IPCR uses oligonucleotides that face outwards from each other, which are designed in regions of previously characterised DNA sequences (Figure 2-2). For linear DNA fragments, this approach would only allow for a linear increase in the number of copies since there is no priming of DNA synthesis in the reverse direction (Ochman, Gerber and Hartl, 1988). However, the addition of a ligation step prior to PCR amplification produces circularised fragments of DNA. Therefore, when ligated

fragments are amplified, the primers extend away from each other allowing amplification of the entire circular DNA fragment containing 'unknown' upstream or downstream DNA sequences.

The feasibility of this approach was originally shown by Ochman, Gerber and Hartl (1988) by amplifying sequences that flank an insertion element (*ISI*) of *Escherichia coli* (*E.coli*). The application of IPCR has since also been used for mutation detection (Leclerc *et al.*, 1996; Liu *et al.*, 2004; Rossetti *et al.*, 2005). Rossetti *et al.* (2005) described the application of IPCR for the genotyping of Factor VIII intron 22 inversions (Inv22), which cause 40-45% of severe cases of haemophilia A. The results corresponded with Southern blotting analysis, which is more time consuming; illustrating that IPCR provided a rapid and robust Inv22 genotyping assay. However, standard IPCR approaches were limited since larger DNA fragments ligate and amplify less efficiently. Therefore, fragments of interest amplified by IPCR should optimally be no greater than 2-3 Kb in length (Ochman, Gerber and Hartl, 1988). Long range PCR (LR-PCR), which use modified protocols with Taq enzyme, can enable amplification of targets up to 50Kb in size (Cheng *et al.*, 1994). Benkel and Fong (1996) identified that by combining long range PCR (LR-PCR) with IPCR (LR-IPCR) led to a dramatic increase in gene characterisation by genome walking. Although the article only amplified fragments up to 6Kb long, the upper limit of LR-IPCR was not determined.

Contrastingly, PCR amplification of cfDNA from maternal plasma for *RHD* genotyping, fetal sexing and aneuploidy determination do not require detection of unknown DNA sequences. Alternatively, the application of IPCR in this approach was to selectively amplify shorter 'fetal' DNA fragments. The application of size selective amplification using COLD-PCR has been previously described (Chapter 3), which uses lower  $T_d$ s to selectively amplify shorter pseudo-fetal DNA fragments. Instead of altering the

denaturation temperature, we hypothesized that by optimising dilute ligation reactions, which encourages self-ligation, selective ligation of shorter (fetal) fragments could be achieved, since larger fragment ligate less efficiently (see above). Consequently, IPCR would allow for selective amplification of the circularised (fetal) DNA fragments (refer to Figure 2-4 in materials and methods chapter).

The aims of this study are:

- To produce pure *RH* exon 7 colonies from amplified products using primers consensus for *RHD* and *RHCE* (refer to Table 2-3 in materials and methods chapter).
- To optimise IPCR using purified *RH* psfDNA fragments expressing sticky-ends following *EcoR1* restriction digest, which produce a 5'-AATT overhang (refer to Figure 2-3 in materials and methods chapter).
- To optimise IPCR using purified *RH* psfDNA fragments with blunt-ends. This is more challenging since the ends terminate in a single base pair with no cohesive overhang as seen with sticky-ends. Though ligation yield are significantly lower compared to sticky ends, blunt ended fragments are always compatible.
- To develop IPCR experiment for the selective amplification of shorter fetal fragments from actual maternal blood samples.



## 4.2 Results

### 4.2.1 Production of purified 285bp *RHD* and *RHCE* fragments

#### 4.2.1.1 *PCR amplification using consensus primers for *RHD* and *RHCE* exon 7*

External primers for a consensus region of *RHD* and *RHCE* on exon 7 (Table 2-2) were used to amplify a 285bp fragment from a male gDNA sample (2.10.1). The external primers were tested at a higher final concentration (500nM) in addition to the 100nM final concentration to ensure high product amplification in preparation for gel extraction. The primers were tested against NTC and Male gDNA (20ng/  $\mu$ L (S1), 2ng/  $\mu$ L (S2) and 0.2ng/  $\mu$ L (S3)) In addition the samples were tested at 56.4°C T<sub>a</sub>, 58.4°C T<sub>a</sub> and 60.4°C T<sub>a</sub>. The results illustrated in Figure 4-1 show a faint band at ~50bp for all samples, which could indicate possible primer-dimer formation. With the exception of one of the NTC replicates, which produced an additional band between 50-100bp (Q), all the other NTCs tested did not show any contamination since no additional bands were present (A, B, I, J, and R). The male gDNA (S3) sample amplified using 500nM of each primer at 60.4°C did not illustrate PCR product (W), however since a band ~300bp is formed when amplified using the lower primer concentration (X) this is likely due to pipetting error. All the other male gDNA samples across all temperatures show amplification of a product just below 300bp for both primer concentrations (C-H, K-P, S-V and X). Samples C and V (highlighted) were randomly selected for gel extraction (refer to 2.5) and quantification (refer to 2.6.1), which yielded DNA concentrations of 18.75 ng/  $\mu$ L and 7.65 ng/  $\mu$ L, respectively.

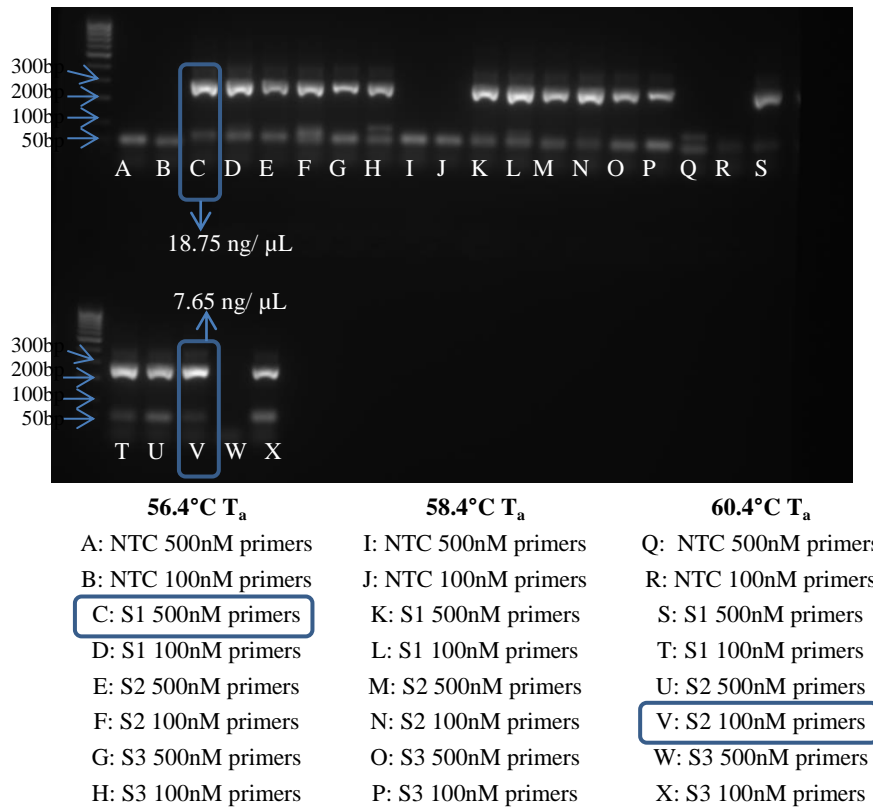


**Figure 4-1: 2% (w/v) agarose gel electrophoresis showing PCR products amplified at multiple T<sub>a</sub>s (56.4°C, 58.4°C and 60.4°C) using RH7 external primers (Table 2-2).** Male gDNA samples were tested at 20ng/ μL (S1), 2ng/ μL (S2) and 0.2ng/ μL (S3) with a NTC for all three T<sub>a</sub>s in reactions containing 100nM and 500nM final concentrations of primers. Lanes C and V (highlighted in blue) were randomly selected for gel extraction and quantification. The DNA concentrations for each sample were 18.75 ng/ μL (C) and 7.65 ng/ μL (G).

#### 4.2.1.2 Colony PCR for Fragment Insertion Analysis

Following PCR amplification, the fragments were gel extracted and purified following PCR amplification (refer to 2.4 and 2.5), then individual *RHD* and *RHCE* fragments from the pooled male gDNA sample were subsequently isolated so that we could select pure *RHD* amplicons to spike into pure *RHCE* amplicons at 5% and 95%, respectively, to mock maternal samples once blunt-

ended assays had been optimised. Cloning was carried out using the TOPO TA Cloning® kit (Invitrogen) (refer to 2.10). The external *RH7* 285bp fragments (Figure 4-1, C and V) were cloned into pCR®2.1 vectors and transformed into competent *E.coli* as described in section 2.10.4 and 2.10.5, respectively.

Directly after cloning, PCR amplification using M13 primers (refer to 2.10.6) was carried out to ensure that the fragments had been inserted into the MCS of the pCR®2.1 vector (Figure 2-9) (refer to 2.10.6). This was completed for 15 white colonies, which should have expressed plasmids containing recombinant DNA and one blue colony. The blue colony acted as a negative control since this shows bacteria which have been transformed with non-recombinant plasmids. Figure 4-2 illustrates the 2% (w/v) agarose gel results which were run alongside the 200bp Step Ladder Marker (Promega) for all 16 colonies. The blue colony (well 1) illustrates amplification at ~200bp, which is expected since amplification of the MCS using M13 primers without the PCR fragment insert should generate a product 199bp in length. Colonies 2, 4-6, 9 and 12 all produce PCR products between 400-500bp, which is also expected since these colonies contains the MCS region (199 bases) and the PCR product (285 bases), which results in amplification of a 484bp product. However, colonies 3, 7, 8, 10, 11 and 13-16 show a smaller product closer to that expressed by the blue colony, which indicates that 285bp *RH* exon 7 fragment has not been inserted into the pCR®2.1 vector. It is possible that longer time was needed for the blue colour to develop for these colonies or alternatively may have been caused by smaller products being cloned into the pCR®2.1 vector. Colonies 2, 4-6, 9 and 12, were subsequently purified (refer to 2.10.7) and quantified using the NanoVue™ Plus Spectrophotometer (GE Healthcare) (refer to 2.6.1). The DNA concentrations identified for colonies 2, 4, 5, 6, 9 and 12, were 99.25ng/μl, 83.25ng/μl, 92.75ng/μl, 5.3ng/μl, 87.25ng/μl and 60ng/μl, respectively.

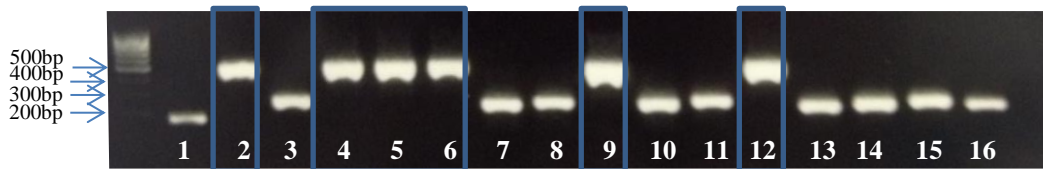


**Figure 4-2: 2% (w/v) agarose gel electrophoresis using M13 primers to check for product insert in 15 white colonies.** Lane 1 illustrates results for a single blue colony, which was used as a negative control. The blue colony (1) illustrates product at ~200bp. Colonies 2, 4-6, 9 and 12 all show a single band between 400bp and 500bp indicating successful uptake of product insert into the pCR@2.1 vector. Colonies 3, 7, 8, 10, 11 and 13-16 all demonstrate amplification close to 200bp indicating unsuccessful uptake of the 285bp *RH* exon 7 fragment.

#### 4.2.1.3 Sequencing results of single white colonies

The 2% (w/v) agarose gel shown in figure 4-2, illustrates that colonies 2, 4-6, 9 and 12 contain *RH* fragments, however samples were subsequently sequenced to determine which colonies contained the *RHD* external fragment and which contained the *RHCE* external fragment (refer to 2.10.7). Initially, all colonies were sequenced in house with only the M13 forward primer on the Applied Biosystems ABI 3130 Genetic Analyzer (Applied Biosystems) (refer to 2.10.7.1). However, colonies 4, 5 and 9 in house sequencing results were unsuccessful. Therefore, these samples were sent to Eurofins Genomics (Ebersberg, Germany) with both the forward and reverse M13 primers for sequencing (refer to 2.10.7.1). Both sets of sequencing results were aligned to the *RHD* and *RHCE* exon 7 285bp external fragments (Table 2-2) using ClustalW2 Multiple

Sequence Alignment (<http://www.ebi.ac.uk/Tools/msa/clustalw2/>) and GeneDoc Software (v2.7.000). The in house sequencing results are shown in Figure 4-3 and the out of house sequencing results are shown in Figure 4-4. There are 17 SNPs in total between *RHD* and *RHCE* within the 285bp external amplicon. Table 4-1 summarises SNP alignment for each colony and consequently the determined *RH* genotype of each colony.

### A) Colony 2 alignment (using M13 forward primer)

```

RHD : GAAGGGCTTCCTTTGAGGTGAGCCTTAGTGCCATCCCTTTGGTGGCCCGGATACCAAGGGTGTGTGAAAGGGGTGGGTAGGGAATAT : 90
RHCE : GAAGGGCTTCCTTTGAGGTGAGCCTTAGTGCCATCCCTTTGGTGGCCCGGATACCAAGGGTGTGTGAAAGGGGTGGGTAGGGAATAT : 90
Col2 : ----GGCCCAATT---T---CCT-----C-T---CTTCTTGGGTGGCCCGGATACCAAGGGTGTGTGAAAGGGGTGGGTAGGGAATAT : 71
      gaagGGcttCtTtgagg*****GAAAGGGGTGGGTAGGGAATAT

RHD : GGGTCTCACCTGCCAATCTGCTTATAATAACACTTGTCACAGGGGTGTGTGTAACCGAGTGTGGGGATTCCACAGCTCCATCATGGG : 181
RHCE : GGGTCTCACCTGCCAATCTGCTTATAATAACACTTGTCACAGGGGTGTGTGTAACCGAGTGTGGGGATTCCACAGCTCCATCATGGG : 181
Col2 : GGGTCTCACCTGCCAATCTGCTTATAATAACACTTGTCACAGGGGTGTGTGTAACCGAGTGTGGGGATTCCACAGCTCCATCATGGG : 162
      GGGTCTCACCTGCCAATCTGCTTATAATAACACTTGTCACAGGGGTGTGTGTAACCGAGTGTGGGGATTCCcCCACAgTCCaTCATGggC

RHD : TCAACTTTCAGCTTGTCTGGGTCTGCTTGGAGAGATCATCTACATTGTGCTGCTGGTGTGATACCGTCCGAGCCGGCAATGGCATGTGG : 272
RHCE : TCCACTTTCAGCTTGTCTGGGTCTGCTTGGAGAGATCACCTACATTGTGCTGCTGGTGTGATACCGTCCGAGCCGGCAATGGCATGTGG : 272
Col2 : TCAACTTTCAGCTTGTCTGGGTCTGCTTGGAGAGATCATCTACATTGTGCTGCTGGTGTGATACCGTCCGAGCCGGCAATGGCATGTGG : 252
      TaCAaCTTcAGCTTGTCTGGGTCTGCTTGGAGAGATCATCTACATTGTGCTGCTGGTGTGATACCGTCCGAGCCGGCAATGGCATGTGGG

RHD : TCACTGGGCTTAC----- : 285
RHCE : TCACTGGGCTTAC----- : 285
Col2 : TCACTGGGCTTACAAGCCGAATTCCACACACTGGCGGCCGTTACTATGATCCGACTCTACCTAGCTTGGGTAATCTGGTATAGCTGTTTC : 343
      TCACTGGGCTTAC

RHD : ----- : 380
RHCE : ----- : 380
Col2 : TGTGTGAAATGTTATCCGCTCACAAATCCACCAACATACGACCCGGAAGCATAAAAGTGGAAA : 407

```

### B) Colony 6 alignment (using M13 forward primer)

```

RHD : GAAGGGCTTCCTTTGAGGTGAGCCTTAGTGCCATCCCTTTGGTGGCCCGGATACCAAGGGTGTGTGAAAGGGGTGGGTAGGGAATAT : 90
RHCE : GAAGGGCTTCCTTTGAGGTGAGCCTTAGTGCCATCCCTTTGGTGGCCCGGATACCAAGGGTGTGTGAAAGGGGTGGGTAGGGAATAT : 90
Col16 : -----CTTAGTGCCCATCCCTTTGGTGGCCCGGATACCAAGGGTGTGTGAAAGGGGTGGGTAGGGAATAT : 68
      gaagggcttctttgaggtgagcCTTAGTGCCCATCCCTTTGGTGGCCCGGATACCAAGGGTGTGTGAAAGGGGTGGGTAGGGAATAT

RHD : GGGTCTCACCTGCCAATCTGCTTATAATAACACTTGTCACAGGGGTGTGTGTAACCGAGTGTGGGGATTCCACAGCTCCATCATGGG : 180
RHCE : GGGTCTCACCTGCCAATCTGCTTATAATAACACTTGTCACAGGGGTGTGTGTAACCGAGTGTGGGGATTCCACAGCTCCATCATGGG : 180
Col16 : GGGTCTCACCTGCCAATCTGCTTATAATAACACTTGTCACAGGGGTGTGTGTAACCGAGTGTGGGGATTCCACACACTCCATCATGGG : 158
      GGGTCTCACCTGCCAATCTGCTTATAATAACACTTGTCACAGGGGTGTGTGTAACCGAGTGTGGGGATTCCcCCACAgTCCaTCATGgg

RHD : CTAACCTTCAGCTTGTCTGGGTCTGCTTGGAGAGATCATCTACATTGTGCTGCTGGTGTGATACCGTCCGAGCCGGCAATGGCATGTG : 270
RHCE : CTAACCTTCAGCTTGTCTGGGTCTGCTTGGAGAGATCACCTACATTGTGCTGCTGGTGTGATACCGTCCGAGCCGGCAATGGCATGTG : 270
Col16 : CTAACCTTCAGCTTGTCTGGGTCTGCTTGGAGAGATCATCTACATTGTGCTGCTGGTGTGATACCGTCCGAGCCGGCAATGGCATGTG : 248
      CTAaCaCTTcAGCTTGTCTGGGTCTGCTTGGAGAGATCATCTACATTGTGCTGCTGGTGTGATACCGTCCGAGcCGGCAATGGCATGTG

RHD : GGTCACTGGGCTTAC----- : 285
RHCE : GGTCACTGGGCTTAC----- : 285
Col16 : GGTCACTGGGCTTACAAGCCGAATTCTGCAGATATCCATCACACTGGCGGCCGCTCGAGCATGCATCTAGAGGGCCCAATTCGCCCTATA : 338
      GGTCACTGGGCTTAC

RHD : ----- : 380
RHCE : ----- : 380
Col16 : GTGAGTCGTATTACAATTCAGTGGCCGTCGTTTACAAACGTCGTGACTGGGAAAACCCCTGGCGTTTACCAACTTTAATCGCCTTGCAC : 428

```



C) Colony 12 alignment (using M13 forward primer)

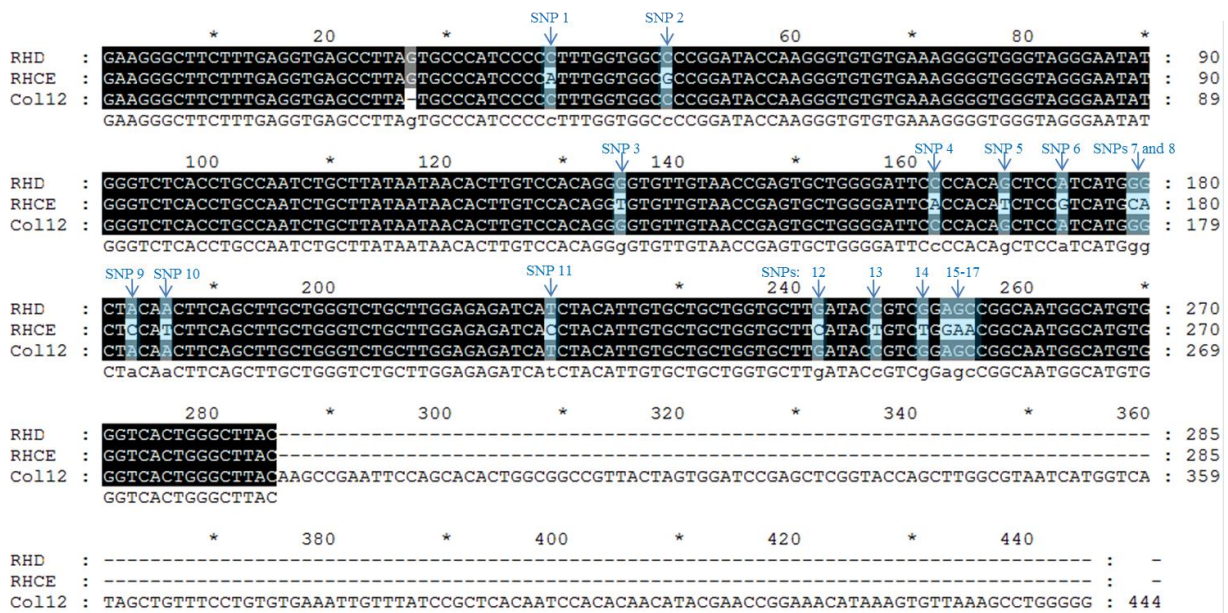


**Figure 4-3: Alignment of in-house sequencing results for colonies 2 (A), 6 (B) and 12**

**(C) against *RHD* and *RHCE* exon 7 285bp fragments.** A) Colony 2 shows that out of the seventeen SNPs, one SNP does not align to *RHD* or *RHCE* (SNP 1), two SNPs align to *RHCE* (SNPs 2 and 16) and fourteen SNPs align to *RHD* (3-15 and 17), therefore this fragment was classified as *RHD*. In addition, a base deletion and mismatch base was also identified. B) Colony 6 was determined to be containing the *RHD* fragment as it illustrated 100% alignment with the 285bp *RHD* sequence. C) Colony 12 was also considered *RHD* since all seventeen SNPs aligned to the *RHD* fragment. However, 100% alignment was not achieved due to a non-SNP region ‘G’ nucleotide base deletion within the cloned sequence.

A) Colony 4 alignment (using M13 forward primer)

```

      *           20           *           40           *           60           *           80           *
RHD : ----- : 15
F4  : CTATAGGGCGAATGGGCCCTCTAGATGCATGCTCGAGCGGCCGCGAGTGTGATGGATATCTGCAGAATTCGGCTT : 90
RHCE : ----- : 15
      GAAGGGCTTCTTTGA
      GAAGGGCTTCTTTGA

      100           *           SNP 1           SNP 2           *           140           *           160           *           180
RHD : GGTGAGCCTTAGTGCCCATCCCCCTTTGGTGGCCCGGATACCAAGGGTGTGTGAAAGGGTGGGTAGGGAATATGGGTCTCACCTGCCA : 105
F4  : GGTGAGCCTTAGTGCCCATCCCCCTTTGGTGGCCCGGATACCAAGGGTGTGTGAAAGGGTGGGTAGGGAATATGGGTCTCACCTGCCA : 180
RHCE : GGTGAGCCTTAGTGCCCATCCCCCTTTGGTGGCCCGGATACCAAGGGTGTGTGAAAGGGTGGGTAGGGAATATGGGTCTCACCTGCCA : 105
      GGTGAGCCTTAGTGCCCATCCCCaTTTGGTGGCgCCGGATACCAAGGGTGTGTGAAAGGGTGGGTAGGGAATATGGGTCTCACCTGCCA

      *           200           *           SNP 3           220           *           SNP 4           SNP 5           SNP 6           SNPs: 7/8           9           10           *
RHD : ATCTGCTTATAATAACACTTGTCCACAGGGGTGTTGTAACCGAGTGTCTGGGGATTCCCCACAGCTCCATCATGGGCTACACTTCAGCTT : 195
F4  : ATCTGCTTATAATAACACTTGTCCACAGGGGTGTTGTAACCGAGTGTCTGGGGATTCCCCACAGCTCCATCATGGGCTACACTTCAGCTT : 270
RHCE : ATCTGCTTATAATAACACTTGTCCACAGGGGTGTTGTAACCGAGTGTCTGGGGATTCCCCACAGCTCCATCATGGGCTACACTTCAGCTT : 195
      ATCTGCTTATAATAACACTTGTCCACAGGGgTGTGTAACCGAgTGTCTGGGGATTCCCCACAgTCCaTCATGggCTaCAaCTTCAGCTT

      280           *           SNP 11           300           *           SNPs: 12           13           14           15-17           340           *           360
RHD : GCTGGGTCTGCTTGGAGAGATCACTACATTGTGCTGCTGGTGTCTGATACCGTCCGAGCGGCAATGGCATGTGGGTCACTGGGCTTAC : 285
F4  : GCTGGGTCTGCTTGGAGAGATCACTACATTGTGCTGCTGGTGTCTGATACCGTCCGAGCGGCAATGGCATGTGGGTCACTGGGCTTAC : 360
RHCE : GCTGGGTCTGCTTGGAGAGATCACTACATTGTGCTGCTGGTGTCTGATACCGTCCGAGCGGCAATGGCATGTGGGTCACTGGGCTTAC : 285
      GCTGGGTCTGCTTGGAGAGATCaTCTACATTGTGCTGCTGGTGTCTGATACCGTcGgAgcCGGCAATGGCATGTGGGTCACTGGGCTTAC

      *           380           *           400           *           420           *           440           *
RHD : ----- : -
F4  : AAGCCGAATTCAGCACACTGGCGGCCGTTACTAGTGGATCCGAGCTCGGTACCAAGCTTGGCGTAATCATGGTCATAGCTGTTTCCTGT : 450
RHCE : ----- : -

      460           *           480           *           500           *           520           *           540
RHD : ----- : -
F4  : GTGAAATGTTATCCGCTCACAATTCCACACAACATACGAGCCGGAAGCATAAAGTGTAAGCCTGGGGTGCCTAATGAGTGAGCTAACT : 540
RHCE : ----- : -
  
```

B) Colony 4 alignment (using M13 reverse primer)

```

      *           560           *           580           *           600           *           620           *
RHD : ----- : 12
R4  : CACTATAGGGCGAATGGGCCCTCTAGATGCATGCTCGAGCGGCCGCGAGTGTGATGGATATCTGCAGAATTCGGCTT : 630
RHCE : ----- : 12
      GAAGGGCTTCTTT
      GAAGGGCTTCTTT

      640           *           SNP 1           SNP 2           *           680           *           700           *           720
RHD : TGAGGTGAGCCTTAGTGCCCATCCCCCTTTGGTGGCCCGGATACCAAGGGTGTGTGAAAGGGTGGGTAGGGAATATGGGTCTCACCTG : 102
R4  : TGAGGTGAGCCTTAGTGCCCATCCCCCTTTGGTGGCCCGGATACCAAGGGTGTGTGAAAGGGTGGGTAGGGAATATGGGTCTCACCTG : 720
RHCE : TGAGGTGAGCCTTAGTGCCCATCCCCCTTTGGTGGCCCGGATACCAAGGGTGTGTGAAAGGGTGGGTAGGGAATATGGGTCTCACCTG : 102
      TGAGGTGAGCCTTAGTGCCCATCCCCaTTTGGTGGCgCCGGATACCAAGGGTGTGTGAAAGGGTGGGTAGGGAATATGGGTCTCACCTG

      *           740           *           SNP 3           760           *           SNP 4           SNP 5           SNP 6           SNPs: 7/8           9           10           *
RHD : CCAATCTGCTTATAATAACACTTGTCCACAGGGGTGTTGTAACCGAGTGTCTGGGGATTCCCCACAGCTCCATCATGGGCTACACTTCAG : 192
R4  : CCAATCTGCTTATAATAACACTTGTCCACAGGGGTGTTGTAACCGAGTGTCTGGGGATTCCCCACAGCTCCATCATGGGCTACACTTCAG : 810
RHCE : CCAATCTGCTTATAATAACACTTGTCCACAGGGGTGTTGTAACCGAGTGTCTGGGGATTCCCCACAGCTCCATCATGGGCTACACTTCAG : 192
      CCAATCTGCTTATAATAACACTTGTCCACAGGGgTGTGTAACCGAgTGTCTGGGGATTCCCCACAgTCCaTCATGggCTaCAaCTTCAG

      820           *           SNP 11           840           *           SNPs: 12           13           14           15-17           880           *           900
RHD : CTTGCTGGGTCTGCTTGGAGAGATCACTACATTGTGCTGCTGGTGTCTGATACCGTCCGAGCGGCAATGGCATGTGGGTCACTGGGCT : 282
R4  : CTTGCTGGGTCTGCTTGGAGAGATCACTACATTGTGCTGCTGGTGTCTGATACCGTCCGAGCGGCAATGGCATGTGGGTCACTGGGCT : 900
RHCE : CTTGCTGGGTCTGCTTGGAGAGATCACTACATTGTGCTGCTGGTGTCTGATACCGTCCGAGCGGCAATGGCATGTGGGTCACTGGGCT : 282
      CTTGCTGGGTCTGCTTGGAGAGATCaTCTACATTGTGCTGCTGGTGTCTGATACCGTcGgAgcCGGCAATGGCATGTGGGTCACTGGGCT

      *           920           *           940           *
RHD : TAC----- : 285
R4  : TACAGCCGAATTCAGCACACTGGCGGCCGTTACTAGTGGATCCGAGCTCGTAG : 954
RHCE : TAC----- : 285
      TAC
  
```



### C) Colony 5 alignment (using M13 forward primer)

```

RHCE : -----*-----20-----*-----40-----*-----60-----*-----80-----*-----
F5 : ATAGGGCGAATGGGCCCTCTAGATGCATGCTCGAGCGGCCGCCAGTGTGATGGATATCTGCAGAAATTCGGCTTGAAGGGCTTCTTTGAGG : 17
RHD : -----*-----20-----*-----40-----*-----60-----*-----80-----*-----
                                           GAAGGGCTTCTTTGAGG : 17
                                           GAAGGGCTTCTTTGAGG

          100          SNP 1          120          SNP 2          *          140          *          160          *          180
RHCE : TGAGCCTTAGTGCCCATCCCCATTTGGTGGCCCGGATACCAAGGGTGTGTGAAAGGGGTGGGTAGGGAATATGGGTCTCACCTGCCAAT : 107
F5 : TGAGCCTTAGTGCCCATCCCCATTTGGTGGCCCGGATACCAAGGGTGTGTGAAAGGGGTGGGTAGGGAATATGGGTCTCACCTGCCAAT : 180
RHD : TGAGCCTTAGTGCCCATCCCCATTTGGTGGCCCGGATACCAAGGGTGTGTGAAAGGGGTGGGTAGGGAATATGGGTCTCACCTGCCAAT : 107
          TGAGCCTTAGTGCCCATCCCCATTTGGTGGCCCGGATACCAAGGGTGTGTGAAAGGGGTGGGTAGGGAATATGGGTCTCACCTGCCAAT

          *          200          SNP 3          *          220          *          SNP 4          SNP 5          SNP 6          SNPs: 7/8          9          10          *
RHCE : CTGCTTATAATAAACAACACTTGTCACAGGCTGTGTGTAACCGAGTGTGGGGATTCACCACATCTCCCTCATGCACTCCACTTTAGCTTGC : 197
F5 : CTGCTTATAATAAACAACACTTGTCACAGGCTGTGTGTAACCGAGTGTGGGGATTCACCACATCTCCCTCATGCACTCCACTTTAGCTTGC : 270
RHD : CTGCTTATAATAAACAACACTTGTCACAGGCTGTGTGTAACCGAGTGTGGGGATTCACCACAGCTCCCTCATGCGCTCCACTTTAGCTTGC : 197
          CTGCTTATAATAAACAACACTTGTCACAGGCTGTGTGTAACCGAGTGTGGGGATTCACCACATCTCCCTCATGCACTCCACTTTAGCTTGC

          280          SNP 11          300          SNPs: 12          13          14          15-17          *          340          *          360
RHCE : TGGGTCTGCTTGGAGAGATCACTACATTGTGCTGCTGGTGTCTCATACTGCTCGGAAACGGCAATGGCATGTGGGTCACTGGGCTTAC-- : 285
F5 : TGGGTCTGCTTGGAGAGATCACTACATTGTGCTGCTGGTGTCTCATACTGCTCGGAAACGGCAATGGCATGTGGGTCACTGGGCTTACAA : 360
RHD : TGGGTCTGCTTGGAGAGATCACTACATTGTGCTGCTGGTGTCTCATACTGCTCGGAAACGGCAATGGCATGTGGGTCACTGGGCTTAC-- : 285
          TGGGTCTGCTTGGAGAGATCACTACATTGTGCTGCTGGTGTCTCATACTGCTCGGAAACGGCAATGGCATGTGGGTCACTGGGCTTAC

          *          380          *          400          *          420          *          440          *
RHCE : -----*-----*-----*-----*-----*-----*-----*-----*-----*-----*-----
F5 : GCCGAATTCAGCACACTGGCGGCCGTTACTAGTGGATCCGAGCTCGGTACCAAGCTTGGCGTAATCATGGTCATAGCTGTTTCTGTGT : 450
RHD : -----*-----*-----*-----*-----*-----*-----*-----*-----*-----*-----

          460          *          480          *          500          *          520          *          540
RHCE : -----*-----*-----*-----*-----*-----*-----*-----*-----*-----*-----
F5 : GAAATGTTATCCGCTCACAATTCACACAAACATACGAGCCGGAAGCATAAAGTGTAAAGCCTGGGGTGCCTAATGAGTGAGCTAACTCA : 540
RHD : -----*-----*-----*-----*-----*-----*-----*-----*-----*-----*-----

```

### D) Colony 5 alignment (using M13 reverse primer)

```

RHCE : -----*-----560-----*-----580-----*-----600-----*-----620-----*-----
R5 : GGCCAGTGAATGTAAATACGACTCATAAGGGCGAATGGGCCCTCTAGATGCATGCTCGAGCGGCCGCCAGTGTGATGGATATCTGCA : 630
RHD : -----*-----560-----*-----580-----*-----600-----*-----620-----*-----

          640          *          660          *          SNP 1          SNP 2          *          700          *          720
RHCE : -----*-----*-----*-----*-----*-----*-----*-----*-----*-----*-----
R5 : GAAATTCGGCTTGAAGGGCTTCTTTGAGGTGAGCCTTAGTGCCCATCCCCATTTGGTGGCCCGGATACCAAGGGTGTGTGAAAGGGGTGG : 720
RHD : -----*-----*-----*-----*-----*-----*-----*-----*-----*-----*-----
          GAAGGGCTTCTTTGAGGTGAGCCTTAGTGCCCATCCCCATTTGGTGGCCCGGATACCAAGGGTGTGTGAAAGGGGTGG

          *          740          *          760          *          SNP 3          780          *          SNP 4          SNP 5          *
RHCE : GTAGGGAATATGGGTCTCACCTGCCAATCTGCTTATAATAAACAACACTTGTCACAGGCTGTGTTGTAACCGAGTGTGGGGATTCACCACATC : 169
R5 : GTAGGGAATATGGGTCTCACCTGCCAATCTGCTTATAATAAACAACACTTGTCACAGGCTGTGTTGTAACCGAGTGTGGGGATTCACCACATC : 810
RHD : GTAGGGAATATGGGTCTCACCTGCCAATCTGCTTATAATAAACAACACTTGTCACAGGCTGTGTTGTAACCGAGTGTGGGGATTCACCACATC : 169
          GTAGGGAATATGGGTCTCACCTGCCAATCTGCTTATAATAAACAACACTTGTCACAGGCTGTGTTGTAACCGAGTGTGGGGATTCACCACATC

          SNP 6          SNPs: 7/8          9          10          *          840          *          SNP 11          SNPs: 12          13          14          15-17          900
RHCE : TCCCTCATGCACTCCACTTTAGCTTGTGGTCTGCTGGGTCGCTTGGAGAGATCACTACATTGTGCTGCTGGTGTCTCATACTGCTCGGAAACGGC : 259
R5 : TCCCTCATGCACTCCACTTTAGCTTGTGGTCTGCTGGGTCGCTTGGAGAGATCACTACATTGTGCTGCTGGTGTCTCATACTGCTCGGAAACGGC : 900
RHD : TCCCTCATGCACTCCACTTTAGCTTGTGGTCTGCTGGGTCGCTTGGAGAGATCACTACATTGTGCTGCTGGTGTCTCATACTGCTCGGAAACGGC : 259
          TCCCTCATGCACTCCACTTTAGCTTGTGGTCTGCTGGGTCGCTTGGAGAGATCACTACATTGTGCTGCTGGTGTCTCATACTGCTCGGAAACGGC

          *          920          *          940          *          960          *
RHCE : AATGGCATGTGGGTCACTGGGCTTAC-----*-----*-----*-----*-----*-----*-----*-----
R5 : AATGGCATGTGGGTCACTGGGCTTACAGCCGAATTCAGCACACTGGCGGCCGTTACTAGTGGATCCGAGCTCGTA : 977
RHD : AATGGCATGTGGGTCACTGGGCTTAC-----*-----*-----*-----*-----*-----*-----*-----
          AATGGCATGTGGGTCACTGGGCTTAC

```



E) Colony 9 alignment (using M13 forward primer)

```

RHCE : -----*-----20-----*-----40-----*-----60-----*-----80-----*----- : 17
F9 : ATAGGGCGATTGGGCCCTCTAGATGCATGCTCGAGCGGCCGCCAGTGTGATGGATATCTGCAGAATTCGGCTTGAAGGGCTTCTTTGAGG : 90
RHD : -----*-----20-----*-----40-----*-----60-----*-----80-----*----- : 17
                                           GAAGGGCTTCTTTGAGG
                                           GAAGGGCTTCTTTGAGG

          100          SNP 1          SNP 2          *          140          *          160          *          180
RHCE : TGAGCCTTAGTGCCCATCCCCATTGGTGGCCCGGATACCAAGGGTGTGTGAAAGGGGTGGGTAGGGAATATGGGTCTCACCTGCCAAT : 107
F9 : TGAGCCTTAGTGCCCATCCCCATTGGTGGCCCGGATACCAAGGGTGTGTGAAAGGGGTGGGTAGGGAATATGGGTCTCACCTGCCAAT : 180
RHD : TGAGCCTTAGTGCCCATCCCCATTGGTGGCCCGGATACCAAGGGTGTGTGAAAGGGGTGGGTAGGGAATATGGGTCTCACCTGCCAAT : 107
          TGAGCCTTAGTGCCCATCCCCATTGGTGGCCCGGATACCAAGGGTGTGTGAAAGGGGTGGGTAGGGAATATGGGTCTCACCTGCCAAT

          *          200          SNP 3          *          220          *          SNP 4          SNP 5          SNP 6          SNPs: 7/8          9          10          *
RHCE : CTGCTTATAATAACACTTGTCCACAGGGTGTGTTGTAACCGAGTGTGGGGATTCACCACATCTCCCTCATGCACTCCACTTTCAGCTTGC : 197
F9 : CTGCTTATAATAACACTTGTCCACAGGGTGTGTTGTAACCGAGTGTGGGGATTCACCACATCTCCCTCATGCACTCCACTTTCAGCTTGC : 270
RHD : CTGCTTATAATAACACTTGTCCACAGGGTGTGTTGTAACCGAGTGTGGGGATTCACCACATCTCCCTCATGCACTCCACTTTCAGCTTGC : 197
          CTGCTTATAATAACACTTGTCCACAGGGTGTGTTGTAACCGAGTGTGGGGATTCACCACATCTCCCTCATGCACTCCACTTTCAGCTTGC

          280          SNP 11          300          SNPs: 12          13          14          15-17          340          *          360
RHCE : TGGGCTGCTTGGAGAGATCAcCTACATTGTGCTGCTGGTGCTTcATACTGTCtGgaaCGGCAATGGCATGTGGGTCACTGGGCTTAc-- : 285
F9 : TGGGCTGCTTGGAGAGATCAcCTACATTGTGCTGCTGGTGCTTcATACTGTCtGgaaCGGCAATGGCATGTGGGTCACTGGGCTTAcAA : 360
RHD : TGGGCTGCTTGGAGAGATCAcCTACATTGTGCTGCTGGTGCTTcATACTGTCtGgaaCGGCAATGGCATGTGGGTCACTGGGCTTAc-- : 285
          TGGGCTGCTTGGAGAGATCAcCTACATTGTGCTGCTGGTGCTTcATACTGTCtGgaaCGGCAATGGCATGTGGGTCACTGGGCTTAc

          *          380          *          400          *          420          *          440          *
RHCE : -----*-----380-----*-----400-----*-----420-----*-----440-----*----- : -
F9 : GCCGAATTCAGCACACTGGCGGCCGTACTAGTGGATCCGAGCTCGGTACCAAGCTTGGCGTAATCATGGTCATAGCTGTTTCCTGTGT : 450
RHD : -----*-----380-----*-----400-----*-----420-----*-----440-----*----- : -

          460          *          480          *          500          *          520          *          540
RHCE : -----*-----460-----*-----480-----*-----500-----*-----520-----*-----540----- : -
F9 : GAAATTGTTATCCGCTCACAATTCACACACATACGAGCCGGAAGCATAAAGTGTAAAGCCTGGGGTGCCTAATGAGTGAGCTAACTCA : 540
RHD : -----*-----460-----*-----480-----*-----500-----*-----520-----*-----540----- : -

```

F) Colony 9 alignment (using M13 reverse primer)

```

RHCE : -----*-----560-----*-----580-----*-----600-----*-----620-----*----- : -
R9 : GCCAGGGTTTTCCAGTCACGACGTTGTAAAACGACGGCCAGTGAATGTAAATACGACTCACTATAGGGCGAATGGGCCCTCTAGATGC : 630
RHD : -----*-----560-----*-----580-----*-----600-----*-----620-----*----- : -

          640          *          660          *          680          *          700          *          SNP 1          720
RHCE : -----*-----640-----*-----660-----*-----680-----*-----700-----*-----720-----*----- : 43
R9 : ATGCTCGAGCGCCGCCAGTGTGATGGATATCTGCAGAATTCGGCTTGAAGGGCTTCTTTGAGGTGAGCCTTAGTGCCCAATCCCAATTTC : 720
RHD : -----*-----640-----*-----660-----*-----680-----*-----700-----*-----720-----*----- : 43
                                           GAAGGGCTTCTTTGAGGTGAGCCTTAGTGCCCAATCCCAATTTC
                                           GAAGGGCTTCTTTGAGGTGAGCCTTAGTGCCCAATCCCAATTTC

          SNP 2          *          740          *          760          *          780          *          800          *
RHCE : GTGGCCCGGATACCAAGGGTGTGTGAAAGGGGTGGGTAGGGAATATGGGTCTCACCTGCCAATCTGCTTATAATAACACTTGTCCACAG : 133
R9 : GTGGCCCGGATACCAAGGGTGTGTGAAAGGGGTGGGTAGGGAATATGGGTCTCACCTGCCAATCTGCTTATAATAACACTTGTCCACAG : 810
RHD : GTGGCCCGGATACCAAGGGTGTGTGAAAGGGGTGGGTAGGGAATATGGGTCTCACCTGCCAATCTGCTTATAATAACACTTGTCCACAG : 133
          GTGGCCCGGATACCAAGGGTGTGTGAAAGGGGTGGGTAGGGAATATGGGTCTCACCTGCCAATCTGCTTATAATAACACTTGTCCACAG

          SNP 3          *          SNP 4          SNP 5          SNP 6          SNPs: 7/8          9          10          *          880          *          SNP 11          900
RHCE : GGTGTTGTAACCGAGTGTGGGGATTCACCACATCTCCCTCATGCACTCCACTTTCAGCTTGGTGGTCTGCTGGAGAGATCAcCTAC : 223
R9 : GGTGTTGTAACCGAGTGTGGGGATTCACCACATCTCCCTCATGCACTCCACTTTCAGCTTGGTGGTCTGCTGGAGAGATCAcCTAC : 900
RHD : GGTGTTGTAACCGAGTGTGGGGATTCACCACATCTCCCTCATGCACTCCACTTTCAGCTTGGTGGTCTGCTGGAGAGATCAcCTAC : 223
          GgTGTGTAACCGAGTGTGGGGATTCACCACATCTCCCTCATGCACTCCACTTTCAGCTTGGTGGTCTGCTGGAGAGATCAcCTAC

          *          SNPs: 12          13          14          15-17          940          *          960          *          980          *
RHCE : ATTGTGCTGCTGGTGCTTcATACTGTCtGgaaCGGCAATGGCATGTGGGTCACTGGGCTTAc----- : 285
R9 : ATTGTGCTGCTGGTGCTTcATACTGTCtGgaaCGGCAATGGCATGTGGGTCACTGGGCTTAcAAGCCGAATTCAGCACACTGGCGGCCG : 990
RHD : ATTGTGCTGCTGGTGCTTcATACTGTCtGgaaCGGCAATGGCATGTGGGTCACTGGGCTTAc----- : 285
          ATTGTGCTGCTGGTGCTTcATACTGTCtGgaaCGGCAATGGCATGTGGGTCACTGGGCTTAc

          1000          *
RHCE : -----*-----1000-----*----- : -
R9 : TTACTAGTGATCCGAGCTCGTAT : 1013
RHD : -----*-----1000-----*----- : -

```

Figure 4-4: Alignment of external sequencing results for colonies 4 (A and B), 5 (C and D) and 9 (E and F) against *RHD* and *RHCE* exon 7 285bp fragments using M13

**forward and reverse primers, respectively.** The results illustrated here and the final classification of each colony are summarised in table 4-1. No other base deletions or base additions were identified however, colony 4 sequenced with the M13 reverse primer showed one non-SNP region mismatch base (G<A).

**Table 4-1: *RH* determination of six colonies (2, 4-6, 9 and 12) by alignment of in house and external sequencing data to the external *RHD* and *RHCE* exon 7 285bp fragments**

Colony	M13 primer	<i>RHD</i> SNPs /17	<i>RHD</i> SNP alignment (%)	<i>RHCE</i> SNPs /17	<i>RHCE</i> SNP alignment (%)	Mismatch or base deletion/ addition SNPs	Mismatch or base deletion/ addition (%)	<i>RHD</i> or <i>RHCE</i> fragment
2 <sup>a</sup>	F	14	82.4	2	11.8	1	5.8	<i>RHD</i>
6 <sup>a</sup>	F	17	100	0	0	0	0	<i>RHD</i>
12 <sup>a</sup>	F	17	100	0	0	0	0	<i>RHD</i>
4 <sup>b</sup>	F	17	100	0	0	0	0	<i>RHD</i>
4 <sup>b</sup>	R	15	88.2	2	11.8	0	0	<i>RHD</i>
5 <sup>b</sup>	F	2	11.8	15	88.2	0	0	<i>RHCE</i>
5 <sup>b</sup>	R	2	11.8	15	88.2	0	0	<i>RHCE</i>
9 <sup>b</sup>	F	1	5.8	16	94.2	0	0	<i>RHCE</i>
9 <sup>b</sup>	R	1	5.8	16	94.2	0	0	<i>RHCE</i>

Legend- F: Forward; R: Reverse.

<sup>a</sup> Sequenced in house using ABI 3130 Genetic Analyzer.

<sup>b</sup> Sequence external (sent to Eurofins Genomics).

The results illustrated that out of the six colonies collected, four contained an *RHD* fragment within the pCR®2.1 vector (2, 4, 6 and 12) and two contained an *RHCE* fragment within the pCR®2.1 vector (5 and 9). For colonies 4 (Figure 4-5 A), 6 (Figure 4-4 A) and 12 (Figure 4-4 C), when sequenced with the M13 forward primer, 100% *RHD* SNP alignment was achieved (17/17 SNPs) (Table 4-1). Since colony 4 was sent for sequencing, an additional sequencing result using the M13 reverse primer was also

generated. The results for colony 4 using the M13 reverse primer illustrated a reduction in *RHD* specific SNP alignment (88.2%) since two SNPs (1 and 2) aligned to the *RHCE* fragment instead (Figure 4-5 B) (Table 4-1). Colony 2 in house sequencing results using the M13 forward primer provided the most varied results (Figure 4-4 A). Fourteen SNPs aligned to the *RHD* fragment (82.4%), hence why this colony was classified as containing an *RHD* fragment within the pCR@2.1 vector (Table 4-1). However, two SNPs (2 and 3) also aligned to the *RHCE* fragment and one SNP (SNP 1) also produced a mismatch ‘G’ nucleotide that did not align to the *RHD* ‘C’ nucleotide or the *RHCE* ‘A’ nucleotide (Figure 4-4A). In addition, the sequencing results for colony 2 also displayed multiple base deletions in the M13 forward primer binding site (Figure 4-4 A). The sequencing results for colony 5 generated by the forward and reverse M13 primers both demonstrated 88.2% SNP alignment to *RHCE* and both sets of results illustrated alignment of SNPs 1 and 2 to *RHD* (Figure 4-5 C and D) (Table 4-1). The external sequencing data for colony 9 generated by the forward and reverse M13 primers also show homogeneity since both sets of results show 94.2% SNP alignment to *RHCE* with one SNP (3) aligning to *RHD* (Figure 4-5 E and F) (Table 4-1). Since these colonies were produced from pooled samples of male gDNA (promega) it is possible that for colonies 5 and 9 where both the forward and reverse show the same polymorphism alignment that the colony selected for sequences may include a novel variant, although error in sequencing alignment is more feasible.

#### 4.2.2 IPCR analysis of sticky-ended fragments

##### 4.2.2.1 *EcoR1 digest*

Once sequencing had been completed to determine the *RH* status of each purified fragment, the purified plasmid DNA aliquots for colonies 2, 4, 5, 9 and 12 were digested

with restriction enzyme *EcoRI* (refer to 2.8.1). Colony 6 was not included due to the low yield of DNA determined in alternative experiment (5.3 ng/  $\mu\text{L}$ ) (4.2.2). Figure 4-6 demonstrates the 2% (w/v) agarose gel for all colonies following restriction digest. The restriction digest, should yield two bands; one smaller band (~300bp) containing the 285bp fragment and a small portion of the vector, and one larger band (>1 kb) representing the rest of the 3.9 kb vector (Figure 2-3). In addition, undigested samples of each colony were also tested and used as a negative control, since these samples should not produce a band of ~300bp. Colonies 2, 5, 9 and 12, which underwent restriction digestion, successfully illustrated two bands, one at >1 kb and one at ~300bp. The digested colony 4 sample did not show any bands, however, since the undigested sample produced one clear band >1 kb it is likely that the sample was loaded incorrectly or not enough DNA was added to the restriction digest (refer to 2.8.1). Consequently, only colonies 2, 5, 9 and 9 were used for subsequent ligation and IPCR.

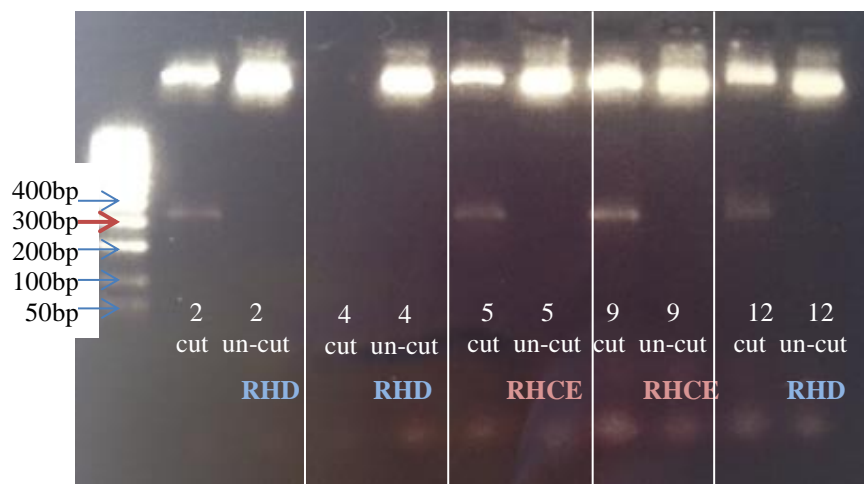


**Figure 4-5: 2% (w/v) agarose gel demonstrating restriction digested (*EcoRI*) and non-digested results for colonies 2, 4, 5, 9 and 12.** The samples that did not undergo restriction digest (un-cut) show a single band at >1kb. In contrast the samples that did undergo restriction digest (cut) with *EcoRI* illustrate two bands, one >1kb and another just above 300bp (thicker red arrow).

#### 4.2.2.2 Ligation and IPCR

Proceeding on from the restriction digest, the 300bp band of colonies 2, 5, 9 and 12 were gel extracted and ethanol precipitated to produce purified *RHD* and *RHCE* fragments. Prior to ligation the extracted 'cut' fragments for all colonies were quantified on the NanoView™ Spectrophotometer. The DNA concentrations identified for colonies 2, 9 and 12, were 23.5ng/μl, 29.5ng/μl and 27ng/μl, respectively. Colony 5 'cut' fragment gel extraction yielded lower DNA (<5 ng/ μL) and consequently was not used in the ligation experiment. The *RH* fragments were then ligated (2.8.2) to produce circularised DNA and IPCR was completed directly after ethanol precipitation of the ligated *RH* fragments. The results indicated that only colony 12 produced a band between 200bp and 300bp with all three ligations (2.8.2) (Figure 4-6). Additionally colony 12 also produced a second, larger band between 500 and 600bp, which was presumed to be a result of two fragments ligating together just prior to self-ligation. Colony 2 and colony 9 only show amplification of one product (between 200bp and 300bp) for ligation 1, and ligations 1 and 3, respectively. The internal IPCR primers (Table 2-2) should produce a fragment 218bp in length. However, because part of the MCS of the pCR®2.1 vector was also incorporated into the circularised sequence (15bp), a band ~233bp was expected (Figure 2-5). Therefore, the results demonstrated successful ligation and subsequent amplification for all colonies at varying ligation reaction concentrations (Figure 4-6). Colony 12, ligation reaction 3 (4 Weiss-units) was selected for sequencing.

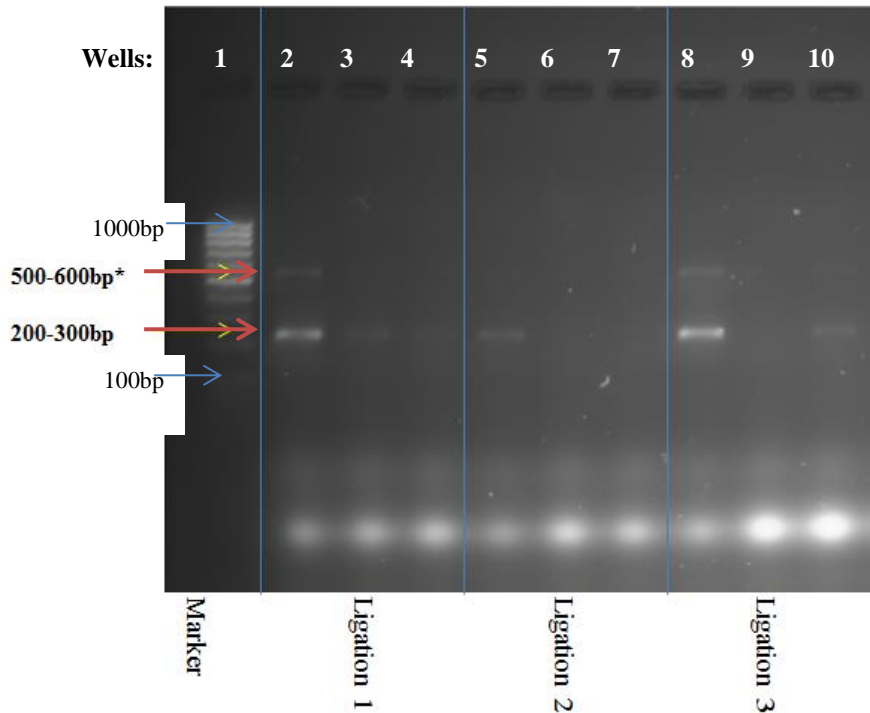


**Figure 4-6: 2% (w/v) agarose gel illustrating IPCR amplification of ligated *RH* fragments for three ligation dilutions (refer to 2.8.2).** The *RHD* fragment from colony 12 is represented in wells 2, 5 and 8 for each ligation. All ligation experiments show an amplified product at ~200-300bp. In addition, for ligation 1 and ligation 3, the colony 12 *RHD* fragment also illustrates a second band between 500-600bp. The *RHD* fragment for colony 2 is represented in wells 3, 6 and 9 for each ligation. This sample only illustrates a faint PCR product at 200-300bp for ligation 1. The *RHCE* fragment from colony 9 is represented in wells 4, 7 and 10. PCR product is visible for this sample at ligation 1 and ligation 3. However, at ligation 2 no band is present.

#### 4.2.2.3 Sequencing results of IPCR product

The IPCR product from the colony 12 *RHD* fragment (ligation 3) (Figure 4-6 well 8) produced the strongest band. Therefore, the unpurified PCR product for this sample was sent to Eurofins Genomics (refer to 2.10.8.1) for sequencing along with the forward

internal IPCR primer (Table 2-2). The sequencing results were aligned to the inverse internal product for both *RHD* and *RHCE* exon 7 insets (Figure 2-2) (Figure 4-7). Figure 2-5 illustrates the product that should have been generated following successful self-ligation of the *EcoRI* restriction site and amplification using consensus internal inverse primers (Table 2-2). Because the internal inverse primers were designed facing away from each other a small section of the fragment is not amplified, resulting in the exclusion of 8 SNP's (Figure 2-2). However, the *RH* status of colony 12 was confirmed using the 9 SNPs that remained (Figure 4-7). The results illustrated in Figure 4-7 show the point at which ligation occurred (*EcoRI* site) and the surrounding 15bp MCS sequence included in the amplification (highlighted orange). The remaining sequence demonstrates 100% SNP alignment to *RHD*. These results demonstrated the ability to self-ligate shorter ('fetal') DNA fragments with successful inverse amplification of circularised fragment for samples that express sticky ends.







This initial optimisation process to analyse the ability of shorter molecules to self-ligate was carried out using *EcoRI* restriction digest, which produced sticky-ended fragments. Sticky ends can ligate more efficiently than blunt-ends and therefore blunt ended fragments will require higher concentrations of ligase. The nature of cfDNA ends is unknown but it is more feasible that cfDNA fragments express blunt-ends as opposed to sticky ends, since this is the simplest DNA end of a double stranded molecule. Therefore, experiments were repeated using a restriction endonuclease that produced blunt-ends (*EcoRV*), before testing real maternal samples.

#### 4.2.3 Self-ligation of blunt ends

Colonies 2 and 5 from glycerol stocks (refer to 2.10.7) were amplified using primers that contained *EcoRV* restriction sites (Table 4-2). However, there is only a single *EcoRV* restriction site within the pCR<sup>®</sup>2.1 MCS and the nucleotide sequence on the alternative side of the product insert region expresses six restriction enzyme sites (*HindIII*, *BamHI*, *KpnI*, *SacI*, *SpeI* and *BstXI*), which all produce sticky-ends (Figure 2-9). Therefore, the forward primer created in house using Primer3 Software and OligoAnalyzer 3.1 (refer to 2.2.2) was designed to contain an additional *EcoRV* restriction site at the 5' end (Table 4-2 shown in red). Despite optimisation of PCR conditions, including annealing temperature gradient (Figure 4-8) and primer concentrations (not shown), the 300bp product was not amplified using these oligonucleotides. Instead of producing new primers, which would require further optimisation or analysis on spike samples, due to the availability of maternal samples obtained from Dr Svetlana Trivodalieva (Macedonian Academy of Sciences and Arts Krste Misirkov 2), subsequent experiments were carried out using real samples as opposed to spiked samples.

**Table 4-2: *EcoRV* oligonucleotides for MCS of pCR®2.1.** The primers used to amplify product insert in the pCR®2.1 vector containing *EcoRV* restriction site in the forward primer (shown in red).

Oligonucleotide	5' → 3' sequence
Forward <i>EcoRV</i>	TCGATATCGCTGGAATTCGG
Reverse <i>EcoRV</i>	CCAGTGTGATGGATATCTGCA

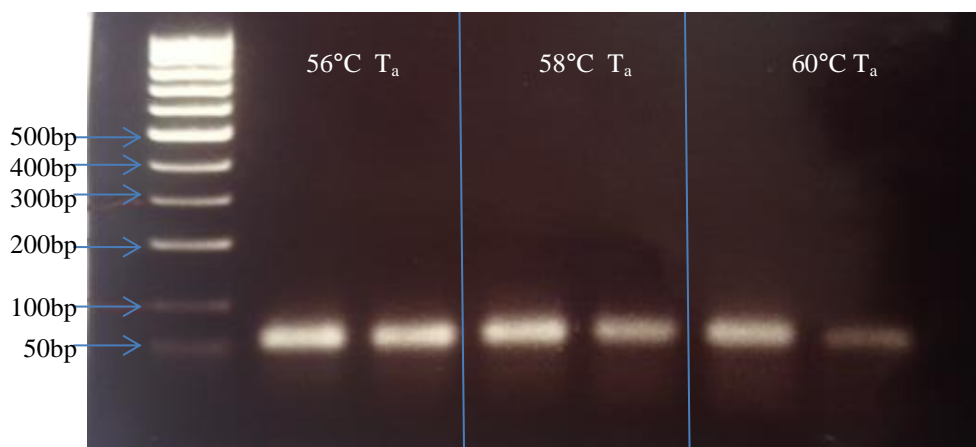


**Figure 4-8: 2% (w/v) agarose gel illustrating annealing temperature gradient (56 - 60°C) for colonies 2 and 5 using oligonucleotides containing *EcoRV* restriction sites.** All temperatures illustrated smaller product at ~50bp as opposed to 300bp expected product.

As previously mentioned, the fragmentation pattern of cfDNA is uncertain, and it is possible that the ends may be incompatible. Therefore, following DNA extraction and quantification of maternal samples Rh47 (15.2 ng/  $\mu$ L) and Rh61 (12.3 ng/  $\mu$ L) (2.1.5) (2.6.1), T4 DNA Polymerase (Thermo Scientific) was added to half of each sample using two concentrations (1 unit and 5 units) (Table 4-3). The polymerase reaction enables blunting of DNA ends, which is necessary if incompatible ends are expressed. However, it is also possible that

cfDNA typically exhibits blunt-ended DNA. Therefore, ligations reactions were also carried out for samples without the pre-polymerisation step.

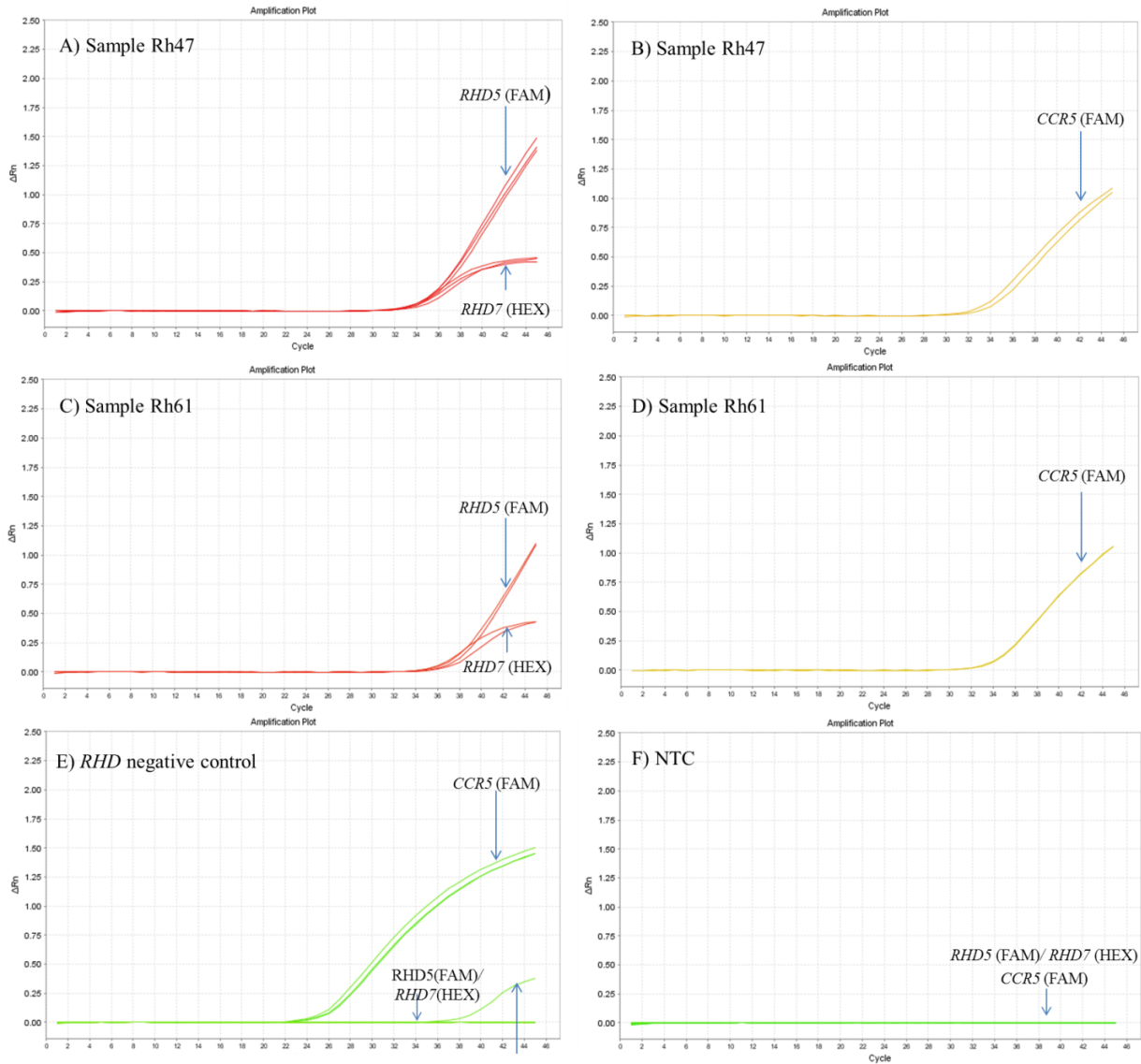
**Table 4-3: T4 DNA Polymerisation reaction.**

	<b>Polymerisation 1</b>	<b>Polymerisation 2</b>
5X Reaction Buffer	4 $\mu\text{L}$	20 $\mu\text{L}$
Linear DNA (Rh47/ Rh61)	150 ng	150 ng
dNTP Mix 2mM each	1 $\mu\text{L}$	1 $\mu\text{L}$
T4 DNA Polymerase (5u/ $\mu\text{L}$ )	0.2 $\mu\text{L}$	1 $\mu\text{L}$
Nuclease free water	Make up to 200 $\mu\text{L}$	Make up to 200 $\mu\text{L}$

The ligation and IPCR experiments were carried out as previously described (refer to 2.8.2 and 2.8.3). Following IPCR amplification, fragments were separated and purified by non-denaturing polyacrylamide gel electrophoresis using a mini-PROTEAN TBE Precast Gel (10% acrylamide) (Bio-Rad). 3  $\mu\text{L}$  of loading dye (12.5 mM Tris pH 8, 30% (v/v) glycerol, 0.25% (w/v) bromophenol blue) was added to 15  $\mu\text{L}$  of PCR product and the total volume (18  $\mu\text{L}$ ) was added to the gel alongside 12  $\mu\text{L}$  of marker (PCR Ranger 100bp DNA Ladder, Norgen). The gel was run using a mini PROTEAN Tetra System (Bio-Rad) in 1x TBE (89 mM Tris, 89 mM Boric acid and 2mM EDTA Buffer) (10x TBE (Bio-Rad)) for 2.5 hours at 60 volts. Following electrophoresis, the gel was transferred to a gel tray with 20 mL 1x TBE and 7.5  $\mu\text{L}$  GelRed (Biotium) (1:10 000 dilution). This was incubated at room temperature on a gyro-rocker for 90 mins. The gel was viewed using the EC3 imaging System (UVP BioImaging system) and results were analysed using Launch Vision WorksLS Program (Chemi Doc 410). The results were unsuccessful since no bands (except the marker) were visible (results not shown). Despite quantification using the NanoVue™ showing the presence of DNA qPCR was carried out to ensure presence of *RHD* specific targets within the sample (*RHD5* (FAM) and *RHD7* (HEX)) (2.7.1). The oligonucleotides for *RHD5* and *RHD7* are illustrated in Table 2-1, although in this instance the *RHD7* target was labelled with HEX

as opposed to FAM, so that both *RHD* targets could be multiplex (2.7.1). In addition, amplification of a reference region on chromosome 3 (*CCR5* (FAM)) was also tested and the oligonucleotides for the *CCR5* target are illustrated in Table 2-2. Samples were run at 60°C  $T_a$  (2.7.1) and the results are illustrated in Figure 4-9.

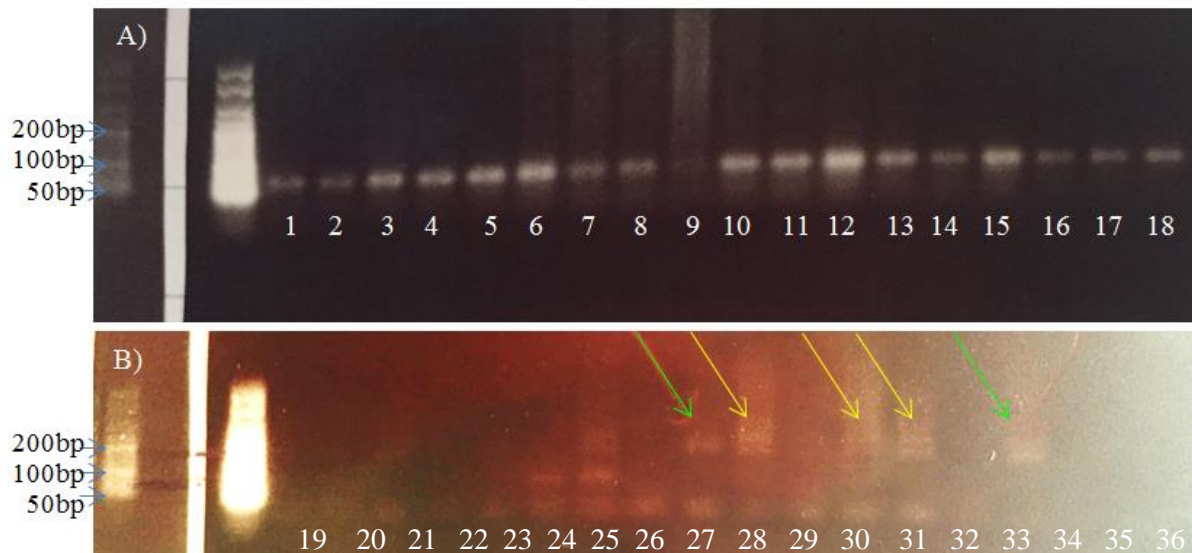
The results showed successful amplification of all three targets, demonstrating that DNA was present in both maternal samples (Figure 4-9 A-D). NTC replicates were clean (Figure 4-9 F), but the results illustrated contamination of one *RHD7* replicate for the *RHD* negative sample (Figure 4-9 E). It is possible that the IPCR was unsuccessful, but it is most likely that the ligation step was ineffective due to the limited amount of cffDNA available, preventing amplification using IPCR primers (Table 2-3).



At 37 Ct the third replicate of the *RHD7* target was amplified but the remaining two replicates illustrated no amplification.

**Figure 4-9: qPCR analysis to determine the presence of DNA in maternal samples Rh47 and Rh61 (non-ligated).** Sample Rh47 shows amplification of both *RHD5* (FAM) and *RHD7* (HEX) (A) and the reference gene *CCR5* (FAM) (B). C) Sample Rh61 also illustrates successful amplification of *RHD5* (FAM) and *RHD7* (HEX) (C) and the reference gene *CCR5* (FAM) (D). The *RHD* negative control shows successful *CCR5* (FAM) amplification and no amplification of *RHD5* (FAM), but did show amplification of one (out of three) replicate for *RHD7* (HEX) (37 Ct) (E). All NTCs were clean (F).

The IPCR was repeated using the same polymerase (2x Fast TaqMan Universal MasterMix (Applied Biosystems)) (2.8.3) (Figure 4-10 A) and an alternative polymerase, which produces high yields and improved specificity, (IMMOLASE™ DNA Polymerase (Bioline)) to determine if this would enable PCR amplification (Figure 4-10 B). The results in Figure 4-10 only show amplification of product ~50-100bp for the 2x Fast TaqMan Universal MasterMix, which is likely to be a result of primer dimerization since this product is also visible in the NTC (well 18). The results for the IMMOLASE™ DNA polymerase show no bands for most samples (Figure 4-10 B). However, samples Rh61 Dilution 1 (non-polymerised) (well 28) and Rh61 Dilution 2 (non-polymerised) (well 29) illustrate a very faint single band ~200bp (Figure 2-4 and Figure 4-10 (yellow arrows)). In addition, samples Rh47 Dilution 1 (polymerised) (well 31), Rh47 Dilution 2 (polymerised) (well 32) and Rh61 Dilution 1 (polymerised) (well 34) all demonstrate two faint bands between 200-300bp (Figure 2-4 and Figure 4-10 (green arrows)). However, the amount of DNA present was minimal and consequently sequencing of the unpurified PCR products (well 28 and well 34) was unsuccessful. The experiment was repeated using IMMOLASE™ DNA polymerase for higher ligation concentrations (6 Weiss units/ reaction) (Figure 2-4), but the 2% (w/v) agarose gel electrophoresis results of repeated IPCR illustrated no product amplification (data not shown). Time constraints prevented further optimisation but due to the limited amount of cffDNA present in maternal samples it is conceivable that detection methods that express higher levels of sensitivity are required.



2x Fast TaqMan Universal MasterMix	IMMOLASE™ DNA Polymerase
1. Rh47 Ligation 2 Polymerisation 1	19. Rh47 Ligation 2 Polymerisation 1
2. Rh47 Ligation 3 Polymerisation 1	20. Rh47 Ligation 3 Polymerisation 1
3. Rh61 Ligation 1 Polymerisation 1	21. Rh61 Ligation 1 Polymerisation 1
4. Rh61 Ligation 2 Polymerisation 1	22. Rh61 Ligation 2 Polymerisation 1
5. Rh61 Ligation 3 Polymerisation 1	23. Rh61 Ligation 3 Polymerisation 1
6. Rh47 Ligation 1 (non-polymerised)	24. Rh47 Ligation 1 (non-polymerised)
7. Rh47 Ligation 2 (non-polymerised)	25. Rh47 Ligation 2 (non-polymerised)
8. Rh47 Ligation 3 (non-polymerised)	26. Rh47 Ligation 3 (non-polymerised)
9. Rh61 Ligation 1 (non-polymerised)	27. Rh61 Ligation 1 (non-polymerised)
10. Rh61 Ligation 2 (non-polymerised)	28. Rh61 Ligation 2 (non-polymerised)
11. Rh61 Ligation 3 (non-polymerised)	29. Rh61 Ligation 3 (non-polymerised)
12. Rh47 Ligation 1 Polymerisation 2	30. Rh47 Ligation 1 Polymerisation 2
13. Rh47 Ligation 2 Polymerisation 2	31. Rh47 Ligation 2 Polymerisation 2
14. Rh47 Ligation 3 Polymerisation 2	32. Rh47 Ligation 3 Polymerisation 2
15. Rh61 Ligation 1 Polymerisation 2	33. Rh61 Ligation 1 Polymerisation 2
16. Rh61 Ligation 2 Polymerisation 2	34. Rh61 Ligation 2 Polymerisation 2
17. Rh61 Ligation 3 Polymerisation 2	35. Rh61 Ligation 3 Polymerisation 2
18. NTC	36. NTC

**Figure 4-10: 2% (w/v) agarose gel for IPCR amplification of maternal samples Rh47 and Rh61 using 2x Fast TaqMan Universal MasterMix (top row) and IMMOLASE™ DNA Polymerase (bottom row).** Amplification using 2x Fast TaqMan Universal MasterMix only illustrates amplification ~50bp. Amplification using IMMOLASE™ DNA Polymerase shows no amplification for most samples. However, samples Rh61 Ligation 1 (non-polymerised) (27), Rh61 Ligation 2 (non-polymerised) (28), Rh47 Ligation 1 (polymerised)

(30), Rh47 Ligation 2 (polymerised) (31) and Rh61 Ligation 1 (polymerised) (33), show a faint band at 200-300bp.

### 4.3 Discussion

The results illustrated successful cloning of pure *RH* fragments, and consequently, initial experiments using sticky ended fragments showed the feasibility of IPCR for self-ligation and amplification of fragments ~218bp in length (Figure 4-6). The 200-300bp fragment was visible for all colony IPCRs when previously ligated with the highest T4 DNA ligase concentration (4 Weiss units/ reaction (ligation reaction 1)). Therefore, ligation reaction 1 was considered to be the optimum conditions for ligation and IPCR amplification, despite the secondary band visible for colony 12 (Figure 4-6). The secondary bands visible in well 2 and well 8 for colony 12 (Figure 4-6) is likely to be a result of intermolecular ligation of two fragments, since the product is double the size of the expected fragment (500-600bp).

Higher DNA concentrations are associated with the formation of intermolecular ligation, whereas lower DNA concentrations (<10ng/  $\mu$ L) preferentially produce intramolecular connections (self-ligation), forming circularised DNA (Sambrook, Fritsch and Maniatis, 1989). Colonies 2 and 9 only demonstrate intramolecular (self) ligation (200-300bp), whereas colony 12 also demonstrates intermolecular ligation to another 200-300bp fragment producing a product between 500-600bp in size (Figure 4-6). Though this occurred for the least dilute ligation reaction (1) (4 Weiss units/ reaction) and the most dilute ligation reaction (3) (1 Weiss unit/ reaction), it is possible that slightly higher DNA concentrations of colony 12 were added to ligation these reactions. Despite adding 0.5-1 ng/  $\mu$ L of DNA to each ligation reaction, small pipetting errors could have resulted in increased volume added to reaction. Although lower concentrations were used, sticky ended fragments are more readily ligated due to the cohesive nature of the overhang (5'-AATT overhang for *Eco*RI).



Quantification of each colony was carried out using NanoVue™ Spectrophotometry. This method is commonly used, however, it can be unreliable and inaccurate, since UV absorbance cannot distinguish between DNA, RNA or protein and results are affected by contaminants such as free nucleotides and salts (Glasel, 1995). Therefore, the sensitivity of this approach is insufficient, preventing accurate quantification of DNA at low concentrations. Consequently, future experiments were carried out using Qubit® dsDNA HS assay kit, which uses fluorescent dyes to accurately quantify DNA nucleic acids only.

Sticky ended-fragments produce cohesive ends that can readily ligate, whereas blunt ended fragments join less efficiently because they do not express complementary overhanging base termini but self-ligate purely by phosphodiester bonds between the 3'hydroxyl ends and 5' phosphate ends of each strand. Since it is expected that cffDNA fragments will be found as blunt ended fragments, consequent experiments were carried out using adapted primers (with *EcoRV* site) (Table 4-2) to produce blunt ended *RH* exon 7 fragments. This was important, as ligating PCR-generated DNA fragments without the restriction enzyme digest step would produce dephosphorylated blunt ended fragments that are unable to self-ligate. In addition, PCR-generated fragments produced for ligation using *Taq* polymerase can leave an A-overhang on the 3'end of the PCR product, which inhibits self-ligation without the *EcoRV* restriction digest. However, the restriction digest (*EcoRV*), ligation and IPCR amplification steps for pseudo-fetal DNA (colony 12 (*RHD* exon 7)) fragment proved unsuccessful so experiments were optimised using donated maternal samples (Rh47 and Rh61).

When ligating DNA extracted from maternal samples, it was expected that 100-300bp bands would be visible for fetal fragments and bands >500bp would be visible for maternal fragments. Consequently, selective enrichment of the shorter cffDNA fragments could be achieved through optimisation of the dilute ligation reaction. However, as described in the previous chapter (Chapter 3), recent studies have determined smaller size differences between

cffDNA and maternal cfDNA (higher proportion at 147bp and higher proportion at 166bp, respectively) (Lo *et al.*, 2010) making differentiation challenging. The results illustrated unsuccessful IPCR amplification of maternal samples using 2x Fast TaqMan Universal MasterMix (Applied Biosystems) but IMMOLASE™ DNA Polymerase (Bioline) demonstrated faint bands between 100-200bp. Although these bands were only visible when the image contrast and brightness was increased to +40%, illustrating limited amplification. The results revealed a single faint band between 100 and 200bp for samples Rh61 non-polymerised DNA (ligation 2 (2 Weiss units)) and Rh61 polymerisation reaction 2 (5 units) (ligation 2). However, for samples; Rh61 non-polymerised DNA (ligation 3 (1 Weiss unit/ reaction)), Rh47 polymerisation 2 (ligation 2) and Rh47 polymerisation 2 (ligation 3), a secondary band ~200bp was also visible. It is possible that the smaller band illustrates amplification of the shorter fetal fragments and the longer DNA represent the slightly larger maternal fragments, however not enough DNA was present for sequencing analysis. Consequently, the experiment was repeated using high concentrations of T4 DNA ligase (up to 20 Weiss units/ reaction) but results were also unsuccessful. As described in the introduction the sensitivity of end-point conventional PCR is lower than for other approaches such as qPCR and dPCR, which use fluorescent labelled probes for detection of specific targets. For future experiments it would be beneficial to design fluorescent labelled probes within the IPCR product to allow target detection on a digital format, since this platform is associated with higher sensitivity (Strain *et al.*, 2013).

Studies have shown that the presence of cffDNA within the maternal plasma is caused by the apoptosis of cyto- and syncytiotrophoblastic cells, which released fetal specific fragmented DNA into the circulation (Bianchi, 2004; Tjoa *et al.*, 2006; Alberry *et al.*, 2007). Whereas, the maternal portion of cfDNA predominantly originates from apoptosis of hematopoietic cells (Sekizawa *et al.*, 2000; Lui *et al.*, 2002). Although apoptosis is the most viable, other

mechanisms such as active secretion of DNA and terminal differentiation have also been suggested as sources of circulating DNA. Because of the structured and non-chaotic nature of apoptosis, specific stages occur in succession, including the formation of apoptotic bodies, which contain either DNA or RNA (Halicka, Bedner and Darzynkiewicz, 2000). The ability to detect stabilized circulating RNA within patients suffering from malignant melanoma and breast cancer provides evidence that cell-free nucleotides are contained in protective vesicles or apoptotic bodies, since plasma is rich in RNase activity (Kopreski *et al.*, 1999; qi Chen *et al.*, 2000). However, alternative forms can also be present within the maternal circulation including shed cells, nucleosomes and free DNA (Bischoff, Lewis and Simpson, 2005). The concern for cffDNA, if assuming blunt-ended form of fragments, is that the maternal plasma may contain phosphatases which will remove the 5'-PO<sub>4</sub> from the fragments preventing ligation, a necessary step for IPCR.

DNA is found tightly coiled around histone proteins to form chromatin. In 1974 Roger Kornberg proposed that chromatin is made up of repeating units that contain two copies each of H2A, H2B, H3 and H4 and 200bp of DNA (histone octamer) (Kornberg, 1974). Apoptotic DNA fragmentation is caused by endogenous endonuclease activity, primarily Caspase-Activated DNase (CAD), which is usually inactivated by the Inhibitor of CAD (ICAD) (Enari *et al.*, 1998). The activation of caspase 3 during programme cell death results in the cleavage of ICAD and subsequent activation of CAD, which digest chromatin. Consequently, CAD cleaves DNA at internucleosomal linker sites between nucleosomes (found in parts of the DNA that are not wrapped around the histone) and produces fragments around 180bp and multiples of 180bp (for example 360bp, 540bp and 720bp) (Widlak *et al.*, 2000). The endonuclease activity is likely to be similar to deoxyribonuclease I (DNase I), which is also involved in DNA fragmentation during apoptosis by cutting non-specifically, yielding 5'-phosphate-terminated polynucleotides with a free hydroxyl group on position 3' (Samejima

and Earnshaw, 2005). DNase I results in random cleavage of both DNA strands at roughly the same site, generating blunt ends or fragments with 1-2 base overhangs (incompatible ends). Because it is unknown as to whether cfDNA is present with blunt ends or incompatible ends, an additional polymerase step was carried out prior to ligation for half of each sample to produce blunt ended fragments if necessary. A previous study that used an alternative endonuclease for DNA fragmentation (MNase) for the investigation of nucleosome mapping also reported a pre-processing step, which involved blunt-ending DNA by filling in (Allan *et al.*, 2012). The results in Figure 4-10 (B) highlight the potential of this approach, but not enough DNA was amplified for further sequencing analysis. However, detection using conventional PCR was unexpected since cffDNA represents a small fraction of the total cfDNA (3-6%) and it is likely that only a proportion of these fetal fragments will undergo successful ligation and IPCR amplification. As previously stated, the incorporation of this technique onto a digital platform would increase sensitivity. Rare sequence detection (RSD) can be determined by using a probe specific to a fetal target (e.g. *SRY* in mothers carrying male fetuses) against an alternatively labelled probe for a reference target. Consequently, through ratio analysis the amount of selective enrichment using *IPCR* can be determined. Ratio's  $<0.1$  would indicate little selective enrichment, since a high proportion of maternal cfDNA is still being amplified. Alternatively, a ratio of  $>0.5$  demonstrate a more equal proportion of the fetal target to the reference target, indicating that *IPCR* is selectively amplifying the shorter fetal fragments. In order to confirm selective enrichment, fetal fractions obtained by non-inverse PCR can be compared to *IPCR* cffDNA fraction results.

Alternatively, it is possibly that the blunt-end formation of samples is preventing optimal ligation of fragments, therefore for future experiments the inclusion of linkers or adapters, which create sticky-ends, could help to improve self-ligation. Linkers are short oligonucleotides (8-12 base pairs in length), which ligate via blunt ends to a DNA molecule

and create restriction enzyme sites upon annealing (Greene, 1998). Once cleaved this produces stick-ended molecules, thus enabling optimal self-ligation. Unlike linkers, adapters, which also bind to DNA molecules, express a cohesive end that encodes a predetermined restriction enzyme site allowing for direct ligation (Greene, 1998). Thus, the addition of adapters to the circulating DNA molecules prevents an additional restriction enzyme digests. The use of adapters is commonly seen in the field of MPS, where the fragmented DNA sequences undergo adapter ligation during library preparation ready for PCR amplification. To prevent dimer formation of adaptor molecules enzymatic treatment (Polynucleotide kinase) is used to alter the 5'-terminus (from 5'-P to 5'-OH), thus preventing the formation of phosphodiester bonds between the 5'OH and 3'OH ends (Chawla, 2002). This is beneficial as it prevents adaptors forming base pairs with themselves, which would create new DNA molecules that remain blunt-ended. However, for our application, self-ligation is necessary and therefore this enzymatic treatment should not be included within the protocol.

The application of selective enrichment of shorter fetal-DNA for improved NIPD has been previously discussed (3.3.2). However, due to the limited amount of cfDNA present little success has been achieved and consequently a viable technique for clinical practice has not been determined. COLD-PCR based approaches for enrichment (Chapter 3) are associated with alterations in efficiencies of primers at the lower  $T_d$ s, particularly for multiplexing experiments. The selective amplification of one target over another prevents accurate quantification, impeding the application of this approach as a reliable test for the NIPD of aneuploidy until optimal assays are achieved. IPCR for selective amplification of shorter fragments via self-ligation can be carried out at the optimal  $T_d$  (95°C), which prevents bias in amplification between targets, assuming cfDNA fragments are fragmented equally and will consequently ligate under the same conditions.

The results illustrate the feasibility of IPCR for pure colony DNA fragments that express sticky ends. However, further testing is required to determine the utility of this approach with actual maternal samples. Due to time constrictions further testing was not conducted, but future experiments combining linkers/ adaptors with highly sensitive ddPCR detection, could potentially enable the analysis of selective enrichment of IPCR for shorter fetal fragments. If future tests prove successful further large scale validation of this approach would need to be conducted before clinical implementation. However, if cffDNA can be increased to >25% using IPCR (Lo *et al.*, 2007), dPCR analysis in conjunction with IPCR selective enrichment could provide a cheaper NIPD test for fetal aneuploidy compared to current MPS approaches.

# Chapter 5

*RHD* zygosity testing for non-maternal samples and maternal *RHD* genotyping using droplet digital PCR (ddPCR)

## 5.1 Introduction

### 5.1.1 RHD Zygosity Testing

Of the 35 blood group systems, Rh is the most complex at the genetic level and is coded for by two paralogous genes (*RHD* and *RHCE*). Multiple combinations of SNPs in *RHCE* are responsible for the C/c and E/e polymorphisms. Although anti-c and anti-E can cause HDFN, events are rare since these antibodies (along with anti-K) only occur in 1 in 300 pregnancies and risk of HDFN for women carrying these antibodies is only 1 in 500 (Koelewijn *et al.*, 2008). Contrastingly, anti-D is one of the most immunogenic antibodies as it is a major cause of HDFN and transfusion reactions during alloimmunisation events. Variation in expression of the *RHD* antigen can cause further complications for obstetric patients and transfusion recipients. Total *RHD* gene deletion, the *RHD* $\Psi$  and some hybrid *RHD-RHCE* genes are responsible for D-negative phenotypes, but SNPs and other hybrid *RHD-RHCE* genes are responsible for D-positive phenotypic D-variants (Avent and Reid, 2000). All known mutations in both *RHD* and *RHCE* have been well catalogued (Reid, Lomas-Francis and Olsson, 2012), however, each year the number of variants can increase as novel alleles emerge.

D-variants can be categorised into two classes: weak D and partial D (Daniels, 2013). Even though weak D antigens express all D epitopes and as a consequent rarely produce anti-D, negative results can still arise using serological testing with a particular monoclonal antibody or procedure. Contrastingly, patients with partial D have the potential to make anti-D since antigens are lacking one or more epitopes. However, in rare cases some variants classified as weak D (such as types 4.2 and 15) have also been shown to produced alloanti-D in numerous patients (Wagner *et al.*, 2000). Initially it was thought that the amino acid substitutions that occur in weak D individuals appear within



the membrane-spanning domains or the cytoplasmic loop and are therefore not expressed externally (Flegel, 2007; Wagner *et al.*, 1999). However, the exact locations of the amino acid residues are not known and different models predict different locations, which could result in the lack of at least one D epitope and consequent anti-D production (Daniels, 2013). Prior to blood transfusion, determining the D antigen status of individuals can help to identify individuals with D variants who can safely receive D+ blood, and also determine individuals with a partial D type that are at risk of anti-D alloimmunisation and therefore require D- blood (Denomme *et al.*, 2005). Alternatively, determining D antigen status in pregnancy can allow for RAADP treatment to be targeted to women at risk of alloimmunisation. Since women who are weak D express all D epitopes and display a reduction in the D antigen rather than complete or partial deletion, it is recommended that anti-D is not given. However, as previously stated some rare weak D-variants can produce alloanti-D (Wagner *et al.*, 2000). Therefore, providing accurate maternal *RHD* genotyping using molecular techniques, which can detect various exons, as opposed to serological testing, could be used to detect the D-variant, and thus determine risk of alloimmunisation.

Paternal zygosity testing to define hemi- or homozygosity of *RHD* can allow clinical management to be focused on pregnancies that are at risk of HDFN, with the assumption of paternity. Further fetal *RHD* genotyping is not required in pregnancies with *RHD* homozygous fathers, and anti-D can be given since the fetus will be hemizygous *RHD* positive. Further testing is only required if the father is *RHD* hemizygous as the fetus has a 50% chance of being *RHD* negative, and thus, anti-D treatment is not required. Previously published methods to determine paternal zygosity have included real-time PCR assessment of *RHD* gene dosage, assessment of the hybrid Rhesus box found in D-negative individuals with the *RHD* gene deletion genotype and allele-specific PCR

methods (Perco *et al.*, 2003; Grootkerk - Tax *et al.*, 2005; Pirelli *et al.*, 2010; Haer - Wigman *et al.*, 2013b). However, it is important to note that zygosity testing by targeting the hybrid Rhesus box found in *RHD*-deletion type cde haplotypes is complicated because of differences in the hybrid box amongst individuals of African descent (Matheson and Denomme, 2002; Grootkerk - Tax *et al.*, 2005).

Determining the precise population frequencies of the different Rh haplotypes (CDE, cDE, CDe, cDe, cde, Cde, cdE, CdE) is complicated due to the inability to differentiate between CDe/Cde; cDE/cdE; cDe/cde; CDE/CdE haplotypes. Differentiation is not possible between these haplotypes since the hemi- or homozygosity of the *RHD* gene in individuals with any of these phenotypes has not been established. For example an individual with the haplotype CDe would be designated as the most common presumed genotype CDe/CDe rather than CDe/Cde. Thus presumed genotype, based on probability, is the manner in which donor and patient red cells are labelled. Zygosity determination of the above would define which haplotype (D-positive or D-negative) is carried by a particular individual. In this study, the ability of ddPCR, a more accurate quantitative PCR platform than conventional qPCR to determine patient *RHD* zygosity in a relatively small cohort of samples was evaluated.

### 5.1.2 Fetal *RHD* genotyping

Initially, definitive diagnosis of fetal sex and *RHD* status could only be achieved through invasive procedures such as amniocentesis and chorionic villus sampling (CVS), which are both associated with a small but significant risk of miscarriage. However, since the discovery of cffDNA within the maternal circulation non-invasive prenatal testing (NIPT) is now a clinical reality (Lo *et al.*, 1997; Avent and Chitty, 2006). Unlike fetal cells, which are also found in the maternal circulation and can persist for many years

postpartum, cffDNA is rapidly cleared following delivery (around 20 minutes) (Bianchi *et al.*, 1996; Nelson, 1996; Rijnders *et al.*, 2003).

Fetal sex determination using non-invasive methods through the analysis of cffDNA is currently available for families at risk of X-linked genetic disorders, such as haemophilia and DMD using qPCR platforms (Lewis *et al.*, 2012). Fetal sexing is especially beneficial in cases of congenital adrenal hyperplasia (CAH), which enables treatment to be targeted to female fetuses only (refer to 1.3.3.1). Many labs worldwide currently provide non-invasive fetal *RHD* genotyping (refer to 1.3.3.2) for alloimmunised women as part of routine practice, allowing the necessary management to be targeted to pregnancies at risk of HDFN (Gautier *et al.*, 2005; Van der Schoot *et al.*, 2006; Daniels *et al.*, 2009). Currently, most non-alloimmunised *RHD* negative mothers carrying *RHD* negative fetuses still receive RAADP unnecessarily. However, routine NIPT of fetal *RHD* genotype using qPCR is now implemented in the Netherlands and Denmark for the targeted administration of RAADP (De Haas *et al.*, 2012; Banch Clausen *et al.*, 2014). The cost analysis of introducing RAADP has seen mixed results. While some studies state that routine testing is cost effective since it will reduce the amount of Anti-D IgG administered thus lowering assay costs (refer to 1.3.3.2) (Chilcott *et al.*, 2003; Chilcott *et al.*, 2004; Van der Schoot *et al.*, 2006), others have argued that the introduction of this service would not result in the reduction in use of Anti-D IgG since postnatal serological testing may also be required for *RHD* negative fetuses determined by NIPD (Szczepura, Osipenko and Freeman, 2011). The second study only recorded savings for the introduction of RAADP if genotyping assays were also used to determine *RHD* status for postnatal analysis as opposed to serological testing. This highlights the requirement for consistencies for the application of cost-analysis decision making within the NHS. Though most cases do illustrate financial benefits and also illuminate the risk of infection

for *RHD*-negative mothers with *RHD*-negative fetuses (refer to 1.3.3.2), it is important to note that risk of sensitisation is reduced from 1.9-2.2% to 0.2% when prophylaxis is administered to all pregnancies (Liumbruno *et al.*, 2010).

Streck BCTs have been shown to increase the relative proportion of cffDNA compared to EDTA tubes (Wong *et al.*, 2013; Sillence *et al.*, 2015) (refer to 1.3.3.5). In this study, initial experiments were conducted to optimise the ddPCR platform for sexing and *RHD* genotyping of non-maternal samples. Consequently, the approach was developed for NIPT of fetal sex and *RHD* status, comparing the sensitivity of this approach to current qPCR based approaches. Due to technical reasons samples collected in EDTA tubes, despite being third trimester, expressed suboptimal cffDNA fractions (<2%). Whereas samples collected in Streck BCTs expressed optimal cffDNA fractions (>3%). However, all samples were included to thoroughly test the capability of the ddPCR assay against the current gold-standard qPCR approach.

The aims of this study were:

- To optimise the ddPCR platform for two sexing multiplex reactions and two *RHD* genotyping multiplex reactions.
- To test the sensitivity of ddPCR for low level copy target detection using spiked samples.
- To determine the ratio of each single-copy target multiplex reaction on individual (non-pooled) samples (refer to 2.1.2).
- To determine the *RHD* zygosity of known and unknown DNA samples extracted from both the plasma and buffy coat of human whole blood (refer to 2.1.2).
- To compare the sensitivity of qPCR to ddPCR for the NIPD of fetal sex and *RHD* status for samples expressing optimal (>3%) and suboptimal (<3%) cffDNA fractions.

## 5.2 Results

### 5.2.1 Optimising of ddPCR multiplex reactions

For sex and *RHD* determination four multiplex reactions were designed (Figure 5-1). Initial experiments were carried out to define the optimum annealing temperature for each reaction, which was decided based on the separation of positive droplets and the ratio achieved for single-copy target genes (See 2.9). For multiplex reaction 1 (*SRY*<sup>(H.P.T)</sup> (FAM)/ Xp22.3 (HEX)) an annealing temperature gradient from 62°C down to 56°C was tested. Separation of the *SRY*<sup>(H.P.T)</sup> target was visible from annealing temperature 58.4°C and below, whereas the Xp22.3 target illustrated visible separation from 59.8°C and below (Figure 5-2). The best ratio was seen when amplifying multiplex reaction at 56.5°C (0.978), and therefore this temperature was determined to be the optimum annealing temperature. However, acceptable ratios were also visible at 58.4°C (0.927) and 56°C (0.975) (Figure 5-2). The annealing temperature gradient for the second multiplex reaction for detection of the 30x multiple copy target region (*TSPY1*) against the Xp22.3 reference was also tested from 62°C down to 56°C. The results illustrated droplet separation for both amplicons at 59.8°C, however; improved separation was visible at 58.4°C and 56°C (Figure 5-3).

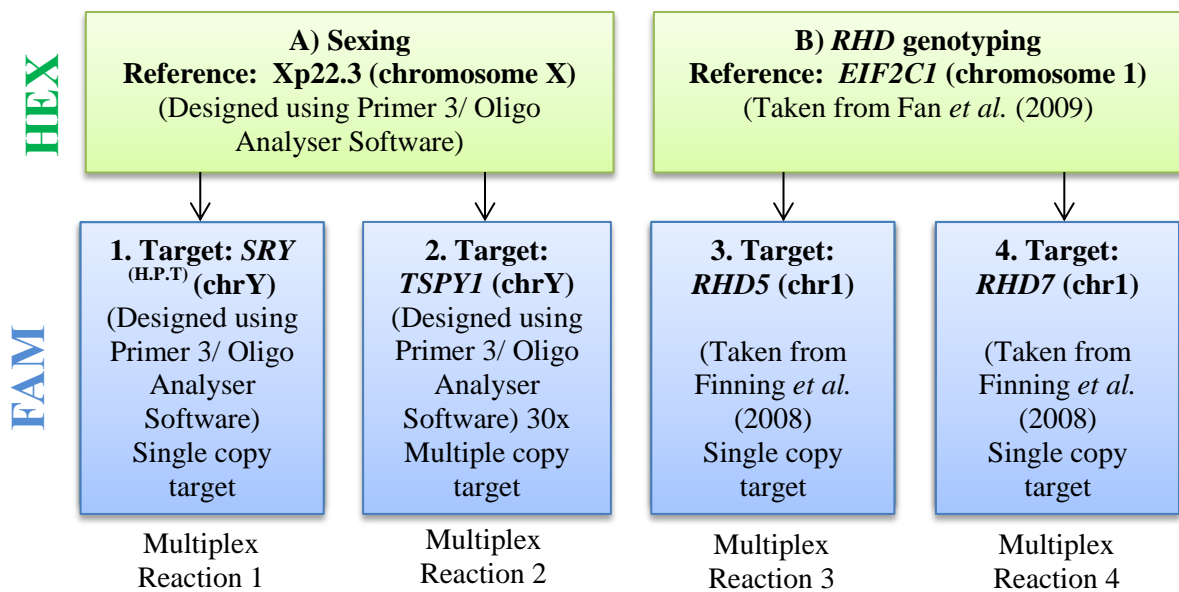


**Figure 5-1: The four multiplex reactions used for sexing (multiplex reactions 1 and 2) and RHD genotyping (multiplex reactions 3 and 4).** For both sexing experiments, the Xp22.3 (HEX-labelled) internal oligonucleotides were used as a reference for a single copy target (*SRY*) (multiplex reaction 1) and a multiple copy target (*TSPY1*) (multiplex reaction 2). For both *RHD* genotyping experiments, the *EIF2C1* (HEX-labelled) oligonucleotides were used as a reference for two single copy targets located on *RHD* exon 5 (multiplex reaction 3) and *RHD* exon 7 (multiplex reaction 4). All target genes (blue) were labelled with FAM fluorescent dye.

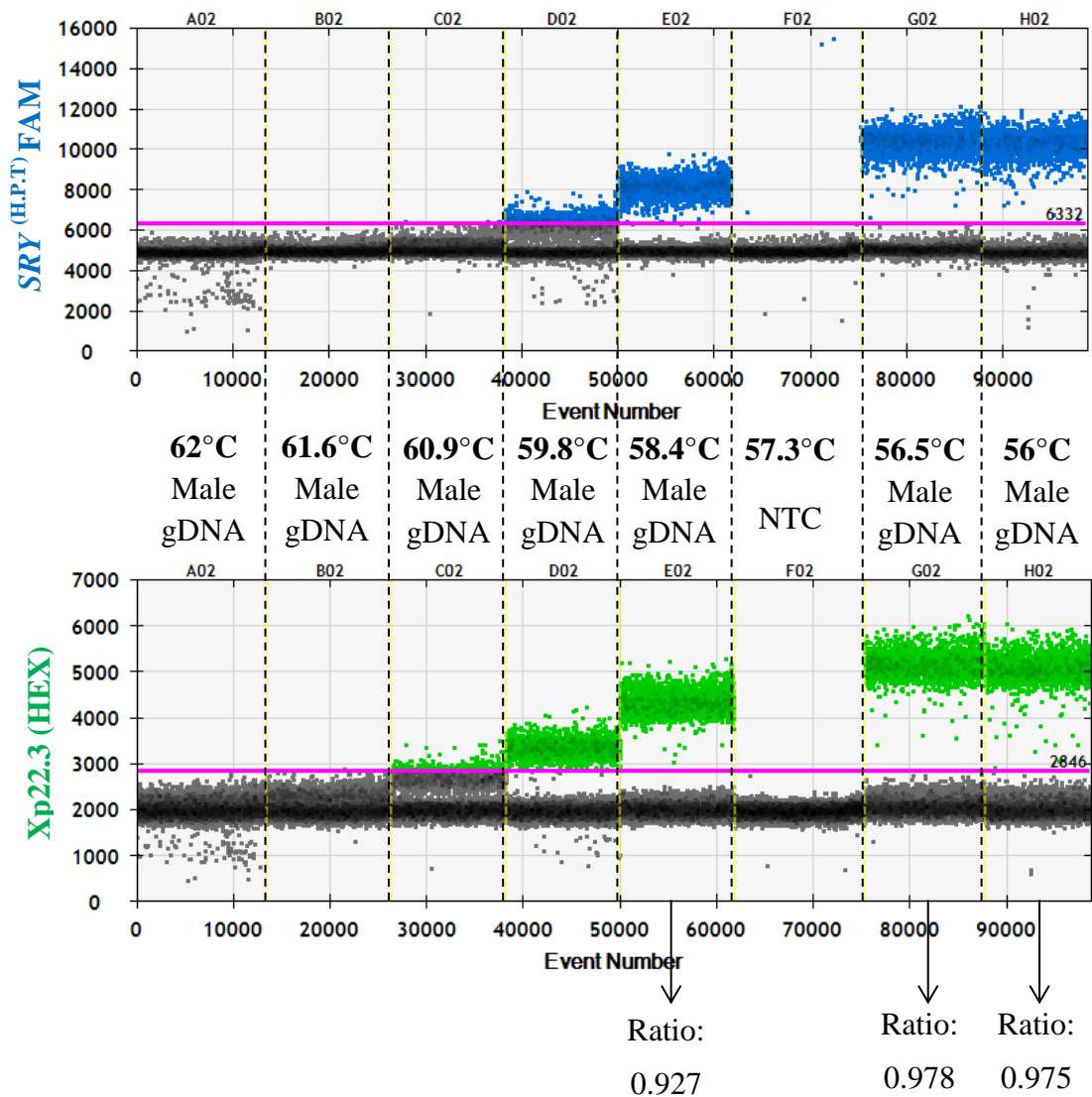


**Figure 5-2: ddPCR data showing annealing temperature gradient (from 62°C down to 56°C) results for *SRY*<sup>(H.P.T)</sup> (FAM) and Xp22.3 (HEX) multiplex reactions. One NTC was tested at 57.3°C T<sub>a</sub> and Male gDNA was tested at all other T<sub>a</sub>s. The result illustrated clear separation of positive and negative droplets begins at 59.8°C and 58.4°C for Xp22.3 and *SRY*, respectively. The ratio was determined by dividing *SRY* positive droplets by Xp22.3 droplets for at each annealing temperature. The results revealed ratios 0.927, 0.978 and 0.975 when amplified at T<sub>a</sub> 58.4°C, 56.5°C and 56°C, respectively.**



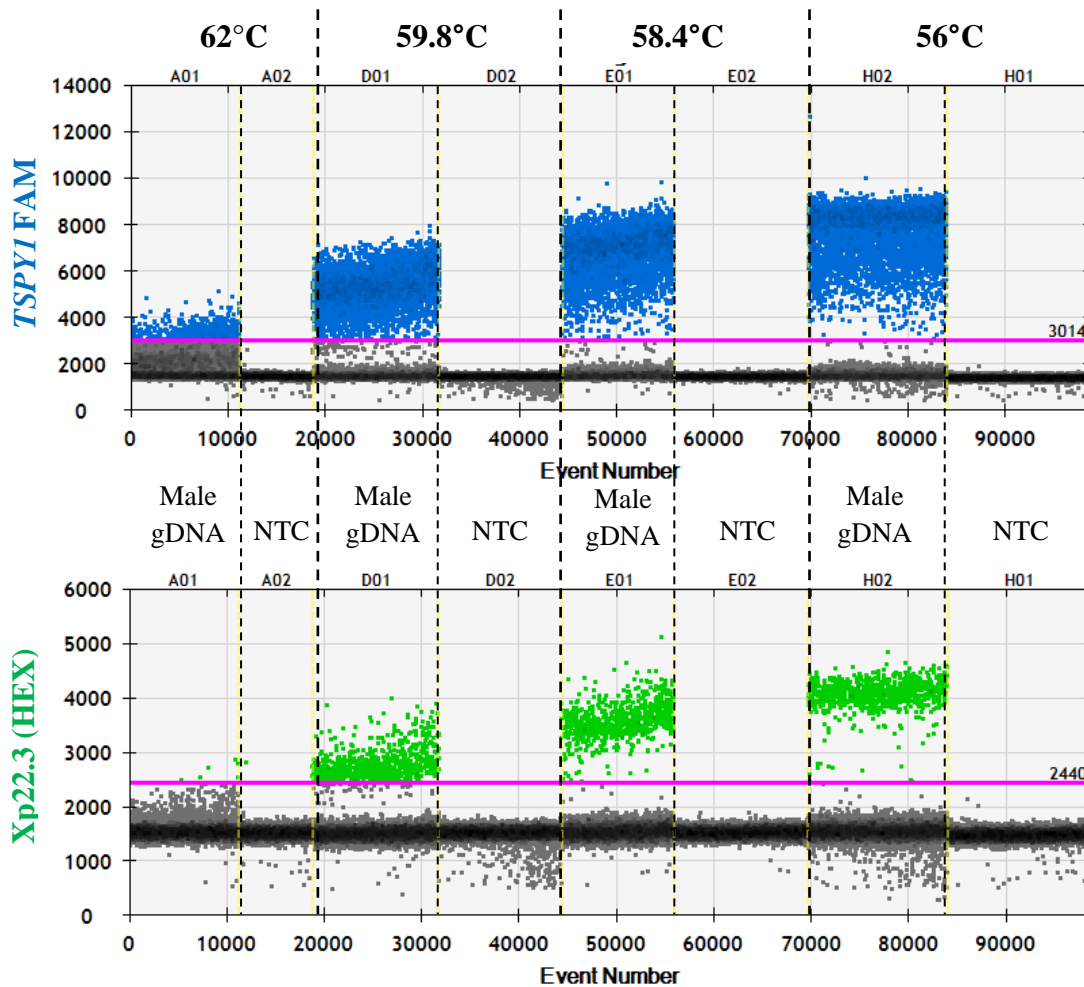


**Figure 5-3: ddPCR data showing the annealing temperature gradient (62°C, 59.8°C, 58.4°C and 56°C) results for *TSPY1* (FAM) and *Xp22.3* (HEX) multiplex reactions. Male gDNA and a NTC were tested at each temperature. The results illustrate that separation is visible from 59.8°C and lower, however optimal separation is seen at 58.4°C and 56°C.**

The annealing temperature was then optimised for both *RHD* genotyping experiments. Since poor droplet separation was visible for both previous reaction at 62 °C, for multiplex reactions 3 and 4, a gradient was tested from 60°C down to 56°C. The results in Figure 5-4 showed successful droplet separation of the *RHD5* (FAM) target at all annealing temperatures, but the *EIF2C1* (HEX) reference showed less optimal

separation at 60°C. The NTC controls tested were clean for all temperatures and the ratios for each annealing temperature were only 0.03-0.04 away from a ratio of 1, which was expected. This illustrated acceptable amplification at all temperatures. Droplet separation for multiplex reaction 4 (*RHD7* (FAM)/ *EIF2C1* (HEX)) demonstrated the same pattern as previously discussed for the *RHD5/EIF2C1* multiplex reaction (Figure 5-5). However, the optimal ratio was visible at 58.4°C (0.995). Therefore, for future experiments all multiplex reactions were tested at 58°C since this temperature illustrated successful droplet separation for all target and reference regions and also enabled all four multiplex reactions to be tested on a single plate.

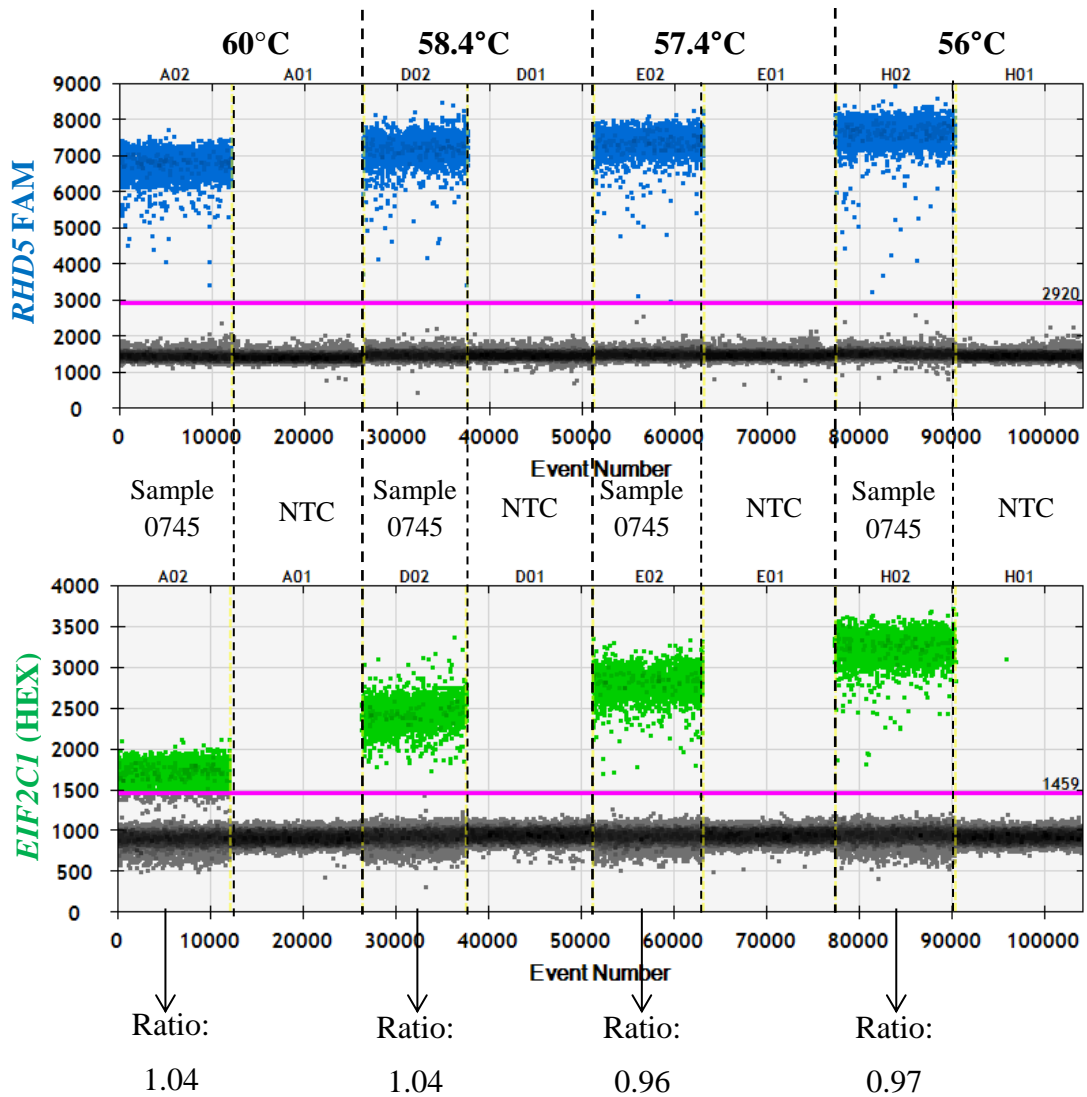


**Figure 5-4: ddPCR data showing the annealing temperature gradient (62°C, 58.4°C, 57.4°C and 56°C) results for *RHD5* (FAM) and *EIF2C1* (HEX) multiplex reactions.** Sample 1347 (homozygous for *RHD*) extracted from human whole blood (refer to 2.1.2) and a NTC were tested. The results illustrate that separation is visible for both targets at all annealing temperatures. Marginally higher separation is visible at 56°C, but all annealing temperatures give a ratio (determined by: *RHD5* (FAM) positive droplets / *EIF2C1* (HEX) positive droplets) close to a ratio of 1.

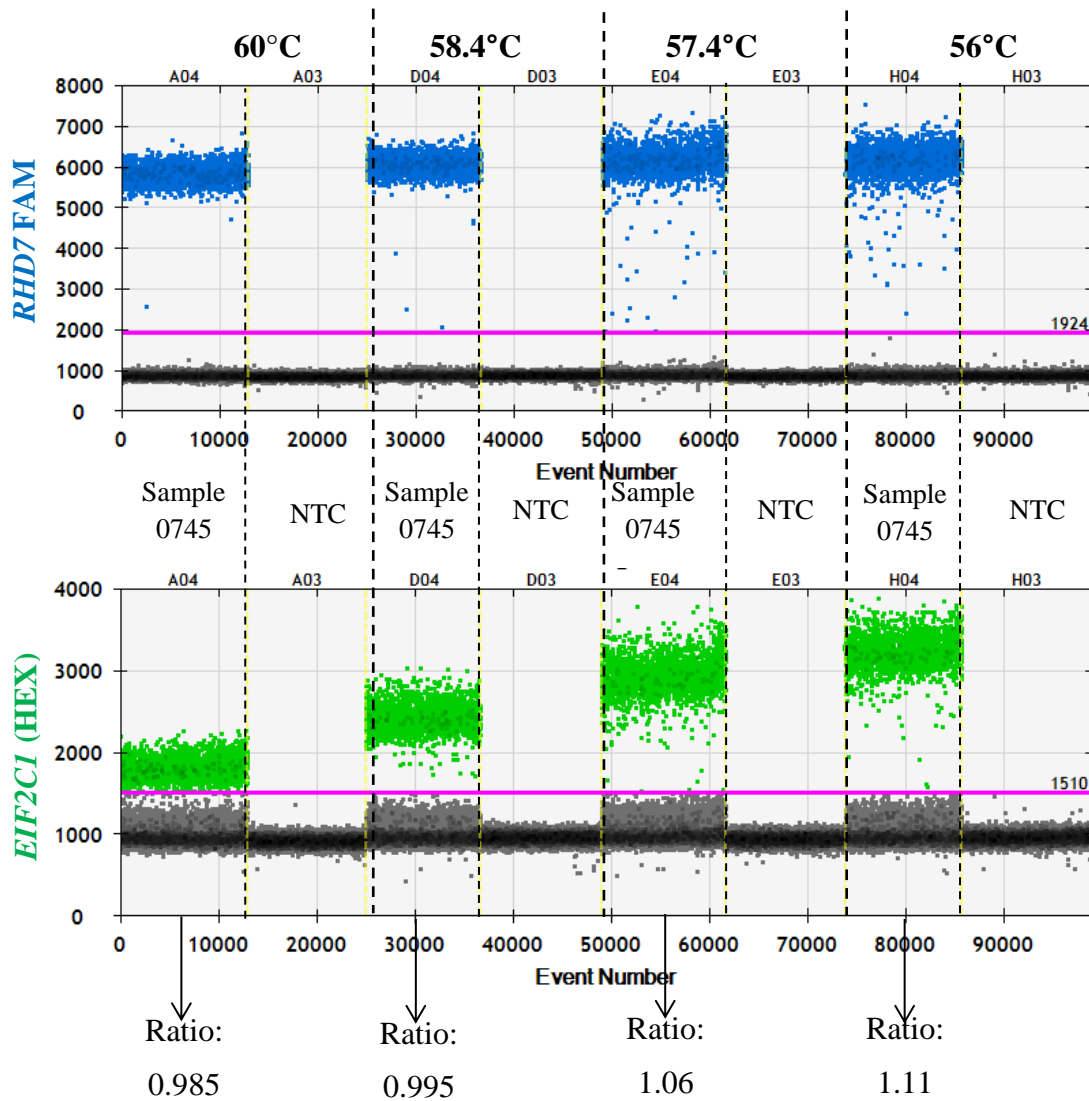
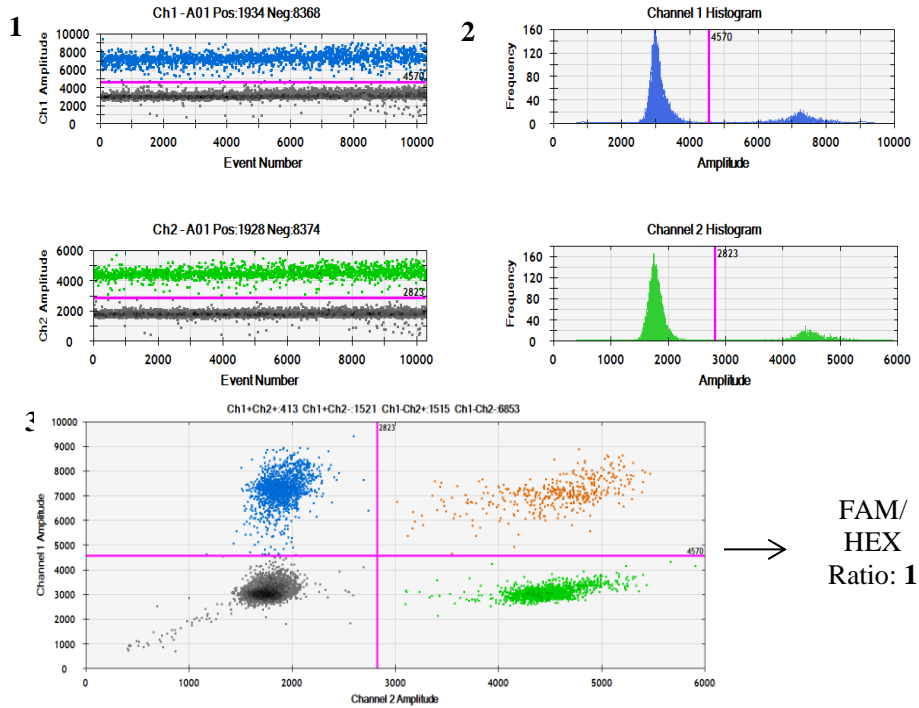


**Figure 5-5: ddPCR data showing the annealing temperature gradient (62°C, 58.4°C, 57.4°C and 56°C) results for *RHD7* (FAM) and *EIF2C1* (HEX) multiplex reactions. Sample 1437 (homozygous for *RHD*) extracted from human whole blood (refer to 2.1.2) and a NTC were tested. The results illustrate that separation is visible for both targets at all annealing temperatures. However, optimal separation was determined to be 58.4°C since this temperature expressed a ratio closer to 1 (0.995). Ratio determined by; *RHD7* (FAM) positive droplets / *EIF2C1* (HEX) positive droplets.**

In previous experiments a final concentration of 300nM of each primer was used. However, other dPCR studies have reported using higher primer concentrations (900nM) (Lo *et al.*, 2007b). Therefore, both primer concentrations (300nM and 900nM) were tested using multiplex reaction 1 (*SRY*<sup>(H.P.T)</sup> (FAM) and Xp22.3 (HEX)) using a constant concentration of each probe (250nM final concentration). The results in Figure 5-6 illustrate effective droplet separation for both primer concentrations. However, a ratio of 1 was achieved when using 300nM of each primer, whereas higher primer concentration (900nM) expressed a ratio of 1.07. Consequently, all future experiments were carried out using the lower (300nM) final primer concentration, since higher concentrations did not improve the assay.

**A) 300nM final concentration of each primer**



**B) 900nM final concentration of each primer**

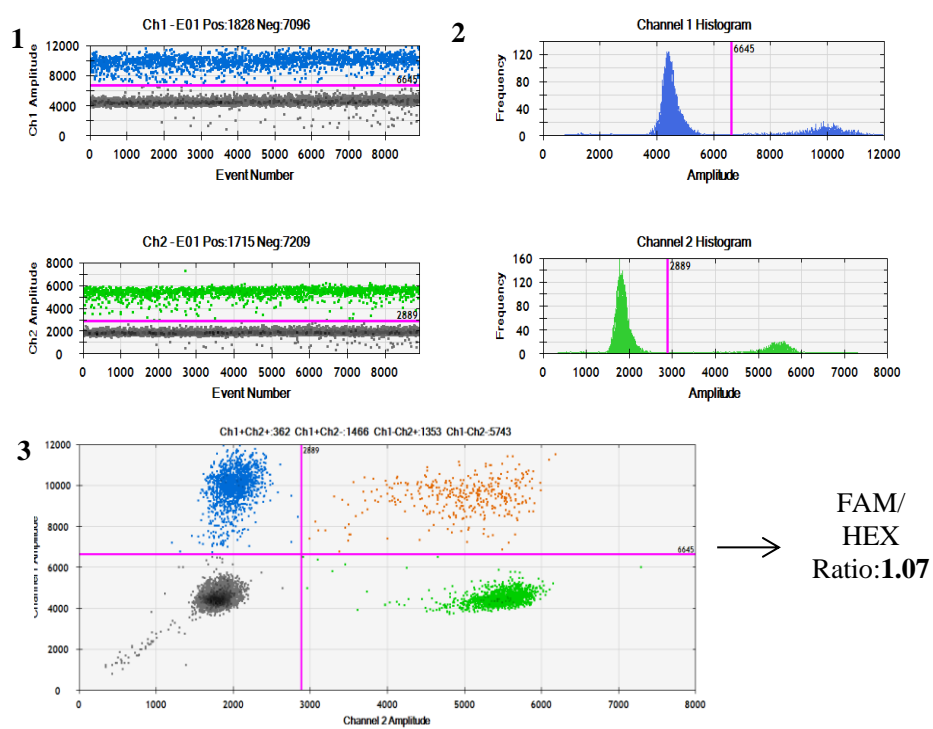


Figure 5-6: ddPCR 1D amplitude plots (1), histogram plots (2) and 2D amplitude plots (3) showing results for lower (300nM) and higher (900nM) primer

**concentrations for *SRY*<sup>(H.P.T)</sup> (FAM) and Xp22.3 (HEX) targets.** The results illustrate effective size separation for both primer concentrations and achieved a ratio of 1 and 1.07 for 300nM (A) and 900nM (B) final primer concentrations, respectively. Since an improved ratio was seen when using the lower concentration and no improvements were recorded with higher primer concentrations, 300nM final primer concentrations were used throughout.

### 5.2.2 Sex determination of non-maternal samples and spiked samples using ddPCR

Previous optimisation experiments using sexing multiplex reactions (Figure 5-1) were carried out using pooled Male gDNA (refer to 2.1.1). Therefore, analysis of plasma extracted DNA from human whole blood samples was carried out following the same ddPCR procedure (refer to 2.9) to determine the ratios of individual samples. The results for three male samples (8023, 936C and 768A), a Female gDNA (Y-negative) control and a Male gDNA (Y-positive) control are illustrated in Figure 5-7. For these initial experiments a single reaction was carried out for each sample. The results only demonstrated amplification of the reference (Xp22.3) for the female control sample, but expressed amplification of both targets for all male samples tested. The Male gDNA control expressed a ratio of 0.94, and the ratio for the individual male sample; 8023, 936C and 768A were 1.08, 1.03 and 1.05, respectively.

Consequently, spike experiments were carried out using Male gDNA, but to increase reliability of result and encourage more accurate ratio analysis each sample was tested in duplicate. Prior to ddPCR experiments, male and Female gDNA were diluted to 2ng/  $\mu$ L and diluted Male gDNA was spiked into the diluted Female gDNA at 50%, 10%, 5%, 3% and 1%. The results for the initial spike experiment using multiplex reaction 1 (*SRY*<sup>(H.P.T)</sup> (FAM)/ *EIF2C1* (HEX)) are illustrated in Figure 5-8. The NTC showed no amplification

and the Male gDNA control sample illustrated an equal representation (ratio of 0.98) of *SRY* and Xp22.3. The Female gDNA control sample only demonstrated amplification of the Xp22.3 target, which expressed twice the number of positive droplets (2359 events) compared to number of positive droplets for Xp22.3 amplification from the Male gDNA sample (1194 events). This is expected since females express two copies of X and males only express one copy of X. The expected fractional abundance of Y-target was determined by dividing the spike percentage by two, since males express one copy of the Y-target and one copy of the X-target. The actual fractional abundance and ratio achieved for each samples are summarised in table 5-1. The results illustrated that all samples were within 0.6% of the expected fractional abundance, illustrating the ability of ddPCR for highly precise quantification even when the target region is present at 1% (compared to 99% of the reference region).

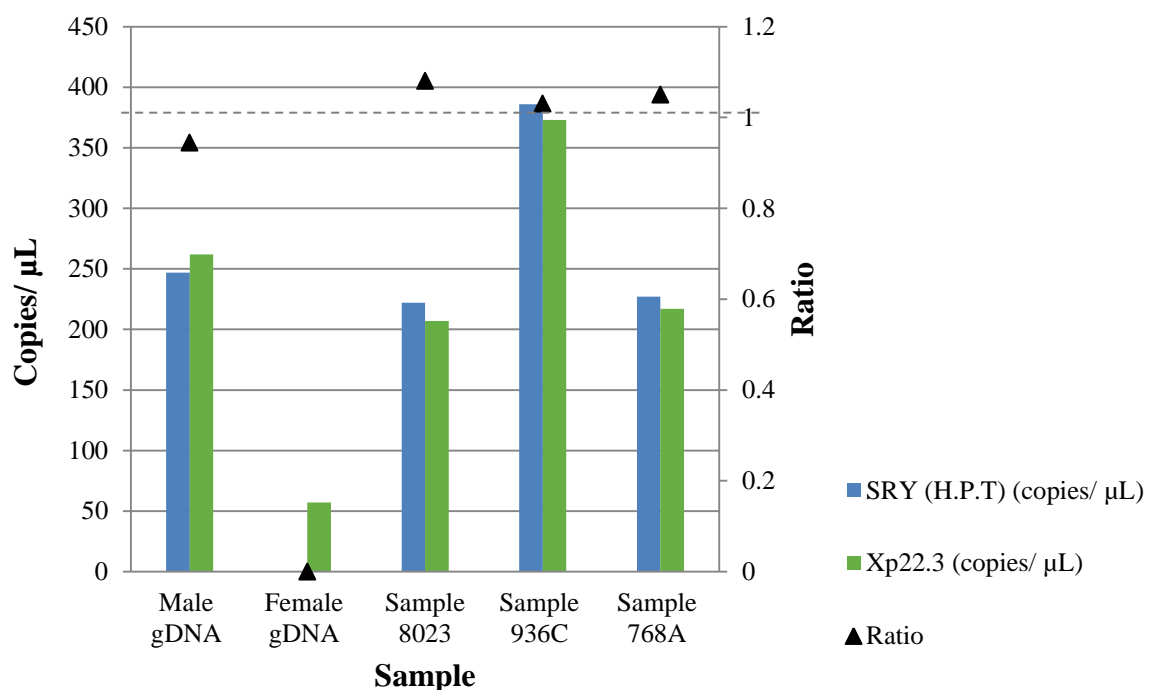


**Figure 5-7: Bar chart illustrating the concentration (copies/ μL) of the *SRY* <sup>(H.P.T)</sup> (FAM) target (blue) and the Xp22.3 (HEX) reference (green). The scatter plot**



**illustrates the ratio of *SRY*/Xp22.3 (black).** The Male gDNA control and the human whole blood samples (8023, 936C and 768A) all illustrate a ratio ~1 (0.94 – 1.08), whereas the Female gDNA control gave a ratio of 0 since no *SRY* target was amplified. The female aliquot gives a significantly lower concentration for the Xp22.3 reference compared to Male gDNA. Although 10ng/  $\mu$ L concentration, female sample had been freeze-thawed multiple times which could explain lower amount of available target DNA.

**Table 5-1: *SRY* (FAM) and Xp22.3 (HEX) multiplex ddPCR results for control samples<sup>1</sup> and female samples spiked with Male gDNA (50% (wt/wt) down to 1% (wt/wt)).** The results show the number of positive events for *SRY* (FAM) and Xp22.3 (HEX), the ratio calculated (*SRY*/ Xp22.3), expected fractional abundance of *SRY* and actual fractional abundance of *SRY*.

	<b>SRY (H.P.T) FAM (events)</b>	<b>Xp22.3 HEX (events)</b>	<b>Ratio</b>	<b>Expected fractional abundance of <i>SRY</i> (H.P.T)</b>	<b>Actual fractional abundance of <i>SRY</i> (H.P.T)</b>
<b>NTC<sup>1</sup></b>	1	1	-	-	-
<b>Male 2ng/<math>\mu</math>l (100%)<sup>1</sup></b>	1181	1207	0.98	50%	49.46%
<b>Female 2ng/<math>\mu</math>l<sup>1</sup></b>	0	2359	-	0%	0%
<b>50% Spike</b>	604	1849	0.31	25%	24.62%
<b>10% Spike</b>	118	2363	0.05	5%	4.76%
<b>5% Spike</b>	49	2427	0.02	2.5%	1.98%
<b>3% Spike</b>	55	2660	0.02	1.5%	2.03%
<b>1% Spike</b>	17	2167	0.01	0.5%	0.79%

On average around 11,000 – 12,000 droplets were produced per well. The results reveal that out of these droplets only around 25% of these droplets were positive for each sample (e.g. 2359 for female sample). To further increase the sensitivity, more sample per well could be loaded or the number of targets included in each multiplex reaction could be increased to expand the number of informative droplets. However, this approach is limited since only two fluorescent dyes can be detected (FAM and HEX/VIC), although variations in assay dilutions can enable amplitude separation using the same fluorophore.

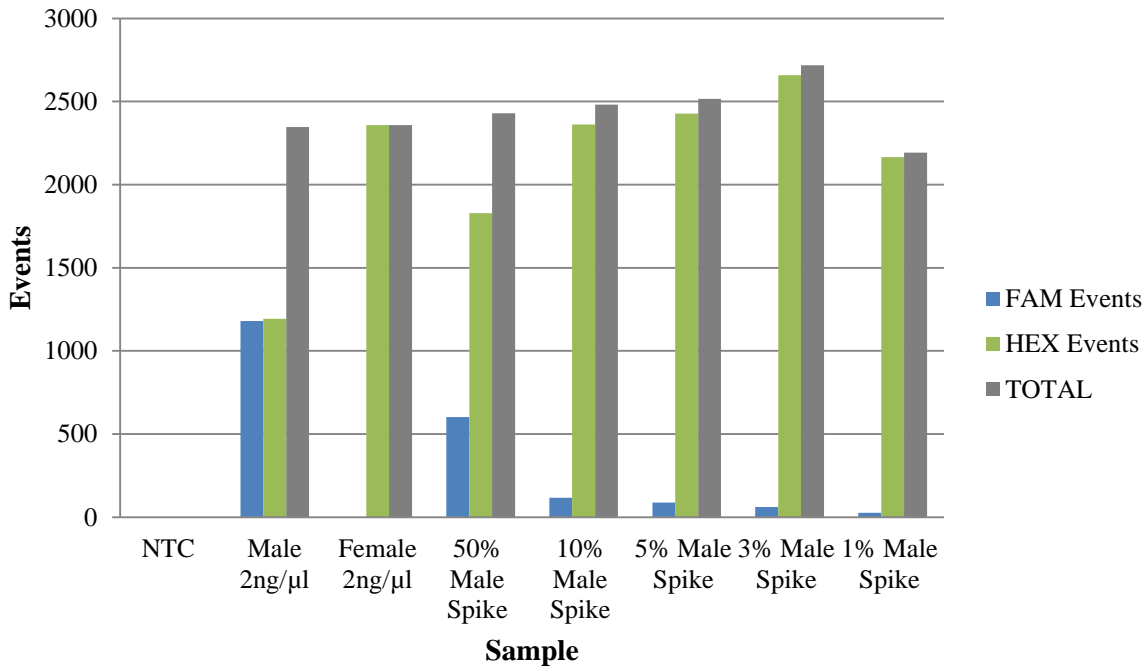


**Figure 5-8: Bar chart illustrating the number of events (positive droplets) for *SRY* (H.P.T) (FAM), Xp22.3 (HEX) and the total (FAM + HEX positive droplets) in a generated by ddPCR in a multiplex experiment.** Female gDNA samples spiked with a decreasing proportion of Male gDNA (50% down to 1%) were tested against the following control samples; pure Male gDNA, pure Female gDNA and NTC. The results illustrated no amplification for the NTC and only amplification of Xp22.3 (HEX) for the female control samples. The number of positive events for the Male gDNA control sample was roughly equal for Xp22.3 (1194) and *SRY* (1180), as expected. The reduced amount of Male gDNA spiked into Female gDNA is shown, and even when spike in at 1% (wt/wt) 26 copies of the *SRY* target were still detected.

The spike experiment was subsequently repeated. However, in this instance the multiple copy target, *TSPY1* (multiplex reaction 2 (Figure 5-1) was tested. Since this target is presented multiple times within the genome, spike samples (using the same diluted Male and Female gDNA) were produced starting at 50% (wt/wt) Male gDNA down to 0.1% (wt/wt) Male gDNA. The results are illustrated in Figure 5-9. The results illustrated a

decrease in number of events for the *TSPY1* target (Figure 5-9 A and B) but still showed successful detection of the Y-specific target even when present at 0.1%. The concentration of Male gDNA at 100% was 812 copies/  $\mu$ L, which continued to decrease in relation to each spike down to 0.1% Male gDNA, which expressed a concentration of 1.22 copies/  $\mu$ L (Figure 5-9 (C)). In contrast, the Xp22.3 concentration remained close to 200 copies/  $\mu$ L for all samples except the 100% and 50% Male gDNA samples, which express higher concentrations of the *TSPY1* target (Figure 5-9 (C)).

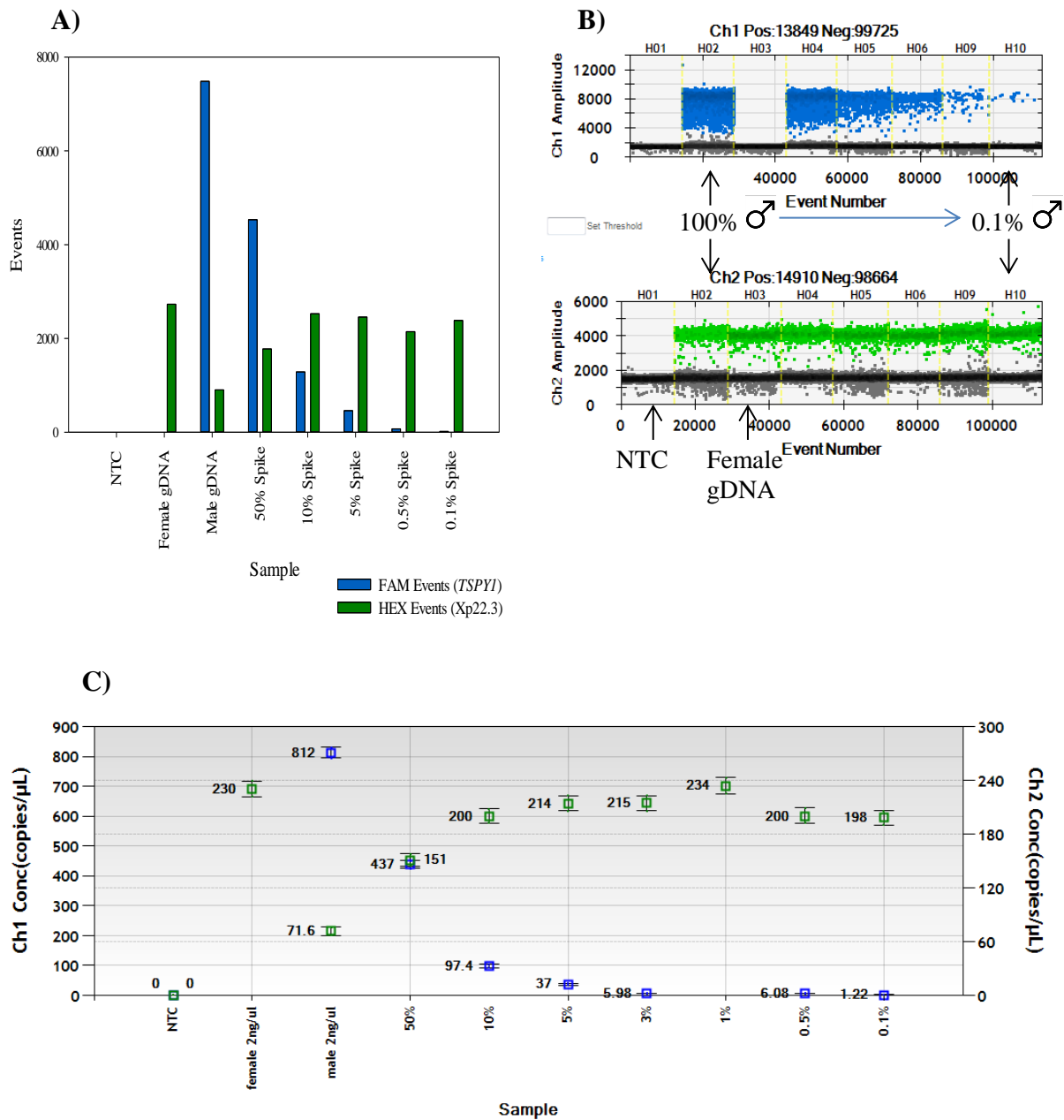


**Figure 5-9: ddPCR results for *TSPY1* Spike experiments.** A) Bar chart illustrating the events (positive droplets) for *TSPY1* (FAM) and Xp22.3 (HEX) for NTC, Female gDNA (2ng/  $\mu$ L), Male gDNA and Female gDNA spiked with a decreasing proportion of Male gDNA (50% down to 1%). B) 1D amplitude plot for all samples, which illustrated a relatively constant number of droplets for the Xp22.3 (HEX) reference and a decreasing number of droplets for the *TSPY1* (FAM) target. C) Concentration (copies/  $\mu$ L) of each

sample for Ch1 (TSPY1 (FAM)) and Ch2 (Xp22.3 (HEX)). The result illustrated that the concentration of the Xp22.3 reference increased and the concentration of the TSPY1 target decreased as the proportion of Male gDNA declined.

### 5.2.3 Determination of *RHD* zygosity for non-maternal samples

Multiplex reactions 3 and 4 (Figure 5-1) were designed to determine the presence of *RHD* in a number of samples. Before zygosity testing, to determine ratio analysis of both multiplex reactions on the ddPCR platform, a D-negative sample (831G (rr)) and three samples thought to be homozygous ( $R_1R_1$ ) D-positive (464E, 9393, 694Y and 778B) were tested. Male gDNA was used as a positive control (since previous experiments optimised using this sample) alongside a NTC. The results for the *RHD5* (FAM) / *EIF2C1* (HEX) multiplex reaction are illustrated in Figure 5-10 and the results for the *RHD7* (FAM) / *EIF2C1* (HEX) multiplex reaction are illustrated in Figure 5-11. Both experiments exhibit no amplification for the NTC. Multiplex reaction 3 (*RHD5*/ *EIF2C1*) and multiplex reaction 4 (*RHD7*/ *EIF2C1*) expressed ratios of 0.69 and 0.70, respectively, for the Male gDNA sample. Since the Male gDNA positive control sample (Promega) is produced from multiple donors, some of which are likely to be D-negative, but all of which will express two copies of the *EIF2C1* reference gene, a ratio of less than 1 was expected. However, the individual samples, which were, homozygous for *RHD* all illustrated a ratio close to 1 (See Figure 5-10 C and Figure 5-11 C). Sample 831G, which was homozygous D-negative, only illustrated amplification of the reference gene (*EIF2C1*). The concentration of each target for both multiplex reactions and ratio produced are summarised in Table 5-2.

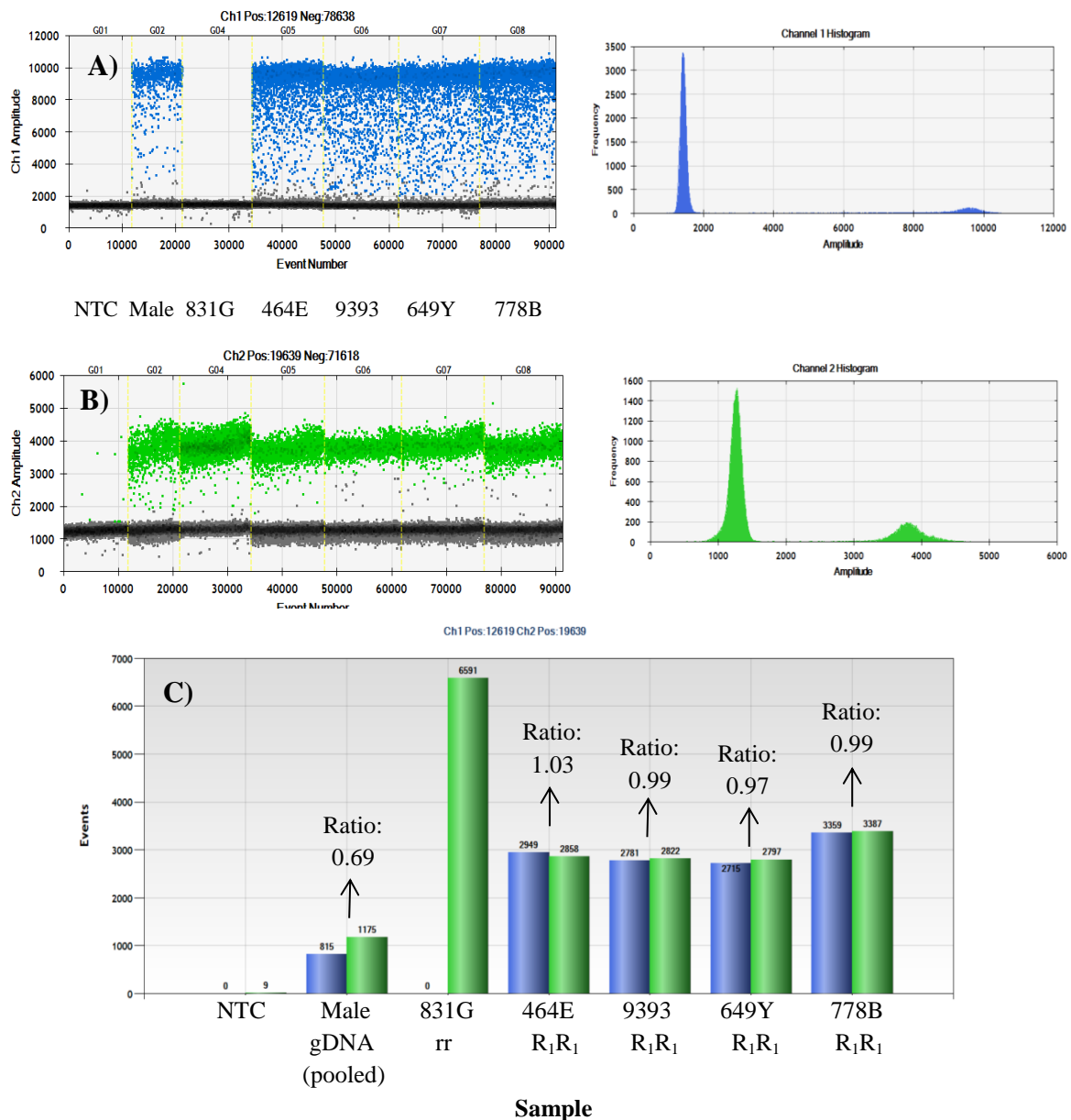


**Figure 5-10: ddPCR data for *RHD5* (FAM)/ *EIF2C1* (HEX) multiplex reaction for control samples (NTC, Male gDNA and Female gDNA) and four unknown DNA samples extracted from plasma of human whole blood (refer to 2.1.2). A) 1D amplitude plot for *RHD5* (FAM) target, B) 1D amplitude plot for *EIF2C1* (HEX) reference and C) Bar chart illustrating the number of *RHD5* (FAM) and *EIF2C1* (HEX) positive droplets (events) for all samples. The results illustrated that sample 831G was *RHD* negative, since no *RHD5* target was amplified and the remaining samples (464E, 9393, 649Y and 778B) were all *RHD* positive, since the *RHD5* target is expressed. The**

results also illustrate that that 464E, 9393, 649Y and 778B are all homozygous for the *RHD* gene since ratios (*RHD5/ EIF2C1*) close to 1 were recorded for all samples (1.03, 0.99, 0.97 and 0.99, respectively). The ratio and concentration of each target for all samples is recorded in Table 5-2.

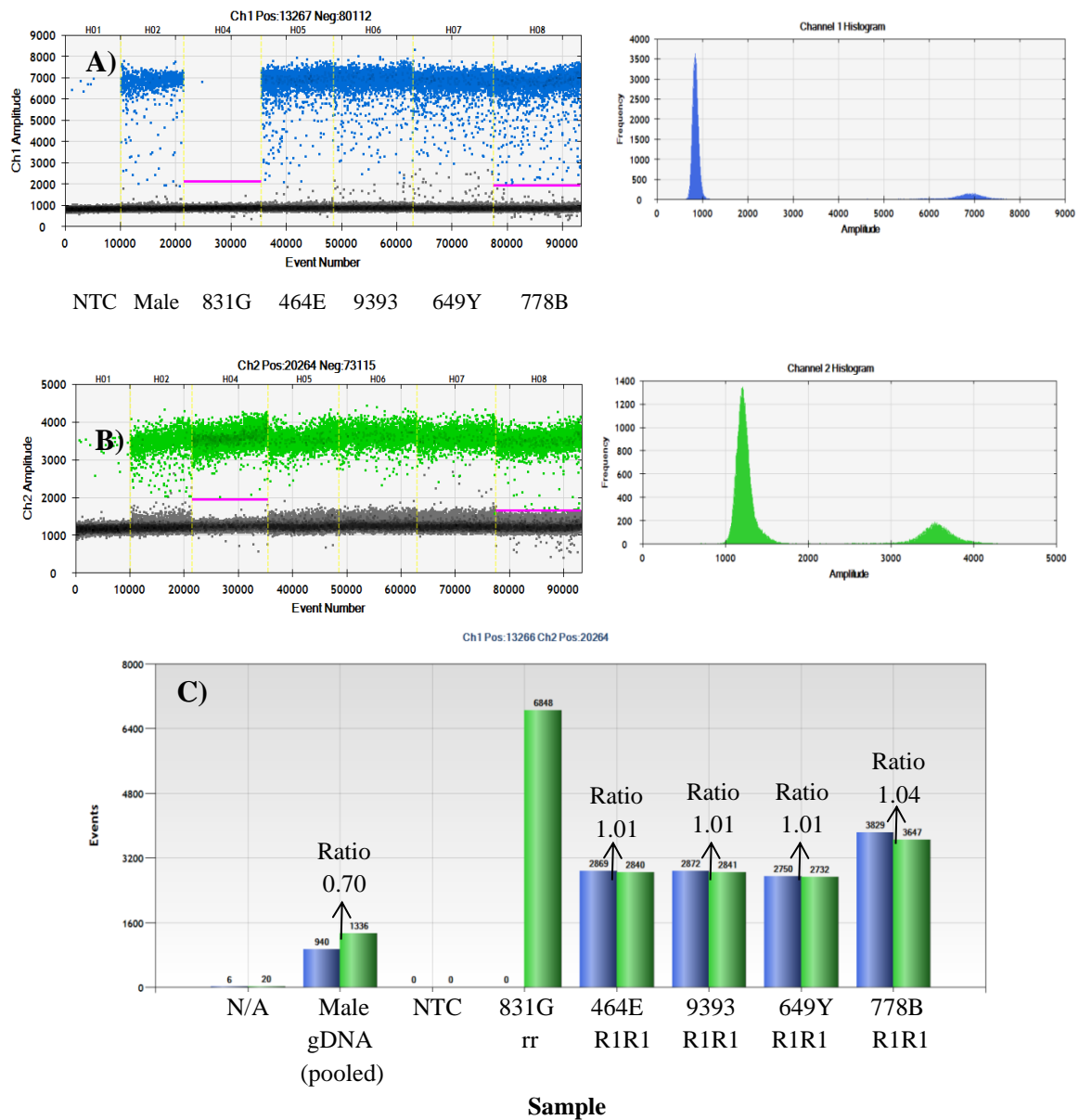


**Figure 5-11: ddPCR data for *RHD7* (FAM)/ *EIF2C1* (HEX) multiplex reaction for control samples (NTC, Male gDNA and Female gDNA) and four unknown DNA samples extracted from plasma of human whole blood (refer to 2.1.2). A) 1D amplitude plot for *RHD7* (FAM) target, B) 1D amplitude plot for *EIF2C1* (HEX)**

reference and C) Bar chart illustrating the number of *RHD5* (FAM) and *EIF2C1* (HEX) positive droplets (events) for all samples. The results illustrated that sample 831G is *RHD* negative, since no *RHD7* target is amplified and the remaining samples (464E, 9393, 649Y and 778B) are all *RHD* positive, since the *RHD7* target is detected. The results also illustrate that samples 464E, 9393, 649Y and 778B are all homozygous for the *RHD* gene since ratios close to 1 were recorded for all samples (1.01, 1.01, 1.01 and 1.04, respectively) N/A well loaded incorrectly.

**Table 5-2: The concentration of each target and the ratio generated for each multiplex reaction; *RHD5* (FAM)/ *EIF2C1* (HEX) and *RHD7* (FAM)/ *EIF2C1* (HEX).** Summary of data shown in Figure 5-9 and Figure 5-10.

Sample	<i>RHD5</i> (copies/ $\mu$ L)	<i>EIF2C1</i> (copies/ $\mu$ L)	Ratio ( <i>RHD5</i> / <i>EIF2C1</i> )	<i>RHD7</i> (copies/ $\mu$ L)	<i>EIF2C1</i> (copies/ $\mu$ L)	Ratio ( <i>RHD5</i> / <i>EIF2C1</i> )
NTC	0	0	0	0	0	0
Male gDNA	98.2	144	0.69	95.2	138	0.70
831G	0	777	0	0	732	0
464E	274	264	1.04	274	271	1.01
9393	242	246	0.99	243	240	1.01
649Y	216	224	0.97	231	229	1.01
778B	297	299	0.99	306	293	1.04

For zygosity testing experiments DNA was extracted from both the buffy coat (carried out by Amr Halawani) and the plasma fraction of separate batches of human whole blood samples (refer to 2.1.2). Samples extracted from buffy coat were quantified using the NanoVue™ Plus Spectrophotometer (GE Healthcare) (refer to 2.6.1) and diluted to 10ng/  $\mu$ L. Some of the samples extracted from the plasma were quantified using the Qubit (refer to 2.6.2) and due to lower yields of DNA concentrations (Table 5-3) none of the plasma-extracted samples were diluted. Subsequently, samples were run on the ddPCR platform as described in section 2.9.



**Table 5-3: Concentration of DNA extracted from the plasma of human whole blood.**

Sample	Presumed <i>RHD</i> genotype determined by serological analysis <sup>1</sup>	Concentration (ng/ $\mu$ L)
065S	R <sub>1</sub> r	7.82
118Z	R <sub>1</sub> r	6.58
1226	R <sub>1</sub> r	10.3
1306	R <sub>1</sub> r	3.35
0670	R <sub>1</sub> R <sub>1</sub>	3.53
1347	R <sub>1</sub> R <sub>1</sub>	2.72
138R	R <sub>1</sub> R <sub>1</sub>	6.24
9673	R <sub>0</sub> r	2.54
069F	R <sub>0</sub> r	6.73
740B	R <sub>0</sub> r	5.26

<sup>1</sup>Determined by NHS BT (Filton).

The presence or absence of the *RHD* genes was used to determine whether the sample was *RHD* positive or *RHD* negative, respectively. The ratio of *RHD5/ EIF2C1* and *RHD7/ EIF2C1* was used to determine whether the samples were hemizygous or homozygous for the *RHD* gene. Samples homozygous for *RHD* would have expressed ratios close to one, since they have two copies of *RHD5* and *RHD7* and two copies of *EIF2C1*. Samples hemizygous for the *RHD* gene would express ratios closer to 0.5, since they only express one copy of *RHD5* and *RHD7* and two copies of *EIF2C1*. Twenty plasma-samples (refer to 2.1.2.1) were tested all with known serologically determined *RH* status (as given by NHS BT (Filton)) and the ddPCR zygosity testing results are illustrated in Figure 5-12 (A). Three rr presumed genotypes were tested (147J, 1660, 7807) and results show no amplification of either D-specific target (Figure 5-12 (A)). Three R<sub>0</sub>r and seven R<sub>1</sub>r presumed genotypes were also tested and all samples, except sample 1777, expressed a ratio close to 0.5 (Figure 5-12 (A) and Figure 5-13) (Table 5-4). Sample 1777, which was previously classified as being R<sub>1</sub>r, expressed ratios of 0.97 and 1.04 for multiplex reactions 3 and 4, respectively. This result contradicted previous

classification and indicated that the sample expressed two copies of the *RHD* gene. Therefore, it is possible that this sample may actually carry the  $R_1R_0$  genotype.

DNA extracted from twenty buffy coat samples were also tested (refer to 2.1.2.2), but in this instance only 9 were analysed with known Rh haplotypes and 11 were tested blind. Of the nine known samples the following Rh haplotypes were tested; two  $R_1R_1$ , three  $R_2R_2$  and three  $R_1r$  (Figure 5-12 (B)). The  $R_1R_1$  samples and the  $R_1r$  samples expressed ratios close to 1 and 0.5, respectively (Figure 5-12 (B) and Figure 5-13) (Table 5-4). Two of the  $R_2R_2$  samples expressed a ratio close to one, but sample 729M ( $R_1R_2$ , weak D) illustrated a ratio of 0.49 and 0.5 for the *RHD5/ EIF2C1* and *RHD7/ EIF2C1* multiplex reactions, respectively (Figure 5-12 (A) and Figure 5-13) (Table 5-4). This indicated that sample 729M only expresses one copy of the *RHD* gene, and could also have been previously misclassified as  $R_1R_2$  and actually express the  $R_1r''$  (DcE/dcE) or  $R_2r'$  (DcE/dCe) genotype.

The amplification and ratio analysis of all unknown targets are illustrated in Figure 5-12 (B) and Table 5-4. Seven of these samples expressed ratios close to 1 for both multiplex reactions (Figure 5-13) (Table 5-4). Four of these samples were confirmed to express the  $R_1R_1$  haplotype (078U, 103N, 1461 and 877L), two were confirmed to express the  $R_2R_2$  haplotype (132H and 689Y) and one was confirmed to express the  $R_2R_Z$  haplotype (746P) (Figure 5-13) (Table 5-4). The remaining four samples (3093, 572R, 7687 and 087W) all expressed ratios closer to 0.5 for both multiplex reactions (Figure 5-13) (Table 5-4). Three of these samples were confirmed to express the  $R_1r$  haplotype (3093, 572R and 7687), but sample 087W had been previously classified as having an  $R_2R_2$  haplotype. The ddPCR results demonstrate that sample 087W is actually hemizygous for the D-antigen and is likely to exhibit the  $R_2r''$  Rh haplotype as opposed to the  $R_2R_2$  haplotype initially stated.

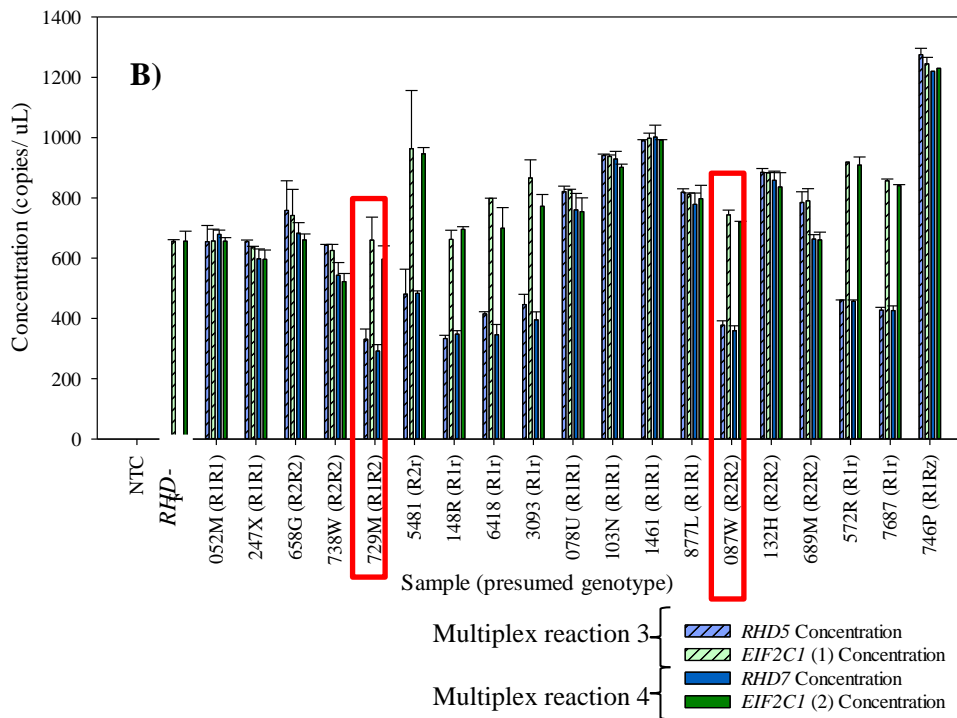
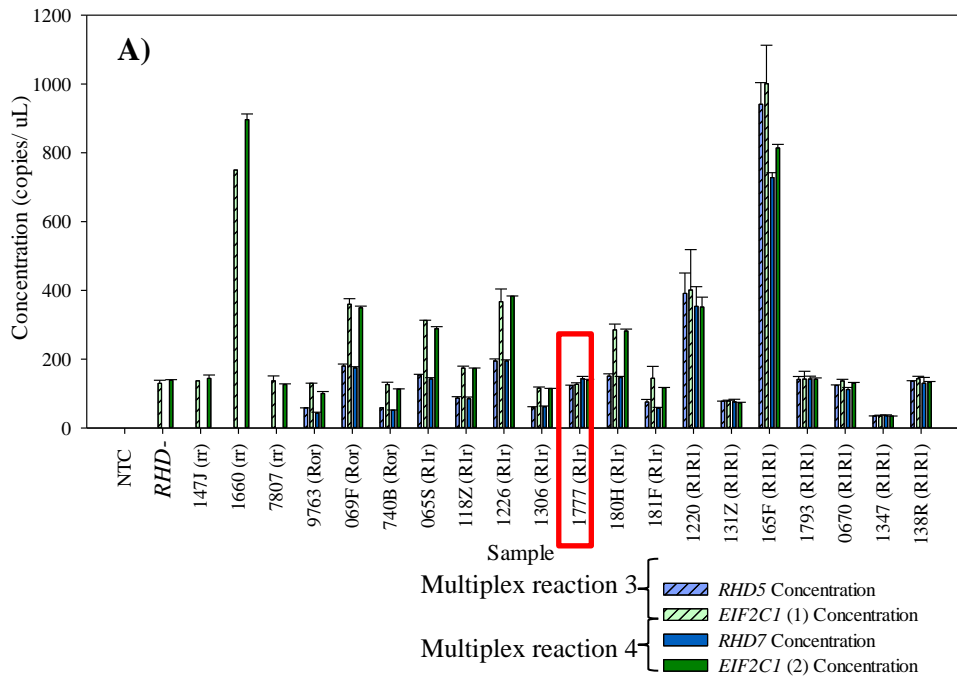


**Figure 5-12: Bar chart demonstrating the mean concentration (copies/  $\mu$ L) and SD for  $RHD5$  (FAM),  $RHD7$  (FAM) and  $EIF2C1$  (HEX) for DNA samples extracted from the plasma (A) and buffy coat (B) of human whole blood (2.1.2 and 2.1.3). The**

*RHD* status of each sample was determined by the presence of *RHD5* (FAM) and *RHD7* (FAM) in multiplex reaction 3 (*RHD* (FAM) / *EIF2C1* (HEX)) and multiplex reaction 4 (*RHD7* (FAM) / *EIF2C1* (HEX)), respectively. Positive samples that illustrated a ratio close to 1 for both multiplex reactions were classified as homozygous for the *RHD* gene and samples that expressed a ratio closer to 0.5 were classified as being hemizygous for the *RHD* gene. These results are summarised in Table 5-4. Samples 1777, 729M and 087W all show disparity with NHS BT (Filton) presumed genotype (red). Sample 1777 (R<sub>1</sub>r) showed an equal amount of both *RHD* targets against the reference (*EIF2C1*), which indicated that this case was *RHD* homozygous. Alternatively, samples 729M (R<sub>1</sub>R<sub>2</sub>) and 087W (R<sub>2</sub>R<sub>2</sub>) showed half the concentration of both *RHD* targets compared to the reference (*EIF2C1*), which demonstrated that these samples were hemizygous for *RHD* (refer to table 5-4 for ratio analysis of each *RHD* target (FAM/HEX)).

**Table 5-4: Zygosity testing results for multiple samples extracted from both the plasma and buffy coat of human whole blood samples.** The *RHD* ratios (*RHD5* and *RHD7*) for each sample was calculated by dividing the *RHD* (FAM) concentration (copies/  $\mu$ L) by the reference (*HEX*) concentration (copies/  $\mu$ L). Sample zygosity (homozygous *RHD* positive, hemizygous *RHD* positive or homozygous *RHD* negative) was determined by the detecting whether the *RHD* targets displayed equal representation (ratio ~1), 50% representation (ratio ~0.5) or 0% representation (ratio 0) compared to the reference (*EIF2C1*), respectively. These results were compared against the presumed genotype determined by NHS BT (Filton) and for three cases (red) the *RHD* genotype was altered.

Sample	Ratio ( <i>RHD5</i> (FAM) / <i>EIF2C1</i> ( <i>HEX</i> ))	Ratio ( <i>RHD7</i> (FAM) / <i>EIF2C1</i> ( <i>HEX</i> ))	ddPCR defined genotype (Hemizygous or homozygous)	Presumed <i>RH</i> genotype determined by serological analysis	Altered genotype based on ddPCR data
147J <sup>1</sup>	0	0	Homozygous <i>RHD</i> negative	rr	n/a
1660 <sup>1</sup>	0	0	Homozygous <i>RHD</i> negative	rr	n/a
7807 <sup>1</sup>	0	0	Homozygous <i>RHD</i> negative	rr	n/a
9763 <sup>1</sup>	0.45	0.43	Hemizygous	R0r	n/a
069F <sup>1</sup>	0.5	0.49	Hemizygous	R0r	n/a
740B <sup>1</sup>	0.47	0.46	Hemizygous	R0r	n/a
065S <sup>1</sup>	0.49	0.49	Hemizygous	R <sub>1</sub> r	n/a
118Z <sup>1</sup>	0.5	0.49	Hemizygous	R <sub>1</sub> r	n/a
1226 <sup>1</sup>	0.52	0.51	Hemizygous	R <sub>1</sub> r	n/a
1306 <sup>1</sup>	0.51	0.53	Hemizygous	R <sub>1</sub> r	n/a
1777 <sup>1</sup>	0.97	1.04	Homozygous <i>RHD</i> positive	R <sub>1</sub> r	R <sub>1</sub> R <sub>0</sub>
180H <sup>1</sup>	0.52	0.52	Hemizygous	R <sub>1</sub> r	n/a
181F <sup>1</sup>	0.52	0.49	Hemizygous	R <sub>1</sub> r	n/a

1220 <sup>1</sup>	0.98	1.01	Homozygous <i>RHD</i> positive	R <sub>1</sub> R <sub>1</sub>	n/a
131Z <sup>1</sup>	0.99	1.04	Homozygous <i>RHD</i> positive	R <sub>1</sub> R <sub>1</sub>	n/a
165F <sup>1</sup>	0.94	0.9	Homozygous <i>RHD</i> positive	R <sub>1</sub> R <sub>1</sub>	n/a
1793 <sup>1</sup>	0.99	1	Homozygous <i>RHD</i> positive	R <sub>1</sub> R <sub>1</sub>	n/a
0670 <sup>1</sup>	0.91	0.85	Homozygous <i>RHD</i> positive	R <sub>1</sub> R <sub>1</sub>	n/a
1347 <sup>1</sup>	0.99	1.03	Homozygous <i>RHD</i> positive	R <sub>1</sub> R <sub>1</sub>	n/a
138R <sup>1</sup>	0.95	0.98	Homozygous <i>RHD</i> positive	R <sub>1</sub> R <sub>1</sub>	n/a
052M <sup>2</sup>	0.99	1.03	Homozygous <i>RHD</i> positive	R <sub>1</sub> R <sub>1</sub>	n/a
247X <sup>2</sup>	1.02	1	Homozygous <i>RHD</i> positive	R <sub>1</sub> R <sub>1</sub>	n/a
658G <sup>2</sup>	1.02	1.03	Homozygous <i>RHD</i> positive	R <sub>2</sub> R <sub>2</sub>	n/a
738W <sup>2</sup>	1.02	1.04	Homozygous <i>RHD</i> positive	R <sub>2</sub> R <sub>2</sub>	n/a
729M <sup>2,3</sup>	0.5	0.49	Hemizygous	R <sub>1</sub> R <sub>2</sub>	R <sub>1</sub> r'' or R <sub>2</sub> r'
5481 <sup>2,3</sup>	0.5	0.51	Hemizygous	R <sub>2</sub> r	n/a
148R <sup>2,3</sup>	0.5	0.5	Hemizygous	R <sub>1</sub> r	n/a
6418 <sup>2,3</sup>	0.51	0.49	Hemizygous	R <sub>1</sub> r	n/a
3093 <sup>2,4</sup>	0.51	0.51	Hemizygous	R <sub>1</sub> r	n/a
078U <sup>2,4</sup>	0.99	1.01	Homozygous <i>RHD</i> positive	R <sub>1</sub> R <sub>1</sub>	n/a
103N <sup>2,4</sup>	1	1.03	Homozygous <i>RHD</i> positive	R <sub>1</sub> R <sub>1</sub>	n/a
1461 <sup>2,4</sup>	0.99	1.01	Homozygous <i>RHD</i> positive	R <sub>1</sub> R <sub>1</sub>	n/a
877L <sup>2,4</sup>	1.01	0.98	Homozygous <i>RHD</i> positive	R <sub>1</sub> R <sub>1</sub>	n/a
087W <sup>2,4</sup>	0.51	0.49	Hemizygous	R <sub>2</sub> R <sub>2</sub>	R <sub>2</sub> r''
132H <sup>2,4</sup>	1	1.03	Homozygous <i>RHD</i> positive	R <sub>2</sub> R <sub>2</sub>	n/a
689M <sup>2,4</sup>	0.99	1	Homozygous <i>RHD</i> positive	R <sub>2</sub> R <sub>2</sub>	n/a
572R <sup>2,3,4</sup>	0.5	0.5	Hemizygous	R <sub>1</sub> r	n/a
7687 <sup>2,3,4</sup>	0.5	0.51	Hemizygous	R <sub>1</sub> r	n/a
746P <sup>2,4</sup>	1.02	0.99	Homozygous <i>RHD</i> positive	R <sub>2</sub> R <sub>z</sub>	n/a

<sup>1</sup> DNA extracted from either plasma of human whole blood samples (refer to 2.1.2).

<sup>2</sup> DNA extracted from buffy coat of human whole blood samples (refer to 2.1.2).

<sup>3</sup> Sample is Weak D.

<sup>4</sup> Sample was tested blind.

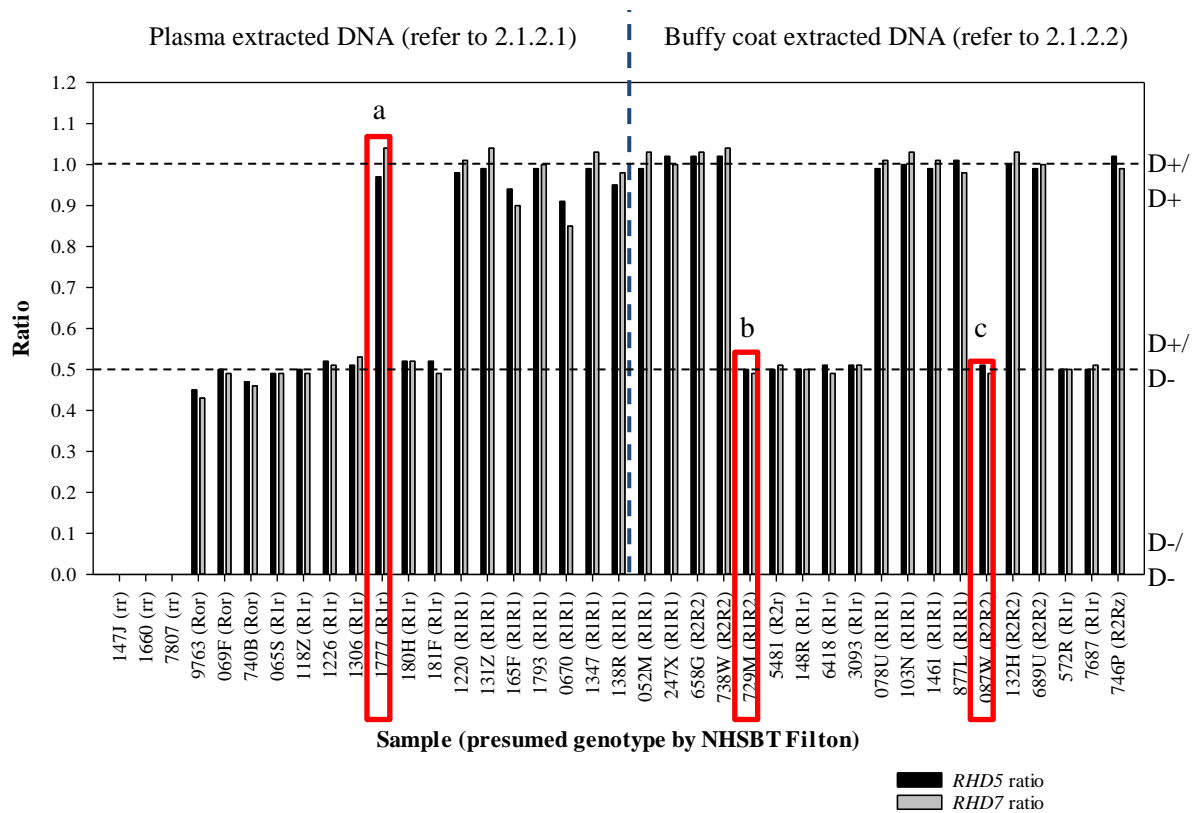


**Figure 5-13: Bar chart illustrated ratio analysis generated by ddPCR to determine *RHD* zygosity using multiplex reaction 3 (*RHD5* (FAM) / *EIF2C1* (HEX)) (grey) and multiplex reaction 4 (*RHD7* (FAM) / *EIF2C1* (HEX)) (black). DNA samples extracted from plasma (right) and buffy coat (left) of whole human blood samples with varying rhesus status were tested. The data illustrates three significant data sets, hemizygous *RHD* negative (D+/ D+, dashed line at ratio 1), hemizygous *RHD* positive (D+/ D-, dashed line at ratio 0.5) and homozygous *RHD* positive (D-/ D-, at ratio 0) ( $p < 0.001$ ). Three samples illustrated discordant results (shown in red). For sample 1777 (a) the presumed genotype was R<sub>1</sub>r (DCE/dce), but the ddPCR data illustrated that this sample was homozygous for D, and is therefore more likely to have the R<sub>1</sub>R<sub>0</sub> (DCE/Dce) genotype. The presumed genotype for sample 729M (b) was R<sub>1</sub>R<sub>2</sub> (DCE/DcE). However, ddPCR showed that this**

sample is hemizygous for *RHD*, and thus will display either the R<sub>1</sub>r'' (DcE/dcE) or R<sub>2</sub>r' genotype (DcE/dCe). Finally sample 087W (c), presumed to express the R<sub>2</sub>R<sub>2</sub> (DcE/DcE) genotype, illustrated hemizygous inheritance of *RHD*, which indicates that this sample actually expresses the R<sub>2</sub>r'' (DcE/dcE).

#### 5.2.4 Testing sensitivity of ddPCR and qPCR for fetal sex determination and *RHD* genotyping in samples expressing optimal and suboptimal cfDNA fractions

DNA was extracted from 2ml of maternal plasma from peripheral blood samples collected in both EDTA tubes (n= 22) and Streck BCTs (n= 24) (refer to 2.1.5). Consequently, four multiplex reactions were tested to determine fetal sex (multiplex reaction 1 and 2) and fetal *RHD* genotype (multiplex reaction 3 and 4) (Figure 5-14). The multiplex reactions used are the same as described previously (Figure 5-1); however, due to repeated amplification of *SRY*<sup>(H.P.T)</sup> in female samples for initial optimisation experiments (data not shown), the primers for the single copy *SRY* target was changed and in this experiment; *SRY* oligonucleotides were taken from Lo *et al.* (1997) (Figure 5-14). All samples were then tested (in duplicated) on the qPCR platform and the ddPCR platform on the same day (refer to 2.7 and 2.9, respectively).



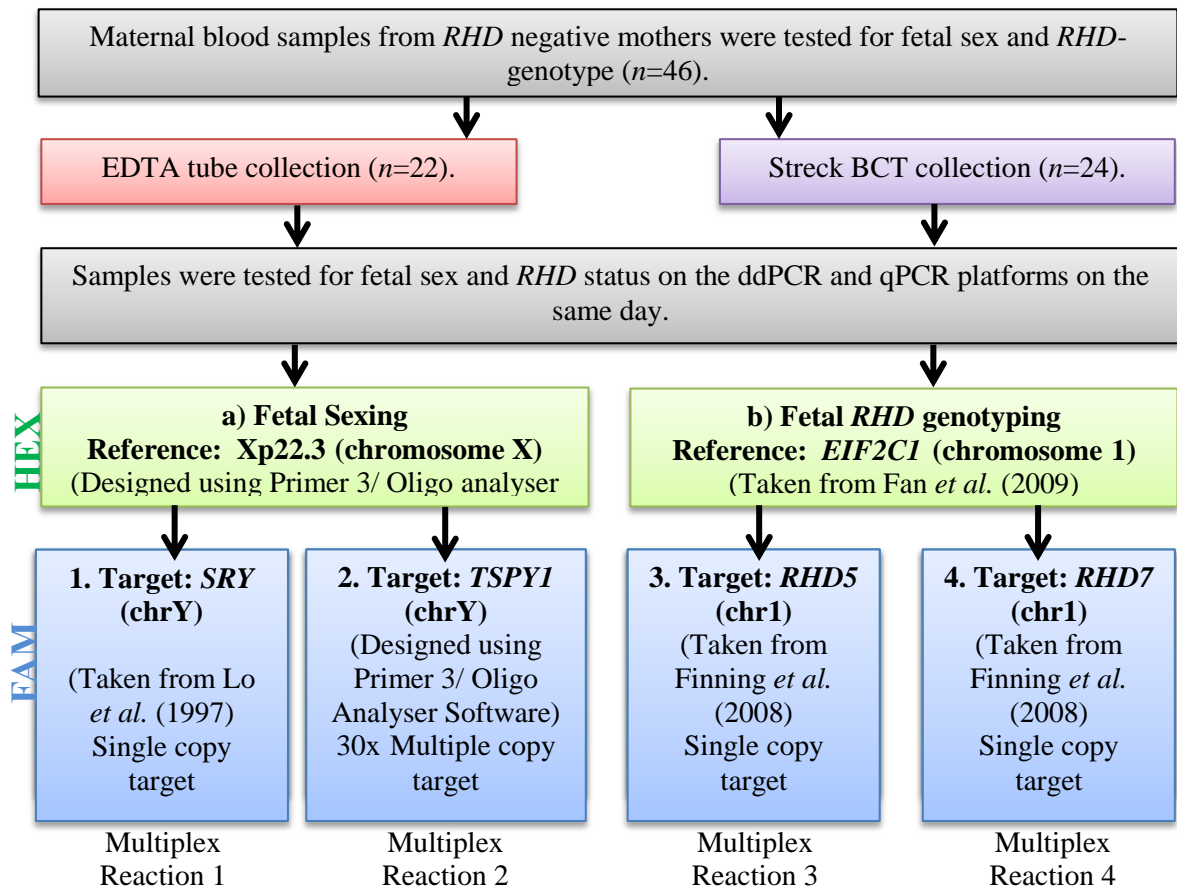


**Figure 5-14: Experimental overview of fetal sex determination and fetal *RHD* genotyping for maternal samples collected in both EDTA tubes ( $n=22$ ) and Streck BCTs ( $n=24$ ).** Four multiplex reactions were used to determine fetal sex (multiplex reaction 1 and 2) and fetal *RHD* genotype (multiplex reaction 3 and 4). All four reactions were tested on the ddPCR and qPCR platform to compare sensitivity for samples with optimal cfDNA fractions ( $\geq 3\%$ ) (Streck BCTs) and suboptimal cfDNA fractions ( $< 3\%$ ) (EDTA tubes).

For ddPCR in 100% of cases the fetal sex predicted by the presence of Y-specific targets was the same as determined by physical examination at birth. Both the single target gene (*SRY*) and the multiple-copy target gene (*TSPY1*) were correctly identified in all male fetuses and absent in all female cases for all samples (EDTA and Streck BCTs) (Table 5-5). Because *SRY* was not detected for any samples (except male positive control) on the

qPCR platform, fetal sex was ascertained by the presence *TSPY1* only (Table 2). The results also illustrated 100% accuracy (Table 5-5) in this instance when only the multiple-copy target gene was considered. Since, the samples collected in Streck BCTs expressed higher cffDNA fractions (4-24%), whereas the samples collected in EDTA tubes illustrated lower cffDNA fractions (0.1%-2%) each sub-set of samples were classified as optimal and suboptimal, respectively.

Fetal *RHD* genotyping on the qPCR platform demonstrated accuracies of 100% and 83% for the *RHD7* and *RHD5* target assays, respectively when testing optimal (Streck BCT) samples. Four samples (16.6%) were classified as inconclusive since qPCR did not detect the *RHD5* target but did show acceptable amplification (<45 Ct) of the *RHD7* target (Table 5-6). The qPCR platform was unable to detect both *RHD*-specific markers (*RHD7* and *RHD5*) in the suboptimal samples (<2% cffDNA) despite serological and ddPCR analysis confirming that 59% (13/22) of these EDTA-collected samples were carrying an *RHD*-positive fetus. Figure 5-15 illustrates the mean Ct value and upper and lower interquartile ranges (IQR) for all targets (*SRY*, *TSPY1*, *RHD5* and *RHD7*) generated by qPCR for maternal samples collected in EDTA tubes (A) and Streck BCTs (B).

**Table 5-5: Fetal sexing and *RHD* genotyping results obtained from both ddPCR and qPCR against results recorded following delivery.**

	Gestation weeks	EDTA/ Streck	gDNA (ng/μl)	qPCR fetal sexing results <sup>a</sup>		ddPCR fetal sexing results			Fetal Sex at Birth <sup>b</sup>	qPCR Fetal <i>RHD</i> Genotyping			ddPCR Fetal <i>RHD</i> Genotyping			Fetal <i>RHD</i> Status <sup>c</sup>
				<i>TSPY1</i>	Sex	<i>SRY</i>	<i>TSPY1</i>	Sex		<i>RHD5</i>	<i>RHD7</i>	<i>RHD</i> Status	<i>RHD5</i>	<i>RHD7</i>	<i>RHD</i> Status	
<b>+ve control</b>	N/A	EDTA	2.0	POS	M	POS	POS	M	N/A	POS	POS	POS	POS	POS	POS	N/A
<b>-ve control</b>	N/A	EDTA	2.0	NEG	F	NEG	NEG	F	N/A	NEG	NEG	NEG	NEG	NEG	NEG	N/A
<b>NTC</b>	N/A	N/A	N/A	NEG	-	NEG	NEG	N	N/A	NEG	NEG	NEG	NEG	NEG	NEG	N/A
<b>1</b>	30+0	EDTA	7.91	NEG	F	NEG	NEG	F	F	NEG	NEG	NEG	POS	POS	POS	POS
<b>2</b>	29+0	EDTA	14.76	NEG	F	NEG	NEG	F	F	NEG	NEG	NEG	NEG	NEG	NEG	NEG
<b>3</b>	29+2	EDTA	9.72	POS	M	POS	POS	M	M	NEG	NEG	NEG	NEG	NEG	NEG	NEG
<b>4</b>	27+6	EDTA	7.15	NEG	F	NEG	NEG	F	F	NEG	NEG	NEG	POS	POS	POS	POS
<b>5</b>	28+2	EDTA	12.01	NEG	F	NEG	NEG	F	F	NEG	NEG	NEG	POS	POS	POS	POS
<b>6</b>	28+0	EDTA	6.72	POS	M	POS	POS	M	M	NEG	NEG	NEG	NEG	NEG	NEG	NEG
<b>7</b>	29	EDTA	27.11	NEG	F	NEG	NEG	F	F	NEG	NEG	NEG	POS	POS	POS	POS
<b>8</b>	28	EDTA	6.61	POS	M	POS	POS	M	M	NEG	NEG	NEG	NEG	NEG	NEG	NEG
<b>9</b>	28+1	EDTA	12.03	POS	M	POS	POS	M	M	NEG	NEG	NEG	NEG	NEG	NEG	NEG
<b>10</b>	28+3	EDTA	6.97	NEG	F	NEG	NEG	F	F	NEG	NEG	NEG	POS	POS	POS	POS
<b>11</b>	27+6	EDTA	9.36	NEG	F	NEG	NEG	F	F	NEG	NEG	NEG	NEG	NEG	NEG	NEG
<b>12</b>	28+1	EDTA	9.03	NEG	F	NEG	NEG	F	F	NEG	NEG	NEG	NEG	POS	INC	NEG
<b>13</b>	28+0	EDTA	10.22	POS	M	POS	POS	M	M	NEG	NEG	NEG	NEG	NEG	NEG	NEG
<b>14</b>	28+0	EDTA	12.25	NEG	F	NEG	NEG	F	F	NEG	NEG	NEG	NEG	NEG	NEG	NEG
<b>15</b>	28+5	EDTA	16.88	POS	M	POS	POS	M	M	NEG	NEG	NEG	POS	POS	POS	POS

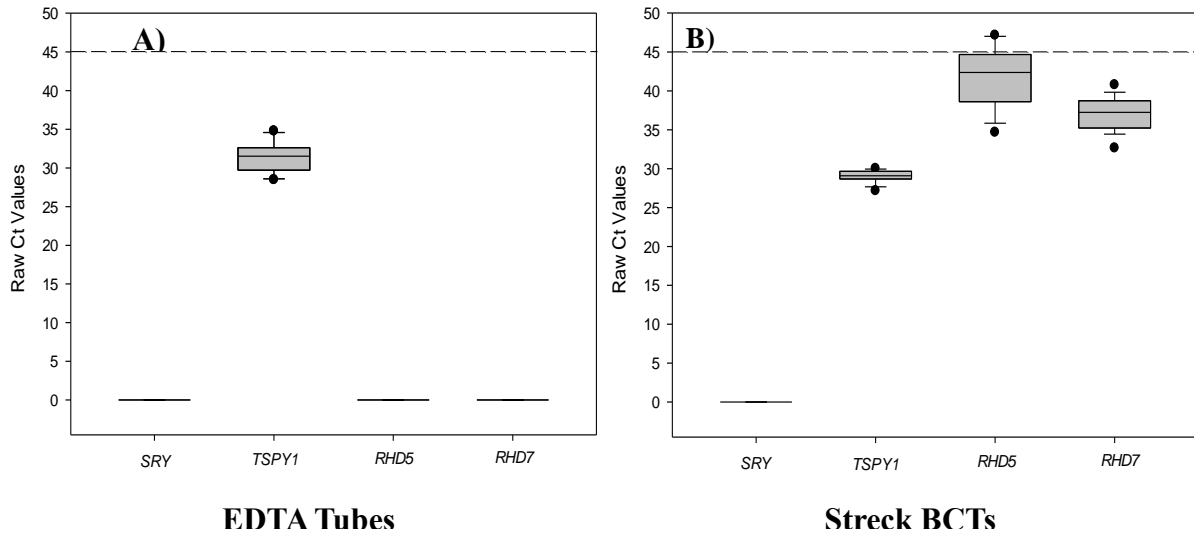
16	28+1	EDTA	13.01	POS	M	POS	POS	M	M	NEG	NEG	NEG	POS	POS	POS	POS
17	28+5	EDTA	15.72	POS	M	POS	POS	M	M	NEG	NEG	NEG	POS	POS	POS	POS
18	28+0	EDTA	19.09	POS	M	POS	POS	M	M	NEG	NEG	NEG	POS	POS	POS	POS
19	28	EDTA	11.51	POS	M	POS	POS	M	M	NEG	NEG	NEG	POS	POS	POS	POS
20	28+5	EDTA	11.87	NEG	F	NEG	NEG	F	F	NEG	NEG	NEG	NEG	NEG	NEG	NEG
21	28+0	EDTA	15.02	NEG	F	NEG	NEG	F	F	NEG	NEG	NEG	POS	POS	POS	POS
22	28+5	EDTA	20.59	NEG	F	NEG	NEG	F	F	NEG	NEG	NEG	POS	POS	POS	POS
23	30+3	Streck	0.74	NEG	F	NEG	NEG	F	F	POS	POS	POS	POS	POS	POS	POS
24	28+3	Streck	0.798	POS	M	POS	POS	M	M	NEG	NEG	NEG	NEG	NEG	NEG	NEG
25	27+5	Streck	0.524	POS	M	POS	POS	M	M	POS	POS	POS	POS	POS	POS	POS
26	28+2	Streck	0.68	POS	M	POS	POS	M	M	POS	POS	POS	POS	POS	POS	POS
27	28+2	Streck	0.552	POS	M	POS	POS	M	M	NEG	NEG	NEG	NEG	NEG	NEG	NEG
28	28+2	Streck	0.607	NEG	F	NEG	NEG	F	F	NEG	POS	INC	POS	POS	POS	POS
29	28+4	Streck	0.729	NEG	F	NEG	NEG	F	F	POS	POS	POS	POS	POS	POS	POS
30	28+2	Streck	0.605	NEG	F	NEG	NEG	F	F	POS	POS	POS	POS	POS	POS	POS
31	27+5	Streck	0.666	POS	M	POS	POS	M	M	POS	POS	POS	POS	POS	POS	POS
32	38+1	Streck	0.643	POS	M	POS	POS	M	M	POS	POS	POS	POS	POS	POS	POS
33	29+2	Streck	0.656	POS	M	POS	POS	M	M	NEG	POS	INC	POS	POS	POS	POS
34	29+2	Streck	0.515	NEG	F	NEG	NEG	F	F	NEG	POS	INC	POS	POS	POS	POS
35	28+2	Streck	0.664	POS	M	POS	POS	M	M	POS	POS	POS	POS	POS	POS	POS
36	29+0	Streck	0.622	POS	M	POS	POS	M	M	NEG	POS	INC	POS	POS	POS	POS
37	28+1	Streck	0.573	NEG	F	NEG	NEG	F	F	POS	POS	POS	POS	POS	POS	POS
38	28+2	Streck	0.521	NEG	F	NEG	NEG	F	F	POS	POS	POS	POS	POS	POS	POS

<b>39</b>	28+1	Streck	0.506	NEG	F	NEG	NEG	F	F	POS	POS	POS	POS	POS	POS	POS
<b>40</b>	28+6	Streck	0.465	POS	M	POS	POS	M	M	NEG	NEG	NEG	NEG	NEG	NEG	NEG
<b>41</b>	28+4	Streck	0.405	POS	M	POS	POS	M	M	NEG	NEG	NEG	NEG	NEG	NEG	NEG
<b>42</b>	28	Streck	0.657	NEG	F	NEG	NEG	F	F	NEG	NEG	NEG	NEG	NEG	NEG	NEG
<b>43</b>	27+5	Streck	0.707	POS	M	POS	POS	M	M	POS	POS	POS	POS	POS	POS	POS
<b>44</b>	28+4	Streck	0.444	NEG	F	NEG	NEG	F	F	POS	POS	POS	POS	POS	POS	POS
<b>45</b>	28+5	Streck	0.401	POS	M	POS	POS	M	M	POS	POS	POS	POS	POS	POS	POS
<b>46</b>	28+6	Streck	0.558	NEG	F	NEG	NEG	F	F	POS	POS	POS	POS	POS	POS	POS

Legend: M, male; F, female; POS, positive; NED, negative.

**Table 5-6: Sensitivity, specificity and accuracy results of maternal samples collected in EDTA tubes and Streck BCTs on both ddPCR and qPCR platforms for fetal sex and *RHD* genotyping.**

Platform	Blood Collection Tube	cffDNA (%) in maternal plasma <sup>a</sup>	Target	Sensitivity	False Negative Results	Specificity	False Positive Results	Accuracy (%) <sup>b</sup>
ddPCR	Streck BCTs	4 - 24%	<i>TSPY1</i>	100%	-	100%	-	100%
			<i>SRY</i>	100%	-	100%	-	100%
			<i>RHD5</i>	100%	-	100%	-	100%
			<i>RHD7</i>	100%	-	100%	-	100%
	EDTA Tubes	0.1 - 2%	<i>TSPY1</i>	100%	-	100%	-	100%
			<i>SRY</i>	100%	-	100%	-	100%
			<i>RHD5</i>	100%	-	95.5%	4.5% (1/22)	95.6%
			<i>RHD7</i>	100%	-	95.5%	4.5% (1/22)	95.6%
qPCR	Streck BCTs	4 - 24%	<i>TSPY1</i>	100%	-	100%	-	100%
			<i>SRY</i>	50%	54.2% (13/24)	100%	-	45.8%
			<i>RHD5</i>	83.4%	16.6% (4/24)	100%	-	83.4%
			<i>RHD7</i>	100%	-	100%	-	100%
	EDTA Tubes	0.1 - 2%	<i>TSPY1</i>	100%	-	100%	-	100%
			<i>SRY</i>	0%	45.5% (10/22)	100%	-	54.5%
			<i>RHD5</i>	0%	59.1% (13/22)	100%	-	40.9%
			<i>RHD7</i>	0%	59.1% (13/22)	100%	-	40.9%

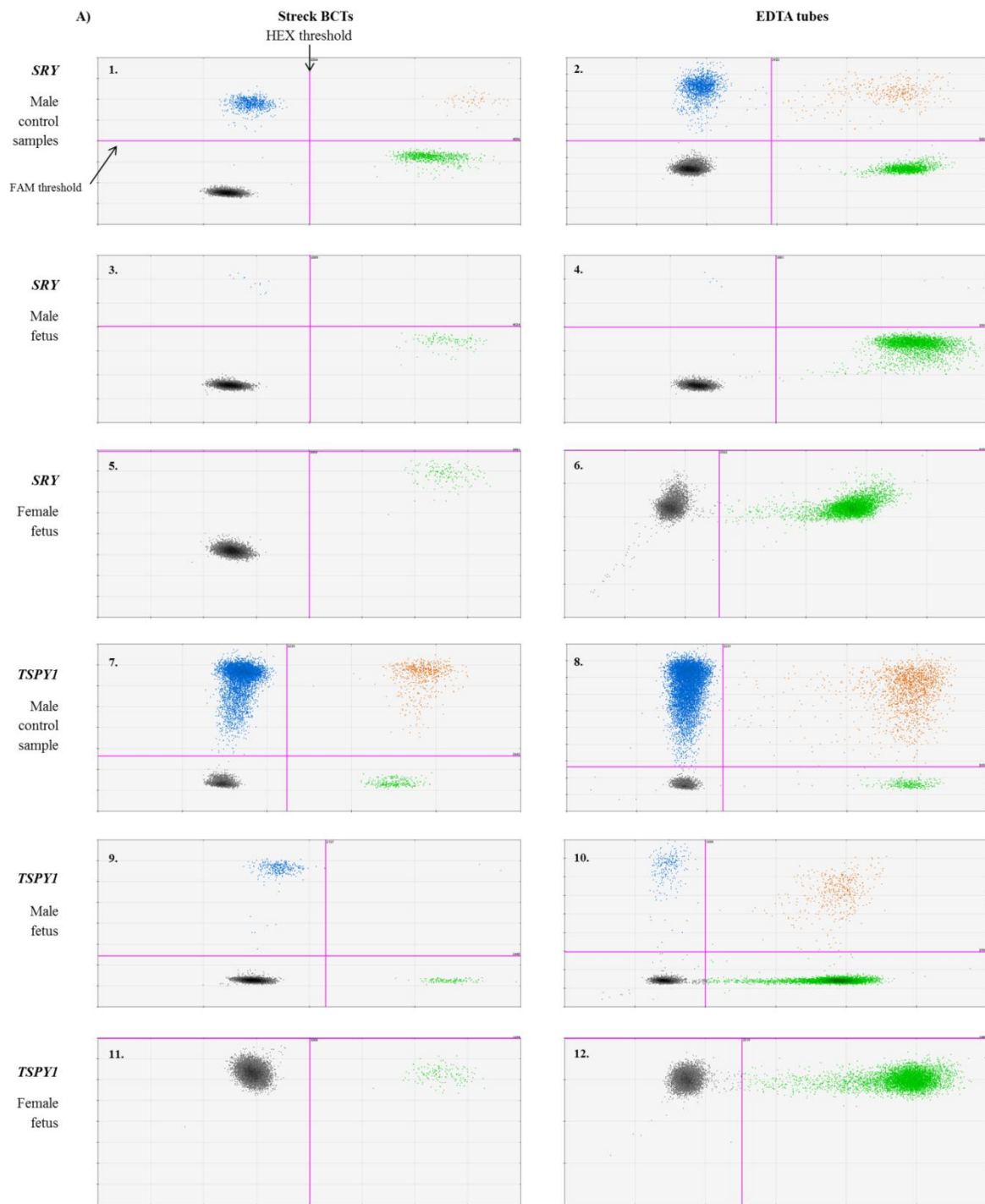


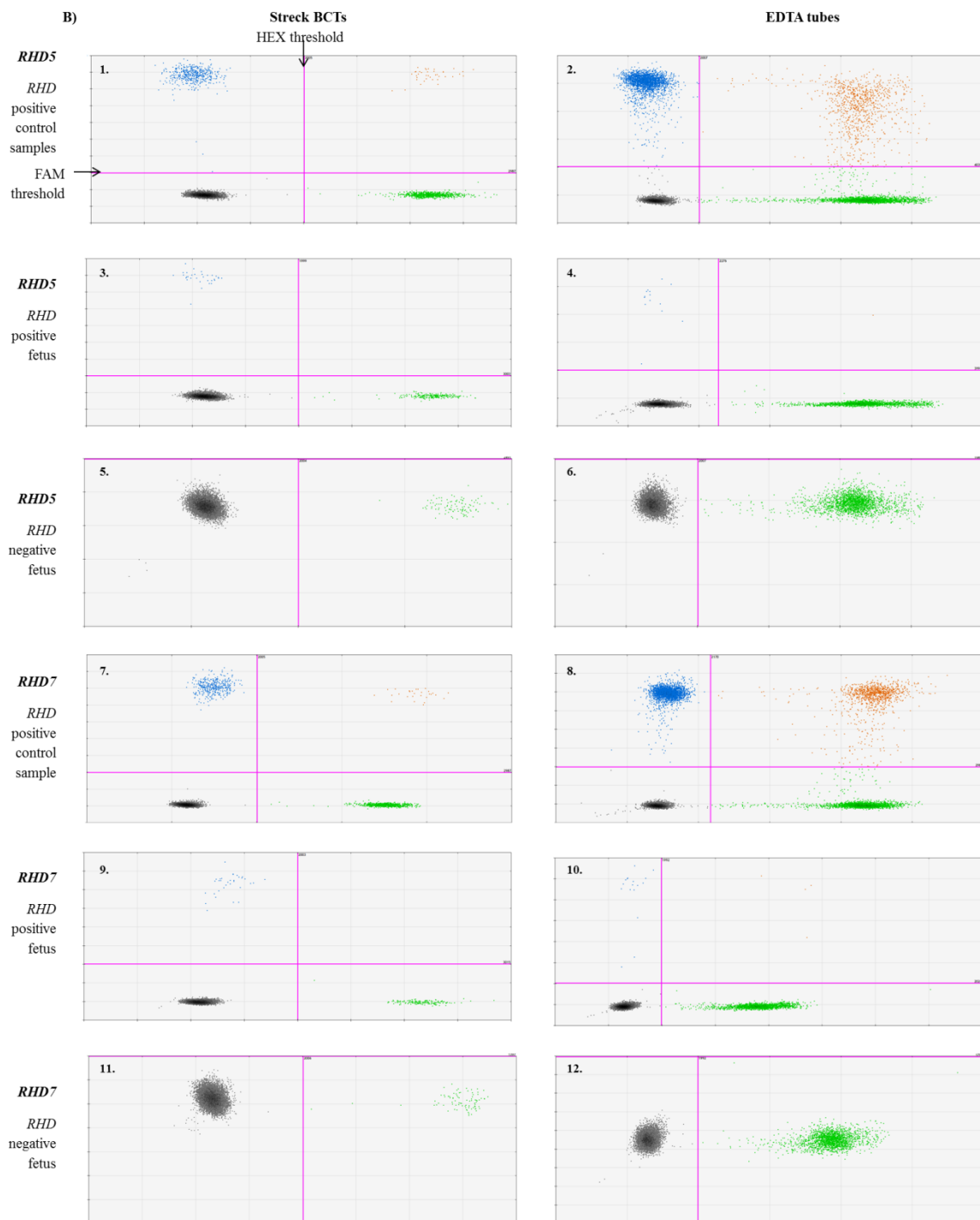
**Figure 5-15: Box Plot of raw Ct values obtained from qPCR analysis showing *SRY*, *TSPY1* (multiple copy target), *RHD5* and *RHD7* targets for A) samples collected in EDTA tubes and B) samples collected in Streck BCTs.** The horizontal line central to each box represents the median of; 10 samples for *TSPY1* (EDTA), 13 samples for *TSPY1* (Streck BCTs) and 18 samples for *RHD5* and *RHD7* (Streck BCTs). The limits of each box denotes the 25<sup>th</sup> and 75<sup>th</sup> percentiles. The whiskers signify the 5<sup>th</sup> and 95<sup>th</sup> percentiles and the circles mark the outliers. Note: Four samples (28, 33, 34, 36) collected in Streck BCTs expressed Ct values above the upper baseline threshold (45 Ct) for target *RHD5* and were therefore determined as negative.

Figure 5-16 illustrates droplet separation for male fetuses (maternal samples 18 and 27), female fetuses (maternal samples 20 and 30), *RHD* positive fetuses (maternal samples 15 and 32) and *RHD* negative fetuses (maternal samples 11 and 27) for samples collected in both EDTA tubes and Streck BCTs, respectively. Samples were classified as positive depending on the presence of each FAM-labelled target (Figure 5-14). The fetal *RHD* genotype was correctly identified in 100% (24/24) and 95.5% (21/22) of cases by ddPCR for samples collected in Streck BCTs and EDTA tubes, respectively (Table 5-5 and Table 5-6). One EDTA-collected sample (sample 12) produced a false positive result, since serological

analysis revealed the fetus to be *RHD*-negative but ddPCR showed clear amplification of the *RHD7* target (18 droplets) and minimal amplification of the *RHD5* target (3 droplets) (Figure 5-16). The concentration (copies/  $\mu$ L) obtained from both target genes (*RHD5* and *RHD7*) and the reference gene (*EIF2C1*) for control samples (NTC, *RHD*+ control, *RHD*- control) and 2b), EDTA-collected samples and Streck BCTs-collected samples are illustrated in Figure 5-17 (A) and 5-17 (B), respectively. The results show successful amplification of all three targets for the *RHD* positive control sample and only show amplification of the reference *EIF2C1* gene for the *RHD*-negative control sample, whereas the NTC sample showed no amplification (Figure 5-17). In addition to the false positive result (1/46 (2%)), 31 samples were correctly classified as *RHD*-positive (67%) and 14 samples were correctly classified as *RHD*-negative (31%) (Figure 5-17).







**Figure 5-16: ddPCR 2D amplitude plots for fetal sex determination (A) and *RHD* genotype (B) for samples collected in Streck BCTs (left) and EDTA tubes (right). A) Fetal sex determination for control positive male sample, male and female fetus. Plots 1 to 6 shows the 2D amplification plot for *SRY*-FAM against Xp22.3-HEX and plots 7 to 12 shows the 2D amplification plot for *TSPY1*-FAM against Xp22.3-HEX. Plots 3 and 9 represent**

maternal sample 27 and plots 4 and 10 represent maternal sample 18 for Streck BCT and EDTA collected samples, respectively. The results for these plots (3, 9, 4, and 10) illustrate male fetuses since there is amplification of both the Y-specific (FAM) targets alongside the reference (Xp22.3-HEX) target. Plots 5 and 11 represent maternal sample 30 and plots 6 and 12 represent maternal sample 20 for Streck BCT and EDTA collected samples, respectively. These results illustrate female fetuses since only the reference (Xp22.3-HEX) is successfully amplified. B) Fetal *RHD* genotyping for control *RHD*-positive sample, *RHD* positive fetuses and *RHD* negative fetuses. Plots 1 to 6 shows the 2D amplification plot for *RHD5*-FAM against *EIF2C1*-HEX and plots 7 to 12 shows the 2D amplification plot for *RHD7*-FAM against *EIF2C1*-HEX. Plots 3 and 9 represent maternal sample 32 and plots 4 and 10 represent maternal sample 15 for Streck BCT and EDTA collected samples, respectively. The results for these plots (3, 9, 4, and 10) illustrate *RHD*-positive fetuses since there is amplification of both the *RHD*-specific (FAM) targets alongside the reference (*EIF2C1*-HEX) target. Plots 5 and 11 represent maternal sample 27 and plots 6 and 12 represent maternal sample 11 for Streck BCT and EDTA collected samples, respectively. These results illustrate *RHD*-negative fetuses since only the reference (*EIF2C1*-HEX) is successfully amplified. Clusters did not show any outlying results were observed for any samples.

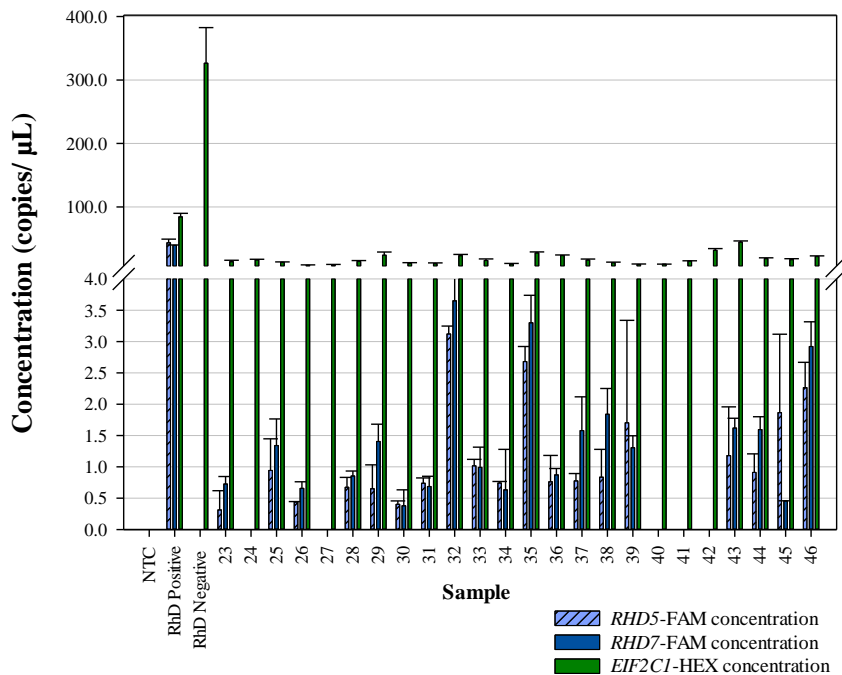
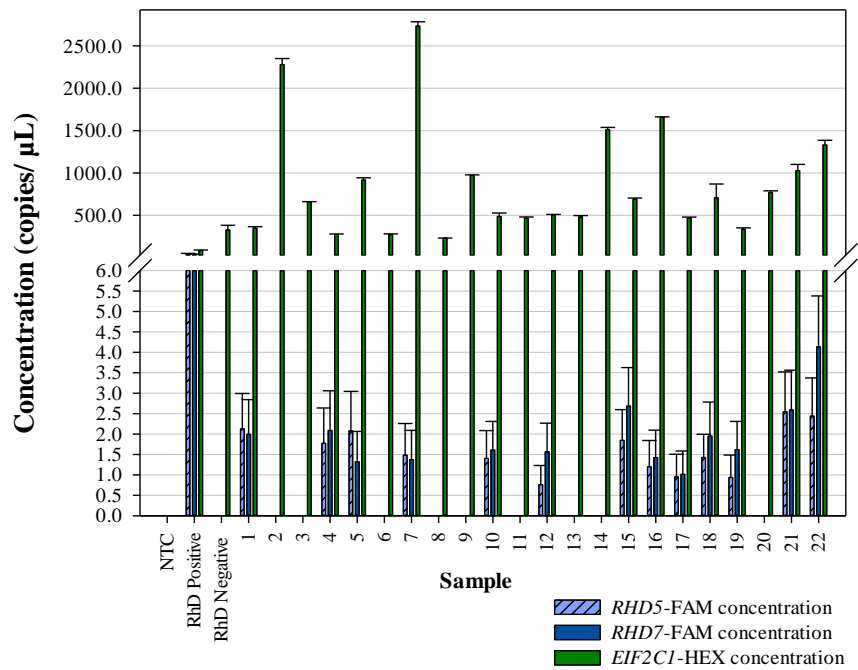


**Figure 5-17: ddPCR results showing concentration (copies/  $\mu\text{L}$ ) of *RHD5*, *RHD7* and *EIF2C1* to determine the fetal *RHD* genotyping from 46 maternal plasma samples. The concentration (copies/ $\mu\text{l}$ ) (+SD) was identified for both target regions (*RHD5* and *RHD7*) and the reference region (*EIF2C1*) for multiplex reactions 3 and 4 (Figure 5-14). The presence or**

absence of the target regions were used to determine fetal status (*RHD*<sup>+</sup> or *RHD*<sup>-</sup>, respectively). a) Maternal Samples collected in EDTA tubes ( $n = 22$ ). b) Maternal samples collected in Streck BCTs ( $n = 24$ ). The same controls were represented in both graphs. The control non-maternal cfDNA *RHD* positive sample (399X) exhibit a ratio of 0.51 and 0.47 for *RHD5/EIF2C1* and *RHD7/EIF2C1*, respectively.

The cffDNA fraction using both Y-specific and *RHD*-specific targets was calculated based on the concentration (copies/  $\mu\text{L}$ ) generated by ddPCR for each multiplex reaction. According to Poisson distribution, the original number of molecules derived from each chromosome can be calculated using the following equation:

$$\text{Number of Molecules} = -\ln [(N - n)/N] \times N$$

Where  $N$  is the total number of wells counted and  $n$  is the number of target or reference positive wells.

The fractions of positive counts were fitted to a Poisson algorithm automatically by the software (Bio-Rad QuantaSoft v1.2) to determine the absolute concentration (presented as copies per  $\mu\text{L}$ ). Once the concentration had been determined for all target and reference regions, the cffDNA fraction within the maternal plasma (%) was calculated. For single-copy targets (*SRY*, *RHD5* and *RHD7*) the following equation was used:

$$\left( \frac{2 \times \text{Target-FAM (copies/ } \mu\text{L)}}{\text{Total copies/ } \mu\text{L}^*} \right) \times 100$$

The multiple copy target cffDNA calculations were based on the assumption that there are 30 copies of DYS14 (on the *TSPY1* gene) in the genome (Barrett *et al.*, 2012).

$$\left( \frac{2 \times (\text{Target-FAM (copies/}\mu\text{l)} / 30)}{\text{Total copies/ } \mu\text{L}^*} \right) \times 100$$

\*Target-FAM (copies/ $\mu$ l) + Reference-HEX (copies/ $\mu$ l).

The cffDNA fractions (%) and concentration of reference targets for blood collection methods using EDTA tubes and Streck BCTs were compared using ddPCR results. Figure 5-8 (A) shows the average cffDNA fraction (%) in maternal plasma for all four target regions (*SRY*, *TSPY1*, *RHD5* and *RHD7*) for both collection methods. The Streck BCT-collected samples show significantly higher cffDNA fraction means (9-16%) for all target regions compared to EDTA collected samples (0.5-1%) ( $p < 0.001$ ). The mean cffDNA fractions generated by the EDTA-collected samples shows no significant difference between all four targets ( $p > 1$ ). However, the cffDNA fraction calculated based on the *SRY*-target is significantly lower than the *TSPY1*- and *RHD7*- cffDNA fractions generated ( $p < 0.01$ ).

The concentration (copies/ $\mu$ L) of each reference gene, Xp22.3 and *EIF2C1* (Figure 5-18 (B)), is a combination of maternal and fetal cfDNA, however is predominantly maternal in origin (90-95%). Samples collected in Streck BCTs showed similar mean concentrations for the Xp22.3 and the *EIF2C1* reference genes (16.18 copies/ $\mu$ L and 17.39 copies/ $\mu$ L, respectively ( $p > 0.1$ )) (Figure 2b). The concentrations (copies/  $\mu$ L) of both reference targets (Xp22.3 and *EIF2C1*) were over 40-fold higher for maternal samples collected in EDTA tubes compared to Streck BCTs (mean concentrations 548.04 copies/  $\mu$ L and 869.25 copies/  $\mu$ L, respectively), suggesting maternal leucocyte degradation (Figure 5-18 (B)). The 2D amplification plots (Figure 5-16) also show a significantly higher number of reference (HEX-labelled) droplets for maternal samples collected in EDTA tubes compared to maternal

samples collected in Streck BCTs ( $p < 0.001$ ). The fetal concentration determined from the *RHD5* and *RHD7* multiplex reactions showed no significant difference for samples collected in EDTA tubes or Streck BCTs ( $p > 0.1$ ), ranging from 0.9 to 4.2 copies/  $\mu\text{L}$  and 0.3 to 3.7 copies/  $\mu\text{L}$ , respectively (Figure 5-17).

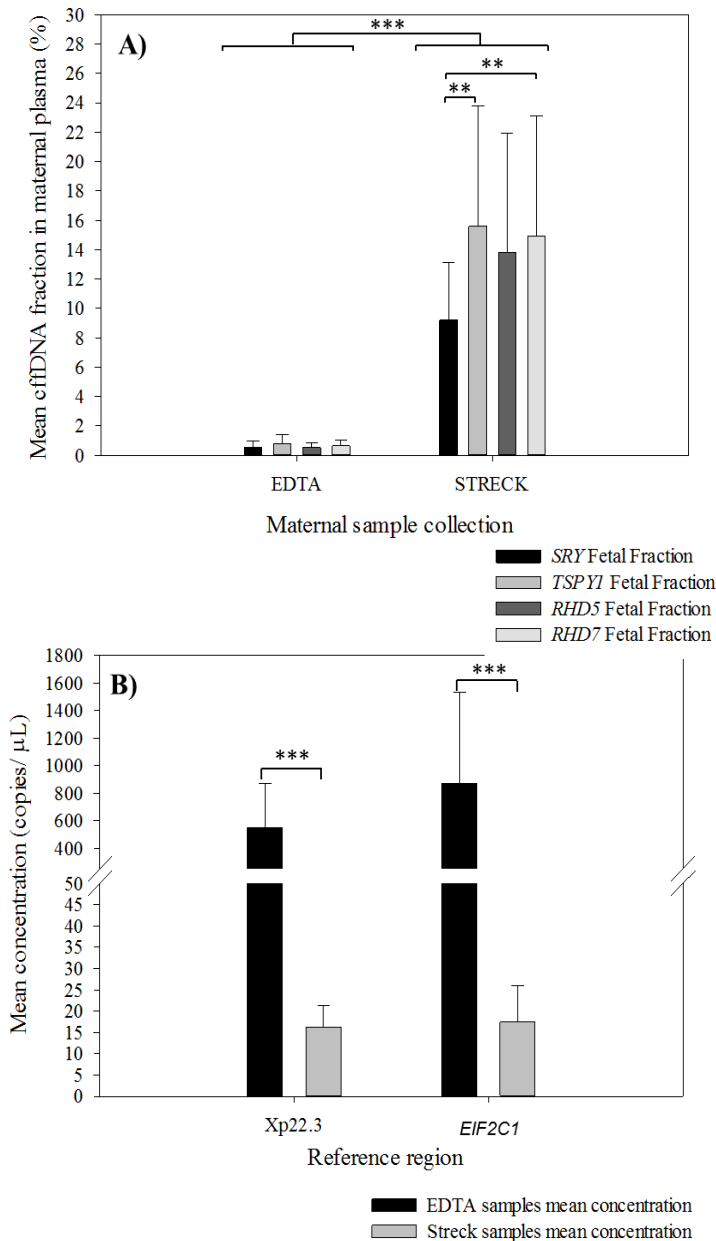


**Figure 5-18: A comparison of mean cfDNA fractions (based on *SRY*, *TSPY1*, *RHD5* and *RHD7* fetal targets) and mean concentrations of the reference targets (*Xp22.3* and *EIF2C1*) for maternal samples collected in EDTA tubes and Streck BCTs. A) Mean cfDNA fraction in maternal plasma calculated by each target gene (refer to 2.9.4). The Streck BCT collected samples show a significantly higher mean cfDNA fraction compared to samples collected in EDTA tubes for all four target regions (\*\*\*,  $p < 0.001$ ). The**

cfDNA fraction based on the *RHD7* and *TSPY1* target genes are significantly higher than the cfDNA fraction determined by the *SRY* target gene (\*\*,  $p < 0.01$ ). B) Mean concentration of reference gene regions *Xp22.3* and *EIF2C1* for maternal samples collected in EDTA tubes and Streck BCTs. The average concentration of both regions were significantly higher in EDTA tube samples than in Streck BCTs (\*\*\*,  $p < 0.001$ ). There was no significant difference between mean concentrations of *Xp22.3* and *EIF2C1* within each sample collection method.



## 5.3 Discussion

### 5.3.1 RH zygosity testing for non-maternal samples

The Rh blood group system is the most polymorphic of the human blood groups, and second to ABO, it is the most clinically significant in transfusion medicine and the primary cause of HDNF (Avent and Reid, 2000). The principle antigen of the *RH* system is the D antigen and the majority of D-negative phenotypes, particularly in Caucasian populations, are a result of complete deletion of the *RHD* gene (Westhoff, 2004). The *RHCE* gene of the Rh blood group system encodes for the C, c, E and e antigens, however, patients are not routinely typed for these antigens. The determination of whether a patient is homozygous (D/D) or hemizygous (D/d) for *RHD* cannot be determined using serological analysis since the difference in reactivity between RBCs with a single or double dose of D-antigen is not reliably detected (Hillyer *et al.*, 2008). Table 5-7 illustrates the various Rh nomenclature and incidence of common haplotypes in Caucasian, African black and Asians populations. Serological analysis will often predict the *RH* genotype based on the frequency of each haplotype within a specific population. Here we have described a rapid approach to determine *RHD* zygosity using ddPCR for the accurate determination of *RHD* genotype.

**Table 5-7: Rh Nomenclature and incidence of common haplotypes for Caucasian, African black and Asian populations.** [Adapted from Provan, Newland and Court (2015)].

Fisher-Race haplotype	Modified Wiener haplotype	Incidence (%)		
		Caucasian	African Black	Asian
<b><i>RHD</i> positive</b>				
DcE	R <sub>1</sub>	42	17	70
DcE	R <sub>2</sub>	14	11	21
Dce	R <sub>0</sub>	4	44	3
DCE	R <sub>Z</sub>	<0.01	<0.01	1
<b><i>RHD</i> negative</b>				
ce	r	37	26	3
Ce	r <sup>'</sup>	2	2	2
cE	r <sup>'2</sup>	1	<0.01	<0.01
CE	r <sup>y</sup>	<0.01	<0.01	<0.01

To determine the *RHD* zygosity, DNA molecular testing by assaying for *RHD* deletions or inactive *RHD* is required and is currently available in specialised blood bank laboratories. Molecular genotyping for transfusion medicine has been available since the mid 1990's and its application enables zygosity to be determined by assaying for the presence of a recessive allele (Westhoff, 2006). In a prenatal setting, paternal zygosity testing can be important to predict the fetal D status when the mother is given RAADP, since multiple genetic events other than complete deletion can result in a D-negative phenotype. These assays must include detection of the 37-bp insertion present in *RHD* pseudogene samples and the D-negative *RHD-CE-D* hybrid gene common in African black populations (Westhoff, 2006). If the father is homozygous for *RHD* then the fetus will be *RHD* positive and anti-D is required. In cases where fathers exhibit heterozygosity of the *RHD* gene, the fetal *RHD* status should be determined.

Determination of human *RHD* gene rhesus box has also been used for determination of zygosity. In one study, a PCR- sequence-specific polymorphism (PCR-SSP) approach was used to determine the upstream box, downstream box and hybrid box of *RHD* (Zhou *et al.*, 2005). The results revealed that only the hybrid box could be determined in homozygous

*RHD*- samples, all the upstream, downstream and hybrid box could be detected in hemizygous *RHD*+ samples and in homozygous *RHD*+ samples the upstream box and downstream box (but not the hybrid box) could be detected. In a more recent study the PCR-SSP approach was also tested against a qPCR approach specific for *RHD* exon 5 (Kacem *et al.*, 2012). The results illustrated that qPCR was the most convenient method with the highest positive and negative predictive values (100% and 98%, respectively). However, it is important to note that out of the 370 samples tested, the zygosity of 32 patients remained unknown because of a lack of heterozygous SNPs or technical failure (Kacem *et al.*, 2012). In addition, as previously stated (refer to 5.1.1), zygosity testing is complicated due to differences in the hybrid Rhesus box found in African populations. (Matheson and Denomme, 2002; Grootkerk - Tax *et al.*, 2005).

The results from the current study show that ddPCR provides a novel method for the determination of *RHD* zygosity, without the need for targeting recessive D-negative alleles. By using ratio analysis, the concentration of fetal specific targets can be compared to a conserved reference gene (such as *EIF2C1*) to identify whether the patient expresses one or two copies of the *RHD* gene. The buffy-coat and plasma samples tested were collected from the NHS BT (Filton), which provided information on the presumed *RH* status of each sample based upon serological testing. The results illustrated 92.5% concordance with the original serological information provided, showing either a ratio of 0, 0.5 or 1 for homozygous *RHD* negative samples, hemizygous *RHD* positive samples or homozygous *RHD* positive samples, respectively. However, three samples (1777, 729M and 087W) illustrated discrepancies in results. Serological and allele frequency analysis determined sample 1777, 729M and 087W to be  $R_1r$ ,  $R_1R_2$  and  $R_2R_2$ , respectively. However, the ddPCR *RHD* zygosity results revealed ratios close to 1 for sample 1777 indicating that this sample is homozygous for the *RHD* gene and therefore is likely to exhibit the  $R_1R_0$  haplotype (Table5-4). Alternatively, samples 729M

and 087W expressed ratios closer to 0.5 indicating RHD hemizyosity (Table 5-4). These results indicate that samples 729M and 087W are likely to exhibit R<sub>1</sub>r<sup>''</sup>/ R<sub>2</sub>r<sup>'</sup> and R<sub>2</sub>r<sup>''</sup> genotypes, respectively, rather than serologically predicted genotypes (R<sub>1</sub>R<sub>2</sub> and R<sub>2</sub>R<sub>2</sub>, respectively). Sample 729M was recorded as being weak D, and therefore it is likely that only one haplotype exhibits a mutation encoding an amino acid change (Westhoff, 2007), indicating incorrect serological classification for this sample. Position effects can alter anti-D expression, for instance the amount of D-antigen in the membrane is reduced when a Ce allele is found in trans to RHD (Westhoff, 2007). Samples that exhibit this phenomenon either have R<sub>1</sub>r<sup>'</sup> (DCe/dCe), R<sub>0</sub>r<sup>'</sup> (Dce/dCe) or R<sub>2</sub>r<sup>'</sup> (DcE/dCe). Sample 729M was mistyped serologically as R<sub>1</sub>R<sub>2</sub>, and the ddPCR results also revealed that this sample was hemizygous for RHD (Figure 5-13). It is difficult to tell whether this sample is R<sub>1</sub>r<sup>''</sup> or R<sub>2</sub>r<sup>'</sup> since both will possess the DdCcEe genotype. However, as sample 729M was also typed as weak D, since the phenomenon of reduced anti-D expression is commonly found in R<sub>2</sub>r<sup>'</sup> and not R<sub>1</sub>r<sup>''</sup>, we can predict R<sub>2</sub>r<sup>''</sup> as the most likely genotype. Consequently, sequencing data carried out by Amr Halawani (unpublished) revealed that sample 729M displayed the exon 9 Gly385Ala 1154G>C SNP, and thus was classified as weak D type 2. In addition the sample illustrated multiple intronic SNPs which appear to be associated with the R<sub>2</sub> haplotype, which demonstrates that sample 729M is likely to be R<sub>2</sub>r<sup>'</sup>.

For accurate determination, developing assays which include R<sub>1</sub> and R<sub>2</sub> SNPs will be required to differentiate between the two haplotypes using ddPCR, or alternatively, diagnosis could be achieved by sequencing the *RHD*/*RHCE* genes as described above (Halawani *et al.*, 2014). In cases where samples inherit hybrid genes, in which portions of the RHD are replaced with portions of the *RHCE* gene, RBCs can display partial D phenotypes. Developing highly accurate ddPCR/ MPS assays to detect all types of D-variants will prevent

wrongful classification of these samples as *RHD*-, and thus avoid sensitisation during pregnancy or blood transfusion.

Routine testing for C, c, E and e antigens is not available and is only offered in cases where the patient has developed atypical antibodies or if they are facing long-term transfusing (for example sickle cell disease patients) (Avent and Reid, 2000). The assay described in this chapter is specific for *RHD* genotyping, however developing specific targets for C and E would enable the same approach to be applied for reliable *RH* genotyping. In addition, the Kell antigen system is important in transfusion medicine and HDFN since anti-Kell can be produced. The *KEL1* antigen is determined in all blood donors in the Netherlands, in a genotyping experiment it was identified two variants (*KEL\*02null* or *KEL\*02mod* allele) in 7.4% of Dutch donors (Ji *et al.*, 2015). By designing an assay included a wild-type *KEL*-target and a target for both mutations; ddPCR genotyping could enable rapid determination of zygosity and thus could be used to accurately determine the frequency of various Kell haplotypes within multiple populations.

This method is relatively cheap, being only marginally more expensive than qPCR (£6.25 and £5.27 per sample, respectively) and can be carried out rapidly for multiple samples. In addition, due to the linear nature of quantification on the ddPCR platform, two-fold increases are more reliably detected compared to qPCR approaches that detect exponential increases in copy number. MLPA was initially described as the first assay able to determine the copy number of blood group alleles. The MPLA approach can multiplex up to 50 targets in a single tube, which enables an extensively large number of blood groups to be tested (Haer - Wigman *et al.*, 2013a). Currently, the blood-MLPA can determine the largest set of blood groups antigens in a single test out of all available genotyping assays (Hashmi *et al.*, 2007; Gassner *et al.*, 2013; Haer - Wigman *et al.*, 2013a; Haer - Wigman *et al.*, 2013b). However,

the total time to generate these results takes a minimum of 25 hours. Though, ddPCR cannot detect all blood group antigens on a single plate, it provides a quick response to *RHD* genotyping and like MPLA, ddPCR can also reliably determine copy number of *RH* blood group alleles in the same test.

Serological RBC agglutination tests have many limitations, including; tests cannot determine *RHD* zygosity, discordant results can occur when patients are multiply transfused, there is a reduced availability of specific reagents and also reports have identified discrepancies in serologic reactivity between different manufacturers', which complicates *RH* determination (Legler *et al.*, 1999; Liu *et al.*, 1999). While blood-MLPA approaches can be used for extensive typing of a patient, *RH* genotyping using dPCR will enable for rapid determination of *RHD* zygosity and fetal typing from amniocytes or cffDNA. This study illustrates high reproducibility and reliability, since different sample types tested on different days all exhibit a significant difference between hemizygous *RHD* positive and homozygous *RHD* positive samples ( $p < 0.01$ ) (Figure 5-13).

To summarise, these results demonstrate that ddPCR provides a reliable platform for the determination of *RHD* zygosity from both buffy-coat and plasma DNA extractions. The application of this assay in a clinical setting would allow for rapid paternal zygosity testing, in cases where the mother is *RHD* negative. In addition, developing further assay targets would enable accurate analysis of partial D genotyping, preventing the risk of HDFN or the production of anti-D in cases transfused with *RHD* positive blood. Since serological agglutination tests cannot distinguish D-variants, this ddPCR provides a novel test for *RH* genotyping, although further assay targets need to be included for complete *RH* profiling.

### 5.3.2 ddPCR vs qPCR for the NIPT of fetal sex and *RHD* genotyping

We have shown that ddPCR could be used to provide a more sensitive and robust platform for routine antenatal *RHD* genotyping. Both the fetal sexing and *RHD* genotyping assays included in this study illustrated 100% sensitivity despite low levels of cfDNA being expressed by a number of samples (<2%) (Table 5-6) (Figure 5-18A). We tested 46 samples and achieved concordance between presumed genotype (from NHS BT (Filton)) and ddPCR defined genotype in 97.8% of test samples using ddPCR (EDTA and Streck samples combined). One sample (2.2%) was classified as inconclusive since the concentration of *RHD7* was seven-fold higher than *RHD5*, which exhibited a very low concentration (<0.3 copies/  $\mu\text{L}$ ). Fetal sexing illustrated 100% accuracy since all 46 samples were correctly classified and no false-positive or false-negative results were recorded for any of the assays on the ddPCR platform.

Non-invasive fetal *RHD* genotyping from maternal serum or plasma using qPCR analysis has shown high levels of accuracy (average 97.4%) for many studies and is currently implemented in the Netherlands and Denmark for targeted administration of prophylaxis anti-D (Gautier *et al.*, 2005; Van der Schoot *et al.*, 2006; Finning *et al.*, 2008; De Haas *et al.*, 2012). However, in a prospective multicentre cohort study it was determined that for samples taken before 11 weeks gestations 16/865 samples (1.8%) were incorrectly classified as *RHD*-negative and fetal *RHD* genotyping was also inconclusive for 393/4913 samples tested (8%) (Chitty *et al.*, 2014). Studies have also shown that false negative results can occur using qPCR when low cfDNA fractions are present, limiting the sensitivity of this platform (Lo *et al.*, 2000; Zhong *et al.*, 2000; Müller *et al.*, 2008). In this study we have shown that for suboptimal samples the single copy targets (*SRY*, *RHD5* and *RHD7*) were not detectable by qPCR, but we achieved 100% sensitivity (95% CI) on the ddPCR platform. Contrastingly, the qPCR results displayed 100% and 83.4% accuracy for fetal sexing (*TSPY1* only) and *RHD*

genotyping, respectively, for samples that expressed optimal cfDNA fractions (>3%) (collected in Streck BCTs).

The cfDNA fraction of these third trimester samples are expected to be >5% (Lo *et al.*, 1997). However, the results indicate maternal DNA degradation for EDTA-collected samples (Figure 5-18), which is likely to have caused the low cfDNA fractions. Fetal DNA in maternal plasma is relatively stable but the amount of total cell-free DNA has been shown to increase in positive correlation with time before processing (Angert *et al.*, 2003). The cfDNA fraction can be preserved for samples collected in EDTA tubes by quick processing (<6 hours) and storing the samples at 4°C before plasma extraction. However, though samples were processed within 6 hours, due to logistical reasons samples were transported and extracted at room temperature. The results for samples collected in Streck BCTs, which contain cell-preserving reagents, show a significant reduction in maternal red blood cell degradation compared to samples collected in EDTA tubes ( $p < 0.001$ ) (Figure 5-18B).

The EDTA tubes are currently standard practice as they contain chelating agents which prevent blood coagulation. One study identified that EDTA blood samples stored at 4-8°C led to remarkable changes in morphology and osmotic fragility over a four day period (Antwi-Baffour *et al.*, 2013). Other animal studies have also identified an increase in red blood cell size over time, due to changes in morphology which permit osmosis into the cell, subsequently leading to haemolysis (Gulati *et al.*, 2002; Walencik and Witeska, 2007). This effect of prolonged time between venepuncture and cfDNA recovery has also shown increases in haemolysis for studies analysing maternal plasma (Houfflin-Debarge *et al.*, 2000; Finning and Chitty, 2008; Hidestrand *et al.*, 2012). Although the samples in this current study were processed within 6 hours, the increased temperature is likely to speed up this process of maternal erythrocyte degradation. Norton *et al.* (2013) determined that Streck BCTs minimize cellular DNA release during sample storage and shipping compared to standard



EDTA tubes. The result illustrated that samples collected in Streck BCTs remain stable for up to 14 days at all temperatures (6°C, 22°C and 37°C). Within a four-day window the EDTA tube samples showed a significant increase in cfDNA when incubated at the higher temperature (22°C and 37°C). The amount of total cfDNA also increased for samples stored at 6°C but not as dramatically (Norton *et al.*, 2013).

This novel ddPCR data indicates that qPCR false negative results were not caused by low absolute cffDNA concentrations, since levels are similar to that expressed by optimal samples (Figure 5-17), but are instead a result of low relative concentrations of cffDNA. The assay used is highly specific and theoretically non-specific amplification should not occur, but since *RHD5* and *RHD7* probes are 96.5% and 100% consensus to the *RHCE* gene, respectively, it is possible that the probes are binding to the abundant maternal *RHCE*, depleting probe availability for fetal-specific *RHD*-targets. Nonetheless, when the cffDNA copy number is very low false negative results are more likely, particularly for the detection of fetal single nucleotide polymorphisms (SNPs) for rare mutation detection. qPCR is more susceptible to non-specific amplification of the maternal allele, and ddPCR maybe more powerful in the detection of alleles associated with conditions such as  $\beta$ -thalassemia and cystic fibrosis.

Manual extractions of Streck-collected samples generated low gene copy numbers (Table 5-5). Brojer *et al.* (2005) determined that Ct values for automated extractions were significantly lower than that for manual extractions (indicating increased gene copy number) when starting with  $\leq 2$ ml of maternal plasma. However, if larger starting quantities of maternal plasma are used (4-5ml), higher concentrations can be achieved using the QIAamp Circulating Nucliec Acid Kit (Qiagen) (Devonshire *et al.*, 2014). Previous analysis has identified that manual extractions yield 23.4% more total cell-free DNA (cffDNA and

maternal cfDNA), however, automated approaches yield 40.7% more cffDNA fraction (Huang *et al.*, 2005). Despite following the manufacturer's instructions for extraction, the manual approach of extraction used in this study combined with the initiation of maternal sample experimentation for this institution, yielded variable samples some of which were suboptimal for qPCR analysis.

The ddPCR data was used to determine cffDNA fraction, as it is associated with higher levels of sensitivity and improved accuracy for low template copy numbers (Jones *et al.*, 2014). Since some droplets may contain multiple targets, Poisson statistics were incorporated to determine the copy number (Pinheiro *et al.*, 2011). The proportion of the fetal specific targets were relatively low (average number of droplets; 12084, average number of *RHD* molecules; 20.8 and 17.8 for samples from EDTA tubes and Streck BCTs, respectively (refer to Figure 5-16)). However, higher proportions of dual positive droplets are visible for EDTA samples since the reference targets (*EIF2C1* or Xp22.3) express a higher number of mean copies per partition (e.g. 0.62 mean copies per partition of *EIF2C1* for sample 15) compared to Streck BCTs (e.g. 0.023 mean copies per partition of *EIF2C1* for sample 32) (Figure 5-16).

Multiple studies have been carried out since the release of the QX100™ ddPCR system in 2012 to compare whether its application can enhance or replace conventional qPCR-based approaches (Hindson *et al.*, 2011; Dodd, Gagnon and Corey, 2013; Hayden *et al.*, 2013; Hindson *et al.*, 2013; Strain *et al.*, 2013; Kim, Jeong and Cho, 2014). While some studies revealed equal sensitivities for ddPCR and qPCR (Hayden *et al.*, 2013; Hindson *et al.*, 2013), a number of studies in various biomedical, pharmaceutical and biotechnological fields have shown considerable improvements of sensitivity and specificity on the ddPCR platform compared to qPCR approaches (Hindson *et al.*, 2011; Dodd, Gagnon and Corey, 2013; Strain *et al.*, 2013; Kim, Jeong and Cho, 2014). This study also illustrates significant improvements

in sensitivity for the ddPCR platform, particularly for samples expressing low cfDNA (<3%) (Table 5-6).

In a previous study, unequal representation of reference targets (*TERT* and *ERV*) was shown in cfDNA compared to genomic DNA (Devonshire *et al.*, 2014). The chosen references (*Xp22.3* and *EIF2C1*) were based on assumptions that cfDNA is fragmented equally across the genome. The ddPCR data demonstrated a ratio close to 1 for all target and reference multiplex reactions, which shows they are present in equal abundance (Figure 5-2, Figure 5-4 and Figure 5-5). In addition, the equal representation of targets for the *RHD5/ EIF2C1* and *RHD7/ EIF2C1* multiplex reactions has been shown, since ratio analysis to determining whether samples in a previous study were hemizygous or homozygous for *RHD* was highly accuracy (Figure 5-13).

Based on the qPCR data, false negative results were shown in 54% of patients. In a clinical setting these cases would not of received RAADP, and thus could potentially lead to the onset of HDFN. Contrastingly, no false negative results were recorded when analysed using the ddPCR, and as a consequence, if applied routinely, administration of this assay would have prevented 31.1% of patients receiving anti-D unnecessarily in our study cohort. Not only would this approach prevent around 1/3 women having to receive the anti-D, it would provide financial benefits. One published study looking at the cost analysis of mass testing for the targeted administration of RAADP in England and Wales identified that if non-invasive testing replaced currently serological tests an annual saving of £507,154 could be achieved (Szczepura, Osipenko and Freeman, 2011). However, this is only achieved if NIPD is also used to replace postnatal serology testing if an *RHD* negative fetus is determined. If NIPD is used in conjunction with postnatal serological testing, no savings were recorded (Szczepura, Osipenko and Freeman, 2011). In addition, previous studies have also reported false positive/ inconclusive results when the fetus expresses D-variants (Rouillac-Le Sciellour

*et al.*, 2004; Finning *et al.*, 2008; De Haas *et al.*, 2012). In contrast to false negative results, false positive results do not lead to alloimmunisation and subsequent HDFN onset. Instead anti-D is administered unnecessarily. For qPCR analysis, four inconclusive results would have received anti-D, which in this instance was necessary since fetuses were confirmed to be *RHD* positive. Based on the ddPCR data only one mother (2%) would have received anti-D that was not required.

The oligonucleotide primers used in this study for the *RHD* targets (Finning *et al.*, 2008) should distinguish between *RHD* positive and *RHD* $\Psi$ / DVI (type 1-4) fetal genotypes, by amplifying exon 7 but not exon 5 for the latter (Figure 5-17). From this study, based on the ddPCR data, only one sample (sample 12) would have received anti-D unnecessarily. However, the true *RHD* genotype could not be confirmed due to constraints on ethical approval which prevented follow up. To improve the sensitivity of *RHD* $\Psi$  detection additional experiments could also include primers designed to incorporate the C674T missense and T807G nonsense mutations in exon 6 (Daniels *et al.*, 1998). In this instance the *RHD* $\Psi$  would present only amplification of exon 7, with no amplification of *RHD* exon 5 or 6. Both ddPCR and qPCR will express similar levels of false positive results due to D-variants, however, this study illustrates that ddPCR has the potential to eliminate or reduce the occurrence of false negative results, particularly for samples with suboptimal cfDNA fractions (<2%). First trimester testing is preferable since it can be carried out with other routine blood test, but as long as a diagnosis is determined before 28 weeks gestation prophylaxis anti-D can be successfully targeted to mothers carrying D-positive fetuses. Currently, around 40% of women in the UK still receive anti-D unnecessarily. Our results show that the sensitivity of ddPCR is considerably higher, particularly for suboptimal samples (<2% cfDNA). Therefore, this ddPCR assay should be able to accurately and reliably determine fetal *RHD* genotype from an EDTA-collected maternal blood sample from

as early as 8 weeks gestation. Women receive their initial blood tests to check for immunization against rubella and other infections (syphilis, hepatitis B and HIV) at 8-10 weeks gestation and this this test could be carried out at the same time. The Rh status of the mother is also determined and to distinguish between *RHD*-positive mothers and *RHD*-positive fetuses carried by *RHD*-negative mothers would be relatively easy. The *RHD*-positive mother would express high concentrations of the *RHD*-target gene that are very close to the concentrations of the reference gene. The *RHD*-positive fetus (carried by an *RHD*-negative mother) would express a significantly lower concentration of *RHD*-target compared to the reference gene. Future experiments will examine the feasibility of ddPCR for first and second trimester samples.

In conclusion, these results show that ddPCR illustrates improved accuracy compared to qPCR for fetal sex determination and *RHD* genotyping. Though this assay demonstrated improved sensitivity of ddPCR compared to qPCR it is important to note that our qPCR assays do not reflect the sensitivity levels commonly achieved (>99%). Initially it was thought that the reduced quality of maternal samples resulted in lower qPCR accuracies, although it could also be a result of lower PCR efficiencies, indicating that further assay optimisation is required. Therefore, an improved method for comparing the sensitivity of ddPCR to qPCR, could be achieved by spiking male gDNA/ *RHD* positive gDNA into female genomic DNA/ *RHD* negative gDNA, respectively, at different ratios, all the way down to 0.1%, which would enable a comparison of sensitivity without the external influence of maternal sample quality. The low but significant presence of false negatives in current qPCR assays for samples expressing low cfDNA fractions demonstrate the need for improved accuracy, which could be achieved using ddPCR. This preliminary data highlights of ddPCR for targeted administration of RAADP. However, validation studies are now required to determine the feasibility and cost-effectiveness of ddPCR for larger cohorts of samples.

## Chapter 6

Determining the feasibility of Pippin Prep™ size selective gel electrophoresis for cffDNA enrichment in conjunction with ddPCR analysis for the detection of T21 in spiked samples

## 6.1 Introduction

The size difference between maternal cfDNA and cffDNA has been previously discussed (refer to 1.3.3.5), and initial approaches for size-selective amplification of the shorter cffDNA fragments using COLD-PCR (refer to Chapter 3) and IPCR (refer to Chapter 4) have been examined. Despite the initial success associated with the COLD-PCR approach using pseudo-maternal samples (refer to 3.2.4), transferring this protocol to real maternal samples revealed too much variation in amplification efficiencies between the reference and target genes at the lower  $T_{ds}$  (refer to 3.2.5). In contrast, the inverse PCR approach is dependent upon the DNA exhibiting cohesive ends. Further investigations are required to initially define the properties of cfDNA ends before optimisation of the selective IPCR approach can be continued (refer to 4.3). In this chapter the application of a third alternative selective-enrichment approach, using the Pippin Prep™ (PP) DNA Size Selective System (Sage Science) is described.

The PP System is an automated preparative gel electrophoresis system, which contains a fluorescent-based DNA detection unit. During electrophoresis, the optical system enables detection of DNA fractions within a particular size range set up by the user. By altering the voltage, the system allows for selected DNA fragments to be electroeluted into a buffer-filled elution module. The principle application of this platform is for facilitating library construction for MPS since target sizes or even ranges of target sizes can be selected without the need for gel extraction (Borgstrom, Lundin and Lundeberg, 2011; Duhaime *et al.*, 2012; Quail *et al.*, 2012). One study, focusing on the optimization of quantitative metagenomics of ultra-low concentration samples, compared three size fractioning methods to test for target recovery efficiency, throughput and risk of cross-sample contamination. These methods included; PP, Solid Phase Reversible Immobilization (SPRI) (using Agencourt AmPure XP beads) and standard gel extraction.

The results illustrated that the PP was the most efficient and reproducible (94-96% of input DNA) with the most specific sizing. In contrast standard gel extraction exhibited moderate target recovery efficiency (64-74%) and the SPRI was the least efficient, only recovering 46-50% of the targeted size fraction (Duhaime *et al.*, 2012).

In this study, the PP gel electrophoresis was used as a tool for size selective enrichment of shorter cffDNA fragments over maternal fragments rather than as a platform for library preparation. The system was set to collect DNA fragments within the range of 100-200bp, with a target of 150bp. Based upon the principles discussed in Chapter 3 (refer to 3.1), it was hypothesized that this would enable selection and enrichment of the shorter fetal-DNA fragments, whilst larger maternal DNA fragments >200bp would be depleted. Unlike previous enrichment strategies, this technique did not require alteration to the PCR  $T_d$  and was not dependent on specific characteristics of cffDNA, such as cohesive ends for self-ligation.

The aims of this study were:

- To selectively enrich shorter fetal DNA fragments using the PP Size Selective System.
- To determine enrichment by analysing the cffDNA fraction (%) before and after PP gel electrophoresis using the ddPCR platform.
- To produce pseudo-maternal samples carrying a 'T21' fetus at varying cffDNA fractions in order to determine the minimal cffDNA fraction required for reliable diagnosis using ddPCR.



## 6.2 Results

### 6.2.1 Pippin Prep™ gel electrophoresis enrichment

#### 6.2.1.1 *Initial PP size-selective experiments using qPCR and ddPCR analysis*

Two maternal samples, one carrying a female fetus (maternal sample 8) and one carrying a male fetus (maternal sample 9) were run on the PP gel electrophoresis System with a target size selection of 150bp (refer to 6.2.1). The eluted PP samples were then collected and analysed using qPCR and ddPCR platforms (refer to 6. 2.2) against non-Pippin Prep (non-PP) aliquots of the same sample, male gDNA, female gDNA and a NTC. The non-PP samples were extracted from a single 1mL aliquot of plasma (8A and 9A) and the PP samples were extracted from three 1mL aliquots of plasma (8BCD and 9BCD), since it was anticipated that a relative proportion of cell-free DNA would be lost following PP gel electrophoresis. The concentration of each aliquot determined by Qubit analysis is illustrated in Table 6-1 and is higher for both maternal samples when extracted from 3 mL of plasma as expected. Due to limited amounts of sample available and previous low levels of sensitivity achieved with qPCR (see Chapter 5), the multiple copy target (*TSPY1* (FAM)) was multiplexed with the *HBB* (HEX) reference on the qPCR platform, while the single copy target multiplex assay (*SRY*<sup>(H.P.T)</sup> (FAM)/ Xp22.3 (HEX)) was tested on the ddPCR platform for this initial experiment (2.9).

**Table 6-1: DNA concentration of maternal sample aliquots.**

Sample	Concentration (ng/ $\mu$ L)
8A	0.82
8BCD	1.61
9A	0.42
9BCD	2.33

The qPCR data revealed amplification of both targets for the male control sample, while the female control and NTC illustrated *HBB* amplification only and no amplification, respectively. The non-maternal (female) sample (147W) illustrated no *TSPY1* amplification but did illustrate successful amplification of the reference gene (*HBB*). The *HBB* amplification for sample 147W demonstrated reduced amplification for the PP aliquot (29.71 Ct) compared to the non-PP aliquot (25.14 Ct). The results also demonstrated a decline in amplification of all targets following PP electrophoresis (Figure 6-1), which led to lower concentration yields (Table 6-2) despite higher starting concentrations (Table 6-1). This result was expected since DNA is lost with additional processing. Maternal sample 8 (female fetus) illustrated contamination on the qPCR platform since late amplification of the Y-specific target (*TSPY1*) was detected (Figure 6-1). Maternal sample 9 (male fetus) illustrated reduced amplification of the *TSPY1* target gene for the PP aliquot (30.51 Ct) compared to the non-PP aliquot (29.65 Ct), but demonstrated an even greater decline in amplification of the *HBB* reference gene for the PP aliquot (27.39 Ct) compared to the non-PP aliquot (25.11 Ct). However, despite higher depletion of ‘maternal’ reference, the cffDNA fraction calculated (refer to 2.9.4) was higher for maternal sample 9A non-PP (1.54%) compared to maternal sample 9BCD PP (1.17%). This result illustrated that the sample had not been successfully enriched.

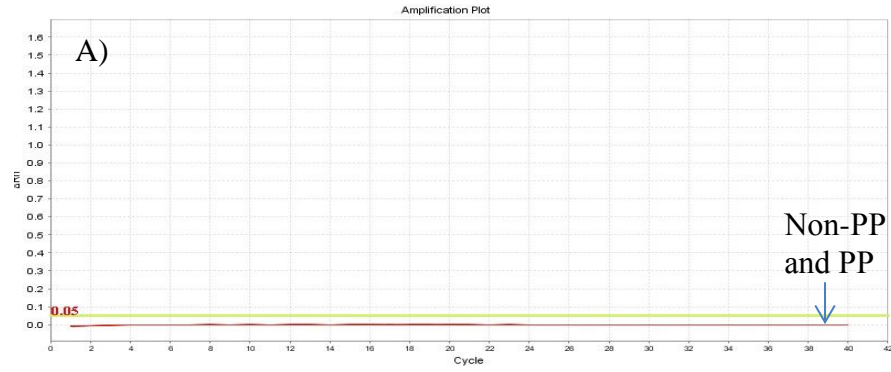
Contrastingly, the ddPCR results illustrated >3-fold increase in cffDNA fraction for maternal sample 9 following PP enrichment when using the single copy target assay (*SRY*<sup>(H.P.T)</sup> (FAM) / Xp22.3 (HEX)) (Figure 6-2). The male gDNA control demonstrated a ratio of 0.99, showing equal proportion of the Y-specific (*SRY*) and X-specific (Xp22.3) targets. The female control sample only illustrated amplification of the Xp22.3 target and the NTC was clean since no amplification was visible. Similarly to qPCR, the PP aliquots of maternal sample

8 (BCD) and maternal sample 9 (BCD) illustrated a decline in concentration compared to the non-PP aliquots (8A and 9A) (Figure 6-2). Due to limited quantities, non-maternal sample (147W) was not analysed on the ddPCR platform. Maternal sample 8BCD (PP) showed low amplification of Y-specific target despite carrying a female fetus indicating sample contamination as seen in qPCR (Figure 6-2 compared to Figure 6-1).

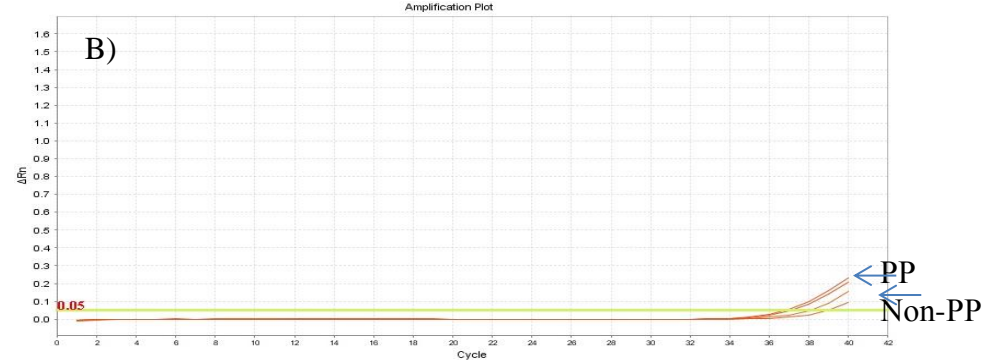
The results illustrated higher cffDNA fractions when using ddPCR analysis with the single copy Y-specific target. Due to the partitioning nature of the ddPCR platform precise quantification of nucleic acid can be achieved allowing small percentage differences in cffDNA fractions to be detected. Therefore, all subsequent experiments to determine PP gel electrophoresis enrichment were conducted using ddPCR. In addition, to reduce variability, DNA was extracted from the same maternal plasma aliquots and later separated for PP and non-PP analysis (unless stated otherwise).

# TSPY1

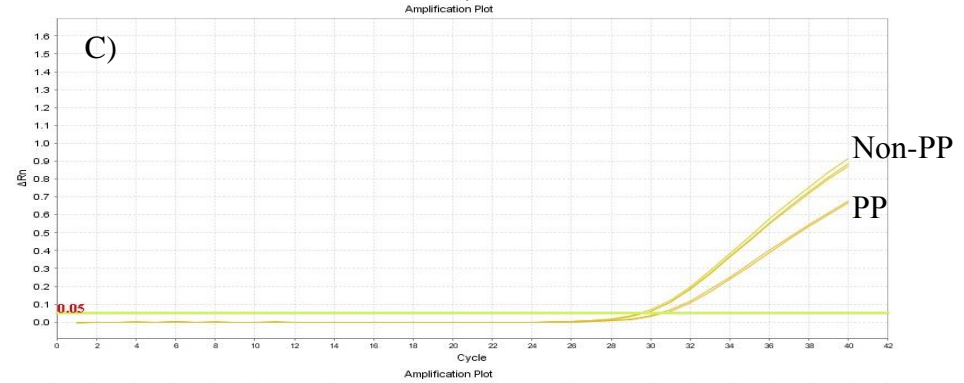
**Non-maternal female sample (147W)**



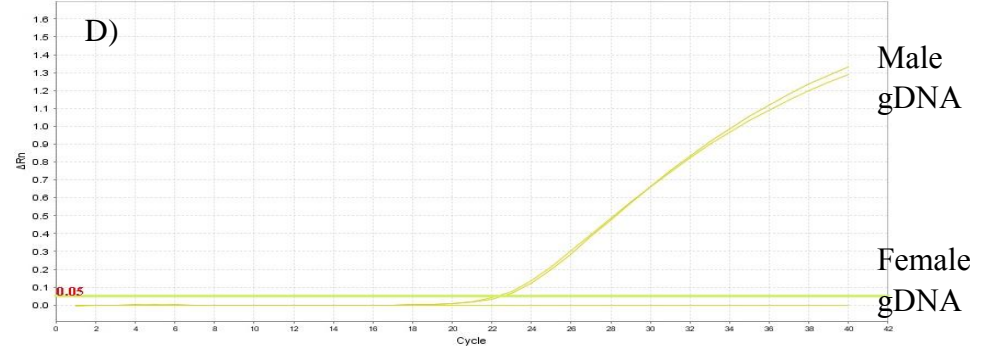
**Maternal Sample 8 (female fetus)**



**Maternal Sample 9 (male fetus)**



**Male and Female Control Samples**



## HBB

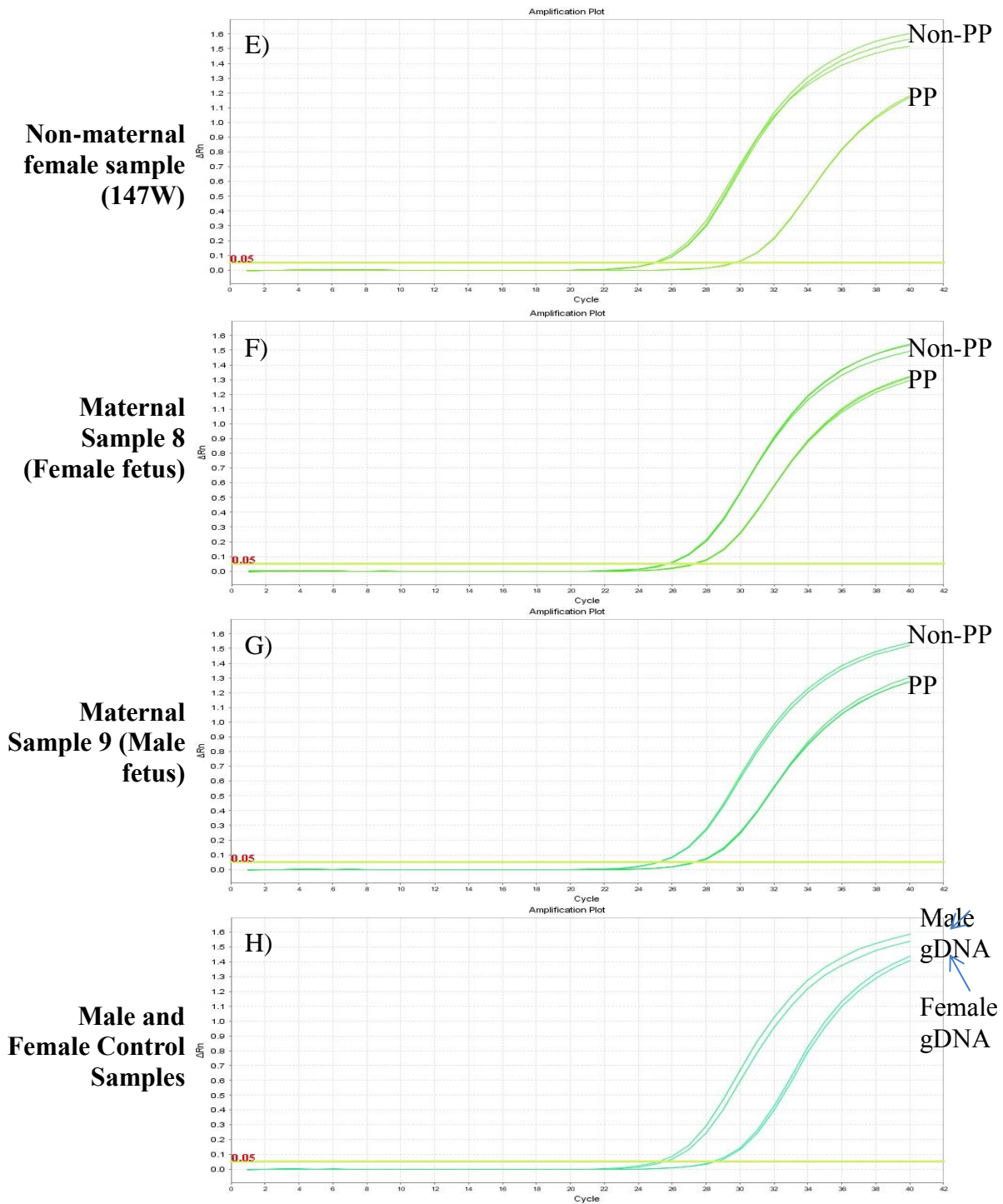
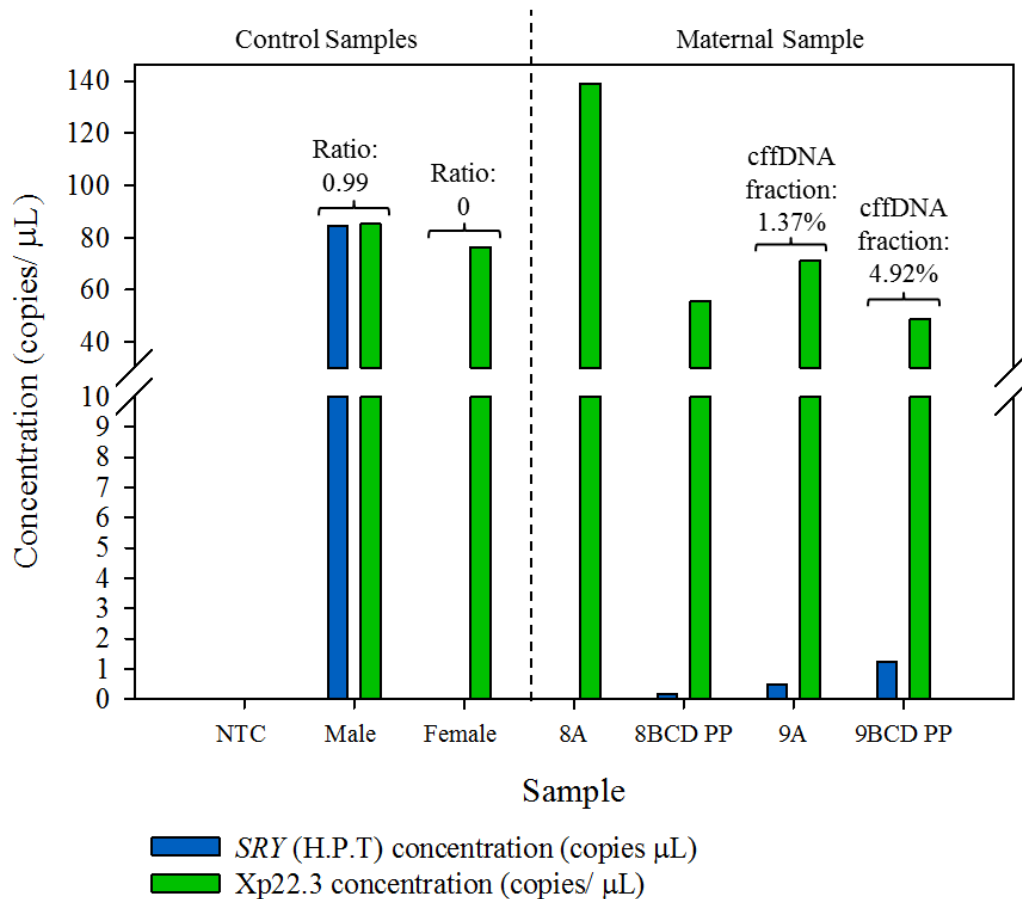


Figure 6-1: qPCR amplification of *TSPY1* (A-D) and *HBB* (E-H) for non-maternal sample 147W (A and E), maternal sample 8 (female fetus) (B and F), maternal sample 9 (male fetus) (C and G) and Male and Female gDNA control samples (D and H). Samples were tested prior to PP-enrichment

(labelled non-PP) and after PP size selective gel electrophoresis (labelled PP). Threshold was set at 0.05 for both assays for consistency when quantifying samples (refer to Table 6-2). Female sample 147W illustrated no amplification of *TSPY1* but did illustrate a reduction in amplification for the *HBB* reference following PP gel electrophoresis (29.71Ct) compared to the non-PP sample (25.14Ct). Both maternal samples also illustrated a decline (~2Ct) in amplification following PP gel electrophoresis (Sample 8 (F) and Sample 9 (G)). Maternal sample 8 illustrated contamination since Y-specific amplification was visible at 37.67Ct and 39.14 for PP and non-PP aliquots, respectively (B). Maternal sample 9 showed a less substantial reduction in amplification for the *SRY* target between the non-PP aliquot (29.65 Ct) and the PP aliquot (30.51 Ct) (C) compared to the decline in amplification visible for the *HBB* reference (G). The male control illustrated successful amplification of both targets, while the female control only illustrated successful amplification of the reference (*HBB*) (D and H).

**Table 6-2: Sample concentration following qPCR analysis and cffDNA fractions for maternal sample 9.**

Sample	<i>TSPY1</i> Concentration (ng/ $\mu$ L)	<i>HBB</i> Concentration (ng/ $\mu$ L)	cffDNA fraction (%)
147W	0	2.92	N/A
147W PP	0	1.32	N/A
8A non-PP	<0.01	2.68	N/A
8BCD PP	<0.01	2.13	N/A
9A non-PP	0.66	2.85	1.54
9BCD PP	0.37	2.11	1.17
Male gDNA	3.2	2.55	N/A
Female gDNA	0	1.77	N/A
NTC	0	0	N/A



**Figure 6-2: Bar Chart illustrating the concentration (copies/ μL) of *SRY*<sup>(H.P.T)</sup> (FAM) target (blue) and Xp22.3 (HEX) reference (green) generated by ddPCR platform.** The following samples were tested; control samples (NTC, Male gDNA and Female gDNA), a maternal sample carrying a female fetus with no selective PP enrichment (8A) and following PP enrichment (8BCD PP), and a maternal sample carrying a male fetus with no selective PP enrichment (9A) and following PP enrichment (9BCD). The result illustrated a ratio of 0.99 for the Male gDNA (*SRY* (copies/ μL) divided by *EIF2C1* (copies/ μL)), which is expected since males will carry a single *SRY*<sup>(H.P.T)</sup> target region and a single Xp22.3 target region. The Female control did not show any *SRY*<sup>(H.P.T)</sup> amplification and the NTC showed no amplification. Sample 8A did not show any amplification following extraction from 1 mL of maternal plasma, but sample 9

showed an increase in cffDNA fraction from 1.37% to 4.92%. However, since samples were extracted from varying volumes of maternal plasma.

#### 6.2.1.2 *ddPCR analysis of PP gel electrophoresis cffDNA enrichment using a multiple-copy Y-specific target (TSPY1)*

Since the initial qPCR results did not illustrate an increase in cffDNA fraction when using the multiple-copy Y-target (*TSPY1*), this experiment was repeated on the ddPCR platform with four new maternal samples carrying a male fetus (13AB, 24AB, 36AB and 43AB). However, since previous ddPCR experiments had been optimised using the *TSPY1* (FAM)/ Xp22.3 (HEX) assay, the Xp22.3 reference was used in replacement of *HBB*.

Prior to PP gel electrophoresis, DNA was extracted from two 1mL aliquots of plasma and eluted in 70  $\mu$ L of Buffer AVE (refer to 2.1.5). The maternal samples were then equally split into two aliquots. One aliquot, labelled 'PP', was run on the PP System, while the second aliquot, labelled 'non-PP', was stored at 4°C. To pre-determine any drop out of larger DNA fragments and assess sample quality, both maternal sample aliquots (PP and non-PP) were run on the Bioanalyzer (refer to 2.6.3) prior to ddPCR analysis. The electropherograms for each sample are illustrated in Figure 6-3 and the electrophoresis gel-like image generated by the Bioanalyzer is shown in Figure 6-4. The results demonstrated that all PP maternal aliquots only showed a single peak/band between 187-208bp, whereas non-PP maternal samples also illustrated multiple peaks/ bands between 350-400bp, 500-600bp and <850bp (Figure 6-3 and 6-4). For unknown reasons maternal sample 13AB PP, did not align to the Ladder and therefore the size (bp) of peak/ band generated could not be determined (Figure 6-3 and 6-4).



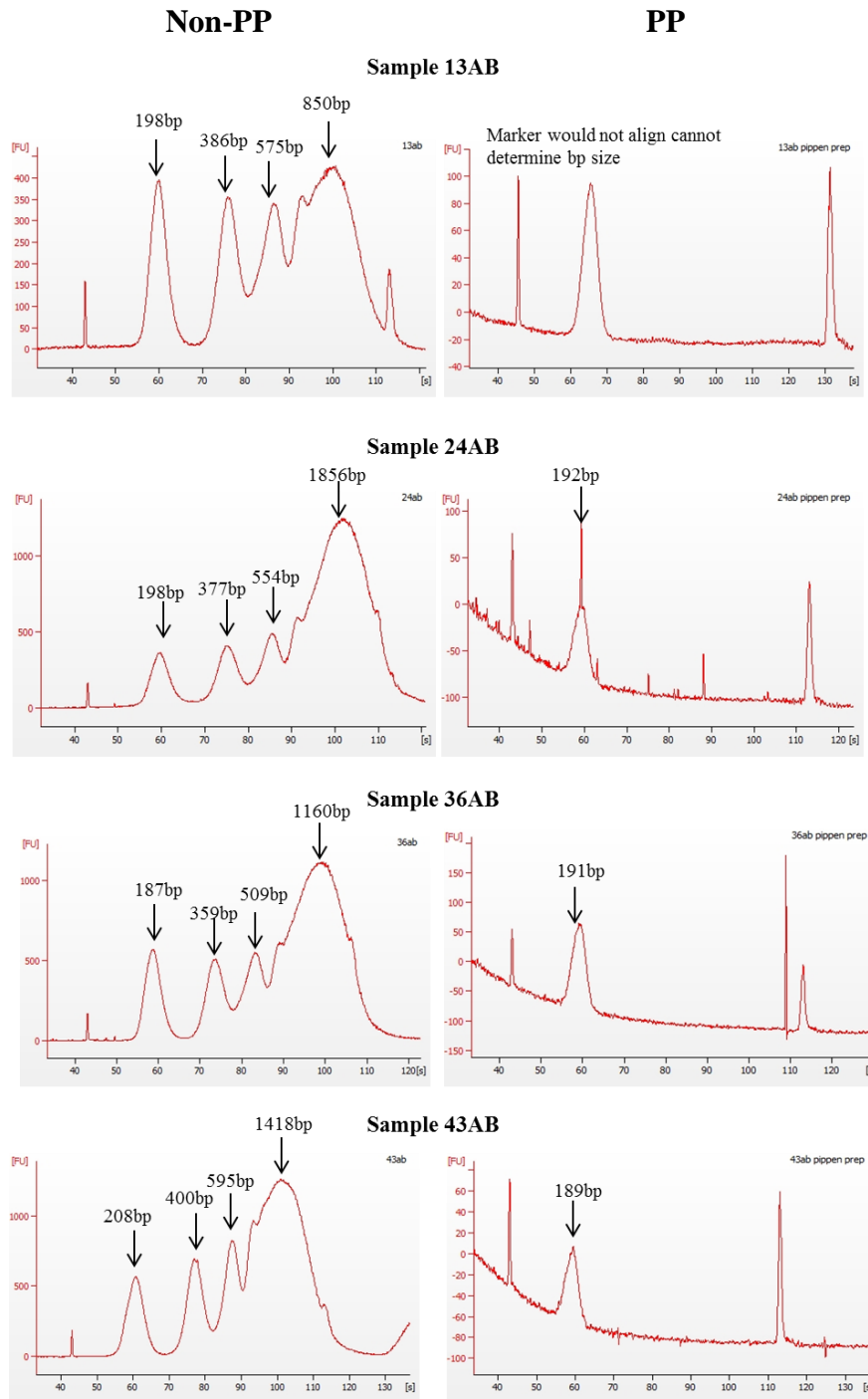


**Figure 6-3: Agilent 2100 Bioanalyzer electropherograms for four maternal samples (13AB, 24AB, 36AB and 43AB) before (non-PP, left column) and after (PP, right column) PP gel electrophoresis. The non-PP aliquots show multiple peaks (4), whereas the PP aliquots only show a single peak (between 189bp to 192 bp) for all samples. The peak generated by maternal sample 13AB (PP) could not be determined.**

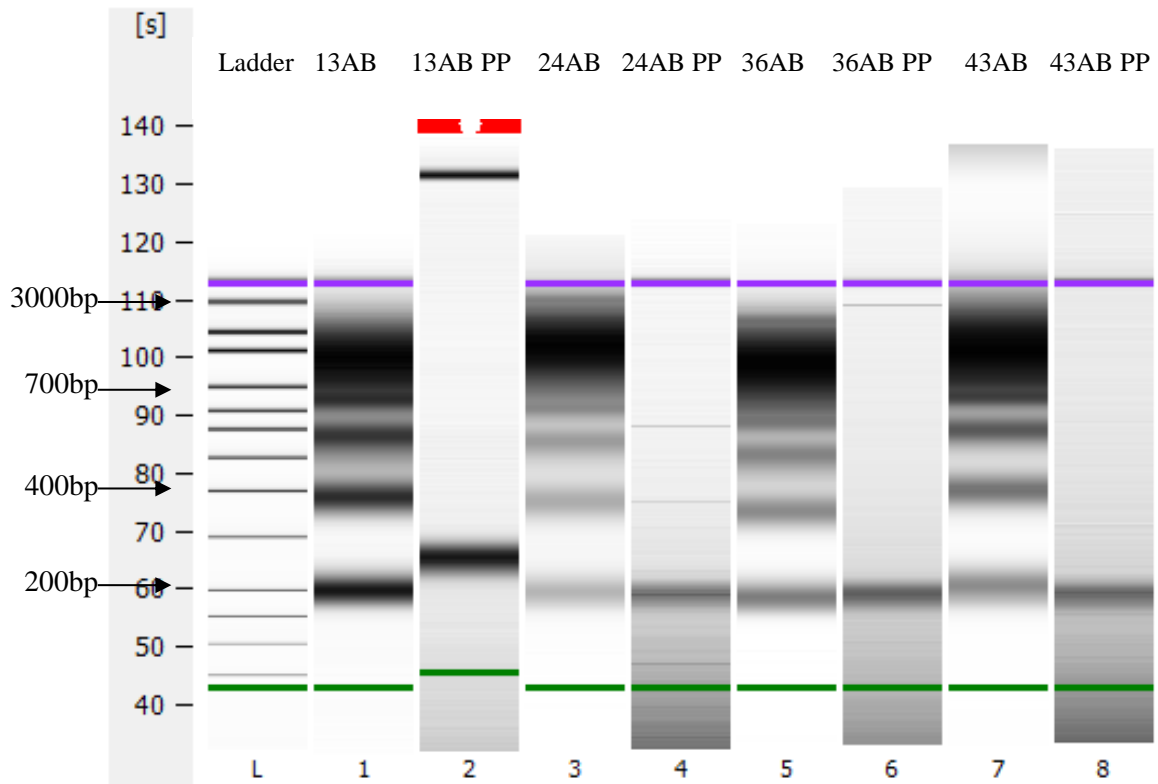


**Figure 6-4: Electrophoresis gel-like image generated by the Bioanalyzer showing the ladder (L) and results for all four maternal samples (13AB, 24AB, 36AB and 43AB) before (non-PP) and after PP gel electrophoresis (PP).** The non-PP maternal samples aliquots (Lane 1 (13AB), Lane 3 (24AB), Lane 5 (36AB) and Lane 7 (43AB)) demonstrated multiple bands at around 200bp, 400bp, 500bp, 700bp and 1000bp. Contrastingly, the PP maternal samples (Lane 4 (24AB PP), Lane 6 (36AB PP) and Lane 8 (43AB PP)) only show a strong band at around 200bp, all the larger fragments are absent or very faint. The results illustrated that sample 13AB PP (Lane 2) did not align to the Ladder and therefore peak size was not determined. However, the gel-like image illustrated that the larger bands present for the non-PP aliquot (Lane 1) were also absent. Following the Bioanalyzer run, maternal samples were analysed on the ddPCR platform to determine if selective enrichment of shorter fetal fragments had been achieved using PP size selective gel electrophoresis (2.9). The results illustrated that all maternal samples illustrated a dramatic drop in number of Events for the reference gene (Xp22.3) and a

declined reduction in number of Events for the fetal Y-specific target (*TSPY1*) for samples that had undergone PP gel electrophoresis (Figure 6-5). The fold-decrease from non-PP to PP aliquot of each maternal sample was consequently calculated and the mean  $\pm$ SD fold-decrease in number of Events for both *TSPY1* and Xp22.3 are illustrated in Figure 6-6. The results demonstrated that the decline in number of positive droplets (Events) was significantly higher for the Xp22.3 reference (Figure 6-6). This illustrated that despite losing some of the fetal specific target through PP gel electrophoresis, the gel was successfully and selectively depleting the larger maternal DNA fragments.

To confirm if enrichment had been achieved the cffDNA fraction using the *TSPY1* multiple-copy target equation was calculated for PP and non-PP maternal DNA aliquots (refer to 2.9.4). The results illustrated that all PP maternal samples expressed a 2- to 5-fold increase in cffDNA fraction (Figure 6-7). Maternal sample 43AB illustrated the highest increase in cffDNA (5-fold increase) from 2.67% to 13.43% for non-PP and PP aliquots, respectively. Before PP enrichment, maternal samples 24AB, 36AB and 43AB all illustrated cffDNA fractions of <1%. These maternal samples were collected in EDTA tubes, which have shown previous low cffDNA fractions (Chapter 5). Therefore, subsequent experiments to test enrichment following PP gel electrophoresis were conducted using maternal samples collected in Streck BCTs, which are associated with higher cffDNA fractions (Chapter 5) (Sillence *et al.*, 2015). Despite extremely low starting quantities of cffDNA, these results illustrate that the PP System can successfully enrich the proportion of cffDNA through size selective gel electrophoresis.

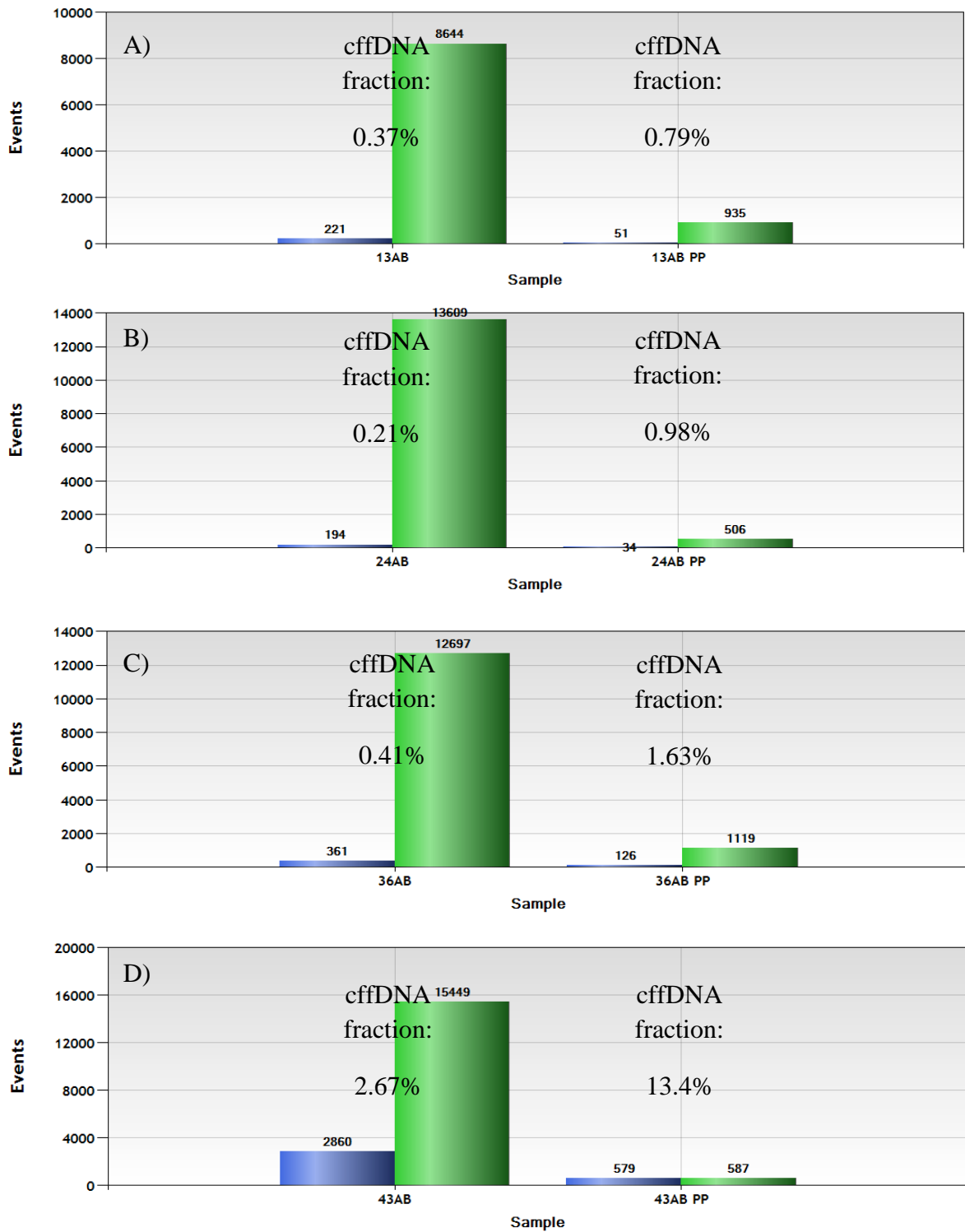


**Figure 6-5: Bar chart illustrating the number of Events (positive droplets) for *SRY* (H.P.T) (FAM, blue) and Xp22.3 (HEX, green) generated by ddPCR for maternal samples 13AB (A), 24AB (B), 36AB (C) and 43AB (D) before and after PP selective enrichment. The results clearly show an increase in cffDNA fraction for all samples following PP gel electrophoresis.**

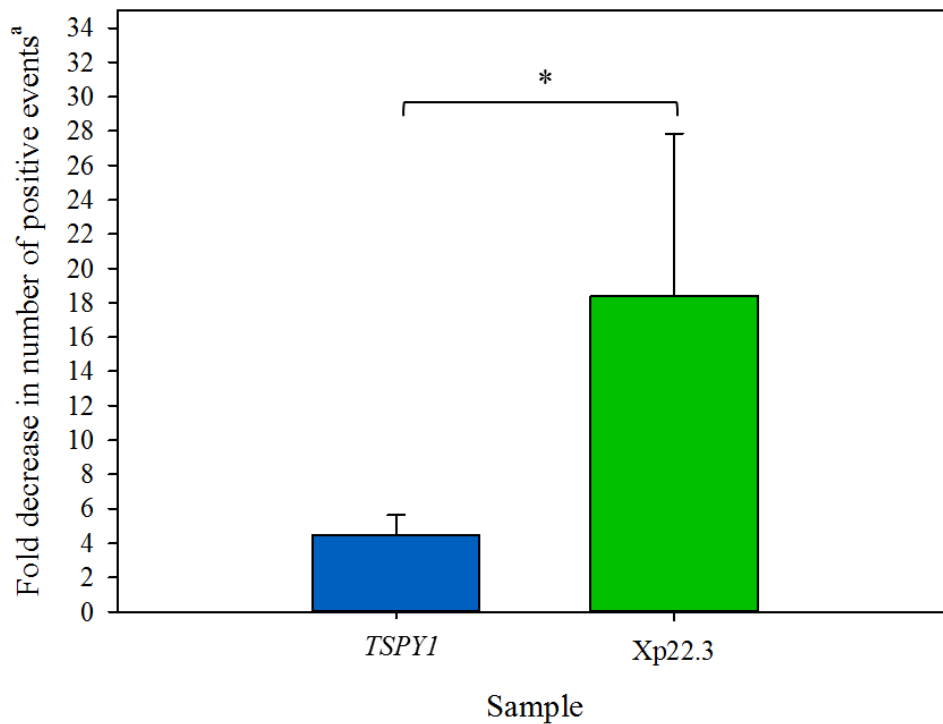


**Figure 6-6** Bar chart illustrated the mean  $\pm$ SD fold-decrease in number of Events (positive droplets) for *TSPY1* (FAM, blue) and Xp22.3 (HEX, green) generated by ddPCR following PP size selective gel electrophoresis. The results illustrated that the number of Events for the reference gene were significantly lower following PP gel electrophoresis compared to the decline in Events for the fetal-specific *TSPY1* target (\* $p < 0.05$ ).

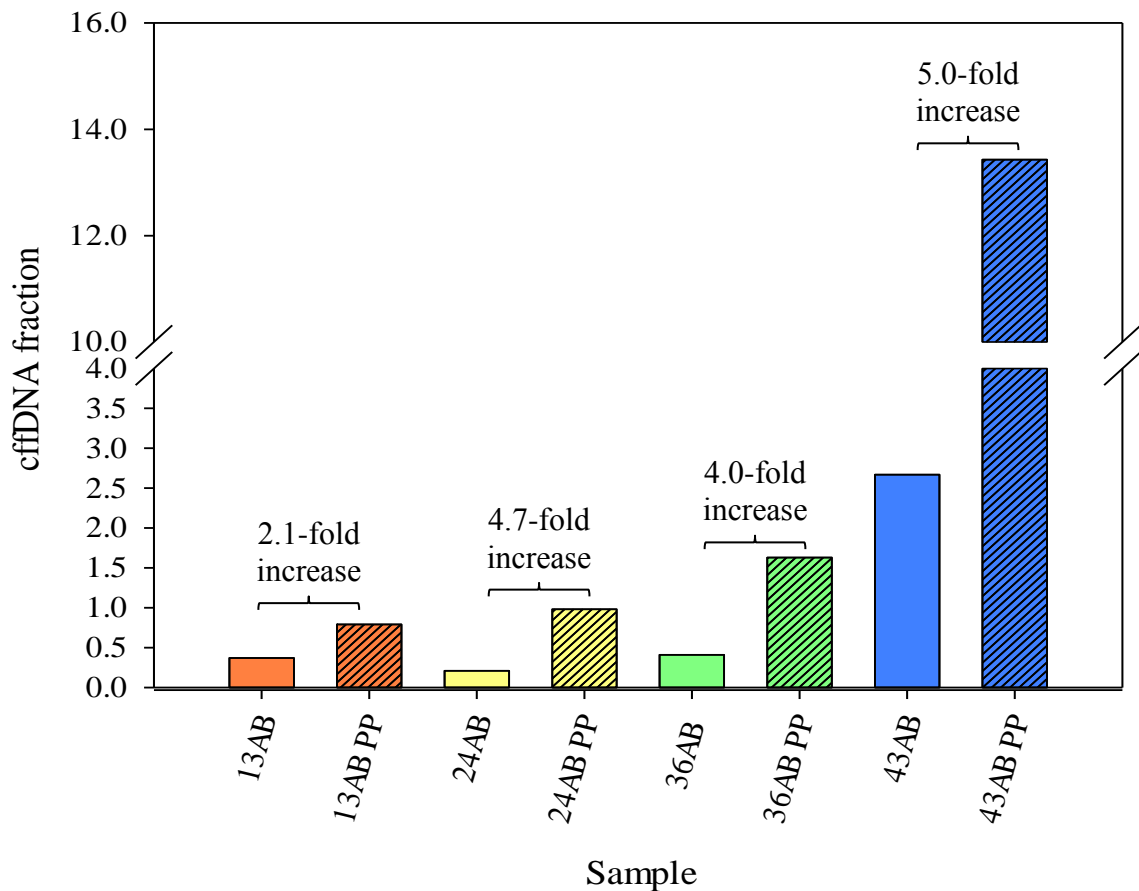


**Figure 6-7:** Bar chart illustrating the cffDNA fraction calculated using the *TSPY1* multiple-copy target equation (refer to 2.9.4) for maternal samples before (non-PP, plain colour) and after (PP, striated colour) PP gel electrophoresis. The results illustrate a 2.1-fold increase, 4.7-fold increase, 4-fold increase and 5-fold increase following PP size selective enrichment for maternal samples 13AB, 24AB, 36AB and 43AB, respectively.

*6.2.1.3 ddPCR analysis of PP gel electrophoresis cffDNA enrichment using a single copy RHD specific targets for samples extracted using Streck BCTs*

To analyse the increase in cffDNA fractions through PP gel electrophoresis using fetal targets specific for the *RHD* gene, DNA was extracted from 2x three 1 mL maternal plasma aliquots. In the previous experiment DNA was extracted from 1x two 1 mL

maternal plasma aliquots and separated. However, since each maternal sample was going to be analysed by two assays (*RHD5* (FAM) / *EIF2C1* (HEX) and (*RHD7* (FAM) / *EIF2C1* (HEX)) an increased amount of DNA was required. Therefore, DNA was extracted from two sets of three 1 mL plasma aliquots. The aliquot showing the highest concentration following Qubit quantification was run on the PP System, while the aliquot expressing the lower concentration was stored at -4°C (non-PP) (Table 6-3). For this experiment eleven maternal samples were tested, ten of these samples (117, 118, 119, 120, 122, 123, 124, 131, 132 and 133) were carrying an *RHD* positive fetus and one sample (130) was carrying an *RHD* negative fetus.

Table 6-3 summarises the results for control samples and all maternal samples before (non-PP) and after (PP) PP gel electrophoresis, including; sample concentration (ng/  $\mu$ L), *RHD5*, *RHD7* and *EIF2C1* concentration (copies/  $\mu$ L) following ddPCR amplification for each multiplex reaction and calculated cffDNA fraction (refer to 2.9.4). The results show that both NTC samples tested illustrated no contamination. Each repeat of the *RHD* negative control (7807) only showed amplification of the reference gene (*EIF2C1*), while each repeat of the *RHD* positive control (131Z) showed amplification of the *RHD* target genes and the reference gene in both assays.

The *RHD5*/ *EIF2C1* assay demonstrated ratios of 1.04 and 1.01 for experiment 1 and experiment 2, while the *RHD7*/ *EIF2C1* assay illustrated a ratio of 0.99 for both experiments. This illustrates that the control sample is homozygous and has two copies of the *RHD* gene, since all ratios are close to 1 (Table 6-3). Maternal sample 130 did not illustrate *RHD* amplification since this sample was carrying an *RHD*- fetus. Sample 119 only detected a small number of *RHD7* targets and no *RHD5* targets following PP gel electrophoresis, illustrating depletion of all cffDNA. Maternal sample 133 was the only

sample to show a reduction in cfDNA fraction, while the remaining maternal samples ( $n=8$ ), all demonstrated an increase in cffDNA fraction (Table 6-3).



**Table 6-3: cffDNA fractions for maternal samples before (non-PP) and after (PP) PP gel electrophoresis.** The cffDNA fractions were calculated based on the concentration (copies/  $\mu$ L) of each target for multiplex reaction 3 (*RHD5* (FAM)/*EIF2C1* (HEX) and multiplex reaction 4 (*RHD7* (FAM)/*EIF2C1* (HEX) (refer to 2.9.4). control samples (*RHD*+ (131Z), *RHD*- (7807) and NTC) were also tested.

	Sample	Conc (ng/ $\mu$ L)	<i>RHD5/ EIF2C1</i>			<i>RHD7/ EIF2C1</i>		
			<i>RHD5</i> -FAM (copies/ $\mu$ l)	<i>EIF2C1</i> -HEX (copies/ $\mu$ l)	Fetal Fraction /*ratio	<i>RHD7</i> -FAM (copies/ $\mu$ l)	<i>EIF2C1</i> -HEX (copies/ $\mu$ l)	Fetal Fraction /*ratio
Controls 05/03/15	NTC	-	0	0	-	0	0	-
	7807 -	-	0	132	-	0	133	-
	131Z +	-	81.7	78.6	1.04*	72.1	72.8	0.99*
Controls 06/03/15	NTC	-	0	0	-	0	0	-
	7807 -	-	0	119	-	0	116	-
	131Z +	-	77.2	76.7	1.01*	77.9	78.2	0.99*
Maternal Samples 05/03/15	120HIJ	2.79	2.91	23.2	25.09	2.93	23.10	25.37
	120EFG PP	3.53	0.503	2.79	36.06	0.72	3.52	40.85
	122EFG	0.476	0.31	6.84	9.06	0.59	5.76	21.07
	122HIJ PP	3.43	0.0406	0.325	24.98	0.05	0.24	41.75
	123EFG	3.53	0.751	22.7	6.62	1.26	23.00	10.96
	123HIJ PP	4.06	0.253	2.07	24.44	0.34	1.26	53.49
	124EFG	2.05	1.25	26.9	9.29	0.97	27.10	7.17
	124HIJ PP	2.13	0.505	3.58	28.21	0.31	3.38	18.40
Maternal Samples 06/03/15	130DEF	0.893	0	22	0	0	19.00	0
	130ABC PP	4.49	0	28.4	0	0	28.90	0
	131DEF	2.36	1.22	61.8	3.95	2.06	58.21	6.83
	131ABC PP	5.57	0.248	7.03	7.06	0.29	7.43	7.51
	132DEF	4.26	1.85	50.8	7.28	30.50	48.70	125.26
	132ABC PP	4.9	0.34	4.14	16.43	3.93	4.79	164.09
	133ABC	3.71	1.08	23.1	9.35	1.31	22.2	11.80
	133DEF PP	3.77	0.106	3.08	6.88	0.31	3.37	18.46
Maternal Samples 02/02/15	117HIJ	0.92	0.752	51	2.95	1.41	48.00	5.88
	117EFG PP	1.06	0.348	3.22	21.61	0.47	3.22	29.38
	118EFG	0.55	2.02	25.5	15.84	2.70	26.60	20.30
	118HIJ PP	0.55	0.99	3.24	61.11	1.62	4.79	67.64
	119EFG	0.50	1.31	27.5	9.53	0.55	23.90	4.59
	119HIJ PP	0.57	0	0.54	0.00	0.11	1.11	20.00

Prior to ddPCR analysis, maternal samples were run on the Agilent 2100 Bioanalyzer. However, despite multiple attempts, only one experiment was successful, all other runs were unsuccessful due to a problem associated with the alignment of the ladder. The Bioanalyzer results for maternal samples 117- 119 are illustrated in Figure 6-8 6-9 alongside a non-maternal control sample (2454). For non-maternal sample 2454 and maternal sample 118 the Agilent Bioanalyzer results revealed four peaks/bands (at 189bp, 381bp, 570bp and 1,379bp) and three peaks/ bands (181bp, 359bp and 494bp) respectively, before (non-PP) PP gel electrophoresis (Figure 6-8 and 6-9). Following PP gel electrophoresis (PP) all peaks/ bands >200bp were removed (Figure 6-8 and 6-9). Maternal sample 117 showered clear peaks/ bands before (non-PP) PP gel electrophoresis at 181bp, 359bp and 494bp, but following PP gel electrophoresis (PP), although a clear peak/ band is shown around 180bp a result (bp) the Agilent 2100 Bioanalyzer did not generate a bp result (Figure 6-8 and 6-9). Finally, the results for maternal sample 119 showed no peaks/ bands for the PP aliquot (Figure 6-8 and 6-9). This indicated that potentially the entire cell-free DNA, including shorter fetal DNA, had been depleted following PP gel electrophoresis.

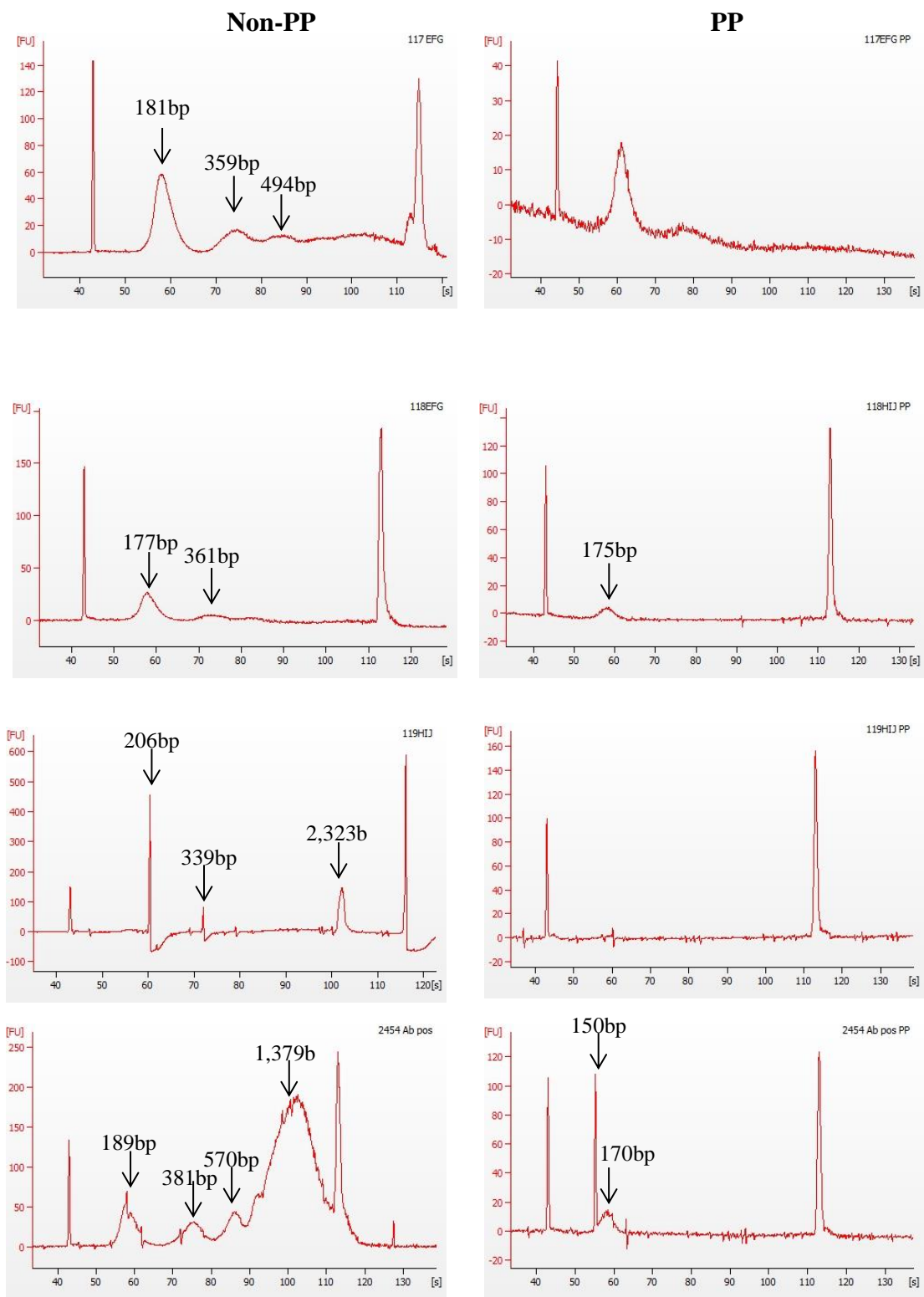


**Figure 6-8: Agilent 2100 Bioanalyzer electropherograms for three maternal samples (117, 118 and 119) and non-maternal sample (2454) before (non-PP, left column) and after (PP, right column) PP gel electrophoresis. The peak generated by maternal sample 117 (PP) could not be determined.**

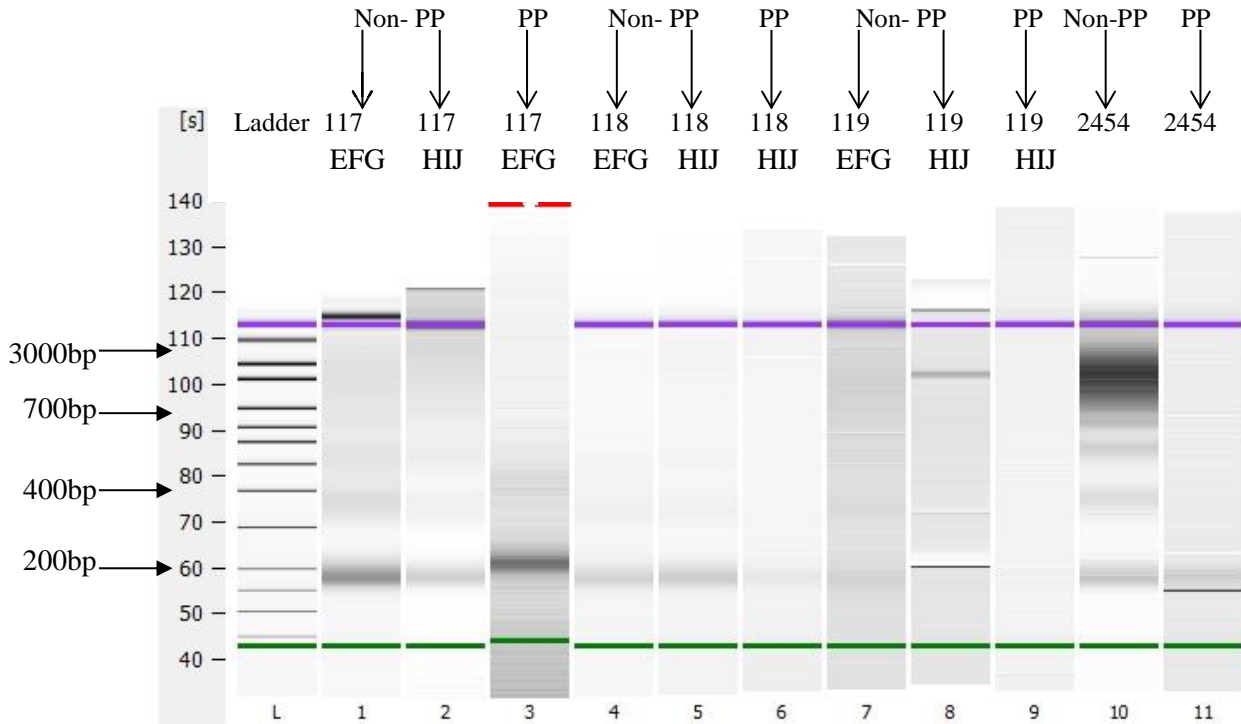


**Figure 6-9: Electrophoresis gel-like image generated by the Agilent 2100 Bioanalyzer showing the ladder (L) and results for three maternal samples (117, 118 and 119) and one non-maternal sample (2454) before (non-PP) and after (PP) PP gel electrophoresis.**

The non-PP aliquots of maternal samples 117 (Lane 1 and 2) and 118 (Lane 4 and 5) all demonstrated multiple bands at around 200bp, 400bp and 500bp. Non-PP aliquot of sample 117 was unsuccessful and the non-PP aliquot of maternal sample 118 only demonstrated a clear band at ~200bp. The non-PP aliquots of maternal sample 119 (Lane 7 and 8) illustrated variations in banding patterns. Sample 119EFG showed a similar pattern to non-PP aliquots of samples 118 and 119. However, the 119HIJ aliquot demonstrated two clear bands at 200bp and 1000bp. The PP aliquot of sample 119HIJ illustrated no clear banding. Non-maternal sample 2454 illustrated bands at 200bp, 400bp, 500bp and 700bp, but also illustrated a thick band at 1000bp for the non-PP aliquot. In contrast, the PP aliquot of non-maternal sample 2454 only demonstrated a fine clear band at 150bp and a thicker less intense band at 170bp.

The cffDNA fractions were calculated based on the concentration of the *RHD* target in comparison the reference gene (*EIF2C1*) and the results are shown in Table 6-3 and Figure 6-10. The results illustrated no *RHD* amplification for maternal sample 130 as expected since both the mother and the fetus are *RHD* negative. Eight of the Maternal samples (117, 118, 120, 122, 123, 124, 131 and 132) illustrated an increase in cffDNA fraction for both target assays (*RHD5/ EIF2C1* and *RHD7/ EIF2C1*) (Table 6-3) (Figure 6-10). The increase in cffDNA fraction was highly varied (Figure 6-11), ranging from 1.9% (maternal sample 131) to 46.3% (maternal sample 118) based on the mean of both assays. Maternal sample 133 illustrated a 6.7% increase in cffDNA fraction following PP gel electrophoresis when calculated using the *RHD7/ EIF2C1* assay, but demonstrated a 2.7% decrease in cffDNA when calculated using the *RHD5/ EIF2C1* assay (Figure 6-11). However, the non-PP aliquot of maternal sample 133 illustrated similar cffDNA fractions of 9.35% and 11.80% for the *RHD5* and *RHD7* multiplex assays, respectively.

Maternal sample 119 illustrated amplification of *RHD* fetal specific targets for the non-PP aliquot (Table 6-3) (Figure 6-12 A and C). However, the PP aliquot of maternal sample 119 only illustrated one positive droplet for the *RHD7* target (Figure 6-12 D) and no positive droplets for the *RHD5* target (Figure 6-12 B). Demonstrating that too much fetal DNA was lost for this sample during PP gel electrophoresis, which is likely to be attributed to low starting concentrations of total cell-free DNA (Table 6-3).

Maternal sample 132 illustrated typical cffDNA fractions when calculated based upon the *RHD5/ EIF2C1* assay (7.28% and 16.43% for non-PP and PP aliquots, respectively) (Figure 6-12 E and F). However, the cffDNA fractions calculated using the *RHD7/ EIF2C1* assay illustrated cffDNA >100% (125.26% and 164.09%, respectively) (Table 6-3). Figure 6-12 E-H demonstrates the increased number of *RHD7* positive droplets in comparison to the number of *RHD5* positive droplets. These results illustrated that maternal sample 132 expresses more

than one copy of the *RHD7* target region, one of which must be maternal in origin. This demonstrates that the mother from sample 132 must be a carrier for an *RHD* variant (the *RHD* $\Psi$  or DVI type 1-3) since only *RHD7* is expressed. By using the concentrations of each target gene and the reference gene, we were able to determine that only one of the maternal alleles expressed the variant *RHD* genotype, see below:

- *RHD5* = 1.85 copies/  $\mu$ L
- *RHD7* = 30.5 copies/  $\mu$ L
- *EIF2C1* = 49.75 copies/  $\mu$ L (maternal + fetal)
- *EIF2C1* (maternal only) =  $49.75 - (2 \times 1.85) = 46.05$  copies/  $\mu$ L (assuming *RHD5* and *EIF2C1* are equally expressed).

If we assume that *RHD5* and *RHD7* are present in equal proportions and that the fetus expresses either one or two copies of the *RHD7* target, we can subtract this from the *RHD7* concentration to determine the maternal proportion ( $30.5 - 1.85 = \mathbf{28.65}$  copies/  $\mu$ L (one fetal copy of *RHD7*)) or  $30.5 - (2 \times 1.85) = \mathbf{26.8}$  copies/  $\mu$ L (two fetal copies of *RHD7*)). By using the maternal only concentrations, the maternal specific ratio of *RHD7*/ *EIF2C1* was then calculated:

- Ratio based on single fetal *RHD7* expression calculation: Maternal *RHD7* / Maternal *EIF2C1* =  $28.65$  copies/  $\mu$ L /  $46.05$  copies/  $\mu$ L = **0.62**.
- Ratio based on dual fetal *RHD7* expression calculation: Maternal *RHD7*/ Maternal *EIF2C1* =  $26.8$  copies/  $\mu$ L /  $46.05$  copies/  $\mu$ L = **0.58**.

Since both ratios illustrated a ratio closer to 0.5 than 1, it showed that the mother of sample 132 is hemizygous for the *RHD7* gene loci rather than homozygous. It is difficult to determine whether the fetus expresses one or two copies of the *RHD7* target. However, since the ratio calculated based upon the fetus displaying two copies of *RHD7* is closer to 0.5, it is more feasible that the fetus is homozygous for *RHD7*. In this instance the fetus would have

inherited D-variant allele rather than the D-negative allele from the mother in addition to the paternally inherited *RHD* allele.

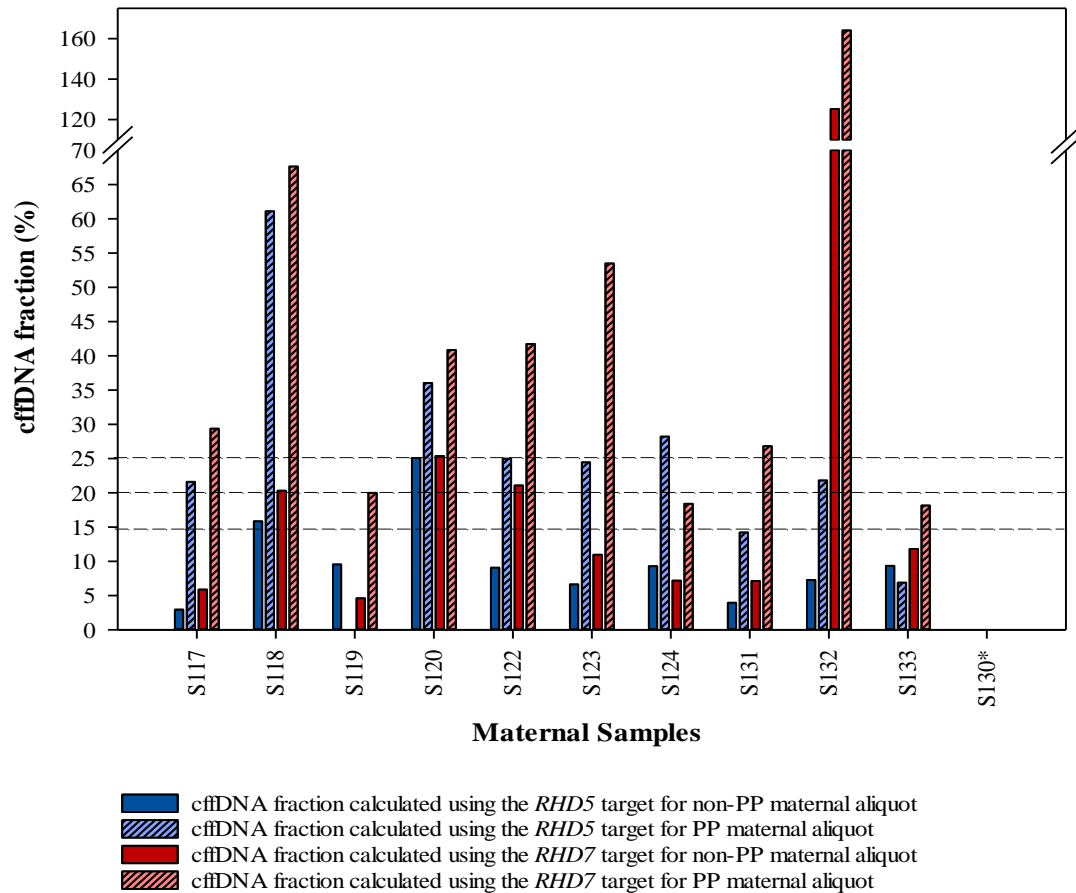


**Figure 6-10: Bar chart illustrating the cffDNA fraction (%) for maternal samples collected in Streck BCTs (n=11) before (non-PP (plain colour)) and after (PP (striated colour)) PP gel electrophoresis using concentrations (copies/  $\mu$ L) generated by ddPCR.** The cffDNA fraction was calculated by dividing each target concentration (copies/  $\mu$ L), *RHD5* (blue) and *RHD7* (red), by the reference (*EIF2C1*) concentration (copies/  $\mu$ L) (refer to 2.9.4). The dashed lines at 15%, 20% and 25% illustrate three cut-off points for fetal T21 NIPD (Table 6-5). For example, all eleven maternal samples (PP) had at least one target above the 15% threshold, whereas the non-PP aliquots only had four maternal samples that

displayed at least one target above the 15% cut-off. At 25% cut-off, none of the non-PP maternal samples displayed cfDNA fractions >25%, whereas seven of the PP aliquots had at least one target above this threshold.

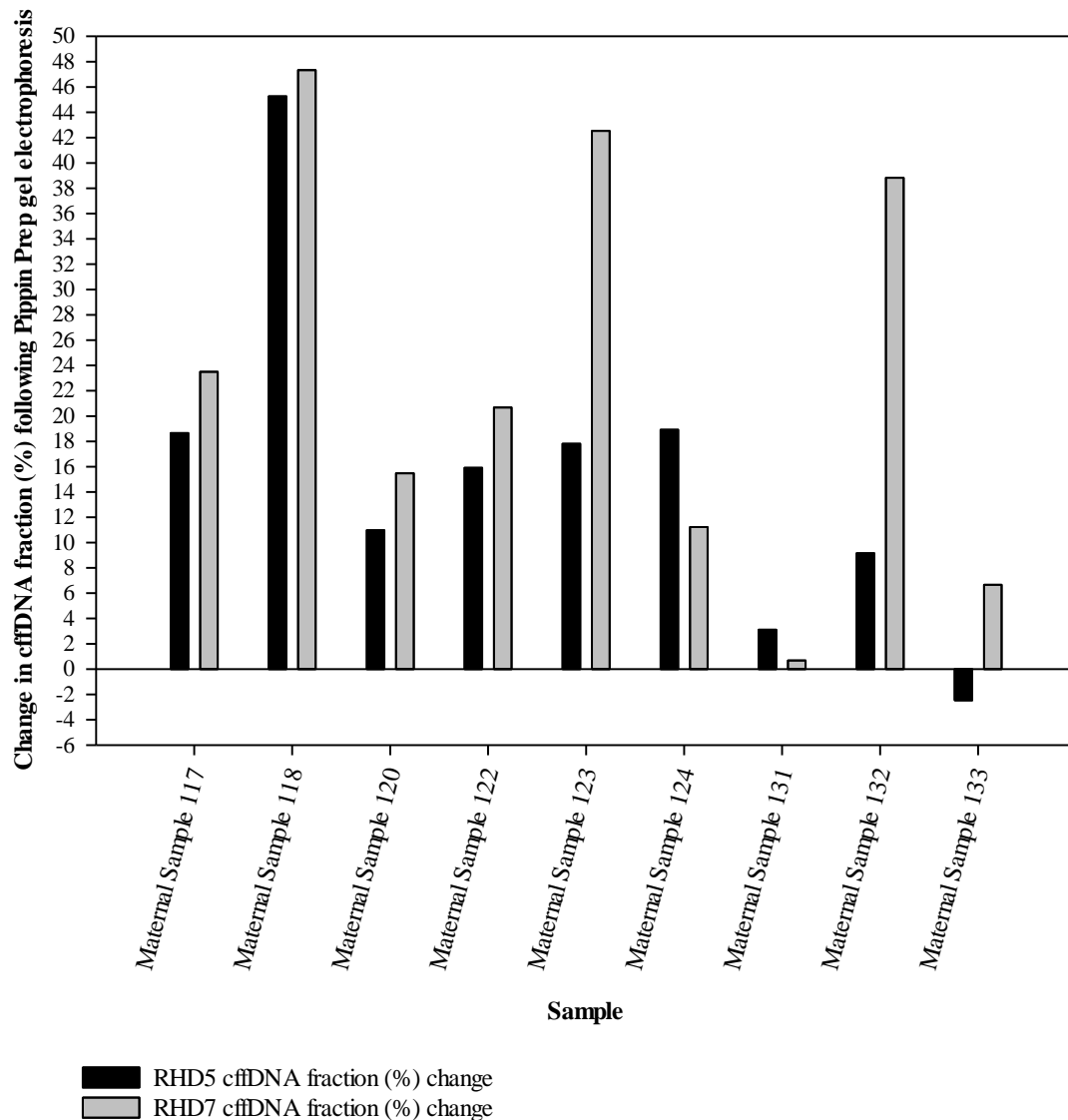
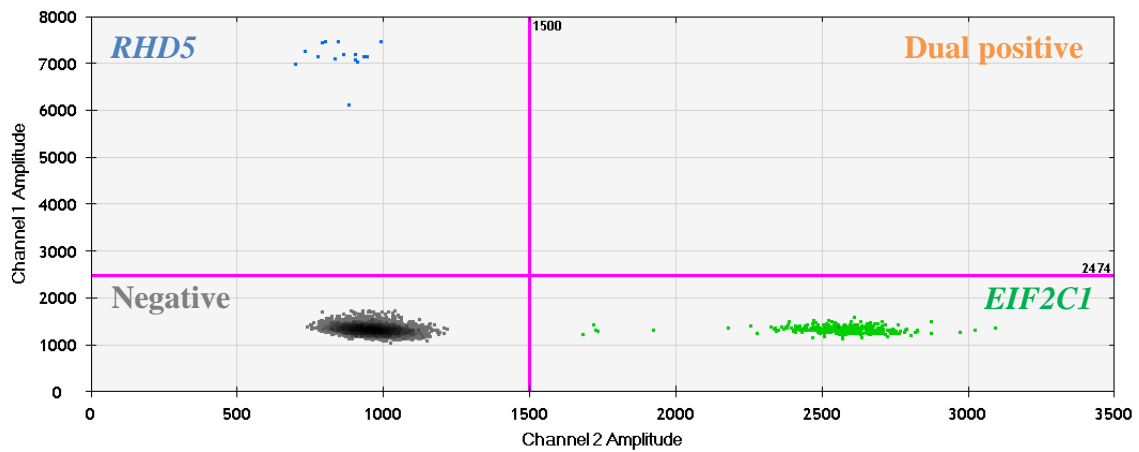


**Figure 6-11: Bar chart illustrating the cfDNA fraction (%) change following PP gel electrophoresis for nine maternal samples (117, 118, 120, 122, 123, 124, 131, 132 and 133). Sample 130 was excluded since this fetus was *RHD*-, and maternal sample 119 was excluded since *RHD5* target was not detected following PP gel electrophoresis. The results illustrated that all cfDNA fractions increased when calculated using the *RHD7/ EIF2C1***

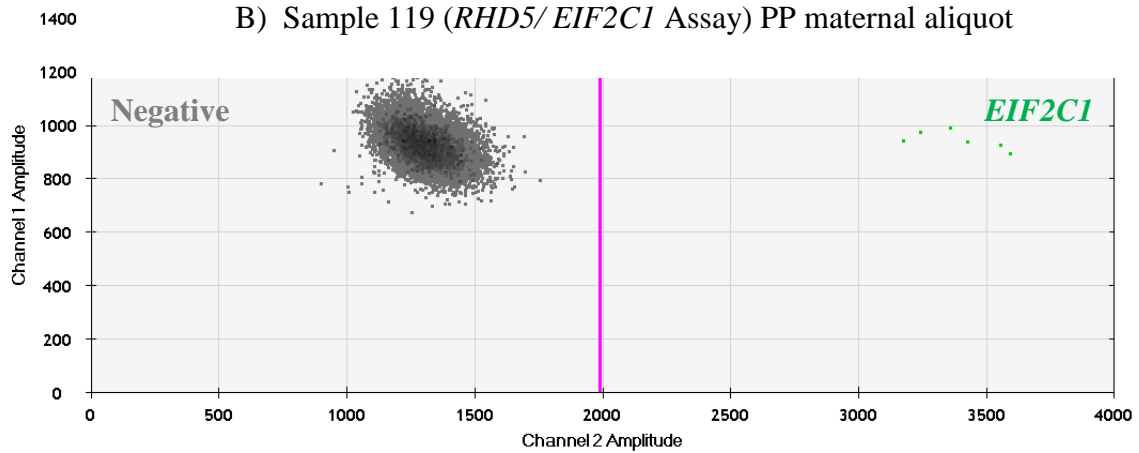


assay. The cffDNA fractions calculated using the *RHD5/ EIF2C1* assay illustrated an increase in cffDNA fractions for eight maternal samples. However, for maternal sample 133 a 2.47% decrease in cffDNA fraction following PP gel electrophoresis was seen.

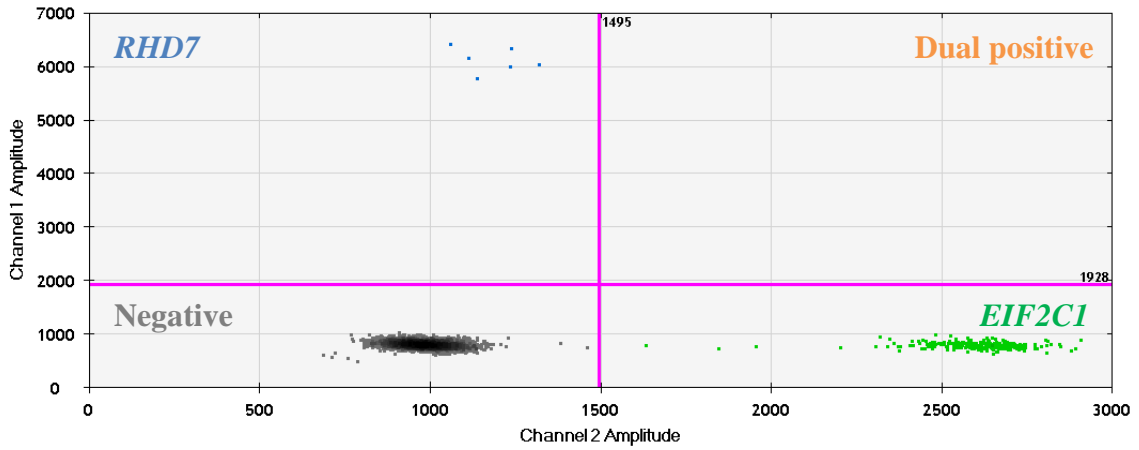
A) Sample 119 (*RHD5/ EIF2C1* Assay) non-PP maternal aliquot



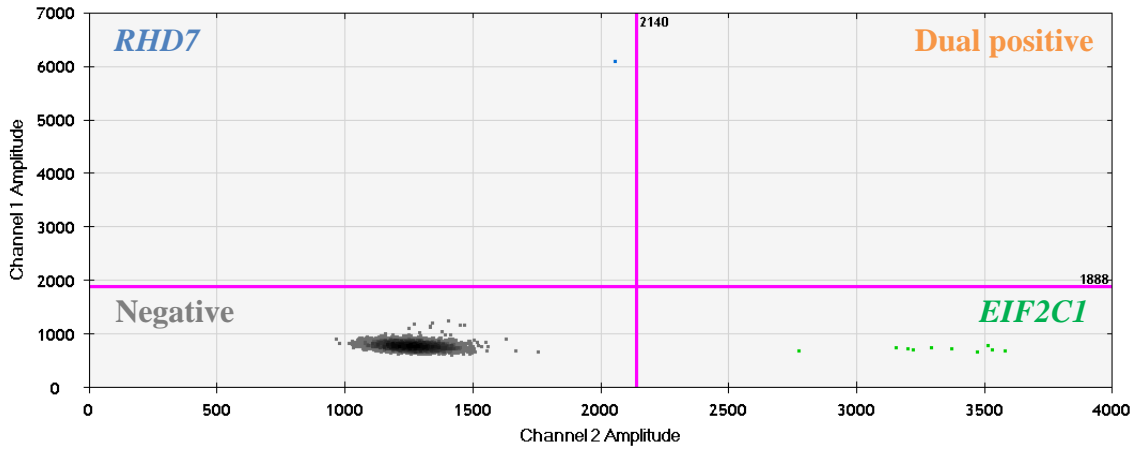
B) Sample 119 (*RHD5/ EIF2C1* Assay) PP maternal aliquot



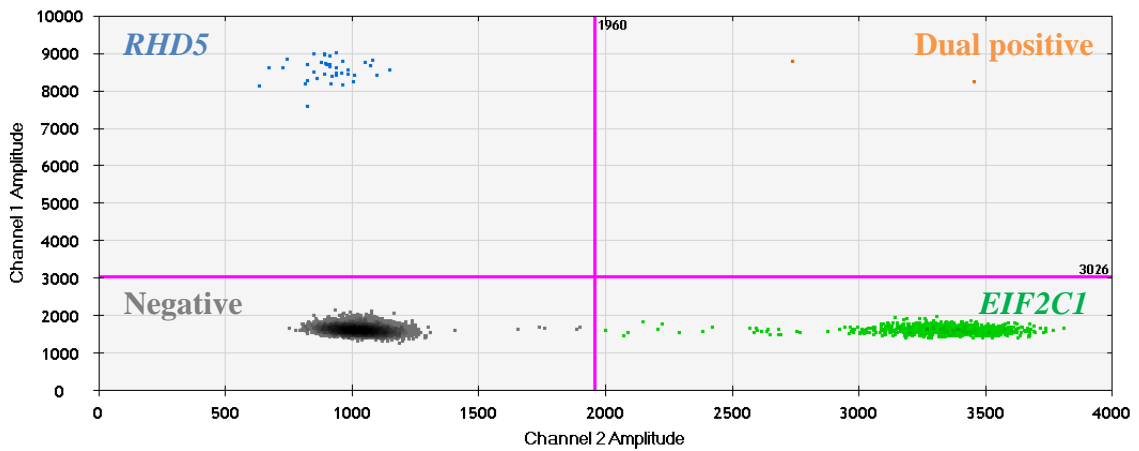
C) Sample 119 (*RHD7/ EIF2C1* Assay) non-PP maternal aliquot



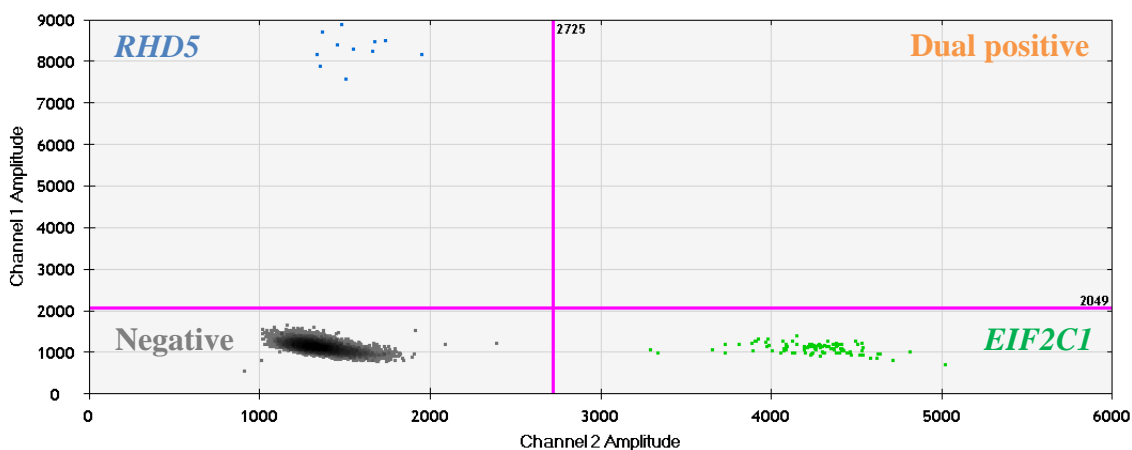
D) Sample 119 (*RHD7/ EIF2C1* Assay) PP maternal aliquot



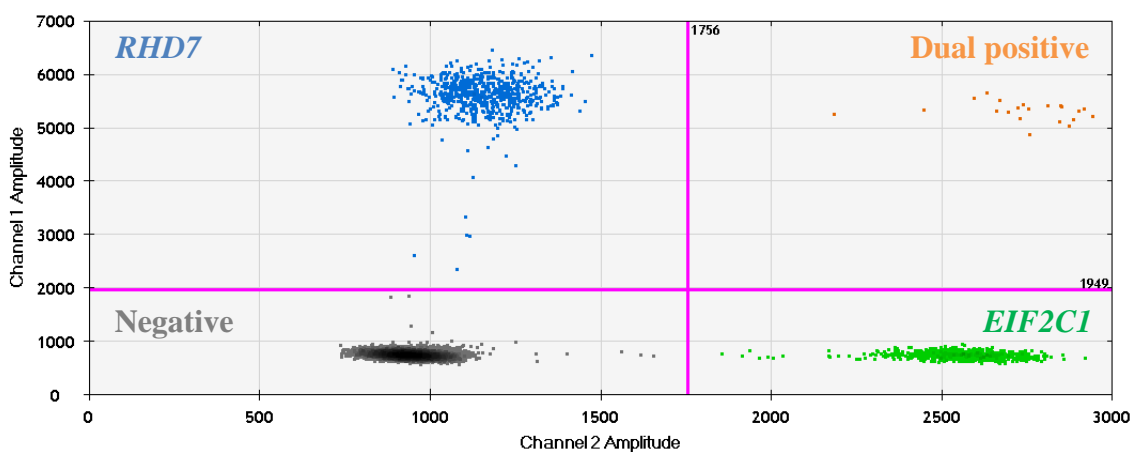
E) Sample 132 (*RHD5/ EIF2C1* Assay) non-PP maternal aliquot



F) Sample 132 (*RHD5*/*EIF2C1* Assay) PP maternal aliquot



G) Sample 132 (*RHD7*/*EIF2C1* Assay) non-PP maternal aliquot



H) Sample 132 (*RHD7*/*EIF2C1* Assay) PP maternal aliquot

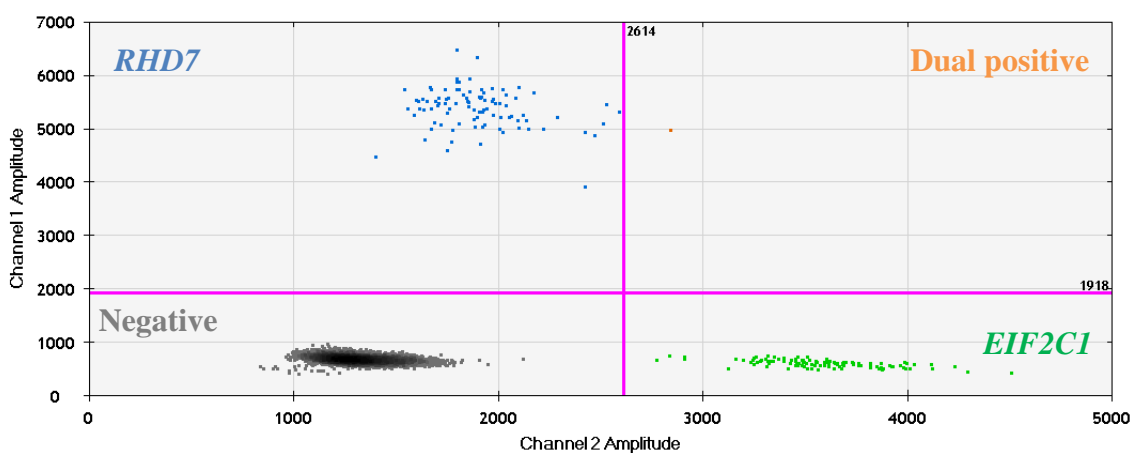


**Figure 6-12: 2D Amplitude plots generated by ddPCR for maternal samples 119 (A-D) and 132 (E-H) for non-PP aliquots (A, C, E and G) and PP aliquots (B, D, F and H).** The Results illustrated that the non-PP aliquot of sample 119 showed positive droplets for both *RHD5* (A) and *RHD7* (C) targets. However, the PP aliquot of sample 119 did not show any positive *RHD5* amplification (B) and only illustrated a single positive droplet for *RHD7* amplification (D). The results for sample 132 illustrated amplification of *RHD5* for both non-PP (E) and PP (F) aliquots indicative of cffDNA fractions (7.28% and 16.4%, respectively). Contrastingly, analysis of maternal sample 132 using the *RH7/ EIF2C1* assay illustrated a dramatic increase in number of positive *RHD7* targets for both non-PP and PP aliquots, resulting in cffDNA fractions >100% (Table 6-3).

The results illustrated low numbers of positive droplets for maternal samples, particularly following PP gel electrophoresis (Figure 6-12), and sample 119 following PP there were no positive fetal specific droplets. Therefore, to enhance sensitivity more data target points need to be determined. This could be achieved in future assays by increasing the starting amount of DNA added, firstly by extracting from larger volumes of maternal plasma (and eluting in the same volume (40  $\mu$ L)) and secondly by increasing primer/ probe starting concentrations so that a larger volume (>5  $\mu$ L) of DNA can be added per 20  $\mu$ L reaction. In addition, merging multiple wells help to increase the number of informative droplets.

PP gel electrophoresis and ddPCR analysis was repeated for three maternal samples: 131HIJ (as previous results illustrated low increase in cffDNA fraction), 132HIJ (as previous result illustrated potential maternal D-variant status) and 133HIJ (as previous result illustrated decline in cffDNA fraction based upon *RHD5* calculation). Previous optimisation experiments using maternal sample 119HIJ prevented repeat experiment for this sample. The results illustrated that maternal sample 133HIJ still illustrated a decline in cffDNA fraction based upon the *RHD5* assay (Table 6-4) (Figure 6-13) and also illustrated a lower increase in cffDNA fraction for the *RHD7* assay (from a 6.7% increase to a 1.7% increase in cffDNA fraction).

The repeat experiment for maternal sample 132HIJ also illustrated cffDNA fractions >100% for the *RHD7* assay and a relatively normal cffDNA for the *RHD5* assay (21.8%) (Table 6-4) (Figure 6-13). The repeat experiment for maternal sample 131HIJ showed an improved increase in cffDNA fraction compared to the initial run for both the *RHD5* assay (from a 3.1% increase to a 7.1% increase in cffDNA fraction) and the *RHD7* assay (from a 0.68% increase to a 19.3% increase in cffDNA fraction) (Figure 6-13).

**Table 6-4: Results for repeat ddPCR experiment for maternal samples 131-133HIJ (PP) showing cffDNA fractions based on concentration of target (FAM) and reference (*EIF2C1*) genes for multiplex reactions *RHD5* (FAM)/ *EIF2C1* (HEX) and *RHD7* (FAM)/ *EIF2C1* (HEX). The results for the first run following PP gel electrophoresis and non-PP aliquots are shown in Table 6-3.**

	Sample	Conc (ng/ul)	RHD5/EIF2C1			RHD7/EIF2C1		
			<i>RHD5</i> -FAM (copies/μl)	<i>EIF2C1</i> -HEX (copies/μl)	Fetal Fraction* /ratio	<i>RHD7</i> -FAM (copies/μl)	<i>EIF2C1</i> -HEX (copies/μl)	Fetal Fraction (%) / *ratio
Controls 12/03/15	NTC	-	0	0	-	0	0	-
	276R -	-	0	72.6	-	0	71.3	
	2470 +	-	110	111	0.994	96.1	93.1	1.03
Maternal Samples 12/03/15	131HIJ PP	5.2	0.221	3.1	<b>14.2</b>	0.363	2.7	<b>26.8</b>
	132HIJ PP	4.4	0.532	4.88	<b>21.8</b>	3.66	3.87	<b>189</b>
	133HIJ PP	2.9	0.0412	2.39	<b>3.44</b>	0.173	2.56	<b>13.5</b>

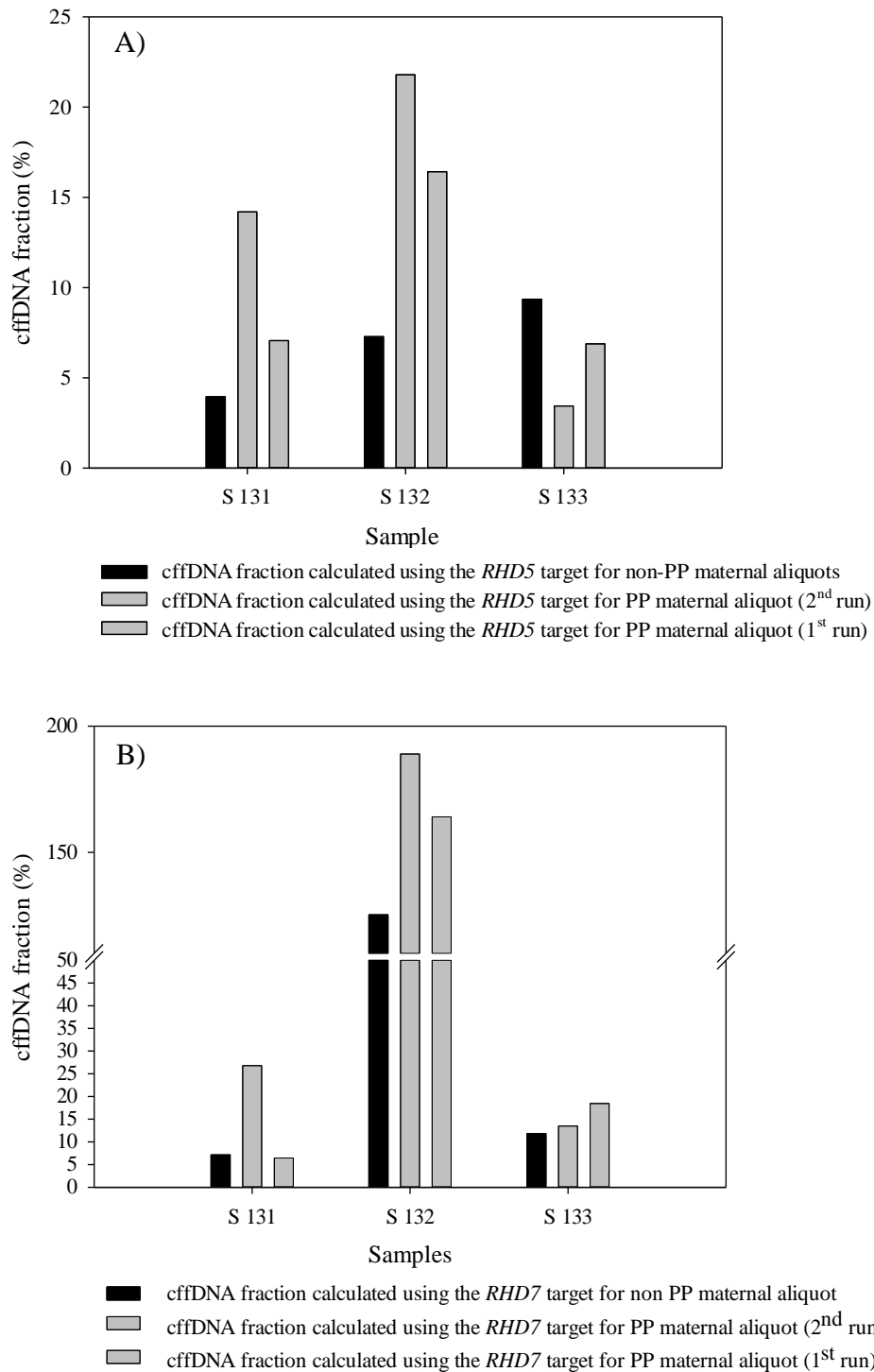


**Figure 6-13: Bar chart illustrating the cffDNA fraction (%) for maternal samples 131HIJ, 132HIJ and 133HIJ based on calculations using the *RHD5* (A) and *RHD7* (B) fetal target concentrations (copies/  $\mu$ L) generated by ddPCR for a single non-PP aliquot (black) and two repeats of the PP aliquot (grey).**

In a previous study, it was determined (using spiked samples) that cffDNA fractions of  $\geq 25\%$  are required to accurately determine fetal trisomy using a digital PCR platform (~770 partitions) (Table 1-4). However, since more partitions are produced using the ddPCR platform (up to 20,000), it is feasible that lower cffDNA fractions could be required for accurate diagnosis of fetal Trisomy from maternal plasma samples. Table 6-5 illustrates the number of samples that would have been feasible for T21 analysis before and after PP gel electrophoresis based on cut off cffDNA fractions at 15%, 20% and 25%. The results illustrated that if cffDNA fractions of 25% were required only 2/10 samples would have been acceptable for T21 analysis. However, following PP gel electrophoresis, 8/10 samples produced cffDNA fractions  $\geq 25\%$ . If the cut off cffDNA fraction could be lowered to 15%, then all samples would have been valid for T21 analysis when enriched using PP gel electrophoresis. Alternatively, a cut off of 15% cffDNA, only 4/10 samples would have been adequate for T21 analysis without any prior enrichment (Table 6-5). To determine the cffDNA fraction required for NIPT of fetal trisomy subsequent spiking experiments were conducted (6.3.2).



**Table 6-5: Number of samples acceptable for T21 analysis (with at least one target above threshold) before (non-PP) and after (PP) PP gel electrophoresis for cffDNA fraction cut-offs of 15%, 20% and 25%. For graphic representation of cffDNA fractions determined for each target (*RHD5* and *RHD7*) against each threshold (dashed line) refer to Figure 6-10.**

<b>cffDNA fraction cut-off (%)</b>	<b>Number of samples with at least 1 target over threshold (before PP)</b>	<b>Number of samples with at least one target over threshold (after PP)</b>
<b>25%</b>	4/10 (maternal samples; 118, 120, 122* and 132*)	10/10 (maternal samples 117, 118, 119*, 120, 122, 123, 124, 131, 132 and 131)
<b>20%</b>	3/10 (maternal samples; 120, 122* and 132*)	10/10 (maternal samples 117, 118, 119*, 120, 122, 123, 124, 131, 132 and 131)
<b>15%</b>	2/10 (maternal samples; 120 and 132*)	10/10 (maternal samples 117, 118, 119*, 120, 122, 123, 124, 131, 132 and 131)

\*Sample only illustrated cffDNA fraction >threshold based on *RHD7* and not *RHD5* calculation (refer to 2.4.9). For sample 119, no *RHD5* target was detected for PP sample.

\*\* Sample only illustrated cffDNA fraction >threshold based on *RHD5* and not *RHD7* calculation (refer to 2.4.9).

## 6.2.2 Spiking Experiments

### 6.2.2.1 *Male gDNA spike experiments to determine detection of low copy targets*

Before determining the cffDNA fraction required for T21 analysis, male gDNA spike experiments were conducted to determine the ability of ddPCR to detect a) a single copy (*SRY*) and b) a multiple-copy (*TSPY1*) Y-specific target, when male gDNA is spiked into female gDNA (3.2.3) down to 1% and 0.1%, respectively. Figure 6-14 illustrates the ddPCR results for the *SRY* (FAM) / Xp22.3 (HEX) multiplex reactions. The results showed one dual positive droplet in the NTC and the 100% male control sample illustrated a 49.46% fractional

abundance of the Y-target (50% expected) (Table 6-6). The results illustrated 1181 *SRY* events and 1207 Xp22.3 events for the male control sample (2388 total) and the female control illustrated twice as many Xp22.3 events (2359) and no *SRY* events as expected (Figure 6-14). Since there was only a 1.2% difference between the total number of events for male and female gDNA control samples, this illustrated accurate dilution of both samples. If the results had revealed slightly higher concentrations of either the male gDNA or the female gDNA the data generated from the spiked samples would have been skewed.

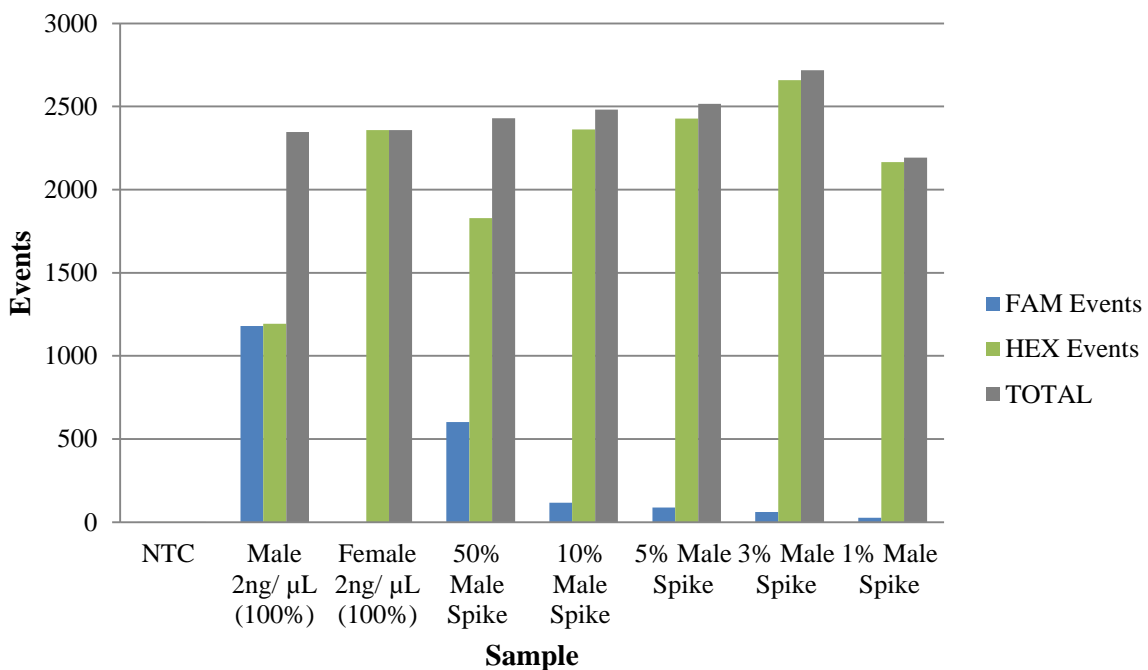


**Figure 6-14: Clustered bar-chart illustrating the number of positive droplets (Events) for *SRY* (FAM) (blue), Xp22.3 (HEX) (green) and the total (grey) generated by ddPCR for NTC, 100% male gDNA, 100% female gDNA and male gDNA spikes from 50% (wt/wt) down to 1% (wt/wt). The NTC shows no amplification and the Female control shows only amplification of the Xp22.3 (HEX) reference, which generated roughly twice as many positive droplets compared to the Xp22.3 number of events generated by the Male control (refer to Table 6-6). The Male control also illustrated a similar number of events for**

*SRY* and Xp22.3 (refer to Table 6-6). The spikes demonstrated a decrease in *SRY* events, but still detect 16 positive droplets for the 1% Male to 99% Female gDNA spike (wt/wt).

Table 6-6 summarises the number of events for *SRY* and Xp22.3 (Figure 6-14) for all samples and also illustrated the expected and actual fractional abundance of *SRY*. The results demonstrated that even when spiked into female gDNA at 1%, the ddPCR platform could still detect 17 droplets containing The Y-specific target. Chi-squared analysis of the expected and observed *SRY* fractional abundance (Table 6-6) revealed that only the 100%, 50% and 10% (wt/wt) Male gDNA spikes illustrated no significant difference. Although, the 5%, 3% and 1% (wt/wt) Male gDNA spiked samples showed similar expected and observed values (Table 6-6), the Chi-squared test revealed that there was significant differences between the observed and expected *SRY* fractional abundance for the 5% (wt/wt) Male spike (<0.05), the 3% Male spike (<0.001) and the 1% Male spike (<0.001). This indicates that more care is required when producing spikes <10%. However, it is important to note that for values less than 5, the Chi-squared test can be quite inaccurate. Lower droplet amplification was visible for the 5% spike compared to the 3% spike. This is likely to be due to handling error rather than decreased sensitivity, therefore it may be beneficial to include more replicates and exclude outlying results as commonly practiced with qPCR.

**Table 6-6: Events (positive droplets) for *SRY* (FAM) and Xp22.3 (HEX) illustrating the actual fractional abundance of *SRY* against the expected fractional abundance.**

	<b>SRY (H.P.T) FAM (events)</b>	<b>SD</b>	<b>Xp22.3 HEX (events)</b>	<b>SD</b>	<b>Ratio</b>	<b>Expected Fractional abundance of <i>SRY</i> (%)</b>	<b>Actual fractional abundance of <i>SRY</i> (%)</b>
<b>NTC</b>	1	-	1	-	-	-	-
<b>Male 2ng/ <math>\mu</math>L (100%)</b>	1181	18.33	1207	21.21	0.977	50%	49.46%
<b>Female 2ng/<math>\mu</math>L</b>	0	-	2359	52.27	-	0%	0%
<b>50% Male Spike</b>	604	5.53	1849	12.77	0.31	25%	24.62%

<b>10% Male Spike</b>	118	5.29	2363	22.34	0.0457	5%	4.76%
<b>5% Male Spike</b>	49	5.29	2427	32.51	0.0183	2.5%	1.98%
<b>3% Male Spike</b>	55	7.21	2660	51.97	0.0184	1.5%	2.03%
<b>1% Male Spike</b>	17		2167		0.00711	0.5%	0.79%

Figure 6-15 shows the 1D amplitude plots for *SRY* (A) and Xp22.3 (B) for all samples. The plots highlight the decline in number of positive droplets for the *SRY* target as the proportion of male gDNA is reduced from 50% down to 1% and the relative stability of positive droplets (events) for the Xp22.3 reference. In addition to being able to detect low levels of copy target number, these results also show the ability of ddPCR to accurately calculate the abundance of target in relation to the reference gene.

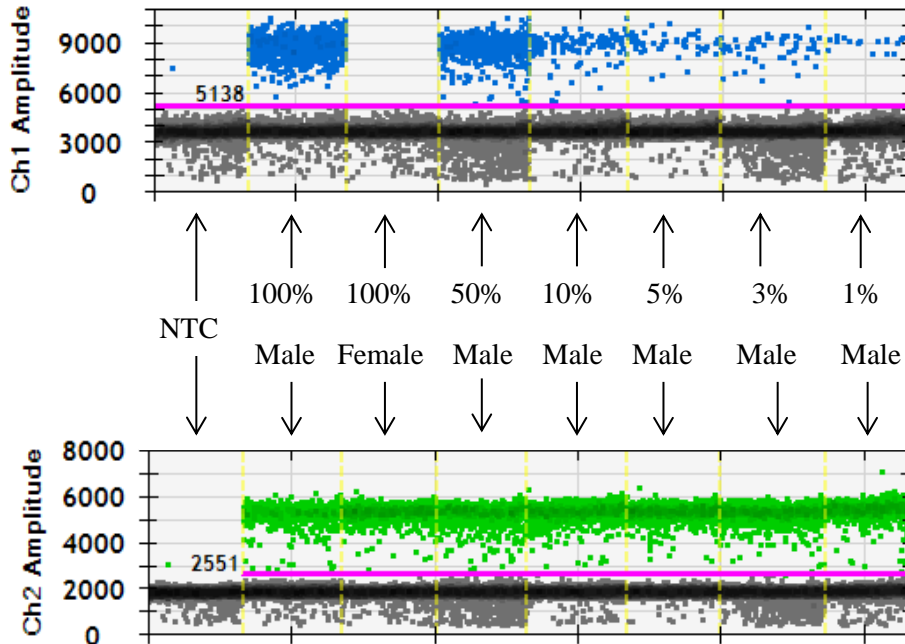


**Figure 6-15: 1D amplitude plots showing *SRY* (FAM) (blue) and Xp22.3 (HEX) (green) positive droplets (events) for NTC, female gDNA (100%), male gDNA (100%), 50% male spike, 10% male spike, 5% male spike, 3% male spike and 1% male spike. The**

pink line in each plot demonstrated the threshold set manual to best discriminate between positive (blue/ green) and negative (grey) droplets.

Subsequently, male gDNA was spiked into female gDNA at the following concentrations: 50%, 10%, 5%, 0.5% and 0.1%. These spiked samples, along with NTC, 100% male gDNA and 100% female gDNA were analysed on the ddPCR platform using the *TSPY1* (FAM)/ Xp22.3 (HEX) multiplex assay. In this assay lower fetal fractions were tested (0.5% and 0.1%) since the *TSPY1* is a multiple-copy target, and thus more droplets should be detectable at lower 'cffDNA fractions'. However, the data was only used to detect presence of *TSPY1* down to 0.1%, fractional abundance was not calculated due to the repetitive nature (up to 30 repeats, (Barrett *et al.*, 2012)) of the *TSPY1* fragment, and thus more reliable 'cffDNA fractions' are likely to be calculated using single-copy targets. Figure 6-16 illustrates the number of events for amplicon. The 100% female gDNA (2ng/  $\mu$ L) sample only showed amplification of the Xp22.3 reference and the NTC did not show any amplification. The 100% male gDNA sample and the male-spiked samples illustrated a decline in number of events as the fraction of male gDNA decreased as expected. The results demonstrated that even when male gDNA was spiked into female gDNA at 0.1%, the ddPCR platform could still detect 16 positive droplets.

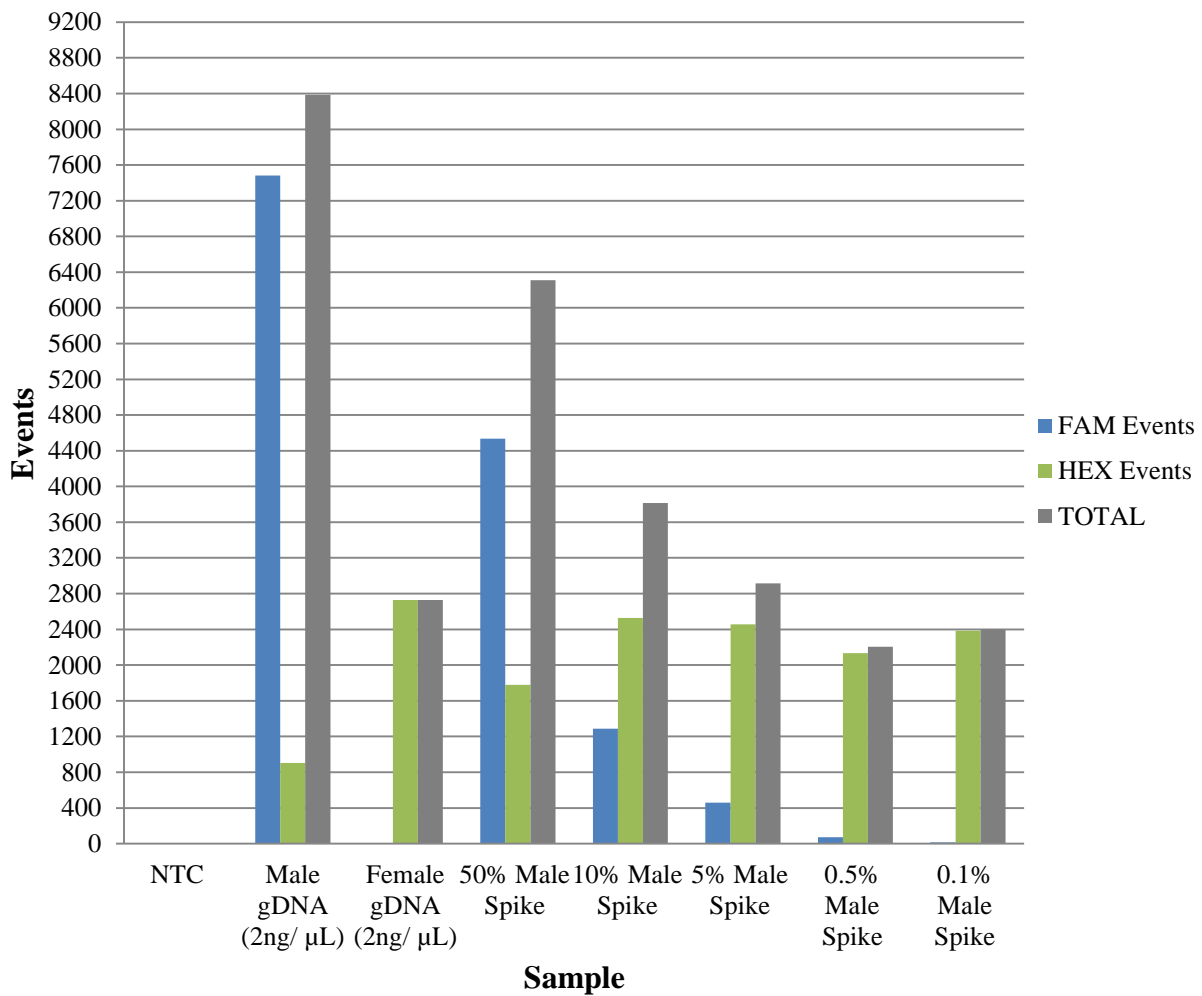


**Figure 6-16: Clustered bar-chart illustrating the number of positive droplets (Events) for *TSPY1* (FAM) (blue), Xp22.3 (HEX) (green) and the total (grey) generated by ddPCR for NTC, 100% male gDNA, 100% female gDNA and male gDNA spikes from 50% down to 0.1%. The results illustrate no amplification for the NTC and only amplification of Xp22.3 for the Female gDNA control sample. Though, 30 copies of *TSPY1* were expected, the Male gDNA control sample only illustrated ~10x the number of events for the *TSPY1* target against the single-copy reference target (Xp22.3). The spike samples illustrate a decline in the number of positive droplets as the percentage (wt/wt) of Male**

gDNA decreases. However, even when spiked at 0.1%, 16 *TSPY1* positive droplets were detected.

The concentration (copies/  $\mu\text{L}$ ) of *TSPY1* and Xp22.3 for each sample is shown in Figure 6-17. The results demonstrated an 11.3-fold increase in the proportion of *TSPY1* compared to the reference (Xp22.3) for the 100% male gDNA (2ng/  $\mu\text{L}$ ) sample (Figure 6-17). This is lower than expected since previous studies have identified that 30 repeats of the DYS14 region on the *TSPY1* gene are present (Barrett *et al.*, 2012). Based on the concentration of *TSPY1* at 100% (812 copies/  $\mu\text{L}$ ), Table 6-7 illustrates the expected and actual concentration of *TSPY1* for the 50%, 10%, 0.5% and 0.1% male-spiked samples. The results illustrated that larger variations in actual concentrations relative to the expected value were seen when lower amounts of male gDNA were present (Table 6-7). Figure 6-18 shows the 1D amplitude plots for *TSPY1* (A) and Xp22.3 (B) for all samples. The plots highlight the decline in number of positive droplets for the *TSPY1* target as the proportion of male gDNA is reduced from 50% down to 1% and the relative stability of positive droplets (events) for the Xp22.3 reference.

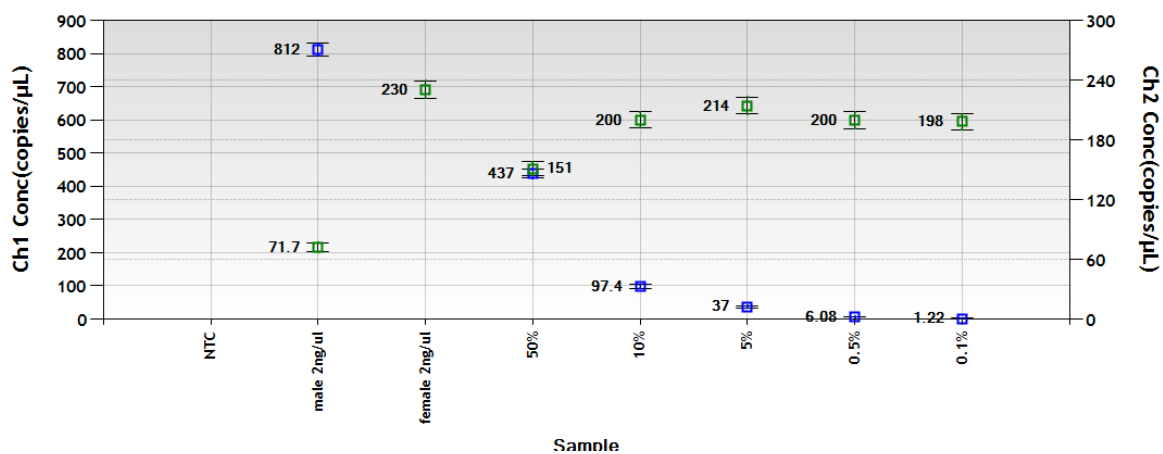


**Figure 6-17: Concentration (copies/  $\mu\text{L}$ ) of *TSPY1* (blue) and Xp22.3 (green) for NTC, 100% female gDNA, 100% male gDNA, 50% male spike, 10% male spike, 5% male spike, 0.5% male spike and 0.1% male spike.**

**Table 6-7: Expected concentrations (copies/  $\mu\text{L}$ ) of *TSPY1* based on concentration value for 100% male gDNA and actual concentration (copies/  $\mu\text{L}$ ).**

Sample	Actual concentration (A) (copies/ $\mu\text{L}$ )	Expected concentration (E) (copies/ $\mu\text{L}$ ) <sup>a</sup>	Difference $((A-E)/A)*100$ (%) <sup>b</sup>
100% male gDNA	812	812	n/a
50% male gDNA	437	406	7.1% increase
10% male gDNA	97.4	81.2	16.7% increase
5% male gDNA	37	40.6	8.9% decrease
0.5% male gDNA	6.08	4.06	33.2% increase
0.1% male gDNA	1.22	0.812	33.4% increase

<sup>a</sup> based on 100% male gDNA

<sup>b</sup> Change in concentration (copies/  $\mu\text{L}$ ) from expected concentration (based upon result for 100% male gDNA) to actual concentration.

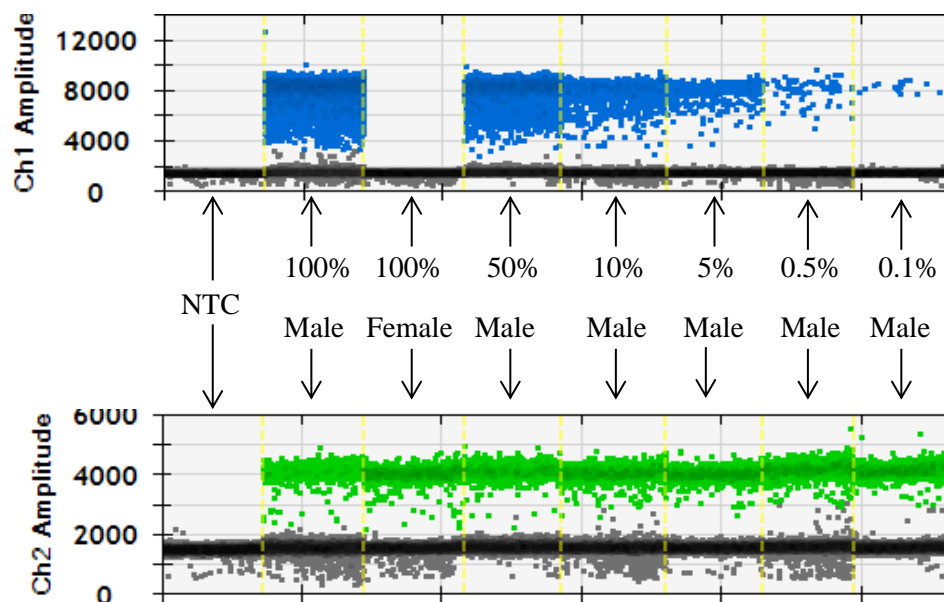


**Figure 6-18: 1D amplitude plots showing *TSPY1* (FAM) (blue) and Xp22.3 (HEX) (green) positive droplets (events) for NTC, female gDNA (100%), male gDNA (100%), 50% (wt/wt) Male gDNA spike down to 0.1% (wt/wt) Male gDNA spike.**



#### 6.2.2.2 T21 gDNA spike experiment to determine the minimal cfDNA fraction required for NIPT of fetal T21

To determine the minimal cfDNA fraction required to detect a significant difference between the T21 gDNA spike samples and the control D21 sample, two multiplex reactions were used. The first reaction involved a previously optimised ddPCR assay (*APP* (FAM)/ *EIF2C1* (HEX)) and the second introduced a new chromosome 21 target, *DSCR3*, also labelled with FAM and multiplexed against the *EIF2C1* (HEX) reference gene. Final concentrations of 300nM and 250nM were used for all primers and probes, respectively, for oligonucleotide information refer to Table 2-1. To evaluate the new chromosome 21 target amplicon (*DSCR3*), singleplex and multiplex reactions for *DSCR3* (FAM) and *EIF2C1* (HEX), were initially carried out at 60°C T<sub>a</sub>. The results illustrated a ratio of 1.46 for the T21 gDNA for both the singleplex and multiplex reactions, but a ratio closer to 1 was observed for the D21 cfDNA sample when carried out in a singleplex reaction (0.98) compared to the multiplex reaction (0.91) (Figure 6-19). Consequently, an annealing temperature gradient (from 57.8°C down to 55°C) was run to determine the optimum T<sub>a</sub> for the multiplex reaction. The clarity of droplet separation and the *DSCR3*/ *EIF2C1* ratio achieved for D21 sample (110W) was analysed to determine the optimum T<sub>a</sub>. The results illustrated that a ratio of 1 was achieved when amplified at 56°C and slightly higher ratios were obtained for the other T<sub>a</sub>'s (Figure 6-20). Since 57.8°C illustrated the second best ratio (1.01), droplet separation at this T<sub>a</sub> was compared to droplet separation at 56°C (Figure 6-21). The results demonstrated superior droplet separation at 56°C and therefore this T<sub>a</sub> was determined to be optimum for the *DSCR3* (FAM)/ *EIF2C1* (HEX) multiplex assay.

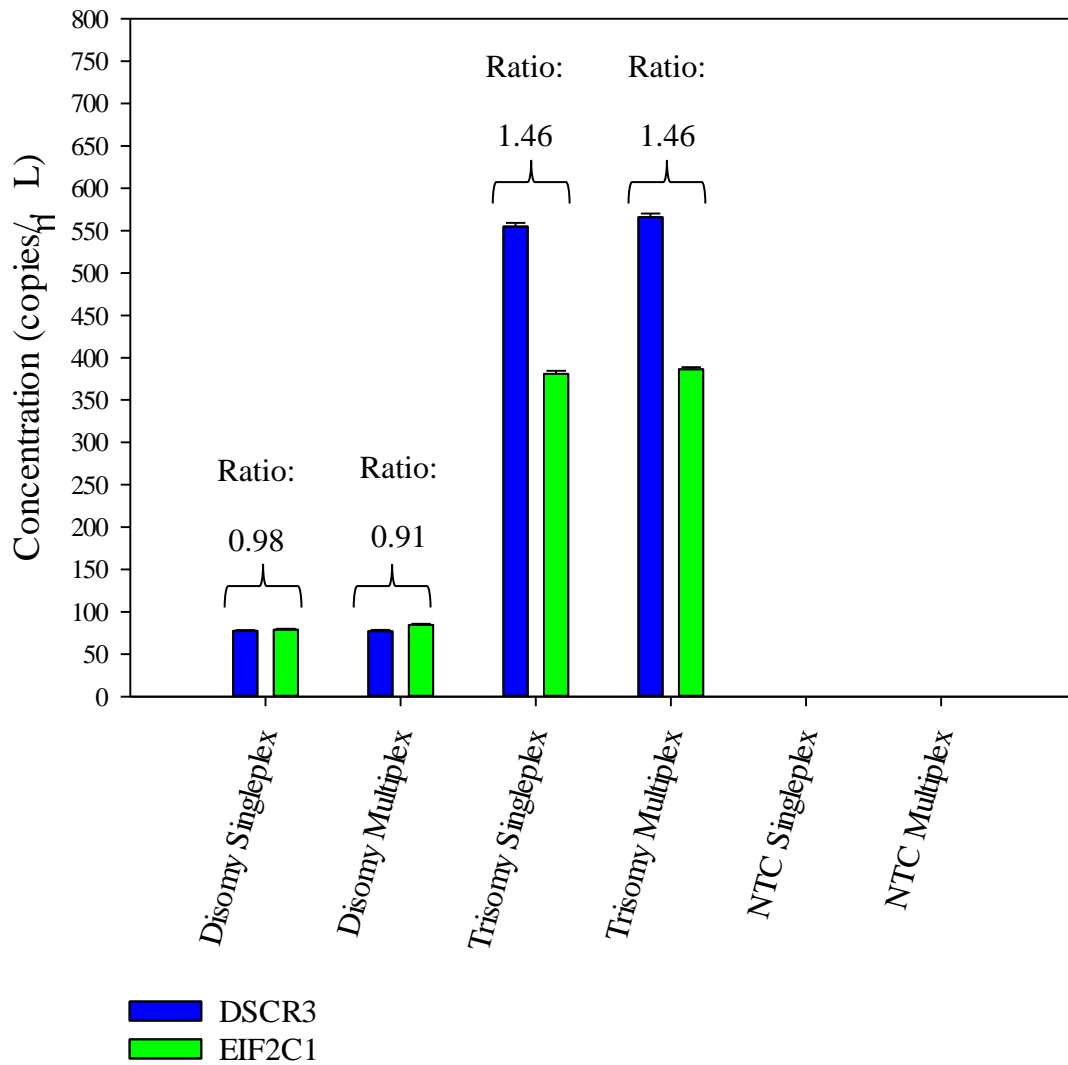


**Figure 6-19: Concentration (copies/  $\mu\text{L}$ ) of *DSCR3* (FAM) (blue) and *EIF2C1* (HEX) generated by ddPCR for D21 and T21 samples set up in both singleplex and multiplex reactions. The graph also illustrated the *DSCR3/ EIF2C1* ratio for all samples. This reaction was carried out at  $60^{\circ}\text{C}$   $T_a$ . The NTC did not illustrate any amplification. The T21 singleplex and multiplex reactions both generated a ratio (*DSCR3/ EIF2C1*) of 1.46, whereas the singleplex reaction for the D21 sample expressed a ratio closer to 1 (0.98) than the D21 multiplex reaction (0.91).**

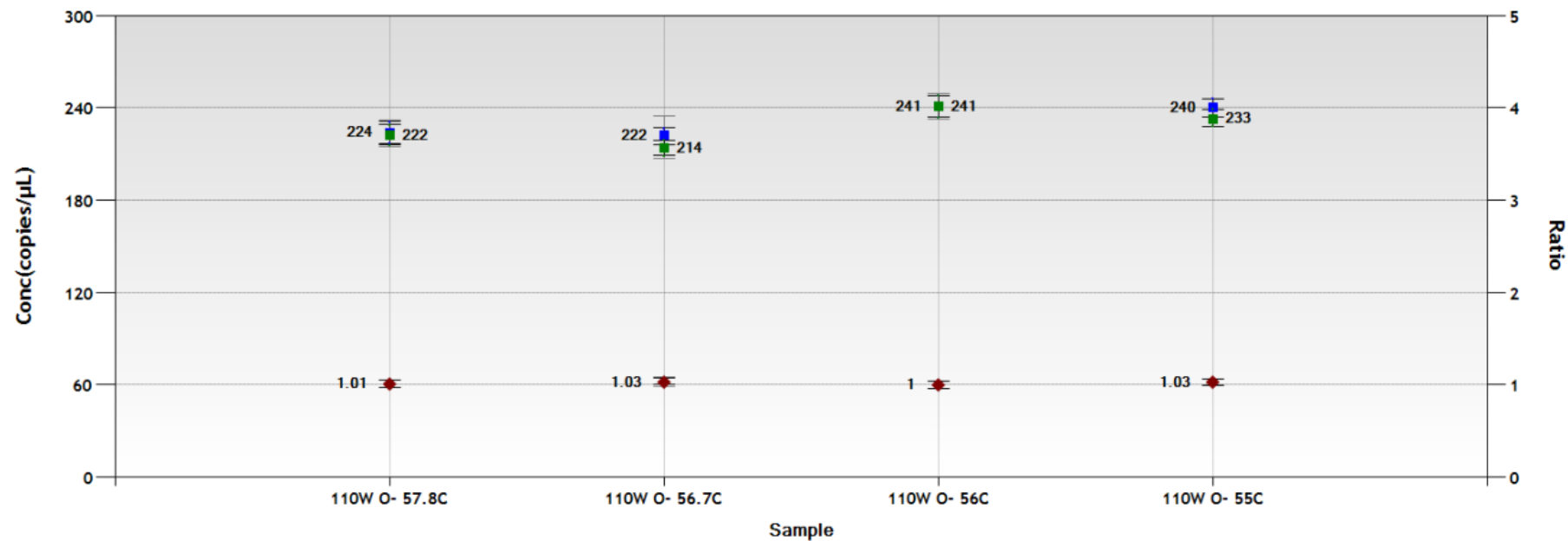


**Figure 6-20: Concentration (copies/  $\mu\text{L}$ ) of *DSCR3* (blue) and *EIF2C1* (green), and the *DSCR3/ EIF2C1* ratio (red) generated by ddPCR for disomy sample 110W at 57.8°C, 56.7°C, 56°C and 55°C. The results showed that the optimum ratio (closest to 1) was achieved at 56°C, which demonstrated 241 copies/  $\mu\text{L}$  of *DSCR3* and 241 copies/  $\mu\text{L}$  of *EIF2C1*, giving a ratio of exactly 1 (241/241).**

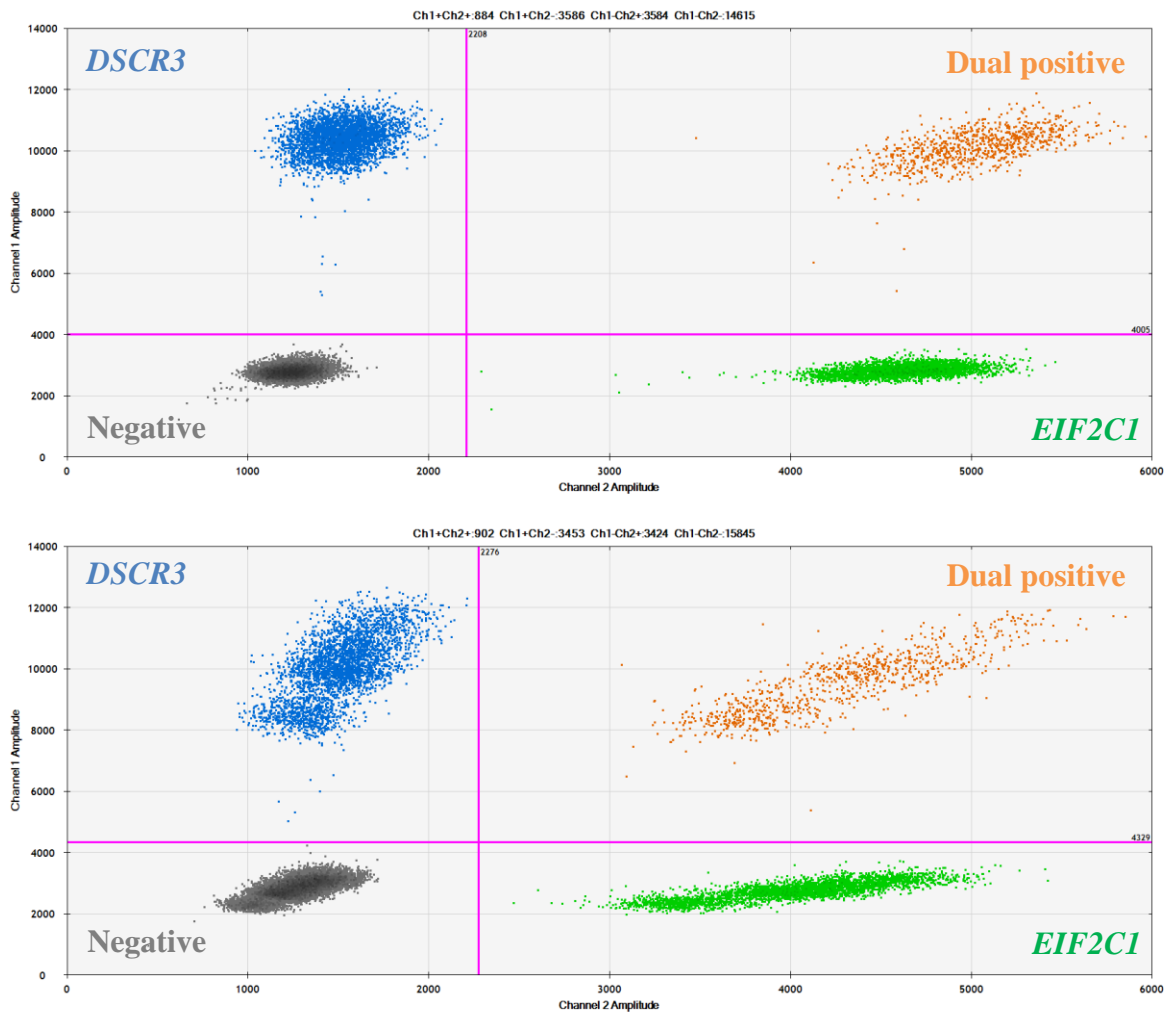


**Figure 6-21: 2D amplitude plot for multiplex reaction (*DSCR3* (FAM)/ *EIF2C1* (HEX)) showing droplet separation for Male gDNA amplification at 56°C  $T_a$  (top) and 57.8°C  $T_a$  (bottom).**

The primer aliquots of the *APP*-FAM/ *EIF2C1*-HEX multiplex assay were re-tested against pooled male (D21) and pooled female (D21) gDNA. The ddPCR run was carried out at 56.5°C, since this was determined to be optimum temperature in previous experiments (3.2.5). Both samples were tested in triplicate against NTC and the mean ( $\pm$ SD) concentration for the chr21-specific (*APP*) and chr1-specific (*EIF2C1*) target for each sample is illustrated in Figure 6-22. The results illustrated a ratio of 1.03 for both male and female gDNA

samples, which illustrated effective amplification since a ratio of 1 was expected. Previous  $T_a$  optimisation experiments illustrated a less desirable ratio (1.11) at 56°C (3.2.5). It is likely that the improved ratios could have been attributed to increased experience, since previous results were obtained shortly after the instillation of the ddPCR system or alternatively slight contamination of sample used in previous experiments. In addition, in this experiment results were carried out in triplicate, whereas the initial experiment was only carried out in duplicate.

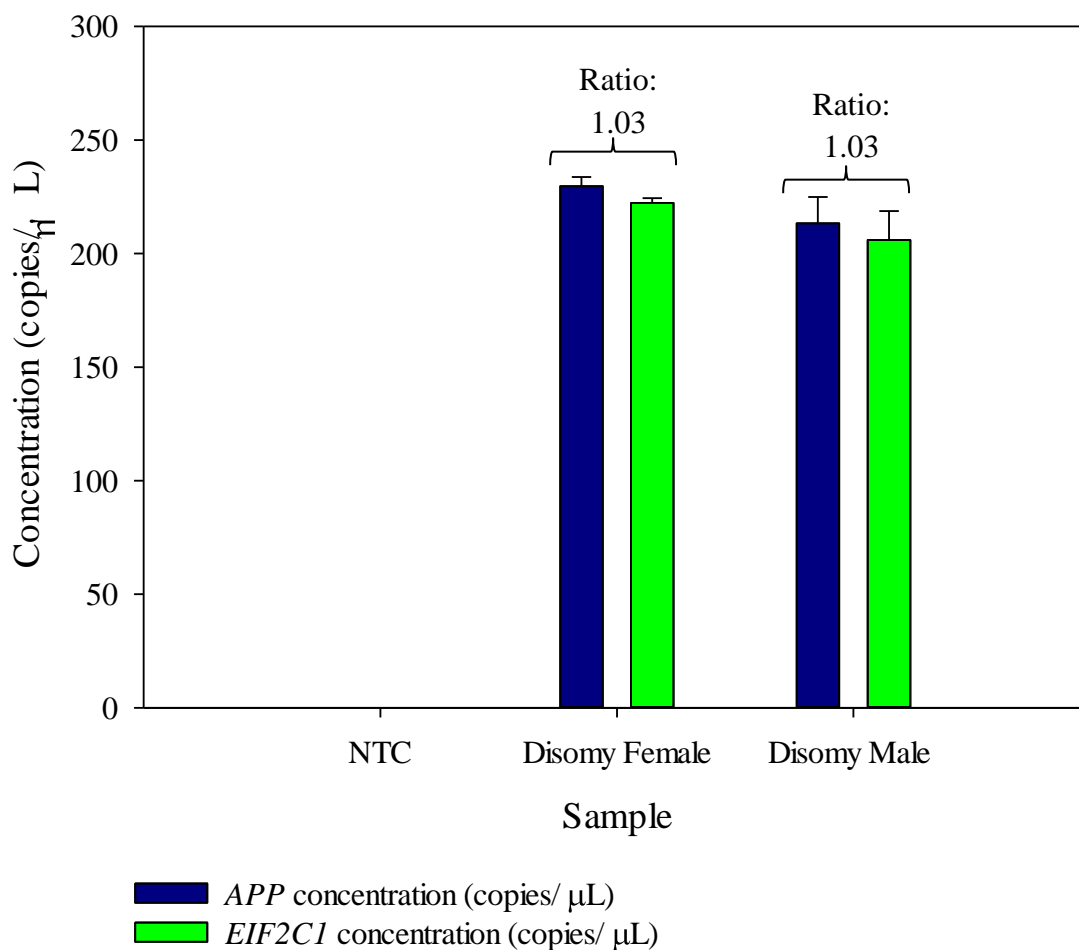


**Figure 6-22: Mean concentration (copies/ μL) ±SD of APP (FAM) (dark blue) and EIF2C1 (HEX) (green) generated by ddPCR for disomy (pooled) female gDNA (2ng/ μL) and disomy (pooled) male gDNA (2ng/ μL). The results illustrated a ratio (APP/ EIF2C1) of 1.03 for both male and female gDNA.**

Once both multiplex assays had been optimised, DNA was extracted from the buffy coat of human whole blood from sample 3135 (refer to 2.1.2), which was used for spiking experiments as opposed to pooled male or female gDNA samples (refer to 2.1.1). This is preferred since the T21 gDNA, obtained from a single patient, can be spiked into a single D21 sample, which is more representative of a maternal sample than pooled Female gDNA. The D21 sample (3135) was spiked with T21gDNA (refer to 6.2.3) from 50% down to 10%. These spiked samples were then tested in triplicate, alongside 100% D21 cfDNA (3135), 100% T21 gDNA and NTC. The first experiment was carried out for the *DSCR3*-FAM/*EIF2C1*-HEX multiplex assay, which was amplified at 56°C T<sub>a</sub>. Consequently, the experiment was repeated (using the same samples) but this time using the *APP*-FAM/*EIF2C1*-HEX multiplex assay, which was run at previously optimised T<sub>a</sub> (56.5°C). The concentration (copies/ µL) of each target and the consequent ratio (and ratio means) calculated for each sample are summarised in Table 6-8 and Table 6-9 for the *DSCR3*/*EIF2C1* and *APP*/*EIF2C1* assays, respectively. The expected ratio for each spiked and non-spiked sample are also shown (Table 6-8 and Table 6-9).

**Table 6-8: Summary of results illustrating the concentration (copies/  $\mu$ L) of *DSCR3* (FAM) and *EIF2C1* (HEX) and the ratios calculated based upon concentration for each triplicate reaction and the mean concentration. The mean ratio calculated (blue) is shown next to the expected ratio (green) for each non-spiked and T21 gDNA –spiked sample (from 50% down to 10%).**

<i>DSCR3/ EIF2C1</i>							
Samples	<i>DSCR3</i> - FAM (copies/ $\mu$ l)	Mean	<i>EIF2C1</i> - HEX (copies/ $\mu$ l)	Mean	Ratio	Mean Ratio*	Expected Ratio*
NTC	0	0	0	0	-	-	-
NTC	0		0		-		
NTC	0		0		-		
Disomy	455	406	446	388	1.02	1.05	1.00
Disomy	320		304		1.05		
Disomy	454		422		1.07		
T21 100%	602	606	394	394	1.53	1.54	1.50
T21 100%	613		388		1.58		
T21 100%	603		400		1.51		
T21 50%	546	536	424	427	1.29	1.26	1.25
T21 50%	533		437		1.22		
T21 50%	530		421		1.26		
T21 25%	526	503	455	444	1.16	1.13	1.13
T21 25%	496		432		1.15		
T21 25%	486		444		1.09		
T21 20%	484	478	428	430	1.13	1.11	1.10
T21 20%	462		432		1.07		
T21 20%	487		430		1.13		
T21 15%	489	489	438	435	1.11	1.12	1.08
T21 15%	493		436		1.13		
T21 15%	485		429		1.13		
T21 10%	472	462	438	438	1.08	1.05	1.05
T21 10%	455		436		1.04		
T21 10%	460		441		1.04		

\* To 2 decimal places

**Table 6-9: Summary of results illustrating the concentration (copies/  $\mu$ L) of *APP* (FAM) and *EIF2C1* (HEX) and the ratios calculated based upon concentration for each triplicate reaction and the mean concentration. The mean ratio calculated (blue) is shown next to the expected ratio (green) for each non-spiked and T21 gDNA –spiked sample (from 50% down to 10%).**

<i>APP/ EIF2C1</i>							
Samples	<i>APP</i> -FAM (copies/ $\mu$ l)	Mean	<i>EIF2C1</i> -HEX (copies/ $\mu$ l)	Mean	Ratio	Mean Ratio*	Expected Ratio*
NTC	0.117	0.208	0	0.0297	-	-	-
NTC	0.186		0.093		-		
NTC	0.257		0		-		
Disomy	352	368	369	367	0.955	1.00	1.00
Disomy	374		369		1.01		
Disomy	374		367		1.02		
T21 100%	520	515	349	347	1.49	1.49	1.50
T21 100%	509		345		1.48		
T21 100%	-		-		-		
T21 50%	440	440	355	356	1.24	1.24	1.25
T21 50%	440		357		1.23		
T21 50%	-		-		-		
T21 25%	397	397	345	353	1.15	1.13	1.13
T21 25%	396		360		1.10		
T21 25%	-		-		-		
T21 20%	402	404	367	365	1.09	1.11	1.10
T21 20%	406		364		1.12		
T21 20%	-		-		-		
T21 15%	377	381	354	353	1.06	1.08	1.08
T21 15%	385		351		1.1		
T21 15%	-		-		-		
T21 10%	367	369	352	353	1.04	1.05	1.05
T21 10%	371		354		1.05		
T21 10%	-		-		-		

\* To 2 decimal places

The results illustrated that the ratios generated for both multiplex assays were extremely close to the expected ratio for all spiked and non-spiked samples (Table 6-8 and Table 6-9) (Figure 6-21). The results illustrated no amplification of targets for the NTC in both assays and THE D21 control demonstrated ratios of 1.05 and 1 for the *DSCR3/ EIF2C1* multiplex assay and the *APP/ EIF2C1* multiplex assay, respectively. The 100% T21 gDNA control sample also illustrated a ratio closer to 1.5 for the *APP/ EIF2C1* assay compared to the *DSCR3/ EIF2C1*



assay (1.49 and 1.54, respectively). The *DSCR3/ EIF2C1* assay ratios for the 50%, 25%, 20% and 10% spiked samples were within 0.01 of the expected ratio (Table 6-8). The result for the 15% spike was slightly higher than expected (Table 6-8) (Figure 6-23). The results for all spiked (and non-spiked) samples generated from the *APP/ EIF2C1* assay all demonstrated ratios within 0.01 of what was expected, with three spiked samples (10%, 15% and 25%) giving the exact expected ratio. Since the 100% D21 sample and 10% spike sample gave the same ratio (1.05) for the *DSCR3/ EIF2C1* assay, but the *APP/EIF2C1* assay achieved a ratio of 1 for the 100% D21 sample, statistical analysis was carried on the second assay.

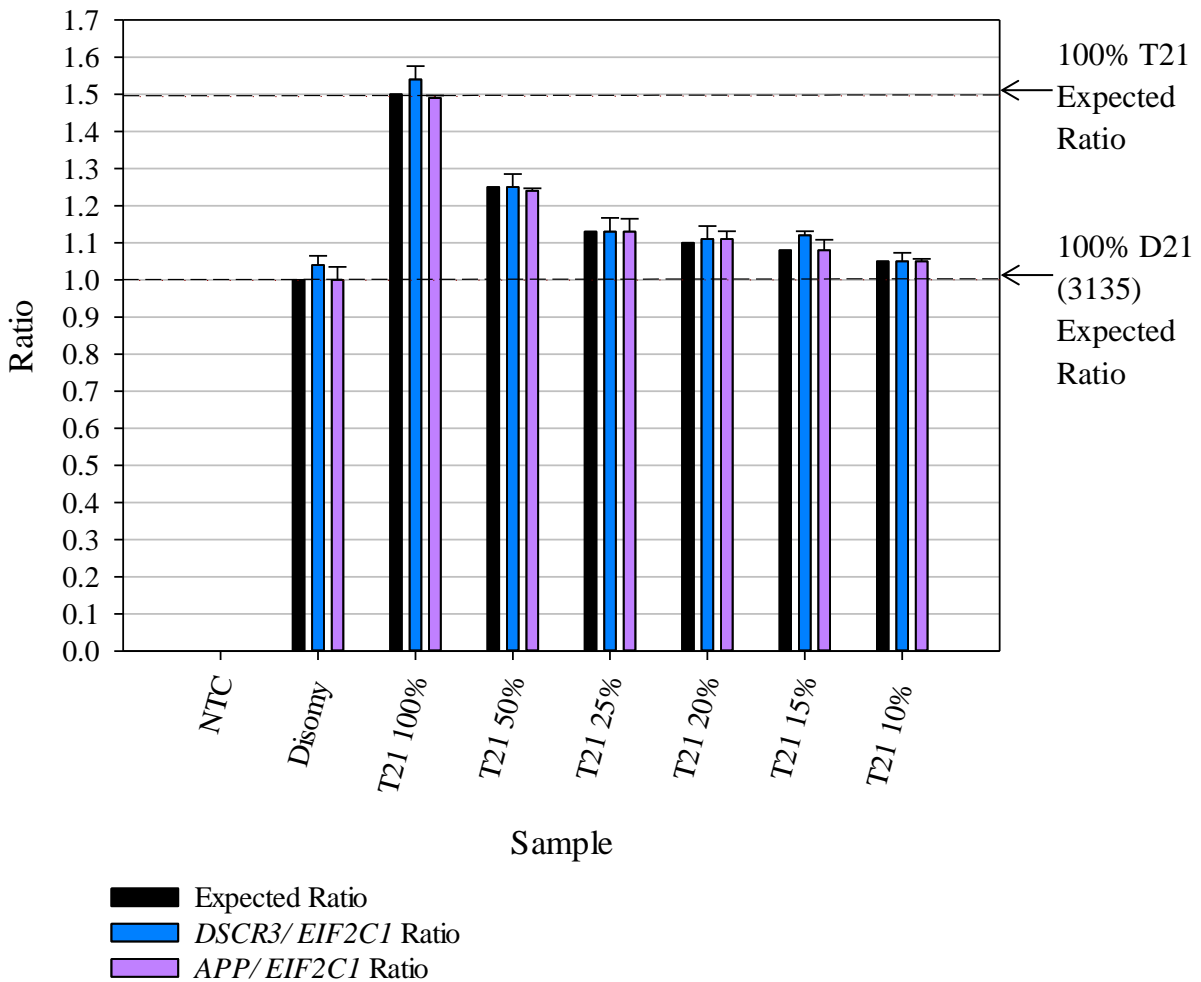


**Figure 6-23: Clustered bar chart illustrating the mean ratio  $\pm$ SD calculated from quadruplet replicates based upon the *DSCR3/ EIF2C1* (blue) assay and the *APP/EIF2C1* assay (purple) compared to the expected ratio for each T21 spike and controls (black). The following samples were tested; NTC, 100% D21 cfDNA (3135) (2ng/  $\mu$ L), 100% T21 gDNA (2ng/  $\mu$ L), and D21 cfDNA (3135) spiked with 50%, 25%, 20% 15% and 10% T21 gDNA. The dashed lines illustrate the expected ratio for 100% D21 gDNA (bottom) at ratio 1 and the expected ratio for 100% T21 gDNA (top) at ratio 1.5.**

Statistical analysis using a comparative t-test on SigmaPlot v13.0 was used to compare ratio results achieved for the D21 cfDNA sample against all other samples containing 100% T21gDNA down to 10% T21gDNA. The results revealed that a significant increase in ratio

was observed for samples that expressed 100% T21 gDNA down to 15% T21 gDNA (Figure 6-22). The 10% T21 gDNA sample did not show a significant increase in ratio compared to the D21 gDNA sample ( $p>0.05$ ) (Figure 6-22). This preliminary data, using pseudo-maternal samples in triplicate indicated that when using the *APP/ EIF2C1* assay T21 could be detected when the pseudo-fetal proportion constituted  $\geq 15\%$  of the total sample.

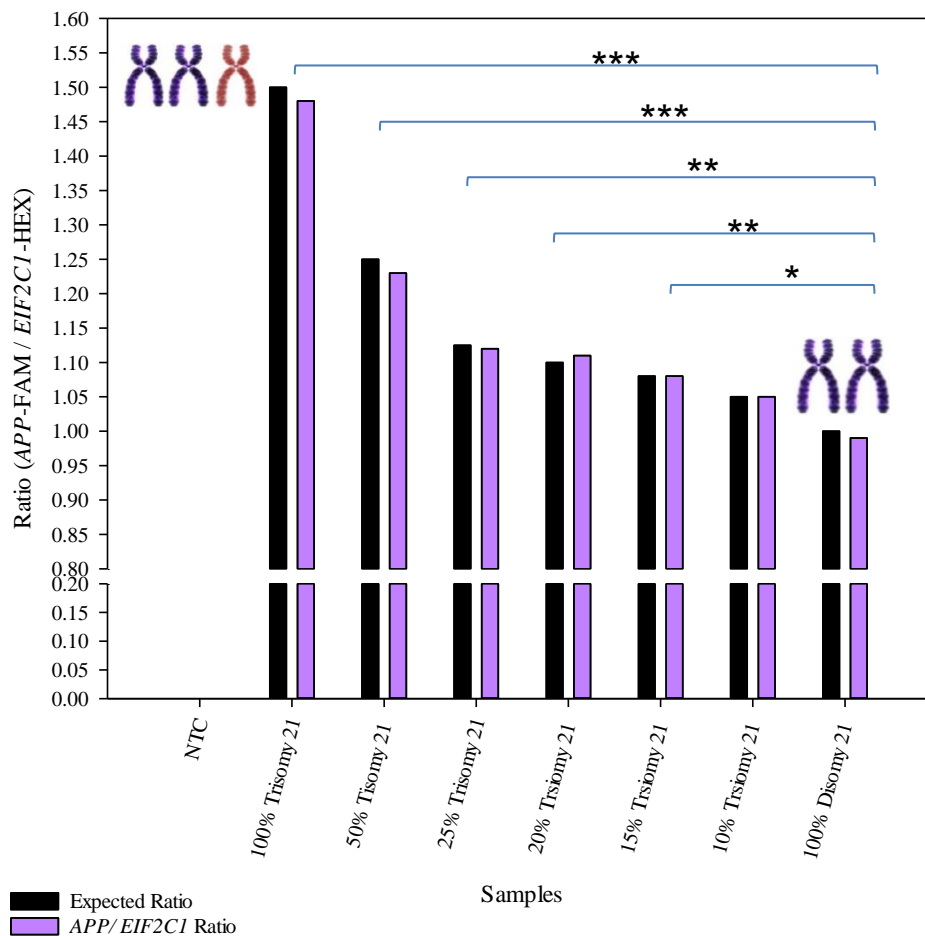


**Figure 6-24: Bar chart illustrating the *APP/ EIF2C1* expected ratio (black) and actual ratio (purple) for NTC, 100% D21, 100% T21 and spike samples (50% down to 10%).** Comparative t-tests revealed a significant increase in ratio value (compared to the 100% D21 gDNA) for the following samples: 100% T21 gDNA ( $P<0.001$ ) 50% T21 gDNA ( $p<0.001$ ), 25% T21 gDNA ( $p<0.005$ ), 20% T21 gDNA ( $p<0.005$ ) and 15% T21 gDNA ( $p<0.05$ ). The 10% spiked-sample did not illustrate a significant increase in ratio compared to the D21 control sample.

## 6.3 Discussion

### 6.3.1 Pippin Prep™ Size Selective Enrichment

The results illustrated successful cffDNA enrichment for all samples (excluding 119) when analysed using the *SRY* (maternal sample 9), *TSPY1* (maternal sample 13, 24, 36 and 43) and the *RHD7* (maternal samples 117, 118, 120, 122, 123, 124, 131, 132 and 133) assays (Figure 6-2, Figure 6-5 and Figure 6-11) (Table 6-3). Despite previous studies identifying high target recovery efficiencies using the PP size-selective approach (refer to 6.1) (Duhaime *et al.*, 2012), one maternal sample (119) illustrated total loss of cffDNA following PP gel electrophoresis when analysed using the *RHD5/ EIF2C1* assay. The aliquot analysed directly following DNA extraction illustrated cffDNA fractions of 9.53% and 4.59% for the *RHD5* and *RHD7* assay, respectively. However, analysis of the aliquot that was run on the PP platform only illustrated amplification of a single *RHD7* target (Figure 6-12). Automated DNA extractions from maternal plasma/ serum have been shown to achieve significantly higher yields of cffDNA (Huang *et al.*, 2005; Müller *et al.*, 2008). By combining this automated approach with increased starting quantities of maternal plasma (up to 5 mL) higher yields of cfDNA (particularly fetal) can be achieved. Consequently, by loading higher quantities of total cfDNA, the amount of cfDNA eluted following PP gel electrophoresis is also likely to increase.

The Agilent 2100 Bioanalyzer results illustrated drop out of larger fragments following PP gel electrophoresis (Figure 6-3, Figure 6-4, Figure 6-8 and Figure 6-9). Consequently, the ddPCR analysis revealed a significant decrease in concentration of the reference gene (Xp22.3) compared to the fetal specific target (*TSPY1*) (Figure 6-6) confirming selective enrichment of cffDNA. This results

reveals that whilst maternal DNA exhibits fragments at <200bp (Stephanie *et al.*, 2014), when additional maternal DNA is released by degradation of leucocytes, as seen with EDTA collected samples (refer to 1.3.3.5), a higher abundance of larger fragments are visible (Figure 6-3 and Figure 6-4) than when samples are collected in Streck BCTs (Figure 6-8 and Figure 6-9).

In contrast, the *RHD5* assay illustrated a decrease in cffDNA fraction (2.47%) for maternal sample 133, but did show successful enrichment for all other *RHD+* fetuses tested ( $n=8$ ) (Figure 6-11). The variation in cffDNA fraction for maternal sample 133 could be due to differences in assay efficiencies, since cffDNA fraction for all samples except 124 was higher based on the *RHD7* assay (Figure 6-10). Previous results revealed similar cffDNA fractions, but illustrated a slightly higher average for the *RHD7* assay also (Figure 5-18). It is possible that a SNP within the exon 5 target is affecting amplification. However, this does not explain the increase in cffDNA fraction seen for maternal sample 124. Whole genome sequencing has revealed that the entire fetal genome is present within the maternal circulation (Lo *et al.*, 2010; Snyder *et al.*, 2013) with predominant size-peaks for fetal (~143 bp) and maternal cfDNA (~166 bp) fragments (Lo *et al.*, 2010). The increase in cffDNA was predominantly improved for samples using the *RHD7* assay ( $n=7$ ), however, two maternal samples (124 and 131) did illustrate greater improvements in cffDNA fraction for the *RHD5* assay (Figure 6-11).

It is possible that fragmentation differs between individuals; however, this preliminary data only illustrates the feasibility of PP gel electrophoresis for selective enrichment. Further larger scale studies are required to validate the reproducibility of this enrichment method. Consequently, visibility of patterns of selective enrichment of one target over the other would be enhanced with increased

sample size. Alternatively, it is likely that variation in enrichment between assays is a result of initiation of such a novel procedure and further testing is required to define the optimum parameters. To increase the reliability of the current PP experiments there are multiple steps that can be carried out in future experiments. Firstly, increasing the amount of cfDNA ran on the PP would increase in proportion collected in the elution phase. In addition, performing a brief current reversal at the end of sample elution can help to increase sample recovery by up to 10% for 100-200bp fragments. Alternatively, increasing the amount of DNA added per well for ddPCR analysis and increasing the number of replicates for each sample could increase the number of data points generated and improve detection and subsequent cfDNA fraction analysis. In the previous chapter it was determined that manual extractions led to reduced quality of maternal samples. Therefore, by implementing an automated approach may help to improve cfDNA recovery at the initial phase, which is likely to improve downstream ddPCR detection of fetal specific targets even following PP gel electrophoresis. It is important that fetal specific targets are identified for all samples to accurately determine cfDNA fraction and ensure that a false negative result is truly false negative and not a result of low cfDNA levels.

Maternal sample 132 illustrated a dramatic increase in cfDNA fraction (>100%) for the *RHD7* multiplex assay only. This indicated that the mother of this sample was not homozygous for a complete deletion of *RHD* since the *RHD* exon 7 amplicon was clearly expressed fetal from and maternal origin. In discordance, the *RHD* exon 5 only illustrated fetal origin since cfDNA fractions of 7.28% and 16.43% were seen before and after PP, respectively. It is likely that patient 132 expressed either an *RHD* pseudogene or D variant allele (refer to 5.1.1). The *RHD* pseudogene is prevalent in Rh D- negative Africans (67%) (Singleton *et al.*, 2000); however, the

ethnicity of maternal sample 132 is recorded as white British and is therefore unlikely to exhibit this genotype.

Figure 6-25 illustrates the *RHD* and *RHCE* hybrid genes in some D variants. Since the results illustrated presence of maternal *RHD* exon 7, but not *RHD* exon 5, it is likely the mother expresses either a DVI or DVa variant (highlighted in red). Based on the genotype, *RHD* DVI has been subdivided into four types (1-4), which express variations in *RHCE* derived exons (Figure 6-25). The encoded phenotype of each DVI variant all differ, which consequently alters the strength and expression of the BARC antigen (Mouro *et al.*, 1994; Avent *et al.*, 1997). BARC was first reported in 1989 as a low-prevalence antigen associated with some DVI RBCs occurring in <0.01% of all populations (Reid, Lomas-Francis and Olsson, 2012). In European populations, DVI types 1 and 2 are more prevalent, whereas DVI type 3 and DVI type 4 are more predominant in specific regions such as Germany and Spain, respectively (Reid, Lomas-Francis and Olsson, 2012). Further analysis of maternal sample 132 using commercially available kits, which test for a number of partial and D alleles, would have been desirable for confirmation of D variant. If we assume maternal sample expresses either a D<sup>VI</sup> type 1 or type 2 variant, determining the presence of the BARC antigen would have enabled confirmation since type 1 does not express BARC and type 2 does express BARC (Avent *et al.*, 1997; Reid, Lomas-Francis and Olsson, 2012). However, lack of ethical approval for collection and storage of maternal buffy coat prevented further analysis.

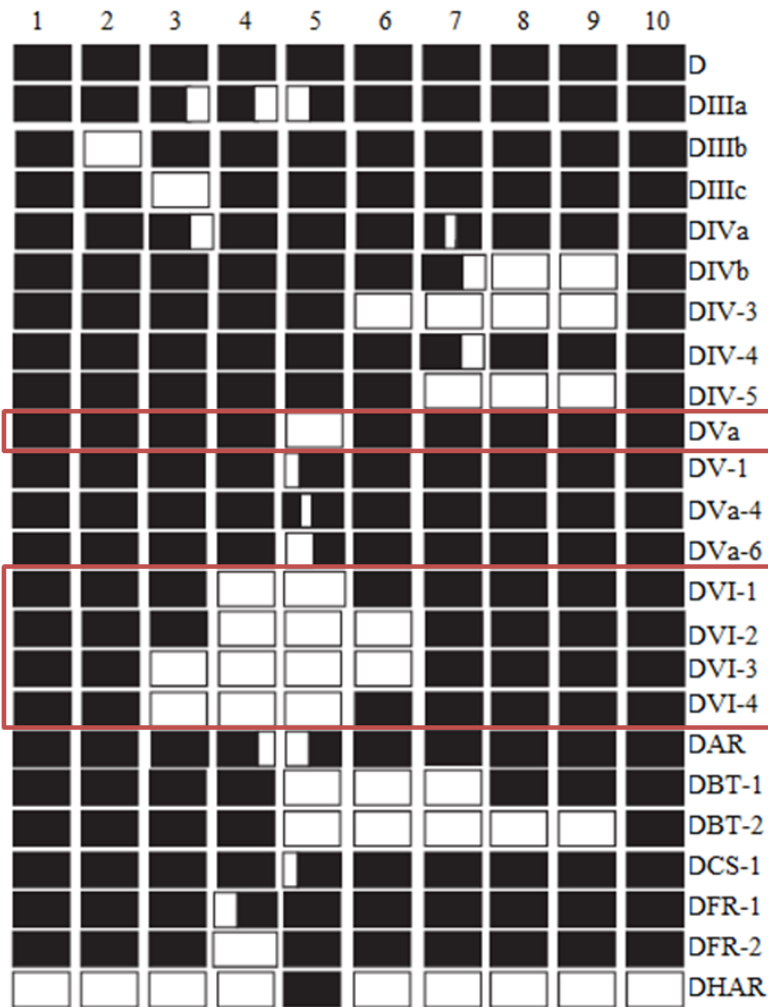


**Figure 6-25: *RHD* exons (black) and *RHCE* exons (white) of hybrid genes in some D variants.** [Adapted from Daniels (2013)].

### 6.3.2 Determining cfDNA fraction for aneuploidy detection

The results illustrated successful detection of single-copy target (*SRY*) even when spiked at 1% into female gDNA (151 GE's of male DNA) and the multiple-copy target was detectable even when spiked at 0.01% (454.5 GE's of male DNA). The digital PCR managed to detect 48.4 copies and 24.4 copies per 20  $\mu$ L reaction for the *SRY*-spike (1%) and *TSPY1*-spike (0.1%), respectively. Many studies have researched the capability of dPCR to detect rare or low copy targets in comparison to qPCR approaches (Pinheiro *et al.*, 2011; Hayden *et al.*, 2013; Hindson *et al.*, 2013; Strain *et al.*, 2013; Kim, Jeong and Cho, 2014; Miotke *et al.*,



2014; Sillence *et al.*, 2015). While some studies illustrated improved precision and reproducibility of dPCR but similar levels of sensitivity (Hayden *et al.*, 2013; Hindson *et al.*, 2013), many studies have shown improved sensitivity using dPCR over qPCR approaches (Pineiro *et al.*, 2011; Strain *et al.*, 2013; Kim, Jeong and Cho, 2014; Miotke *et al.*, 2014; Sillence *et al.*, 2015). Previous data has also revealed the improved sensitivity of ddPCR (100%) to determine fetal sex and *RHD* genotype for samples expressing low cfDNA fractions (<2%) compared to qPCR (0%) (Chapter 5) (Sillence *et al.*, 2015). Whilst this demonstrated the ability of ddPCR to detect low copy targets, determination of fetal aneuploidy is considerably more complicated since reliable and accurate quantification of small copy number changes between target and reference DNA is required.

In addition to detection of low copy number targets, dPCR also enables accurate quantification using both microfluidic (Pineiro *et al.*, 2011; Sanders *et al.*, 2011) and droplet-based (Strain *et al.*, 2013; Ludlow *et al.*, 2014; Miotke *et al.*, 2014; Contente-Cuomo and Murtaza, 2015; Tsao *et al.*, 2015) techniques. In one study, multiplex primers were designed to amplify short (67-71 bp) and long (439-522 bp) PCR products from independent regions of the human genome each labelled with FAM and TET, respectively (Contente-Cuomo and Murtaza, 2015). Through analysis using picoliter ddPCR, the study revealed that the relative quantities of short and long fragments mirrored the integrity of sheared DNA input and accurate quantification could be achieved when using as few as 200 pg of cell-free DNA. In an alternative study, microfluidic dPCR was able to measure a smaller CNV compared to conventional qPCR for the investigation of *HER2* gene amplification in breast cancer cell lines (Whale *et al.*, 2012). This research was conducted using the BioMark HD (Fluidigm) dPCR instrument, which partitions each reaction into 770 x 0.84 nL chambers. Data published by Lo *et al.* (2007b), which produced simulations of pseudo-maternal samples containing 50%, 25% and 10% fetal DNA (obtained from placenta), used 384-well reaction

plates to carry out digital RCD using SPRT analysis. By constructing a range of SPRT curves based on the number of reference molecules per well ( $m_r$ ), chromosomal imbalance could be determined by plotting the proportion of informative wells containing the over-represented allele ( $P_r$ ) against the total number of informative wells. The study revealed that at 25% 'cffDNA', with a combined total of 7,680 PCR analyses, 97% of both euploid and aneuploidy cases would be classifiable, with 3% requiring further analyses until classification can be achieved (Lo *et al.*, 2007b). The results revealed that with a decreasing fractional concentration of fetal DNA, a larger number of informative counts are required for digital RCD. However, to obtain cffDNA fractions of  $\geq 25\%$ , selective enrichment methods are required (Li *et al.*, 2004).

For samples expressing 100% T21, the RCD ratio should be 1.5, since there are three copies of chromosome 21 and two copies of any other autosomal reference chromosome. For maternal samples containing 10% cffDNA the RCD decreases to 1.05 (Lo *et al.*, 2007b). The results in this study reveal accurate quantification on the QX100 ddPCR System, since all T21 spiked samples from 100% down to 10% illustrated the expected RCD ratio (or within 0.01) (Figure 6-23 and Figure 6-24). Rather than carry out SPRT analysis, a comparative t-test was used to determine significant difference between each individual spike sample against the 100% disomy control sample. The results illustrated that significant difference between the disomy sample (ratio: 1) and spiked samples were detectable down to 15% 'cffDNA' using the QX100 (Bio-Rad) ddPCR platform for samples tested in triplicate ( $p < 0.05$ ) (Figure 6-24). In future experiments, increasing the number of replicates per run could help to decrease the minimal cffDNA fraction required for aneuploidy detection since averaging across more replicates reduces variability, improves precision and allows smaller changes to be detected (Yang and Speed, 2002).

The QX100 ddPCR System, which was used in this study, generates a 20-fold increase in the number of partitions (14,000 to 16,000 droplets per sample) compared to the Fluidigm BioMark HD platform (770 chambers). In addition, this method allows for increased sample partitions and higher throughput compared to the 384-well approach as described by Lo *et al.* (2007b). Alternatively, the RainDrop Digital PCR (RainDance™ Technologies, MA, USA) produces the highest number of partitions with up to 10,000,000 droplets per sample. Increasing the number of partitions per reactions enables detection of lower copy number targets and allows for improved quantification and subsequent detection of low level CNV. Our results illustrated that when tested in triplicate on the QX100 ddPCR System a minimum of 15% cffDNA fraction is required. As previously mentioned this could be improved by increasing the number of replicates or alternatively by transferring the assay onto the RainDrop Digital PCR (RainDance). However, the RainDance platform is costly (£7-£20 per sample) with lower throughput (8 samples per run) in comparison to the QX100 ddPCR system (£2 per sample; 96 samples per run) (Baker, 2012).

### 6.3.3 Future work

To achieve a fetal fraction of 25%, enrichment techniques are required in most cases. The initial data from our research highlights the capability of PP gel electrophoresis to increase the cffDNA fractions. In addition, spike experiments conducted on the QX100 ddPCR System have identified that significant differences between disomy control samples and 15% T21 spiked samples are capable of being detected. The results from this study reveal that if a cut-off of 15% was accepted all maternal samples collected in Streck BCTs (117, 118, 119, 120, 122, 123, 124, 131, 132 and 133) would have been eligible for aneuploidy analysis following PP enrichment (Table 6-5).

Future experiments combining multiple repeats per sample and higher starting quantities of maternal plasma could help to further reduce the minimum cfDNA fraction required for reliable detection of foetal aneuploidy using the QX100 ddPCR system. The enrichment results in this study were obtained from a maximum of 3 mL of maternal plasma. However, this can be further increased to up to 8 mL of plasma when collecting around 15mL of maternal blood, which is at the limit of routine practice (Lo *et al.*, 2007).

Alternatively, MLPA approaches have been used to determine aneuploidy from CVS, which revealed over 95% concordance with traditional karyotyping (Koober *et al.*, 2009). The advantage of MLPA is that many targets can be multiplexed in a single reaction, which makes it ideal for blood group typing, including *RHD* zygosity testing (Haer - Wigman *et al.*, 2013a). The advantage of including multiple target loci is that if fragmentation does differ between individuals selective bias is reduced, increasing quantification reliability and consequently the digital RCD calculated. However, the approach is associated with lower sample throughput and longer run times (up to 25 hours) (Haer - Wigman *et al.*, 2013a). The results shown here illustrated excellent ratio analysis for the *APP/ EIF2C1* multiplex reaction, but revealed slightly less optimal digital RCD using the *DSCR3/ EIF2C1* multiplex reaction (Figure 6-23). Rather than develop MLPA based approaches for aneuploidy determination, future ddPCR experiments could combine multiple chromosome 21 targets (all labelled with FAM) against multiple references targets (all labelled with VIC/ HEX) to reduce fragmentation bias. Consequently, it is fundamental that the ddPCR RCD approach following PP enrichment is validated for actual maternal samples carrying T21 fetuses.

It has been previously discussed that despite declines in the cost of NGS for NIPT of fetal aneuploidy, tests are still too expensive for implementation into routine clinical practice (refer to 1.3.3.3.2). The total cost of the PP enrichment assay combined with ddPCR analysis

(<£13.00 per sample) is considerably cheaper than commercial NIPT, which ranges from £400-£900 in the UK (Morris *et al.*, 2014) making it a more economically viable test.

#### 6.3.4 Conclusion

This data highlights the application of ddPCR for the detection of ‘fetal’ aneuploidy in samples expressing  $\geq 15\%$  ‘cffDNA’. Consequently, by using 15% cffDNA fraction as a cut-off, all maternal samples (collected in Streck BCTs) enriched by PP gel electrophoresis would have been viable for aneuploidy analysis. Further optimisation studies are required to define the limits of this ddPCR system for the determination of aneuploidy for spiked samples, and consequently actual maternal samples carrying T21 fetuses. However, the preliminary data demonstrates the feasibility of combining PP enrichment with ddPCR for the detection of fetal aneuploidy. The reduced costs associated with this procedure compared to established targeted MPS approaches, along with rapid turn-around times, makes this concept a legitimate competitor for routine testing.

# Chapter 7

## Discussion

## 7.1 Size-selective enrichment of cffDNA

The discovery of cffDNA within the maternal circulation revolutionised prenatal testing and created a platform for NIPD (Lo *et al.*, 1997). NIPD of fetal sex and *RHD* status is already available (Chitty *et al.*, 2008) and platforms to test for aneuploidy are also available commercially as secondary screening tests (Benn, 2014). Providing NIPD for such conditions eradicates the need for invasive tests, which are associated with a small but significant risk of miscarriage. While MPS approaches currently provide highly sensitive commercially available screening, developing a cost effective platform to accurately test for aneuploidy and single gene disorders, which can be applied to routine testing, is highly sought after. While NIPD is effective for fetal specific targets, detection of fetal chromosomal abnormalities cannot be used as a definitive diagnostic platform at present due to the small but significant risk of discordant results, which often arise due to low cffDNA fractions (refer to 1.3.3). Therefore, we set out to analyse a number of molecular techniques, other than gel extraction methods previously described (Li *et al.*, 2004), which could be used to size-select smaller fragments and consequently enrich cffDNA.

Initially, it was determined that cffDNA was considerably shorter (<300bp) than maternal cfDNA (>1kb) (Li *et al.*, 2004). Fragmentation differences were exploited for the selective enrichment of cffDNA (up to 50% total cffDNA), permitting the detection of fetal genetic loci, such as SNPs and paternally inherited mutations, which would have been undetectable prior to selective amplification (Li *et al.*, 2004). However, since these initial studies, it has been determined that the variation between cffDNA and maternal cfDNA is lower (143bp to 166bp, respectively) than first described (Stephanie *et al.*, 2014). Consequently, enrichment approaches have not been used for detection of any genetic condition (Liao *et al.*, 2011). Though the maternal cfDNA also constitutes smaller

fragments that are closer to the fragment sizes expressed by the fetus, the concept of size-selective enrichment is still feasible since samples that show degradation can express a higher proportion of larger maternal cfDNA fragments (Qin, Williams and Fernando, 2013; Qin, Bassett and Fernando, 2014; Sillence *et al.*, 2015). The data in this thesis analyses the development of three different strategies to increase the relative proportion of cffDNA, including COLD-PCR (Chapter 3), IPCR (Chapter 4) and PP size-selective gel electrophoresis (Chapter 6).

The initial COLD-PCR data using fragments containing STRs demonstrated that at lower denaturation temperatures shorter products were formed, most likely as a result of hairpin formation (refer to 3.3.1). Consequently, experiments were conducting on pseudo-maternal DNA samples for sequences that contained non-polymorphic sites of interest. The results highlighted the success of this approach on a qPCR platform since non-maternal samples showed no amplification and pseudo-maternal samples illustrated late amplification (Figure 3-16). The procedure was subsequently transferred onto a ddPCR platform to improve counting of the Chr21 target against the Chr1 target for accurate ratio analysis. Further optimisation on the ddPCR platform was carried out using actual maternal samples due to the recent availability of these samples within the department at this time. However, the results did not show variation in dropout for maternal and non-maternal samples, though smaller temperature differences ( $<1^{\circ}\text{C}$ ) were not tested. This suggests that the temperature dropout ( $T_c$ ) for larger maternal fragments is likely to be marginally higher, if at all, compared to temperature drop out ( $T_c$ ) for slightly short cffDNA fragments.

The concept of the IPCR method was successfully shown using pure Rh fragments (refer to 4.2.2). However, time constraints prevented further developments to determine the nature of cfDNA fragment ends and subsequently optimise dilute ligation reactions.



Although the true capability for selective enrichment using this technique was not fully established, the advantage of IPCR as opposed to COLD-PCR is that selective enrichment does not require amplification at lower  $T_d$ 's, which is associated with alterations in efficiencies of primers, particularly for multiplexing experiments. Consequently, if one target amplifies more efficiently at the critical  $T_d$  this creates a bias which alters the RCD calculated for determination of fetal aneuploidy. Target amplification at lower  $T_d$ 's is feasible, but only if reactions are carried out separately at individual optimum conditions not in a multiplex reaction. Alternatively, IPCR selective amplification is achieved by determining a dilute ligase reaction, which allows for self-ligation of shorter fragments only, and thus reaction can be carried out at optimal  $T_d$  (95°C). This prevents bias amplification assuming equal fragmentation of cffDNA, which will enable ligation of all fragments under the same conditions. However, it is likely that small variations in concentrations of DNA ligase will lead to ligation of both maternal and fetal cfDNA fragments as opposed to just smaller fetal DNA fragments, and therefore, very precise and accurate laboratory conduct is required in future experiments.

Enrichment using size-selective gel electrophoresis on the PP System was also carried out using actual maternal samples. By using a size selective range of 100bp to 200bp the data illustrated that on average the PP approach increased the cffDNA by 16.1% and 18.8% when using the *RHD5* and *RHD7* assays, respectively (Table 6-3). Figure 6-5 highlights the loss of both cffDNA fragments and maternal cfDNA fragments following PP size-selective gel electrophoresis for samples collected in EDTA tubes, which are more susceptible to maternal DNA degradation as opposed to Streck BCTs. Though this approach does lose valuable fetal DNA (average of 4-fold decrease), this decrease is significantly lower than the loss of the reference target (Xp22.3, average of 18-fold decrease), which is predominantly maternal ( $p < 0.001$ ) (Figure 6-6). This suggests that

even though the PP system selects both maternal and fetal cfDNA fragments since size differences are minimal, a greater proportion of maternal DNA is being removed compared to cffDNA prior to ddPCR amplification. The initial data demonstrates successful fetal enrichment and its application for T21 detection in spike samples is promising (refer to 7.4). However, extracting from larger volumes of maternal plasma or altering the size range on the PP system could increase the amount of cffDNA available and improve cffDNA enrichment in future experiments, respectively.

Despite the relative success of gel-extraction based methods for the selective enrichment of cffDNA (Li *et al.*, 2004), these approaches are labour-intensive, inefficient and prone to contamination (Eslami and Salehi, 2014). Consequently, enrichment approaches have not been implemented in a clinical setting for NIPD of genetic disorders in conjunction with MPS analysis (Liao *et al.*, 2011). The PP system is less prone to contamination, is relatively easy to carry out with little hands on time, and is more efficient and reproducible than conventional gel extraction (see 6.1) (Duhaime *et al.*, 2012). In addition to the methods described here, alternative methods of enrichment, such as peptide-nucleic acid-mediated PCR enrichment, have also been described (Galbiati *et al.*, 2008). Galbiati *et al.* (2008) focused on the NIPD of  $\beta$ -thalassaemia, which clamped maternal wild-type alleles using peptide nucleic acids (PNAs), allowing mutant enrichment amplification since microchip analysis was not sufficiently sensitive to directly determine fetal mutated alleles in maternal plasma. The results illustrated proportional inhibition and using microarray analysis demonstrated 100% concordance with CVS analysis, but such analysis can only be carried out in couples which express different mutations (Galbiati *et al.*, 2008).

Methylation DNA immunoprecipitation (MeDIP) approaches have also been described, which target differentially methylated regions (DMRs) between the fetus and mother, to

increase the proportion of DMRs that are specifically hypermethylated in the fetal DNA (Papageorgiou *et al.*, 2009; Papageorgiou *et al.*, 2011; Tsaliki *et al.*, 2012; Kyriakou *et al.*, 2013; Ioannides *et al.*, 2014). Consequently, following on from DNA methylation enrichment ratio analysis can be used to determine the overrepresentation of chr21 for NIPD of DS with 100% sensitivity and 100% specificity (Papageorgiou *et al.*, 2011). In a recent study, the robustness of the current methodology was improved by identifying further DMRs within intergenic and intragenic regions to expand the DMR panel available for use with MeDIP qPCR (Ioannides *et al.*, 2014). However, in an alternative study concerns about the robustness of this approach were raised, and also determined that there were theoretical deficiencies (Tong *et al.*, 2012). However, at present no large-scale validation studies using this approach have been reported. In addition, the implementation of MeDIP-qPCR approaches for routine use within the clinic is limited by labour-intensive and time-consuming bisulphite conversion or restriction enzyme digestion, which makes this approach less practical (Twiss *et al.*, 2014).

On the other hand, methods to deplete maternal cfDNA using formaldehyde have been developed, but since the initial experiment (Dhallan *et al.*, 2004), subsequent evaluation studies have not seen great improvements in cffDNA fraction (Chinnapapagari *et al.*, 2005; Chung *et al.*, 2005) (refer to 1.3.3.5). Streck BCTs contain unknown cell preserving agents that prevent maternal leukocyte degradation and preserve higher cffDNA fragments (refer to 1.3.3.5). Though my study revealed great improvements in cffDNA fraction for Streck BCTs compared to EDTA tubes within 6 hours of extraction (Figure 5-18) (Sillence *et al.*, 2015), most studies have determined that Streck BCTs are most effective for preservation when extracting DNA/RNA from older samples collected  $\geq 7$  days earlier (Wong *et al.*, 2013; Qin, Bassett and Fernando, 2014; El Messaoudi and Thierry, 2015). However, we did not test variation in sample storage times.

Determining fetal genetic conditions, such as aneuploidy, during the first trimester is advantageous since it allows a longer time frame for prospective parents to receive genetic counselling and make an informed decision. Consequently, if parents choose to abort pregnancy, earlier determination is often seen as more acceptable, but only if a gradualist view is adopted (refers to 1.1). Despite the widespread analysis of NIPD using MPS techniques (refer to 1.3.3.3.2), at present, diagnosis is only achieved using invasive procedures, which are associated with a 1% risk of miscarriage (Ehrich *et al.*, 2011) (refer to 1.2). Currently, one of the major disadvantages of NIPD/ NIPT of fetal conditions, such as T21, is that inconclusive and false negative results can arise due to low levels of cffDNA within the maternal circulation, particularly during the first trimester (cffDNA ~3%) (Wright and Burton, 2009). In addition, the fraction of cffDNA during early pregnancy and throughout pregnancy can also vary depending on multiple factors including maternal weight, ethnicity and other pregnancy related disorders, such as pre-eclampsia as described in section 1.3.3.

Once a reliable method for cffDNA enrichment or maternal depletion can be identified, size fractioning methods can be used in conjunction with highly sensitive detection systems, such as the ddPCR, for the NIPD of fetal aneuploidy at a fraction of the cost compared to MPS techniques (refer to 7.4). The amount of cffDNA enrichment required for accurate analysis is dependent upon the number of events for each gene region; the higher the number of data points, the less cffDNA is required for diagnosis. For example, one study determined that a cffDNA fraction of 5% requires a minimum of 100,000 data points (Sun, Jiang and Chan, 2015). Initially it was described that cffDNA must be increased to  $\geq$  25% to enable accurate determination of T21 (Lo *et al.*, 2007b). However, when using more sophisticated, digital platforms, which generate a significantly higher

number of reads per sample, less enrichment is required (Sun, Jiang and Chan, 2015) (refer to 7.4).

## 7.2 Determination of *RHD* zygosity

Serological testing of patient red blood cells readily defines each sample as D-positive or D-negative in the majority of cases. However, some patients carry *RHD* genetic variant alleles, which produce a range of partial D, weak D or severely weak D (Del) phenotypes (Hyland, 2013). Therefore, it is important to select the appropriate monoclonal antibodies for typing and develop strategies to efficiently detect partial and weak D phenotypes with high sensitivity. With current serological testing, patients with weak D are typed D-positive via direct agglutination when using anti-D testing. However, studies have shown that serology can often type variant patients as D-negative, either due to insufficient antibody selection or variation in interpretation of the data, which can initiate immunisation upon transfusion (Sandler *et al.*, 2014). The D<sup>VI</sup> variant is the clinically most important and most frequent partial D (Wagner *et al.*, 1998). Some studies have identified that D<sup>VI</sup> (and some other variants) do not react with monoclonal antibodies, such as RUM-1, and can therefore often be mistyped as D-negative (Polin *et al.*, 2009; Credidio, Pellegrino Jr and Castilho, 2011). This is detrimental for blood transfusion since D<sup>VI</sup> variants incorrectly typed as negative should not be given to D-negative recipients as some of the D-epitopes that are expressed may lead to alloimmunisation. In addition, for institutes that target anti-D administration, incorrect classification (D-negative) of a D<sup>VI</sup> fetus could lead to HDFN. However, for prenatal testing, D<sup>VI</sup> variant mothers are typed D-negative deliberately to ensure that anti-D is administered since the absence of some D-epitopes, which will be present on fetal RBCs (if D-positive),

could lead to sensitisation and haemolysis of fetal RBCs. Routine serological methods can determine most weak D's, but the Del RBCs can only be detected by absorption and elution tests, which are time consuming and consequently not feasible for routine testing (Sun *et al.*, 2008). Therefore, qPCR methods have been developed to identify SNPs for biallelic discrimination of genomic sequences (Gibson, 2006). In this study we used a ddPCR platform, which has been shown to express higher levels of sensitivity and precision than qPCR (Baker, 2012), combined with a standard assay for two *RHD* exons (5 and 7) to determine zygosity (Finning *et al.*, 2008). These alleles are often chosen since *RHD* 7 is amplified in wild-type D+, D<sup>VI</sup> variant and *RHD* pseudogene samples, whereas *RHD* exon 5 is only amplified in wild-type D+ samples.

The results revealed 92.5% concordance with the original serological information for determination of homozygous and hemizygous *RHD* positive individuals. Figure 5-13 illustrates the ratios generated by each sample, and the data displayed shows an instant and clear diagnosis of zygosity. Three samples, 1777, 729M and 087W, illustrated discrepancies between serological phenotype and molecular genotype (Table 5-4) (refer to 5.2.3). Sample 729M was typed serologically as weak D with the phenotype R<sub>1</sub>R<sub>2</sub>. Since serological data only provides qualitative results, determining the actual phenotyping is often achieved based on frequency of particular alleles within a population. However, the ddPCR data illustrated a ratio close to 0.5 for both the exon 5 and exon 7 *RHD* targets, illustrating that this sample was hemizygous for *RHD* and therefore is more likely to express the R<sub>1</sub>r'' or R<sub>2</sub>r' phenotype. Designing an assay which amplifies SNPs for R<sub>2</sub> would enable determination of actual phenotype. Since sample 729M is classified as weak D and D-variant haplotypes are rare within

the population (2.2%) (Wang, Lane and Quillen, 2010), it is unlikely this individual is homozygous for weak D. If the patient expressed a normal *RHD* positive allele then serological analysis would not have typed this sample as weak D. This supports the result obtained by ddPCR and suggests that the most likely phenotype determined serologically was incorrect for sample 729M. Therefore, this suggest that the ddPCR provides a more accurate and reliable platform for detection of partial and weak D variants, and provides accurate assessment of *RHD* zygosity. Including more targets to detect all known *RHD*/*RHCE* variants would enable accurate determination of the true phenotype, and this may indicate that the frequencies of r', r'' and R0 haplotypes may be higher than previously suspected based on serological data.

The ddPCR provides an accurate and cost-effective platform for rapid determination of *RHD* zygosity, and has wide implications on current screening used for blood transfusion and administration of anti-D within pregnancy in D-negative mothers. This initial study used two targets which can be used to discriminate between *RHD* positive and *RHD* pseudogene samples. However, there are multiple SNPs and hybrid *RHD-RHCE* genes that are responsible for D-variants (Figure 6-25). Developing a broad spectrum of exon targets would enable detection of multiple D-variant haplotypes for a reliable and accurate determination of all weak, partial and Del variants. Alternative approaches using microarrays, MLPA based approaches or NGS sequencing may prove to be better platforms for accurate analysis of the entire *RHD* gene or multiple exon analysis. However, for quick zygosity determination, ddPCR provide the most rapid and cost effective technique currently available.

MLPA based approaches can multiplex up to 50 targets in a single tube, and can therefore detect multiple *RHD* targets. In one study, 70 *RHD* and 17 *RHCE* variant targets were used for *RHD* genotyping. The results revealed correct classification in 99% of cases, three cases were not determined due to the presence of two new *RHD* variant alleles (*RHD\*DCS2* (a novel partial *RHD* allele) and *RHD\*443G* (a novel D-null allele) and consequent lack of detecting probes (Haer - Wigman *et al.*, 2013b). In addition, this study also revealed that MLPA is effective for zygosity testing since the *RHD* copy number is determined on the signals generated from 17 *RHD* wild-type probe combinations. Thus, the *RH*-MLPA assay is more suitable for detecting zygosity than qPCR (Krog, Clausen and Dziegiel, 2007b) or amplification of the hybrid Rh box (Grootkerk - Tax *et al.*, 2005). The MLPA approach can determine exon copy number to detect hybrid *RHD/RHCE* alleles compared to normal *RHD* alleles, but whilst multiple targets can be run in a single reaction results take a minimum of two days to obtain (Haer - Wigman *et al.*, 2013b).

Alternatively, this exon-targeted approach is transferable to a ddPCR platform. Though this platform may only be able to detect a smaller number of exon targets, since some variants are very rare in certain ethnic groups, population specific assays could be used for rapid (<4 hours) zygosity testing. The importance of zygosity testing is clinically relevant in pregnancies for women who are *RHD* negative. In such cases the paternal zygosity can be determined to assess whether *RHD* typing is required in RhD alloimmunised women (Haer - Wigman *et al.*, 2013b). Sample 1777 was mistyped serologically as R1r, whereas the digital PCR data demonstrated a ratio of close to 1, which indicates



that this sample is actually  $R_1R_0$ . If we hypothesise that sample 1777 was being tested to determine paternal zygosity, the homozygous status of *RHD* determined using molecular ddPCR analysis would have indicated that the fetus would be *RHD*-positive, whereas the hemizygous status determined serologically would have led to unnecessary additional *RHD* typing.

### 7.3 NIPD of fetal sex and *RHD* genotype

Fetal sex and *RHD* genotyping using maternal plasma samples is already implemented within the clinic (Chitty *et al.*, 2008; De Haas *et al.*, 2012). However, within the UK routine prenatal genotyping is not enforced across all hospitals, and as a result all *RHD* negative mothers receive anti-D (The UK National Screening Committee, 2015). This is undesirable since anti-D treatment is costly, and the intramuscular injection in *RHD* negative mothers carrying *RHD* negative fetuses (~30%) exposes them to potential pathogens and causes unnecessary discomfort. Though qPCR approaches for determination of fetal sex and *RHD* status are highly sensitive, false negative or inconclusive results can arise when samples express low cffDNA fractions (Daley, Hill and Chitty, 2014). Therefore, we developed an assay which compared sensitivity of ddPCR vs qPCR for the NIPD of fetal sex and *RHD* genotype in samples expressing optimal (>3%) and sub-optimal (<3%) levels of cffDNA.

The qPCR results were only successful for samples expressing cffDNA fractions >3% (excluding the multiple copy target *TSPY1*) and achieved sensitivities of 100% (*TSPY1* only) and 83.4% for fetal sex and *RHD* genotype for optimal samples, respectively. In contrast ddPCR achieved 100% sensitivity for fetal sex and *RHD* genotype in all samples. This data highlights that for

samples expressing low cfDNA fractions, ddPCR provides a more robust platform with improved accuracy. One sample did illustrate an inconclusive result, which was indicative of an *RHD* $\Psi$  or DVI (type 1-4) variant (refer to 5.3.2). By including a wider range of targets across all exons of the *RHD* gene would enable accurate determination of multiple *RHD* variants (refer to 7.2). MPLA methods can be used to select a wider range of *RHD* and *RHCE* exon targets, among other blood group antigens (such as KEL) in a single run, and in a prenatal sense is advantageous for broad screening of multiple RBC antigens, not just RhD, that could initiate HDFN (Haer - Wigman *et al.*, 2013a). However, digital approaches may be advantageous to MPLA assays for quick determination of the presence of *RHD* using standard assays that include *RHD* exon 5, 7 and 10. In addition, digital PCR approaches can be used to develop population specific assays for rapid analysis of most frequent *RH* variant alleles (refer to 7.2).

Reliable and accurate determination of fetal *RHD* status including detection of weak, partial and Del variants enables anti-D treatment to be targeted to women that require treatment. One study that looked at the cost analysis of implementing NIPD for the targeted administration of anti-D, revealed that only minor savings would be achieved (Szczepura, Osipenko and Freeman, 2011). It is also predicted that generation of false negative or inconclusive results associated with qPCR analysis, particularly during the first trimester, will increase maternal sensitisation events. The study concluded that the reliability of NIPD must be demonstrated in various ethnic minority populations, and in regard to first trimester testing it is likely that emerging technologies may need to be developed to improve accuracy (Szczepura, Osipenko and Freeman, 2011).

It is important that the systems available for the NIPD of fetal *RHD* status are highly sensitive, since false positive results are not detrimental, but incorrectly diagnosing a fetus as *RHD* negative can lead to a sensitisation event and subsequent HDFN. The results in this study highlight the application of ddPCR for the highly sensitive detection of *RHD* specific targets compared to conventional qPCR approaches. Since the cost of each ddPCR assay is similar to qPCR, it is feasible that this platform could replace current qPCR methods for routine testing prior to the decision of whether to administer anti-D within the clinic.

#### **7.4 NIPD/ NIPT of fetal aneuploidy**

Routine definitive diagnosis of fetal aneuploidy is achieved using invasive testing for women considered high risk, but non-invasive tests are being developed to improve the sensitivity and specificity of current screening approaches (refer to 1.1). NIPT using MPS based approaches are available within the private sector, but presently these methods are too costly (>£400) to replace current DS screening tests (Allyse *et al.*, 2015) (refer to 1.3.3.3.2). In this study we developed an alternative method for the NIPD/ NIPT of fetal aneuploidy by combining a selective enrichment strategy using the PP size selective gel electrophoresis with a highly sensitive molecular detection system (QX100 ddPCR).

Firstly, the results demonstrated that the PP successfully enriched cffDNA (up to 45%) for the majority of samples (14/16) (Table 6-3) (refer to 7.1). However, due to depletion of cffDNA following PP enrichment one sample lost all cffDNA and one sample showed a decrease in cffDNA (~3%) (Table 6-3) (Figure 6-10). Despite the relative success of this approach, further optimisation is required to ensure reliability of cffDNA enrichment (refer to 7.5).

Secondly, spike samples were used to represent maternal samples containing various levels of cffDNA (from 10% to 50%) to determine the lowest cffDNA fraction that is required to determine significant difference between the ratio achieved for a T21 fetus and a reference euploid fetus. The experiment revealed that a significant difference ( $<0.05$ ) could be detected for pseudo-maternal samples containing 15% or higher cffDNA (Figure 6-24). The 10% pseudo-cffDNA spike sample did not express a significant difference. Though further optimisation tests are required to improve sensitivity to detect significant difference in samples expressing lower cffDNA fractions ( $<15\%$ ), this initial data improves on previous methods which suggest 25% cffDNA is required (Lo *et al.*, 2007b).

Theoretically, if we applied the 15% cffDNA fraction cut off, 100% of samples would have been acceptable for T21 detection following PP enrichment (Table 6-5). Alternatively, only 40% of samples illustrated  $>15\%$  cffDNA fraction without selective enrichment (Table 6-5). Though this data is promising, it is vital that tests are optimised to increase accuracy and reliability. Consequently, testing novel assays on actual maternal samples is essential to truly determine the feasibility of this approach (refer to 7.5).

Initially, in 2008 s-MPS was the first proof of concept study for the introduction of NIPT for T21 (Fan *et al.*, 2008). Since then, more cost-effective t-MPS approaches have been validated for NIPT of T21 showing high levels of sensitivity (98.6%-100%) and specificity (97.9%-100%) (Boon and Faas, 2013). These targeted approaches have also been described for other aneuploidies including T13, T18 and sex chromosome anomalies, although the accuracy of these tests are often lower than for T21 testing (Bianchi *et al.*, 2012; Futch *et al.*, 2013). NIPT is not considered to be diagnostic since confined placental mosaicism (Lau *et al.*, 2013), maternal chromosome rearrangements

(Osborne *et al.*, 2013) and low cfDNA fractions (refer to 1.3.3.3.2) can result in conflicting results.

Currently, establishing MPS-based approaches that can detect unbalanced chromosomal aberrations, such as duplications or deletions, is under development. Despite incorporation of these approaches within the private sector, the limits of detection have not been defined, making pre-test counselling challenging (Daley, Hill and Chitty, 2014). NIPT of aneuploidy is only available privately, and as previously mentioned high costs prevent implementation to all pregnancies as an alternative to current screening tests. Alternatively, providing NIPT as a secondary test following current DS screening tests may prove to be more cost effective (Chitty *et al.*, 2012). However, at present uptake of NIPT as a secondary screening tool is only available to higher income families raising concerns for equality of access for all women. Developing our NIPT, which uses cfDNA enrichment (if required) in conjunction with ddPCR, provides a considerably cheaper alternative to MPS (refer to 1.3.3.3.1), and thus could potentially be employed as a secondary screening tool for T21. In addition to T21, this approach can also be developed for other aneuploidies, and is currently already being developed for single gene disorders, such as haemophilia (Tsui *et al.*, 2011) and sickle cell anaemia (Barrett *et al.*, 2012) (refer to 1.3.3.4). The approach for detecting single gene disorders can be universally applied for any type of disorder provided assays for wild-type and mutated alleles can be developed. Consequently this highlights the capability of digital PCR for determination of cancer biomarkers, which could allow for early diagnosis and consequently improved prognosis (Dawson *et al.*, 2013; Taly *et al.*, 2013; White *et al.*, 2014).

Studies have also developed assays that can analyse the entire fetal genome, which enables diagnosis of multiple conditions in a single run (Lo, 2013). However, not only is this approach expensive and time-consuming, but it also raises a wide number of ethical

concerns since extensive data on multiple disorders can hinder both pre-test and post-test counselling (refer to 1.4). This illustrates that it would be more cost-effective, and ethically and socially acceptable, to offer testing for analysis of fetal genetic material for certain disorders in families with a previous history or that are shown to be at high risk for specific genetic conditions. The dPCR platforms are not capable of analysing the entire fetal genome. However, if targeted testing is required for distinct single gene disorders, dPCR has the capability to provide a rapid and cheaper alternative to MPS-based methods.

### **7.5 Potential gene therapy for fetal aneuploidy**

Currently, NIPT is carried out to determine fetal aneuploidy during early pregnancy to allow prospective parents a longer period of time to seek counselling and come to a difficult decision. However, the long-term aim is that non-invasive diagnosis can be used to detect affected pregnancies and target therapeutic treatment to prenatally reduce symptoms associated with aneuploidies such as congenital anomalies of the heart, immunodeficiencies and developmental delay in DS (Epstein, 2013). The most promising results have been provided by a research group in Worcester, who have determined that the additional chromosome in T21 can be silenced by inserting a large (non-coding) RNA gene, known as *XIST*, into the extra chr21 in human stem cells (Jiang *et al.*, 2013). *XIST* is crucial during pregnancy since it modifies chromatin and architecture by silencing one X chromosome (in females) to compensate for differences in X-linked genes between males and females (Levenson, 2013). Jiang *et al.* (2013, used zinc finger nucleases (ZFNs), which enable genome editing by generating a double-stranded DNA break at specific sites to target the insertion of the *XIST* gene ,and subsequently silence all genes across the chromosome. Though these results make prenatal gene therapy for DS conceivable, its application is not certain. However, this method will at least provide an

improved understanding behind the biology involved in the onset of DS and possibly allow for determination of certain genes responsible for multiple dysfunctional developments. This may enable administration of drugs that can alleviate the effects of the condition.

## **7.6 Future Work**

Future experiments to optimise COLD-PCR conditions and IPCR conditions are required to fully determine the feasibility of these two enrichment strategies. It is important that initial test focus on the nature of cffDNA fragment ends, which will determine whether additional steps are required prior to self-ligation. The relative size difference between cffDNA and maternal cfDNA is not as significant as previously thought (refer to 7.1). Therefore, both the COLD-PCR and IPCR approaches may only be feasible for enrichment when maternal leukocyte degradation has occurred and larger maternal fragments are visible. However, with regard to IPCR it is feasible that if all fragments are ligated following IPCR, sequencing smaller fetal product against larger maternal products could provide additional information on how DNA is fragmented. This may provide information on pattern variation between maternal cfDNA fragments and cffDNA fragments, and thus help provide an explanation as to why size variations are visible.

Though the PP approach was relatively successful, further optimisations are likely to improve overall cfDNA yield and consequent downstream analysis. This could be achieved by extracting from 5mL of maternal plasma as opposed to 3mL, in conjunction with optimisation of size range selected to see if smaller ranges could further deplete maternal fraction. Once optimal conditions have

been defined for maximum cffDNA enrichment on this platform, the reliability and accuracy of this assay for size-selective enrichment must be analysed by testing larger cohorts of maternal samples.

The initial spiking data demonstrated significant variation between euploid control and pseudo-T21 pregnancy cases when cffDNA fractions of 15% were visible. This was achieved by carrying out each reaction in quadruplet. Including multiple repeats (up to 10) of each sample is one way in which this assay could be developed to improve test reliability and sensitivity. Not only will this increase the number of data sets per sample, but by combining multiple wells more target reads can be generated. An alternative approach to increase number of reads per sample in future experiments is to combine multiple Chr21-targets (FAM-labelled) against multiple reference targets (HEX-labelled) in a single reaction. Increasing the number of reads will reduce the cffDNA fraction required for T21 detection. If this can be achieved for samples containing 5% cffDNA, then additional enrichment will not be required. Once T21 detection can be reliably determined in spike samples, tests must be repeated for actual maternal samples. Unless the fetus expresses triploidy, it is highly unlikely a fetus will express T21 and T18, therefore, labelling Chr21-targets with FAM and 18-targets with HEX could allow for the simultaneous diagnosis of T21 and T18. In addition, Chr21 is the smallest chromosome (represents 1.5% of the total DNA) and Chr18 is also one of the smallest (represents 2.5% of the total DNA), whereas Chr1 is the largest chromosome (represents 9% of the total DNA) (Genetics Home Reference, 2014). Multiplexing Chr18 and Chr21 is likely to give more reliable results since it is possible that the difference in size may alter the amount of cffDNA fragments released into the maternal circulation.



Alternatively, Chr21 could also be multiplex with Chr13 (represents 3.5% of the total DNA) to detect for DS and Patau's syndrome simultaneously.

## 7.7 Conclusion

The size-selective enrichment of cffDNA is complicated by the limited variation in maternal cfDNA and cffDNA fragment size, which is possibly why COLD-PCR and IPCR experiments using actual maternal samples were unsuccessful. However, despite the size limitations, the PP assay did express successful enrichment in the majority of samples, and thus is the most likely approach for future selective-enrichment experiments, although IPCR could provide a valuable technique for analysing cfDNA fragments. The identification of fetal specific targets can be detected with improved accuracy using ddPCR as opposed to qPCR for the determination of fetal sex, *RHD* status and potentially certain single gene disorders. Though MPS is the current gold standard for non-invasive detection of fetal aneuploidy, the combination of ddPCR along with selective enrichment (if required) has the potential to provide a cheaper alternative that could be offered to all high-risk cases following initial screening. Alternatively, it is more financially feasible that this digital-PCR approach could be used to replace current screening tests as opposed to MPS-based NIPT, which is only commercially available. Providing a highly accurate, low cost first trimester screening test, would reduce the number of mothers offered invasive testing and reduce the number of affected pregnancies missed. Consequently, if consistently high PPVs can be achieved in large scale validation studies it is possible that this technique could be used to replace invasive testing.

## APPENDICES 1

### Genome Equivalent Calculations for 21APP and 1EIF2C1 for a 5% Spike

- Plasma sample 936C (R2R2) = 16.4 ng/  $\mu\text{L}$
  - Fetal Chr 21 *APP* sample A (1) = 14.5 ng/  $\mu\text{L}$
  - Fetal Chr 1 *EIF2C1* sample B (2) = 17.5 ng/  $\mu\text{L}$
1. Plasma DNA sample 936C and pseudo-fetal DNA samples were diluted to 2ng/  $\mu\text{L}$ .
  2. The molecular equivalent of genomic DNA and fake fetal DNA for a 5% spike was calculated as follows:

Note: To work this out you need to know the concentration of plasma, and you also need to know that 1 genome equivalent is 6.6pg of genomic DNA.

For example, if the plasma is 16.4ng/  $\mu\text{L}$  (aka 16400 pg/  $\mu\text{L}$ ) then we can calculate the genome equivalent for plasma by dividing 16400 pg/  $\mu\text{L}$  by 6.6pg:

$$16400 / 6.6 = 2485 \text{ genome equivalents per microliter}$$

Therefore, we can calculate the following spike genome equivalents:

$$5\% \text{ fetal spike} = 124.25 \text{ genome equivalents per microliter}$$

3. Calculate the molecular mass of the fake fetal fragment

Each base pair = 650 Da therefore for a 286 bp fragment (chromosome 21) the molecular mass =

$$\text{Chr 21 } APP: 650 \times 286 = 1.86 \times 10^5$$

$$\text{Chr 1 } EIF2C1: 650 \times 317 = 2.06 \times 10^5$$

4. Calculate moles per litre of fetal fragment:

To calculate moles/ L you need to know the concentration of the fake fetal fragment (e.g. Chr 21 *APP* = 14.5 ng/  $\mu\text{L}$ , Chr 1 *EIF2C1* = 17.5 ng/  $\mu\text{L}$ ), you then divide this by the molecular mass (above answer in step 2). (Convert ng/ul to grams e.g. 14.5 ng/  $\mu\text{L}$  = 14.5 x 10<sup>-9</sup> g/  $\mu\text{L}$ ):

$$\text{Chr 21 } APP: (14.5 \times 10^{-9} \text{ g}) / (1.86 \times 10^5 \text{ g/ litre}) = 7.79 \times 10^{-14} \text{ moles/ litre}$$

$$\text{Chr 1 } EIF2C1: (17.5 \times 10^{-9} \text{ g}) / (2.06 \times 10^5 \text{ g/ litre}) = 8.49 \times 10^{-14} \text{ moles/ litre}$$

4. Then calculate molecules per microliter of fetal fragment:

To do this you need to multiply moles/litre (above answer for step 3) by Avogadro's Constant ( $6.023 \times 10^{23}$ ):

$$\text{Chr 21 APP: } (7.79 \times 10^{-14}) \times (6.023 \times 10^{23}) = 4.7 \times 10^{10}$$

$$\text{Chr 1 EIF2C1: } (8.49 \times 10^{-14}) \times (6.023 \times 10^{23}) = 5.1 \times 10^{10}$$

5. Dilute fetal fragment:

Complete a serial dilution by taking 1uL of fake fetal DNA ( $4.6 \times 10^{10}$  molecules/uL) and add to 1mL of water, then take 1uL of that solution and add to 1mL of water etc....

**Chr 21 APP:**

$$4.7 \times 10^{10} \text{ molecules/ } \mu\text{L}$$

$$\text{Dilute 1:1000} = 4.7 \times 10^7$$

$$\text{Dilute 1:1000} = 4.7 \times 10^4$$

$$\text{Dilute 1:1000} = \mathbf{47 \text{ molecules/ } \mu\text{L}}$$

**Chr 1 EIF2C1:**

$$5.1 \times 10^{10} \text{ molecules/ } \mu\text{L}$$

$$\text{Dilute 1:1000} = 5.1 \times 10^7$$

$$\text{Dilute 1:1000} = 5.1 \times 10^4$$

$$\text{Dilute 1:1000} = \mathbf{51 \text{ molecules/ } \mu\text{L}}$$

6. Work out how much fetal fragment you need to add to 1  $\mu\text{L}$  of plasma (based on genomic equivalents (GEs)).

For this you need to refer back to calculation 1. You need to divide the molecular equivalent value for each spike by the number of molecules per microliter.

$$\text{Chr 21 APP: 5\% Spike} = 124.25 / 47 = \mathbf{2.64 \mu\text{L}}$$

Therefore add 2.64  $\mu\text{L}$  to every 1  $\mu\text{L}$  of plasma

We need 33  $\mu\text{L}$  (30  $\mu\text{L}$  +10%) of spike therefore multiple both by 10: (1  $\mu\text{L}$  of plasma x 10 = 10  $\mu\text{L}$ ) + (2.33  $\mu\text{L}$  of diluted fetal fragment x 10 = 23.3  $\mu\text{L}$ ) = 33.3  $\mu\text{L}$  in total for experiment 1.

$$\text{Chr 1 EIF2C1: 5\% Spike} = 124.25 / 51 = \mathbf{2.44 \mu\text{L}}$$

Therefore add 2.44  $\mu\text{L}$  to every 1  $\mu\text{L}$  plasma

We need 33  $\mu\text{L}$  (30ul +10%) of spike therefore multiple both by 10: (1ul of plasma x 10 = 10  $\mu\text{L}$ ) + (2.33  $\mu\text{L}$  of diluted fetal fragment x 10 = 23.3  $\mu\text{L}$ ) = 33.3  $\mu\text{L}$  in total for experiment 1.

**To produce fake trisomy spike:**

$$\text{Chr 21 APP: } (124.25 \text{ GE's} / 5) \times 3 = 74.55 \text{ GE's/ Spike}$$

Therefore for 21 (*APP*) to 1  $\mu\text{L}$  of plasma add:

$$74.55 / 47 \text{ molecules/ } \mu\text{L} = 1.59 \mu\text{L}$$

$$\text{Chr 1 EIF2C1: } (124.25 \text{ GE's} / 5) \times 2 = 49.7 \text{ GE's/ Spike}$$

Therefore for 1 (*EIF2C1*) to 1  $\mu\text{L}$  of plasma add:

$$49.7 / 51 = 0.97 \mu\text{L}$$

5% 'DS'-spike: 1  $\mu\text{L}$  genomic plasma DNA, 1.59  $\mu\text{L}$  of chromosome 21 fetal DNA fragment (*APP*) and 0.97  $\mu\text{L}$  of chromosome 1 pseudo-fetal DNA fragment (*EIF2C1*). This was then multiplied by volume required per assay.

**To produce normal spike:**

$$\text{Chr 21 APP } (124.25 \text{ GE's} / 5) \times 2.5 = 62.125 \text{ GE's/ Spike}$$

Therefore for 21 (*APP*) to 1  $\mu\text{L}$  of plasma add:

$$62.125 / 47 \text{ molecules/ } \mu\text{L} = 1.32 \mu\text{L}$$

$$\text{Chr 1 EIF2C1 } (124.25 \text{ GE's} / 5) \times 2.5 = 62.125 \text{ GE's/ Spike}$$

Therefore for 1 (*EIF2C1*) to 1  $\mu$  of plasma add:

$$62.125 / 51 = 1.22 \mu\text{L}$$

5% 'normal'-spike: 1  $\mu\text{L}$  genomic plasma DNA, 1.32  $\mu\text{L}$  of chromosome 21 pseudo-fetal DNA fragment (*APP*) and 1.22  $\mu\text{L}$  chromosome 1 pseudo-fetal DNA fragment (*EIF2C1*). This was then multiplied by volume required per assay.

**APPENDICES 2 – Primer Analysis (Legend: Int, Internal; Ext, External)**

Chromosome 21 Primer Analysis

	<i>DSCR3</i> Ext Forward	<i>DSCR3</i> Ext Reverse	<i>DSCR3</i> Int Forward	<i>DSCR3</i> Int Reverse	<i>RCANI</i> Ext Forward	<i>RCANI</i> Ext Reverse	<i>RCANI</i> Int Forward	<i>RCANI</i> Int Reverse	<i>APP</i> Ext Forward	<i>APP</i> Ext Reverse	<i>APP</i> Int Forward	<i>APP</i> Int Reverse
<b>Primer Length (bp)</b>	20	20	20	21	20	19	19	20	20	20	20	20
<b>Tm °C</b>	57	55.4	57.1	56.2	52.8	56.7	58.5	58.4	56.3	51	54.7	57
<b>Annealing Temp °C</b>	60.96	59.82	56.13	55.86	59.74	60.91	40.90	40.87	60.79	59.2	57.51	58.2
<b>GC content %</b>	55	50	55	47.6	45	57.9	57.9	55	55	40	50	55
<b>GC clamp (need to be ≤ 4)</b>	3	3	2	3	2	3	3	1	3	3	3	3
<b>Hairpins (Delta G)</b>	-0.47	-0.28	-1.36	2.89-2.98	1.58-2.55	-1.65	1.69-1.99	1.1-1.99	1.04-1.6	2.16-2.79	-0.54	-0.54
<b>Self-Dimer (Delta G)</b>	<u>-6.76</u>	-3.14	-4.64	-3.14	-3.61	-5.19	-4.62	-3.14	-3.14	-1.94	-3.61	-3.14
<b>Cross-Dimer (Delta G)</b>	-5.99	-5.99	<u>-6.24</u>	<u>-6.24</u>	-5.19	-5.19	-3.14	-3.14	-1.94	-1.94	-5.12	-5.12
<b>Repeats</b>	None	None	1 (2)	1 (2)	None	1 (2)	1 (2)	1 (2)	None	None	None	1 (2)
<b>Runs (need to be ≤ 4)</b>	2	4	3	3	3	2	2	2	2	<u>5</u>	2	2
<b>3' End Stability (Max Delta G)</b>	-8.13	-9.47	-6.84	-6.46	-8.53	-7.87	-7.96	-5.85	-3.14	-8.19	-3.61	-8.65
<b>BLASTed to test specificity</b>	<a href="#">NC_018932.2</a> (0.017 100%)	<a href="#">NC_000022.11</a>	<a href="#">NC_018932.2</a> (0.017 100%)	<a href="#">NC_018932.2</a> (0.006 100%)	<a href="#">NC_018932.2</a> (0.017 100%)	<a href="#">NC_018932.2</a> (0.044 100%)	<a href="#">NC_018932.2</a> (0.044 100%)	<a href="#">NC_018932.2</a> (0.017 100%)	<a href="#">NC_018932.2</a> (0.017 100%)	<a href="#">NC_018932.2</a> (0.006 100%)	<a href="#">NC_018932.2</a> (0.017 100%)	<a href="#">NC_018932.2</a> (0.017 100%)
<b>Product size</b>	315		87		292		97		286		96	

Chromosome 18 Primer Analysis

	<i>APCDD1</i> Ext Forward	<i>APCDD1</i> Ext Reverse	<i>APCDD1</i> Int Forward	<i>APCDD1</i> Int Reverse	<i>TTR</i> Ext Forward	<i>TTR</i> Ext Reverse	<i>TTR</i> Int Forward	<i>TTR</i> Int Reverse	<i>TNFRSF- IIA, Ext</i> Forward	<i>TNFRSF- IIA, Ext</i> Reverse	<i>TNFRSF- IIA,Int</i> Forward	<i>TNFRSF- IIA,Int</i> Reverse
<b>Primer Length (bp)</b>	20	20	20	22	20	20	19	22	20	20	20	20
<b>T<sub>m</sub> °C</b>	55.9	55.6	55.9	54.5	53.4	55.3	56.4	55.8	55.4	55.2	54.6	55.6
<b>Annealing Temp °C</b>	62.77	62.68	61.37	60.95	55.72	56.29	56.62	56.44	61.22	61.16	56.78	57.08
<b>GC content %</b>	55	50	55	45.5	50	50	57.9	45.5	55	55	50	50
<b>GC clamp (need to be ≤ 3)</b>	3	3	1	2	2	1	3	2	3	3	2	3
<b>Hairpins (Delta G)</b>	-1.22 - - 0.39	-0.23 - 0.4	-0.23 - 0.4	1.96 - 2.89	-0.49 - - 0.33	-0.38 - - 0.14	-1.38 - - 0.42	0.08 - 0.59	-0.27- 0.53	-0.99	-0.71	-0.67
<b>Self-Dimer (Delta G)</b>	-4.67	-3.14	-1.47	-3.61	-4.64	-5.13	-4.67	-5.09	-3.17	-5.38	-3.14	-3.14
<b>Cross-Dimer (Delta G)</b>	-5.02	-5.02	-3.52	-3.52	-3.54	-3.54	-5.12	-5.12	-5.02	-5.02	<u>-6.21</u>	<u>-6.21</u>
<b>Repeats</b>	None	None	None	None	None	None	None	None	1 (2)	None	None	None
<b>Runs (need to be ≤ 4)</b>	3	3	4	3	3	3	3	2	2	3	3	3
<b>3' End Stability (Max Delta G)</b>	-8.07	-6.85	-5.61	-6.46	-6.6	-6.83	-8.07	-7.65	-6.35	-7.58	-6.58	-6.85
<b>BLASTed to test specificity</b>	<a href="#">NC_0189</a> <a href="#">29.2</a> (0.017 100%)	<a href="#">NC_0189</a> <a href="#">29.2</a> (0.017 100%)	<a href="#">NC_0189</a> <a href="#">29.2</a> (0.017 100%)	<a href="#">NC_018929</a> <a href="#">2</a> (0.001 100%)	<a href="#">NC_0189</a> <a href="#">29.2</a> (0.017 100%)	<a href="#">NC_0189</a> <a href="#">29.2</a> (0.017 100%)	<a href="#">NC_0189</a> <a href="#">29.2</a> (0.044 100%)	<a href="#">NC_0189</a> <a href="#">29.2</a> (0.001 100%)	<a href="#">NC_018929.2</a> (0.017 100%)	<a href="#">NC_018929.2</a> (0.017 100%)	<a href="#">NC_0189</a> <a href="#">29.2</a> (0.017 100%)	<a href="#">NC_018929</a> <a href="#">2</a> (0.017 100%)
<b>Product size</b>	297		97		282		98		285		85	

Chromosome 13 Primer Analysis

	<i>SPG20</i> Ext Forward	<i>SPG20</i> Ext Reverse	<i>SPG20</i> Int Forward	<i>SPG20</i> Int Reverse	<i>ZIC2</i> Ext Forward	<i>ZIC2</i> Ext Reverse	<i>ZIC2</i> Int Forward	<i>ZIC2</i> Int Reverse	<i>ATP7B</i> Ext Forward	<i>ATP7B</i> Ext Reverse	<i>ATP7B</i> Int Forward	<i>ATP7B</i> Int Reverse
<b>Primer Length (bp)</b>	20	20	19	21	20	20	21	20	20	20	20	20
<b>Tm °C</b>	60.07	59.14	60.21	58.92	59.21	59.99	60.80	60.40	60.07	59.83	59.09	59.28
<b>Annealing Temp °C</b>			56.3	56.0			59.34	59.22			56.07	56.08
<b>GC content %</b>	55	50	52.63	47.62	55	60	47.62	50	50	50	<u>35</u>	45
<b>GC clamp (need to be ≤ 4)</b>	2	4	1	3	3	3	1	2	2	3	2	none
<b>Hairpins (Delta G)</b>	0.44- 1.39	-0.55	-1.58	-1.53	0.31-0.83	0.63-1.49	0.25	-0.58 to 0.35	0.58 to 1.53	-0.37	0.35 to 1.04	-1.49
<b>Self-Dimer (Delta G)</b>	-4.16	-5.24	-6.62	-3.91	-3.65	-3.14	-3.91	-3.14	-5.38	-6.34 (in central region)	-5.36	-3.91
<b>Cross-Dimer (Delta G)</b>	-3.14	-3.14	-5.02	-5.02	-3.14	-3.14	-4.64	-4.64	-3.9	-3.9	-5.02	-5.02
<b>Repeats</b>	3	3	3	3	none	none	2	none	3	2	3	2
<b>Runs (need to be ≤ 4)</b>	2	none	none	2	2	2	<u>5</u>	3	none	2	none	2
<b>3' End Stability (Max Delta G)</b>	-5.48	<u>-9.76</u>	-6.59	-7.58	-7.26	-6.47	-6.82	-3.14	-6.84	-7.96	-6.96	-5.85
<b>BLASTed to test specificity</b>	<a href="#">NC_01892</a> 4.2 (0.017 100%)	<a href="#">NC_0189</a> 24.2 (0.017 100%)	<a href="#">NC_0189</a> 24.2 (0.044 100%)	<a href="#">NC_018924</a> .2 (0.006 100%)	<a href="#">NC_0189</a> 24.2 (0.017 100%)	<a href="#">NC_018924</a> .2 (0.017 100%)	<a href="#">NC_0189</a> 24.2 (0.006 100%)	<a href="#">NC_0189</a> 24.2 (0.017 100%)	<a href="#">NC_018924</a> .2 (0.017 100%)	<a href="#">NC_018924</a> .2 (0.017 100%)	<a href="#">NC_0189</a> 24.2 (0.017 100%)	<a href="#">NC_018924</a> .2 (0.017 100%)
<b>Product size</b>	297		80		297		90		300		82	

### Chromosome X Primer Analysis

	<i>FOXP3</i> Ext Forward	<i>FOXP3</i> Ext Reverse	<i>FOXP3</i> Int Forward	<i>FOXP3</i> Int Reverse	<i>NROB1</i> Ext Forward	<i>NROB1</i> Ext Reverse	<i>NROB1</i> Int Forward	<i>NROB1</i> Int Reverse	<i>PRPS1</i> Ext Forward	<i>PRPS1</i> Ext Reverse	<i>PRPS1</i> Int Forward	<i>PRPS1</i> Int Reverse
<b>Primer Length (bp)</b>	20	20	19	20	19	20	19	18	20	20	22	20
<b>T<sub>m</sub> °C</b>	60.05	60.35	60.24	60.69	60.25	61.79	58.98	57.48	59.96	58.52	60.88	60.13
<b>Annealing Temp °C</b>			60.6	60.7			60.9	60.44			56.6	56.3
<b>GC content %</b>	50	55	57.89	55.0	52.63	60	57.89	55.56	55	45	50	60
<b>GC clamp (need to be ≤ 4)</b>	2	2	3	2	2	2	3	1	2	2	3	3
<b>Hairpins (Delta G)</b>	1.04	0.98 to 1.94	-1.44	-0.54	1.04	-0.1 to 0.83	-0.1 to 0.72	-0.81 to -0.23	-0.14 to -0.98	-0.2 to 0.79	0.52 to 0.97	-0.79 to -0.35
<b>Self-Dimer (Delta G)</b>	-3.61	-3.14	-3.55	-3.14	-3.61	-3.61	-3.61	-3.55	-3.14	-3.53	-3.14	-4.64
<b>Cross-Dimer (Delta G)</b>	-3.3	-3.3	-4.89	-4.89	-6.31 (at 5' end)	-6.31 (at 5' end)	-6.6 (at 5' end)	-6.6 (at 5' end)	-3.53	-3.53	-4.74	-4.74
<b>Repeats</b>	none	2	2	none	2	2	2	none	2	2	3	none
<b>Runs (need to be ≤ 4)</b>	3	2	3	3	3	2	2	3	2	2	2	3
<b>3' End Stability (Max Delta G)</b>	-6.82	-7.07	-6.73	-8.3	-7.07	-6.24	-7.96	-5.85	-6.46	-6.7	-8.2	-8.03
<b>BLASTed to test specificity</b>	<a href="#">NC_018934</a> _2 (0.017 00%)	<a href="#">NC_018934</a> _34.2 (0.017 100%)	<a href="#">NC_018934</a> _34.2 (0.044 100%)	<a href="#">NC_018934</a> _34.2 (0.017 100%)	<a href="#">NC_018934</a> _34.2 (0.044 100%)	<a href="#">NC_018934</a> _2 (0.017 100%)	<a href="#">NC_018934</a> _34.2 (0.044 100%)	<a href="#">NC_018934</a> _2 (0.17 100%)	Multiple binding do not use			
<b>Product size</b>	288		94		293		89		259		88	



### Chromosome Y Primer Analysis

	<i>SRY*</i> Ext F	<i>SRY*</i> Ext R	<i>SRY*</i> Int F	<i>SRY*</i> Int R	<i>SRY**</i> Ext F	<i>SRY**</i> Ext R	<i>SRY**</i> Int F	<i>SRY**</i> Int R	<i>TSPY1</i> Ext F	<i>TSPY1</i> Ext R	<i>TSPY1</i> Int F	<i>TSPY1</i> Int R	<i>DDX3Y</i> Ext F	<i>DDX3Y</i> Ext R	<i>DDX3Y</i> Int F	<i>DDX3Y</i> Int R	
Primer Length (bp)	20	20	20	20	21	20	20	20	20	20	20	20	20	20	20	22	
Tm °C	52.8	52.8	56.3	56.2	52.6	54.8.	52.3	54.2	58	55.9	53.6	55.8	57.1	57.3	56.8	54.9	
Annealing Temp °C	58.34	58.34	55.19	55.16	47.99	48.65	51.41	51.97	60.6	59.97	55.08	55.74	61.03	61.09	58.14	57.57	
GC content %	45	45	55	50	42.9	50	45	50	55	55	50	55	55	60	55	50	
GC clamp (need to be ≤ 4)	2	2	2	1	1	3	1	3	3	3	0	2	2	3	3	3	
Hairpins (Delta G)	0.02	-0.31 -0.07	-0.98- -0.14	0.05	0.17	-0.95	-2.57	1.01	-0.65- 0.15	1.47- 2.02	2.36- 2.96	0.57- 1.26	-0.21- 0.55	0.65-2.5	0.72- 1.54	1.19- 1.85	
Self-Dimer (Delta G)	-5.36	-3.61	<u>-6.34</u>	<u>-6.3</u>	-4.62	-5.02	-5.02	-3.61	-5.38	-1.95	-1.47	-3.14	-3.55	-4.16	<u>-6.34</u>	-1.95	
Cross-Dimer (Delta G)	-3.61	-3.61	-4.64	-4.64	<u>-6.95</u>	<u>-6.95</u>	<u>-6.85</u>	<u>-6.85</u>	<u>-6.6</u>	<u>-6.6</u>	-1.34	-1.34	-3.14	-3.14	<u>-6.24</u>	<u>-6.24</u>	
Repeats	None	None	2(2)	None	2 (2)	None	None	2 (3)	None	None	None	None	2 (3)	None	None	None	
Runs (need to be ≤ 4)	3	3	2	3	3	2	4	3	2	2	4	3	3	2	3	3	
3' End Stability (Max Delta G)	-8.48	-6.69	-8.19	-5.85	-6.58	-6.47	-7.32	-3.14	-7.58	-8.2	-6.32	-8.63	-7.07	-6.97	-7.96	-7.96	
BLASTed to test specificity	<a href="#">NC_000024</a> <a href="#">.10</a> (0.017 100%)	<a href="#">NC_000024</a> <a href="#">.10</a> (0.017 100%)	<a href="#">NC_000024</a> <a href="#">.10</a> (0.017 100%)	<a href="#">NC_000024</a> <a href="#">.10</a> (0.017 100%)	<a href="#">NC_000024</a> <a href="#">.10</a> (0.006 100%)	<a href="#">NC_000024</a> <a href="#">.10</a> (0.017 100%)	<a href="#">NC_000024</a> <a href="#">.10</a> (0.017 100%)	<a href="#">NC_000024</a> <a href="#">.10</a> (0.017 100%)	<a href="#">NC_000024</a> <a href="#">.10</a> (0.017 100%)	<a href="#">NC_000024</a> <a href="#">.10</a> (0.017 100%)	<a href="#">NC_000024</a> <a href="#">.10</a> (0.017 100%)	<a href="#">NC_000024</a> <a href="#">.10</a> (0.017 100%)	<a href="#">NC_000024</a> <a href="#">.10</a> (0.017 100%)	<a href="#">NC_000024</a> <a href="#">.10</a> (0.017 100%)	<a href="#">NC_000024</a> <a href="#">.10</a> (0.017 100%)	<a href="#">NC_000024</a> <a href="#">.10</a> (0.017 100%)	<a href="#">NC_000024</a> <a href="#">.10</a> (0.001 100%)
Product size	300		89		287			96		293			88		296		89

Legend: F, Forward; R, Reverse.

\*Designed in house by Kelly Sillence. \*\* Designed in house by Hannah Thompson.

## References

Abele, H., Wagner, P., Sonek, J., Hoopmann, M., Brucker, S., Artunc-Ulkumen, B. and Kagan, K. O. (2015) 'First trimester ultrasound screening for Down syndrome based on maternal age, fetal nuchal translucency and different combinations of the additional markers nasal bone, tricuspid and ductus venosus flow'. *Prenatal Diagnosis*, 35 (12). pp 1182-1186.

Agarwal, A., Sayres, L. C., Cho, M. K., Cook-Deegan, R. and Chandrasekharan, S. (2013) 'Commercial landscape of noninvasive prenatal testing in the United States'. *Prenatal Diagnosis*, 33 (6). pp 521-531.

Akinlade, F., Cowans, N., Kisanga, M. and Spencer, K. (2012) 'Maternal serum CA 19-9 and CA 15-3 levels in pregnancies affected by trisomy 21'. *Prenatal Diagnosis*, 32 pp 644-648.

Akolekar, R., Zaragoza, E., Poon, L., Pepes, S. and Nicolaides, K. (2008) 'Maternal serum placental growth factor at 11+ 0 to 13+ 6 weeks of gestation in the prediction of pre-eclampsia'. *Ultrasound in Obstetrics and Gynecology*, 32 (6). pp 732-739.

Alfirevic, Z. and Callaghan, T. (2014) 'Anti-RhD prophylaxis for RhD negative pregnant women'. *BMJ*, 349 pp g5437.

Alberry, M., Maddocks, D., Jones, M., Abdel Hadi, M., Abdel-Fattah, S., Avent, N. and Soothill, P. (2007) 'Free fetal DNA in maternal plasma in anembryonic pregnancies: confirmation that the origin is the trophoblast'. *Prenatal Diagnosis*, 27 (5). pp 415-418.

Allan, J., Fraser, R. M., Owen-Hughes, T. and Keszenman-Pereyra, D. (2012) 'Micrococcal nuclease does not substantially bias nucleosome mapping'. *Journal of Molecular Biology*, 417 (3). pp 152-164.

Allyse, M., Minear, M. A., Berson, E., Sridhar, S., Rote, M., Hung, A. and Chandrasekharan, S. (2015) 'Non-invasive prenatal testing: a review of international implementation and challenges'. *International Journal of Woman's Health*, 7 pp 113.

American College of Obstetricians and Gynecologists (2012) 'Genetics, society for maternal-fetal medicine publications committee. Committee Opinion No. 545:

Noninvasive prenatal testing fo fetal aneuploidy'. *Obstetrics and Gynecology*, 120 pp 1532-1534.

Angert, R. M., LeShane, E. S., Lo, Y. D., Chan, L. Y., Delli-Bovi, L. C. and Bianchi, D. W. (2003) 'Fetal cell-free plasma DNA concentrations in maternal blood are stable 24 hours after collection: analysis of first-and third-trimester samples'. *Clinical Chemistry*, 49 (1). pp 195-198.

Antenatal Results and Choices (2013) 'Non-invasive prenatal testing for Down's syndrome (NIPT)'. [Online]. Available at: <http://www.arc-uk.org/tests-explained/down-syndrome-screening/non-invasive-prenatal-testing-for-down-s-syndrome> (Accessed: November 2nd 2015).

Antwi-Baffour, S., Quao, E., Kyeremeh, R. and Mahmood, S. A. (2013) 'Prolong storage of blood in EDTA has an effect on the morphology and osmotic fragility of erythrocytes'. *International Journal of Biomedical Science and Engineering*, 1(2). pp 20-23.

Ashoor, G., Syngelaki, A., Wagner, M., Birdir, C. and Nicolaides, K. (2012) 'Chromosome-selective sequencing of maternal plasma cell-free DNA for first trimester detection of trisomy 21 and trisomy 18'. *America Journal of Obstetrics and Gynecology*, 206 pp 322.e321-325.

Ashoor, G., Syngelaki, A., Poon, L., Rezende, J. and Nicolaides, K. (2013a) 'Fetal fraction in maternal plasma cell-free DNA at 11–13 weeks' gestation: relation to maternal and fetal characteristics'. *Ultrasound in Obstetrics and Gynecology*, 41 (1). pp 26-32.

Ashoor, G., Syngelaki, A., Wang, E., Struble, C., Oliphant, A., Song, K. and Nicolaides, K. H. (2013b) 'Trisomy 13 detection in the first trimester of pregnancy using a chromosome-selective cell-free DNA analysis method'. *Ultrasound in Obstetrics and Gynecology*, 41 (1). pp 21-25.

Auer, T., Sninsky, J. J., Gelfand, D. H. and Myers, T. W. (1996) 'Selective amplification of RNA utilizing the nucleotide analog dITP and *Thermus thermophilus* DNA polymerase'. *Nucleic Acids Research*, 24 (24). pp 5021-5025.

Avent, N. D., Liu, W., Jones, J. W., Scott, M. L., Voak, D., Pisacka, M., Watt, J. and Fletcher, A. (1997) 'Molecular analysis of Rh transcripts and polypeptides from individuals expressing the DVI variant phenotype: an RHD gene deletion event does not generate all DVIccEe phenotypes'. *Blood*, 89 (5). pp 1779-1786.

Avent, N. D. and Reid, M. E. (2000) 'The Rh blood group system: a review'. *Blood*, 95 (2). pp 375-387.

Avent, N. D. and Chitty, L. S. (2006) 'Non-invasive diagnosis of fetal sex; utilisation of free fetal DNA in maternal plasma and ultrasound'. *Prenatal Diagnosis*, 26 (7). pp 598-603.

Avent, N. D. (2008) 'RHD genotyping from maternal plasma: guidelines and technical challenges'. *Prenatal Diagnosis*. Springer, pp 185-201.

Baker, M. (2012) 'Digital PCR hits its stride'. *Nature Methods*, 9 (6). pp 541-544.

Banch Clausen, F., Steffensen, R., Christiansen, M., Rudby, M., Jakobsen, M., Jakobsen, T., Krog, G., Madsen, R., Nielsen, K. and Rieneck, K. (2014) 'Routine noninvasive prenatal screening for fetal RHD in plasma of RhD-negative pregnant women—2 years of screening experience from Denmark'. *Prenatal Diagnosis*, 3 (10). pp 1000-1005.

Barrett, A. N., Zimmermann, B. G., Wang, D., Holloway, A. and Chitty, L. S. (2011) 'Implementing prenatal diagnosis based on cell-free fetal DNA: accurate identification of factors affecting fetal DNA yield'. *PLoS One*, 6 (10). pp e25202.

Barrett, A. N., McDonnell, T. C., Chan, K. A. and Chitty, L. S. (2012) 'Digital PCR analysis of maternal plasma for noninvasive detection of sickle cell anemia'. *Clinical Chemistry*, 58 (6). pp 1026-1032.

Bartel, D. P. (2009) 'MicroRNAs: target recognition and regulatory functions'. *Cell*, 136 (2). pp 215-233.

Benacerraf, B., Frigoletto, F. J. and Cramer, D. (1987) 'Down syndrome: sonographic sign for diagnosis in the second-trimester fetus'. *Radiology*, 163 pp 811.

Benn, P. A. (2002) 'Advances in prenatal screening for Down syndrome: II first trimester testing, integrated testing, and future directions'. *Clinica Chimica Acta*, 324 (1). pp 1-11.

Benn, P., Cuckle, H. and Pergament, E. (2013) 'Non-invasive prenatal testing for aneuploidy: current status and future prospects'. *Ultrasound in Obstetrics and Gynecology*, 42 (1). pp 15-33.

Benn, P. (2014) 'Non-invasive prenatal testing using cell free DNA in maternal plasma: recent developments and future prospects'. *Journal of Clinical Medicine*, 3 (2). pp 537-565.

Benn, P. (2015) 'Recent publication supports the cost effectiveness of NIPT for all pregnant women, regardless of prior risk'. Natera, Inc., [Online]. Available at: <http://natera.mediaroom.com/2015-08-10-Recent-Publication-Supports-the-Cost-Effectiveness-of-NIPT-for-All-Pregnant-Women-Regardless-of-Prior-Risk>. (Accessed: September 29<sup>th</sup> 2015).

Benn, P., Curnow, K. J., Chapman, S., Michalopoulos, S. N., Hornberger, J. and Rabinowitz, M. (2015) 'An Economic Analysis of Cell-Free DNA Non-Invasive Prenatal Testing in the US General Pregnancy Population'. *Public Library of Sciences ONE*, 10 (7). e0132313.

Benkel, B. F. and Fong, Y. (1996) 'Long range-inverse PCR (LR-IPCR): extending the useful range of inverse PCR'. *Genetic Analysis: Biomolecular Engineering*, 13 (5). pp 123-127.

Bertero, M., Camaschella, C., Serra, A., Bergui, L. and Caligaris-Cappio, F. (1988) 'Circulating 'trophoblast' cells in pregnancy have maternal genetic markers '. *Prenatal Diagnosis*, 8 pp 588-590.

Bianchi, D. W., Zickwolf, G. K., Weil, G. J., Sylvester, S. and DeMaria, M. A. (1996) 'Male fetal progenitor cells persist in maternal blood for as long as 27 years postpartum'. *Proceedings of the National Academy of Sciences*, 93 (2). pp 705-708.

Bianchi, D. W. (1999) 'Fetal cells in the maternal circulation: feasibility for prenatal diagnosis'. *British Journal of Haematology*, 105 (3). pp 574-583.

Bianchi, D. (2004) 'Circulating fetal DNA: its origin and diagnostic potential—a review'. *Placenta*, 25 pp S93-S101.

Bianchi, D. W., Avent, N. D., Costa, J. M. and Van der Schoot, C. E. (2005) 'Noninvasive Prenatal Diagnosis of Fetal Rhesus D: Ready for Prime(r) Time'. *Obstetrics and Gynecology*, 106 (4). pp 841-844.

Bianchi, D. W., Platt, L., Goldberg, J. D., Z, A. A., Sehnert, A. J. and Rava, R. P. (2012) 'Genome-wide fetal aneuploidy detection by maternal plasma DNA sequencing'. *Obstetrics and Gynecology*, 119 pp 890-901.

Bianchi, D. W., Parker, R. L., Wentworth, J., Madankumar, R., Saffer, C., Das, A. F., Craig, J. A., Chudova, D. I., Devers, P. L. and Jones, K. W. (2014) 'DNA sequencing versus standard prenatal aneuploidy screening'. *New England Journal of Medicine*, 370 (9). pp 799-808.

Bischoff, F. Z., Lewis, D. E. and Simpson, J. L. (2005) 'Cell-free fetal DNA in maternal blood: kinetics, source and structure'. *Human Reproductive Update*, 11 (1). pp 59-67.

Blaas, H.-G. K. (2014) 'Detection of structural abnormalities in the first trimester using ultrasound'. *Best Practice and Research in Clinical Obstetrics and Gynaecology*, 28 (3). pp 341-353.

Boon, E. M. J. and Faas, B. H. W. (2013) 'Benefits and limitations of whole genome versus targeted approaches for noninvasive prenatal testing for fetal aneuploidies. '. *Prenatal Diagnosis*, pp DOI: 10.1002/pd.4111.

Boormans, E. M., Birnie, E., Wildschut, H. I., Schuring-Blom, H. G., Oepkes, D., van Oppen, C. A., Nijhuis, J. G., Macville, M. V., Kooper, A. J. and Huijsdens, K. (2008) 'Multiplex ligation-dependent probe amplification versus karyotyping in prenatal diagnosis: the MAKE study'. *BioMed Central Pregnancy and Childbirth*, 8 (1). pp 18.

Borgstrom, E., Lundin, S. and Lundeberg, J. (2011) 'Large scale library generation for high throughput sequencing'. *Public Library of Sciences ONE*, 6 (4). pp e19119.

Bowman, J. (1996) 'Hemolytic disease of the newborn'. *Vox Sanguinis*, 70 (S3). pp 62-67.

Brojer, E., Żupanska, B., Guz, K., Orzinska, A. and Kalinska, A. (2005) 'Noninvasive determination of fetal RHD status by examination of cell-free DNA in maternal plasma'. *Transfusion*, 45 (9). pp 1473-1480.

Buckley, F. and Buckley, S. (2008) 'Wrongful deaths and rightful lives—screening for Down syndrome'. *Down Syndrome Research and Practice*, 12 (2). pp 79-86.

Burger, N. B., Bekker, M. N., Groot, C. J., Christoffels, V. M. and Haak, M. C. (2015) 'Why increased nuchal translucency is associated with congenital heart disease: a systematic review on genetic mechanisms'. *Prenatal Diagnosis*, 35 (6). pp 517-528.

Cameron, M. and Moran, P. (2009) 'Prenatal screening and diagnosis of neural tube defects'. *Prenatal Diagnosis*, 29 (4). pp 402-411.

Cavanagh, C., McHugh, A. and Coppinger, C. (2015) 'Improving outcomes for babies with genetic disorders '. Public Health England (PHE) screening: NHS Blot Spot Screening Programme. [Online]. Available at: [www.publichealth.org.uk](http://www.publichealth.org.uk). (Accessed: November 1<sup>st</sup> 2015).

Chan, K. A., Zhang, J., Hui, A. B., Wong, N., Lau, T. K., Leung, T. N., Lo, K.-W., Huang, D. W. and Lo, Y. D. (2004) 'Size distributions of maternal and fetal DNA in maternal plasma'. *Clinical Chemistry*, 50 (1). pp 88-92.

Chan, K. A., Ding, C., Gerovassili, A., Yeung, S. W., Chiu, R. W., Leung, T. N., Lau, T. K., Chim, S. S., Chung, G. T. and Nicolaides, K. H. (2006) 'Hypermethylated RASSF1A in maternal plasma: a universal fetal DNA marker that improves the reliability of noninvasive prenatal diagnosis'. *Clinical Chemistry*, 52 (12). pp 2211-2218.

Chang, Y.-H., Lee, G.-B., Huang, F.-C., Chen, Y.-Y. and Lin, J.-L. (2006) 'Integrated polymerase chain reaction chips utilizing digital microfluidics'. *Biomedical Microdevices*, 8 (3). pp 215-225.

Chawla, H. (2002) *Introduction to plant biotechnology*. Science Publishers Inc. New Hampshire, USA.

Cheng, S., Fockler, C., Barnes, W. M. and Higuchi, R. (1994) 'Effective amplification of long targets from cloned inserts and human genomic DNA'. *Proceedings of the National Academy of Sciences*, 91 (12). pp 5695-5699.

Childbirth Connection (2012) 'Planning pregnancy genetic counselling and testing'. National Partnership for women and families. [Online]. Available at: <http://www.childbirthconnection.org/article.asp?ck=10310> (Accessed: November 24<sup>th</sup> 2015).

Chilcott, J., Jones, M. L., Wight, J., Forman, K., Wray, J., Beverley, C. and Tappenden, P. (2003) 'A review of the clinical effectiveness and cost-effectiveness of routine anti-D prophylaxis for pregnant women who are rhesus-negative'. *Health Technological Assessment*, 7 (4). pp ii-62.

Chilcott, J., Tappenden, P., Lloyd Jones, M., Wight, J., Forman, K., Wray, J. and Beverley, C. (2004) 'The economics of routine antenatal anti-D prophylaxis for pregnant women who are rhesus negative'. *BJOG: An International Journal of Obstetrics and Gynaecology*, 111 (9). pp 903-907.

Chim, S. S., Tong, Y. K., Chiu, R. W., Lau, T. K., Leung, T. Y., Chan, L. Y. S., Oudejans, C. B. M., Ding, C. and Lo, Y. M. (2005) 'Detection of the placental epigenetic signature of the maspin gene in maternal plasma'. *Proceedings of the National Academy of Sciences of the United States of America*, 11 pp 14753-14758.

Chim, S. S., Jin, S., Lee, T. Y., Lun, F. M., Lee, W. S., Chan, L. Y., Jin, Y., Yang, N., Tong, Y. K. and Leung, T. Y. (2008a) 'Systematic search for placental DNA-methylation markers on chromosome 21: toward a maternal plasma-based epigenetic test for fetal trisomy 21'. *Clinical Chemistry*, 54 (3). pp 500-511.

Chim, S. S., Shing, T. K., Hung, E. C., Leung, T.-y., Lau, T.-k., Chiu, R. W. and Lo, Y. D. (2008b) 'Detection and characterization of placental microRNAs in maternal plasma'. *Clinical Chemistry*, 54 (3). pp 482-490.



Chinnapapagari, S. K. R., Holzgreve, W., Lapaire, O., Zimmermann, B. and Hahn, S. (2005) 'Treatment of maternal blood samples with formaldehyde does not alter the proportion of circulatory fetal nucleic acids (DNA and mRNA) in maternal plasma'. *Clinical Chemistry*, 51 (3). pp 652-655.

Chitty, L. S., van der Schoot, C. E., Hahn, S. and Avent, N. D. (2008) 'SAFE-The Special Non-invasive Advances in Fetal and Neonatal Evaluation Network: aims and achievements'. *Prenatal Diagnosis*, 28 pp 83-88.

Chitty, L. S., Hill, L., White, H., Wright, D. and Morris, S. (2012) 'Noninvasive prenatal testing for aneuploidy-ready for prime time? '. *American Journal of Obstetrics and Gynecology*, pp 269-275.

Chitty, L. S., Finning, K., Wade, A., Soothill, P., Martin, B., Oxenford, K., Daniels, G. and Massey, E. (2014) 'Diagnostic accuracy of routine antenatal determination of fetal RHD status across gestation: population based cohort study'. *British Medical Journal*, 349 pp g5243.

Chiu, R. W., Poon, L. L., Lau, T. K., Leung, T. N., Wong, E. M. and Lo, Y. D. (2001) 'Effects of blood-processing protocols on fetal and total DNA quantification in maternal plasma'. *Clinical Chemistry*, 47 (9). pp 1607-1613.

Chiu, R. W., Lau, T. K., Leung, T. N., Chow, K. C., Chui, D. H. and Lo, Y. D. (2002) 'Prenatal exclusion of  $\beta$  thalassaemia major by examination of maternal plasma'. *Lancet*, 360 (9338). pp 998-1000.

Chiu, R. W. K., Cantor, C. R. and Lo, Y. M. D. (2009) 'Non-invasive prenatal diagnosis by single molecule counting technologies '. *Trends in Genetics*, 25 (7). pp 324-331.

Chiu, R. W., Akolekar, R., Zheng, Y. W., Leung, T. Y., Sun, H., Chan, K. C., Lun, F. M., Go, A. T., Lau, E. T., To, W. W. and AL, E. (2011) 'Non-invasive prenatal assessment of trisomy 21 by multiplexed maternal plasma DNA sequencing: large scale validity study'. *British Medical Journal*, 11 pp 342:c7401.

Choi, H., Lau, T., Jiang, F., Chan, M., Zhang, H., Lo, P., Chen, F., Zhang, L. and Wang, W. (2013) 'Fetal aneuploidy screening by maternal plasma DNA sequencing: 'false positive' due to confined placental mosaicism'. *Prenatal Diagnosis*, 33 (2). pp 198-200.

Choolani, M., Mahyuddin, A. P. and Hahn, S. (2012) 'The promise of fetal cells in maternal blood'. *Best Practice and Research Clinical Obstetrics and Gynaecology*, 26 (5). pp 655-667.

Choy, K., Kwok, Y., Cheng, Y., Wong, K., Wong, H., Leung, K., Suen, K., Adler, K., Wang, C. and Lau, T. (2014) 'Diagnostic accuracy of the BACs-on-Beads™ assay versus karyotyping for prenatal detection of chromosomal abnormalities: a retrospective consecutive case series'. *British Journal of Obstetrics and Gynaecology*, 121 (10). pp 1245-1252.

Christiansen, M., Pihl, K., Hedley, P. L., Gjerris, A. C., Lind, P. Ø., Larsen, S. O., Krebs, L. and Larsen, T. (2010) 'ADAM 12 may be used to reduce the false positive rate of first trimester combined screening for Down syndrome'. *Prenatal Diagnosis*, 30 (2). pp 110-114.

Chung, G. T., Chiu, R. W., Chan, K. A., Lau, T. K., Leung, T. N. and Lo, Y. D. (2005) 'Lack of dramatic enrichment of fetal DNA in maternal plasma by formaldehyde treatment'. *Clinical Chemistry*, 51 (3). pp 655-658.

Ciaranfi, A., Curchod, A. and Odartchenko, N. (1977) '[Post-partum survival of fetal lymphocytes in the maternal blood]'. *Schweizerische Medizinische Wochenschrift*, 107 (5). pp 134-138.

Cicero, S., Sacchini, C., Rembouskos, G. and Nicolaides, K. (2003) 'Sonographic markers of fetal aneuploidy—a review'. *Placenta*, 24 pp S88-S98.

Comas, C., Bermejo, B., Hilari, J. and Echevarria, M. (2014) 'OP03. 03: Implementation of non-invasive prenatal testing (NIPT) for fetal aneuploidy in a general screening population in two European centres'. *Ultrasound in Obstetrics and Gynecology*, 44 (S1). pp 69-69.

Contente-Cuomo, T. and Murtaza, M. (2015) 'Quality assessment of circulating cell-free DNA using multiplexed droplet-digital PCR'. *Cancer Research*, 75 (15 Supplement). pp 2404-2404.

Costa, J. M., Benachi, A., Gautier, E., Jouannic, J. M., Ernault, P. and Dumez, Y. (2001) 'First-trimester fetal sex determination in maternal serum using real-time PCR'. *Prenatal Diagnosis*, 21 (12). pp 1070-1074.

Cowans, N., Stamatopoulou, A., Tørring, N. and Spencer, K. (2011) 'Early first-trimester maternal serum placental growth factor in trisomy 21 pregnancies'. *Ultrasound in Obstetrics and Gynecology*, 37 (5). pp 515-519.

Credidio, D., Pellegrino Jr, J. and Castilho, L. (2011) 'Serologic and molecular characterization of D variants in Brazilians: impact for typing and transfusion strategy'. *Immunohematology*, 27 (1). pp 6-11.

Crosley, E., Durland, U., Seethram, K., MacRae, S., Gruslin, A. and Christians, J. (2013) 'First trimester maternal circulating levels of pregnancy-associated plasma protein A2 (PAPP-A2) are elevated in pregnancies that subsequently develop preeclampsia'. *Placenta*, 9 (34). pp A53.

Cupp, J. E., Leary, J. F., Cernichiari, E., Wood, J. and Doherty, R. A. (1984) 'Rare-event analysis methods for detection of fetal red blood cells in maternal blood'. *Cytometry*, 5 (2). pp 138-144.

Daley, R., Hill, M. and Chitty, L. S. (2014) 'Non-invasive prenatal diagnosis: progress and potential'. *Archives of Disease in Childhood-Fetal and Neonatal Edition*, pp fetalneonatal-2013-304828.

Daniels, G., Faas, B., Green, C., Smart, E., Maaskant-van Wijk, P., Avent, N., Zondervan, H., Borne, A. and Schoot, C. v. d. (1998) 'The VS and V blood group polymorphisms in Africans: a serologic and molecular analysis'. *Transfusion*, 38 (10). pp 951-958.

Daniels, G., Finning, K., Martin, P. and Massey, E. (2009a) 'Noninvasive prenatal diagnosis of fetal blood group phenotypes: current practice and future prospects'. *Prenatal Diagnosis*, 29 (2). pp 101-107.

Daniels, G., Van Der Schoot, C., Gassner, C. and Olsson, M. L. (2009b) 'Report of the third international workshop on molecular blood group genotyping'. *Vox Sanguinis*, 96 (4). pp 337-343.

Daniels, G. (2013) 'Variants of RhD—current testing and clinical consequences'. *British Journal of Haematology*, 161 (4). pp 461-470.

Dawson, S.-J., Tsui, D. W., Murtaza, M., Biggs, H., Rueda, O. M., Chin, S.-F., Dunning, M. J., Gale, D., Forshew, T. and Mahler-Araujo, B. (2013) 'Analysis of circulating tumor DNA to monitor metastatic breast cancer'. *New England Journal of Medicine*, 368 (13). pp 1199-1209.

Das, K., Dumais, J., Basiaga, S. and Krzyzanowski, G. D. (2013) 'Carbon-13 nuclear magnetic resonance analysis of formaldehyde free preservatives'. *Acta histochemica*, 115 (5). pp 481-486.

De Haas, M., Van der Ploeg, C., Scheffer, P., Verlinden, D., Hirschberg, H., Abbink, F. and van der Schoot, C. (2012) 'A nation-wide fetal RHD screening programme for targeted antenatal and postnatal anti-D'. *ISBT Science Series*, 7 (1). pp 164-167.

de Jong, A., Dondorp, W. J., de Die-Smulders, C. E., Frints, S. G. and de Wert, G. M. (2010) 'Non-invasive prenatal testing: ethical issues explored'. *European Journal of Human Genetics*, 18 (3). pp 272-277.

Deng, Y.-H., Yin, A.-H., He, Q., Chen, J.-C., He, Y.-S., Wang, H.-Q., Li, M. and Chen, H.-Y. (2011) 'Non-invasive prenatal diagnosis of trisomy 21 by reverse transcriptase multiplex ligation-dependent probe amplification'. *Clinical Chemistry and Laboratory Medicine*, 49 (4). pp 641-646.

Denomme, G. A., Wagner, F. F., Fernandes, B. J., Li, W. and Flegel, W. A. (2005) 'Partial D, weak D types, and novel RHD alleles among 33,864 multiethnic patients: implications for anti-D alloimmunization and prevention'. *Transfusion*, 45 (10). pp 1554-1560.

Devers, P. L., Cronister, A., Ormond, K. E., Facio, F., Brasington, C. K. and Flodman, P. (2013) 'Noninvasive prenatal testing/noninvasive prenatal diagnosis: the position of the

National Society of Genetic Counselors'. *Journal of Genetic Counseling*, 22 (3). pp 291-295.

Devonshire, A. S., Whale, A. S., Gutteridge, A., Jones, G., Cowen, S., Foy, C. A. and Huggett, J. F. (2014) 'Towards standardisation of cell-free DNA measurement in plasma: controls for extraction efficiency, fragment size bias and quantification'. *Analytical and Bioanalytical Chemistry*, 406 (26). pp 6499-6512.

Dhallan, R., Au, W.-C., Mattagajasingh, S., Emche, S., Bayliss, P., Damewood, M., Cronin, M., Chou, V. and Mohr, M. (2004) 'Methods to increase the percentage of free fetal DNA recovered from the maternal circulation'. *Journal of the Medical Association*, 291 (9). pp 1114-1119.

Diehl, F., Li, M., Dressman, D., He, Y., Shen, D., Szabo, S., Diaz, L. A., Goodman, S. N., David, K. A. and Juhl, H. (2005) 'Detection and quantification of mutations in the plasma of patients with colorectal tumors'. *Proceedings of the National Academy of Sciences of the United States of America*, 102 (45). pp 16368-16373.

Dodd, D. W., Gagnon, K. T. and Corey, D. R. (2013) 'Digital quantitation of potential therapeutic target RNAs'. *Nucleic Acid Therapeutics*, 23 (3). pp 188-194.

Dondorp, W., de Wert, G., Bombard, Y., Bianchi, D. W., Bergmann, C., Borry, P., Chitty, L. S., Fellmann, F., Forzano, F. and Hall, A. (2015) 'Non-invasive prenatal testing for aneuploidy and beyond: challenges of responsible innovation in prenatal screening'. *European Journal of Human Genetics*, 23 (11). Pp 1438-1450.

Driscoll, D. A. and Gross, S. (2009) 'Prenatal screening for aneuploidy'. *New England Journal of Medicine*, 360 (24). pp 2556-2562.

Du, Y., Zhang, J., Wang, H., Yan, X., Yang, Y., Yang, L., Luo, X., Chen, Y., Duan, T. and Ma, D. (2011) 'Hypomethylated DSCR4 is a placenta-derived epigenetic marker for trisomy 21'. *Prenatal Diagnosis*, 31 (2). pp 207-214.

Duhaime, M. B., Deng, L., Poulos, B. T. and Sullivan, M. B. (2012) 'Towards quantitative metagenomics of wild viruses and other ultra-low concentration DNA samples: a rigorous assessment and optimization of the linker amplification method'. *Environmental Microbiology*, 14 (9). pp 2526-2537.

Eder, A. (2006) 'Update on HDFN: new information on long-standing controversies'. *Immunohematology-Washington DC*, 22 (4). pp 188.

Ehrich, M., Deciu, C., Zwiefelhofer, T., Tynan, J. A., Cagasan, L., Tim, R., Lu, V., McCullough, R., McCarthy, E. and Nygren, A. O. (2011) 'Noninvasive detection of fetal trisomy 21 by sequencing of DNA in maternal blood: a study in a clinical setting'. *American Journal of Obstetrics and Gynecology*, 204 (3). pp 205. e201-205. e211.

El Messaoudi, S. and Thierry, A. R. (2015) 'Pre-analytical Requirements for Analyzing Nucleic Acids from Blood'. *Circulating Nucleic Acids in Early Diagnosis, Prognosis and Treatment Monitoring*. Springer, pp 45-69.

Elnifro, E. M., Ashshi, A. M., Cooper, R. J. and Klapper, P. E. (2000) 'Multiplex PCR: optimization and application in diagnostic virology'. *Clinical Microbiology Reviews*, 13 (4). pp 559-570.

Emad, A., Bouchard, E. F., Lamoureux, J., Ouellet, A., Dutta, A., Klingbeil, U. and Drouin, R. (2014) 'Validation of automatic scanning of microscope slides in recovering rare cellular events: application for detection of fetal cells in maternal blood'. *Prenatal Diagnosis*, 34 (6). pp 538-546.

Enari, M., Sakahira, H., Yokoyama, H., Okawa, K., Iwamatsu, A. and Nagata, S. (1998) 'A caspase-activated DNase that degrades DNA during apoptosis, and its inhibitor ICAD'. *Nature*, 391 (6662). pp 43-50.

Epstein, C. J. (2013) 'of Down Syndrome'. *Molecular Genetic Medicine*, 2 pp 105.

Eslami, G. and Salehi, R. (2014) 'Development of a chamber system for rapid, high yield and cost-effective purification of deoxyribonucleic acid fragments from agarose gel'. *Advanced biomedical research*, 3

Fairbrother, G., Johnson, S., Musci, T. J. and Song, K. (2013) 'Clinical experience of noninvasive prenatal testing with cell-free DNA for fetal trisomies 21, 18, and 13, in a general screening population'. *Prenatal Diagnosis*, 33 (6). pp 580-583.

Fairbrother, G., Burigo, J., Sharon, T. and Song, K. (2015) 'Prenatal screening for fetal aneuploidies with cell-free DNA in the general pregnancy population: a cost-effectiveness analysis'. *The Journal of Maternal-Fetal and Neonatal Medicine*, (ahead-of-print). pp 1-5.

Fan, H. C., Blumenfeld, Y. J., Chitkara, U., Hudgins, L. and Quake, S. R. (2008) 'Noninvasive diagnosis of fetal aneuploidy by shotgun sequencing DNA from maternal blood'. *Proceedings of National Academy of Sciences of the United States of America*, 105 (42). pp 16266-16271.

Fan, H. C., Blumenfeld, Y. J., El-Sayed, Y. Y., Chueh, J. and Quake, S. R. (2009) 'Microfluidic digital PCR enables rapid prenatal diagnosis of fetal aneuploidy'. *American Journal of Obstetrics and Gynecology*, 200 (5). pp 543. e541-543. e547.

Fan, H. C., Blumenfeld, Y. J., Chitkara, U., Hudgins, L. and Quake, S. R. (2010) 'Analysis of the size distributions of fetal and maternal cell-free DNA by paired-end sequencing'. *Clinical Chemistry*, 56 (8). pp 1279-1286.

Farina, A., LeShane, E. S., Romero, R., Gomez, R., Chaiworapongsa, T., Rizzo, N. and Bianchi, D. W. (2005) 'High levels of fetal cell-free DNA in maternal serum: a risk factor for spontaneous preterm delivery'. *American Journal of Obstetrics and Gynecology*, 193 (2). pp 421-425.

Ferguson-Smith, M. A. (2003) 'Placental mRNA in maternal plasma: prospects for fetal screening'. *Proceedings of the National Academy of Sciences of the United States of America*, 100 (8). pp 4360-4362.

Fichou, Y., Audrézet, M., Guéguen, P., Dupont, I., Jamet, D., Le Maréchal, C. and Ferec, C. (2013) 'Next-Generation Sequencing (NGS) for blood group genotyping', *Vox Sanguinis*. Wiley-Blackwell 111 River St, Hoboken 07030-5774, NJ USA, pp. 59-59.

Finning, K. M. and Chitty, L. S. (2008) 'Non-invasive fetal sex determination: impact on clinical practice', *Seminars in Fetal and Neonatal Medicine*. Elsevier, pp. 69-75.

Finning, K., Martin, P., Summers, J., Massey, E., Poole, G. and Daniels, G. (2008) 'Effect of high throughput RHD typing of fetal DNA in maternal plasma on use of anti-RhD

immunoglobulin in RhD negative pregnant women: prospective feasibility study'. *British Medical Journal*, 336 (7648). pp 816-818.

Flegel, W. A. (2007) 'The genetics of the Rhesus blood group system'. *Blood Transfusion*, 5 (2). pp 50.

Forest, M. G., Morel, Y. and David, M. (1998) 'Prenatal treatment of congenital adrenal hyperplasia'. *Trends in Endocrinology and Metabolism*, 9 (7). pp 284-289.

Fung, K. F. K., Eason, E., Crane, J., Armson, A., De La Ronde, S., Farine, D., Keenan-Lindsay, L., Leduc, L., Reid, G. and Aerde, J. (2003) 'Prevention of Rh alloimmunization'. *Journal of obstetrics and gynaecology Canada: JOGC= Journal d'obstetrique et gynecologie du Canada: JOGC*, 25 (9). pp 765-773.

Futch, T., Spinosa, J., Bhatt, S., Feo, E., Rava, R. P. and Sehnert, A. J. (2013) 'Initial clinical laboratory experience in noninvasive prenatal testing for fetal aneuploidy from maternal plasma DNA samples'. *Prenatal Diagnosis*, 33 (6). pp 569-574.

Fyfe, T. M., Ritchey, M. J., Taruc, C., Crompton, D., Galliford, B. and Perrin, R. (2014) 'Appropriate provision of anti-D prophylaxis to RhD negative pregnant women: a scoping review'. *BMC pregnancy and childbirth*, 14 (1). pp 411.

Galbiati, S., Foglieni, B., Travi, M., Curcio, C., Restagno, G., Sbaiz, L., Smid, M., Pasi, F., Ferrari, A. and Ferrari, M. (2008) 'Peptide-nucleic acid-mediated enriched polymerase chain reaction as a key point for non-invasive prenatal diagnosis of  $\beta$ -thalassemia'. *Haematologica*, 93 (4). pp 610-614.

Galbiati, S., Brisci, A., Lalatta, F., Seia, M., Makrigiorgos, G. M., Ferrari, M. and Cremonesi, L. (2011) 'Full COLD-PCR protocol for noninvasive prenatal diagnosis of genetic diseases'. *Clinical Chemistry*, 57 (1). pp 136-138.

Gänshirt, D., Smeets, F. W., Dohr, A., Walde, C., Steen, I., Lapucci, C., Falcinelli, C., Sant, R., Velasco, M. and Garritsen, H. S. (1998) 'Enrichment of fetal nucleated red blood cells from the maternal circulation for prenatal diagnosis: experiences with triple density gradient and MACS based on more than 600 cases'. *Fetal Diagnosis and Therapy*, 13 (5). pp 276-286.



Gassner, C., Meyer, S., Frey, B. M. and Vollmert, C. (2013) 'Matrix-assisted laser desorption/ionisation, time-of-flight mass spectrometry-based blood group genotyping—the alternative approach'. *Transfusion Medicine Reviews*, 27 (1). pp 2-9.

Gautier, E., Benachi, A., Giovangrandi, Y., Ernault, P., Olivi, M., Gaillon, T. and Costa, J.-M. (2005) 'Fetal RhD genotyping by maternal serum analysis: a two-year experience'. *American Journal of Obstetrics and Gynecology*, 192 (3). pp 666-669.

Genetics Home Reference (2014) 'Chromosomes'. [Online]. Available at: <http://ghr.nlm.nih.gov/chromosome/> (Accessed: December 3<sup>rd</sup> 2015).

Ghi, T., Huggon, I., Zosmer, N. and Nicolaides, K. (2001) 'Incidence of major structural cardiac defects associated with increased nuchal translucency but normal karyotype'. *Ultrasound in Obstetrics and Gynecology*, 18 (6). pp 610-614.

Gibson, N. J. (2006) 'The use of real-time PCR methods in DNA sequence variation analysis'. *Clinica Chimica Acta*, 363 (1). pp 32-47.

Gil, M., Quezada, M., Bregant, B., Ferraro, M. and Nicolaides, K. (2013) 'Implementation of maternal blood cell-free DNA testing in early screening for aneuploidies'. *Ultrasound in Obstetrics and Gynecology*, 42 (1). pp 34-40.

Glaab, W. E. and Tindall, K. R. (1997) 'Mutation rate at the hprt locus in human cancer cell lines with specific mismatch repair-gene defects'. *Carcinogenesis*, 18 (1). pp 1-8.

Glasel, J. (1995) 'Validity of nucleic acid purities monitored by 260nm/280nm absorbance ratios'. *BioTechniques*, 18 (1). pp 62-63.

Go, A. T., van Vugt, J. M. and Oudejans, C. B. (2010) 'Non-invasive aneuploidy detection using free fetal DNA and RNA in maternal plasma: recent progress and future possibilities'. *Human Reproduction Update*, 17 (3). pp 372-382.

Grande, M., Ordoñez, E., Cirigliano, V., Cid, J., Grau, E., Pericot, A., Teixido, I., Marin, J. and Borrell, A. (2013) 'Clinical application of midtrimester non-invasive fetal RHD

genotyping and identification of RHD variants in a mixed-ethnic population'. *Prenatal Diagnosis*, 33 (2). pp 173-178.

Green, J. M., Hewison, J., Bekker, H. L., Bryant, L. D. and Cuckle, H. S. (2004) 'Psychosocial aspects of genetic screening of pregnant women and newborns: a systematic review'. *National Institute for Health Research Journals Library*, 8 (33). pp 1366-5278.

Greene, J. (1998) *Recombinant DNA principles and methodologies*. CRC Press. Florida, USA.

Grootkerk-Tax, M. G., Maaskant-van Wijk, P. A., Van Drunen, J., Der Schoot, V. and Ellen, C. (2005) 'The highly variable RH locus in nonwhite persons hampers RHD zygosity determination but yields more insight into RH-related evolutionary events'. *Transfusion*, 45 (3). pp 327-337.

Groves, R., Sunderajan, L., Khan, A. R., Parikh, D., Brain, J. and Samuel, M. (2006) 'Congenital anomalies are commonly associated with exomphalos minor'. *Journal of Pediatric Surgery*, 41 (2). pp 358-361.

Gulati, G. L., Hyland, L. J., Kocher, W. and Schwarting, R. (2002) 'Changes in automated complete blood cell count and differential leukocyte count results induced by storage of blood at room temperature'. *Archives of pathology and laboratory medicine*, 126 (3). pp 336-342.

Haak, M. C., Bartelings, M. M., Jackson, D. G., Webb, S., van Vugt, J. M. and Gittenberger-de Groot, A. C. (2002) 'Increased nuchal translucency is associated with jugular lymphatic distension'. *Human Reproduction*, 17 (4). pp 1086-1092.

Haddad, G., Favre, X., Briere, N., Aloin, M., Chretien, S., Develay-Morice, J. and Ghanimeh, J. (2015) 'EP06. 02: Automated measurement of nuchal translucency by volume NT<sup>TM</sup>(3D ultrasound): feasibility and reproducibility about 100 consecutive measurements by five physicians'. *Ultrasound in Obstetrics and Gynecology*, 46 (S1). pp 201-202.

Haddow, J. E., Palomaki, G. E., Knight, G. J., Williams, J., Pulkkinen, A., Canick, J. A., Saller Jr, D. N. and Bowers, G. B. (1992) 'Prenatal screening for Down's syndrome with use of maternal serum markers'. *New England Journal of Medicine*, 327 (9). pp 588-593.

Haer-Wigman, L., Ji, Y., Lodén, M., Haas, M., Schoot, C. E. and Veldhuisen, B. (2013a) 'Comprehensive genotyping for 18 blood group systems using a multiplex ligation-dependent probe amplification assay shows a high degree of accuracy'. *Transfusion*, 53 (11pt2). pp 2899-2909.

Haer-Wigman, L., Veldhuisen, B., Jonkers, R., Lodén, M., Madgett, T. E., Avent, N. D., Haas, M. and Schoot, C. E. (2013b) 'RHD and RHCE variant and zygosity genotyping via multiplex ligation-dependent probe amplification'. *Transfusion*, 53 (7). pp 1559-1574.

Hahn, M., Wilhelm, J. and Pingoud, A. (2001) 'Influence of fluorophor dye labels on the migration behavior of polymerase chain reaction-amplified short tandem repeats during denaturing capillary electrophoresis'. *Electrophoresis*, 22 (13). pp 2691-2700.

Hahn, S., Huppertz, B. and Holzgreve, W. (2005) 'Fetal cells and cell free fetal nucleic acids in maternal blood: new tools to study abnormal placentation?'. *Placenta*, 26 (7). pp 515-526.

Halawani, A., Altayar, M., Kiernan, M., Reynolds, A. and Kaushik, N. (2014) 'Can nextgeneration DNA sequencing solve the RH complexity for genotyping'. *Vox Sang*, 107 (S1). pp 196.

Halicka, H. D., Bedner, E. and Darzynkiewicz, Z. (2000) 'Segregation of RNA and separate packaging of DNA and RNA in apoptotic bodies during apoptosis'. *Experimental cell research*, 260 (2). pp 248-256.

Hall, A., Bostanci, A. and Wright, C. (2010) 'Non-invasive prenatal diagnosis using cell-free fetal DNA technology: applications and implications'. *Public Health Genomics*, 13 (4). pp 246-255.

Hallak, M., Johnson, M., Pryde, P., Isada, N., Zador, I. and Evans, M. (1992) 'Chorionic villus sampling: transabdominal versus transcervical approach in more than 4000 cases'. *Journal of Obstetrics and Gynaecology*, 80 (3, Part 2). pp 349-352.

Hartl, D. and Jones, E. (2005) *Genetics: Analysis of Genes and Genomes*. Sixth edn. Sudbury, MA Jones and Bartlett Publishes

Herzenberg, L. A., Bianchi, D. W., Schröder, J., Cann, H. M. and Iverson, G. M. (1979) 'Fetal cells in the blood of pregnant women: detection and enrichment by fluorescence-

activated cell sorting'. *Proceedings of the National Academy of Sciences of the United States of America*, 76 (3). pp 1453-1455.

Hashmi, G., Shariff, T., Zhang, Y., Cristobal, J., Chau, C., Seul, M., Vissavajhala, P., Baldwin, C., Hue-Roye, K. and Charles-Pierre, D. (2007) 'Determination of 24 minor red blood cell antigens for more than 2000 blood donors by high-throughput DNA analysis'. *Transfusion*, 47 (4). pp 736-747.

Hayden, R., Gu, Z., Ingersoll, J., Abdul-Ali, D., Shi, L., Pounds, S. and Caliendo, A. (2013) 'Comparison of droplet digital PCR to real-time PCR for quantitative detection of cytomegalovirus'. *Journal of Clinical Microbiology*, 51 (2). pp 540-546.

Heywood, W. E., Madgett, T. E., Wang, D., Wallington, A., Hogg, J., Mills, K. and Avent, N. D. (2011) '2D DIGE analysis of maternal plasma for potential biomarkers of Down Syndrome'. *Proteome Science*, 9 (1). pp 56.

Heywood, W., Mills, K., Wang, D., Hogg, J., Madgett, T. E., Avent, N. D. and Chitty, L. S. (2012) 'Identification of new biomarkers for Down's syndrome in maternal plasma'. *Journal of Proteomics*, 75 (9). pp 2621-2628.

Hidestrand, M., Stokowski, R., Song, K., Oliphant, A., Deavers, J., Goetsch, M., Simpson, P., Kuhlman, R., Ames, M. and Mitchell, M. (2012) 'Influence of temperature during transportation on cell-free DNA analysis'. *Fetal Diagnosis and Therapy*, 31 (2). pp 122-128.

Hill, L. (1996) 'The sonographic detection of trisomies 13, 18 and 21'. *Clinical Obstetrics and Gynecology*, 39 pp 831-850.

Hill, M., Finning, K., Martin, P., Hogg, J., Meaney, C., Norbury, G., Daniels, G. and Chitty, L. (2011) 'Non-invasive prenatal determination of fetal sex: translating research into clinical practice'. *Clinical Genetics*, 80 (1). pp 68-75.

Hill, M., Wright, D., Daley, R., Lewis, C., McKay, F., Mason, S., Lench, N., Howarth, A., Boustred, C. and Lo, K. (2014) 'Evaluation of non-invasive prenatal testing (NIPT) for aneuploidy in an NHS setting: a reliable accurate prenatal non-invasive diagnosis (RAPID) protocol'. *BioMed Central Pregnancy and Childbirth*, 14 (1). pp 229.

Hillyer, C. D., Shaz, B. H., Winkler, A. M. and Reid, M. (2008) 'Integrating molecular technologies for red blood cell typing and compatibility testing into blood centers and transfusion services'. *Transfusion Medicine Reviews*, 22 (2). pp 117-132.

Hindson, B. J., Ness, K. D., Masquelier, D. A., Belgrader, P., Heredia, N. J., Makarewicz, A. J., Bright, I. J., Lucero, M. Y., Hiddessen, A. L. and Legler, T. C. (2011) 'High-throughput droplet digital PCR system for absolute quantitation of DNA copy number'. *Analytical Chemistry*, 83 (22). pp 8604-8610.

Hindson, C. M., Chevillet, J. R., Briggs, H. A., Gallichotte, E. N., Ruf, I. K., Hindson, B. J., Vessella, R. L. and Tewari, M. (2013) 'Absolute quantification by droplet digital PCR versus analog real-time PCR'. *Nature Methods*, 10 (10). pp 1003-1005.

Honda, H., Mihar, N., Ohashi, Y., Samura, O., Kinutani, M., Hara, T. and Ohama, K. (2002) 'Fetal gender determination in early pregnancy through qualitative and quantitative analysis of fetal DNA in maternal serum'. *Human Genetics*, 110 (1). pp 75-79.

Houfflin-Debarge, V., Ronique, E., O'donnell, H., Overton, T., Bennett, P. R. and Fisk, N. M. (2000) 'High sensitivity of fetal DNA in plasma compared to serum and nucleated cells using un-nested PCR in maternal blood'. *Fetal Diagnosis and Therapy*, 15 (2). pp 102-107.

Hua, R., Barrett, A. N., Tan, T. Z., Huang, Z., Mahyuddin, A. P., Ponnusamy, S., Sandhu, J. S., Ho, S. S., Chan, J. K. and Chong, S. (2014) 'Detection of aneuploidy from single fetal nucleated red blood cells using whole genome sequencing'. *Prenatal Diagnosis*, 35 pp 637-644.

Huang, D. J., Zimmermann, B. G., Holzgreve, W. and Hahn, S. (2005) 'Use of an automated method improves the yield and quality of cell-free fetal DNA extracted from maternal plasma'. *Clinical Chemistry*, 51 (12). pp 2419-2420.

Huang, Z., Fong, C. Y., Gauthaman, K., Sukumar, P., Choolani, M. and Bongso, A. (2011) 'Novel approaches to manipulating foetal cells in the maternal circulation for non-invasive prenatal diagnosis of the unborn child'. *Journal of Cellular Biochemistry*, 112 (6). pp 1475-1485.

Huettel, B., Kreil, D. P., Matzke, M. and Matzke, A. J. (2008) 'Effects of aneuploidy on genome structure, expression, and interphase organization in *Arabidopsis thaliana*'. *Public Library of Sciences Genetics*, 4 (10). pp e1000226.

Human Genetics Commission and the UK National Screening Committee (2005) *Profiling the newborn: a prospective gene technology?* London: Human Genetics Commission.

Hussein, N., Qureshi, N., Weng, S. F., Kleijnen, J. and Kai, J. (2013) 'Preconception risk assessment for thalassaemia, sickle cell disease, cystic fibrosis and Tay-Sachs disease'. *The Cochrane Library*, 12 (8). DOI: 10.1002/14651858.CD010849.

Hyett, J., Moscoso, G. and Nicolaides, K. (1995) 'Increased nuchal translucency in trisomy 21 fetuses: relationship to narrowing of the aortic isthmus'. *Human Reproduction*, 10 (11). pp 3049-3051.

Hyett, J., Moscoso, G., Papapanagiotou, G., Perdu, M. and Nicolaides, K. (1996) 'Abnormalities of the heart and great arteries in chromosomally normal fetuses with increased nuchal translucency thickness at 11–13 weeks of gestation'. *Ultrasound in Obstetrics and Gynecology*, 7 (4). pp 245-250.

Hyett, J., Moscoso, G. and Nicolaides, K. (1997) 'Abnormalities of the heart and great arteries in first trimester chromosomally abnormal fetuses'. *American Journal of Medical Genetics*, 69 (2). pp 207-216.

Hyett, J., Perdu, M., Sharland, G., Snijders, R. and Nicolaides, K. (1997) 'Increased nuchal translucency at 10—14 weeks of gestation as a marker for major cardiac defects'. *Ultrasound in Obstetrics and Gynecology*, 10 (4). pp 242-246.

Hyland, C. A. (2013) 'The challenge and paradox in serology RhD typing for blood donors and patients'. *Blood Transfusion*, 11 (1). pp 4.

Iles, R. K., Shahpari, M. E., Cuckle, H. and Butler, S. A. (2015) 'Direct and rapid mass spectral fingerprinting of maternal urine for the detection of Down syndrome pregnancy'. *Clinical Proteomics*, 12 (1). pp 9.

Illumina® (2015) 'HiSeq® 2500 sequencing system: Unsurpassed power and sufficiency for production scale sequencing'. [Online]. Available at: [http://www.illumina.com/documents/products/datasheets/datasheet\\_hiseq2500.pdf](http://www.illumina.com/documents/products/datasheets/datasheet_hiseq2500.pdf) (Accessed: November 8th 2015).

Innis, M. A., Gelfand, D. H. and Sninsky, J. J. (1999) *PCR applications: protocols for functional genomics*. Academic Press. Elsevier. Massachusetts, USA.

International Society for Prenatal Diagnosis (2013) 'Position Statement from the aneuploidy screening committee on behalf of the board of the International Society for Prenatal Diagnosis (ISPD)'. International Society for Prenatal Diagnosis [Online]. Available at: <http://ispdhome.org/public/news/2013/PositionStatementAneuploidy4apr2013.pdf> (Accessed: November 14th 2015).

Ioannides, M., Papageorgiou, E. A., Keravnou, A., Tsaliki, E., Spyrou, C., Hadjidaniel, M., Sismani, C., Koumbaris, G. and Patsalis, P. C. (2014) 'Inter-individual methylation variability in differentially methylated regions between maternal whole blood and first trimester CVS'. *Molecular cytogenetics*, 7 (1). pp 1-8.

Jaques, A., Halliday, J., Francis, I., Bonacquisti, L., Forbes, R., Cronin, A. and Sheffield, L. (2007) 'Follow up and evaluation of the Victorian first-trimester combined screening programme for Down syndrome and trisomy 18'. *British Journal of Obstetrics and Gynaecology: An International Journal of Obstetrics and Gynaecology*, 114 (7). pp 812-818.

Jiang, J., Jing, Y., Cost, G. J., Chiang, J.-C., Kolpa, H. J., Cotton, A. M., Carone, D. M., Carone, B. R., Shivak, D. A. and Guschin, D. Y. (2013) 'Translating dosage compensation to trisomy 21'. *Nature*, 500 (7462). pp 296-300.

Jiang, P., Chan, C. W., Chan, K. A., Cheng, S. H., Wong, J., Wong, V. W.-S., Wong, G. L., Chan, S. L., Mok, T. S. and Chan, H. L. (2015) 'Lengthening and shortening of plasma DNA in hepatocellular carcinoma patients'. *Proceedings of the National Academy of Sciences of the United States of America*, 112 (11). pp E1317-E1325.

Jones, M., Williams, J., Gärtner, K., Phillips, R., Hurst, J. and Frater, J. (2014) 'Low copy target detection by Droplet Digital PCR through application of a novel open access bioinformatic pipeline, 'definetherain''. *Journal of Virological Methods*, 202 (100). pp 46-53.

Jouannic, J. M., Thioulin, A. C., Bonnet, D., Houyel, L., Lelong, N., Goffinet, F. and Khoshnood, B. (2011) 'Measurement of nuchal translucency for prenatal screening of congenital heart defects: a population-based evaluation'. *Prenatal Diagnosis*, 31 (13). pp 1264-1269.

Kacem, N., Chakroun, T., Moussa, H., Abdelkefi, S., Houissa, B., Chiaroni, J. and Jemni Yacoub, S. (2012) 'RHD zygosity assignments based on most probable genotype and hybrid Rhesus box detection in Tunisia'. *Transfusion Medicine*, 22 (5). pp 362-366.

Kagan, K. O., Etchegaray, A., Zhou, Y., Wright, D. and Nicolaides, K. H. (2009) 'Prospective validation of first-trimester combined screening for trisomy 21'. *Ultrasound in Obstetrics and Gynecology*, 34 (1). pp 14-18.

Kagan, K., Staboulidou, I., Cruz, J., Wright, D. and Nicolaides, K. (2010) 'Two-stage first-trimester screening for trisomy 21 by ultrasound assessment and biochemical testing'. *Ultrasound in Obstetrics and Gynecology*, 36 (5). pp 542-547.

Kang, Y., Dong, X., Zhou, Q., Zhang, Y., Cheng, Y., Hu, R., Su, C., Jin, H., Liu, X., Ma, D., Tian, W. and Li, X. (2012) 'Identification of novel candidate maternal serum protein markers for Down syndrome by integrated proteomic and bioinformatic analysis'. *Prenatal Diagnosis*, 32 (3). pp 284-292.

Kaur, M., Zhang, Y., Liu, W.-H., Tetradis, S., Price, B. D. and Makrigiorgos, G. M. (2002) 'Ligation of a primer at a mutation: a method to detect low level mutations in DNA'. *Mutagenesis*, 17 (5). pp 365-374.

Kellogg, D., Rybalkin, I., Chen, S., Mukhamedova, N., Vlasik, T., Siebert, P. and Chenchik, A. (1994) 'TaqStart Antibody:" hot start" PCR facilitated by a neutralizing monoclonal antibody directed against Taq DNA polymerase'. *BioTechniques*, 16 (6). pp 1134-1137.

Kellogg, G., Slattery, L., Hudgins, L. and Ormond, K. (2014) 'Attitudes of mothers of children with Down syndrome towards noninvasive prenatal testing'. *Journal of Genetic Counseling*, 23 (5). pp 805-813.



Kermekchiev, M. B., Tzekov, A. and Barnes, W. M. (2003) 'Cold - sensitive mutants of Taq DNA polymerase provide a hot start for PCR'. *Nucleic Acids Research*, 31 (21). pp 6139-6147.

Kim, T. G., Jeong, S.-Y. and Cho, K.-S. (2014) 'Comparison of droplet digital PCR and quantitative real-time PCR in *mcrA*-based methanogen community analysis'. *Biotechnology Reports*, 4 pp 1-4.

Koelewijn, J., Vrijkotte, T., Van der Schoot, C., Bonsel, G. and De Haas, M. (2008) 'Effect of screening for red cell antibodies, other than anti-D, to detect hemolytic disease of the fetus and newborn: a population study in the Netherlands'. *Transfusion*, 48 (5). pp 941-952.

Koo, M. (2014) 'Droplet digital PCR introduction'. Life Science Group, Inc. [Online]. Available at: <http://cgs.hku.hk/portal/files/GRC/Events/Seminars/2012/20120502/qx100%20digital%20qpcr%20introduction%20mikki%20koo.pdf> (Accessed: November 3<sup>rd</sup> 2015).

Kooper, A. J., Faas, B. H., Feuth, T., Creemers, J. W., Zondervan, H. H., Boekkooi, P. F., Quartero, R. W., Rijnders, R. J., van der Burgt, I. and van Kessel, A. G. (2009) 'Detection of chromosome aneuploidies in chorionic villus samples by multiplex ligation-dependent probe amplification'. *The Journal of Molecular Diagnostics*, 11 (1). pp 17-24.

Kopreski, M. S., Benko, F. A., Kwak, L. W. and Gocke, C. D. (1999) 'Detection of tumor messenger RNA in the serum of patients with malignant melanoma'. *Clinical Cancer Research*, 5 (8). pp 1961-1965.

Kornberg, R. D. (1974) 'Chromatin structure: a repeating unit of histones and DNA'. *Science*, 184 (4139). pp 868-871.

Koster, M., Heetkamp, K. M., Pennings, J. L., de Vries, A., Visser, G. H. and Schielen, P. C. (2010) 'Down syndrome screening: imagining the screening test of the future'. *Expert Review of Molecular Diagnostics*, 10 (4). pp 445-457.

Kotlabova, K., Doucha, J. and Hromadnikova, I. (2011) 'Placental-specific microRNA in maternal circulation—identification of appropriate pregnancy-associated microRNAs with diagnostic potential'. *Journal of Reproductive Immunology*, 89 (2). pp 185-191.

Krog, G. R., Clausen, F. B. and Dziegiel, M. H. (2007) 'Quantitation of RHD by real-time polymerase chain reaction for determination of RHD zygosity and RHD mosaicism/chimerism: an evaluation of four quantitative methods'. *Transfusion*, 47 (4). pp 715-722.

Krone, N. and Arlt, W. (2009) 'Genetics of congenital adrenal hyperplasia'. *Best Practice and Research in Clinical Endocrinology and Metabolism*, 23 (2). pp 181-192.

Kumar, S. and Regan, F. (2005) 'Management of pregnancies with RhD alloimmunisation'. *British Medical Journal*, 330 (7502). pp 1255-1258.

Kyriakou, S., Kypri, E., Spyrou, C., Tsaliki, E., Velissariou, V., Papageorgiou, E. A. and Patsalis, P. C. (2013) 'Variability of cfDNA in maternal plasma does not prevent correct classification of trisomy 21 using MeDIP-qPCR methodology'. *Prenatal Diagnosis*, 33 (7). pp 650-655.

Ladomery, M. R., Maddocks, D. G. and Wilson, I. D. (2011) 'MicroRNAs: their discovery, biogenesis, function and potential use as biomarkers in non-invasive prenatal diagnostics'. *International Journal of Molecular Epidemiology and Genetics*, 2 (3). pp 253.

Lam, K.-W. G., Jiang, P., Liao, G. J., Chan, K. A., Leung, T. Y., Chiu, R. W. and Lo, Y. D. (2012) 'Noninvasive prenatal diagnosis of monogenic diseases by targeted massively parallel sequencing of maternal plasma: application to  $\beta$ -thalassemia'. *Clinical Chemistry*, 58 (10). pp 1467-1475.

Langbehn, D. R., Brinkman, R. R., Falush, D., Paulsen, J. S. and Hayden, M. (2004) 'A new model for prediction of the age of onset and penetrance for Huntington's disease based on CAG length'. *Clinical Genetics*, 65 (4). pp 267-277.

Langlois, S., Brock, J., Wilson, R., Audibert, F., Carroll, J., Carter, L. and al, e. (2013) 'Society of Obstetricians and Gynaecologists of Canada Committee Opinion No. 287. Current status in non-invasive prenatal detection of Down syndrome, trisomy 18, and trisomy 13 using cell-free DNA in maternal plasma'. *Journal of Obstetrics and Gynaecology Canada*, 35 pp 177-181.

Lau, T. K., Chan, M. K., Salome Lo, P. S., Connie Chan, H. Y., Kim Chan, W. S., Koo, T. Y., Ng, H. Y. J. and Pooh, R. K. (2012) 'Clinical utility of noninvasive fetal trisomy (NIFTY) test—early experience'. *The Journal of Maternal-Fetal and Neonatal Medicine*, 25 (10). pp 1856-1859.

Lau, T. K., Jiang, F. M., Stevenson, R. J., Lo, T. K., Chan, L. W., Chan, M. K., Lo, P. S. S., Wang, W., Zhang, H. Y. and Chen, F. (2013) 'Secondary findings from non-invasive prenatal testing for common fetal aneuploidies by whole genome sequencing as a clinical service'. *Prenatal Diagnosis*, 33 (6). pp 602-608.

Lazaros, L., Hatzi, E., Bouba, I., Makrydimas, G., Dalkalitsis, N., Stefos, T., Paraskevaidis, E. and Georgiou, I. (2008) 'Non-invasive first-trimester detection of paternal beta-globin gene mutations and polymorphisms as predictors of thalassemia risk at chorionic villous sampling'. *European Journal of Obstetrics and Gynecology and Reproductive Biology*, 140 (1). pp 17-20.

Leclerc, D., Campeau, E., Goyette, P., Adjalla, C., Christensen, B., Ross, M., Eydoux, P., Rosenblatt, D., Rozen, R. and Gravel, R. (1996) 'Human methionine synthase: cDNA cloning and identification of mutations in patients of the cblG complementation group of folate/cobalamin disorders'. *Human Molecular Genetics*, 5 (12). pp 1867-1874.

Lee, T., LeShane, E. S., Messerlian, G. M., Canick, J. A., Farina, A., Heber, W. W. and Bianchi, D. W. (2002) 'Down syndrome and cell-free fetal DNA in archived maternal serum'. *American Journal of Obstetrics and Gynecology*, 187 (5). pp 1217-1221.

Legler, T., Eber, S., Lakomek, M., Lynen, R., Maas, J., Pekrun, A., Repas-Humpe, M., Schröter, W. and Köhler, M. (1999) 'Application of RHD and RHCE genotyping for correct blood group determination in chronically transfused patients'. *Transfusion*, 39 (8). pp 852-855.

Lench, N., Barrett, A., Fielding, S., McKay, F., Hill, M., Jenkins, L., White, H. and Chitty, L. S. (2013) 'The clinical implementation of non-invasive prenatal diagnosis for single-gene disorders: challenges and progress made'. *Prenatal Diagnosis*, 33 (6). pp 555-562.

Levenson, D. (2013) 'Extra chromosome in trisomy 21 silence d in stem cells: Findings raise potential for new insights into Down syndrome and other chromosomal disorders'. *American Journal of Medical Genetics Part A*, 161 (11). pp vii-viii.

Lewis, C., Hill, M., Skirton, H. and Chitty, L. S. (2012) 'Non-invasive prenatal diagnosis for fetal sex determination: benefits and disadvantages from the service users' perspective'. *European Journal of Human Genetics*, 20 (11). pp 1127-1133.

Li, Y., Zimmermann, B., Rusterholz, C., Kang, A., Holzgreve, W. and Hahn, S. (2004) 'Size separation of circulatory DNA in maternal plasma permits ready detection of fetal DNA polymorphisms'. *Clinical Chemistry*, 50 (6). pp 1002-1011.

Li, Y., Di Naro, E., Vitucci, A., Zimmermann, B., Holzgreve, W. and Hahn, S. (2005) 'Detection of paternally inherited fetal point mutations for  $\beta$ -thalassemia using size-fractionated cell-free DNA in maternal plasma'. *Journal of the American Medical Association*, 293 (7). pp 843-849.

Li, Y., Di Naro, E., Vitucci, A., Grill, S., Zhong, X. Y., Holzgreve, W. and Hahn, S. (2009) 'Size fractionation of cell-free DNA in maternal plasma improves the detection of a paternally inherited  $\beta$ -thalassemia point mutation by MALDI-TOF mass spectrometry'. *Fetal Diagnosis and Therapy*, 25 (2). pp 246-249.

Li, J., Berbeco, R., Distel, R. J., Jänne, P. A., Wang, L. and Makrigiorgos, G. M. (2007) 's-RT-MELT for rapid mutation scanning using enzymatic selection and real time DNA-melting: new potential for multiplex genetic analysis'. *Nucleic Acids Research*, 35 (12). pp e84.

Li, J., Wang, L., Mamon, H., Kulke, M. H., Berbeco, R. and Makrigiorgos, G. M. (2008) 'Replacing PCR with COLD-PCR enriches variant DNA sequences and redefines the sensitivity of genetic testing'. *Nature Medicine*, 14 (5). pp 579-584.

Li, W.-H., Wang, P.-H., Chuang, C.-M., Chang, Y.-W., Yang, M.-J., Chen, C.-Y., Chao, K.-C. and Yen, M.-S. (2015) 'Noninvasive prenatal testing for fetal trisomy in a mixed risk factors pregnancy population'. *Taiwanese Journal of Obstetrics and Gynecology*, 54 (2). pp 122-125.

Liang, D., Lv, W., Wang, H., Xu, L., Liu, J., Li, H., Hu, L., Peng, Y. and Wu, L. (2013) 'Non-invasive prenatal testing of fetal whole chromosome aneuploidy by massively parallel sequencing'. *Prenatal Diagnosis*, 33 (5). pp 409-415.

Liao, G. J., Lun, F. M., Zheng, Y. W., Chan, K. A., Leung, T. Y., Lau, T. K., Chiu, R. W. and Lo, Y. D. (2011) 'Targeted massively parallel sequencing of maternal plasma DNA permits efficient and unbiased detection of fetal alleles'. *Clinical Chemistry*, 57 (1). pp 92-101.

Liew, M., Pryor, R., Palais, R., Meadows, C., Erali, M., Lyon, E. and Wittwer, C. (2004) 'Genotyping of single-nucleotide polymorphisms by high-resolution melting of small amplicons'. *Clinical Chemistry*, 50 (7). pp 1156-1164.

Liu, W., Avent, N. D., Jones, J. W., Scott, M. L. and Voak, D. (1999) 'Molecular configuration of Rh D epitopes as defined by site-directed mutagenesis and expression of mutant Rh constructs in K562 erythroleukemia cells'. *Blood*, 94 (12). pp 3986-3996.

Liu, W.-H., Kaur, M., Wang, G., Zhu, P., Zhang, Y. and Makrigiorgos, G. M. (2004) 'Inverse PCR-based RFLP scanning identifies low-level mutation signatures in colon cells and tumors'. *Cancer Research*, 64 (7). pp 2544-2551.

Liumbruno, G. M., D'Alessandro, A., Rea, F., Piccinini, V., Catalano, L., Calizzani, G., Pupella, S. and Grazzini, G. (2010) 'The role of antenatal immunoprophylaxis in the prevention of maternal-foetal anti-Rh (D) alloimmunisation'. *Blood Transfusion*, 8 (1). pp 8.

Lichtenbelt, K., Diemel, B., Koster, M., Manten, G., Siljee, J., Schuring-Blom, G. and Page-Christiaens, G. (2015) 'Detection of fetal chromosomal anomalies: does nuchal translucency measurement have added value in the era of non-invasive prenatal testing?'. *Prenatal Diagnosis*,

Lichtenstein, A. V., Melkonyan, H. S., Tomei, L. D. and Umansky, S. R. (2001) 'Circulating nucleic acids and apoptosis'. *Annals of the New York Academy of Sciences*, 945 (1). pp 239-249.

Lim, J. H., Kim, S. Y., Park, S. Y., Lee, S. Y., Kim, M. J., Han, Y. J., Lee, S. W., Chung, J. H., Kim, M. Y., Yang, J. H. and Ryu, H. M. (2011) 'Non-Invasive Epigenetic Detection

of Fetal Trisomy 21 in First Trimester Maternal Plasma'. *Public Library of Sciences ONE*, 6 (11). pp e27709.

Lim, J. H., Lee, D. E., Kim, K. S., Kim, H. J., Lee, B. Y., Park, S. Y., Ahn, H. K., Lee, S. W., Kim, M. Y. and Ryu, H. M. (2014) 'Non-invasive detection of fetal trisomy 21 using fetal epigenetic biomarkers with a high CpG density'. *Clinical Chemistry and Laboratory Medicine*, 52 (5). pp 641-647.

Lim, J. H., Kim, S. Y., Kim, H. J., Kim, K. S., Han, Y. J., Kim, M. H., Choi, J. S., Kim, M. Y., Ryu, H. M. and Park, S. Y. (2015) 'MicroRNAs as potential biomarkers for noninvasive detection of fetal trisomy 21'. *Journal of Assisted Reproduction and Genetics*, 32 (5). pp 827-837.

Lim, T. H., Tan, A. and Goh, V. H. H. (1999) 'Enrichment of fetal trophoblasts and nucleated erythrocytes from maternal blood by an immunomagnetic colloid system'. *Human Genetics*, 104 (5). pp 399-404.

Lo, Y. M., Corbetta, N., Chamberlain, P. F., Rai, V., Sargent, I. L., Redman, C. W. and Wainscoat, J. S. (1997) 'Presence of fetal DNA in maternal plasma and serum'. *Lancet*, 350 (9076). pp 485-487.

Lo, Y., Tein, M. S., Lau, T. K., Haines, C. J., Leung, T. N., Poon, P. M., Wainscoat, J. S., Johnson, P. J., Chang, A. M. and Hjelm, N. M. (1998a) 'Quantitative analysis of fetal DNA in maternal plasma and serum: implications for noninvasive prenatal diagnosis'. *The American Journal of Human Genetics*, 62 (4). pp 768-775.

Lo, Y. D., Tein, M. S., Lau, T. K., Haines, C. J., Leung, T. N., Poon, P. M., Wainscoat, J. S., Johnson, P. J., Chang, A. M. and Hjelm, N. M. (1998b) 'Quantitative analysis of fetal DNA in maternal plasma and serum: implications for noninvasive prenatal diagnosis'. *The American Journal of Human Genetics*, 62 (4). pp 768-775.

Lo, Y. M. D., Hjelm, M., Fidler, C., Sargent, I. L., Murphy, M. F., Chamberlain, P. F., Poon, P. M. K., Redman, C. W. G. and Wainscoat, J. S. (1998c) 'Prenatal diagnosis of fetal RhD status by molecular analysis of maternal plasma'. *New England Journal of Medicine*, 339 pp 1734-1738.

Lo, Y. D., Zhang, J., Leung, T. N., Lau, T. K., Chang, A. M. and Hjelm, N. M. (1999) 'Rapid clearance of fetal DNA from maternal plasma'. *The American Journal of Human Genetics*, 64 (1). pp 218-224.

Lo, Y. D., Lau, T. K., Chan, L. Y., Leung, T. N. and Chang, A. M. (2000) 'Quantitative analysis of the bidirectional fetomaternal transfer of nucleated cells and plasma DNA'. *Clinical Chemistry*, 46 (9). pp 1301-1309.

Lo, Y. D., Tsui, N. B., Chiu, R. W., Lau, T. K., Leung, T. N., Heung, M. M., Gerovassili, A., Jin, Y., Nicolaides, K. H. and Cantor, C. R. (2007a) 'Plasma placental RNA allelic ratio permits noninvasive prenatal chromosomal aneuploidy detection'. *Nature Medicine*, 13 (2). pp 218-223.

Lo, Y. D., Lun, F. M., Chan, K. A., Tsui, N. B., Chong, K. C., Lau, T. K., Leung, T. Y., Zee, B. C., Cantor, C. R. and Chiu, R. W. (2007b) 'Digital PCR for the molecular detection of fetal chromosomal aneuploidy'. *Proceedings of the National Academy of Sciences of the United States of America*, 104 (32). pp 13116-13121.

Lo, Y. D., Chan, K. A., Sun, H., Chen, E. Z., Jiang, P., Lun, F. M., Zheng, Y. W., Leung, T. Y., Lau, T. K. and Cantor, C. R. (2010) 'Maternal plasma DNA sequencing reveals the genome-wide genetic and mutational profile of the fetus'. *Science Translational Medicine*, 2 (61). pp 61ra91-61ra91.

Lo, Y. D. (2013) 'Non-invasive prenatal testing using massively parallel sequencing of maternal plasma DNA: from molecular karyotyping to fetal whole-genome sequencing'. *Reproductive Biomedicine Online*, 27 (6). pp 593-598.

Lo, Y. D., Chiu, R. W. K. and Chan, K. C. (2014) 'Diagnosing fetal chromosomal aneuploidy using massively parallel genomic sequencing'. [in US Patent 20,140,329,696.] (Accessed: October 26<sup>th</sup> 2015).

Lo, Y. D. (2015) 'Noninvasive prenatal diagnosis: from dream to reality'. *Clinical Chemistry*, 61 (1). pp 32-37.

Loeb, L. A. and Christians, F. C. (1996) 'Multiple mutations in human cancers'. *Mutation Research/Fundamental and Molecular Mechanisms of Mutagenesis*, 350 (1). pp 279-286.

Los, F. J., van den Berg, C., Wildschut, H. I., Brandenburg, H., den Hollander, N. S., Schoonderwaldt, E. M., Pijpers, L., Galjaard, J. H. and Van Opstal, D. (2001) 'The diagnostic performance of cytogenetic investigation in amniotic fluid cells and chorionic villi'. *Prenatal Diagnosis*, 21 (13). pp 1150-1158.

Ludlow, A. T., Robin, J. D., Sayed, M., Litterst, C. M., Shelton, D. N., Shay, J. W. and Wright, W. E. (2014) 'Quantitative telomerase enzyme activity determination using droplet digital PCR with single cell resolution'. *Nucleic Acids Research*, 42 (13). pp e104-e104.

Lui, Y. Y., Chik, K.-W., Chiu, R. W., Ho, C.-Y., Lam, C. W. and Lo, Y. D. (2002) 'Predominant hematopoietic origin of cell-free DNA in plasma and serum after sex-mismatched bone marrow transplantation'. *Clinical Chemistry*, 48 (3). pp 421-427.

Lun, F. M., Chiu, R. W., Chan, K. C., Leung, T. Y., Lau, T. K. and Lo, Y. M. (2008) 'Microfluidics digital PCR reveals a higher than expected fraction of fetal DNA in maternal plasma.'. *Clinical Chemistry*, 54 pp 1664-1672.

Lun, F. M., Chiu, R. W., Sun, K., Leung, T. Y., Jiang, P., Chan, K. A., Sun, H. and Lo, Y. D. (2013) 'Noninvasive prenatal methylomic analysis by genomewide bisulfite sequencing of maternal plasma DNA'. *Clinical Chemistry*, 59 (11). pp 1583-1594.

Lurie, S. (1990) 'Age distribution of erythrocyte population in late pregnancy'. *Gynecologic and obstetric investigation*, 30 (3). pp 147-149.

Macher, H. C., Martinez-Broca, M. A., Rubio-Calvo, A., Leon-Garcia, C., Conde-Sanchez, M., Costa, A., Navarro, E. and Guerrero, J. M. (2012) 'Non-invasive prenatal diagnosis of multiple endocrine neoplasia type 2A using COLD-PCR combined with HRM genotyping analysis from maternal serum'. *Public Library of Sciences ONE*, 7 (12). pp e51024.

Maddocks, D., Alberry, M., Attilakos, G., Madgett, T., Choi, K., Soothill, P. and Avent, N. (2009) 'The SAFE project: towards non-invasive prenatal diagnosis'. *Biochemical Society Transactions*, 37 (2). pp 460.



Malhotra, N., Singh, K., Tomar, S., Malhotra, J., Rao, J. and Malhotra, N. (2014) Color Doppler and 3D and 4D Ultrasound in Screening for Birth Defects. *Ultrasound in Obstetrics and Gynecology* Forth Edition. Jaypee Brother Medical Publishers (P) Ltd. New Delhi, India.

Matheson, K. A. and Denomme, G. A. (2002) 'Novel 3' Rhesus box sequences confound RHD zygosity assignment'. *Transfusion*, 42 (5). pp 645-650.

McBean, R., Hyland, C. and Flower, R. (2014) 'Molecular genotyping platforms for blood group antigen prediction'. *Pathology-Journal of the RCPA*, 46 pp S87.

McEwan, A., Godfrey, A. and Wilkins, J. (2012) 'Screening for Down syndrome'. *Obstetrics, Gynaecology and Reproductive Medicine*, 22 (3). pp 70-75.

McMurray, C. T. (1999) 'DNA secondary structure: a common and causative factor for expansion in human disease'. *Proceedings of the National Academy of Sciences of the United States of America*, 96 (5). pp 1823-1825.

Merz, E. and Pashaj, S. (2015) 'OP12. 04: The frontal fetal facial (FFF) angle in the second trimester measured by 3D ultrasound in normal fetuses and fetuses with Trisomy 21'. *Ultrasound in Obstetrics and Gynecology*, 46 (S1). pp 88-88.

Migueluez, J., Moskovitch, M., Cuckle, H., Zugaib, M., Bunduki, V. and Maymon, R. (2010) 'Model-predicted performance of second-trimester Down syndrome screening with sonographic prenatal thickness'. *Journal of Ultrasound in Medicine*, 29 (12). pp 1741-1747.

Miotke, L., Lau, B. T., Rumma, R. T. and Ji, H. P. (2014) 'High sensitivity detection and quantitation of DNA copy number and single nucleotide variants with single color droplet digital PCR'. *Analytical Chemistry*, 86 (5). pp 2618-2624.

Miran, T. (2012) 'Enrichment of minority DNA in admixes of DNA samples: potential use in non-invasive prenatal diagnosis (NIPD), of Down syndrome'.

Morris, J., Mutton, D. and Alberman, E. (2002) 'Revised estimates of the maternal age specific live birth prevalence of Down's syndrome'. *Journal of Medical Screening*, 9 (1). pp 2-6.

Morris, S., Karlsen, S., Chung, N., Hill, M. and Chitty, L. S. (2014) 'Model-based analysis of costs and outcomes of non-invasive prenatal testing for Down's syndrome using cell free fetal DNA in the UK National Health Service'. *Public Library of Sciences ONE*, 9 (4). pp e93559.

Mouro, I., Le Van Kim, C., Rouillac, C., Van Rhenen, D., Le Pennec, P., Bailly, P., Cartron, J. and Colin, Y. (1994) 'Rearrangements of the blood group RhD gene associated with the D<sup>+</sup> V<sup>+</sup> I category phenotype'. *Blood*, 83 (4). pp 1129-1135.

Müller, S. P., Bartels, I., Stein, W., Emons, G., Gutensohn, K., Köhler, M. and Legler, T. J. (2008) 'The determination of the fetal D status from maternal plasma for decision making on Rh prophylaxis is feasible'. *Transfusion*, 48 (11). pp 2292-2301.

Mullis, K., Faloona, F., Scharf, S., Saiki, R., Horn, G. and Erlich, H. (1986) 'Specific enzymatic amplification of DNA in vitro: the polymerase chain reaction', *Cold Spring Harbor Symposia on Quantitative Biology*. Cold Spring Harbor Laboratory Press, pp. 263-273.

Murray, V., Monchawin, C. and England, P. R. (1993) 'The determination of the sequences present in the shadow bands of a dinucleotide repeat PCR'. *Nucleic Acids Research*, 21 (10). pp 2395-2398.

Munnangi, S., Gross, S. J., Madankumar, R., Salcedo, G. and Reznik, S. E. (2014) 'Pregnancy associated plasma protein-A2: A novel biomarker for down syndrome'. *Placenta*, 35 (11). pp 900-906.

Narasimhan, K., Lin, S. L., Tong, T., Baig, S., Ho, S., Sukumar, P., Biswas, A., Hahn, S., Bajic, V. B. and Choolani, M. (2013) 'Maternal serum protein profile and immune response protein subunits as markers for non-invasive prenatal diagnosis of trisomy 21, 18, and 13'. *Prenatal Diagnosis*, 33 (3). pp 223-231.

Natera (2015) 'Panorama Natera Prenatal screen'. [Online]. Available at: <http://global.panoramatest.com/uk> (Accessed: November 24th 2015).

National Institute for Health and Care Excellence (NICE) (2008) 'Technological appraisal guidance 156. Routine antenatal anti-D prophylaxis for women who are rhesus D negative'. NICE. [Online]. Available at: <http://www.nice.org.uk/guidance/TA156/chapter/1-guidance> (Accessed: October 27th 2015).

Nelson, J. L. (1996) 'Maternal–fetal immunology and autoimmune disease. Is some autoimmune disease auto-alloimmune or allo-autoimmune?'. *Arthritis and Rheumatism*, 39 (2). pp 191-194.

Nelson, J. L. (2008) 'Your cells are my cells'. *Scientific American*, 298 (2). pp 72-79.

New, M. I., Carlson, A., Obeid, J., Marshall, I., Cabrera, M. S., Goseco, A., Lin-Su, K., Putnam, A. S., Wei, J. Q. and Wilson, R. C. (2001) 'Extensive personal experience: prenatal diagnosis for congenital adrenal hyperplasia in 532 pregnancies'. *Journal of Clinical Endocrinology and Metabolism*, 86 (12). pp 5651-5657.

New, M. I., Tong, Y. K., Yuen, T., Jiang, P., Pina, C., Chan, K. A., Khattab, A., Liao, G. J., Yau, M. and Kim, S.-M. (2014) 'Noninvasive Prenatal Diagnosis of Congenital Adrenal Hyperplasia Using Cell-Free Fetal DNA in Maternal Plasma'. *Journal of Clinical Endocrinology and Metabolism*,

NHS (2010) 'Cell-free fetal DNA for fetal sex determination in sex-linked genetic disorders'. [Online]. Available at: <http://www.rapid.nhs.uk/wp-content/uploads/2013/12/RAPID-commissioning-guide.pdf> (Accessed: October 21st 2015).

Nicolaidis, K., Azar, G., Byrne, D., Mansur, C. and Marks, K. (1992) 'Fetal nuchal translucency: ultrasound screening for chromosomal defects in first trimester of pregnancy'. *British Medical Journal*, 304 (6831). pp 867-869.

Nicolaidis, K., Spencer, K., Avgidou, K., Faiola, S. and Falcon, O. (2005) 'Multicenter study of first-trimester screening for trisomy 21 in 75 821 pregnancies: results and estimation of the potential impact of individual risk-orientated two-stage first-trimester screening'. *Ultrasound in Obstetrics and Gynecology*, 25 (3). pp 221-226.

Nicolaidis, K. (2011) 'Screening for fetal aneuploidies at 11 to 13 weeks'. *Prenatal Diagnosis*, 31 pp 7-15.

Nicolaidis, K., Syngelaki, A., Ashoor, G., Birdir, C. and Touzet, G. (2012) 'Noninvasive prenatal testing for fetal trisomies in a routinely screened first-trimester population'. *American Journal of Obstetrics and Gynecology*, 207 pp 374.e371-376.

Nicolaidis, K., Syngelaki, A., Gil, M., Atanasova, V. and Markova, D. (2013a) 'Validation of targeted sequencing of single-nucleotide polymorphisms for non-invasive prenatal detection of aneuploidy of chromosomes 13, 18, 21, X, and Y'. *Prenatal Diagnosis*, 33 (6). pp 575-579.

Nicolaidis, K. H., Syngelaki, A., Gil, M. d. M., Quezada, M. S. and Zinevich, Y. (2013b) 'Prenatal detection of fetal triploidy from cell-free DNA testing in maternal blood'. *Fetal Diagnosis and Therapy*, 35 (3). pp 212-217.

Nicolaidis, K. H., Musci, T. J., Struble, C. A., Syngelaki, A. and Gil, M. d. M. (2014) 'Assessment of fetal sex chromosome aneuploidy using directed cell-free DNA analysis'. *Fetal Diagnosis and Therapy*, 35 (1). pp 1-6.

Nigam, A., Saxena, P., Prakash, A. and Acharya, A. S. (2012) 'Detection of fetal nucleic acid in maternal plasma: A novel noninvasive prenatal diagnostic technique'. *Journal International Medical Sciences Academy*, 25 (3). pp 119-200.

Norton, M. E., Brar, H., Weiss, J., Karimi, A., Laurent, L. C., Caughey, A. B., Rodriguez, H., Williams, J. I., Mitchell, M. E. and Adair, C. D. (2012) 'Non-invasive Chromosomal Evaluation (NICE) Study: results of a multicenter prospective cohort study for detection of fetal trisomy 21 and trisomy 18.'. *American Journal of Obstetrics and Gynecology*, 207 pp 137.e131-137.e138.

Norton, S. E., Luna, K. K., Lechner, J. M., Qin, J. and Fernando, M. R. (2013) 'A New Blood Collection Device Minimizes Cellular DNA Release During Sample Storage and Shipping When Compared to a Standard Device'. *Journal of Clinical Laboratory Analysis*, 27 (4). pp 305-311.

Nussbaum, R., McInnes, R., Willard, H. and Hamosh, A. (2007) *Genetics of common disorders with complex inheritance*. 7th edn. Philadelphia: Thompson and Thompson Genetics in Medicine. Elsevier Saunders.

Nyberg, D. and Souter, V. (2001) 'Sonographic markers of fetal trisomies: second trimester'. *Journal of Ultrasound in Medicine*, 20 pp 655-674.

Ochman, H., Gerber, A. S. and Hartl, D. L. (1988) 'Genetic applications of an inverse polymerase chain reaction'. *Genetics*, 120 (3). pp 621-623.

Ogilvie, C. M., Yaron, Y. and Beaudet, A. L. (2009) 'Current controversies in prenatal diagnosis 3: for prenatal diagnosis, should we offer less or more than metaphase karyotyping?'. *Prenatal Diagnosis*, 29 (1). pp 11-14.

Olney, R. S., Moore, C. A., Khoury, M. J., Erickson, J. D., Edmonds, L. D., Botto, L. D., Atrash, H. K., control, C. f. d. and prevention (1995) *Chorionic villus sampling and amniocentesis: recommendations for prenatal counseling*. US Department of Health and Human Services, Public Health Service, Centers for Disease Control and Prevention (CDC).

Oregon Health and Science University (OHSU) (2005) *Department of Health Services (DHS): genetics and primary care what's new in prenatal genetic screening*. Available at: <http://slideplayer.com/slide/5128318/> (Accessed: October 6<sup>th</sup> 2015).

Osborne, C. M., Hardisty, E., Devers, P., Kaiser-Rogers, K., Hayden, M. A., Goodnight, W. and Vora, N. L. (2013) 'Discordant noninvasive prenatal testing results in a patient subsequently diagnosed with metastatic disease'. *Prenatal Diagnosis*, 33 (6). pp 609-611.

Palomaki, G. E., Kloza, E. M., Lambert-Messerlian, G. M., Haddow, J. E., Neveux, L. M., Ehrich, M., van den Boom, D., Bombard, A. T., Deciu, C. and Grody, W. W. (2011) 'DNA sequencing of maternal plasma to detect Down syndrome: an international clinical validation study'. *Genetics in Medicine*, 13 (11). pp 913-920.

Palomaki, G. E., Deciu, C., Kloza, E. M., Lambert-Messerlian, G. M., Haddow, J. E., Neveux, L. M., Ehrich, M., van den Boom, D., Bombard, A. T. and Grody, W. W. (2012)

'DNA sequencing of maternal plasma reliably identifies trisomy 18 and trisomy 13 as well as Down syndrome: an international collaborative study'. *Genetics in Medicine*, 14 (3). pp 296-305.

Papageorgiou, E. A., Fiegler, H., Rakyán, V., Beck, S., Hultén, M., Lamnissou, K., Carter, N. P. and Patsalis, P. C. (2009) 'Sites of differential DNA methylation between placenta and peripheral blood: molecular markers for noninvasive prenatal diagnosis of aneuploidies'. *American Journal of Pathology*, 174 (5). pp 1609-1618.

Papageorgiou, E. A., Karagrigoriou, A., Tsaliki, E., Velissariou, V., Carter, N. P. and Patsalis, P. C. (2011) 'Fetal-specific DNA methylation ratio permits noninvasive prenatal diagnosis of trisomy 21'. *Nature Medicine*, 17 (4). pp 510-513.

Papasavva, T., Kalakoutis, G., Kalikas, I., Neokli, E., Papacharalambous, S., Kyrri, A. and Kleanthous, M. (2006) 'Noninvasive Prenatal Diagnostic Assay for the Detection of  $\beta$ -Thalassemia'. *Annals of the New York Academy of Sciences*, 1075 (1). pp 148-153.

Parikh, B., Brody, M. D., Stone, J. & Halderman, J. D. Google Patents, (2014) Method and device for identification of nucleated red blood cells from a maternal blood sample. Available at: <https://www.google.com/patents/US8426122>. (Accessed October 2<sup>nd</sup> 2015).

Pencina, M. J., D'Agostino, R. B., D'Agostino, R. B. and Vasan, R. S. (2008) 'Evaluating the added predictive ability of a new marker: from area under the ROC curve to reclassification and beyond'. *Statistics in medicine*, 27 (2). pp 157.

Perco, P., Shao, C. P., Mayr, W. R., Panzer, S. and Legler, T. J. (2003) 'Testing for the D zygosity with three different methods revealed altered Rhesus boxes and a new weak D type'. *Transfusion*, 43 (3). pp 335-339.

Pergament, E., Cuckle, H., Zimmermann, B., Banjevic, M., Sigurjonsson, S., Ryan, A., Hall, M. P., Dodd, M., Lacroute, P. and Stosic, M. (2014) 'Single-nucleotide polymorphism-based noninvasive prenatal screening in a high-risk and low-risk cohort'. *Obstetrics and Gynecology*, 124 (2, PART 1). pp 210-218.

Petruska, J., Goodman, M. F., Boosalis, M. S., Sowers, L. C., Cheong, C. and Tinoco, I. (1988) 'Comparison between DNA melting thermodynamics and DNA polymerase

fidelity'. *Proceedings of the National Academy of Sciences of the United States of America*, 85 (17). pp 6252-6256.

Phylipsen, M., Yamsri, S., Treffers, E. E., Jansen, D. T., Kanhai, W. A., Boon, E. M., Giordano, P. C., Fucharoen, S., Bakker, E. and Harteveld, C. L. (2012) 'Non-invasive prenatal diagnosis of beta-thalassemia and sickle-cell disease using pyrophosphorolysis-activated polymerization and melting curve analysis'. *Prenatal Diagnosis*, 32 (6). pp 578-587.

Pinheiro, L. B., Coleman, V. A., Hindson, C. M., Herrmann, J., Hindson, B. J., Bhat, S. and Emslie, K. R. (2011) 'Evaluation of a droplet digital polymerase chain reaction format for DNA copy number quantification'. *Analytical Chemistry*, 84 (2). pp 1003-1011.

Pirelli, K. J., Pietz, B. C., Johnson, S. T., Pinder, H. L. and Bellissimo, D. B. (2010) 'Molecular determination of RHD zygosity: predicting risk of hemolytic disease of the fetus and newborn related to anti-D'. *Prenatal diagnosis*, 30 (12-13). pp 1207-1212.

Polin, H., Danzer, M., Gaszner, W., Broda, D., St-Louis, M., Pröll, J., Hofer, K. and Gabriel, C. (2009) 'Identification of RHD alleles with the potential of anti-D immunization among seemingly D- blood donors in Upper Austria'. *Transfusion*, 49 (4). pp 676-681.

Ponnusamy, S., Zhang, H., Kadam, P., Lin, Q., Lim, T. K., Sandhu, J. S., Kothandaraman, N., Mahyuddin, A. P., Biswas, A. and Venkat, A. (2012) 'Membrane proteins of human fetal primitive nucleated red blood cells'. *Journal of Proteomics*, 75 (18). pp 5762-5773.

Poon, L. L., Leung, T. N., Lau, T. K. and Lo, Y. D. (2000) 'Presence of fetal RNA in maternal plasma'. *Clinical Chemistry*, 46 (11). pp 1832-1834.

Poon, L. C., Dumidrascu-Diris, D., Francisco, C., Fantasia, I. and Nicolaides, K. H. (2015) 'The IONA® test for first-trimester detection of trisomy 21, 18 and 13'. *Ultrasound in Obstetrics and Gynecology*, doi: 10.1002/uog.15749.

Porreco, R. P., Garite, T. J., Maurel, K., Marusiak, B., Network, O. C. R., Ehrich, M., van den Boom, D., Deciu, C. and Bombard, A. (2014) 'Noninvasive prenatal screening for fetal trisomies 21, 18, 13 and the common sex chromosome aneuploidies from maternal

blood using massively parallel genomic sequencing of DNA'. *American Journal of Obstetrics and Gynecology*, 211 (4). pp 365. e361-365. e312.

Provan, D., Newland, A. and Court, D. S. (2015) *Medical Sciences*. eds. Naish, J. and Court, D.S., Haematology. vol. 2. UK: Elsevier Ltd.

Premaitha Health PLC (2015) 'Premaita Health launches the IONA® test, the first ever CE-marked NIPT Product for pregnant women'. [Online]. Available at: <http://www.premaitha.com/news/press-releases/18-news/138-premaitha-health-launches-the-iona-test-the-first-ever-ce-marked-nipt-product-for-pregnant-women> (Accessed: November 8th 2015).

Public Health England (2015) *Fetal Anomaly Screening Programme - Standards 2015-2016*. Department of Health. London. (Accessed: October 16<sup>th</sup> 2015).

qi Chen, X., Bonnefoi, H., Pelte, M.-F., Lyautey, J., Lederrey, C., Movarekhi, S., Schaeffer, P., Mulcahy, H. E., Meyer, P. and Stroun, M. (2000) 'Telomerase RNA as a detection marker in the serum of breast cancer patients'. *Clinical Cancer Research*, 6 (10). pp 3823-3826.

Qin, J., Williams, T. L. and Fernando, M. R. (2013) 'A novel blood collection device stabilizes cell-free RNA in blood during sample shipping and storage'. *BMC research notes*, 6 (1). pp 380.

Qin, J., Bassett, C. and Fernando, M. (2014) 'Preservation of circulating cell-free fetal RNA in maternal blood using a blood collection device containing a stabilizing reagent'. *Journal of Molecular and Genetic Medicine*, 14 pp 23-28.

Quail, M. A., Gu, Y., Swerdlow, H. and Mayho, M. (2012) 'Evaluation and optimisation of preparative semi-automated electrophoresis systems for Illumina library preparation'. *Electrophoresis*, 33 (23). pp 3521-3528.

Quezada, M. S., Gil, M., Francisco, C., Oròsz, G. and Nicolaidis, K. H. (2015) 'Screening for trisomies 21, 18 and 13 by cell - free DNA analysis of maternal blood at 10 - 11



weeks' gestation and the combined test at 11 - 13 weeks'. *Ultrasound in Obstetrics and Gynecology*, 45 (1). pp 36-41.

Reid, M. E., Lomas-Francis, C. and Olsson, M. L. (2012) *The blood group antigen factsbook*. Academic Press.

Rijnders, R., Van Der Luijt, R., Peters, E., Goeree, J., Van Der Schoot, C., Ploos Van Amstel, J. and Christiaens, G. (2003) 'Earliest gestational age for fetal sexing in cell-free maternal plasma'. *Prenatal Diagnosis*, 23 (13). pp 1042-1044.

Risberg, B. (2013) 'Establishment of PCR based methods for detection of ctDNA in blood'.

Rizzo, C., Castiglia, L., Arena, E., Gangi, S., Mazzola, G., Caruso, C. and Vasto, S. (2012) 'Weak D and partial D: our experience in daily activity'. *Blood Transfusion*, 10 (2). pp 235.

Roberts, J. (2014) 'Count your nucleic acids with these digital PCR systems '. Biocompare. [Online]. Available at: <http://www.biocompare.com/Editorial-Articles/154784-Count-Your-Nucleic-Acids-with-These-Digital-PCR-Systems/> (Accessed: November 3<sup>rd</sup> 2015).

Romitti, P. A., Zhu, Y., Puzhankara, S., James, K. A., Nabukera, S. K., Zamba, G. K., Ciafaloni, E., Cunniff, C., Druschel, C. M. and Mathews, K. D. (2015) 'Prevalence of Duchenne and Becker Muscular Dystrophies in the United States'. *Pediatrics*, 135 (3). pp 513-521.

Rong, Y., Gao, J., Jiang, X. and Zheng, F. (2012) 'Multiplex PCR for 17 Y-chromosome specific short tandem repeats (STR) to enhance the reliability of fetal sex determination in maternal plasma'. *International Journal of Molecular Sciences*, 13 (5). pp 5972-5981.

Rossetti, L. C., Radic, C. P., Larripa, I. B. and De Brasi, C. D. (2005) 'Genotyping the hemophilia inversion hotspot by use of inverse PCR'. *Clinical Chemistry*, 51 (7). pp 1154-1158.

Rouillac-Le Sciellour, C., Puillandre, P., Gillot, R., Baulard, C., Métral, S., Le Van Kim, C., Cartron, J.-P., Colin, Y. and Brossard, Y. (2004) 'Large-scale pre-diagnosis study of fetal RHD genotyping by PCR on plasma DNA from RhD-negative pregnant women'. *Molecular Diagnosis*, 8 (1). pp 23-31.

Rouillac-Le Sciellour, C., Sérazin, V., Brossard, Y., Oudin, O., Le Van Kim, C., Colin, Y., Guidicelli, Y., Menu, M. and Cartron, J.-P. (2007) 'Noninvasive fetal RHD genotyping from maternal plasma: Use of a new developed Free DNA Fetal Kit RhD®'. *Transfusion Clinique et Biologique*, 14 (6). pp 572-577.

Rozenberg, P., Bussi eres, L., Chevret, S., Bernard, J. P., Malagrida, L., Cuckle, H., Chabry, C., Durand-Zaleski, I., Bidat, L. and Lacroix, I. (2006) 'Screening for Down syndrome using first-trimester combined screening followed by second-trimester ultrasound examination in an unselected population'. *American Journal of Obstetrics and Gynecology*, 195 (5). pp 1379-1387.

Saiki, R. K., Scharf, S., Faloona, F., Mullis, K. B., Horn, G. T., Erlich, H. A. and Arnheim, N. (1985) 'Enzymatic amplification of beta-globin genomic sequences and restriction site analysis for diagnosis of sickle cell anemia'. *Science*, 230 (4732). pp 1350-1354.

Sambrook, J., Fritsch, E. F. and Maniatis, T. (1989) *Molecular cloning*. vol. 2. Cold spring harbor laboratory press New York.

Samejima, K. and Earnshaw, W. C. (2005) 'Trashing the genome: the role of nucleases during apoptosis'. *Nature Reviews Molecular Cell Biology*, 6 (9). pp 677-688.

Sanders, R., Huggett, J. F., Bushell, C. A., Cowen, S., Scott, D. J. and Foy, C. A. (2011) 'Evaluation of digital PCR for absolute DNA quantification'. *Analytical Chemistry*, 83 (17). pp 6474-6484.

Sandler, S. G., Roseff, S. D., Domen, R. E., Shaz, B. and Gottschall, J. L. (2014) 'Policies and procedures related to testing for weak D phenotypes and administration of Rh immune globulin'. *Arch Pathol Lab Med*, 138 (5). pp 620-625.

Sargent, I. L., Johansen, M., Chua, S. and Redman, C. W. (1994) 'Clinical Experience: Isolating Trophoblasts from Maternal Blooda'. *Annals of the New York Academy of Sciences*, 731 (1). pp 154-161.

Scheffer, P., Ait Soussan, A., Verhagen, O., Page-Christiaens, G., Oepkes, D., de Haas, M. and Van der Schoot, C. (2011) 'Noninvasive fetal genotyping of human platelet antigen-1a'. *British Journal of Obstetrics and Gynaecology: An International Journal of Obstetrics and Gynaecology*, 118 (11). pp 1392-1395.

Schlütter, J. M., Hatt, L., Bach, C., Kirkegaard, I., Kølvråa, S. and Uldbjerg, N. (2014) 'The cell-free fetal DNA fraction in maternal blood decreases after physical activity'. *Prenatal Diagnosis*, 34 (4). pp 341-344.

Schmitz, D., Netzer, C. and Henn, W. (2009) 'An offer you can't refuse? Ethical implications of non-invasive prenatal diagnosis'. *Nature Reviews Genetics*, 10 (8). pp 515-515.

Schroder, J., Tilikai, A. and Chapelle, A. (1974) 'fetal leukocytes in maternal circulation after delivery. 1. cytological aspects'. *Transplantation*, 17 (4). pp 346-354.

Sehnert, A. J., Rhees, B., Comstock, D., de Feo, E., Heilek, G., Burke, J. and Rava, R. P. (2011) 'Optimal detection of fetal chromosomal abnormalities by massively parallel DNA sequencing of cell-free fetal DNA from maternal blood'. *Clinical Chemistry*, 57 (7). pp 1042-1049.

Sekizawa, A., Samura, O., Zhen, D., Falco, V., Farina, A. and Bianchi, D. W. (2000) 'Apoptosis in fetal nucleated erythrocytes circulating in maternal blood'. *Prenatal Diagnosis*, 20 (11). pp 886-889.

Sekizawa, A., Kondo, T., Iwasaki, M., Watanabe, A., Jimbo, M., Saito, H. and Okai, T. (2001) 'Accuracy of fetal gender determination by analysis of DNA in maternal plasma'. *Clinical Chemistry*, 47 (10). pp 1856-1858.

Seo, S. B., Ge, J., King, J. L. and Budowle, B. (2014) 'Reduction of stutter ratios in short tandem repeat loci typing of low copy number DNA samples'. *Forensic Science International: Genetics*, 8 (1). pp 213-218.

Sherod, C., Sebire, N., Soares, W., Sniijders, R. and Nicolaidis, K. (1997) 'Prenatal diagnosis of trisomy 18 at the 10–14-week ultrasound scan'. *Ultrasound in Obstetrics and Gynecology*, 10 (6). pp 387-390.

Shi, Z., Xu, W., Loechel, F., Wewer, U. M. and Murphy, L. J. (2000) 'ADAM 12, a disintegrin metalloprotease, interacts with insulin-like growth factor-binding protein-3'. *Journal of Biological Chemistry*, 275 (24). pp 18574-18580.

Sillence, K. A., Madgett, T. E., Roberts, L. A., Overton, T. G. and Avent, N. D. (2013) 'Non-invasive screening tools for down's syndrome: a review'. *Diagnostics*, 3 (2). pp 291-314.

Sillence, K. A., Roberts, L. A., Hollands, H. J., Ross Welch, C., Thompson, H. P., Keirnan, M., Madgett, T. E. and Avent, N. D. (2015) 'Fetal sex and *RHD* genotyping with digital PCR demonstrates greater sensitivity than real-time PCR'. *Clinical Chemistry*, 61 (11). pp 1399-1407.

Singleton, B. K., Green, C. A., Avent, N. D., Martin, P. G., Smart, E., Daka, A., Narter-Olaga, E. G., Hawthorne, L. M. and Daniels, G. (2000) 'The presence of an *RHD* pseudogene containing a 37 base pair duplication and a nonsense mutation in Africans with the Rh D-negative blood group phenotype'. *Blood*, 95 (1). pp 12-18.

Skirton, H., Goldsmith, L. and Chitty, L. S. (2014) 'An easy test but a hard decision: ethical issues concerning non-invasive prenatal testing for autosomal recessive disorders'. *European Journal of Human Genetics*, 23 (8). pp 1004-1009.

Snyder, M. W., Simmons, L. E., Kitzman, J. O., Santillan, D. A., Santillan, M. K., Gammill, H. S. and Shendure, J. (2013) 'Noninvasive fetal genome sequencing: a primer'. *Prenatal Diagnosis*, 33 (6). pp 547-554.

Sonek, J., Molina, F., Kinney Hiatt, A., Glover, M., McKenna, D. and Nicolaides, K. (2012) 'Paper abstracts of the ISPD 16th international conference on prenatal diagnosis and therapy'. *Prenatal Diagnosis*, 32 (Suppl. 1). pp 1-128.

Song, Y., Liu, C., Qi, H., Zhang, Y., Bian, X. and Liu, J. (2013) 'Noninvasive prenatal testing of fetal aneuploidies by massively parallel sequencing in a prospective Chinese population'. *Prenatal Diagnosis*, 33 (7). pp 700-706.

Soothill, P. (2014) 'Non-invasive Prenatal Testing for Chromosomal Abnormalities using Maternal Plasma DNA'. Scientific Impact Paper No. 15 (March 2014). Royal College of Obstetricians and Gynaecologists. Kent, UK.

Souka, A., Snijders, R., Novakov, A., Soares, W. and Nicolaides, K. (1998) 'Defects and syndromes in chromosomally normal fetuses with increased nuchal translucency thickness at 10-14 weeks of gestation'. *Ultrasound in Obstetrics and Gynecology*, 11 (6). pp 391-400.

Souka, A. P., von Kaisenberg, C. S., Hyett, J. A., Sonek, J. D. and Nicolaides, K. H. (2005) 'Increased nuchal translucency with normal karyotype'. *American Journal of Obstetrics and Gynecology*, 192 (4). pp 1005-1021.

Sparks, A. B., Struble, C. A., Wang, E. T., Song, K. and Oliphant, A. (2012a) 'Noninvasive prenatal detection and selective analysis of cell-free DNA obtained from maternal blood: evaluation for trisomy 21 and trisomy 18'. *American Journal of Obstetrics and Gynecology*, 206 pp 319e311-319e319.

Sparks, A. B., Wang, E. T., Struble, C. A., Barrett, W., Stokowski, R., McBride, C., Zahn, J., Lee, K., Shen, N. and Doshi, J. (2012b) 'Selective analysis of cell-free DNA in maternal blood for evaluation of fetal trisomy'. *Prenatal diagnosis*, 32 (1). pp 3-9.

Speiser, P. W. and White, P. C. (2003) 'Congenital adrenal hyperplasia'. *New England Journal of Medicine*, 349 (8). pp 776-788.

Spencer, K., Liao, A. W., Skentou, H., Cicero, S. and Nicolaides, K. H. (2000) 'Screening for triploidy by fetal nuchal translucency and maternal serum free b-hCG and PAPP-A at 10±14 weeks of gestation'. *Prenat Diagn*, 20 (6). pp 495-499.

Spencer, K. and Nicolaides, K. H. (2003) 'Screening for trisomy 21 in twins using first trimester ultrasound and maternal serum biochemistry in a one-stop clinic: a review of three years experience'. *British Journal of Obstetrics and Gynaecology: An International Journal of Obstetrics and Gynaecology*, 110 (3). pp 276-280.

Spencer, K., Cowans, N. J. and Nicolaides, K. H. (2008) 'Low levels of maternal serum PAPP-A in the first trimester and the risk of pre-eclampsia'. *Prenatal Diagnosis*, 28 (1). pp 7-10.

Stephanie, C. Y., Chan, K. A., Zheng, Y. W., Jiang, P., Liao, G. J., Sun, H., Akolekar, R., Leung, T. Y., Go, A. T. and van Vugt, J. M. (2014) 'Size-based molecular diagnostics

using plasma DNA for noninvasive prenatal testing'. *Proceedings of the National Academy of Sciences of the United States of America*, 111 (23). pp 8583-8588.

Stokowski, R., Wang, E., White, K., Batey, A., Jacobsson, B., Brar, H., Balanarasimha, M., Hollemon, D., Sparks, A. and Nicolaides, K. (2015) 'Clinical performance of non-invasive prenatal testing (NIPT) using targeted cell-free DNA analysis in maternal plasma with microarrays or next generation sequencing (NGS) is consistent across multiple controlled clinical studies'. *Prenatal Diagnosis*, doi: 10.1002/pd.4686.

Stoll, C., Dott, B., Alembik, Y. and Roth, M. (1993) 'Evaluation of routine prenatal ultrasound examination in detecting fetal chromosomal abnormalities in a low risk population'. *Human Genetics*, 91 pp 37-41.

Strain, M. C., Lada, S. M., Luong, T., Rought, S. E., Gianella, S., Terry, V. H., Spina, C. A., Woelk, C. H. and Richman, D. D. (2013) 'Highly precise measurement of HIV DNA by droplet digital PCR'. *Public Library of Sciences ONE*, 8 (4). pp e55943.

Stressig, R., Kozlowski, P., Froehlich, S., Siegmann, H. J., Hammer, R., Blumenstock, G. and Kagan, K. O. (2011) 'Assessment of the ductus venosus, tricuspid blood flow and the nasal bone in second-trimester screening for trisomy 21'. *Ultrasound in Obstetrics and Gynecology*, 37 (4). pp 444-449.

Stumm, M., Entezami, M., Haug, K., Blank, C., Wüstemann, M., Schulze, B., Raabe-Meyer, G., Hempel, M., Schelling, M. and Ostermayer, E. (2014) 'Diagnostic accuracy of random massively parallel sequencing for non-invasive prenatal detection of common autosomal aneuploidies: a collaborative study in Europe'. *Prenatal Diagnosis*, 34 (2). pp 185-191.

Su, B. and Macer, D. R. (2003) 'Chinese people's attitudes towards genetic diseases and children with handicaps'. *Law and Human Genome Review*, 18 pp 191-210.

Sun, C.-F., Liu, J.-P., Chen, D.-P., Wang, W.-T. and Yang, T.-T. (2008) 'Use of real time PCR for rapid detection of Del phenotype in Taiwan'. *Annals of Clinical and Laboratory Science*, 38 (3). pp 258-263.

Sun, K., Jiang, P. and Chan, K. A. (2015) 'The impact of digital DNA counting technologies on noninvasive prenatal testing'. *Expert Review of Molecular Diagnostics*, 15 (10). pp 1261-1268.

Sykes, P., Neoh, S., Brisco, M., Hughes, E., Condon, J. and Morley, A. A. (1992) 'Quantitation of targets for PCR by use of limiting dilution'. *BioTechniques*, 13 (3). pp 444-449.

Szczepura, A., Osipenko, L. and Freeman, K. (2011) 'A new fetal RHD genotyping test: costs and benefits of mass testing to target antenatal anti-D prophylaxis in England and Wales'. *BioMed Central Pregnancy and Childbirth*, 11 (1). pp 5.

Taly, V., Pekin, D., Benhaim, L., Kotsopoulos, S. K., Le Corre, D., Li, X., Atochin, I., Link, D. R., Griffiths, A. D. and Pallier, K. (2013) 'Multiplex picodroplet digital PCR to detect KRAS mutations in circulating DNA from the plasma of colorectal cancer patients'. *Clinical Chemistry*, 59 (12). pp 1722-1731.

Tang, N., Tornatore, P. and Weinberger, S. R. (2004) 'Current developments in SELDI affinity technology'. *Mass Spectrometry Reviews*, 23 (1). pp 34-44.

Teeuw, M. E., Henneman, L., Bochdanovits, Z., Heutink, P., Kuik, D. J., Cornel, M. C. and ten Kate, L. P. (2010) 'Do consanguineous parents of a child affected by an autosomal recessive disease have more DNA identical-by-descent than similarly-related parents with healthy offspring? Design of a case-control study'. *BioMed Central Medical Genetics*, 11 (1). pp 113.

Tjoa, M. L., Cindrova-Davies, T., Spasic-Boskovic, O., Bianchi, D. W. and Burton, G. J. (2006) 'Trophoblastic oxidative stress and the release of cell-free feto-placental DNA'. *American Journal of Pathology*, 169 (2). pp 400-404.

The UK National Screening Committee (2008) *Fetal Anomaly Screening Programme - Screening for Down's Syndrome: UK NSC Policy recommendations 2007-2010: Model of Best Practice*. Department of Health. London: Public Health England (PHE).

The UK National Screening Committee (2011) *NHS Fetal Anomaly Screening Programme - Screening for Down's syndrome: UK NSC Policy recommendations 2011-2014: Model of Best Practice*. Department of Health. London: Public Health England (PHE).

The UK National Screening Committee (2013) Antenatal screening for Rhesus D status and red cell allo-antibodies. Department of Health London, UK: Public Health England (PHE).

The UK National Screening Committee (2015) *Fetal Anomaly Screening Programme- Programme Handbook June 2015*. Department of Health. London: Public Health England (PHE).

Thurik, F., Ait Soussan, A., Bossers, B., Woortmeijer, H., Veldhuisen, B., Page-Christiaens, G., Haas, M. and Schoot, C. (2015) 'Analysis of false-positive results of fetal RHD typing in a national screening program reveals vanishing twins as potential cause for discrepancy'. *Prenatal Diagnosis*, 35 (8). pp 754-760.

Togrul, C., Ozaksit, G. M., Seckin, K. D., Baser, E., Karsli, M. F. and Gungor, T. (2014) 'Is there a role for fetal ductus venosus and hepatic artery Doppler in screening for fetal aneuploidy in the first trimester?'. *The Journal of Maternal-Fetal and Neonatal Medicine*, (0). pp 1-4.

Tong, Y. K., Jin, S., Chiu, R. W., Ding, C., Chan, K. A., Leung, T. Y., Yu, L., Lau, T. K. and Lo, Y. D. (2010) 'Noninvasive prenatal detection of trisomy 21 by an epigenetic-genetic chromosome-dosage approach'. *Clinical Chemistry*, 56 (1). pp 90-98.

Tong, Y. K., Chiu, R. W. K., Chan, K. C. A., Leung, T. Y. and Lo, Y. M. D. (2012) 'Technical concerns about immunoprecipitation of methylated fetal DNA for noninvasive trisomy 21 diagnosis'. *Nature Medicine*, 18 (9). pp 1327-1328.

Tsaliki, E., Papageorgiou, E. A., Spyrou, C., Koumbaris, G., Kypri, E., Kyriakou, S., Sotiriou, C., Touvana, E., Keravnou, A. and Karagrigoriou, A. (2012) 'MeDIP real-time qPCR of maternal peripheral blood reliably identifies trisomy 21'. *Prenatal Diagnosis*, 32 (10). pp 996-1001.

Tsao, S. C.-H., Weiss, J., Hudson, C., Christophi, C., Cebon, J., Behren, A. and Dobrovic, A. (2015) 'Monitoring response to therapy in melanoma by quantifying circulating tumour DNA with droplet digital PCR for BRAF and NRAS mutations'. *Scientific Reports*, 5 pp doi:10.1038/srep11198.



Tsui, N. B., Kadir, R. A., Chan, K. A., Chi, C., Mellars, G., Tuddenham, E. G., Leung, T. Y., Lau, T. K., Chiu, R. W. and Lo, Y. D. (2011) 'Noninvasive prenatal diagnosis of hemophilia by microfluidics digital PCR analysis of maternal plasma DNA'. *Blood*, 117 (13). pp 3684-3691.

Turan, N., Katari, S., Gerson, L. F., Chalian, R., Foster, M. W., Gaughan, J. P., Coutifaris, C. and Sapienza, C. (2010) 'Inter- and Intra-Individual Variation in Allele-Specific DNA mMethylation and Gene Expression in Children Conceived using Assisted Reproductive Technology'. *Public Library of Sciences Genetics*, 6 (7). pp e1001033.

Twiss, P., Hill, M., Daley, R. and Chitty, L. S. (2014) 'Non-invasive prenatal testing for Down syndrome', *Seminars in Fetal and Neonatal Medicine*. Elsevier, pp. 9-14.

Ünlü, M., Morgan, M. E. and Minden, J. S. (1997) 'Difference gel electrophoresis. A single gel method for detecting changes in protein extracts'. *Electrophoresis*, 18 (11). pp 2071-2077.

Urbaniak, S. and Greiss, M. (2000) 'RhD haemolytic disease of the fetus and the newborn'. *Blood Reviews*, 14 (1). pp 44-61.

Valinen, Y., Rapakko, K., Kokkonen, H., Laitinen, P., Tekay, A., Ahola, T. and Ryyananen, M. (2007) 'Clinical first-trimester routine screening for Down syndrome in singleton pregnancies in northern Finland'. *American Journal of Obstetrics and Gynecology*, 196 (3). pp 278. e271-278. e275.

Van den Hof, M. C., Nicolaidis, K. H., Campbell, J. and Campbell, S. (1990) 'Evaluation of the lemon and banana signs in one hundred thirty fetuses with open spina bifida'. *American Journal of Obstetrics and Gynecology*, 162 (2). pp 322-327.

van der Schoot, C. E., Tax, G. M., Rijnders, R. J., de Haas, M. and Christiaens, G. C. (2003) 'Prenatal typing of Rh and Kell blood group system antigens: the edge of a watershed'. *Transfusion Medicine Reviews*, 17 (1). pp 31-44.

van der Schoot, C., Soussan, A. A., Koelewijn, J., Bonsel, G., Paget-Christiaens, L. and De Haas, M. (2006) 'Non-invasive antenatal RHD typing'. *Transfusion Clinique et Biologique*, 13 (1). pp 53-57.

Verweij, E., Jacobsson, B., Scheltema, P., Boer, M., Hoffer, M., Hollemon, D., Westgren, M., Song, K. and Oepkes, D. (2013) 'European Non-Invasive Trisomy Evaluation (EU-NITE) study: a multicenter prospective cohort study for non-invasive fetal trisomy 21 testing'. *Prenatal Diagnosis*, 33 (10). pp 996-1001.

Wachtel, S. S., Sammons, D., Twitty, G., Utermohlen, J., Tolley, E., Phillips, O. and Shulman, L. P. (1998) 'Charge flow separation: quantification of nucleated red blood cells in maternal blood during pregnancy'. *Prenatal Diagnosis*, 18 (5). pp 455-463.

Wagner, F. F., Gassner, C., Müller, T. H., Schönitzer, D., Schunter, F. and Flegel, W. A. (1998) 'Three molecular structures cause Rhesus D category VI phenotypes with distinct immunohematologic features'. *Blood*, 91 (6). pp 2157-2168.

Wagner, F. F. and Flegel, W. A. (2000) 'RHD gene deletion occurred in the Rhesus box'. *Blood*, 95 (12). pp 3662-3668.

Wagner, F. F., Frohmajer, A., Ladewig, B., Eicher, N. I., Lonicer, C. B., Müller, T. H., Siegel, M. H. and Flegel, W. A. (2000) 'Weak D alleles express distinct phenotypes'. *Blood*, 95 (8). pp 2699-2708.

Wailoo, K. and Pemberton, S. (2008) *The troubled dream of genetic medicine: ethnicity and innovation in Tay-Sachs, cystic fibrosis, and sickle cell disease*. JHU Press.

Wald, N. J., Kennard, A., Hackshaw, A. and McGuire, A. (1996) 'Antenatal screening for Down's syndrome'. *Journal of Medical Screening*, 4 (4). pp 181-246.

Wald, N. and Hackshaw, A. (1997) 'Combining Ultrasound and Biochemistry in First-Trimester Screening for Down's syndrome'. *Prenatal Diagnosis*, 17 (9). pp 821-829.

Wald, N., Rodeck, C., Hackshaw, A., Walters, J., Chitty, L. and Mackinson, A. (2003) 'First and second trimester antenatal screening for Down's syndrome: the results of the Serum, Urine and Ultrasound Screening Study (SURUSS)'. *Journal of Medical Screening*, 10 (2). pp 56-87.

Wald, N., Rodeck, C., Hackshaw, A. and Rudnicka, A. (2004) 'SURUSS in perspective'. *British Journal of Obstetrics and Gynecology: An International Journal of Obstetrics and Gynaecology*, 111 (6). pp 521-531.

Wald, N. (2008) 'Guidance on terminology'. *Journal of Medical Screening*, 15 (1). pp 50-50.

Wald, N., Huttly, W., Murphy, K., Ali, K., Bestwick, J. and Rodeck, C. (2009) 'Antenatal screening for Down's syndrome using the Integrated test at two London hospitals'. *Journal of Medical Screening*, 16 (1). pp 7-10.

Walencik, J. and Witeska, M. (2007) 'The effects of anticoagulants on hematological indices and blood cell morphology of common carp (< i> *Cyprinus carpio*</i> L.)'. *Comparative Biochemistry and Physiology Part C: Toxicology and Pharmacology*, 146 (3). pp 331-335.

Walker, B. S., Nelson, R. E., Jackson, B. R., Grenache, D. G., Ashwood, E. R. and Schmidt, R. L. (2015) 'A Cost-Effectiveness Analysis of First Trimester Non-Invasive Prenatal Screening for Fetal Trisomies in the United States'. *Public Library of Sciences ONE*, 10 (7). 0131402.

Walknowska, J., Conte, F. and Grumbach, M. (1969) 'Practical and theoretical implications of fetal/maternal lymphocyte transfer'. *Lancet*, 293 (7606). pp 1119-1122.

Walsh, P. S., Fildes, N. J. and Reynolds, R. (1996) 'Sequence analysis and characterization of stutter products at the tetranucleotide repeat locus vWA'. *Nucleic Acids Research*, 24 (14). pp 2807-2812.

Wang, D., Lane, C. and Quillen, K. (2010) 'Prevalence of RhD variants, confirmed by molecular genotyping, in a multiethnic prenatal population'. *American journal of clinical pathology*, 134 (3). pp 438-442.

Wang, E., Batey, A., Struble, C., Musci, T., Song, K. and Oliphant, A. (2013) 'Gestational age and maternal weight effects on fetal cell-free DNA in maternal plasma'. *Prenatal diagnosis*, 33 (7). pp 662-666.

Wang, P. and Michaels, C. A. (2010) 'Chinese families of children with severe disabilities: Family needs and available support'. *Research and Practice for Persons with Severe Disabilities*, 34 (2). pp 21-32.

Wapner, R. J., Babiarz, J. E., Levy, B., Stosic, M., Zimmermann, B., Sigurjonsson, S., Wayham, N., Ryan, A., Banjevic, M. and Lacroute, P. (2015) 'Expanding the scope of noninvasive prenatal testing: detection of fetal microdeletion syndromes'. *American Journal of Obstetrics and Gynecology*, 212 (3). pp 332. e331-332. e339.

Wataganara, T., Peter, I., Messerlian, G. M., Borgatta, L. and Bianchi, D. W. (2004) 'Inverse correlation between maternal weight and second trimester circulating cell-free fetal DNA levels'. *Journal of Obstetrics and Gynecology*, 104 (3). pp 545-550.

Weiss, J., Schwechheimer, K., Cavenee, W. K., Herlyn, M. and Arden, K. C. (1993) 'Mutation and expression of the p53 gene in malignant melanoma cell lines'. *International Journal of Cancer*, 54 (4). pp 693-699.

Westhoff, C. M. (2004) 'The Rh blood group system in review: a new face for the next decade'. *Transfusion*, 44 (11). pp 1663-1673.

Westhoff, C. M. (2006) 'Molecular testing for transfusion medicine'. *Current Opinion in Hematology*, 13 (6). pp 471-475.

Wetterstrand, K. (2015) 'DNA Sequencing Costs: Data from the NHGRI Genome Sequencing Program (GSP)'. [Online]. Available at: <http://www.genome.gov/sequencingcosts/> (Accessed: November 8<sup>th</sup> 2015).

Whale, A. S., Huggett, J. F., Cowen, S., Speirs, V., Shaw, J., Ellison, S., Foy, C. A. and Scott, D. J. (2012) 'Comparison of microfluidic digital PCR and conventional quantitative PCR for measuring copy number variation'. *Nucleic Acids Research*, 40 (11). pp e82-e82.

White, T. B., McCoy, A. M., Streva, V. A., Fenrich, J. and Deininger, P. L. (2014) 'A droplet digital PCR detection method for rare L1 insertions in tumors'. *Mobile DNA*, 5 (1). pp 30.

Widlak, P., Li, P., Wang, X. and Garrard, W. T. (2000) 'Cleavage preferences of the apoptotic endonuclease DFF40 (caspase-activated DNase or nuclease) on naked DNA and chromatin substrates'. *Journal of Biological Chemistry*, 275 (11). pp 8226-8232.

Wong, D., Moturi, S., Angkachatchai, V., Mueller, R., DeSantis, G., van den Boom, D. and Ehrich, M. (2013) 'Optimizing blood collection, transport and storage conditions for cell free DNA increases access to prenatal testing'. *Clinical Biochemistry*, 46 (12). pp 1099-1104.

Woods, C. G., Cox, J., Springell, K., Hampshire, D. J., Mohamed, M. D., McKibbin, M., Stern, R., Raymond, F. L., Sandford, R. and Sharif, S. M. (2006) 'Quantification of homozygosity in consanguineous individuals with autosomal recessive disease'. *The American Journal of Human Genetics*, 78 (5). pp 889-896.

Wright, C. (2009) 'Cell-free fetal nucleic acids for non-invasive prenatal diagnosis: report of the UK expert working group'. Report of the UK expert working group, PHG Foundation (2009). Available at <http://www.phgfoundation.org/reports/4985/> (Accessed: August 24<sup>th</sup> 2015).

Wright, C. and Burton, H. (2009) 'The use of cell-free fetal nucleic acids in maternal blood for non-invasive prenatal diagnosis'. *Human Reproduction Update*, 15 (1). pp 139-151.

Yakovchuk, P., Protozanova, E. and Frank-Kamenetskii, M. D. (2006) 'Base-stacking and base-pairing contributions into thermal stability of the DNA double helix'. *Nucleic Acids Research*, 34 (2). pp 564-574.

Yang, Y. H. and Speed, T. (2002) 'Design issues for cDNA microarray experiments'. *Nature Reviews Genetics*, 3 (8). pp 579-588.

Yu, B., Zhang, B., Wang, J., Wang, Q.-w., Huang, R.-p., Yang, Y.-q. and Shao, S.-h. (2012) 'Preliminary proteomic-based identification of a novel protein for Down's syndrome in maternal serum'. *Experimental Biology and Medicine*, 237 (5). pp 530-539.

Zechner, U., Wilda, M., Kehrer-Sawatzki, H., Vogel, W., Fundele, R. and Hameister, H. (2001) 'A high density of X-linked genes for general cognitive ability: a run-away process shaping human evolution?'. *Trends in Genetics*, 17 (12). pp 697-701.

Zhao, C., Tynan, J., Ehrich, M., Hannum, G., McCullough, R., Saldivar, J.-S., Oeth, P., van den Boom, D. and Deciu, C. (2015) 'Detection of fetal subchromosomal abnormalities by sequencing circulating cell-free DNA from maternal plasma'. *Clinical Chemistry*, 61 (4). pp 608-616.

Zhong, X. Y., Bürk, M. R., Troeger, C., Kang, A., Holzgreve, W. and Hahn, S. (2000) 'Fluctuation of maternal and fetal free extracellular circulatory DNA in maternal plasma'. *Obstetrics and Gynecology*, 96 (6). pp 991-996.

Zhou, H., Lan, J., Wang, X., Fan, H., Wang, Y., Meng, Q., Zhao, X. and Zhang, Y. (2005) '[Determination of human RHD gene rhesus box and its significance]'. *Journal of Experimental Hematology*, 13 (1). pp 130-134.

Zimmermann, B., Holzgreve, W., Wenzel, F. and Hahn, S. (2002) 'Novel real-time quantitative PCR test for trisomy 21'. *Clinical Chemistry*, 48 pp 362-363.

Zimmermann, B., El-Sheikhah, A., Nicolaides, K., Holzgreve, W. and Hahn, S. (2005) 'Optimized real-time quantitative PCR measurement of male fetal DNA in maternal plasma'. *Clinical Chemistry*, 51 (9). pp 1598-1604.

Zimmermann, B., Hill, M., Gemelos, G., Demko, Z., Banjevic, M., Baner, J., Ryan, A., Sigurjonsson, S., Chopra, N. and Dodd, M. (2012) 'Noninvasive prenatal aneuploidy testing of chromosomes 13, 18, 21, X, and Y, using targeted sequencing of polymorphic loci'. *Prenatal Diagnosis*, 32 (13). pp 1233-1241.

Zosmer, N., Souter, V., Chan, C., Huggon, I. and Nicolaides, K. (1999) 'Early diagnosis of major cardiac defects in chromosomally normal fetuses with increased nuchal translucency'. *British Journal of Obstetrics and Gynaecology: An International Journal of Obstetrics and Gynaecology*, 106 (8). pp 829-833.

Zuo, Z., Chen, S. S., Chandra, P. K., Galbincea, J. M., Soape, M., Doan, S., Barkoh, B. A., Koeppen, H., Medeiros, L. J. and Luthra, R. (2009) 'Application of COLD-PCR for improved detection of KRAS mutations in clinical samples'. *Modern Pathology*, 22 (8). pp 1023-1031.



# Fetal Sex and *RHD* Genotyping with Digital PCR Demonstrates Greater Sensitivity than Real-time PCR

Kelly A. Sillence,<sup>1</sup> Llinos A. Roberts,<sup>2</sup> Heidi J. Hollands,<sup>2</sup> Hannah P. Thompson,<sup>1</sup> Michele Kiernan,<sup>1</sup> Tracey E. Madgett,<sup>1</sup> C. Ross Welch,<sup>2</sup> and Neil D. Avent<sup>1\*</sup>

**BACKGROUND:** Noninvasive genotyping of fetal *RHD* (Rh blood group, D antigen) can prevent the unnecessary administration of prophylactic anti-D to women carrying *RHD*-negative fetuses. We evaluated laboratory methods for such genotyping.

**METHODS:** Blood samples were collected in EDTA tubes and Streck<sup>®</sup> Cell-Free DNA<sup>™</sup> blood collection tubes (Streck BCTs) from *RHD*-negative women (n = 46). Using Y-specific and *RHD*-specific targets, we investigated variation in the cell-free fetal DNA (cffDNA) fraction and determined the sensitivity achieved for optimal and suboptimal samples with a novel Droplet Digital<sup>™</sup> PCR (ddPCR) platform compared with real-time quantitative PCR (qPCR).

**RESULTS:** The cffDNA fraction was significantly larger for samples collected in Streck BCTs compared with samples collected in EDTA tubes ( $P < 0.001$ ). In samples expressing optimal cffDNA fractions ( $\geq 4\%$ ), both qPCR and digital PCR (dPCR) showed 100% sensitivity for the *TSPY1* (testis-specific protein, Y-linked 1) and *RHD7* (*RHD* exon 7) assays. Although dPCR also had 100% sensitivity for *RHD5* (*RHD* exon 5), qPCR had reduced sensitivity (83%) for this target. For samples expressing suboptimal cffDNA fractions ( $< 2\%$ ), dPCR achieved 100% sensitivity for all assays, whereas qPCR achieved 100% sensitivity only for the *TSPY1* (multiplex target) assay.

**CONCLUSIONS:** qPCR was not found to be an effective tool for *RHD* genotyping in suboptimal samples ( $< 2\%$  cffDNA). However, when testing the same suboptimal samples on the same day by dPCR, 100% sensitivity was achieved for both fetal sex determination and *RHD* genotyping. Use of dPCR for identification of fetal specific markers can reduce the occurrence of false-negative and

inconclusive results, particularly when samples express high levels of background maternal cell-free DNA.

© 2015 American Association for Clinical Chemistry

Diagnosis of fetal sex, *RHD* (Rh blood group, D antigen)<sup>3</sup> genotype, and chromosomal abnormalities can be achieved only through analysis of fetal DNA. Initially, this could be achieved through invasive procedures such as amniocentesis and chorionic villus sampling, quoted as having a 1% risk of miscarriage (1). Since the discovery of cell-free fetal DNA (cffDNA)<sup>4</sup> in maternal plasma, noninvasive prenatal testing is now a clinical reality (1–5). Fetal sex determination is offered in the clinic for families at risk of X-linked disorders, such as Duchenne muscular dystrophy (6). Determination of fetal sex is especially beneficial in cases of congenital adrenal hyperplasia, to allow therapy to be targeted to female fetuses only (7). Fetal aneuploidy detection requires accurate quantification and presently can only be determined by next-generation sequencing, which is too costly for routine testing (8).

The antigens of the Rh blood group system are coded for by 2 genes, *RHD* and *RHCE* (Rh blood group, CcEe antigens), which are located on chromosome 1 (p34–p36) (9). In white populations, most D-negative phenotypes result from a complete *RHD* deletion (10). For D-negative individuals of African descent, only 18% are a result of *RHD* deletion. Instead, 66% and 15% of D-negative Africans have an inactive *RHD* gene (*RHD* $\Psi$ ) or a hybrid gene (*RHD-CE-D<sup>S</sup>* or *r<sup>S</sup>*), which do not produce any RhD protein (10, 11). Many laboratories currently provide noninvasive fetal *RHD* genotyping for alloimmunized women as routine practice to manage hemolytic disease of the fetus and newborn (HDFN)

<sup>1</sup> School of Biomedical and Healthcare Sciences, Plymouth University, Plymouth University Peninsula Schools of Medicine and Dentistry, Plymouth, UK; <sup>2</sup> Department of Fetal Medicine, Plymouth Hospitals National Health Service Trust, Plymouth, UK.

\* Address correspondence to this author at: School of Biomedical and Healthcare Sciences, Plymouth University, Plymouth, UK PL4 8AA. E-mail neil.avent@plymouth.ac.uk.  
Received January 28, 2015; accepted August 24, 2015.

Previously published online at DOI: 10.1373/clinchem.2015.239137

© 2015 American Association for Clinical Chemistry

<sup>3</sup> Human genes: *RHD*, Rh blood group, D antigen; *RHCE*, Rh blood group, CcEe antigens; *SRY*, sex-determining region Y; *TSPY1*, testis-specific protein, Y-linked 1; *AGO1*, argo-

nate RISC catalytic component 1 (formerly *EIF2C1*); *TERT*, telomerase reverse transcriptase; *ERV3-1*, endogenous retrovirus group 3, member 1.

<sup>4</sup> Nonstandard abbreviations: cffDNA, cell-free fetal DNA; HDFN, hemolytic disease of the fetus and newborn; qPCR, real-time quantitative PCR; dPCR, digital PCR; BCT, blood collection tube; cfDNA, cell-free DNA; *RHD5*, Rh blood group, D antigen exon 5; *RHD7*, Rh blood group, D antigen exon 7; FAM, carboxyfluorescein; HEX, hexachlorofluorescein; BLAST, Basic Local Alignment Search Tool; gDNA, genomic DNA; ddPCR, droplet digital PCR; Cq, quantification cycle; Ta, annealing temperature; NTC, no-template control; 2D, 2-dimensional.

**Table 1. Summary of amplicon location, length, and fluorescent label for each multiplex reaction.**

Multiplex reaction	Amplicon	Chromosome	Gene	Exon/intron	Fluorescent reporter dye	Length, bp	Origin
1	Target	Y	<i>SRY</i>	Exon	FAM	137	Lo et al. (22)
2	Target	Y	<i>TSPY1</i>	Exon	FAM	88	In-house
1 and 2	Reference	X	Xp22.3	Intron	HEX	95	Fan et al. (23)
3	Target	1	<i>RHD5</i>	Exon (5)	FAM	82	Finning et al. (24)
4	Target	1	<i>RHD7</i>	Exon (7)	FAM	75	Finning et al. (24)
3 and 4	Reference	1	<i>AGO1</i>	Exon	HEX	81	Fan et al. (23)

(4, 12–14). Before 1970, HDFN was a major cause of fetal mortality (46/100 000 births in the UK alone) (15), but since the introduction of routine antenatal anti-D prophylaxis, incidence has decreased nearly 10-fold (16). Currently, all *RHD*-negative women in the West are offered this prophylaxis, which is costly, as it is produced from hyper-immunized male volunteers. Providing a noninvasive test for fetal *RHD* genotyping allows administration to be targeted to *RHD*-negative women who are known to be carrying an *RHD*-positive fetus. This is now routine in the Netherlands and Denmark with real-time quantitative PCR (qPCR) approaches (4, 17, 18). However, recent publications have described the application of digital PCR (dPCR) for the detection of low-level targets with improved precision, resulting in reliable quantification well below the limit of quantification of qPCR (19, 20).

The use of Streck<sup>®</sup> Cell-Free DNA<sup>™</sup> blood collection tubes (BCTs) instead of conventional EDTA tubes has been shown to increase the proportion of cfDNA (21). Streck BCTs contain proprietary cell-preserving reagents, which prevent maternal cell lysis and consequently reduce the amount of maternal cell-free DNA (cfDNA) released into the plasma. In this study, we compared the sensitivity of dPCR and qPCR for the noninvasive determination of fetal sex and *RHD* genotype for samples collected in both Streck BCTs and EDTA tubes. For technical reasons, some samples, despite being collected in the third trimester, expressed suboptimal cfDNA fractions (<2%). However, all samples were included to thoroughly test the capability of the dPCR assay against the current gold standard, qPCR.

## Materials and Methods

### STUDY PARTICIPANTS

*RHD*-negative pregnant women (28–30 weeks' gestation), all of whom met inclusion criteria, were recruited at Plymouth Hospitals NHS Trust, Plymouth, UK, with informed consent, from November 2013 to September 2014. Ethics approval was granted by the United Bristol Healthcare and Trust Research and Ethics Committee (13/SW/0148).

### SAMPLE PROCESSING

Twenty-two maternal peripheral blood samples were collected in EDTA tubes (5–10 mL total blood volume) and centrifuged at 1600g for 10 min at room temperature (samples 1–22). The plasma was carefully removed and transferred to a 15-mL tube. The plasma was then recentrifuged at 16 000g for 10 min. All samples were processed within 4 h of collection, and plasma aliquots (1 mL) were stored at –80 °C. *RHD*<sup>+</sup> and *RHD*<sup>–</sup> human whole blood, collected in EDTA tubes (5 mL total blood volume), was supplied by National Health Service Blood and Transplant (Bristol, UK) as positive and negative controls, respectively. These samples were processed within 48–96 h by following the same double-spin protocol described above.

Twenty-four maternal blood samples collected in Streck BCTs (10–20 mL total blood volume) were centrifuged at 1600g for 15 min at room temperature (samples 23–46). Plasma was carefully removed, transferred to a 50-mL tube, and recentrifuged at 2500g for 10 min. All samples were processed within 48 h of collection, and plasma aliquots (1 mL) were stored at –80 °C.

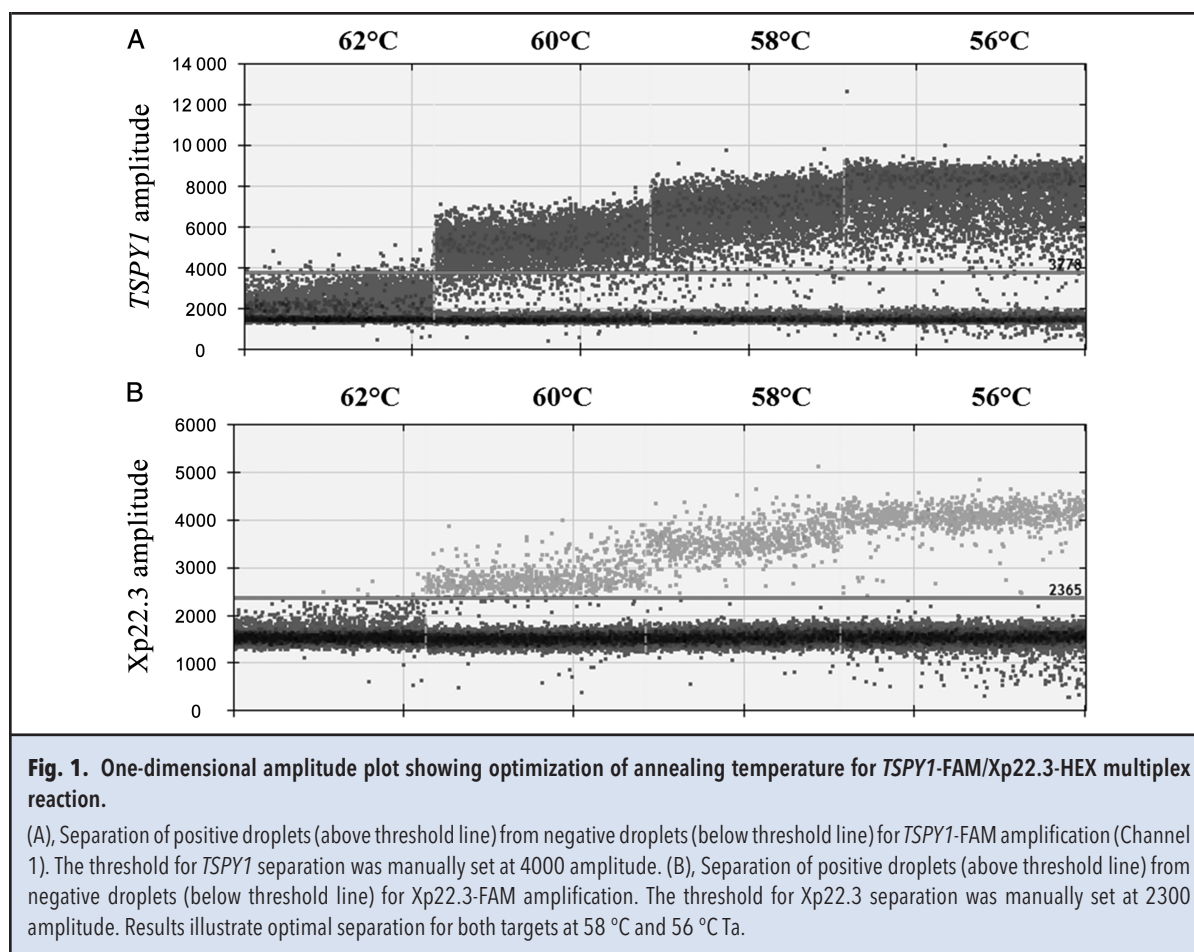
### DNA EXTRACTION

DNA was extracted from two 1-mL aliquots of plasma with the QIAamp Circulating Nucleic Acid kit (Qiagen) and QIAvac 24 Plus (Qiagen). The extraction process followed the manufacturer's protocol, and each sample was eluted in 60 µL Buffer AVE [RNase-free water containing 0.04% (wt/vol) sodium azide]. No DNase or RNase treatment was used. After DNA extraction, we quantified samples on the Qubit<sup>®</sup> 2.0 Fluorometer (Life Technologies) with the Qubit dsDNA HS assay kit (Life Technologies). Samples were stored at –20 °C as 60-µL aliquots for ≤4 weeks.

### PCR PRIMERS AND PROBES

For both dPCR and qPCR, we tested 4 multiplex reactions: 2 for fetal sex determination and 2 for fetal *RHD* genotyping (Table 1). Primer concentrations (300 to 900 nmol/L) and annealing temperatures (56 °C to 62 °C) were optimized for all multiplex reactions. Fig. 1 shows





the optimization process for *TSPY1*-FAM/*Xp22.3*-HEX. We used *Xp22.3* oligonucleotides as a reference for 2 Y-specific targets [*SRY* (sex-determining region Y) (22) and *TSPY1* (testis-specific protein, Y-linked 1)] for fetal sex determination. *AGO1* (argonaute RISC catalytic component 1; formerly *EIF2C1*) primers were taken from Fan et al. (23) and used as a reference for 2 *RHD*-specific targets [*RHD* exon 5 (*RHD5*) and *RHD* exon 7 (*RHD7*)] (24) since *AGO1* is also located on chromosome 1. The oligonucleotide sequences (HPLC purified, Eurofins Genomics) and amplicon sizes for all target [carboxyfluorescein (FAM)-labeled] and reference [hexachlorofluorescein (HEX)-labeled] regions are shown in Supplemental File 1, which accompanies the online version of this article at <http://www.clinchem.org/content/vol61/issue11>. Sequences for the *Xp22.3* reverse primer and all *TSPY1* oligonucleotides were designed with online software (<http://primer3.sourceforge.net> and <http://www.idtdna.com/calc/analyzer>) and subjected to Basic Local Alignment Search Tool (BLAST) analysis against the National Center for Biotechnology Information GenBank DNA database (accession nos. NC\_000024.10 and NC\_000023.11).

#### REAL-TIME qPCR

qPCR reactions were performed in a 20- $\mu$ L solution containing 1 $\times$  TaqMan Universal PCR Master Mix (Life Technologies), 300 nmol/L primers, 250 nmol/L probes, and a standard volume of template DNA (5  $\mu$ L). Sample concentrations are recorded in online Supplemental File 2; because of the low abundance of cfDNA in extracted maternal plasma, the samples were not diluted. Reactions were conducted in duplicate, with positive and negative controls for each assay. After optimization of annealing temperature ( $T_a$ ), cycling was carried out on a Life Technologies StepOnePlus™ qPCR System under the following conditions: 95 °C for 10 min, 50 cycles of 95 °C for 15 s, and 58 °C for 1 min. Fifty cycles were used to ensure amplification of low-copy-number target DNA. We included a standard curve of male genomic DNA (gDNA) (Promega) in triplicate on each plate. We used FAM-labeled fluorescent probes for all target regions (*SRY*, *TSPY1*, *RHD5*, and *RHD7*) and HEX-labeled fluorescent probes for both reference regions (*Xp22.3* and *AGO1*) (Table 1; also see online Supplemental File 1).

**Table 2.** Summary of fetal sex determination and *RHD* genotyping results obtained from both dPCR and qPCR against results recorded after delivery.

Platform	Samples	Sex determination					<i>RHD</i> determination				
		Male		Female		Inconclusive	Positive		Negative		Inconclusive
		Fetus	Newborn	Fetus	Newborn		Fetus	Newborn	Fetus	Newborn	
dPCR	46										
EDTA tubes	22	10	10	12	12	0	12	12	9	10	1
Streck BCTs	24	13	13	11	11	0	19	19	5	5	0
qPCR	46										
EDTA tubes	22	10	10	12	12	0	0	12	22	10	0
Streck BCTs	24	13	13	11	11	0	15	19	5	5	4

#### Digital PCR

dPCR reactions were performed in a 20- $\mu$ L solution containing 10  $\mu$ L droplet digital PCR (ddPCR) Supermix for Probes (Bio-Rad), 300 nmol/L primers, and 250 nmol/L probes. Because samples were not diluted after Qubit quantification, we added a standard volume of template DNA (5  $\mu$ L) with positive and negative controls. All reactions were conducted in duplicate and run on the QX100™ Droplet Generator (Bio-Rad) according to the manufacturer's instructions. By use of an oil emersion approach, the sample was drawn through the cartridge under a vacuum, where approximately 20 000 1-nL droplets were formed. The droplets (40  $\mu$ L total volume) were then transferred to a 96-well plate and covered with a pierceable foil heat seal on the PX1™ Plate Sealer (Bio-Rad). Cycling was carried out on a C1000 Touch™ Thermal Cycler (Bio-Rad) under optimized conditions: 95 °C for 10 min, 40 cycles of 95 °C for 30 s, and 58 °C for 1 min, after which a final 98 °C step for 10 min was carried out (as recommended by Bio-Rad). Samples were analyzed immediately on the QX100™ Droplet Reader (Bio-Rad). To ensure uniformity, samples were extracted and tested by qPCR and dPCR on the same day by the same investigator.

#### DATA ANALYSIS

For qPCR, targets with a mean quantification cycle ( $C_q$ ) of  $<45$  were recorded as positive, provided no-template controls (NTC) remained negative ( $C_q >45$ ), to ensure inclusion of low-copy-number targets. Targets that expressed  $C_q$  values  $>45$  for both duplicates were recorded as negative. Thresholds were set at 0.05 for all targets (StepOne™ Software v2.3).

We analyzed the raw fluorescent data from the dPCR platform with Bio-Rad QuantaSoft v1.2 software. Once thresholds for each sample had been set manually with the 2-dimensional (2D) amplification plot, positive and negative droplets were determined (Fig. 1; also see

online Supplemental File 3). Thresholds were determined when intermediate droplets between 2 clusters did not alter the calculated concentration (Poisson 95% CI) (20). Online Supplemental File 4 shows the calculations used for determining the cfDNA fraction by use of the dPCR results on the basis of the concentration (copies per microliter). All statistical analysis for comparing Streck BCTs vs EDTA tubes for both cfDNA fractions and reference DNA concentration were performed with Mann–Whitney *U* test (SigmaPlot v12.5), and significance was accepted at  $P < 0.05$ .

#### CONFIRMATION OF FETAL SEX AND *RHD* STATUS

The accuracy of dPCR and qPCR for the prenatal detection of fetal sex was ascertained at birth (Table 2). Fetal blood group was verified after delivery through the serology of umbilical cord blood samples.

#### Results

##### FETAL SEX DETERMINATION

For dPCR, in 100% of cases, the fetal sex predicted by using both Y-specific targets (*TSPY1* and *SRY*) was the same as that determined at birth (Table 2). The  $T_a$  gradient was optimized for all targets, and despite Fig. 1 illustrating equal separation at 58 °C and 56 °C, the 2D amplitude plot illustrated better separation at 58 °C (data not shown). In addition, at  $T_a$  58 °C, the *SRY*-FAM/Xp22.3 multiplex reaction produced a ratio closer to 1 than at  $T_a$  56 °C (0.931 and 0.835, respectively). The *SRY* assay was successful only for the male positive control by qPCR. Therefore, fetal sex was ascertained by *TSPY1* only for qPCR (Table 2; also see online Supplemental File 2). The results also illustrated 100% accuracy when only the multiple-copy target gene was considered for qPCR analysis (Table 3). Calibration curves, slopes,  $y$ -intercepts,  $R^2$  values, and efficiencies for qPCR data are shown in online Supplemental File 5.

**Table 3.** Results of testing 22 and 24 maternal samples collected in EDTA tubes and Streck BCTs, respectively, with dPCR and qPCR for fetal sex and *RHD* genotyping.

Platform and target gene	Sensitivity, %	False-negative results, % (n)	Specificity, %	False-positive results, % (n)	Accuracy, % <sup>c</sup>
dPCR					
Streck BCTs <sup>a</sup>					
<i>TSPY1</i>	100		100		100
<i>SRY</i>	100		100		100
<i>RHD5</i>	100		100		100
<i>RHD7</i>	100		100		100
EDTA tubes <sup>b</sup>					
<i>TSPY1</i>	100		100		100
<i>SRY</i>	100		100		100
<i>RHD5</i>	100		95.5	4.5 (1)	95.6
<i>RHD7</i>	100		95.5	4.5 (1)	95.6
qPCR					
Streck BCTs <sup>a</sup>					
<i>TSPY1</i>	100		100		100
<i>SRY</i>	50	54.2 (13)	100		45.8
<i>RHD5</i>	83.4	16.6 (4)	100		83.4
<i>RHD7</i>	100		100		100
EDTA tubes <sup>b</sup>					
<i>TSPY1</i>	100		100		100
<i>SRY</i>	0	45.5 (10)	100		54.5
<i>RHD5</i>	0	59.1 (13)	100		40.9
<i>RHD7</i>	0	59.1 (13)	100		40.9

<sup>a</sup> cfDNA in maternal plasma 4%–24%, calculated from dPCR results.  
<sup>b</sup> cfDNA in maternal plasma 0.1%–2%, calculated from dPCR results.  
<sup>c</sup> Accuracy was calculated as (true positives + true negatives)/(true positives + false positives + false negatives + true negatives).

The cfDNA fraction with both Y-specific and *RHD*-specific targets was calculated on the basis of the concentration (copies per microliter) generated by dPCR for each multiplex reaction (see online Supplemental File 4). The samples collected in Streck BCTs expressed higher cfDNA fractions (4%–24%) and were classed as optimal, whereas the samples collected in EDTA tubes, during the initial stages of sample collection, illustrated lower cfDNA fractions (0.1%–2%) and were classified as suboptimal (Fig. 2A).

#### FETAL *RHD* GENOTYPING

By dPCR, fetal *RHD* genotype was correctly identified in 100% (24/24) and 95.5% (21/22) of cases for samples collected in Streck BCTs and EDTA tubes, respectively (Table 3). One EDTA-collected sample (sample 12) produced a false-positive result, since serological analysis revealed the fetus to be *RHD*-negative but dPCR showed clear amplifi-

cation of the *RHD7* target (18 droplets) and minimal amplification of the *RHD5* target (3 droplets) (Fig. 3A). Fig. 3 illustrates the concentrations obtained from both target genes (*RHD5* and *RHD7*) and the reference gene (*AGO1*) for control samples [NTC, *RHD*<sup>+</sup> control, *RHD*<sup>-</sup> control (Fig. 3, A and B); samples collected in EDTA tubes (Fig. 3A); and samples collected in Streck BCTs (Fig. 3B)]. The results show successful amplification of all 3 targets for the *RHD*-positive control sample and show amplification of only the reference *AGO1* gene for the *RHD*-negative control sample, whereas the NTC sample showed no amplification (Fig. 3). In addition to the false-positive result (1/46, 2%), 31 samples were correctly classified as *RHD* positive (67%) and 14 samples were correctly classified as *RHD* negative (31%) (Fig. 3).

Optimal samples (collected in Streck BCTs), which expressed cfDNA fractions  $\geq 4\%$ , demonstrated accuracies of 100% and 83% on the qPCR platform for the

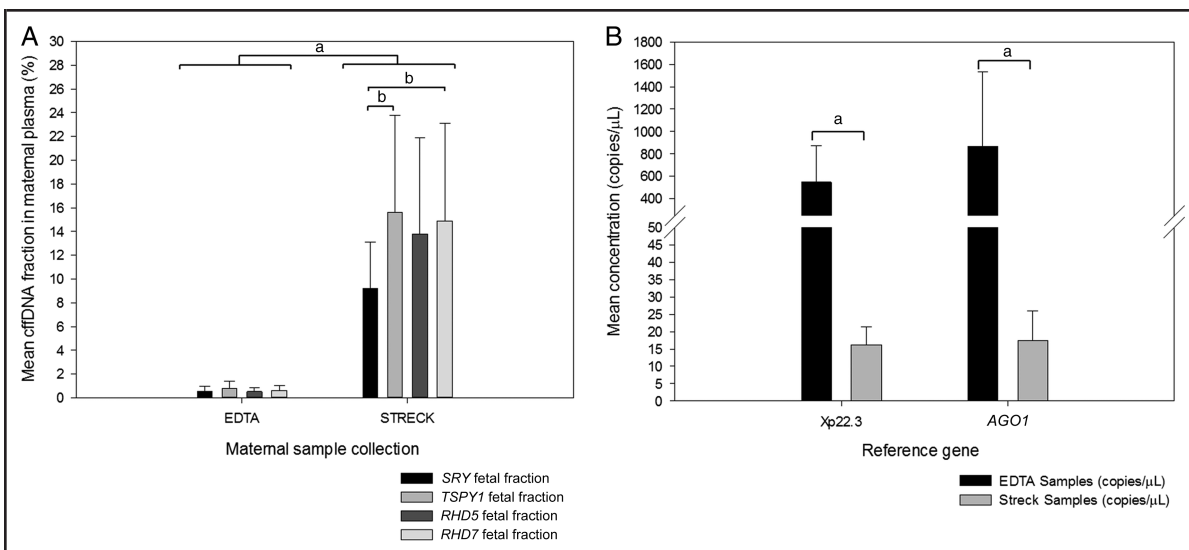


**Fig. 2.** Comparison between maternal samples collected in EDTA tubes and Streck BCTs.

(A), Mean cfDNA fraction in maternal plasma calculated by each target gene (see online Supplemental File 1). The samples collected in Streck BCTs show a significantly higher mean cfDNA fraction compared with samples collected in EDTA tubes for all 4 target regions ( $^aP < 0.001$ ). The cfDNA fractions on the basis of the *RHD7* and *TSPY1* target genes are significantly larger than the cfDNA fraction determined by the *SRY* target gene ( $^bP < 0.01$ ). (B), Mean concentration of reference gene regions Xp22.3 and *AGO1* for maternal samples collected in EDTA tubes and Streck BCTs. The mean concentrations of both regions were significantly higher in EDTA tube samples than in Streck BCTs ( $^aP < 0.001$ ). There was no significant difference between mean concentrations of Xp22.3 and *AGO1* within each sample collection method.

*RHD7* and *RHD5* target assays, respectively. Four samples (16.6%) were classified as inconclusive because qPCR did not detect the *RHD5* target but did show acceptable amplification of the *RHD7* target ( $<45$  Cq) (Table 3). The qPCR platform was unable to detect both *RHD*-specific markers (*RHD7* and *RHD5*) in the suboptimal samples ( $<2\%$  cfDNA), despite serological and dPCR analysis confirming that 59% (13/22) of these EDTA-collected samples were carrying an *RHD*-positive fetus.

#### SAMPLE COLLECTION: EDTA VS STRECK BCT

The cfDNA fractions and concentrations of reference targets for blood collection methods with EDTA tubes and Streck BCTs were compared by use of dPCR results. Fig. 2A shows the mean cfDNA fraction in maternal plasma for all 4 target regions (*SRY*, *TSPY1*, *RHD5*, and *RHD7*) for both collection methods. The samples collected in Streck BCTs showed significantly larger mean cfDNA fractions (9%–16%) for all target regions than those collected in EDTA (0.5%–1%) ( $P < 0.001$ ). The mean cfDNA fractions generated by the EDTA-collected samples demonstrated no significant differences between all 4 targets ( $P > 1$ ). However, the cfDNA fraction calculated on the basis of the *SRY* target was significantly smaller than the *TSPY1* and *RHD7* cfDNA fractions ( $P < 0.01$ ).

Although the concentration of each reference gene (Xp22.3 and *AGO1*) (Fig. 2B) is a combination of maternal and fetal cfDNA, it is predominantly maternal in origin (90%–95%). Samples collected in Streck BCTs showed similar mean concentrations for Xp22.3 and *AGO1* reference genes (16.18 and 17.39 copies/ $\mu$ L, respectively;  $P > 0.1$ ) (Fig. 2B). The concentrations of both reference targets (Xp22.3 and *AGO1*) were  $>40$ -fold higher for maternal samples collected in EDTA tubes compared with Streck BCTs (mean concentrations 548.04 and 869.25 copies/ $\mu$ L, respectively), suggesting maternal leukocyte degradation (Fig. 2B). The 2D amplification plots (see online Supplemental File 3) also showed a significantly higher number of reference (HEX-labeled) droplets for maternal samples collected in EDTA tubes compared with maternal samples collected in Streck BCTs ( $P < 0.001$ ). The fetal concentration determined from *RHD5* and *RHD7* amplification was similar for samples collected in both EDTA and Streck BCTs ( $P > 0.1$ ): 0.9–4.2 copies/ $\mu$ L and 0.3–3.7 copies/ $\mu$ L, respectively (Fig. 3).

#### Discussion

Noninvasive fetal *RHD* genotyping by use of qPCR analysis has shown high levels of accuracy for optimal samples (mean 97.4%) and is currently implemented in the Neth-

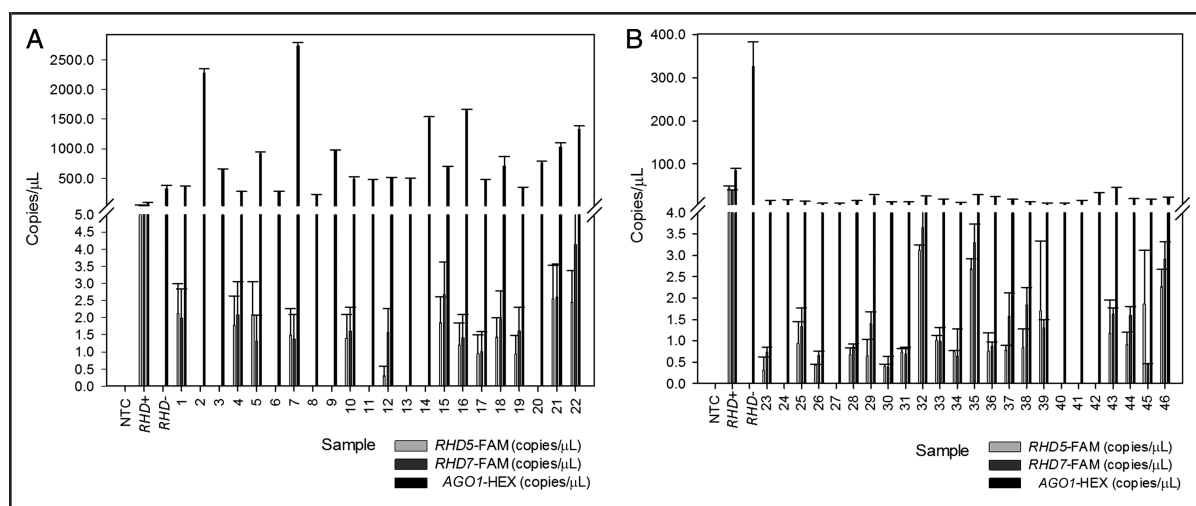


**Fig. 3.** Fetal *RHD* genotyping results from maternal plasma samples.

The concentration (copies per microliter) (plus SD) was identified for both target regions (*RHD5* and *RHD7*) and the reference region (*AGO1*). The presence or absence of the target regions were used to determine fetal status (*RHD*<sup>+</sup> or *RHD*<sup>-</sup>, respectively). (A), Maternal samples collected in EDTA tubes (n = 22). (B), Maternal samples collected in Streck BCTs (n = 24). The same controls are represented in both graphs. The control nonmaternal cfDNA *RHD*-positive sample (399X) exhibited ratios of 0.51 and 0.47 for *RHD5/AGO1* and *RHD7/AGO1*, respectively.

erlands and Denmark for targeted administration of prophylactic anti-D (4, 10, 11, 17, 18, 25). In a recent population-based cohort study, mass-throughput fetal *RHD* genotyping was sufficient from the end of the first trimester with qPCR (26). However, for samples taken at <11 weeks' gestation, 16 of 865 samples (1.8%) were incorrectly classified as *RHD* negative. Fetal *RHD* genotyping was also inconclusive for 393 of 4913 samples tested (8%) (26). Previous studies have identified that low cfDNA fractions can lead to false-negative results by qPCR, limiting the sensitivity of this approach (27–29). The oligonucleotides used in this study for *RHD* genotyping are identical to the sequences used in Finning et al. (24), but for unknown reasons worked less effectively for our qPCR assay. However, our results clearly indicate that for suboptimal samples, the single-copy targets (*SRY*, *RHD5*, and *RHD7*) were not detectable by qPCR but achieved 100% sensitivity (95% CI) on the dPCR platform.

Because of the gestational ages of these samples, cfDNA is expected to be >5% (1). However, results show maternal DNA degradation for EDTA-collected samples, since the number of positive droplets for references (Xp22.3 and *AGO1*) was significantly higher compared with samples collected in Streck BCTs ( $P < 0.001$ ) (Fig. 2B; also see online Supplemental File 3). These novel dPCR data indicate that qPCR false-negative results were not caused by low absolute cfDNA concentrations, since they are similar to those expressed by optimal samples (Fig. 2B), but are instead a result of low relative concentrations of cfDNA. The assay used is

highly specific, and theoretically, nonspecific amplification should not occur, but because *RHD5* and *RHD7* probes have 96.5% and 100% consensus, respectively, with the *RHCE* gene, it is possible that the probes are binding to the abundant maternal *RHCE*, depleting probe availability for fetal-specific *RHD* targets. Nonetheless, when the cfDNA copy number is very low, false-negative results are more likely, particularly for the detection of fetal single nucleotide polymorphisms for rare mutation detection. qPCR is more susceptible to nonspecific amplification of the maternal allele, and dPCR maybe more powerful in the detection of alleles associated with conditions such as  $\beta$ -thalassemia and cystic fibrosis.

The amount of fetal DNA fraction has been shown to increase in positive correlation with time before processing (30). To preserve large cfDNA fractions, it is recommended that samples collected in EDTA tubes should be extracted within 6 h and kept at 4 °C before plasma extraction. Although maternal samples collected in EDTA were processed within 6 h, all transportation of these samples between sites was carried out at room temperature for logistical reasons. The chosen references (Xp22.3 and *AGO1*) were based on assumptions that cfDNA is fragmented equally across the genome, and dPCR analysis showed equal abundance of reference to target loci for nonmaternal cfDNA samples, since a ratio of approximately 1 was expressed (see online Supplemental File 3). This is important, because a previous study has shown unequal representation of reference targets [e.g., *TERT* (telomerase reverse transcriptase) and *ERV3-1*



---

(endogenous retrovirus group 3, member 1)] in cfDNA compared to genomic DNA (31). In addition, the *RHD*<sup>+</sup> control used in Fig. 3 shows a ratio of approximately 0.5, illustrating that the control sample is hemizygous for the *RHD* gene, whereas homozygous *RHD* samples tested with the same assay expressed ratios close to 1 (data not shown).

dPCR data were used to determine the cfDNA fraction, since they are expected to demonstrate higher levels of sensitivity and improved accuracy for low template copy numbers (32). Poisson statistics were incorporated to determine the copy number, since some droplets may have contained multiple targets (33). The proportion of fetal target DNA was relatively low [mean number of droplets 12 084, mean number of *RHD* molecules 20.8 and 17.8 for samples from EDTA tubes and Streck BCTs, respectively (data not shown)]. However, increases in the mean number of copies per partition for the references (e.g., *AGO1*), which is shown in EDTA maternal samples [e.g., 0.62 mean copies per partition (sample 15)], result in higher proportions of dual-positive droplets compared to samples collected in Streck BCTs [e.g., 0.023 mean copies per partition (sample 32)] (see online Supplemental File 3). Since the release of the QX100™ ddPCR system in 2012, various studies have been conducted to find out whether its application can enhance or replace current qPCR-based approaches (19, 20, 33–36). Some studies have shown equal sensitivity for dPCR and qPCR, but with improved levels of precision and day-to-day reproducibility with dPCR approaches (35, 36). However, several studies have shown considerable improvements of sensitivity and specificity on the dPCR platform compared with qPCR approaches (19, 20, 33, 34). The current study also illustrates significant improvements in sensitivity for the dPCR platform, particularly for samples expressing low relative proportions of fetal DNA (<2%) (Table 3).

On the basis of the qPCR data, 54% of patients had false-negative results and in a clinical setting would not have received required anti-D, risking alloimmunization and subsequent HDFN. However, dPCR results revealed no false-negative results, and routine administration of this assay would have prevented unnecessary anti-D administration in 31.1% of patients in our study cohort. Previous studies have also reported false-positive or inconclusive results when the fetus expresses D-variants (4, 20, 24). False-positive results do not pose a risk of alloimmunization but result in unnecessary anti-D administration. If applied to a clinical setting, anti-D would have been administered to the 4 women with inconclusive results found with qPCR for samples collected in Streck BCTs, which in these cases was necessary since the fetuses were *RHD*<sup>+</sup>. On the basis of the dPCR data, only 1

woman (2%) would have received anti-D that was not required. The oligonucleotide primers used in this study for the *RHD* targets were as described by Finning et al. (24). These primers should distinguish between *RHD*-positive and *RHD*Ψ/DVI (type 1–4) fetal genotypes by amplifying exon 7 but not exon 5 for the variant samples. However, constraints on ethics approval prevented follow-up confirmation of the inconclusive result (sample 37) via analysis of fetal cord DNA to determine the true *RHD* genotype of this fetus. Both dPCR and qPCR will express similar levels of false-positive results owing to D-variants, but our results show that dPCR has the potential to eliminate or reduce the occurrence of false-negative results, especially in cases in which low cfDNA fractions (<2%) are expressed.

In conclusion, this study illustrates that dPCR shows improved accuracy for fetal sex determination and *RHD* genotyping compared with qPCR, particularly for suboptimal samples that express low relative proportions of fetal DNA (<2%). Despite the accuracy of qPCR being relatively high in most large-scale validation studies (3, 9, 24), false-negative results are still present and have been attributed to maternal DNA degradation. Further large-scale studies are now necessary to determine the accuracy of dPCR for fetal *RHD* genotyping, but these results illustrate that dPCR has the potential to provide a safer and more reliable noninvasive diagnostic test for the targeted administration of prophylaxis anti-D.

---

**Author Contributions:** All authors confirmed they have contributed to the intellectual content of this paper and have met the following 3 requirements: (a) significant contributions to the conception and design, acquisition of data, or analysis and interpretation of data; (b) drafting or revising the article for intellectual content; and (c) final approval of the published article.

**Authors' Disclosures or Potential Conflicts of Interest:** Upon manuscript submission, all authors completed the author disclosure form. Disclosures and/or potential conflicts of interest:

**Employment or Leadership:** None declared.

**Consultant or Advisory Role:** N.D. Avent, Grifols AG.

**Stock Ownership:** None declared.

**Honoraria:** None declared.

**Research Funding:** K.A. Sillence, bursary from Plymouth University.

**Expert Testimony:** None declared.

**Patents:** None declared.

**Role of Sponsor:** The funding organizations played a direct role in the design of study, choice of enrolled patients, review and interpretation of data, and preparation or approval of manuscript.

**Acknowledgments:** Special thanks to all the pregnant women who took part in this study. We also thank all the staff at Plymouth Hospitals NHS Trust for their advice and support throughout sample collection.

## References

- Lo YM, Corbetta N, Chamberlain PF, Rai V, Sargent IL, Redman CW, et al. Presence of fetal DNA in maternal plasma and serum. *Lancet* 1997;350:485-7.
- Rijnders RJ, Christiaens GC, Bossers B, van der Smagt JJ, van der Schoot CE, de Haas M. Clinical applications of cell-free fetal DNA from maternal plasma. *Obstet Gynecol* 2004;103:157-64.
- Avent ND, Chitty LS. Non-invasive diagnosis of fetal sex; utilisation of free fetal DNA in maternal plasma and ultrasound. *Prenat Diagn* 2006;26:598-603.
- De Haas M, Van der Ploeg C, Scheffer P, Verlinden D, Hirschberg H, Abbink F, et al. A nation-wide fetal RHD screening programme for targeted antenatal and post-natal anti-D. *ISBT Sci Ser* 2012;7:164-7.
- Avent ND. Prenatal testing for hemolytic disease of the newborn and fetal neonatal alloimmune thrombocytopenia: current status. *Expert Rev Hematol* 2014;7:741-5.
- Lewis C, Hill M, Skirton H, Chitty L. Non-invasive prenatal diagnosis for fetal sex determination: benefits and disadvantages from the service users' perspective. *Eur J Hum Genet* 2012;20:1127-33.
- New MI, Tong YK, Yuen T, Jiang P, Pina C, Chan KA, et al. Noninvasive prenatal diagnosis of congenital adrenal hyperplasia using cell-free fetal DNA in maternal plasma. *J Clin Endocrinol Metab* 2014;99:E1022-30.
- Agarwal A, Sayres LC, Cho MK, Cook-Deegan R, Chandrasekharan S. Commercial landscape of noninvasive prenatal testing in the United States. *Prenatal diagnosis* 2013;33:521-31.
- Avent ND. RHD genotyping from maternal plasma: guidelines and technical challenges. *Methods Mol Biol* 2008;444:185-201.
- Wagner FF, Flegel WA. RHD gene deletion occurred in the Rhesus box. *Blood* 2000;95:3662-8.
- Daniels G, Faas B, Green C, Smart E, Maaskant-van Wijk P, Avent N, et al. The VS and V blood group polymorphisms in Africans: a serologic and molecular analysis. *Transfusion* 1998;38:951-8.
- Sillence KA, Madgett TE, Roberts LA, Overton TG, Avent ND. Non-invasive screening tools for Down's syndrome: a review. *Diagnostics* 2013;3:291-314.
- Van der Schoot C, Soussan AA, Koelewijn J, Bonsel G, Paget-Christiaens L, De Haas M. Non-invasive antenatal RHD typing. *Transfus Clin Biol* 2006;13:53-7.
- Gautier E, Benachi A, Giovangrandi Y, Ernault P, Olivi M, Gaillon T, et al. Fetal RhD genotyping by maternal serum analysis: a two-year experience. *Am J Obstet Gynecol* 2005;192:666-9.
- Bowman JM. Hemolytic disease of the newborn. *Vox Sang* 1996;70:62-7.
- Kumar S, Regan F. Management of pregnancies with RhD alloimmunisation. *BMJ* 2005;330:1255-8.
- Rouillac-Le Scieillour C, Puillandre P, Gillot R, Baulard C, Métal S, Le Van Kim C, et al. Large-scale pre-diagnosis study of fetal RHD genotyping by PCR on plasma DNA from RhD-negative pregnant women. *Mol Diagn* 2004;8:23-31.
- Banch Clausen F, Steffensen R, Christiansen M, Rudby M, Jakobsen M, Jakobsen T, et al. Routine noninvasive prenatal screening for fetal RHD in plasma of RhD-negative pregnant women: 2 years of screening experience from Denmark. *Prenat Diagn* 2014;34:1000-5.
- Strain MC, Lada SM, Luong T, Rought SE, Gianella S, Terry VH, et al. Highly precise measurement of HIV DNA by droplet digital PCR. *PLoS one* 2013;8:e55943.
- Miotke L, Lau BT, Rumma RT, Ji HP. High sensitivity detection and quantitation of DNA copy number and single nucleotide variants with single color droplet digital PCR. *Anal Chem* 2014;86:2618-24.
- Wong D, Moturi S, Angkatchai V, Mueller R, DeSantis G, van den Boom D, et al. Optimizing blood collection, transport and storage conditions for cell free DNA increases access to prenatal testing. *Clin Biochem* 2013;46:1099-104.
- Lo Y, Tein MS, Lau TK, Haines CJ, Leung TN, Poon PM, et al. Quantitative analysis of fetal DNA in maternal plasma and serum: implications for noninvasive prenatal diagnosis. *Am J Hum Genet* 1998;62:768-75.
- Fan HC, Blumenfeld YJ, El-Sayed YY, Chueh J, Quake SR. Microfluidic digital PCR enables rapid prenatal diagnosis of fetal aneuploidy. *Am J Obstet Gynecol* 2009;200:543.e1-7.
- Finning K, Martin P, Summers J, Massey E, Poole G, Daniels G. Effect of high throughput RHD typing of fetal DNA in maternal plasma on use of anti-RhD immunoglobulin in RhD negative pregnant women: prospective feasibility study. *BMJ* 2008;336:816-8.
- Brojer E, Zupanska B, Guz K, Orzinska A, Kalinska A. Noninvasive determination of fetal RHD status by examination of cell-free DNA in maternal plasma. *Transfusion* 2005;45:1473-80.
- Chitty LS, Finning K, Wade A, Soothill P, Martin B, Oxenford K, et al. Diagnostic accuracy of routine antenatal determination of fetal RHD status across gestation: population based cohort study. *BMJ* 2014;349:g5243.
- Müller SP, Bartels I, Stein W, Emmons G, Gutensohn K, Köhler M, et al. The determination of the fetal D status from maternal plasma for decision making on Rh prophylaxis is feasible. *Transfusion* 2008;48:2292-301.
- Lo YD, Lau TK, Chan LY, Leung TN, Chang AM. Quantitative analysis of the bidirectional fetomaternal transfer of nucleated cells and plasma DNA. *Clin Chem* 2000;46:1301-9.
- Zhong XY, Bürk MR, Troeger C, Kang A, Holzgreve W, Hahn S. Fluctuation of maternal and fetal free extracellular circulatory DNA in maternal plasma. *Obstet Gynecol* 2000;96:991-6.
- Norton SE, Luna KK, Lechner JM, Qin J, Fernando MR. A new blood collection device minimizes cellular DNA release during sample storage and shipping when compared to a standard device. *J Clin Lab Anal* 2013;27:305-11.
- Devonshire AS, Whale AS, Gutteridge A, Jones G, Cowen S, Foy CA, Huggett JF. Towards standardisation of cell-free DNA measurement in plasma: controls for extraction efficiency, fragment size bias and quantification. *Anal Bioanal Chem* 2014;406:6499-512.
- Jones M, Williams J, Gärtner K, Phillips R, Hurst J, Frater J. Low copy target detection by Droplet Digital PCR through application of a novel open access bioinformatic pipeline, 'definetherain.' *J Virol Methods* 2014;202:46-53.
- Pinheiro LB, Coleman VA, Hindson CM, Herrmann J, Hindson BJ, Bhat S, et al. Evaluation of a droplet digital polymerase chain reaction format for DNA copy number quantification. *Anal Chem* 2011;84:1003-11.
- Kim TG, Jeong S-Y, Cho K-S. Comparison of droplet digital PCR and quantitative real-time PCR in mcrA-based methanogen community analysis. *Biotechnol Rep* 2014;4:1-4.
- Hayden R, Gu Z, Ingersoll J, Abdul-Ali D, Shi L, Pounds S, et al. Comparison of droplet digital PCR to real-time PCR for quantitative detection of cytomegalovirus. *J Clin Microbiol* 2013;51:540-6.
- Hindson CM, Chevillet JR, Briggs HA, Gallichotte EN, Ruf IK, Hindson BJ, et al. Absolute quantification by droplet digital PCR versus analog real-time PCR. *Nat Methods* 2013;10:1003-5.
- Flegel WA. The genetics of the Rhesus blood group system. *Blood Transfus* 2007;5:50.
- Barrett AN, McDonnell TCR, Chan KCA, Chitty LS. Digital PCR analysis of maternal plasma for noninvasive detection of sickle cell anemia. *Clin Chem* 2012;58:1026-32.

*Review*

## Non-Invasive Screening Tools for Down Syndrome: A Review

Kelly A. Sillence, Tracey E. Madgett, Llinos A. Roberts, Timothy G. Overton and  
Neil D. Avent \*

School of Biomedical and Biological Sciences, Plymouth University Peninsula School of Medicine  
and Dentistry, Plymouth University, Plymouth, PL4 8AA, UK;

E-Mails: kelly.sillence@plymouth.ac.uk (K.A.S.); tracey.madgett@plymouth.ac.uk (T.E.M.);  
llinos.roberts@plymouth.ac.uk (L.A.R.); timoverton@me.com (T.G.O.)

\* Author to whom correspondence should be addressed; E-Mail: neil.avent@plymouth.ac.uk;  
Tel.: +44-17-5258-4884.

*Received: 10 April 2013; in revised form: 14 May 2013 / Accepted: 16 May 2013 /*

*Published:*

---

**Abstract:** Down syndrome (DS) is the most common genetic cause of developmental delay with an incidence of 1 in 800 live births, and is the predominant reason why women choose to undergo invasive prenatal diagnosis. However, as invasive tests are associated with around a 1% risk of miscarriage new non-invasive tests have been long sought after. Recently, the most promising approach for non-invasive prenatal diagnosis (NIPD) has been provided by the introduction of next generation sequencing (NGS) technologies. The clinical application of NIPD for DS detection is not yet applicable, as large scale validation studies in low-risk pregnancies, that express the same levels of sensitivity as the existing invasive techniques, need to be completed. Currently, prenatal screening is still the first line test for the detection of fetal aneuploidy. Screening cannot diagnose DS, but developing a more advanced screening program can help to improve detection rates, and therefore reduce the number of women offered invasive tests. This article describes how the prenatal screening program has developed since the introduction of maternal age as the original “screening” test, and subsequently discusses recent advances in detecting new screening markers with reference to both proteomic and bioinformatic techniques.

**Keywords:** screening; Down syndrome; non-invasive; biomarkers; sonographic markers; next-generation-sequencing

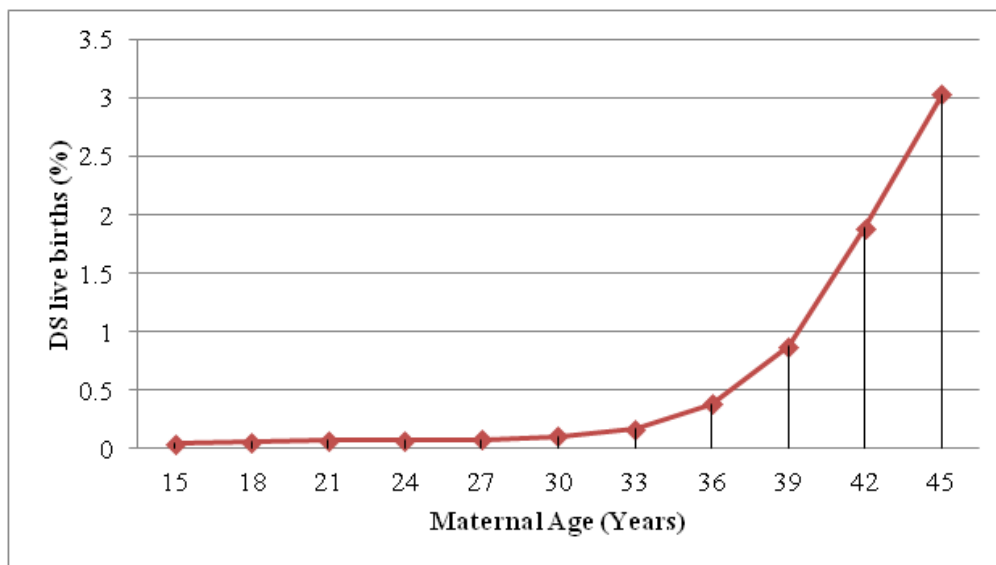
---



## 1. Introduction

Down syndrome (DS) is the most common chromosomal aneuploidy and is the leading genetic cause of developmental delay. The overall incidence of DS is around 1 in 800 live births [1,2], but the risk of fetal trisomy is directly related to maternal age, increasing gradually up to age 33 and subsequently increasing exponentially (Figure 1). Women in their late 40s have an incidence rate of around 1 in 32 live births [3]. Between 1989 and 2008, the percentage of women conceiving aged 35 years and over increased from 9% to 20%, respectively, which led to a 71% rise in the number of DS pregnancies [2,4]. Despite an expected 1.32 fold increase in the number of DS live births as a result of this, the reported rate in England and Wales fell by 1% from 736 live births in 1989 to 750 live births in 2008 [2,5]. In the UK the National Down Syndrome Cytogenetic Register (NDSCR) indicate that without improved screening tools between 1989 and 2008, the continuous rise in maternal age would have caused a 48% increase in live births with DS [3]. Although there are clear ethical issues surrounding prenatal screening, with the majority of women terminating affected pregnancies the evidence provided clearly illustrates the effectiveness of screening for DS.

**Figure 1.** The estimated risk of Down syndrome (DS) according to maternal age (adapted from [3]).



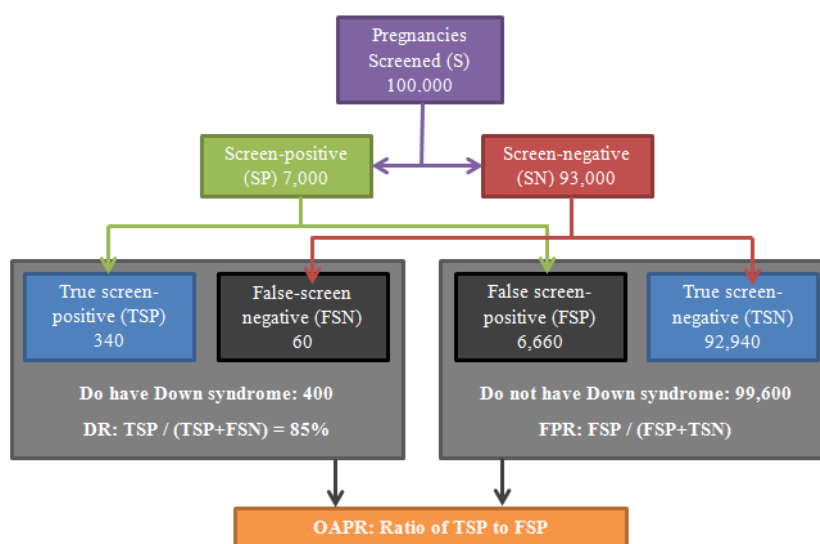
In addition to advanced maternal age, other risk factors include previous family history and gestational age, as 43% of DS pregnancies miscarry between 10 weeks and term [6,7]. The gradual introduction of various biochemical and sonographic markers since the early 1980s, has greatly improved the sensitivity of current screening programs to around 95% [6]. Women with a high risk following screening are offered invasive procedures such as amniocentesis or chorionic villus sampling (CVS) for a definitive diagnosis. However, these invasive procedures are associated with around a 1% risk of iatrogenic fetal loss [1,8,9]. Advances in screening tools could further improve the specificity and sensitivity of current screening methods, thus reducing the number of women offered invasive diagnostic tests. In spite of the huge recent advances in non-invasive prenatal diagnostics using next generation sequencing (NGS) [1], screening will remain an essential first line test in the clinical management of aneuploid pregnancies. This review will outline the development of screening

over the last four decades up to present day and discuss possible new screening tools that could potentially be used in a clinical setting.

## 2. Definitions

There are various measurements that can be used to determine the success of a screening program including; the detection rate (DR), the false positive rate (FPR), screen positive rate (SPR), and the odds of a positive result (OAPR). The DR (sensitivity) of the test identifies the proportion of affected cases successfully identified by the screening program, for example a DR of 90% means that the screening test will successfully detect 9 out of 10 cases of DS. However, high sensitivity alone is not sufficient for DS detection. The test must also display a low FPR, which is defined as the rate of occurrence of positive results in non-affected cases. More recently, the SPR has been used as an alternative to the FPR, The screen positive rate identifies those with a result above the cut off risk (for example 1 in 150) and will include both true positives and false positives [5]. It is important that the FPR/SPR is kept as low as possible so to minimize the number of women offered invasive procedures which will in turn reduce the number of miscarriages of healthy fetuses. The likelihood of a woman having a DS pregnancy confirmed by CVS or amniocentesis if her screen risk is high is known as the OAPR. If a screening test has a high OAPR, more affected pregnancies will be successfully diagnosed for every miscarriage caused by invasive testing [10,11]. Both the DR and the FPR/SPR are influenced by the risk threshold above which invasive testing is offered. In an ideal screening test the DR would be high (>90%) and the SPR would be low (<2%). However, increasing the threshold (for example to 1 in 100) would cause both the DR and the SPR to decline, and decreasing the threshold (for example to 1 in 300) would cause both the DR and SPR to increase [5].

**Figure 2.** The screening process, potential outcomes and measures of accuracy. Detection rate (DR): Proportion of affected cases successfully identified by the screening test.  $TSP / (TSP + FSN) = 85\%$ . False positive rate (FPR): Proportion of positive results in non-affected cases identified by the screening test.  $FSP / (FSP + TSN) = 6.7\%$  (adapted from [10,11]). [get permission from 11. http://www.down-syndrome.org/editorials/2087/?page=1](http://www.down-syndrome.org/editorials/2087/?page=1)



Since the introduction of screening for DS the DR has greatly improved parallel to a decrease in the SPR [10]. Therefore more affected cases of DS are being detected via screening and fewer non-affected cases are being identified as high risk. This has led to an overall increase in OAPR and consequently a decline in the number of invasive tests offered to women. Although there is still room for improvement, Figure 2 illustrates the possible outcomes and measures of accuracy of the screening process [11].

### 3. Screening: Past to Present

#### 3.1. Historical Overview

In the early 1980s, maternal age was effectively the only screening tool available for detection of DS and invasive diagnostic tests were offered to all women aged 35 years and above. These tests were only offered to women younger than 35 years if there was known family history of the disorder [12]. However this approach was inappropriate and unsustainable for numerous reasons. Firstly, maternal age alone is not an effective screening test as it has a DR of less than 35%, meaning that most fetuses with DS were undetected and many women with unaffected fetuses were subjected to unnecessary invasive testing [5,13]. Secondly, as the average maternal age was beginning to rise, resources to perform invasive testing for all these women were unavailable [5].

To improve the sensitivity of screening for DS, sonographic and biochemical screening tests were developed that could be combined with maternal age to increase the accuracy of risk assessment. The initial opportunity to improve screening arose in 1984, when several studies identified an association between low alpha-fetoprotein (AFP) levels (around a 25% reduction) in maternal serum and fetal aneuploidy [14–16]. AFP is a large serum glycoprotein produced by both the yolk sac and the fetal liver, and is considered to function in a similar way as albumin in adults [17]. DiMaio *et al.* identified that using a cut-off for risk at which 5% of women under 35 are offered invasive testing, around 25–30% of pregnancies in which the fetus has DS will be detected using AFP serum biomarker alone [18]. The identification of this marker for DS detection was a serendipitous scientific discovery, initially raised AFP levels were used to identify pregnancies that were potentially affected by fetal neural tube defects particularly anencephaly, it was only during this cohort that the link between low AFP levels and an increased incidence of DS was identified. Now AFP is used clinically worldwide for screening of DS after the first trimester as one of the biochemical serum markers used in the quadruple test.

Since then, various pregnancy-associated maternal serum markers for DS have been evaluated. Key markers that have been incorporated into the screening program include human chorionic gonadotropin (hCG), estriol, inhibin A and pregnancy associated plasma protein A (PAPP-A). hCG is a hormone initially produced by the embryo and later by the syncytiotrophoblast. Its function is to enable the secretion of progesterone, which promotes the maintenance of the corpus luteum [19]. During very early pregnancy hCG levels increase rapidly until 12 weeks gestation, at which point the hCG levels off, normal hCG values during the second trimester range between 4,060 and 165,400 mIU/mL. In 1987, Bogart *et al.* identified an association between an increase in serum levels of hCG and DS pregnancies (approximately double the normal values), which led to the introduction of the second trimester double

test a year later in the UK [20]. This test measured maternal serum concentrations of both AFP and hCG between 15 and 20 weeks gestation alongside maternal age. With a risk threshold of 1 in 250, the DR was approximately 60% with a SPR of 5% [5].

Shortly after the double test was established in the UK, studies reported a 25% reduction of unconjugated estriol in DS pregnancies (normal value at 15 weeks gestation is around 4nmol/L) [21]. The addition of estriol as a third marker was the basis for the “Triple test” [22,23]. In the early 1990s the triple test was adjusted by the replacement of hCG with the free beta subunit of hCG (f $\beta$ -hCG) as it is this which is more markedly increased in DS pregnancies [24]. Although the triple test was associated with higher sensitivity (67% DR), it was not considered to be a great improvement on the double test, as the SPR was not lowered and the costs of screening were increased [25]. However, in the early 1990s, inhibin A was found to be significantly elevated in DS pregnancies, leading to the generation of the quadruple test with an improved DR of 75% [26]. The double, triple and quadruple test all offer a greater DR than maternal age alone but can only be performed during the second trimester.

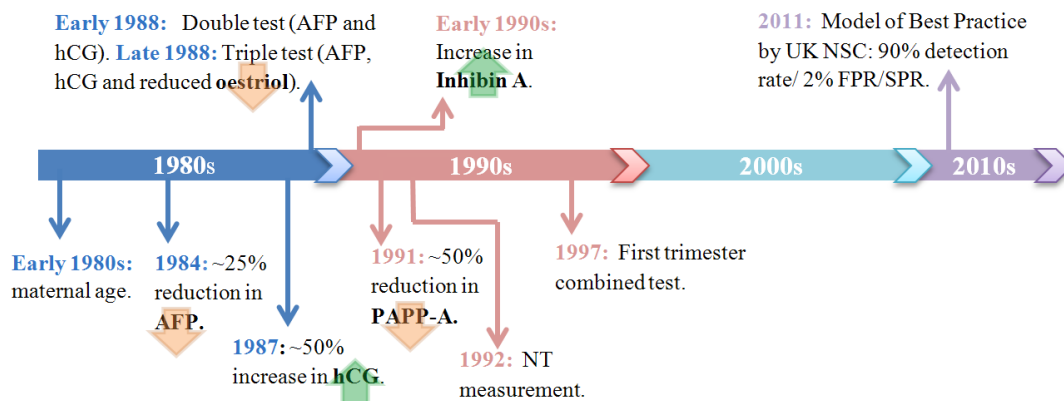
In 1991 maternal serum associated plasma protein-A (PAPP-A) was shown to be reduced by around 50% in DS pregnancies and was detectable from as early as 8 weeks gestation [22,27]. Between 17 and 19 weeks gestation maternal serum PAPP-A levels in DS affected pregnancies returned to those values observed with unaffected pregnancies [28,29]. Throughout the 1990s the emphasis was to perform screening in the first trimester, allowing parents to decide at an earlier stage in the pregnancy whether to undergo invasive testing.

In addition to these biochemical markers, the risk of DS pregnancies can also be evaluated by the identification of physical markers using sonographic imaging. In 1992 the ultrasound screening test of nuchal translucency (NT) was developed by Nicolaides *et al.* [30], the ultrasound NT is the sonographic appearance of a collection of fluid under the skin behind the fetal neck in the first trimester between 11 and 13 weeks gestation. The maturation of the fetal lymphatics often occurs later during the second trimester in fetuses with DS and other chromosomal abnormalities, which causes an increase in fluid collection.

During the early 1990s a number of reports identified an association between DS and increased NT. In 1994, Nicolaides *et al.* reported that an NT value  $\geq 2.5$  mm was seen in 84% of fetuses with DS and 4.5% of normal fetuses in a study involving 1,273 pregnancies [31]. However, it is important that when measuring the NT thickness care is taken when aligning the calipers, as an error of 0.4 mm can significantly alter the risk. For example, at 12 weeks gestation the risk of having a DS fetus when NT values of 2.6 mm and 3.0 mm are recorded is quoted as 1 in 1,394 and 1 in 563, respectively [32]. When maternal age alone was used as a screening tool, only two out of 11 cases of DS were detected, however following the introduction of NT measurement, three out of four cases of DS were detected by karyotyping because of an increased NT, this illustrates then when obtained by well-trained professionals, NT measurement is a highly reproducible screening tool [33,34].

The combination of NT, maternal age and early detectable serum biomarkers (f $\beta$ -hCG and PAPP-A) was referred to as the first trimester combined test [35]. Studies have identified that with the first trimester combined test around 85–90% of all DS cases could be detected with a 5% FPR [36–39]. Figure 3 illustrates a short summary of key DS screening developments incorporated in a clinical setting from the early 1980s to date.

**Figure 3.** Timeline summarising the key developments in UK DS screening, from the early 1980s when maternal age was effectively the only screening tool used up to the identification of the Model of Best Practice identified by the UK National Screening Committee (NSC) in 2011.



### 3.2. Current Methods

In 2008 the UK National Screening Committee's (UK NSC) Model of Best Practice for DS screening set a target for 2010/11 to achieve a DR of 90% and a FPR/SPR of 2%, however this is yet to be achieved (Figure 3). The test currently closest to achieving standards set by the MoBP is the first trimester combined screening test (DR 85–90% and FPR 5%). However, women who miss first trimester screening can only be offered second trimester quadruple testing, which has a slightly lower sensitivity (75% DR) and a higher FPR (6.9%) than the first-trimester combined test [5].

Some hospitals also offer the integrated test [40], which is performed in two stages. Firstly the combined test is performed followed by second-trimester biochemistry (quad test) a few weeks later [41]. This test is used to help reduce the FPR, as women that are high risk following the combined test may become a low risk following the result of the integrated test. In 2013 the International Society for Prenatal Diagnosis (ISPD) identified that integrated screening can be offered when CVS is not available [41]. However, the UK NSC does not recommend integrated testing for two fundamental reasons. Firstly a woman who is considered to be high risk following the combined test may not return for her quad test and therefore may be lost within the system without having been counseled properly and secondly, there are higher cost and service implications associated with combining the two screening tests [42]. A possible compromise to this problem is Contingency screening, which allows pregnant women with a significantly high risk following first-trimester screening to be offered invasive diagnostic tests immediately. In contrast, pregnant women that indicate extremely low risk after first trimester screening are reassured. It is only those women with an intermediate risk value (between 1 in 50 and 1 in 1,000) that are offered further testing with other ultrasound markers including nasal bones, tricuspid regurgitation and ductus venous Doppler to further refine the risk before offering invasive testing. This approach results in a DR of 90% for a FPR of 3% [37]. Currently, the UK NSC has also not supported the Contingency screening test despite improvements to DR and FPR/SPR, because of the complexity associated with the technique and the implications for service reconfiguration [5].

In the United States, the Society for Maternal-Fetal Medicine (SMFM) completed a survey in 2007 to determine changes in screening and numbers of invasive diagnostic procedures performed since 2001. The results showed that over this time frame the evolution and increased uptake of DS screening between 2001 and 2007 led to a 20% reduction in invasive diagnostic procedures [43]. The ISPD recognizes that the use of maternal age alone to assess fetal DS risk in pregnant women is insufficient and has stated that a combination of ultrasound NT measurement and serum markers in the first trimester should be available to all women who desire early risk assessment. For women that first attend their prenatal care after 13 weeks 6 days gestation, the ISPD recommends that the quadruple test should be provided [44].

#### 4. Further Developments

Since the early 1980s enormous progress for DS screening has been made, however further improvements are still required. The problem associated with current screening tests is that 5% or more of screened women need to undergo invasive testing in order to detect 60–80% of fetuses with DS, resulting in large numbers of false screen-positives. In 2008 it was estimated that approximately 400 babies without DS were miscarried following invasive procedures on women with false positive screening results in England and Wales [11]. Here we look at new screening techniques that are being developed that could potentially raise sensitivity of current screening methods (to around 90% DR) and lower the FPR/SPR (to around 2%), allowing more DS cases to be detected and less invasive testing to be offered, thus reducing the number of miscarriages in affected and unaffected pregnancies.

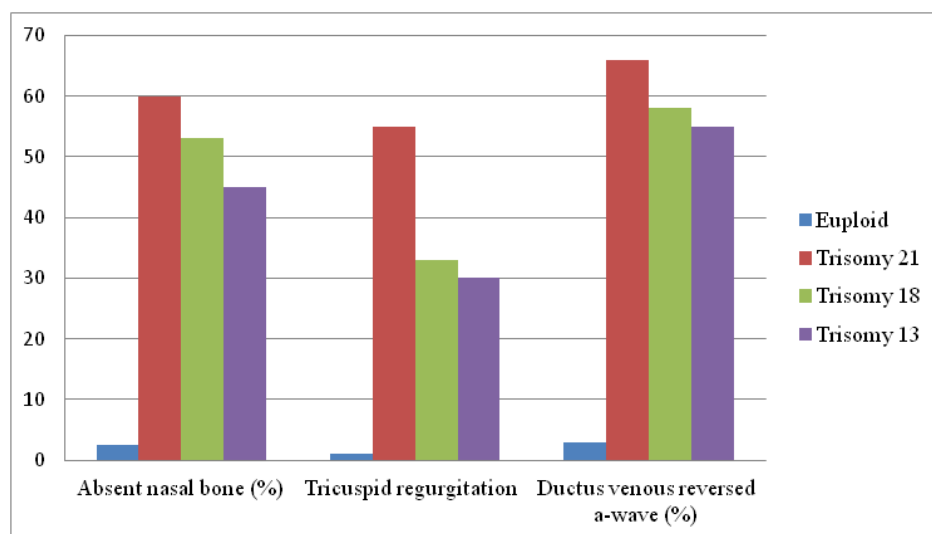
##### 4.1. Sonographic Markers of DS

The role of sonographic markers in the risk assessment of DS has been extensively investigated at the 11–14 week scan and at the time of the mid-trimester fetal anomaly scan. Sonographic markers at the 11–14 week scan include structural abnormalities (exomphalos, cystic hygroma, *etc.*) and more subtle markers such as presence or absence of nasal bones, tricuspid regurgitation and reversed flow in the ductus venosus. Markers at the mid-trimester scan can again be divided into structural anomalies (congenital heart disease, anterior abdominal wall defects, ventriculomegaly, *etc.*) and more subtle markers (choroid plexus cysts, echogenic foci in the heart, increased nuchal fold, *etc.*) traditionally referred to as “soft markers”.

The association between structural anomalies and aneuploidy detected during the first trimester or mid-trimester scan is well established. Fetal exomphalos or Fallot’s tetralogy for example has a significant association with Down’s Syndrome. Detection of structural anomalies at the time of either the 11–14 week scan or the mid-trimester scan should lead to the offer of amniocentesis or CVS. Atrioventricular septal defects (AVSD) are an example of second-trimester structural anomaly. In pregnancies that demonstrate a normal fetal karyotype, the frequency of AVSD is 1 in 10,000 live births, but in DS pregnancies this increases significantly to 2,000 in 10,000 live births (1 in 5 incidence) [45]. However, repeated studies have shown that less than 25% of affected fetuses demonstrate major structural abnormalities, whereas 1 or more “soft markers” could be observed in 50% or more cases [46–48].

The presence or absence of the more subtle features at the 11–14 week scan has been used to refine the risks generated by combined screening. Hypoplasia of the nasal bone is identified in 65% of fetuses with DS between 11 and 14 weeks gestation. However, this marker shows significant inter-racial variation. In Caucasian populations only 1–3% of normal pregnancies have an absent nasal bone during late first-trimester whereas in African populations this increases to around 10% [5]. Incorporating nasal bone assessment into combined screening therefore gives better results in Caucasian populations. Doppler flow examination across the tricuspid valve and in the ductus venosus, have also proved useful markers. In 2009, Kagan *et al.* performed a large scale study involving 20,000 euploid pregnancies which included 122 cases with DS. Reversed flow in the a-wave of the ductus venosus and tricuspid regurgitation were observed in 55% and 60% of DS cases, and in 3.2% and 0.9% of euploid cases, respectively [49]. Incorporation of these markers into a first-trimester combined screening test can increase the DR to 93–96% with a FPR of 2.5% [47]. Figure 4 illustrates the occurrence of these sonographic features in euploid and trisomy foetuses. Checking for these additional markers is not only challenging but also very time-consuming and they have not been adopted into routine clinical practice for widespread screening. They may have a role, however, in a contingent screening model, whereby they are offered to women with an intermediate risk from combined screening who need further information before deciding whether to opt for invasive testing [37].

**Figure 4.** Sonographic features of trisomies 21, 18 and 13 (adapted from [50]).



The significance of the identification of soft markers at the time of the mid-trimester scan has been far more contentious. In the 1990s it was common place for women to be offered invasive procedures when choroid plexus cysts, echogenic foci in the fetal heart, mild renal pelvical dilatation were noted at the time of the 20 week scan. However, a review of the importance of these soft markers in 2001 confirmed their very low sensitivity and specificity for DS with the exception of an increased nuchal fold (the thickness of skin at the back of the fetal neck noted at the time of the mid-trimester scan, not to be confused with nuchal translucency measurements at the time of the first trimester scan) which had a likelihood ratio of 17 for DS [51]. One of the reasons why the importance of soft markers has diminished is because of the widespread adoption of first and second trimester screening over the last 10 years. Poor uptake in screening in the early 1990s meant that the prevalence of DS at the time of the

mid-trimester scan was much greater than in current practice. Screening tests perform better when the prevalence the condition being screened for is high. With the increasing uptake of effective DS screening before 20 weeks the efficacy of screening using soft markers is now much less.

A combination of these factors led to the National Screening Committee in the UK in 2009 recommending that the a prior risk for DS should not be adjusted depending on the presence of absence of single or multiple soft markers (choroid plexus cysts, dilated cisterna magna, echogenic cardiac foci and a 2 vessel cord).

#### 4.2. New Serum Biomarkers

Despite recent advances in ultrasound technology allowing current screening techniques to achieve detection rates >90% with FPRs <5%, improvements to these rates is still a priority for current research in prenatal assessment. In addition to identifying new possible ultrasound markers, novel biochemical screening markers to improve current DRs and FPRs/SPRs have been extensively studied [52–58]. Since the discovery of cell-free fetal DNA (cffDNA) within the maternal circulation many advances have been made in prenatal screening [52]. Recent studies exploring the proteomic profile of maternal serum have identified both non-epigenetic and epigenetic screening markers that could potentially be used as an alternative or in addition to current screening tools to provide greater specificity and lower FPRs/SPRs [53–58]. The SAFE (Special Non-Invasive Advances in Fetal and Neonatal Evaluation) NoE (Network of Excellence) was established by the European Union (EU) in 2004 to implement routine, cost-effective non-invasive prenatal diagnosis (NIPD) and neonatal screening through the formation of long term partnerships worldwide [59,60]. The program played a key role in the standardization of RhD genotyping, and also set out to identify a panel of new, more informative, biomarkers for fetal DS detection. Despite the program ending in March 2009, the long term goals set out by the SAFE NoE are still a key area of research [59].

Non-epigenetic markers, such as maternal serum markers (MSMs) used in the combined screening test, simply show a marked increased or decreased level in affected cases in comparison to normal pregnancies. Novel biochemical markers are currently under investigation but so far there has been no formal large scale evaluation of new markers by the UK NSC to inform policy. Epigenetic approaches have also been examined in an attempt to discriminate the fetal DNA molecules from the high background of maternal DNA fragments (around 90% of total DNA). Difference in DNA methylation between the mother and fetus is currently the most characterized epigenetic modification studied for possible prenatal detection of DS [61,62]. Targeting fetal-specific markers allows for the generated signal to be completely fetal in origin, subsequent chromosomal dosage can then be carried out for trisomy identification. Table 1 illustrates various studies over the past few years that have published results on potential new biomarkers (both non-epigenetic and epigenetic) that could be used to improve the sensitivity of current screening programs. For both PIGF and ADAM12 (Table 1) detection needs to occur prior to 10 weeks gestation, as they are both almost non-existent by this time. Though it would be ideal to screen for DS this early in pregnancy, these tests are fairly unpractical because women have often not had their first pregnancy appointment with either their doctor or midwife. However if early screening is a possible it has been identified that the addition of PIGF to the combined test can help to increase the DR by 4–7% [63]. Alternatively, the results for the CA15-3 and



CA19-9 (Table 1) were not affected by maternal age [54]. Kamyab *et al.* identified that both the accuracy and specificity were improved by using two target genes (*DSCAM* and *DYRK1A*), producing an overall specificity of 96% and sensitivity of 80% [56]. Providing further validation studies are carried out it is possible that these biochemical markers may help to improve current screening tests.

**Table 1.** Summary of studies identifying potential new biochemical markers for prenatal screening of DS.

<i>Non-Epigenetic Markers</i>			
Study	Marker	Assay	Results
Cowens <i>et al.</i> [54]	Placental growth factor (PIGF)	DELFIAXpress immunoassay platform.	Increase during early first trimester in affected DS pregnancies (1 MoM in unaffected pregnancies, 1.3 MoM in DS pregnancies, $p < 0.0001$ ).
Wang <i>et al.</i> [64]	ADAM12	Auto DELFIA/DELFIADAM12 Research kit (PerkinElmer Life and Analytical Sciences, Finland).	Reduction during early first-trimester in affected DS pregnancies (1 MoM in unaffected pregnancies, 1.26 MoM in DS pregnancies, $p < 0.05$ ).
Akinlade <i>et al.</i> [55]	CA15-3 CA19-9	Quantified by the Kryptor Analyzer.	No difference between euploid and DS pregnancies. Significantly elevated in DS pregnancies. (0.98 MoM in euploid, 1.16 MoM in trisomy 21, $p = 0.024$ ).
Kamyab <i>et al.</i> [56]	<i>DSCAM</i> <i>DYRK1A</i>	Multiplex assay with cytogenetic analysis and QF-PCR.	The mean gene dosage rate was significantly increased for both genes in DS pregnancies compared to euploid pregnancies ( $p < 0.001$ ).
<i>Epigenetic Markers</i>			
Lim <i>et al.</i> [57]	<i>PDE9A</i>	Quantitative methylation specific-PCR.	<i>M-PDE9A</i> (maternal) did not differ between pregnancies, but levels of <i>U-PDE9A</i> (fetal) were significantly higher in DS pregnancies.
Du <i>et al.</i> [58]	<i>DSCR4</i>	Methylation specific primers and digital PCR.	Hypomethylated in placental tissue and methylated in maternal cells. Can detect and quantify unmethylated <i>DSCR4</i> in the first-trimester maternal plasma, successfully detect DS by RCD against a reference gene (e.g., <i>ZFY</i> ).
Chim <i>et al.</i> [65]	<i>SERPINB5</i> (coding for Maspin)	Bisulphite genomic sequencing and RT-Quantitative methylation-specific PCR.	Hypomethylated in placental tissue and methylated in maternal cells. <i>SERPINB5</i> was the first fetal-specific hypomethylated gene to be identified in maternal plasma.

The phosphodiesterase gene, *PDE9A*, is an example of an epigenetic marker, as it is completely methylated in maternal blood (*M-PDE9A*) and unmethylated in the placenta (*U-PDE9A*). In 2011, Lim *et al.* report a DR of 77.8% of DS pregnancies for this marker and a 5% FPR, demonstrating that *U-PDE9A* is an effective biomarker for the non-invasive diagnosis of DS during the first-trimester of pregnancy [57]. Other studies have also identified epigenetic markers (Table 1) for DS screening, but before any can be approved by the UK NSC, large validation studies must be carried out.

Currently there are many developments occurring in integrated proteomics and bioinformatics analysis in an attempt to identify multiple candidate protein biomarkers from maternal serum for detection of DS. Kang *et al.* identified 31 DS differentially expressed maternal serum proteins (DS-DEMSPs) using the latest proteomic techniques to identify proteins differentially expressed in the maternal serum of women carrying a DS fetus, ten of which were considered as potential biomarkers (Alpha-2-macroglobulin, Apolipoprotein A1, Apolipoprotein E, Complement C1s subcomponent, Complement component 5, Complement component 8, alpha polypeptide, Complement component 8, beta polypeptide and Fibronectin) [66]. Initial bioinformatics analysis by SAFE NoE has identified differences of known placental and DS markers, such as genes located in the *DSCR* region of chromosome 21. The SAFE project identified that the combination of both bioinformatics and proteomic approaches could be used to find previously unidentified biomarkers of aneuploidy [59]. The integration of proteomics and bioinformatics would not only provide a useful tool for prenatal screening of DS, but would also provide a mechanism for the detection of other birth defects or pregnancy related disorders. However, it is important to appreciate that plasma proteomics is extremely complicated due to the huge “noise” present when looking for new screening targets. Only a small number of studies have attempted to identify new biomarkers for DS, therefore it is essential that larger scale studies are conducted using newer technology, such as liquid chromatography-mass spectrometers, which can identify larger numbers of peptides in one analysis with great sensitivity [67]. It is likely however, that with the rapid advances in DNA technology developments in this area will be somewhat marginalized.

#### 4.3. Digital PCR and Next Generation Sequencing (NGS)

Since the identification of cffDNA in maternal plasma [52], the goal is to detect DS and other aneuploidy disorders, such as trisomy 18 (Edwards syndrome), Trisomy 13 (Patau syndrome) and Monosomy X (Turners syndrome), using NIPD. Unlike screening, NIPD does not identify the risk of DS but allows for a definitive diagnosis. Currently, cffDNA has allowed for successful NIPD of gender determination [68] and RhD status [69,70], and is available on a research basis for some single gene disorders such as sickle cell anemia [71]. Recently, studies have identified new sophisticated analytical methods, such as digital PCR and massively parallel sequencing (MPS) (also known as NGS) which are capable of detecting chromosomal aneuploidy from maternal plasma [1,8,72–74]. However, until these techniques pass the scientific and regulatory hurdles required to be considered diagnostic they could potentially be used to significantly improve current screening strategies.

There have been various molecular techniques developed for non-invasive aneuploidy detection, which are allele dependent and labor intensive [75,76]. As maternal plasma only contains up to 10% fetal DNA, to detect the presence of a DS fetus the screening test would need to be able to detect a 5%

difference in plasma DNA concentrations for a sequence located on chromosome 21. In conventional real-time PCR, a difference of one cycle threshold (Ct) value corresponds to a 2-fold change in copy number, making it very difficult to detect a 1.5-fold increase in only 10% of the total DNA [77]. Digital PCR quantifies nucleic acids by counting amplification from single molecules [78], allowing copy number changes less than 2-fold to be easily detected. Digital PCR can be performed manually, but can be labor intensive and replication levels are limited by format of plate used (96 well or 384 well). Alternatives to the manual approach are now emerging. One of these methods is the use of microfluidic chips, which splits the original sample into 765 reaction chambers [79].

**Figure 5.** False-color images of microfluidic digital PCR chips. FAM signal is shown in green, which represents the target chromosome (chromosome X, Y or 21), and HEX signal is shown in red, which represents the reference chromosome (chromosome 1). Yellow squares indicate overlapping of HEX and FAM. **(A)** Normal female fetus (46 XX). The ratio of chromosomes X and 21 are equal to reference chromosome 1 (2:2). There is no target Y chromosome identified. **(B)** DS male fetus (47 XY + 21). Ratio of chromosomes Y and X is half of reference chromosome 1 (1:2 ratios for X or Y and chromosome 1, respectively). This fetus indicates an increase of chromosome 21 in comparison to reference chromosome 1 (3:2 ratio, respectively), indicating trisomy 21 (adapted from [80]).

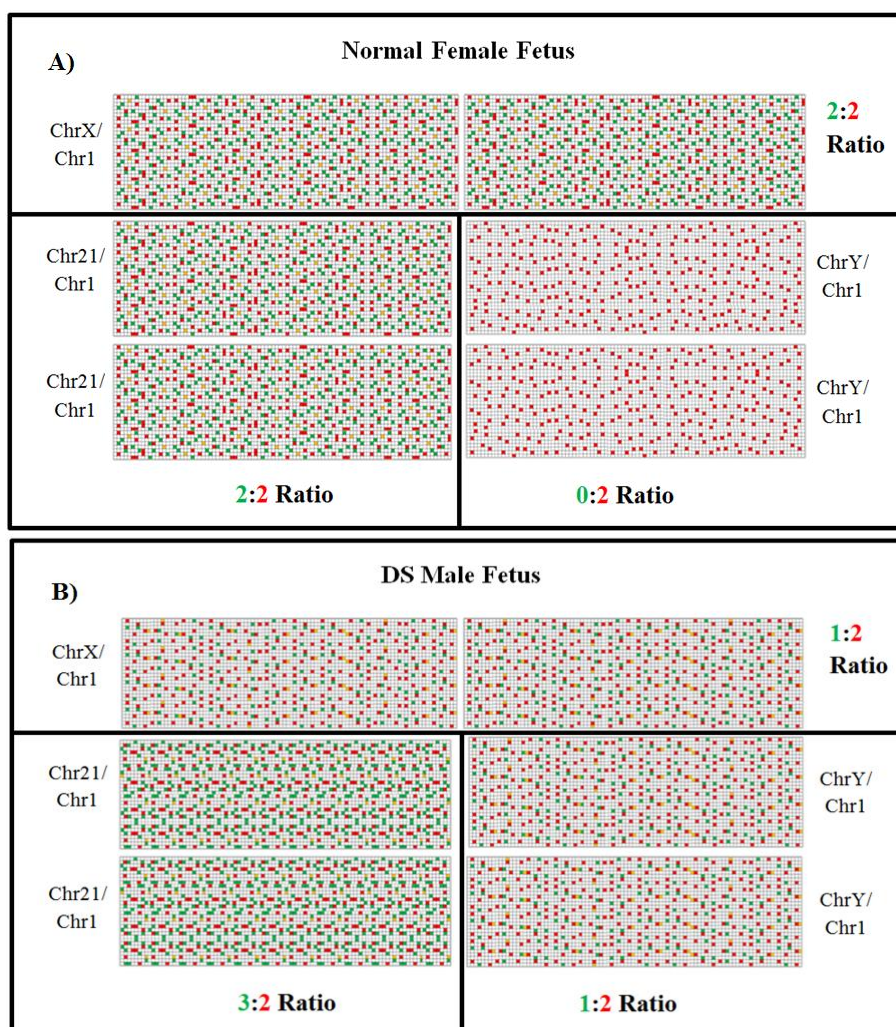


Figure 5, adapted from Fan *et al.* illustrates a mock microfluidic digital PCR chip image of a normal female fetus and a DS male fetus. Detection of DS pregnancies can be identified by determining the allelic ratio. The ratio between the 21-target chromosome (FAM-labeled) against the reference chromosome 1 (HEX-labeled) is 3:2 and 2:2 in DS male fetus and normal female fetus, respectively [80]. However, these results were achieved using CVS samples. To achieve this level of accuracy using maternal plasma samples is more challenging due to the high level of background maternal DNA.

Microfluidic digital PCR does not rely on data that is collected during the exponential PCR phase and it does not require a standard for absolute quantification (unlike RT-PCR), which allows for improved precision and accuracy [81]. Lun *et al.* successfully detected fetal-derived Y-chromosomal DNA in maternal plasma using microfluidic digital PCR, which showed higher sensitivity compared with non-digital real-time PCR, 100% and 90%, respectively, and lower imprecision [82]. Later in 2009, Lo *et al.* identified an approach using digital PCR for the non-invasive detection of DS. Firstly, the report identifies a digital RNA-SNP strategy, which uses digital PCR to determine the imbalance of a single nucleotide polymorphism (SNP) on *PLAC4* mRNA, a placentally-expressed transcript on chromosome 21, in women bearing DS fetuses. Secondly, it identifies an alternative method known as the digital relative chromosome dosage (RCD) method. The RCD method is advantageous to the RNA-SNP approach as it does not require polymorphisms for analysis; it simply detects over- or underrepresented alleles by comparing copy numbers variation between chromosomes. However, DS could only be detected in samples containing 25% fetal DNA [83]. If a 25% fetal enhancement is achieved, 7,680 molecules would need to be analyzed to achieve successful characterization of trisomy status [84]. Evans *et al.* reported that if fetal DNA is enriched to 20%, then 2,609 counts would be sufficient to achieve a 99% DR for a 1% FPR. However, if fetal DNA is only enriched by 2%, over 110,000 counts would be needed to achieve a 95% DR for a 5% FPR [85]. Due to the high level of sensitivity achieved (99% DR), provided efficient prior-fetal enrichment, it is possible that digital PCR could potentially replace current screening methods. However, even though digital PCR could provide a cheaper alternative to NGS-NIPT, confirmation of the high-throughput possibilities and costs of digital PCR by large validation studies are still required.

The development of non-invasive tests based on cffDNA within the maternal circulation provides substantial new opportunities to improve prenatal screening. To date, the most convincing data for a generally applicable test for aneuploidy detection from cffDNA have been generated through MPS. This technology allows cffDNA obtained from maternal plasma to produce millions of short-sequence tags that can be aligned and uniquely mapped to a reference human genome that are by definition mapped to a specific chromosome [86]. The DR for fetal aneuploidy using this method is determined by the depth of sequencing and subsequent counting statistics. Fan *et al.* were the first to propose counting chromosomes using high-throughput massively parallel shotgun sequencing (MPSS) technology. In this study 5 million sequence tags were obtained per patient, providing sufficient data to detect the over- or under- representation of chromosomes and allow for correct classification of an aneuploidy fetus [87]. Table 2 illustrates the DR and FPR associated with large scale clinical trials of NIPT by MPS for fetal DS detection.

Ehrich *et al.* revealed that MPSS managed to detect all 39 cases of DS samples (in a cohort of 449); however one normal sample was misclassified as DS (Table 2) [1]. The method described by Chiu *et al.* diagnosed a DS fetus when the Z-score for the proportion of chromosome 21 DNA molecules was  $>3$ , which indicates a 99% chance of statistical significance (Table 2) [8]. This method simply normalizes the number of sequence tags on the chromosome of interest by the number of tags in the sequencing run. However, it has been identified that using MPS, intra-run and inter-run variability can alter the chromosomal distribution of sequence reads for each sample. Some of the variability can come from sample handling, such as the DNA extraction procedure or the sequencing itself can lead to small shifts in the distribution of tags [88]. To minimize the intra- and inter-run sequencing variation, a study by Sehnert *et al.* developed an optimized algorithm by using normalized chromosome values (NCVs) from the sequence data [72]. When chromosome ratios are normally distributed, the NCV is equivalent to a statistical Z-score for the ratios. Threshold values for trisomy were established for all chromosomes of interest (13, 18 and 21). NCV values  $>4.0$  were required for classification of affected aneuploidy state, and NCV values  $<2.5$  were used to classify unaffected cases. NCV values between 2.5 and 4 were classified as “no call”. Using these parameters, this study demonstrated 100% correct classification of samples with DS and Trisomy 18. However, one sample for chromosome 13 was classified as a “no call” [72]. Some speculation exists that the poor detection rate using NGS for trisomy 13 may be due in part to the lesser level of fragmentation of this larger chromosome [89].

**Table 2.** Clinical trials of NIPT by massively parallel sequencing (MPS) for fetal DS (adapted from [41]).

Study	Method	DR (%)	FPR (%)
Chiu <i>et al.</i> [90]	Shotgun (2-plex protocol)	100	2.1
Chiu <i>et al.</i> [90]	Shotgun (8-plex protocol)	79.1	1.2
Ehrich <i>et al.</i> [1]	Shotgun	100	0.2
Bianchi <i>et al.</i> [91]	Shotgun	100	0
Jensen <i>et al.</i> [92]	Shotgun	100	0.9
Sparks <i>et al.</i> [93]	Targeted	100	0.8
Ashoor <i>et al.</i> [88]	Targeted	100	0
Norton <i>et al.</i> [94]	Targeted	100	0.1
Liang <i>et al.</i> [95]	Targeted	100	0

MPS technologies have successfully enabled the NIPT of fetal chromosomal aneuploidies. The identification of DS was primarily identified, and currently many recent clinical studies have indicated detection rates  $>99\%$  [1,90]. The incorporation of MPS for the detection of trisomy 18 and trisomy 13 was proved to be more difficult than detecting DS due to the relatively lower GC content expressed by these two chromosomes in comparison to chromosome 21. However, when the coefficient of variance (CVs) was adjusted with GC content, it was noted that trisomy 18 and trisomy 13 can be detected accurately [87]. Chromosome 21 only represents less than 1.5% of the genome (in disomy cases) and as MPSS is not selective, millions of DNA fragments must be sequenced in order to detect statistically significant differences between trisomic and normal fetuses [96]. Therefore targeted methods have been developed, which count only specific sequences in contrast to shotgun sequencing, which counts all free DNA. In a recent statement from the Aneuploidy Screening Committee on behalf of the ISPD, it was noted that only cfDNA analysis based on MPS with either

“shotgun” or “targeted” counting have been sufficiently validated to be considered analytically sound [41]. Targeted sequencing can allow for more samples to be multiplexed at once, proving a cheaper alternative to whole genome sequencing (WGS). However, the limitation of this method is that only the region of interest can be studied.

Aria Diagnostics (San Jose, CA, USA) have developed a multiplex MPS assay, termed “Digital Analysis of Selected Regions” (DANSR) which sequences regions from target chromosomes. In a study by Sparks *et al.* DANSR was used to develop an algorithm, the Fetal-fraction Optimized Risk of Trisomy Evaluation (FORTE), which combines both the age-related risks and the proportion of cfDNA in the samples to provide an individual risk score for trisomy. The low proportion of cfDNA within the maternal circulation can make quantification of fetal chromosome imbalances difficult and potentially inaccurate, however, the FORTE algorithm factors in the fetal fraction when calculation the risk of aneuploidy. When there is a high proportion of cfDNA the difference between trisomic *versus* disomic chromosomes is greater, making it easier to detect trisomy [93]. This approach was also reported by Ashoor *et al.* which included a cohort of 400 samples from pregnancies with known karyotypes, 300 euploid (normal), 50 trisomy 18 (Edwards syndrome) and 50 trisomy 21 (DS). Both these reports which used the DANSR/FORTE assay identified high degrees of accuracy (Table 2) [88]. However, in these trials the test was only offered to high-risk pregnancies, but the future aim is to deliver this assay to all pregnancies as a highly accurate screening test for aneuploidies [97]. Chui *et al.* identified that if referrals for amniocentesis or CVS were based on sequencing test results; approximately 98% of the invasive diagnostic procedures could be avoided [90]. In 2012 Aria Diagnostics announced the launch of a U.S. clinical study involving 25,000 pregnancies to compare FORTE with the current combined screening test for DS [98].

Table 3 illustrates some of the NGS platforms that are currently available. The HiSeq2000 has a significantly higher number of single end reads per run, which makes this platform very suitable for multiplexing samples and thus high throughput runs. However with the development of targeted counting smaller bench-top platforms such as the MiSeq and Ion Torrent could be used for more rapid testing due to reduced sample-prep time and faster run times, however these platforms will exert lower throughput due to lower number of single end reads per run. Even though the initial costs are cheaper for the bench-top platforms (MiSeq and Ion Torrent), because of the increased number of base reads per run with high throughput platforms (HiSeq2000), the cost per Mb is actually cheaper for the HiSeq2000 (\$0.07) than the Illumina MiSeq (\$0.5) and Ion Torrent (\$0.64) [99,100].

**Table 3.** NGS Platforms suitable for NIPT (adapted from [96,101]).

	PCR-based sequencing	Single end reads per run	Run Time
<b>HiSeq™2000</b> (Illumina, Inc.)	Sequencing-by-synthesis	3 billion	5–14 days
<b>HiSeq™2500</b> (rapid run) (Illumina, Inc.)	Sequencing-by-synthesis	~300 million (10 Gb)	7 h
<b>SOLiD™4</b> (Life Technologies™/ Applied Biosystems™)	Sequencing-by-ligation	~0.7 billion	5–10 days
<b>HeliScope® Single Molecule Sequencer</b> (Helicos™Biosciences)	Single-molecule-sequencing-by-synthesis	~840 million (28 Gb)	8 days
Benchtop: <b>MiSeq™</b> (Illumina, Inc.)	Sequence-by-synthesis	~12 million (3.4 Gb)	16.5 h
Benchtop: <b>Ion Torrent™</b> (Life Technologies™)	Semiconductor sequencing technology	~5 million (1 Gb)	4.4 h

The International Society for Prenatal Diagnosis (ISPD) has reported that before routine MPS population screening can be introduced additional trials are needed. These trials need to confirm that there is efficacy in low-risk populations, that it is cost-effective and suitable for diverse subpopulations (such as twin or IVF pregnancies) [102]. Commercial MPS-based testing for prenatal detection of DS has been introduced into some areas of the United States, China and more recently the European Union (EU). Currently there are three commercial providers of NIPT within the USA who have received Clinical Laboratory Improvement Amendments (CLIA) certification; however more recently an additional competitor, Natera, has entered the market (Table 4) [103,104]. The Harmony test (provided by Aria Diagnostics) is currently the cheapest (\$795); however this test uses selective sequencing in comparison to the Verifi test and the MaterniT21 Plus test, which are MPSS-based test for aneuploidy detection. According to a study published earlier this year, with reference to WGS, the sequencing alone can already be done for less than \$1,000, however soon it is likely the entire process will drop below the \$1,000 mark [105]. The ISPD has outlined that this NIPT should be offered to high-risk pregnancies only and not offered as an initial test as screening via MPS for all pregnancies as it is not currently cost effective [102]. It is vital that all women undergoing MPS-based testing are offered prenatal counseling, so that the benefits and limitations of the test can be explained.

**Table 4.** Commercial tests available for the NIPT of trisomies (adapted from [104]).

Company	Test	Released	Trisomies Tested	Genetic Testing Method	Accuracy	Sensitivity	Cost
Sequenom	MaterniT21 Plus	February 2012	13, 18, 21, sex chromo-somes	MPSS	>99%	92–99%	\$2,762
Verinata	Verifi Prenatal Test	March 2012	13, 18, 21, sex chromo-somes	MPSS	100%	87–99%	\$1,500
Aria Diagnostics	Harmony Prenatal Test	May 2012	13, 18, 21	Chromosome-selective sequencing	>99%	80–99%	\$795
Natera	Panorama	March 2013	13, 18, 21	Single nucleotide polymorph-ism	100%	92–99%	\$1,495

## 5. Conclusions

This review demonstrates how screening for the detection of DS has improved since the early 1980s when maternal age was the only “tool” available. It also provides an insight into how new physical and biochemical markers may play a role in future routine screening to allow for increased test sensitivity with fewer false screen positives. Although this is still a key area of research, the main focus is to provide a definitive diagnosis through non-invasive techniques, such as digital PCR and NGS. A recent trial conducted within the UK to assess the performance of NIPT for fetal trisomy in a routinely screened first-trimester population identified a DR of >99% and a false positive rate of 0.1% for trisomy 21 and trisomy 18, which is a significant improvement on current screening DRs and FPRs (85–90% and 5%, respectively) [50,106]. Although the sensitivity of NGS currently provides DRs



similar to that provided by CVS, before even considering the replacement of IPD with NIPD, further large scale validation studies of low-risk populations are required to confirm that NGS test sensitivity is consistent with current invasive testing (97.8% and 99.4% for CVS and amniocentesis, respectively) [107]. It is also important that the economic aspects, counseling requirements and turnaround times are also considered [97].

The cost of NIPD is likely to vary by country due to variations in the accuracy of the NIPD test, the cost of the NIPD test and the numbers undergoing NIPD [97]. However for fetal aneuploidy testing, whole genome MPS is still quite expensive, therefore to lower costs targeted approaches are being developed [96]. Using MPS in high-risk pregnancies following initial screening increases the OAPR, causing fewer women with unaffected fetuses to miscarry. Furthermore, providing NGS to all pregnancies would not only increase the OAPR but also reduce the number of unidentified trisomy fetuses, however this would be associated with a dramatic increase in cost due to a substantial rise in the numbers undergoing NIPD.

Developments in proteomics to detect multiple novel biomarkers could provide a cheaper screening alternative to NGS but will most likely display a reduction in sensitivity. However, new biomarkers can only be used for screening purposes, whereas MPS directly identifies fetal DNA providing a NIPD approach that could potentially replace current IPD techniques. With the continuous decline in MPS costs, NIPD of fetal aneuploidy is an exciting area of research that could become a clinical reality for all pregnancies in the near future.

## Acknowledgements

??

## Conflict of Interest

The authors declare no conflict of interest.

## References

1. Ehrich, M.; Deciu, C.; Zwiefelhofer, T.; Tynan, J.A.; Cagasan, L.; Tim, R.; Lu, V.; McCullough, R.; McCarthy, E.; Nygren, A.O. Noninvasive detection of fetal trisomy 21 by sequencing of DNA in maternal blood: A study in a clinical setting. *Am. J. Obstet. Gynecol.* **2011**, *204*, 201–211.
2. Egan, J.F.; Benn, P.A.; Zelop, C.M.; Bolnick, A.; Gianferrari, E.; Borgida, A.F. Down syndrome births in the United States from 1989 to 2001. *Am. J. Obstet. Gynecol.* **2004**, *191*, 1044–1048.
3. Morris, J.K.; Mutton, D.E.; Alberman, E. Revised estimates of the maternal age specific live birth prevalence of Down's syndrome. *J. Med. Screen* **2002**, *9*, 2–6.
4. Crane, E.; Morris, J.K. Changes in maternal age in England and Wales—Implications for Down syndrome. *Down Syndr. Res. Pract.* **2006**, *10*, 41–43.
5. McEwan, A.; Godfrey, A.; Wilkins, J. Screening for Down syndrome. *Obstet. Gynaecol. Reprod. Med.* **2012**, *22*, 70–75.
6. Rozenberg, P.; Bussi eres, L.; Chevret, S.; Bernard, J.P.; Malagrida, L.; Cuckle, H.; Chabry, C.; Durand-Zaleski, I.; Bidat, L.; Lacroix, I. Screening for Down syndrome using first-trimester



- combined screening followed by second trimester ultrasound examination in an unselected population. *Gynecol. Obstet. Fertil.* **2007**, *35*, 303–311.
7. Morris, J.K.; Wald, N.J.; Watt, H.C. Fetal loss in Down syndrome pregnancies *Prenat. Diagn.* **1999**, *19*, 142–145.
  8. Chiu, R.W.K.; Cantor, C.R.; Lo, Y.M.D. Non-invasive prenatal diagnosis by single molecule counting technologies. *Trends Genet.* **2009**, *25*, 324–331.
  9. Ferguson-Smith, M.A. Placental mRNA in maternal plasma: Prospects for fetal screening. *Proc. Natl. Acad. Sci. USA* **2003**, *100*, 4360–4362.
  10. Wald, N.J. Guidance on terminology. *J. Med. Screen* **2006**, *13*, 53.
  11. Buckley, F.; Buckley, S. Wrongful deaths and rightful lives—Screening for Down syndrome. *Down Syndr. Res. Prac.* **2008**, *12*, 79–86.
  12. Haddow, J.E.; Palomaki, G.E.; Knight, G.J.; Williams, J.; Pulkkinen, A.; Canick, J.A.; Saller, D.N.; Bowers, G.B. Prenatal screening for Down’s syndrome with use of maternal serum markers. *N. Engl. J. Med.* **1992**, *327*, 588–593.
  13. Benacerraf, B.R.; Gelman, R.; Friholetto, F.D. Sonographic identification of second-trimester fetuses with Down’s syndrome. *N. Engl. J. Med.* **1987**, *317*, 1371–1376.
  14. Merkatz, I.; Nitowsky, H.; Marci, J.; Johnson, W. An association between low maternal serum alpha-fetoprotein and fetal chromosomal abnormalities. *Am. J. Obstet. Gynecol.* **1984**, *148*, 886–894.
  15. Cuckle, H.; Wald, N.; Lindenbaum, R. Maternal serum alpha-fetoprotein measurement: A screening test for Down syndrome. *Lancet* **1984**, *1*, 926–929.
  16. Furhmann, W.; Wendt, P.; Weitzel, H. Maternal serum-AFP as screening test for Down syndrome. *Lancet* **1984**, *2*, doi: 10.1016/S0140-6736(84)92389-4.
  17. Gillespie, G.; Uversky, V. Structure and function of alpha-fetoprotein: A biophysical overview. *Biochem. Biophys. Acta* **2000**, *1480*, 41–56.
  18. DiMaio, M.; Baumgarten, A.; Greenstein, R.; Mahoney, M. Screening for fetal Down’s syndrome in pregnancy by measuring maternal serum alpha-fetoprotein levels. *N. Engl. J. Med.* **1987**, *6*, 342–346.
  19. Cole, L. New discoveries on the biology and detection of human chorionic gonadotrophin. *Reprod. Biol. Endocrinol.* **2009**, *7*, doi: 10.1186/1477-7827-7-8.
  20. Bogart, M.; Pandian, M.; Jones, O. Abnormal maternal serum chorionic gonadotropin levels in pregnancies with fetal chromosome abnormalities. *Prenat. Diagn.* **1987**, *7*, 623–630.
  21. Agarwal, R. Prenatal diagnosis of chromosomal anomalies: Pictorial essay. *Indian J. Radiol. Imaging* **2003**, *13*, 173–188.
  22. Canick, J.; Kellner, L. First trimester screening for aneuploidy: Serum biochemical markers. *Semin. Perinatol.* **1999**, *5*, 359–368.
  23. Crossley, J.; Aitken, D.; Connor, J. Second-trimester unconjugated oestriol levels in maternal serum from chromosomally abnormal pregnancies using an optimized assay. *Prenat. Diagn.* **1993**, *13*, 271–280.
  24. Ryall, R.; Staples, A.; Robertson, E.; Pollard, A. Improved performance in a prenatal screening programme for Down’s syndrome incorporating serum-free hCG subunit analyses. *Prenat. Diagn.* **1992**, *12*, 251–261.

25. Reynolds, T. The triple test as a screening technique for Down syndrome: Reliability and relevance. *Int. J. Wom. Health* **2010**, *2010*, 83–88.
26. Aitken, D.A.; Wallace, E.M.; Crossley, J.A.; Swanston, I.A.; Pareren, Y.V.; Maarle, M.V.; Groome, N.P.; Macri, J.N.; Connor, M.J. Dimeric inhibin A as a marker for Down's syndrome in early pregnancy. *N. Engl. J. Med.* **1996**, *334*, 1231–1236.
27. Brambati, B.; Macintosh, M.C.; Teisner, B.; Maguiness, S.; Shrimanker, K.; Lanzani, A.; Bonacchi, I.; Tului, L.; Chard, T.; Grudzinskas, J.G. Low maternal serum levels of pregnancy associated plasma protein a (PAPP-A) in the first trimester in association with abnormal fetal karyotype. *Br. J. Obstet. Gynaecol.* **1993**, *100*, 324–326.
28. Knight, G.; Palomaki, G.; Haddow, J.E. Pregnancy associated plasma protein A as a marker for Down syndrome in the second trimester of pregnancy. *Prenat. Diagn.* **1993**, *13*, 222–223.
29. Reis, F.; D'Antona, D.; Petraglia, F. Predictive value of hormone measurements in maternal and fetal complications of pregnancy. *Endo Rev.* **2002**, *23*, 230–257.
30. Nicolaides, K.H.; Azar, G.; Byrne, D.; Mansur, C.; Marks, K. Fetal nuchal translucency: Ultrasound screening for chromosomal defects in first trimester of pregnancy. *BMJ* **1992**, *304*, 867–869.
31. Nicolaides, K.H.; Brizot, M.L.; Snijders, R.J. Fetal nuchal translucency: Ultrasound screening for chromosomal defects in first trimester of pregnancy. *J. Obstet. Gynaecol.* **1994**, *101*, 782–786.
32. Committee, T.N.S. National Down's Syndrome Screening Program (DoSYSP). Available online: <http://fetalanomaly.screening.nhs.uk/standardsandpolicies> (accessed on 20 May 2013).
33. Chitty, L.S.; Pandya, P.P. Ultrasound screening for fetal abnormalities in the first trimester. *Prenat. Diagn.* **1997**, *17*, 1269–1281.
34. Pandya, P.P.; Altman, D.G.; Brizot, M.L.; Pettersen, H.; Nicolaides, K.H. Repeatability of measurement of fetal nuchal translucency thickness. *Ultrasound Obstet. Gynecol.* **1995**, *5*, 334–337.
35. Wald, N.; Hackshaw, A.K. Combining ultrasound and biochemistry in first trimester screening for Down's syndrome. *Prenat. Diagn.* **1997**, *17*, 821–829.
36. Spencer, K.; Nicolaides, K.H. Screening for trisomy 21 in twins using first trimester ultrasound and maternal serum biochemistry in a one-stop clinic: A review of three years experience. *Br. J. Obstet. Gynaecol.* **2003**, *110*, 276–280.
37. Nicolaides, K.H.; Spencer, K.; Avqidou, K.; Faiola, S.; Falcon, O. Multicenter study of first-trimester screening for trisomy 21 in 75,821 pregnancies: Results and estimation of the potential impact of individual risk-orientated two-stage first-trimester screening. *Ultrasound Obstet. Gynecol.* **2005**, *25*, 221–226.
38. Jaques, A.M.; Halliday, J.L.; Francis, I.; Bonacquisti, L.; Forbes, R.; Cronin, A.; Sheffield, L.J. Follow up and evaluation of the victorian first-trimester combined screening programme for Down syndrome and trisomy 18. *BJOG* **2007**, *114*, 812–818.
39. Valinen, Y.; Rapakko, K.; Kokkonen, H.; Laitinen, P.; Tekay, A.; Ahola, T.; Ryyananen, M. Clinical first-trimester routine screening for Down syndrome in singleton pregnancies in northern Finland. *Am. J. Obstet. Gynecol.* **2007**, *196*, 278, doi: 10.1016/j.ajog.2006.11.040.

40. Wald, N.J.; Huttly, W.J.; Murphy, K.W.; Ali, K.; Bestwick, J.P.; Rodeck, C.H. Antenatal screening for Down's syndrome using the integrated test at two London hospitals. *J. Med. Screen* **2009**, *16*, 7–10.
41. Benn, P.; Borell, A.; Chiu, R.; Cuckle, H.; Dugoff, L.; Faas, B.; Gross, S.; Johnson, J.; Maymon, R.; Norton, M.; *et al.* Position statement from the aneuploidy screening committee on behalf of the board of the international society for prenatal diagnosis, April 2013. *Prenat. Diagn.* **2013**, *32*, 1–2.
42. NHS Fetal Anomaly Screening Programme. Screening for Down's syndrome: UK NSC Policy Recommendations 2011–2014 Model of Best Practice. Available online: <http://www.fetalanomaly.screening.nhs.uk/getdata.php?id=11393> (accessed on 13 May 2013).
43. Fang, Y.M.V.; Benn, P.; Campbell, W.; Bolnick, J.; Prabulos, A.M.; Egan, J.F.X. Down syndrome screening in the united states in 2001 and 2007: A survey of maternal-fetal medicine specialists. *Am. J. Obstet. Gynecol.* **2009**, *201*, e91–e95.
44. Benn, P.; Borrell, A.; Crossley, J.; Cuckle, H.; Dugoff, L.; Gross, S.; Johnson, J.-A.; Maymon, R.; Odibo, A.; Schielen, P.; *et al.* Aneuploidy screening: A position statement from a committee on behalf of the board of the international society for prenatal diagnosis, January 2011. *Prenat. Diagn.* **2011**, *31*, 519–522.
45. Maslen, C.L.; Babcock, D.; Robinson, S.W.; Bean, L.J.; Dooley, K.J.; Willour, V.L.; Sherman, S.L. Creld1 mutations contribute to the occurrence of cardiac atrioventricular septal defects in Down syndrome. *Am. J. Med. Genet.* **2006**, *140*, 2501–2505.
46. Nyberg, D.; Souter, V. Sonographic markers of fetal trisomies: Second trimester. *J. Ultrasound Med.* **2001**, *20*, 655–674.
47. Stoll, C.; Dott, B.; Alembik, Y.; Roth, M. Evaluation of routine prenatal ultrasound examination in detecting fetal chromosomal abnormalities in a low risk population. *Hum. Genet.* **1993**, *91*, 37–41.
48. Hill, L. The sonographic detection of trisomies 13, 18 and 21. *Clin. Obstet. Gynecol.* **1996**, *39*, 831–850.
49. Kagan, K.O.; Etchegaray, A.; Zhou, Y.; Wright, D.; Nicolaides, K.H. Prospective validation of first-trimester combined screening for trisomy 21. *Ultrasound Obstet. Gynecol.* **2009**, *34*, 14–18.
50. Nicolaides, K. Screening for fetal aneuploidies at 11 to 13 weeks. *Prenat. Diagn.* **2011**, *31*, 7–15.
51. Smith-Bindman, R.; Hosmer, W.; Feldstein, V.A.; Deeks, J.J.; Goldberg, J.D. Second-trimester ultrasound to detect fetuses with Down syndrome: A meta-analysis. *JAMA* **2001**, *285*, 1044–1055.
52. Lo, Y.M.; Corbetta, N.; Chamberlain, P.F.; Rai, V.; Sargent, I.L.; Redman, C.W.; Wainscoat, J.S. Presence of fetal DNA in maternal plasma and serum. *Lancet* **1997**, *350*, 485–487.
53. Tsui, D.W.; Chan, K.C.; Chim, S.S.; Chan, L.W.; Leung, T.Y.; Lau, T.K.; Lo, Y.M.; Chiu, R.W. Quantitative aberrations of hypermethylated RASSF1A gene sequences in maternal plasma in pre-eclampsia. *Prenat. Diagn.* **2007**, *27*, 1212–1218.
54. Cowans, N.; Stamatopoulou, A.; Topping, N.; Spencer, K. Early first trimester maternal serum placental growth factor in trisomy 21 pregnancies. *Ultrasound Obstet. Gynecol.* **2011**, *37*, 515–519.

55. Akinlade, F.; Cowans, N.; Kisanga, M.; Spencer, K., Maternal serum CA 19-9 and CA 15-3 levels in pregnancies affected by trisomy 21. *Prenat. Diagn.* **2012**, *32*, 644–648.
56. Kamyab, A.R.; Shahrokhi, F.; Shamsian, E.; Nosaied, M.H.; Dibajnia, P.; Hashemi, M.; Mahdian, R. Determination of sensitivity and specificity of a novel gene dosage assay for prenatal screening of trisomy 21 syndrome. *Clin. Biochem.* **2012**, *45*, 267–271.
57. Lim, J.H.; Kim, S.Y.; Park, S.Y.; Lee, S.Y.; Kim, M.J.; Han, Y.J.; Lee, S.W.; Chung, J.H.; Kim, M.Y.; Yang, J.H.; *et al.* Non-invasive epigenetic detection of fetal trisomy 21 in first trimester maternal plasma. *PLoS One* **2011**, *6*, doi: 10.1371/journal.pone.0027709.
58. Du, Y.; Zhang, J.; Wang, H.; Yan, X.; Yang, Y.; Yang, L.; Luo, X.; Chen, Y.; Duan, T.; Ma, D. Hypomethylated dscr4 is a placenta-derived epigenetic marker for trisomy 21. *Prenat. Diagn.* **2011**, *31*, 207–214.
59. Maddocks, D.G.; Alberry, M.S.; Attilakos, G.; Madgett, T.E.; Choi, K.; Soothill, P.W.; Avent, N.D. The SAFE project: Towards non-invasive prenatal diagnosis. *Biochem. Soc. Trans.* **2009**, *37*, 460–465.
60. Chitty, L.S.; van der Schoot, C.E.; Hahn, S.; Avent, N.D. SAFE-the special non-invasive advances in fetal and neonatal evaluation network: Aims and achievements. *Prenat. Diagn.* **2008**, *28*, 83–88.
61. Shipp, T.; Benacerraf, B. Second trimester ultrasound screening for chromosomal abnormalities. *Prenat. Diagn.* **2002**, *22*, 296–307.
62. Cicero, S.; Curcio, P.; Papageorghiou, A.; Sonek, J.; Nicolaides, K. Absence of nasal bone in fetuses with trisomy 21 at 11–14 weeks of gestation: An observational study. *Lancet* **2001**, *358*, 1665–1667.
63. Donaldson, K.; Turner, S.; Morrison, L.; Liitte, P.; Nilsson, C.; Cuckle, H. Maternal serum placental growth factor and  $\alpha$ -fetoprotein testing in first trimester screening for Down syndrome. *Prenat. Diagn.* **2013**, *33*, 457–461.
64. Wang, M.; Lu, S.; Zhu, Y.; Li, H. Adam12 is an effective marker in the second trimester of pregnancy for prenatal screening of Down syndrome. *Prenat. Diagn.* **2010**, *30*, 561–564.
65. Chim, S.S.; Tong, Y.K.; Chiu, R.W.; Lau, T.K.; Leung, T.Y.; Chan, L.Y.S.; Oudejans, C.B.M.; Ding, C.; Lo, Y.M. Detection of the placental epigenetic signature of the maspin gene in maternal plasma. *Proc. Natl. Acad. Sci. USA* **2005**, *11*, 14753–14758.
66. Kang, Y.; Dong, X.; Zhou, Q.; Zhang, Y.; Cheng, Y.; Hu, R.; Su, C.; Jin, H.; Liu, X.; Ma, D.; *et al.* Identification of novel candidate maternal serum protein markers for Down syndrome by integrated proteomic and bioinformatic analysis. *Prenat. Diagn.* **2012**, *32*, 284–292.
67. Avent, N.D. Maternal plasma biomarkers for Down syndrome: Present and future. *Drugs Today* **2013**, *49*, 145–152.
68. Honda, H.; Miharu, N.; Ohashi, Y.; Samura, O.; Kinutani, M.; Hara, T.; Ohama, K. Fetal gender determination in early pregnancy through qualitative and quantitative analysis of fetal DNA in maternal serum. *Hum. Genet.* **2002**, *110*, 75–79.
69. Bianchi, D.W.; Avent, N.D.; Costa, J.M.; van der Schoot, C.E. Noninvasive prenatal diagnosis of fetal rhesus D: Ready for prime(r) time. *Obstet. Gynecol.* **2005**, *106*, 841–844.

70. Lo, Y.M.D.; Hjelm, M.; Fidler, C.; Sargent, I.L.; Murphy, M.F.; Chamberlain, P.F.; Poon, P.M.K.; Redman, C.W.G.; Wainscoat, J.S. Prenatal diagnosis of fetal rhd status by molecular analysis of maternal plasma. *N. Engl. J. Med.* **1998**, *339*, 1734–1738.
71. Satio, H.; Sekizawa, A.; Morimoto, T. Prenatal DNA diagnosis of a single-gene disorder from maternal plasma. *Lancet* **2000**, *356*, doi: 10.1016/S0140-6736(00)02767-7.
72. Sehnert, A.J.; Rhees, B.; Comstock, D.; de Feo, E.; Heilek, G.; Burke, J.; Rava, R.P. Optimal detection of fetal chromosomal abnormalities by massively parallel DNA sequencing of cell-free fetal DNA from maternal blood. *Clin. Chem.* **2011**, *57*, 1042–1049.
73. Dan, S.; Chen, F.; Choy, K.W.; Jiang, F.; Lin, J.; Xuan, Z.; Wang, W.; Chen, S.; Li, X.; Jiang, H., *et al.* Prenatal detection of aneuploidy and imbalanced chromosomal parallel sequencing. *PLoS One* **2011**, *7*, doi:10.1371/journal.pone.0027835.
74. Papageorgiou, E.A.; Patsalis, P.C. Non-invasive prenatal diagnosis of aneuploidies: New technologies and clinical applications. *Genom. Med.* **2012**, *4*, doi: 10.1016/j.tig.2009.05.004.
75. Hulten, M.; Dhanjal, S.; Pertl, B. Rapid and simple prenatal diagnosis of common chromosome disorders: Advantages and disadvantages of the molecular methods fish and QF-PCR. *Reproduction* **2003**, *126*, 279–297.
76. Shaffer, L.; Bui, T. Molecular cytogenetic and rapid aneuploidy detection methods in prenatal diagnosis. *Am. J. Med. Genet.* **2007**, *145*, 87–98.
77. Zimmermann, B.; Holzgreve, W.; Wenzel, F.; Hahn, S. Novel real-time quantitative PCR test for trisomy 21. *Clin. Chem.* **2002**, *48*, 362–363.
78. Vogelstein, B.; Kinzler, K.; Digital PCR. *Proc. Natl. Acad. Sci. USA* **1999**, *96*, 9236–9261.
79. White, R.; Blainey, P.; Fan, H.; Quake, S. Digital PCR provides sensitive and absolute calibration for high throughput sequencing. *BMC* **2009**, *10*, 116, doi: 10.1186/1471-2164-10-116.
80. Fan, H.C.; Blumenfeld, Y.J.; El-Sayed, Y.Y.; Chueh, J.; Quake, S.R. Microfluidic digital PCR enables rapid prenatal diagnosis of fetal aneuploidy. *Am. J. Med. Genet.* **2009**, *200*, e541–e547.
81. Zimmermann, B.G.; Grill, S.; Holzgreve, W.; Zhong, X.Y.; Jackson, L.G.; Hahn, S. Digital PCR: A powerful new tool for noninvasive prenatal diagnosis? *Prenat. Diagn.* **2008**, *28*, 1087–1093.
82. Lun, F.M.; Chiu, R.W.; Chan, K.C.; Leung, T.Y.; Lau, T.K.; Lo, Y.M. Microfluidics digital PCR reveals a higher than expected fraction of fetal DNA in maternal plasma. *Clin. Chem.* **2008**, *54*, 1664–1672.
83. Lo, Y.M.D.; Lun, F.M.; Chan, K.C.; Tsui, N.B.Y.; Chong, K.C.; Lau, T.K.; Leung, T.Y.; Zee, T.Y.; Cantor, C.R.; Chiu, R.W. Digital PCR for the molecular detection of fetal chromosomal aneuploidy. *Proc. Natl. Acad. Sci. USA* **2007**, *104*, 13116–13121.
84. Lo, Y.M.; Chan, K.C.; Chiu, R.W. Noninvasive fetal trisomy 21 detection using chromosomal selective sequencing: A variation of the molecular counting theme. *Expert Rev. Mol. Diagn.* **2012**, *12*, 329–331.
85. Evans, M.I.; Wright, D.A.; Pergament, E.; Cuckle, H.S.; Nicolaides, K.H., Digital PCR for noninvasive detection of aneuploidy: Power analysis equations for feasibility. *Fetal Diagn. Ther.* **2012**, *31*, 244–247.
86. Sonek, J.; Molina, F.; Hiatt, A.K.; Glover, M.; McKenna, D.; Nicolaides, K. Paper abstracts of the ISPD 16th international conference on prenatal diagnosis and therapy. *Prenat. Diagn.* **2012**, *32*, 1–128.

87. Fan, H.C.; Blumenfeld, Y.J.; Chitkara, U.; Hudgins, L.; Quake, S.R. Noninvasive diagnosis of fetal aneuploidy by shotgun sequencing DNA from maternal blood. *Proc. Natl. Acad. Sci. USA* **2008**, *105*, 16266–16271.
88. Ashoor, G.; Syngelaki, A.; Wagner, M.; Birdir, C.; Nicolaides, K. Chromosome-selective sequencing of maternal plasma cell-free DNA for first trimester detection of trisomy 21 and trisomy 18. *Am. J. Obstet. Gynecol.* **2012**, *206*, e321–e325.
89. Avent, N.D. Refining noninvasive prenatal diagnosis with single-molecular next-generation sequencing. *Clin. Chem.* **2012**, *58*, 657–658.
90. Chiu, R.W.; Akolekar, R.; Zheng, Y.W.; Leung, T.Y.; Sun, H.; Chan, K.C.; Lun, F.M.; Go, A.T.; Lau, E.T.; To, W.W.; *et al.* Non-invasive prenatal assessment of trisomy 21 by multiplexed maternal plasma DNA sequencing: Large scale validity study. *BMJ* **2011**, *11*, doi: 10.1136/bmj.c7401.
91. Bianchi, D.W.; Platt, L.; Goldberg, J.D.; Abuhamad, A.Z.; Sehnert, A.J.; Rava, R.P. Genome-wide fetal aneuploidy detection by maternal plasma DNA sequencing. *Obstet. Gynecol.* **2012**, *119*, 890–901.
92. Jensen, T.; Zwiefelhofer, T.; Tim, R.; Dzakula, Z.; Kim, S.; Mazloom, A.; Zhu, Z.; Tynan, J.; Lu, T.; McLennan, G. High-throughput massively parallel sequencing for fetal aneuploidy detection from maternal plasma. *PLoS One* **2013**, *8*, doi: 10.1371/journal.pone.0057381.
93. Sparks, A.B.; Struble, C.A.; Wang, E.T.; Song, K.; Oliphant, A. Noninvasive prenatal detection and selective analysis of cell-free DNA obtained from maternal blood: Evaluation for trisomy 21 and trisomy 18. *Am. J. Obstet. Gynecol.* **2012**, *206*, e311–e319.
94. Norton, M.E.; Brar, H.; Weiss, J.; Karimi, A.; Laurent, L.C.; Caughey, A.B.; Rodriguez, H.; Williams, J.I.; Mitchell, M.E.; Adair, C.D. Non-invasive chromosomal evaluation (nice) study: Results of a multicenter prospective cohort study for detection of fetal trisomy 21 and trisomy 18. *Am. J. Obstet. Gynecol.* **2012**, *207*, e131–e138.
95. Liang, D.; Lv, W.; Wang, H.; Xu, L.; Liu, J.; Li, H.; Hu, L.; Peng, Y.; Wu, L. Non-invasive prenatal testing of fetal whole chromosome aneuploidy by massively parallel sequencing. *Prenat. Diagn.* **2013**, *33*, 409–415.
96. Boon, E.M.J.; Faas, B.H.W. Benefits and limitations of whole genome *versus* targeted approaches for noninvasive prenatal testing for fetal aneuploidies. *Prenat. Diagn.* **2013**, doi: 10.1002/pd.4111.
97. Chitty, L.S.; Hill, L.; White, H.; Wright, D.; Morris, S. Noninvasive prenatal testing for aneuploidy-ready for prime time? *Am. J. Obstet. Gynecol.* **2012**, *206*, 269–275.
98. GenomeWeb. Aria Kicks off Clinical Trial for Non-Invasive Down Syndrome Test. Available online: <http://www.genomeweb.com/mdx/aria-kicks-clinical-trial-non-invasive-down-syndrome-test> (accessed on 12 May 2013).
99. Liu, L.; Li, Y.; Li, S.; Hu, N.; He, Y.; Pong, R.; Lin, D.; Lu, L.; Law, M. Comparison of next-generation sequencing systems. *J. Biomed. Biotechnol.* **2012**, doi: 10.1155/2012/251364.
100. Loman, N.J.; Misra, R.V.; Dallman, T.J.; Constantinidou, C.; Gharbia, S.E.; Wain, J.; Pallen, M.J. Performance comparison of benchtop high-throughput sequencing platforms. *Nat. Biotechnol.* **2012**, *30*, 434–439.

101. Pareek, C.S.; Smoczynski, R.; Trefyn, A. Sequencing technologies and genome sequencing. *J. Appl. Genet.* **2011**, *52*, 413–435.

102. Benn, P.; Borrell, A.; Cuckle, H.; Dugoff, L.; Gross, S.; Johnson, J.A.; Maymon, R.; Odibo, A.; Schielen, P.; Spencer, K. Prenatal detection of Down syndrome using massively parallel sequencing (MPS): A rapid response statement from a committee on behalf of the board of the international society for prenatal diagnosis. *Prenat. Diagn.* **2012**, *32*, 1–2.
103. Hui, L. Non-invasive prenatal testing for fetal aneuploidy: Charting the course from clinical validation to clinical utility. *Ultrasound Obstet. Gynecol.* **2013**, *41*, 2–6.
104. Jiang, K. Competition intensifies over market for DNA-based prenatal tests. *Nat. Med.* **2013**, *19*, doi: 10.1038/nm0413–1381.
105. Perkel, J. Finding the true \$1,000 genome. *BioTechniques* **2013**, *54*, 71–74.
106. Nicolaides, K.; Syngelaki, A.; Ashoor, G.; Birdir, C.; Touzet, G. Noninvasive prenatal testing for fetal trisomies in a routinely screened first-trimester population. *Am. J. Obstet. Gynecol.* **2012**, *207*, e371–e376.
107. Anderson, C.; Brown, C. Fetal chromosome abnormalities: Antenatal screening and diagnosis. *Am. Fam. Physic.* **2009**, *79*, 117–123.

© 2013 by the authors; licensee MDPI, Basel, Switzerland. This article is an open access article distributed under the terms and conditions of the Creative Commons Attribution license (<http://creativecommons.org/licenses/by/3.0/>).